CANADIAN THESES ON MICROFICHE

THÈSES CANADIENNES SUR MICROFICHE

National Library of Canada
Collections Development Branch

Canadian Theses on
Microfiche Service

Ottawa, Canada
K1A 0N4

Bibliothèque nationale du Canada
Direction du développement des collections

Service des thèses canadiennes
sur microfiche

NOTICE

The quality of this microfiche is heavily dependent upon the quality of the original thesis submitted for microfilming. Every effort has been made to ensure the highest quality of reproduction possible.

If pages are missing, contact the university which granted the degree.

Some pages may have indistinct print especially if the original pages were typed with a poor typewriter ribbon or if the university sent us an inferior photocopy.

Previously copyrighted materials (journal articles, published tests, etc.) are not filmed.

Reproduction in full or in part of this film is governed by the Canadian Copyright Act, R.S.C. 1970, c. C-30. Please read the authorization forms which accompany this thesis.

AVIS

La qualité de cette microfiche dépend grandement de la qualité de la thèse soumise au microfilmage. Nous avons tout fait pour assurer une qualité supérieure de reproduction.

S'il manque des pages, veuillez communiquer avec l'université qui a conféré le grade.

La qualité d'impression de certaines pages peut laisser à désirer, surtout si les pages originales ont été dactylographiées à l'aide d'un ruban usé ou si l'université nous a fait parvenir une photocopie de qualité inférieure.

Les documents qui font déjà l'objet d'un droit d'auteur (articles de revue, examens publiés, etc.) ne sont pas microfilmés.

La reproduction, même partielle, de ce microfilm est soumise à la Loi canadienne sur le droit d'auteur, SRC 1970, c. C-30. Veuillez prendre connaissance des formules d'autorisation qui accompagnent cette thèse.

THIS DISSERTATION
HAS BEEN MICROFILMED
EXACTLY AS RECEIVED

LA THÈSE A ÉTÉ
MICROFILMÉE TELLE QUE
NOUS L'AVONS REÇUE

NL 339 (r. 86/09)

Canada

0-315-19552-5

National Library of Canada
Canadian Theses Division
Ottawa, Canada
K1A 0N4

Bibliothèque nationale du Canada
Division des thèses canadiennes

67460

PERMISSION TO MICROFILM — AUTORISATION DE MICROFILMER

• Please print or type — Écrire en lettres moulées ou dactylographier

Full Name of Author — Nom complet de l'auteur

GONZALO A. ROJAS

Date of Birth — Date de naissance

Dec. 22 / 1945

Country of Birth — Lieu de naissance

COLOMBIA

Permanent Address — Résidence fixe

Departamento de Petróleo
Universidad de Oriente
Puerto La Cruz
VENEZUELA

Title of Thesis — Titre de la thèse

SCALED MODEL STUDIES OF IMMISCIBLE CARBON DIOXIDE DISPLACEMENT OF HEAVY OIL

University — Université

University of Alberta

Degree for which thesis was presented — Grade pour lequel cette thèse fut présentée

Ph.D

Year this degree conferred — Année d'obtention de ce grade

1985

Name of Supervisor — Nom du directeur de thèse

Dr. S.M. FAROUQ ALI

Permission is hereby granted to the NATIONAL LIBRARY OF CANADA to microfilm this thesis and to lend or sell copies of the film.

The author reserves other publication rights, and neither the thesis nor extensive extracts from it may be printed or otherwise reproduced without the author's written permission.

L'autorisation est, par la présente, accordée à la BIBLIOTHÈQUE NATIONALE DU CANADA de microfilmer cette thèse et de prêter ou de vendre des exemplaires du film.

L'auteur se réserve les autres droits de publication; ni la thèse ni de longs extraits de celle-ci ne doivent être imprimés ou autrement reproduits sans l'autorisation écrite de l'auteur.

Date

Jan. 10 / 1985

Signature

Gonzalo Rojas G

NL-91 (4/77)

THE UNIVERSITY OF ALBERTA

SCALED MODEL STUDIES OF IMMISCIBLE CARBON DIOXIDE DISPLACEMENT OF HEAVY OIL

by

GONZALO A. ROJAS

A THESIS

SUBMITTED TO THE FACULTY OF GRADUATE STUDIES AND RESEARCH

IN PARTIAL FULFILMENT OF THE REQUIREMENTS FOR THE DEGREE

OF DOCTOR OF PHILOSOPHY

IN

PETROLEUM ENGINEERING

DEPARTMENT OF MINERAL ENGINEERING

EDMONTON, ALBERTA

SPRING, 1985

THE UNIVERSITY OF THE ALBERTA

RELEASE FORM

NAME OF AUTHOR . . . . Gonzalo A. Rojas . . . . . .

TITLE OF THESIS Scaled Model Studies of Immiscible Carbon Dioxide . . .
Displacement of Heavy Oil . . . . . .

DEGREE FOR WHICH THESIS WAS PRESENTED . Ph.D. . . . . .

YEAR THIS DEGREE GRANTED 1985. . .

Permission is hereby granted to THE UNIVERSITY OF ALBERTA LIBRARY to reproduce single copies of this thesis and to lend or sell such copies for private, scholarly or scientific research purposes only.

The author reserves other publication rights, and neither the thesis nor extensive extracts from it may be printed or otherwise reproduced without the author's written permission.

(Signed) Gonzalo Rojas G. . . . .

PERMANENT ADDRESS:

Departamento de Petroleo . . . . . .

Universidad de Oriente . . . . . .

Puerto La Cruz, Venezuela . . . . . .

DATED . Jan. 10 1985

THE UNIVERSITY OF ALBERTA

FACULTY OF GRADUATE STUDIES AND RESEARCH

The undersigned certify that they have read, and recommend to the Faculty of Graduate Studies and Research, for acceptance, a thesis entitled SCALED MODEL STUDIES OF IMMISCIBLE CARBON DIOXIDE DISPLACEMENT OF HEAVY OIL . . . submitted by GONZALO A. ROJAS . . . . . in partial fulfilment of the requirements for the degree of Doctor of Philosophy in Petroleum Engineering.

Supervisor

External Examiner

Date Dec. 7/1984

To my mother and my family

Maria de Jesus, Maria Eugenia, Eugenia Maria, and David Alberto

ABSTRACT

This research was directed toward an experimental [illegible] the secondary and tertiary recovery of a medium gravity [illegible] CO_2 under immiscible conditions.

The first task undertaken was to derive a set of scaling groups for immiscible displacement of heavy oil by CO_2 gas alone, and by CO_2 and water, using inspectional and dimensional analyses, and taking into account the mass transfer between CO_2 and oil, and CO_2 and water by solution and diffusion. A broad discussion of the practical application of these scaling groups is presented. The basic prototype scaled down was a quarter of a five-spot (total area 6.4 ha) of an unconsolidated, homogeneous reservoir, with rock and fluid characteristics similar to those of the Abeffeldy field in the Lloydminster area.

A flanged, rectangular, pressure vessel, capable of withstanding pressures up to ∿10MPa was designed following ASME guide lines. It was equipped with nine wells, which permitted the simulation of different horizontal and inclined patterns, such as 5-spot, 9-spot, and line drive if desired. It was operated for two years without any problems.

Experimental evaluation of the mass transfer between subcritical CO_2 and two Aberfeldy oil samples at 5.5 MPag & 21-23°C showed that while the solution of CO_2 was high causing a marked decrease in oil viscosity (> 95%), the amount of diffused CO_2 was not enough to produce a reduction in oil viscosity higher than 50%.

Twenty four experiments were carried out using the scaled model. In all runs, the CO_2 slug volume was 20% HCPV and average displacement

conditions were 5.5 MPag and 22°C. The following parameters were varied: injection rate, oil viscosity, type of sand, and volumetric ratio of CO_2/brine slugs (WAG ratio).

The broad range of velocities used (0.18 - 2.9 m/d) permitted the study of the effects of the viscous, diffusive, and gravitational forces on the CO_2 slug process for heavy oil recovery. It was found that viscous forces completely dominated CO_2 injection, and that the mass transfer between CO_2 and oil, and in situ emulsification of oil had a stabilizing effect on the brine front. The experimental results also showed that oil recoveries at CO_2 and brine breakthroughs were rate-dependent. While recovery at CO_2 breakthrough decreased slightly with increasing rate, recovery at brine breakthrough increased moderately.

Among all secondary oil (1032 mPa.s viscosity) recovery strategies tested, the WAG 4:1 process was found to be the best. The basic economic parameters of this process were: 48% HCPV overall recovery (15% HCPV of extra recovery over a brineflood), 131.5 sm^3 of CO_2 required to produce an extra cubic metre of oil, and production of 32.5% of the injected CO_2. For the more viscous oil (4681 mPa.s viscosity) the overall secondary recovery using the WAG 4:1 was 22% HCPV. In this case the small improvement (5% HCPV) in recovery over brineflooding was achieved mainly in the blowdown phase of the flood.

In all WAG tertiary floods, an oil bank was observed to start producing at moderate water-oil ratios at the same time as the CO_2 breakthrough occurred. Although, there was no apparent difference

in tertiary oil recovery for varying WAG ratios; the WAG 4:1 ratio appeared to be slightly more efficient, recovering 13.5% of the original oil in place (prior to brineflooding).

ACKNOWLEDGEMENTS

The author gratefully appreciate the guidance and encouragement provided by Dr. S.M. Farouq Ali during the course of this investigation.

Thanks are expressed to Dr. D.L. Flock for permitting the use of his laboratory equipment.

The author also thanks Professor P.M. Dranchuk, Dr. D.S. Montgomery, Dr. R.G. Bentsen, and Dr. V.R. Puttagunta for their valuable discussion and constructive criticism of this dissertation.

Appreciation is also expressed to Mr. Bob Smith for his valuable help in the setting up of the model and to the Technical Staff of the Department of Mineral Engineering.

Sincere gratitude is expressed to the University of Oriente for providing the author with a two-year scholarship.

Acknowledgement is also made to Husky Oil Operations Ltd., specially to Dr. W.T. Strickland, Jr., for providing the oil, water, and sand used in this study.

The financial support for this research provided by the Alberta Oil Sands Technology and Research Authority (AOSTRA) is gratefully acknowledged. Special thanks are expressed to Dr. Ted Cyr of AOSTRA for his encouragement and input to this research.

TABLE OF CONTENTS

CHAPTER		PAGE
1.	INTRODUCTION	1
2.	PHASES AND OBJECTIVES OF THIS STUDY	3
3.	LITERATURE REVIEW	6
	3.1. Oil Property Changes	7
	3.1.1. Oil Expansion	8
	3.1.2. Diffusion of CO_2 into Heavy Oil and Water	10
	3.1.3. Viscosity Reduction	12
	3.1.4. Solubility of Oils in Compressed Carbon Dioxide	13
	3.2. Interfacial Tension Reduction	16
	3.2.1. Carbon Dioxide - Crude Oil	16
	3.2.2. Water - Crude Oil	16
	3.3. Blowdown Recovery	17
	3.4. Permeability Changes	19
	3.4.1. Rock Dissolution by Carbonic Acid	19
	3.4.2. Asphaltene Deposition	21
	3.5. Laboratory Investigations on Heavy Oil Recovery by Carbon Dioxide	22
	3.5.1. Continuous CO_2 Injection	22
	3.5.2. CO_2 Slug Process	23
	3.5.3. Injection of Alternate Slugs of CO_2 and Water	24
	3.5.4. Tertiary Heavy Oil Recovery	27
	3.6. Simulation of Heavy Oil Production by CO_2 Injection	30

CHAPTER PAGE

4. DERIVATION OF SCALING GROUPS FOR IMMISCIBLE DISPLACEMENT OF OIL BY CARBON DIOXIDE AND BRINE 32

4.1. Inspectional Analysis. 33

4.1.1. Governing Equations 33

4.1.1.1. Solution, Diffusion, and Dispersion Mechanisms 33

4.1.1.2. Assumptions Made in the Development of the Governing Equations 36

4.1.1.3. Mass Balance Equations 37

4.1.1.4. Mass Transport Equations 39

4.1.1.5. Saturation and Capillary Pressure Equations 41

4.1.1.6. Fractional Flow Equation of Carbon Dioxide 42

4.1.2. Boundary and Initial Conditions 44

4.1.3. Dimensionless Form of the Partial Differential Equations 45

4.1.4. Scaling Groups from Inspectional Analysis . 47

4.2. Dimensional Analysis 48

4.3. Scaling of Unstable Displacements 55

5. RELAXATION OF SCALING REQUIREMENTS 59

5.1. Structure of Porous Medium 59

5.2. Inertial Forces 60

5.3. Capillary Forces, Relative Permeability, and Wettability 62

5.4. Dispersion of Carbon Dioxide into Oil and Water . . 63

5.5. End Effects 64

5.5.1. Gas-Oil System 64

CHAPTER PAGE

5.5.2. Water-Oil System 65

5.6. Scaling Groups After Relaxation 67

6. OPERATING POLICY VARIATIONS 69

7. EXPERIMENTAL APPARATUS 74

7.1. High Pressure Physical Model 74

7.1.1. General Design 74

7.1.2. Pressure Vessel 74

7.1.3. Injection and Production Wells 80

7.1.4. Fluid Injection and Production Systems . . . 84

7.1.5. Oven 85

7.1.6. Data Acquisition System 86

7.2. Diffusion Cell 86

8. MATERIALS, EXPERIMENTAL PROCEDURES, AND DATA PROCESSING . 88

8.1. Fluids 88

8.2. Unconsolidated Sand 88

8.3. Aberfeldy Tank Sand Cleaning Procedure 90

8.4. Diffusion of CO_2 into Oil at High Pressure 93

8.5. Packing, Saturation, and Model Cleaning Procedures 93

8.6. Porosity and Permeability Measurements 96

8.7. Experimental Procedure for the Displacement Tests . 98

8.7.1. CO_2 Slug Process 99

8.7.2. Brine - Alternating - CO_2 Slugs (WAG Process). 99

8.7.3. Brineflood 100

CHAPTER PAGE

8.8. Oil-Water Separation 100

8.9. Additional Tests 100

8.10. Interfacial Tension of Oil-CO_2 Saturated Brine at Different Pressures 101

8.11. Study of Mechanically Prepared Emulsions 102

8.12. Data Processing 103

9. PRESENTATION AND DISCUSSION OF RESULTS 105

9.1. Solution and Diffusion of CO_2 into Aberfeldy Heavy Oil 105

9.1.1. Properties of Aberfeldy Heavy Oil Saturated with CO_2 106

9.1.2. Molecular Diffusion of CO_2 into Aberfeldy Heavy Oil 108

9.2. Heavy Oil-Carbonated Brine Interfacial Tensions . . . 114

9.3. In Situ Emulsification of Aberfeldy Crude Oil 121

9.4. Rheology of Mechanically Prepared Emulsions 128

9.5. Sandpack Properties 133

9.6. Displacement Results 139

9.6.1. Heavy Oil Recovery by Immiscible CO_2 Injection 139

9.6.2. Visualization of Displacement Type 146

9.6.3. Rate-Dependence of CO_2 and Brine Breakthrough Oil Recoveries 147

9.6.3.1. Oil Recovery at CO_2 Breakthrough 149

9.6.3.2. Comparison Between Levels of Dispersion in Model and Prototype . 156

9.6.3.3. Oil Recovery at Brine Breakthrough . 159

CHAPTER PAGE

9.6.4. Stabilizing Effect of CO_2 on the Brine Front . . . 163

9.6.5. Overall Recovery for the CO_2 Slug Process 165

9.6.6. Injection of Alternate Slugs of CO_2 and Brine . . 169

9.6.6.1. Effect of the WAG Ratio on Secondary Oil Recovery 171

9.6.6.2. Optimal WAG Ratio 174

9.6.7. WAG Process Versus CO_2 Slug Process 180

9.6.8. Conventional Brinefloods 182

9.6.9. Mobilization of Viscous Residual Oil 188

9.6.10. Blowdown Recovery 198

9.6.11. Effect of Oil Viscosity 207

9.6.12. Basic Economic Parameters 213

9.6.12.1. CO_2 Requirement 213

9.6.12.2. CO_2 Retention 216

9.6.12.3. Prototype/Model Time Scale 218

9.6.13. Production of Sand Fines and Clay Minerals 222

9.6.14. Reproducibility of Displacement Results 225

10. CONCLUSIONS 229

11. RECOMMENDATIONS FOR FURTHER STUDIES 233

REFERENCES 234

APPENDIX A. MASS BALANCE 246

APPENDIX B. DERIVATION OF THE FRACTIONAL FLOW EQUATION OF CARBON DIOXIDE 251

APPENDIX C. DERIVATION OF EQUATIONS 24, 25 AND 26 257

PAGE

APPENDIX D. DERIVATION OF THE DIMENSIONLESS FORM OF THE FRACTIONAL FLOW AND CONTINUITY EQUATIONS 260

APPENDIX E. DERIVATION OF THE SCALING GROUPS BY DIMENSIONAL ANALYSIS 270

APPENDIX F. CALCULATION EXAMPLE OF THE MOLECULAR DIFFUSION COEFFICIENT 278

APPENDIX G. PRODUCTION HISTORIES OF ALL RUNS IN TABULATED FORM . . 282

APPENDIX H, PRODUCTION HISTORIES OF ALL RUNS IN GRAPHICAL FORM . . 336

LIST OF TABLES

TABLE	CAPTION	PAGE
1	Variables Which Control the Displacement Process	51
2	Comparison Between the Scaling Groups Derived by Inspectional and Dimensional Analyses	56
3	Rock and Fluid Properties of the Prototype	79
4	Characteristics of the High Pressure Vessel	82
5	Properties of Oil and Water Used in the Model	89
6	Bulk Mineralogy of the Sands Used in the Experiments	92
7	Data and Results of the Molecular Diffusion Experiments	113
8	Interfacial Tension of Oil External Emulsion-Brine Produced During the CO_2/Brine Floods	115
9	Interfacial Tension of Heavy Oil-Reservoir Water Saturated with CO_2 at Different Pressures	119
10	Characteristics of Unconsolidated Sandpacks	134
11	Summary of Displacement Tests	140
12	Viscous Oil Recovery Performance During the Continuous Injection of a 20% HCPV Slug of Subcritical CO_2	144
13	Effect of Superficial Velocity on Carbon Dioxide and Brine Breakthrough Oil Recoveries	150
14	Values of $(K/V)_M/(K/V)_P$ for Various Carbon Dioxide and Brine Superficial Velocities	161
15	Effect of Carbon Dioxide on Heavy Oil Recovery at Brine Breakthrough	164
16	Summary of Basic Economic Parameters for Secondary Recovery of Heavy Oil by Injection of a 20% HCPV Slug of CO_2 Driven by Brine	167
17	Summary of Basic Economic Parameters for Secondary Recovery of Heavy Oil Using the WAG Process	175

TABLE	CAPTION	PAGE
18	Comparison of Average Economic Parameters for Secondary Heavy Oil Recovery Using the Slug CO_2 and WAG Processes	182
19	Results of Conventional Brinefloods	183
20	Summary of Basic Economic Parameters for Tertiary Recovery of Heavy Oil by Injection of CO_2 and Brine	190
G1	Results of Run 1	283
G2	Results of Run 3	285
G3	Results of Run 4	288
G4	Results of Run 5	291
G5	Results of Run 6	293
G6	Results of Run 7	295
G7	Results of Run 8	296
G8	Results of Run 9	298
G9	Results of Run 10	300
G10	Results of Run 11	302
G11	Results of Run 12	303
G12	Results of Run 13	305
G13	Results of Run 14	307
G14	Results of Run 15	309
G15	Results of Run 16	311
G16	Results of Run 17	313
G17	Results of Run 18	315
G18	Results of Run 19	317
G19	Results of Run 20	320
G20	Results of Run 21	323

TABLE	CAPTION	PAGE
G21	Results of Run 22	326
G22	Results of Run 23	329
G23	Results of Run 24	331
G24	Results of Run 25	333

LIST OF FIGURES

FIGURE	CAPTION	PAGE
1	Solubility of CO_2 in Wilmington Oil (15°API) and Swelling Factors at Different Temperatures	9
2	Viscosity of CO_2-Saturated Bitumen	14
3	CO_2 Density Required for Miscible Displacement	14
4	Schematic Diagram of the Physical Model	75
5	Cross Sections of the High Pressure Vessel	81
6	Pattern Arrangements for Horizontal Floods. Also Central Well to Simulate the Huff-n-Puff Process	83
7	Schematic Diagram of the Diffusion Cell	87
8	Particle Size Analysis of Three Sand Samples	91
9	Steps of Displacement Experiment Procedure	95
10	Refractive Indices of Aberfeldy Reservoir Water-Distilled Water Mixtures	97
11	Determination of Pore Volume by Miscible Displacement. Run 7	97
12	Effect of Pressure on CO_2 Solubility and Swelling Factor of Two Aberfeldy Heavy Oil Samples	107
13	Effect of CO_2 Solubility and Temperature on the Viscosity of Two Aberfeldy Heavy Oil Samples	109
14	Changes of Viscosity of Heavy Oil-CO_2 Foam Formed by Releasing the Pressure after Diffusion of CO_2 @ 23°C & 5.5 MPag During Eight Days	111
15	Interfacial Tensions of Oil External Emulsion-Brine Produced During the CO_2/Brine Floods	116
16	Time Required to Saturate the Reservoir Water With CO_2 @ 5.59 MPag & 23°C	118
17	Effect of Carbon Dioxide on the Interfacial Tension Between Heavy Oil and Reservoir Water from Aberfeldy Field, Lloydminster Area	120

FIGURE	CAPTION	PAGE
18	Structure of Some Nitrogen Bases Found in Heavy Oils . . .	122
19	Pressure Drop Versus Fluid Injected for Different Processes Using Ottawa Silica Sand	125
20	Pressure Drop Versus Fluid Injected For Different Processes Using Aberfeldy Tank Sand	127
21	Rheology of Mechanically Prepared Emulsions	130
22	Comparison of Pack Properties	138
23	Simulated Distillations of Two Aberfeldy-Lloydminster Heavy Oil Samples	148
24	Rate-Dependence of CO_2 and Brine Breakthrough Oil Recoveries of Heavy Oil in Immiscible Carbon Dioxide Slug Process	151
25	CO_2 and Brine Breakthrough Oil Recoveries as a Function of Model/Prototype Ratios of Gravitational Forces to Viscous Forces	152
26	Effect of Transverse and Longitudinal Dispersion on CO_2 Breakthrough Oil Recovery. Ottawa Silica Sand Packs .	153
27	Effect of Transverse and Longitudinal Dispersion on CO_2 Breakthrough Oil Recovery. Ottawa Silica and Aberfeldy Tank Sand Packs	154
28	CO_2 Breakthrough Oil Recovery as a Function of Model/Prototype Transverse Dispersion Scaling Group. Ottawa Silica Sand Packs	157
29	CO_2 Breakthrough Oil Recovery as a Function of Model/Prototype Transverse Dispersion Scaling Group. Ottawa Silica and Aberfledy Tank Sand Packs	158
30	Effect of Superficial Velocity on the Production History of the CO_2 Slug Process	166
31	Effect of the WAG Ratio on Production Histories of Secondary Heavy Oil Recovery Floods	172
32	Comparison of the WAG 4:1 and CO_2 Slug Processes with Brineflood. Secondary Recovery of 1032 mPa.s Oil	173

FIGURE	CAPTION	PAGE
33	Optimal WAG Ratio for Secondary Recovery of Heavy Oil . .	177
34	Effect of WAG Ratio on Cumulative Water-Oil and Gas-Oil Ratios of Immiscible Displacement of Heavy Oil	178
35	Effect of Type of Sand on the Brineflood Performance of Heavy Oil (1032 mPa.s @ 23°C)	189
36	Increase of Heavy Oil Recovery by Injection of Brine Alternates with Subcritical CO_2 After Brineflooding . . .	192
37	Effect of WAG Ratio on Production Histories of Tertiary Heavy Oil Recovery Floods	193
38	Effect of WAG Ratio on Tertiary Heavy Oil Recovery . . .	194
39	Effect of WAG Ratio on Cumulative Water-Oil and Gas-Oil Ratios of Tertiary Recovery of Heavy Oil	195
40	Comparison of Secondary and Tertiary Heavy Oil Recovery Using the WAG 4:1 Process	199
41	Optimal WAG Ratios for Secondary and Tertiary Recovery of Heavy Oil	200
42	Variation of Recovery with Pressure During the Blowdown Stage of Heavy Oil (1032 mPa.s @ 23°C) Displacements . . .	202
43	Effect of Pressure on Blowdown Recovery and Molar Volume of CO_2	203
44	Variation of Water-Oil Ratio During the Blowdown Stage of the Displacements Using the WAG Process	205
45	Variation of Water-Oil Ratio During the Blowdown Stage of Secondary Recovery Displacements Using the CO_2 Slug Process	206
46	Effect of Viscosity on Heavy Oil Recovery by a 20% HCPV Slug of Subcritical CO_2 Driven by Brine	208
47	Effect of Viscosity on Heavy Oil Recovery Using the WAG 4:1 Process (CO_2 Slug Volumes = 2% HCPV)	209
48	Effect of Viscosity on Tertiary Recovery of Heavy Oil Using the WAG 4:1 Process (CO_2 Slug Volumes = 2% HCPV) . .	210
49	Comparison of WAG 4:1 and CO_2 Slug Processes with Brine-flooding for Secondary Recovery of 4681 mPa.s Oil	211

FIGURE	CAPTION	PAGE
50	Comparison of Economic Parameters for Secondary and Tertiary Recovery of Two Viscous Oils Using the WAG 4:1 Process	215
51	Carbon Dioxide Required to Displace Heavy Oil Using CO_2 Slug and WAG Processes	217
52	Effect of CO_2 Retention on Blowdown Recovery	219
53	Secondary and Tertiary Oil Recovery Versus Model and Prototype Times. WAG 4:1 Process	221
54	Reproducibility of Brinefloods Conducted Under Identical Conditions	226
55	Reproducibility of the WAG 1:1 Process Varying Only the Volume of the CO_2 Slugs	227
A1	Control Volume for Mass Balance of Carbon Dioxide	248
H1	Production History of Run 1	337
H2	Production History of Run 3	338
H3	Production History of Run 4	339
H4	Production History of Run 5	340
H5	Production History of Run 6	341
H6	Production History of Run 7	342
H7	Production History of Run 8	343
H8	Production History of Run 9	344
H9	Production History of Run 10	345
H10	Production History of Run 11	346
H11	Production History of Run 12	347
H12	Production History of Run 13	348
H13	Production History of Run 14	349
H14	Production History of Run 15	350
H15	Production History of Run 16	351

FIGURE	CAPTION	PAGE
H16	Production History of Run 17	352
H17	Production History of Run 18	353
H18	Production History of Run 19	354
H19	Production History of Run 20	355
H20	Production History of Run 21	356
H21	Production History of Run 22	357
H22	Production History of Run 23	358
H23	Production History of Run 24	359
H24	Production History of Run 25	360

LIST OF PHOTOGRAPHIC PLATES

PLATE	CAPTION	PAGE
1	Rectangular, High Pressure Vessel and Sight Glass Equipped High Pressure Separator	76
2	High Pressure Fluid Injection System	77
3	Model and Fluid Production System	78
4	60% Brine-in-Oil Aberfeldy Emulsion. Brine pH = 7.1 Oil Sample 1	132
5	60% Brine-in-Oil Aberfeldy Emulsion. Brine pH = 7.32 Oil Sample 1	132
6	25% Brine-in-Oil Aberfeldy Emulsion. Brine pH = 6.5 Oil Sample 1	132
7	25% Brine-in-Oil Aberfeldy Emulsion. Brine pH = 7.5 Oil Sample 1	132
8	25% Brine-in-Oil Aberfeldy Emulsion. Brine pH = 5.41 Oil Sample 2	132
8	25% Brine-in-Oil Aberfeldy Emulsion. Brine pH = 7.56 Oil Sample 2	132

NOMENCLATURE

A	Cross-Sectional Area (L^2)
Ax, Ay, Az	Cross-Sectional Area Normal to Flow in x, y, and z Directions (L^2)
Bg, Bo, Bw	Volumetric Factor of Carbon Dioxide, Oil and Water (L^3L^{-3})
Cgo, Cgw	Concentration of Carbon Dioxide into Oil and Water Due to Diffusion and Convective Dispersion (L^3L^{-3})
dp	Average Particle Diameter (L)
$\bar{\bar{D}}go$, $\bar{\bar{D}}gw$	Diagonal Tensor of Dispersion Coefficient of Carbon Dioxide into Oil and Water (L^2t^{-1})
Dgox, Dgoy, Dgoz	Dispersion Coefficient of Carbon Dioxide into Oil in x, y, and z Directions (L^2t^{-1})
Dgwx, Dgwy, Dgwz	Dispersion Coefficient of Carbon Dioxide into Water in x, y, and z Directions (L^2t^{-1})
D_{Lgo}, D_{Lgw}	Longitudinal (x-direction) Dispersion Coefficient of Carbon Dioxide into Oil and Water (L^2t^{-1})
Do	Molecular Diffusion of Carbon Dioxide into Oil (L^2t^{-1})

$D_{Tgo}(D_T)$, D_{Tgw}	Transverse (y and z directions) Dispersion Coefficient of Carbon Dioxide into Oil and Water (L^2t^{-1})
$\vec{f_g}$, $\vec{f_o}$, $\vec{f_w}$	Vector of Fractional Flow of Carbon Dioxide, Oil, and Water (Lt^{-1}/Lt^{-1})
$f_{g\xi}$, $f_{g\theta}$, $f_{g\lambda}$	Fractional Flow of Carbon Dioxide in ξ, θ, and λ Directions (Lt^{-1}/Lt^{-1})
$f_{o\xi}$, $f_{o\theta}$, $f_{o\lambda}$	Fractional Flow of Oil in ξ, θ, and λ Directions (Lt^{-1}/Lt^{-1})
$f_{w\xi}$, $f_{w\theta}$, $f_{w\lambda}$	Fractional Flow of Water in ξ, θ, and λ Directions (Lt^{-1}/Lt^{-1})
$\vec{g}$	Vector of Gravity Acceleration (Lt^{-2})
g_x, g_y, g_z	Gravity Acceleration in x, y, and z Directions (Lt^{-2})
$\vec{Ggo}$, $\vec{Ggw}$	Vector of Volumetric Flux of Carbon Dioxide Dispersing into Oil and Water (L^3t^{-1})
Ggox, Ggoy, Ggoz	Volumetric Flux of Carbon Dioxide Dispersing into Oil in x, y, and z Directions (L^3t^{-1})
Ggwx, Ggwy, Ggwz	Volumetric Flux of Carbon Dioxide Dispersing into Water in x, y, and z Directions (L^3t^{-1})
H	Height of the System (L)
H_M, H_p	Height of the Model and Prototype (L)
Isr	Instability Number (Dimensionless)

J(Sg), J(Sg*)	Gas-Oil Leverett J-function (Dimensionless)
J(Sw), J(Sw*)	Oil-Water Leverett J-function (Dimensionless)
K	Absolute (Single Fluid) Permeability (L^2)
$\bar{\bar{K}}$	Diagonal Tensor of Absolute Permeability (L^2)
Kx, Ky, Kz	Absolute Permeability in x, y, and z Directions (L^2)
Kg, Ko, Kw	Effective Permeability to Gas, Oil, and Water (L^2)
Krg(Sg), Krg(Sg*)	Relative Permeability to Gas (Dimensionless)
Kro(Sg,Sw), Kro(Sg*,Sw*)	Relative Permeability to Oil (Dimensionless)
Krw(Sw), Krw(Sw*)	Relative Permeability to Water (Dimensionless)
K_M, K_P	Absolute Permeability of the Model and Prototype (L^2)
Kwor	Permeability to Water at Residual Oil Saturation (L^2)
L	Length of the System (L)
L_M, L_P	Length of the Model and Prototype (L)
m_{CO_2}	Weight of CO_2 in the Foam (M)
m_o	Weight of Oil in the Foam (M)
Mg, M_{CO_2}	Molecular weight of Carbon Dioxide (MM^{-1})
Mgo	Gas-Oil Mobility Ratio (Dimensionless)
Mo	Molecular Weight of Oil (MM^{-1})

Mwo, M	Water-Oil Mobility Ratio (Dimensionless)
Ncgo	Linear Gas-Oil Capillary Number (Dimensionless)
Ncow	Linear Oil-Water Capillary Number (Dimensionless)
Ng	Gravity Number (Dimensionless)
Ng	Molar Flow of Carbon Dioxide (Mt^{-1})
$\vec{N}gog$	Vector of Oil-Gas Gravity Number (Dimensionless)
$\vec{N}gwo$	Vector of Water-Oil Gravity Number (Dimensionless)
P	Pressure ($ML^{-1}t^{-2}$)
Pc	Capillary Pressure ($ML^{-1}t^{-2}$)
Pg, Po, Pw	Pressure in Carbon Dioxide, Oil, and Water Phases ($ML^{-1}t^{-2}$)
q_o, q_w	Oil and Water Flow Rates for Two-Phase Flow (L^3t^{-1})
Q	Injection Flow Rate (L^3t^{-1})
Re	Reynolds Number (Dimensionless)
Rso, Rsw	Solution Carbon Dioxide-Oil and Carbon Dioxide-Water Ratios (L^3L^{-3})
Sg, So, Sw	Gas, Oil, and Water Saturations (L^3L^{-3})
Sg*, So*, Sw*	Normalized Gas, Oil, and Water Saturations (Dimensionless)
Sor	Residual Oil Saturation (L^3L^{-3})

Swi	Irreducible Water Saturation (L^3L^{-3})
t	Time (t)
T	Temperature (T)
t_M, t_P	Time Scale for Model and Prototype (t)
$\overrightarrow{v_g}$	Vector of Composite Carbon Dioxide Velocity (Lt^{-1})
$\overrightarrow{v'_g}$	Vector of Carbon Dioxide Velocity From Darcy's Law (Lt^{-1})
$\overrightarrow{v'_o}$, $\overrightarrow{v_o}$	Vector of Oil Velocity from Darcy's Law (Lt^{-1})
$\overrightarrow{v'_w}$, $\overrightarrow{v_w}$	Vector of Water Velocity from Darcy's Law (Lt^{-1})
v_{gx}, v_{gy}, v_{gz}	Composite Carbon Dioxide Velocity in x, y, and z Directions (Lt^{-1})
v_{ox}, v_{oy}, v_{oz} (v'_{ox}, v'_{oy}, v'_{oz})	Oil Velocity from Darcy's Law in x, y, and z Directions (Lt^{-1})
v_{wx}, v_{wy}, v_{wz} (v'_{wx}, v'_{wy}, v'_{wz})	Water Velocity from Darcy's Law in x, y, and z Directions (Lt^{-1})
$\overrightarrow{v_T}$	Vector of Superficial Velocity (Lt^{-1})
$\lvert\overrightarrow{v_T}\rvert$, V	Superficial Velocity (Lt^{-1})
V_M, V_P	Model and Prototype Superficial Velocities (Lt^{-1})

V_g^*, V_w^*	Slug Volumes of Carbon Dioxide and Water (Fraction of the Hydrocarbon Pore Volume of the System) (L^3L^{-3})
W	Width of the System (L)
x, y, z	Cartesian Coordinates
$\Delta C/\Delta L$	Concentration Gradient of CO_2 in the Oil (ML^{-4})
$\Delta G/\Delta t$	Molar Flux of Carbon Dioxide by Diffusion (Mt^{-1})
$\Delta\rho_{og}$	Oil-Carbon Dioxide Density Difference (ML^{-3})
$\Delta\rho_{wo}$	Water-Oil Density Difference (ML^{-3})
θ	Dimensionless Width
λ	Dimensionless Height
μ_g, μ_o, μ_w	Carbon Dioxide, Oil, and Water Viscosities $(ML^{-1}t^{-1})$
ξ	Dimensionless Length
ρ	Density (ML^{-3})
ρ_g, ρ_o, ρ_w	Carbon Dioxide, Oil, and Water Densities at Reservoir Conditions (ML^{-3})
$\rho_{w\text{-}CO_2}$	Density of Water Saturated with CO_2 (ML^{-3})
ρ_g^*	Carbon Dioxide Density at Standard Conditions (ML^{-3})
σ	Interfacial Tension (Mt^{-2})

σ_e	Effective Interfacial Tension (Mt^{-2})
σ_{go}	Carbon Dioxide-Oil Interfacial Tension (Mt^{-2})
σ_{ow}	Oil-Water Interfacial Tension (Mt^{-2})
σ_m	Inhomogeneity Factor (a measure of the inhomogeneity of the porous medium)
τ	Dimensionless Time
τ_M, τ_P	Model and Prototype Dimensionless Times
ν_f	Specific Volume of the Oil-CO_2 Mixture (L^3M^{-1})
ν_{CO_2}	Specific Volume of CO_2 (L^3M^{-1})
ν_o	Specific Volume of Oil (L^3M^{-1})
ϕ	Porosity (L^3L^{-3})
ϕ_P, ϕ_M	Porosity of Model and Prototype (L^3L^{-3})

1. INTRODUCTION

Two-thirds of the heavy oil deposits of the world cannot be exploited by means of thermal methods, because the energy balance of a field project can be poor for reasons of reservoir depth and thickness, low oil saturation and/or porosity. This huge amount of oil (several trillion barrels) has provided strong motivation for the development of new and improved heavy oil recovery methods. One of the more promising of these techniques uses carbon dioxide and water for immiscible displacement of conventional, not too viscous, heavy oils as has been recently demonstrated by the excellent results of several projects which are being carried out in the United States and Hungary.[1]

In Lloydminster, Canada, there are many heavy, moderately viscous oil reservoirs which do not offer favourable conditions for the application of thermal methods such as steam injection and in situ combustion. Some of them are located in the Aberfeldy field which is one of the largest oil fields in the Lloydminster area. The Aberfeldy reservoirs are characterized by shallow (518 m) and thin (6.1 m) unconsolidated, marine sands, moderate oil viscosity (1000-5000 mPa.s at reservoir conditions), and low reservoir pressure (3.45 MPa). In these thin reservoirs, the thermal methods could yield good technical results but due to the high heat losses their economics may be tenuous. Better results could be obtained with CO_2/water injection under immiscible conditions.

To date, the published laboratory studies of immiscible displacement of heavy oil by CO_2 gas or liquid have been conducted in

unscaled models[2,3,4,5]. Optimistic high recovery is obtained in such models, because in many cases the development of viscous and gravitational instabilities is restricted, and thereby the results obtained are of limited value from the standpoint of field application.

The main objective of this research was to build a high pressure scaled model on the basis of a new set of scaling groups derived by inspectional and dimensional analyses, which included the variables that affect the CO_2/water/oil flow in porous media. Numerous experiments were carried out with a view to investigating the effect of the different forces that control the displacement of heavy oil by subcritical carbon dioxide/brine injection and optimizing Aberfeldy oil recovery through the use of various brine-carbon dioxide injection strategies.

2. PHASES AND OBJECTIVES OF THIS STUDY

The broad objective of this study was to investigate the possible application of the CO_2/water injection process to shallow, thin, heavy oil reservoirs with characteristics similar to the Aberfeldy-Lloydminister reservoirs. To meet this broad objective the research was conducted in several phases:

1. Review of the literature on the current technological research being conducted on immiscible displacement of heavy oil by carbon dioxide and on the changes in oil properties due to solution and diffusion of CO_2 in heavy oils. The information obtained from the review was used in the design and methodology of the laboratory research performed in this study, and as a comparison for the results obtained.
2. Derivation of the scaling groups for three-dimensional, immiscible displacement of heavy oil by CO_2 gas alone and by CO_2 plus water using inspectional and dimensional analyses and taking into account the diffusion and dispersion of carbon dioxide into oil.
3. Design of a flanged rectangular pressure vessel following the design equations of the American Society of Mechanical Engineers, ASME.
4. Setting up the physical model to evaluate various strategies of CO_2/water injection into a reservoir.
5. Evaluation of the Aberfeldy reservoir water and oil properties as well as the volumetric behaviour and viscosity of CO_2-oil mixtures.
6. Conducting a series of displacement tests to simulate physically the injection of carbon dioxide and brine in shallow, thin, heavy oil reservoirs. The following CO_2/brine injection strategies were

studied:

6.1. Secondary Recovery

6.1.1. CO_2 slug-brine flood

6.1.2. Alternate slugs of CO_2 and brine

6.1.3. Brineflood (To have a basis for comparing with oil recoveries obtained by carbon dioxide injection.)

6.2. Tertiary Recovery

6.2.1. Brineflood-CO_2 slug-Brine flood

6.2.2. Brineflood - Alternate slugs of CO_2 and brine.

In all runs, the total slug volume of CO_2 and the average displacement pressure were maintained constant. The following parameters were varied:

- Injection flow rate
- Oil viscosity
- Type of sand
- Volumetric ratio of CO_2/brine slugs (WAG ratio)

This experimental and theoretical study was designed to meet the following objectives:

1. To derive a new set of scaling groups to simulate physically the immiscible displacement of oil by CO_2/water injection, taking into account the mass transfer between CO_2 and oil, and CO_2 and water.
2. To construct a high pressure, rectangular, scaled model, which has been operated for two years without any mechanical problems.
3. To evaluate the effect of injection flow rates on oil recovery.

4. To investigate the role of the viscous, diffusive, and gravitational forces on the immiscible displacement of heavy oil by CO_2 and water.
5. To gain insight into the blowdown recovery mechanism.
6. To select the best CO_2/brine injection strategy for the recovery of viscous oil from shallow, thin reservoirs.
7. To optimize the slug volumes of CO_2 and water in the WAG process in order to maximize secondary and tertiary oil recoveries.

3. LITERATURE REVIEW

A literature survey reveals that up to now all the experimental studies of oil recovery by carbon dioxide at high pressure have been conducted in unscaled models of cylindrical shape, because, as was recognized by Dosher and Gharib[6], "it had been impossible to fabricate a rectangular model free of mechanical problems." These studies permitted insight to be gained into the microscopic displacement mechanisms, which are reviewed in this chapter. However, as the real geometry of the reservoirs was not simulated, in many cases the viscous and gravitational instabilities were restricted, resulting in optimistically high oil recoveries.

Work in the early 1960's by Beeson and Ortloff[2], Dickerson and Crawford[7], and Welker and Dunlop[8] identified the potential for using carbon dioxide as an enhanced heavy oil recovery agent. However, at that time there was little interest in exploiting the heavy oil fields, and usually the cost of CO_2 required was greater than the price of the heavy crude oil. The favourable response from a small-volume, immiscible CO_2 project conducted by U.S. Oil Refining Co. in Arkansas in 1969[9] can be considered as the precursor of field projects of carbon dioxide to recover heavy oil.

Carbon dioxide can be injected into a reservoir in the liquid or the gas phase. Beeson and Ortloff[2] found that the additional heavy oil recovery per unit of carbon dioxide injected (on a mass basis) waa higher when a slug of CO_2 driven by water was injected in as a gas phase rather than as a liquid. Recently, Miller and Jones[10] presented a paper on

the solubility of CO_2 into and swelling of heavy oils (15-17°API). The PVT (Pressure - Volume - Temperature) curves showed a sharp break at approximately the condensation pressure of carbon dioxide when it goes from gas to liquid phase. Very little CO_2 goes into solution after carbon dioxide is in the liquid phase. The above findings indicate that in the case of heavy oils it is better to inject the CO_2 in the gas phase rather than in the liquid phase

To inject CO_2 gas in a shallow, cold reservoir with temperature around 21°C (such as Lloydminster, Saskatchewan, reservoirs) it is necessary that the pressure of CO_2 be lower than 6 MPa. As discussed by Kamath et al.[11], when injecting supercritical CO_2 or CO_2 gas into a reservoir, the carbon dioxide will be in equilibrium with liquid oil so that the flow is essentially two-phase and overall miscibility of the CO_2 - hydrocarbon system in never attained. That is, the displacement mechanism is essentially of the Buckley-Leverett type, with mass transfer[12]. This idea has been supported by the results of several experimental works[4,5,13,14].

3.1. Oil Property Changes

Early work of Beecher and Parkhurst[15] in 1926 showed that the solubility of carbon dioxide in crude oil is higher than that of natural gas. For a particular crude oil of 30.2°API, a natural gas (82.5% CH_4) was found to be approximately four times as soluble as air, but only one-third as soluble as carbon dioxide on a molar basis. Since 1926, several investigators have shown that CO_2 dissolves readily in heavy oil[7,8,10,16,17,18] and bitumen[19,20] increasing the volume and reducing viscosity.

3.1.1. Oil Expansion

Solubility of carbon dioxide in crude oils and expansion of crude oils in equilibrium with CO_2 are governed by three factors: pressure, temperature, and crude oil composition. Miller and Jones[10] found that at supercritical temperature the solubility of CO_2 gas and the expansion of heavy oils increase with increasing pressure and decreasing temperature and density of oil. Figure 1 shows the carbon dioxide solubility and the swelling factor for Wilmington oil (15°API) at different temperatures. The CO_2 solubility is defined as the standard cubic metres of CO_2 in solution in a cubic metre of stock tank oil at certain conditions of pressure (P) and temperature (T). In turn, the swelling factor is defined as:

$$\frac{\text{Volume of oil saturated with } CO_2 \text{ at P and T}}{\text{Volume of oil containing no } CO_2 \text{ at T}}$$

It can be seen in Figure 1 that at 23.9°C, which is less than the critical temperature of carbon dioxide (31.1°C), the curve shows a sharp break in solubility at approximately the condensation pressure of CO_2. The low mass transfer between CO_2 liquid and heavy oil may be the reason for the aforementioned sharp break in the solubility and swelling curve slopes.

Several researchers[8,10,21] have shown that the solubility of carbon dioxide gas in conventional heavy oil (14-17°API) at moderate pressures (4-6 MPa) and temperatures (20-25°C) is of the order of 50-100 sm^3 in a cubic metre of oil, yielding between 10 and 20% increase in volume.

Also, Svrcek and Mehrotra[20] measured the amounts of carbon dioxide,

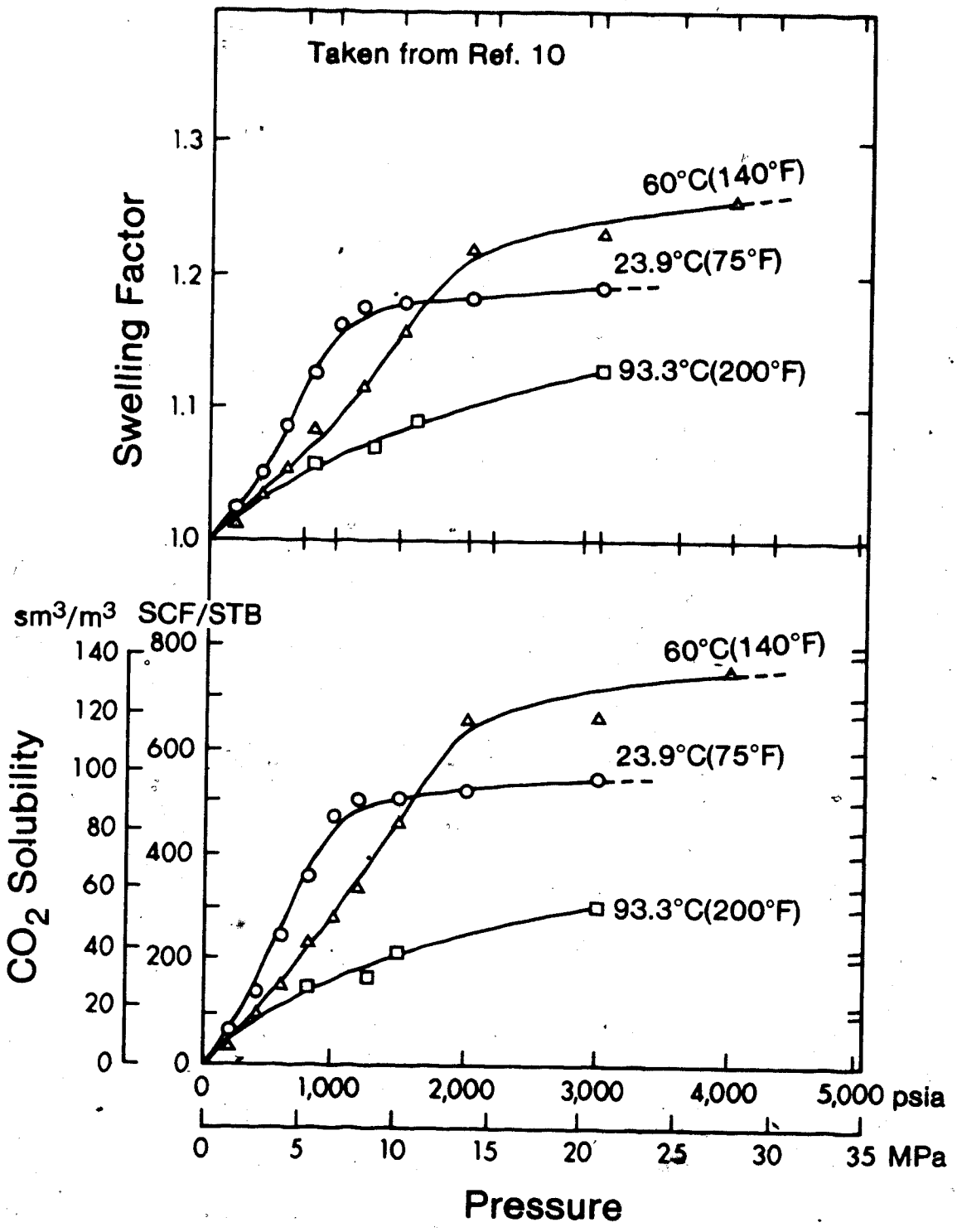


Figure 1 Solubility of CO_2 in Wilmington Oil (15°API) and Swelling Factors at Different Temperatures

methane, and nitrogen in Athabasca bitumen at different pressures and temperatures. They found that the volumetric solubility of carbon dioxide in bitumen varies more or less linearly with pressure in the range of 0-6 MPa investigated by them. They did not find the break in solubility found by Miller and Jones[10], possibly because they worked at relatively low pressures.

The swelling or expansion effect is a very important recovery mechanism because the volume of residual oil left in the reservoir after flooding is inversely proportional to the swelling factor; that is, the greater the swelling, the less is the stock tank oil abandoned in the reservoir.

3.1.2. Diffusion of CO_2 into Heavy Oil and Water

Carbon dioxide mixes with viscous oils not only by solution but also by diffusion. If CO_2 and heavy oil are in contact with an initially sharp interface they will very slowly diffuse into one another. As time passes, the sharp interface between the two fluids will become a diffuse mixed zone. This macroscopic transport of mass, independent of any convection within the system, is defined as molecular diffusion. The diffusion helps carbon dioxide to penetrate into heavy oil and may reduce viscous fingering. Also, in the cyclic CO_2 stimulation process[22], the volume of oil contacted by CO_2 can be increased by diffusion. A precise knowledge of the diffusion coefficient permits the determination of the optimal soaking time.

Very little information is available on the molecular diffusion coefficient of carbon dioxide into oils at reservoir conditions. Most experiments have been performed at atmospheric pressure. Davies et al.[23]

reported a study made on the diffusion of carbon dioxide into a range of organic liquids and hydrocarbon mixtures over a sixty-fold range of solvent viscosity. For a gas oil of 26.5 mPa.s viscosity, the diffusivity was 0.728E - 05 cm^2/s at 25°C and 0 MPag (g indicates gauge pressure).

Rajan and Goren[24], studying the absorption of gas into liquid droplets flowing on a vertical wire, determined the diffusivity of carbon dioxide into high viscosity hydrocarbon oils. They found diffusion coefficients lower than 1.0E - 05 cm^2/s at atmospheric pressure for hydrocarbon oils having viscosities greater than 50 mPa.s.

McManamey and Woolen[25] in 1973 proposed the following equation for the diffusion coefficient of CO_2 in organic liquids at atmospheric conditions

$$Do(cm^2/s) = 1.41 \times 10^{-10} \mu_o^{-0.47} (mPa.s) . \qquad (1)$$

Recently, Denoyellé and Bardon[26] found that the diffusion coefficient of CO_2 increases with increasing pressure. At 15 MPag, diffusion coefficients were found to be more than five times higher than those reported in the literature at atmospheric pressure. For example, they found a diffusion coefficient of 4.6 E - 05 cm^2/s at 15 MPag and 80°C for a 570 mPa.s viscosity oil. Using Equation 1, a value of 0.18E - 05 cm^2/s is obtained for the same crude oil at atmospheric conditions. The authors concluded that there is still an influence of the oil viscosity on diffusivity but it seems to be slightly less pronounced than that at atmospheric pressure.

Schmidt et al.[27] also found high values of carbon dioxide

diffusivity in Athabasca bitumen. At 5 MPag the molecular diffusion coefficient measured was of the order of that observed in most liquid systems (1.0E - 05 cm^2/s). The authors concluded that the high viscosity of bitumen and the fact that diffusivities are not lower than 1.0E - 05 cm^2/s suggest a strong interaction between CO_2 and bitumen.

Although Schmidt et al.[27] and Denoyelle and Bardon[26] used different devices for the diffusion coefficient measurements, the very high values reported by them could have been affected by convection streams induced by density changes and pressure gradients at the beginning of the experiments, and by swelling or expansion of the oil by solution of CO_2.

Water is not as good a solvent as oil for CO_2. Mungan[28] indicated that the change in viscosity, density, and formation volume factor of water, due to the low carbon dioxide solution, can be shown to be less than one percent. However, literature data[25] indicate that diffusion of CO_2 in water at 75°C is faster than diffusion of CO_2 in oil if the oil viscosity is above 0.5 mPa·s. Denoyelle and Bardon[26] also found that CO_2 diffused faster in water than in any of the viscous oils studied by them and that the diffusivity of CO_2 in water varies as the square root of pressure.

3.1.3. Viscosity Reduction

The large reduction in the viscosity of heavy oils when they become saturated with carbon dioxide at increasing pressures is the main mechanism of the immiscible CO_2-flooding process. Viscosity reductions greater than 90% can be obtained by saturating heavy oil with CO_2 at 5.5 MPag[8,16]. Dickerson and Crawford[7] reported that

greater percentage reductions in viscosity occur at lower operating temperatures than at higher temperatures, suggesting that at some high temperature the curves converge to form a single line along which viscosity is a function of temperature alone. Comparing the results obtained by Dickerson and Crawford[7], Jacobs et al.[19], and Bader et al.[29], the above-mentioned temperature is around 150°C for pressures below 6.9 MPa (see Figure 2). Killesreiter[30] also found that at 145°C and above, the effect of dissolved carbon dioxide on oil viscosity is negligible.

Jacobs et al.[19] reported the effect of dissolved carbon dioxide, methane and nitrogen on the viscosity of Athabasca bitumen. Their experimental results show that CO_2 dramatically reduces the viscosity of bitumen, particularly at temperatures lower than 100°C. Methane and nitrogen were found to have a much smaller effect on bitumen viscosity.

Another factor that affects the viscosity of heavy oil-carbon dioxide mixtures is the time to achieve equilibrium (meaning no change of viscosity with time) between the two fluids. At times lower than the equilibrium time, the viscosity of the mixture decreases with time. Goss and Exall[31] showed an example of the viscosity behaviour of a Canadian bitumen sample exposed to a 6.8 MPag carbon dioxide atmosphere at 50°C. The equilibrium was achieved in 12.5 days and the bitumen viscosity decreased from 18000 mPa.s to 8000 mPa.s during that period of time.

3.1.4. Solubility of Oils in Compressed Carbon Dioxide

In 1959, Prausnitz and Benso[32] reported data on the solubility of liquid hydrocarbons in compressed carbon dioxide and used them to

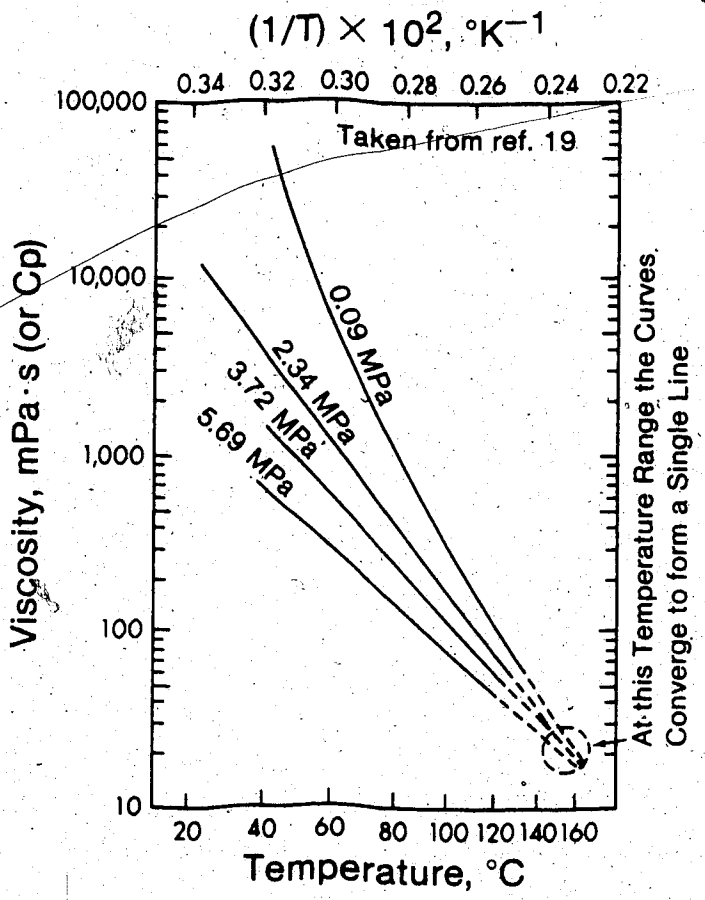


Figure 2 Viscosity of CO_2-Saturated Bitumen

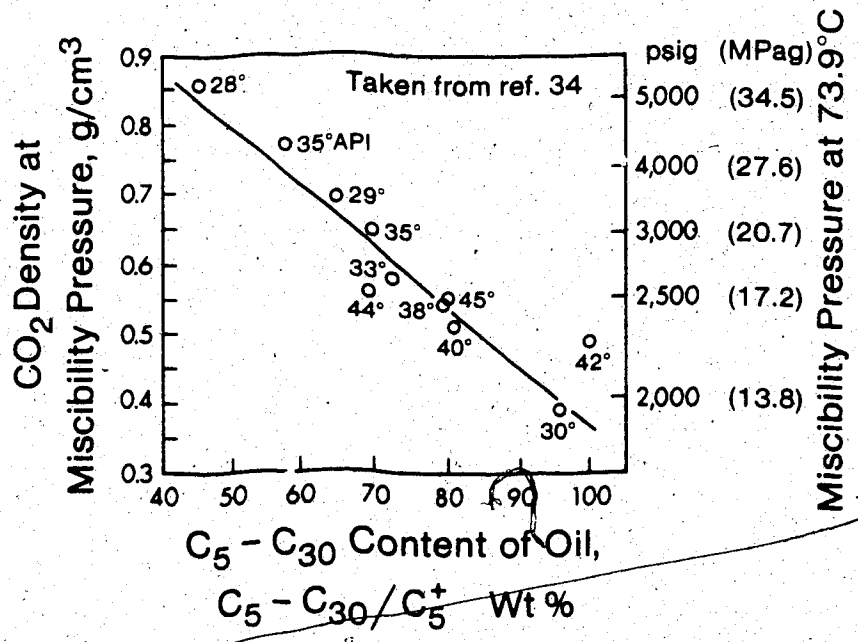


Figure 3 CO_2 Density required for Miscible Displacement

compute virial coefficients for the vapour-phase mixtures. It was found by the authors that at the same temperature and total pressure, a liquid hydrocarbon is more soluble in nitrogen than in hydrogen and more soluble in carbon dioxide than in nitrogen. The difference in physical properties between hydrogen (T_c = 33°K) and a typical liquid hydrocarbon (T_c = 500°K) is certainly larger than that between the physical properties of nitrogen (T_c = 126°K) or carbon dioxide (T_c = 304°K) and a typical liquid hydrocarbon. Later, in 1982, Holm and Josendal[33] found that supercritical CO_2 is a much more powerful solubilizer of hydrocarbons than natural gas; carbon dioxide extracts (or vaporizes) hydrocarbons in the gasoline and gas-oil range (C_5 - C_{30}) rather than only C_2 through C_6 hydrocarbons. The solvent power of CO_2 increases with pressure which is associated with increased CO_2 density. For heavy oils with very small amounts of gasoline and gas-oil range hydrocarbons, higher pressure is required to compress the carbon dioxide to a more dense liquid and to promote greater solubility.

Figure 3, taken from Holm[34], shows that the greater the concentration of extractable hydrocarbons $\left(\frac{C_5 - C_{30}}{C_5^+} \text{ wt\%}\right)$, the lower the minimum miscibility pressure (MMP) between light oils and carbon dioxide should be. For instance, Red Wash oil (28°API) with $\frac{C_5 - C_{30}}{C_5^+}$ wt% = 45% has a MMP higher than 34.5 MPag at 73.9°C; that means that the MMP's for heavy oils with low percentage of extractable hydrocarbons by carbon dioxide would be in excess of 35 MPag, which are impractical pressures for heavy oil reservoirs.

3.2. Interfacial Tension Reduction

It is well known that in immiscible displacements a reduction in interfacial tension between displacing and displaced phases produces a decrease in capillary pressure so that a significant reduction in the residual oil saturation may be achieved. Also, a low oil-water interfacial tension promotes in situ emulsification of oil, which may improve oil recovery.

3.2.1. Carbon Dioxide - Crude Oil

Rosman and Zana[35] reported that the interfacial tensions (0.1 - 0.03 mN/m) between carbon dioxide (displacing phase) and a mixture of CO_2 and crude oil (displaced phase) in a carbon dioxide flood is lower than that between water and oil (24.8 mN/m) in a waterflood. The same researchers determined values of residual saturations of light oils for immiscible CO_2 floods at 15 - 16 MPa & 54.4°C, 10% lower than for waterfloods.

Early work on the surface tension of crude oils in equilibrium with gases (or interfacial tension between crude oils and gases) was done by Beecher and Parkhurst[15]. The results of their experiments indicated a reduction of approximately 20% in the surface tension of crude oils at pressures from 2.8 to 3.4 MPa. Numerous data on surface tension of crude oils at high pressure are presented by Katz et al.[36].

3.2.2. Water - Crude Oil

Several researchers have determined the reduction in interfacial tension between crude oil and water with acid pH. Breston and Macfarlane[37] showed that the interfacial tension between Bradford crude

and water can be reduced from 28.8 to 18.1 mN/m by carbonation at 5.2 MPag. (It is intended to give an explanation for the decrease of the carbonic acid - heavy oil interfacial tension, later in the text.) Farouq Ali et al.[38] and Scott et al.[39] presented curves of interfacial tension of Lloydminster crude oils as function of pH, showing reductions of interfacial tension at low and high pH.

Strassner[40] observed that emulsions commonly encountered in producing crude oils are stabilized by films, which are formed at the water-oil interfaces. It was found by Strassner that the rigid interfacial films formed by asphaltenes are strongest in acid pH and the emulsions produced in this case are water-in-oil type.

Viscous, stable emulsions of acid solutions in Lloydminster crude were employed by Farouq Ali et al.[38] to displace Lloydminster crude from porous media. The breakthrough oil recovery achieved using an acid emulsion slug of 3% pore volume displaced by water was twice that for a waterflood, showing that the acid emulsion was effective in controlling the high mobility of water.

3.3. Blowdown Recovery

Blowdown Recovery is the oil recovered after termination of a flood by depleting the pressure in the reservoir to a low value. The mechanism of blowdown is similar to solution gas drive during the normal production-depletion of an oil field. However, at the same conditions of pressure, temperature, saturations, and crude composition the blowdown recovery in carbon dioxide floods is higher than that in gas floods due to the higher expansion, and solubility of carbon dioxide in oil.

Beeson and Ortloff[2] were the first to show the effectiveness of the blowdown mechanism in recovering oil. They indicated that the additional recovery by solution gas drive is very nearly equal to the additional oil recovery obtained as a result of trapped gas in waterfloods carried out in the presence of a free gas phase.

Using a 22°API stock-tank oil, Holm and Josendal[41] showed that up to 18.6% of the original oil in place can be recovered by CO_2 solution gas drive. Also, results of experiments carried out by Rojas and coworkers[4,42] in Venezuela showed that high recoveries of heavy oil (10-15°API) can be achieved by the blowdown mechanism. For instance, using a 15°API Venezuelan oil up to 31% of the oil in place was recovered by CO_2 solution gas drive from an unconsolidated porous medium with a high initial oil saturation when the pressure was reduced from 20.7 to 0 MPag. In that experiment a high recovery of 25% was obtained when the pressure dropped from 6.9 to 0 MPag. This behaviour is due to the high volume expansion of CO_2 between those pressure levels at 65.6°C. This experiment was repeated using natural gas (85% CH_4) instead of CO_2 and the recovery was only 13% HCPV.

Holm[43] found that the additional oil recovered by pressure-depletion after termination of CO_2-carbonated waterfloods is a direct function of oil saturation at the end of floods. This finding was verified by Rojas and coworkers[4,42], who using the same 15°API oil mentioned above, obtained a low blowdown recovery of 3% after the subordinate phase of a supercritical CO_2 flood (at 20.7 MPag & 65.6°C). The result of this run is similar to that reported by Klins and Farouq Ali[44] using a numerical model. Recently, Bardon et al.[45] using

heavy oils (9-15°API) from Turkey also obtained high oil recovery by depletion after pressurization with CO_2 gas.

The effect of pressure on blowdown recovery was investigated by Henry[46]. He found that after termination of supercritical CO_2 floods, the blowdown recovery slightly increases with increasing flood pressure.

No report has been made of a field application of carbon dioxide using a repressuring-depletion technique, however, the blowdown mechanism has been substantiated in the field by the results of the Mead-Strawn CO_2-waterflood project[47].

3.4. Permeability Changes

The carbonic acid formed when carbon dioxide dissolves in water can react with carbonate minerals in the reservoir rock with resulting permeability increases. On the other hand asphaltene precipitation may occur, which may lower the rock permeability.

3.4.1. Rock Dissolution by Carbonic Acid

The efficiency of an oil recovery process may be affected when the injected fluids react chemically with the reservoir rock. Chemical reaction between the rock and the injected fluids can be in the form of fluid adsorption onto the rock surfaces or rock dissolution by the injected fluids. In CO_2/water floods, chemical reaction may occur in the form of carbonate rock dissolution.

Carbon dioxide dissolves in water to form carbonic acid according to the following reversible reaction:

$$H_2O + CO_2 \rightleftarrows H_2CO_3 \qquad (2)$$

Carbonate rocks contain mainly $CaCO_3$ and $MgCO_3$. The alkali metal carbonates react with CO_2 in the presence of water to form water soluble bicarbonates. The stoichometric equation of the reactions are as follows[48]:

$$H_2O + CO_2 + CaCO_3 \rightleftarrows Ca(HCO_3)_2 \quad (3)$$

$$H_2O + CO_2 + MgCO_3 \rightleftarrows Mg(HCO_3)_2 \quad (4)$$

The factors that affect the equilibrium of the above equations are changes in the concentrations of reactants and products, pressure, and temperature. The calcium and magnesium bicarbonates are quite soluble in water, which may lead to a permeability increase in carbonate rocks.

In 1959, Holm[43] reported a study in which the permeability of a dolomite core increased three-fold at the end of six CO_2-carbonated waterfloods. A total of about 0.7 pore volume of CO_2 and eight pore volumes of carbonated water passed through the core during the floods. Holm[43] concluded that in field applications of CO_2, the increase in permeability would occur primarily in the immediate vicinity of injection wells.

Recently Omole and Osoba[48] showed the positive and negative effects of carbon dioxide on carbonate rocks during CO_2 flooding of petroleum reservoirs. They concluded that CO_2 dissolved some of the rock around the injection well during CO_2 flooding of carbonate reservoirs. However, the dissolved carbonate could be precipitated along the flow path if pressure drop became significant; the greater the pressure drawdown, the greater will be the carbonate precipitation and hence the reduction

in the rock permeability.

Graue and Blevins[49] reported that small channels of high permeability produced by rock dissolution in a tertiary CO_2-waterflood pilot in the Sacroc unit caused early breakthrough of CO_2 (7 days) in one of the producer wells. Because of the carbon dioxide channeling, the volumetric efficiency was estimated to be as low as 33%.

3.4.2. Asphaltene Deposition

One of the problems to be expected in carbon dioxide flooding is asphaltene instability, which might induce plugging. Strausz[50] describes the asphaltenes as high molecular weight materials which, on solvent fractionation, appear as a dark-coloured amorphous solids and are kept in colloidal suspension in the bitumen by the lower molecular weight polar materials. Asphaltene precipitation occurs when the hydrocarbons and polar oil fraction lose their ability to disperse colloidally the asphaltene fraction.

When CO_2 and light oil mix at high pressure, multiple liquid phases may occur in equilibrium. In some instances, a solid phase may appear. The heavy ends of a light oil become less soluble with the addition of CO_2 and precipitate.

Studying the complex phase behaviour of CO_2/light oil systems, Graue and Zana[51] observed a dark solid precipitation at carbon dioxide concentrations of 44% mol. or higher. The solid precipitation was estimated to be 2-5% vol. of the original reservoir oil. It is possible that such precipitation in the reservoir would cause a reduction in rock permeability. However, some researchers[52,53] have speculated on the possibility that the precipitation of solid phases in the CO_2/oil

transition zone might reduce carbon dioxide mobility below the level anticipated from normal viscosity and relative permeability relations which could increase recovery.

3.5. Laboratory Investigations on Heavy Oil Recovery by Carbon Dioxide

Basically three different immiscible CO_2 processes have been investigated in order to enhance heavy oil recovery. They are: straight or continuous CO_2 injection, the CO_2 slug process, and injection of alternate slugs of CO_2 and water (WAG process).

3.5.1. Continuous CO_2 Injection

In this process, CO_2 is injected continuously up to a high producing GOR of the order of 4500 sm^3 CO_2/m^3 oil. This process has been used successfully in light oil reservoirs[54], but a field test in a heavy oil reservoir using this type of process has not been reported. However, continuous CO_2 injection has been investigated in laboratory models by a number of researchers.

Henry[46] carried out a series of displacement tests in a 0.61 m length of 0.635 cm ID tubing packed with 20/40 mesh sand and saturated with heavy oil of 10°API and 16000 mPa.s viscosity at 22.2°C. The tests were made at pressures from 6.9 to 13.8 MPag and at 26.7°C, using one and one-half pore volumes of liquefied gas for each test. Roughly 30% of oil in place was produced at breakthrough and 60% at the end of flood including the blowdown recovery. Westgrowth Petroleums Ltd.[55] reported a slim tube displacement test of Retlaw Mannville "V" recombined reservoir fluid by carbon dioxide. The slim tube had a length of 12.2 m and 0.62 cm internal diameter, was packed with 100 mesh sand and saturated with 22°API (40.8 mPa.s @ 35.5°C) oil.

At test conditions of 11.8 MPag and 35.5°C the oil recoveries at CO_2 B.T. and end of flood were 60% and 80% of the original oil in place, respectively. The high recovery of viscous oil obtained in slim tubes can be attributed to the absence of viscous fingering since the diameter of the tubes used in the reported displacement tests were too small to permit the development of CO_2 fingers.

Rojas and coworkers[4,42] investigated the recovery of a 15°API crude in a supercritical CO_2 flood (at 20.7 MPag & 65.6°C) using an unscaled model which consisted of a pipe 1.0m in length and 10.12 cm ID. The recovery at CO_2 breakthrough was low, only [illegible]%, due to the unfavourable mobility ratio and because the diameter [illegible] was large enough so that viscous fingering could take place. Dur[illegible] the subordinate phase the recovery was almost twice the recovery obtained before breakthrough.

Very poor displacement efficiency of a viscous oil by rapid carbon dioxide injection was indicated by Sayegh and Maini[56]. These authors reported breakthrough recovery of Lloydminster crude (23700 mPa.s @ 20°C) by carbon dioxide at 3.45 MPa & 20°C as low as 3% of pore volume. The tests were carried out in a core of 0.44 m length and 2.8 cm diameter. Very high oil viscosity, low back pressure, and rapid injection rate of the carbon dioxide may be indicated as the reasons for that low recovery efficiency.

3.5.2. CO_2 Slug Process

In 1959, Beeson and Ortloff[2] investigated the use of water-driven carbon dioxide slugs to recover viscous crude oil (20°API, 400 mPa.s at 21.1°C) from small diameter models at low flow rates. The volumetric

sweep efficiency of the injected fluids was close to 100%. Tests were carried out with the carbon dioxide slugs in the liquid (0.09 PV at 6.9 MPa & 21.1°C) and gas (0.08 PV at 6.9 MPa & 54.4°C) states. In both cases the recoveries were around 50% of the original oil in place, much higher than that by waterflood (29%). The authors indicated that the additional heavy oil recovery per unit mass of carbon dioxide injected was higher in the CO_2 gas slug flood than in CO_2 liquid slug floods.

Laboratory studies on a viscous oil (90 mPa.s at 21.1°C) carried out by Holm[53] showed that a CO_2 slug (44.5 sm^3 CO_2/m^3 of oil in place) followed by water achieved an 80% increase in oil recovery over a conventional waterflood. Holm[53] pointed out three reasons by which the use of CO_2 as a slug is superior to the use of carbonated water:

1) carbon dioxide is better than carbonated water in reducing oil saturation;
2) for the same amount of carbon dioxide, the slug process recovers more oil than a carbonated waterflood;
3) the additional oil recovered by a CO_2 slug flood is produced more rapidly than the oil recovered by a carbonated waterflood.

3.5.3. Injection of Alternate Slugs of CO_2 and Water

Here, small slugs of CO_2 and water are injected alternately until the total desired amount of CO_2 is injected. Finally, water is injected continuously until the process is terminated at a producing WOR higher than 20 m^3/m^3.

The principal problem in recovering heavy oil by carbon dioxide is the high mobility ratio between the displacing and displaced fluids. As a consequence, much of the oil is not contacted and thereby not produced. Recently, Holm[34] indicated that alternate injection of water with carbon dioxide (the WAG process) has been the most widely used mobility control method.

In 1957, Caudle and Dyes[57] proposed the control of the gas mobility in a gas-driven displacement by injecting water along with gas. The presence of water in the invaded zone lowers the relative permeability to gas and decreases its mobility, thus the injected water interferes with the flow of carbon dioxide to impede rapid, high rate production of carbon dioxide. As indicated by Stone[58], field tests of this finding showed that it was more feasible to inject water alternately with gas rather than as a mixture; this process became known as the "WAG process."

Several authors have attempted to estimate the optimum H_2O:CO_2 ratio for a WAG process using simple equations[57,59] or complex numerical simulators[60,61]. It seems that the best procedure to estimate the H_2O:CO_2 ratio for a specific reservoir is using a physical model[59,60], which implicitly takes into account the real permeability relations among the phases, including hysteresis of relative permeability curves under drainage or imbibition conditions.

Caudle and Dyes[57] indicated that if too much gas is injected the process can only approach the mechanism of the gas-driven displacement, and if too little gas is injected the worst that can happen is that the reservoir will be subjected to a water drive.

Ko and Stanton[61] from numerical simulation results concluded that in presence of trapped light oil saturation (in tertiary recovery), larger CO_2 slugs are required in a WAG process for more efficient displacement. Conversely, in the absence of light oil trapping (in secondary recovery), smaller CO_2 slugs are required to maintain good mobility control.

Stalkup[52] pointed out that a potential disadvantage of solvent/water injection is trapping of oil by water if over injection of water should cause high water saturation at the displacing front.

Sheldon and Schneider[62] concluded from experimental tests that the miscible displacement of light oil by CO_2/water injection is rate-dependent and oil recovery in the region swept by the solvent decreases with increased displacement rate. They recognized that the contact time needed in a field application generally cannot be obtained in core tests because of the difficulty in scaling core tests to the field. So far no research has been published on the rate dependence of heavy oil recovery by immiscible CO_2/water injection.

Blackwell et al.[59] and Stone[58] studied the negative effect of gravity segregation on oil recovery by the injection of water alternating with gas. Gravity segregation causes the injected gas to rise to the top of the formation and water to migrate to the bottom. Reservoir simulation results obtained by Stone[58] indicated that vertical conformance in a WAG flood can be greatly improved by the use of injection rates that are high relative to well spacing.

Another mechanism by which heavy oil may be recovered in a CO_2/waterflood is known as the trapped-gas effect. The small free gas saturation of carbon dioxide created in the reservoir replaces part of

the residual oil that would have been left in the reservoir. The effect of free gas saturation on oil recovery by waterflooding has been studied by several researchers[63,64,65]. The experimental results show that the production of oil by waterflooding in water-wet rocks can be substantially increased by the maintenance of a free gas saturation in a reservoir during the flooding operation. Craig[66] pointed out that the effect of an initial gas saturation on oil displacement depends upon the magnitude of the trapped gas existing at the waterflood front. If no trapped gas remains in an element of the rock as the waterflood front reaches it, there is no influence on oil displacement.

Very little information from laboratory studies on injection of alternate slugs of CO_2 and water for heavy oil recovery has been published. Some experimental work carried out in Venezuela[67,4] showed the effectiveness of the WAG process in recovering 10°API (2000 mPa.s viscosity at 65.6°C) oil. A high recovery of 65.4% HCPV (Hydrocarbon Pore Volume) was obtained with a 3:1 WAG ratio in a linear cylindrical model. As a tertiary heavy oil recovery method, the WAG process has been studied by researchers of Chevron Oil Field Research Co. Their results are discussed in the following section.

From the point of view of field application, the WAG process as a secondary recovery process is being used with encouraging results in the third phase of the Lick Creek Meakin Sand Unit immiscible CO_2/ waterflood project which is the largest field application of carbon dioxide in recovering heavy oil (17°API, 160 mPa.s at 48°C)[68].

3.5.4. Tertiary Heavy Oil Recovery

Carbon dioxide drive followed by brine injection, WAG drive

process and huff-n-puff technique were studied by Sankur et al.[13,14] for tertiary recovery of 14°API gravity, 283 mPa.s (at 50.6°C) viscosity oil from waterflooded cores (5.08 cm in diameter). Only the ratio of gravitational to viscous forces was scaled down in these experiments. As reservoir and core geometries were not similar, it was assumed that H/L in the similarity group scaled was diameter-to-length for the core and formation thickness-to-well spacing for the reservoir. The authors concluded that the CO_2 drive process was more effective in recovering Wilmington oil than CO_2 huff-n-puff. Also, using two WAG ratios 0.22:1 and 1:1 they concluded that heavy oil recovery can be improved by using smaller slugs of gas alternating with water at higher WAG ratios and pressures. Pressure had a significant effect on the recovery process; for the drive and WAG processes the overall recoveries showed a marked increase with the increase in pressure from 5.2 to 8.6 MPag with run temperatures higher than the critical temperature of CO_2.

High tertiary recoveries of heavy oil (16.9°API, 130 mPa.s at 54.4° C) by CO_2 slugs driven by water were reported by Wang[5] using a slim tube system (0.6 cm. O.D. and 7.3 m. length). Wang[5] investigated the effect of slug size and pressure on CO_2 recovery requirement (or CO_2 consumption factor, sm^3 CO_2/m^3 oil). Increasing the slug size from 0.2 to 1.2 PV the tertiary recovery increased slightly from 26.1 to 31.5% and the CO_2 requirement increased dramatically from 161 to 799.6 sm^3/m^3, indicating that there is an economical, optimum slug size for the recovery of heavy oil by the slug CO_2 process. As in the experiments carried out by Sankur et al.[13] the tertiary recovery was observed to increase with increasing pressure at supercritical CO_2

temperature.

A series of CO_2 flooding tests for the investigation of the effect of CO_2 slug size were also conducted by Wang[5] on a consolidated sandstone core. Oil recoveries for all core tests were lower than the corresponding tests run on the slim tube system. This showed the importance of simulating correctly the reservoir morphology in laboratory experiments. Higher recoveries are obtained when using unconsolidated sand packs to simulate a sandstone reservoir.

Poor results for heavy oil (14.5°API, 23700 mPa.s at 20°C) displacement by carbon dioxide at water saturations higher than the irreducible water saturation and at low pressures (3.5 MPag) were reported by Sayegh and Maini[56]. They indicated that the presence of a low mobile water saturation resulted in preferential displacement of water, the injected gas displaced very little oil. From phase behaviour studies the authors determined that during differential liberation, CO_2 was retained by the oil preferentially to CH_4 and, consequently, reduced viscosities in the huff-n-puff process were maintained down to low pressures.

Bardon et al.[45] also performed a study for evaluating the efficiency of Dodan gas (88% CO_2) injection in recovering viscous oil (290 mPa.s at 65.6°C) from an area of the Bati Raman field (Turkey) previously waterflooded. A decrease in residual oil saturation from 47% to 30% was achieved in a waterflooded core by injecting a 0.1 PV slug of Dodan gas and flooding the core again by water, both under supercritical CO_2 pressure (10.1 MPag).

3.6. Simulation of Heavy Oil Production by CO_2 Injection

Klins and Farouq Ali[44] developed a numerical model that simulates the unsteady-state, two dimensional flow of three phases: oil, water, and gas (CO_2). It was assumed that there was no diffusional mixing, liquids were non-volatile and thermodynamic equilibrium existed between phases without considering transient mass transfer. With the above limitations the results indicated that over the viscosity range of 1 to 1000 mPa.s and pressure range of 7.0 - 7.5 MPa carbon dioxide flooding was superior to natural depletion, nitrogen flooding or waterflooding, for oil viscosities above 70 mPa.s. Oil recovery by carbon dioxide flooding was found to be strongly dependent on initial oil saturation for the 100 and 1000 mPa.s oils tested. In the case of the highest oil viscosity, recovery increased from 3 to 29 percentiles as initial oil saturation was increased from 40 to 70%. It was concluded by the authors that the economics of the immiscible carbon dioxide flooding without injecting water were tenuous.

Reid and Robinson[68] indicated that the Lick Creek Meakin Unit immiscible CO_2/waterflood project was modeled using a three dimensional, three-phase, compressible reservoir simulator. The results indicated that alternate CO_2/water injection with cyclic CO_2 stimulation of the producing wells would be the preferred operating procedure for the field application. The simulator showed that the highest residual oil saturation occurred in the upper reservoir, which was swept by CO_2 but not by water. According to the results, cyclic CO_2 stimulation of the wells prior to the WAG process would improve oil rates, reduce WOR's, increase CO_2 coverage of the reservoir, disperse CO_2 rapidly throughout the

reservoir, and cause wells to flow. Cyclic CO_2 stimulation was regarded as the first stage in the CO_2/waterflood project. However, it is important to bear in mind that field huff-n-puff projects without displacement of oil from well to well have proved to be uneconomic[1].

An equation-of-state compositional simulator was used by Spivak and Chima[12] to assist in the design and monitoring of two projects implemented in the Wilmington field, California[21]. The simulator did not take into account the probable fingering of carbon dioxide, nor the effect of diffusive forces on recovery. They concluded that the process of immiscible CO_2 drive in heavy oil reservoirs can be looked upon as a process of viscosity reduction, followed by waterflooding of the reduced viscosity oil. The authors also found that injecting the CO_2 alternately with water as opposed to injecting it as a slug resulted in improved recoveries.

Patton, Coats, and Spence[69] used a mathematical model for simulating the CO_2 huff-n-puff process. The model numerically simulated 2 or 3D transient multiphase flow in reservoirs by implicitly solving the conventional Darcy flow and mass conservation equations. They found that it was necessary to use the implicit method and a direct solution of the simultaneous equations to simulate the rapid, large transients in pressure, saturation, and dissolved gas at high throughput ratios that occur in the CO_2 cyclic process. The authors concluded that under the following optimal conditions the CO_2 huff-n-puff process could be considered economically attractive: oil viscosities less than 2000 mPa.s at reservoir conditions, no flow blockage around the wellbore, deep reservoirs capable of accepting high pressure, and water-wet reservoirs.

4. DERIVATION OF SCALING GROUPS FOR IMMISCIBLE DISPLACEMENT OF OIL BY CARBON DIOXIDE AND BRINE

The best procedure for deriving an extended set of scaling groups is to combine the two general methods available for the derivation of these groups: dimensional and inspectional analyses.

Dimensional analysis as defined by Langhaar[70] is a method by which information about a phenomenon can be deduced from the single premise that the phenomenon may be described by a dimensionally correct equation among certain variables. In order to know that a certain variable affects a phenomenon, it is necessary to understand enough about the problem to explain why and how the variable influences the phenomenon.

In inspectional analysis, as indicated by Craig et al.[71], all equations describing the process mechanism are combined to form a single equation. The coefficients of this equation are then combined to form the dimensionless scaling groups.

Farouq Ali et al.[72] pointed out the advantages and disadvantages of both methods. The successful application of dimensional analysis requires that a good deal be known about the particular process under consideration. If any single important variable is omitted, it is possible to obtain incorrect results. On the other hand, dimensional analysis permits the derivation of scaling groups that do not appear among those derived by inspectional analysis. The chief advantage of inspectional analysis is that the scaling criteria thus obtained have a clear physical meaning, and their function in the process can be

readily visualized.

4.1. Inspectional Analysis

The following procedure was used to derive the scaling groups by inspectional analysis:

a) Formulation of the governing partial differential equations in dimensionless form;

b) Selection of initial and boundary conditions, and

c) Identification of the similarity groups.

4.1.1. Governing Equations

The processes occurring in heavy oil reservoirs when injecting carbon dioxide and water to displace immiscibly oil are basically fluid flow of three immiscible phases and mass transfer between carbon dioxide and oil, and between carbon dioxide and water. In the zone invaded by carbon dioxide and water mass transfer takes place due to solution, diffusion, and dispersion of CO_2 in oil and water, solution being the most important of all.

4.1.1.1. Solution, Diffusion, and Dispersion Mechanisms

The difference among solution, diffusion, and dispersion can be visualized as follows. According to Hildebrand[73] the solubility of one substance in another depends fundamentally upon the ease with which the two molecular species are able to mix. Thus solubility is proportional to the attractive forces between the molecules of substances under consideration. In the case of two non-polar molecules, such as carbon dioxide and heavy paraffinic hydrocarbons, the intermolecular forces are

usually called van der Waals-London forces and they play a fundamental role in the solubility of carbon dioxide in crude oils.

As explained by Hildebrand, Prausnitz and Scott[74] two radically different theories have been proposed for diffusion in liquids: the hydrodynamical theory (Alder's theory) and the lattice (hole) theory (Eyring's theory). According to the hydrodynamical theory, diffusion takes place by random molecular motions due to concentration, temperature or pressure gradients. This theory is based upon the Stokes-Einsten[75] equation which indicates that the molecular diffusivity of a solute molecule varies inversely with the viscosity of the solvent. Several researchers[23,25] have found that the molecular diffusion coefficient of CO_2 in organic liquids is not a function of μ_o^{-1} as the hydrodynamical theory states but μ_o^{-q}, q being a constant close to 0.5. According to the lattice theory, diffusion occurs by jumps of a molecule from its "cage" within which it has been "oscillating" into a neighboring "hole" or "vacancy." The most interesting aspect of the Eyring's theory is that his equation predicts non-Newtonian behaviour for liquids in general and also it predicts an exponential decrease in viscosity with temperature. It is well known that they are characteristics of some extra-heavy oils. However, the Eyring's theory has not been used as a starting point in developing correlations for diffusion in liquids[76].

An accepted definition of diffusion was given by Crank[77]. He defined diffusion as the process by which matter is transported from one part of a system to another as a result of random molecular motion. Sherwood et al.[78] indicated that diffusion results from the thermal motion of the molecules which are in a state of continuous thermal agitation with

maximum entropy or disorder. Molecules move at high speeds but travel extremely short distances before colliding with other molecules and are deflected in random directions. The migration of individual molecules is slow except at quite low molecular densities such as gas densities. Sherwood et al.[78] also pointed out that molecular diffusion may occur as result of concentration, temperature or pressure gradients, or because a directed external electrical or other potential is applied to a mixture. However, Bird et al.[75] indicated that the effects of temperature and pressure gradients, and external forces are usually minor. The so-called molecular diffusivity is proportional to the concentration gradient of the component being diffused.

The difference between diffusion and solution may be understood through the words written by Hildebrand et al.[74]: "it is significant that diffusion is not related to attractive forces as measured by solubility." The effect of temperature on solution and diffusion of gases into liquids are opposite. While solution decreases, diffusion increases with increasing temperature.

Perkins and Johnston[79] wrote a review of diffusion and dispersion in porous media. They indicated that if there is movement of fluids through the rock, then there may be an additional mixing or dispersion which may be greater than that due to molecular diffusion alone. However, van der Poel[80] pointed out that at flow velocities less than 10^{-3} cm/s (0.864 m/d) which is a high velocity in the field, the width of the transition zone in porous media is still largely dominated by molecular diffusion. In the region where both diffusion and convective dispersion are important, the total dispersion coefficient is the sum of

these two coefficients. At high values of velocity, convective dispersion becomes dominant and both longitudinal and transverse dispersion coefficient increase with increasing values of velocity.

4.1.1.2. Assumptions Made in the Development of the Governing Equations

The partial differential equations for multiphase flow with mass transfer may be derived by combining Darcy's and Fick's laws and the equation of mass conservation.

The following assumptions were made:

1. Homogeneous porous medium.
2. Immiscible fluids.
3. Fluids are of small and constant compressibility at reservoir conditions.
4. Darcy's and Fick's equations are valid. Flow rates are small enough so that the inertial effects are negligible.
5. Flow behaviour of oil is Newtonian.
6. Relative permeabilities depend on saturation according to the channel flow theory.
7. The reservoir temperature remains constant during CO_2/water injection.
8. Three phases may exist: an oleic phase, an aqueous phase, and a carbon dioxide gas phase.
9. There is no solubility of heavy oil and water in subcritical carbon dioxide.

The widely accepted channel flow theory[80] provides a physical basis for the equations used in calculating three phase relative permeabilities.

and capillary pressures. The channel flow theory states that in any flow channel there is at most only one mobile fluid. The wetting phase flows through the small pore spaces and the nonwetting phase in the large pore spaces, and the intermediate phase spatially separates them. This implies that for a water-wet reservoir water relative permeability and water-oil capillary pressure in the three-phase-system are functions of water saturations, and similarly, the gas relative permeability and gas-oil capillary pressure are functions of gas saturation. The oil relative permeability is function of both water and gas saturations. Such dependencies are consistent with experimental results of Leverett and Lewis[81]. Although, relative permeability depends also on pore size distribution, wettability, saturation history, interfacial tension, and temperature, these parameters are considered to be constant in an isothermal displacement of heavy oil by CO_2/water injection in a given reservoir and they are implicitly taken into account in experimental curves of relative permeability versus saturation.

4.1.1.3. Mass Balance Equations

The following mass balance equations are taken from Appendix A where they are derived.

Carbon Dioxide

Using differential operators Equation A-5 takes the following form:

$$\nabla \cdot \left(\frac{\vec{v}'_g}{Bg} + \frac{Rso\ \vec{v}'_o}{Bo} + \frac{1}{Bg}\left(\frac{\vec{G}go}{A}\right) + \frac{Rsw\ \vec{v}'_w}{Bw} + \frac{1}{Bg}\left(\frac{\vec{G}gw}{A}\right) \right)$$

$$+ \frac{\partial}{\partial t}\left[\phi\left(\frac{Sg}{Bg} + \frac{Rso\ So}{Bo} + \frac{Rsw\ Sw}{Bw} + \frac{So\ Cgo}{Bg} + \frac{Sw\ Cgw}{Bg}\right)\right] = 0 \qquad (5)$$

This equation takes into account mass transfer between CO_2 and oil, and CO_2 and water by solution, diffusion and dispersion. While Rso and Rsw are explicit functions of pressure, Cgo and Cgw are explicit functions of distance (from the gas/oil interface) and time for a given reservoir. Cgo and Cgw could be interpreted as "additional solubilities" of carbon dioxide into oil and reservoir water caused by the diffusive forces. Through Cgo and Cgw it may be possible to take into account the transient mass transfer between CO_2 and heavy oil.

Assuming that the mass transfer between CO_2-oil and CO_2-water occurs only by solution as is considered to be the case in the black oil reservoir simulators, Equation 5 can be written as follows:

$$\nabla \cdot \left(\frac{\vec{v}'_g}{Bg} + \frac{Rso\ \vec{v}'_o}{Bo} + \frac{Rsw\ \vec{v}'_w}{Bw} \right) + \frac{\partial}{\partial t} \left[\phi \left(\frac{Sg}{Bg} + \frac{Rso\ So}{Bo} + \frac{Rsw\ Sw}{Bw} \right) \right] = 0 \qquad (6)$$

Oil and Water

The three-dimensional equations of mass transfer for oil and water are much simpler than that for carbon dioxide. They may be derived using a procedure similar to that developed in Appendix A.

Oil
$$\nabla \cdot \left(\frac{\vec{v}'_o}{Bo} \right) + \frac{\partial}{\partial t} \left(\frac{\phi\ So}{Bo} \right) = 0 \qquad (7)$$

Water
$$\nabla \cdot \left(\frac{\vec{v}'_w}{Bw} \right) + \frac{\partial}{\partial t} \left(\frac{\phi\ Sw}{Bw} \right) = 0 \qquad (8)$$

where
$$\nabla = \frac{\partial}{\partial x} \vec{i} + \frac{\partial}{\partial y} \vec{j} + \frac{\partial}{\partial z} \vec{k}$$

$$\nabla \cdot \left(\frac{\vec{v}'_g}{Bg} + \frac{Rso\ \vec{v}'_o}{Bo} + \frac{1}{Bg} \left(\frac{\vec{G}go}{A} \right) + \frac{Rsw\ \vec{v}'_w}{Bw} + \frac{1}{Bg} \left(\frac{\vec{G}gw}{A} \right) \right) = \text{divergence}$$

of the composite carbon dioxide vector (free, dissolved, and dispersed)

$$\nabla \cdot \left(\frac{\vec{v}'_o}{Bo} \right) = \text{divergence of the oil velocity vector}$$

$$\nabla \cdot \left(\frac{\vec{v}'_w}{Bw} \right) = \text{divergence of the water velocity vector}$$

Equations 7 and 8 are much simpler than Equation 6 because the solution and diffusion of oil and water into carbon dioxide at subcritical conditions were neglected.

4.1.1.4. Mass Transport Equations

Reservoir flow rates of the phases can be approximated by two independent processes, mass transport due to flow as governed by Darcy's law and due to dispersion as governed by a modification of Fick's law.

Darcy's Law

Darcy's law for each phase and in a general three-dimensional form can be written as follows:

Carbon dioxide $$\vec{v}'_g = - \frac{\bar{\bar{K}}\, Krg}{\mu_g} (\nabla Pg - \rho_g \vec{g}) \qquad (9)$$

Oil $$\vec{v}'_o = - \frac{\bar{\bar{K}}\, Kro}{\mu_o} (\nabla Po - \rho_o \vec{g}) \qquad (10)$$

Water $$\vec{v}'_w = - \frac{\bar{\bar{K}}\, Krw}{\mu_w} (\nabla Pw - \rho_w \vec{g}) \qquad (11)$$

where for each phase

$$\nabla P = \text{grad } P = \frac{\partial P}{\partial x} \vec{i} + \frac{\partial P}{\partial y} \vec{j} + \frac{\partial P}{\partial z} \vec{k}$$

In Equations 9 to 11 the effective permeabilities are expressed as the product of relative permeabilities by the single-fluid

permeability (Collins[82]).

$\bar{\bar{K}}$ is the diagonal tensor of absolute (single-fluid) permeability, which can be written as

$$\bar{\bar{K}} = \begin{pmatrix} Kx & 0 & 0 \\ 0 & Ky & 0 \\ 0 & 0 & Kz \end{pmatrix}$$

Modified Fick's Law

Perkins and Johnston[79] showed that when fluids are flowing through porous media, dispersion of gas in a liquid may be greater than that due to molecular diffusion alone and in this case it is necessary to use a dispersion coefficient instead of a molecular diffusion coefficient in Fick's equation.

Dispersion of CO_2 into Oil

$$\left(\frac{\vec{G}go}{A}\right) = -\bar{\bar{D}}go \nabla Cgo \qquad (12)$$

Dispersion of CO_2 into Water

$$\left(\frac{\vec{G}gw}{A}\right) = -\bar{\bar{D}}gw \nabla Cgw \qquad (13)$$

where

$$\nabla Cgo = \text{grad } Cgo = \frac{\partial Cgo}{\partial x}\vec{i} + \frac{\partial Cgo}{\partial y}\vec{j} + \frac{\partial Cgo}{\partial z}\vec{k}$$

$$\nabla Cgw = \text{grad } Cgw = \frac{\partial Cgw}{\partial x}\vec{i} + \frac{\partial Cgw}{\partial y}\vec{j} + \frac{\partial Cgw}{\partial z}\vec{k}$$

$\bar{\bar{D}}go$ and $\bar{\bar{D}}gw$ are diagonal tensors of dispersion coefficients given by

$$\bar{\bar{D}}go = \begin{pmatrix} Dgox & 0 & 0 \\ 0 & Dgoy & 0 \\ 0 & 0 & Dgoz \end{pmatrix}, \quad \bar{\bar{D}}gw = \begin{pmatrix} Dgwx & 0 & 0 \\ 0 & Dgwy & 0 \\ 0 & 0 & Dgwz \end{pmatrix}$$

the total velocity of carbon dioxide is obtained by adding Equations 9, 12, and 13

$$\vec{v}_g = \vec{v}'_g + \frac{\vec{G}go}{A} + \frac{\vec{G}gw}{A} \tag{14}$$

or

$$\vec{v}_g = -\frac{\bar{\bar{K}}\, Krg}{g}(\nabla Pg - \rho_g \vec{g}) - \bar{\bar{D}}go \nabla Cgo - \bar{\bar{D}}gw \nabla Cgw \tag{15}$$

Equation 15 may be written in matrix form as:

$$\begin{bmatrix} v_{gx} \\ v_{gy} \\ v_{gz} \end{bmatrix} = -\frac{Krg}{\mu_g}\begin{pmatrix} Kx & 0 & 0 \\ 0 & Ky & 0 \\ 0 & 0 & Kz \end{pmatrix}\begin{bmatrix} \partial Pg/\partial x \\ \partial Pg/\partial y \\ \partial Pg/\partial z \end{bmatrix} + \frac{Krg\ \rho_g}{\mu_g}\begin{pmatrix} Kx & 0 & 0 \\ 0 & Ky & 0 \\ 0 & 0 & Kz \end{pmatrix}\begin{bmatrix} g_x \\ g_y \\ g_z \end{bmatrix}$$

$$-\begin{pmatrix} Dgox & 0 & 0 \\ 0 & Dgoy & 0 \\ 0 & 0 & Dgoz \end{pmatrix}\begin{bmatrix} \partial Cgo/\partial x \\ \partial Cgo/\partial y \\ \partial Cgo/\partial z \end{bmatrix} - \begin{pmatrix} Dgwx & 0 & 0 \\ 0 & Dgwy & 0 \\ 0 & 0 & Dgwz \end{pmatrix}\begin{bmatrix} \partial Cgw/\partial x \\ \partial Cgw/\partial y \\ \partial Cgw/\partial z \end{bmatrix} \tag{16}$$

4.1.1.5. Saturation and Capillary Pressure Equations

As flow of three phases is considered, the saturation identity becomes

$$So + Sg + Sw = 1 \tag{17}$$

Also the porous medium is considered water-wet. Therefore, the oil-water capillary pressure is a function of water saturation, as follows:

$$Pcow(Sw) = Po - Pw \tag{18}$$

and the gas-oil capillary pressure is a function of gas saturation given by

$$Pcgo(Sg) = Pg - Po \tag{19}$$

4.1.1.6. Fractional Flow Equation of Carbon Dioxide

The above equations can be combined to obtain the three-dimensional vector of fractional flow of carbon dioxide ($\vec{f}_g$) when three immiscible phases are flowing in the porous medium (see Appendix B for the derivation):

$$\vec{f}_g = \frac{\vec{v}_g}{|\vec{v}_T|} = \left(\vec{v}_T - \frac{\bar{\bar{K}}\, Krw}{\mu_w} \left(1 + \frac{Kro\ \mu_w}{Krw\ \mu_o} \right) \vec{g}\, \Delta \rho_{og} - \vec{g}\, \Delta \rho_{wo} \frac{\bar{\bar{K}}\, Krw}{\mu_w} \right) \frac{Fg}{|\vec{v}_T|}$$

$$- \left(\left(1 + \frac{Kro\ \mu_w}{Krw\ \mu_o} \right) \frac{dPcgo}{dSg} \nabla Sg - \frac{dPcow}{dSw} \nabla Sw \right) \frac{\bar{\bar{K}}\, Krw\, Fg}{\mu_w |\vec{v}_T|}$$

$$- \left(1 + \frac{Kro\ \mu_w}{Krw\ \mu_o} \right) (\bar{\bar{D}}go \nabla Cgo + \bar{\bar{D}}gw \nabla Cgw) \frac{Krw\ \mu_g}{Krg\ \mu_w} \frac{Fg}{|\vec{v}_T|} \tag{20}$$

where

$$Fg = \left(1 + \frac{Krw\ \mu_g}{Krg\ \mu_w} + \frac{Kro\ \mu_g}{Krg\ \mu_o} \right)^{-1}$$

$$\nabla Sg = \frac{\partial Sg}{\partial x} \vec{i} + \frac{\partial Sg}{\partial y} \vec{j} + \frac{\partial Sg}{\partial z} \vec{k}$$

$$\nabla Sw = \frac{\partial Sw}{\partial x} \vec{i} + \frac{\partial Sw}{\partial y} \vec{j} + \frac{\partial Sw}{\partial z} \vec{k}$$

$$\nabla Cgo = \frac{\partial Cgo}{\partial x} \vec{i} + \frac{\partial Cgo}{\partial y} \vec{j} + \frac{\partial Cgo}{\partial z} \vec{k}$$

$$\nabla Cgw = \frac{\partial Cgw}{\partial x}\vec{i} + \frac{\partial Cgw}{\partial y}\vec{j} + \frac{\partial Cgw}{\partial z}\vec{k}$$

$$\Delta\rho_{og} = \rho_o - \rho_g$$

$$\Delta\rho_{wo} = \rho_w - \rho_o$$

$$\vec{v}_T = \vec{v}_g + \vec{v}_w + \vec{v}_o$$

Equation 20 can be written for the following special cases:

1) Three immiscible phases without considering dispersion of carbon dioxide:

$$\vec{f}_g = \left(\vec{v}_T - \frac{\bar{\bar{K}}\,Krw}{\mu_w}\left(1 + \frac{Kro\ \mu_w}{Krw\ \mu_o}\right)\vec{g}\,\Delta\rho_{og} - \vec{g}\,\Delta\rho_{wo}\,\frac{\bar{\bar{K}}\,Krw}{\mu_w}\right)\frac{Fg}{|\vec{v}_T|}$$

$$- \left(\left(1 + \frac{Kro\ \mu_w}{Krw\ \mu_o}\right)\frac{dPcgo}{dSg}\nabla Sg - \frac{dPcow}{dSw}\nabla Sw\right)\frac{\bar{\bar{K}}\,Krw\,Fg}{\mu_w|\vec{v}_T|} \qquad (21)$$

2) Two immiscible phases (oil-gas) considering dispersion of CO_2 into oil:

$$\vec{f}_g = \left(\vec{v}_T - \frac{\bar{\bar{K}}\,Kro}{\mu_o}\vec{g}\,\Delta\rho_{og} - \frac{\bar{\bar{K}}\,Kro}{\mu_o}\frac{dPcgo}{dSg}\nabla Sg\right)\frac{Fg}{|\vec{v}_T|}$$

$$- \frac{Kro\ \mu_g}{Krg\ \mu_o}\bar{\bar{D}}go\,\nabla Cgo\,\frac{Fg}{|\vec{v}_T|} \qquad (22)$$

3) Two immiscible phases (oil-gas) without considering dispersion of CO_2 into oil:

$$\vec{f}_g = \left(\vec{v}_T - \frac{\bar{\bar{K}}\,Kro}{\mu_o}\left(\frac{dPcgo}{dSg}\nabla Sg + \vec{g}\,\Delta\rho_{og}\right)\right)\frac{Fg}{|\vec{v}_T|} \qquad (23)$$

For Equations 22 and 23

$$Fg \left(+ \frac{Kro\ \mu_g}{Krg\ \mu_o} \right)^{-1}$$

and

$$\vec{v}_T = \vec{v}_o + \vec{v}_g$$

The continuity equations for gas, oil, and water (Equations 5,7, and 8) can be written as functions of fractional flow, as follows (from Appendix C):

$$\frac{1}{Bg} \nabla \cdot \vec{f}_g + \frac{d(1/Bg)}{dPg} \nabla Pg \cdot \vec{f}_g + \frac{Rso}{Bo} \nabla \cdot \vec{f}_o + \frac{d(Rso/Bo)}{dPo} \nabla Po \cdot \vec{f}_o + \frac{Rsw}{Bw} \nabla \cdot \vec{f}_w + \frac{d(Rsw/Bw)}{dPw} \nabla Pw \cdot \vec{f}_w$$

$$= - \frac{1}{|\vec{v}_T|} \frac{\partial}{\partial t} \left(\frac{\phi Sg}{Bg}\right) - \frac{1}{|\vec{v}_T|} \frac{\partial}{\partial t} \left(\frac{\phi So\ Rso}{Bo}\right) - \frac{1}{|\vec{v}_T|} \frac{\partial}{\partial t} \left(\frac{\phi Sw\ Rsw}{Bw}\right) - \frac{1}{|\vec{v}_T|} \frac{\partial}{\partial t} \left(\frac{\phi So\ Cgo}{Bg}\right) - \frac{1}{|\vec{v}_T|} \frac{\partial}{\partial t} \left(\frac{\phi Sw\ Cgw}{Bg}\right) \quad (24)$$

$$\frac{1}{Bo} \nabla \cdot \vec{f}_o + \frac{d(1/Bo)}{dPo} \nabla Po \cdot \vec{f}_o = - \frac{1}{|\vec{v}_T|} \frac{\partial}{\partial t} \left(\frac{\phi So}{Bo}\right) \quad (25)$$

$$\frac{1}{Bw} \nabla \cdot \vec{f}_w + \frac{d(1/Bw)}{dPw} \nabla Pw \cdot \vec{f}_w = - \frac{1}{|\vec{v}_T|} \frac{\partial}{\partial t} \left(\frac{\phi Sw}{Bw}\right) \quad (26)$$

4.1.2. Boundary and Initial Conditions

The boundary and initial conditions must be known to complete the mathematical and physical modelling of the reservoir. There are various ways of specifying the boundary conditions. The most commonly used

procedure[83] is that the reservoir is sealed at all faces across which there is no flow, and fluid injection and production take place at wells which can be represented by point sources or sinks. These boundary conditions may be also applied to the study of mechanically confined physical models. Thus with the exception of the wells, the fractional flow of carbon dioxide is zero at lateral, upper, and lower boundaries; hence,

$$|\vec{f}_{gn}|_{lat.bound.} = |\vec{f}_{gn}|_{up.bound.} = |\vec{f}_{gn}|_{low.bound.} = 0, \quad t \geq 0$$

where the subscript n refers to flow in a direction normal to the boundary.

At the injection wells, the flow rates of CO_2 and water are known. At the production wells, either the total flow rate or the bottomhole pressure can be specified.

Only one initial condition needs to be specified for saturations, pressure, and concentrations of carbon dioxide in oil and water due to dispersion. At initial time (t = 0) we must know the distribution of saturations, pressure, and concentrations of CO_2 due to dispersion in the porous medium. Since at the beginning of a project the carbon dioxide saturation in the reservoir and the concentrations of CO_2 in oil and water due to dispersion are zero, the corresponding fractional flow of CO_2 at t = 0 is also zero.

4.1.3. Dimensionless Form of the Partial Differential Equations

Equations 20, 24, 25, and 26 were normalized in Appendix D following a procedure similar to that of Perkins and Collins[84]. The fractional flow and continuity equations can be written in dimensionless form as follows:

Fractional Flow of Carbon Dioxide

$$\vec{f}_g = \left[\frac{\vec{v}_T}{|\vec{v}_T|} - \vec{N}gog\left(\frac{1+Mwo}{Mgo}\right)Krg(Sg^*) - \vec{N}gwo\ Krw(Sw^*)\right]Fg$$

$$- \left[Ncgo\ Krg(Sg^*)\left(\frac{1+Mwo}{Mgo}\right)\frac{dJ(Sg^*)}{dSg^*}\left(\frac{\partial Sg^*}{\partial\xi}\vec{i} + \frac{L}{W}\frac{\partial Sg^*}{\partial\theta}\vec{j} + \frac{L}{H}\frac{\partial Sg^*}{\partial\lambda}\vec{k}\right)\right.$$

$$\left. - Ncow\ Krw(Sw^*)\ \frac{dJ(Sw^*)}{dSw^*}\left(\frac{\partial Sw^*}{\partial\xi}\vec{i} + \frac{L}{W}\frac{\partial Sw^*}{\partial\theta}\vec{j} + \frac{L}{H}\frac{\partial Sw^*}{\partial\lambda}\vec{k}\right)\right]Fg$$

$$- \left(\frac{1+Mwo}{Mgo}\right)\frac{Dgox}{|\vec{v}_T|L}\left(\frac{\partial Cgo}{\partial\xi}\vec{i} + \frac{Dgoy\ L}{Dgox\ W}\frac{\partial Cgo}{\partial\theta}\vec{j} + \frac{Dgoz\ L}{Dgox\ H}\frac{\partial Cgo}{\partial\lambda}\vec{k}\right)Fg$$

$$- \left(\frac{1+Mwo}{Mgo}\right)\frac{Dgwx}{|\vec{v}_T|L}\left(\frac{\partial Cgw}{\partial\xi}\vec{i} + \frac{Dgwy\ L}{Dgwx\ W}\frac{\partial Cgw}{\partial\theta}\vec{j} + \frac{Dgwz\ L}{Dgwx\ H}\frac{\partial Cgw}{\partial\lambda}\vec{k}\right)Fg \qquad (27)$$

Continuity Equation of Carbon Dioxide

$$\frac{1}{Bg}\left(\frac{\partial f_{g\xi}}{\partial\xi} + \frac{L}{W}\frac{\partial f_{g\theta}}{\partial\theta} + \frac{L}{H}\frac{\partial f_{g\lambda}}{\partial\lambda}\right) + \left(f_{g\xi}\frac{\partial Pg}{\partial\xi} + \frac{L}{W}f_{g\theta}\frac{\partial Pg}{\partial\theta} + \frac{L}{H}f_{g\lambda}\frac{\partial Pg}{\partial\lambda}\right)\frac{d}{dPg}\left(\frac{1}{Bg}\right)$$

$$+ \frac{Rso}{Bo}\left(\frac{\partial f_{o\xi}}{\partial\xi} + \frac{L}{W}\frac{\partial f_{o\theta}}{\partial\theta} + \frac{L}{H}\frac{\partial f_{o\lambda}}{\partial\lambda}\right) + \left(f_{o\xi}\frac{\partial Po}{\partial\xi} + \frac{L}{W}f_{o\theta}\frac{\partial Po}{\partial\theta} + \frac{L}{H}f_{o\lambda}\frac{\partial Pg}{\partial\lambda}\right)\frac{d}{dPo}\left(\frac{Rso}{Bo}\right)$$

$$+ \frac{Rsw}{Bw}\left(\frac{\partial f_{w\xi}}{\partial\xi} + \frac{L}{W}\frac{\partial f_{w\theta}}{\partial\theta} + \frac{L}{H}\frac{\partial f_{w\lambda}}{\partial\lambda}\right) + \left(f_{w\xi}\frac{\partial Pw}{\partial\xi} + \frac{L}{W}f_{w\theta}\frac{\partial Pw}{\partial\theta} + \frac{L}{H}f_{w\lambda}\frac{\partial Pw}{\partial\lambda}\right)\frac{d}{dPw}\left(\frac{Rsw}{Bw}\right)$$

$$= -\frac{1}{Bg}\frac{\partial Sg^*}{\partial\tau} - \left(Sg^* + CgoSo^* + \frac{Sor\ Cgo}{1-Sor-Swi} + Cgw\ Sw + \frac{Swi\ Cgw}{1-Sor-Swi}\right)\frac{d}{dPg}\left(\frac{1}{Bg}\right)\frac{\partial Pg}{\partial\tau}$$

$$- \frac{Rso}{Bo}\frac{\partial So^*}{\partial\tau} - \left(So^* + \frac{Sor}{1-Sor-Swi}\right)\frac{d}{dPo}\left(\frac{Rso}{Bo}\right)\frac{\partial Po}{\partial\tau} - \frac{Rsw}{Bw}\frac{\partial Sw^*}{\partial\tau}$$

$$- \left(Sw^* + \frac{Swi}{1-Sor-Swi}\right)\frac{d}{dPw}\left(\frac{Rsw}{Bw}\right)\frac{\partial Pw}{\partial\tau} - \frac{1}{Bg}\frac{\partial}{\partial\tau}(Cgo\ So^*) - \frac{Sor}{Bg(1-Sor-Swi)}\frac{\partial Cgo}{\partial\tau}$$

$$- \frac{1}{Bg}\frac{\partial}{\partial\tau}(Cgw\ Sw^*) - \frac{Swi}{Bg(1-Sor-Swi)}\frac{\partial Cgw}{\partial\tau} \qquad (28)$$

Continuity Equation of Oil

$$\frac{1}{Bo}\left(\frac{\partial f_{o\xi}}{\partial \xi}+\frac{L}{W}\frac{\partial f_{o\theta}}{\partial \theta}+\frac{L}{H}\frac{\partial f_{o\lambda}}{\partial \lambda}\right)+\left(f_{o\xi}\frac{\partial Po}{\partial \xi}+\frac{L}{W}f_{o\theta}\frac{\partial Po}{\partial \theta}+\frac{L}{H}f_{o\lambda}\frac{\partial Po}{\partial \lambda}\right)\frac{d}{dPo}\left(\frac{1}{Bo}\right)$$

$$=-\frac{1}{Bo}\frac{\partial So^*}{\partial \tau}-\left(So^*+\frac{Sor}{1-Sor-Swi}\right)\frac{d}{dPo}\left(\frac{1}{Bo}\right)\frac{\partial Po}{\partial \tau} \qquad (29)$$

Continuity Equation of Water

$$\frac{1}{Bw}\left(\frac{\partial f_{w\xi}}{\partial \xi}+\frac{L}{W}\frac{\partial f_{w\theta}}{\partial \theta}+\frac{L}{H}\frac{\partial f_{w\lambda}}{\partial \lambda}\right)+\left(f_{w\xi}\frac{\partial Pw}{\partial \xi}+\frac{L}{W}f_{w\theta}\frac{\partial Pw}{\partial \theta}+\frac{L}{H}f_{w\lambda}\frac{\partial Pw}{\partial \lambda}\right)\frac{d}{dPw}\left(\frac{1}{Bw}\right)$$

$$=-\frac{1}{Bw}\frac{\partial Sw^*}{\partial \tau}-\left(Sw^*+\frac{Swi}{1-Sor-Swi}\right)\frac{d}{dPw}\left(\frac{1}{Bw}\right)\frac{\partial Pw}{\partial \tau} \qquad (30)$$

4.1.4. Scaling Groups From Inspectional Analysis

Equations 27, 28, 29, and 30 and appropriate initial and boundary conditions represent a mathematical description of the immiscible displacement of heavy oil by carbon dioxide gas and water. By inspection the dimensionless scaling groups are:

$$\frac{L}{W},\ \frac{L}{H},\ Mwo,\ Mgo,\ \vec{N}gog,\ \vec{N}gwo,\ Ncgo,\ Ncow,\ \frac{dJ(Sg^*)}{dSg^*},\ \frac{dJ(Sw^*)}{dSw^*},\ \frac{Dgox}{|\vec{v}_T|L}$$

$$\frac{Dgwx}{|\vec{v}_T|L},\ \frac{Dgoy}{Dgox}\frac{L}{W},\ \frac{Dgoz}{Dgox}\frac{L}{H},\ \frac{Dgwy}{Dgwx}\frac{L}{W},\ \frac{Dgwz}{Dgwx}\frac{L}{H}$$

Moreover the functions Krg(Sg*), Kro(Sg*,Sw*), Krw(Sw*), J(Sg*), J(Sw*), the concentration gradients of CO_2 due to dispersion, and the PVT properties of the fluids must be the same in the model and in the prototype. Mwo and Mgo must be evaluated at the average saturations of the fluids behind and ahead of the flood front. The names of the scaling groups are given in Table 2.

In applying the rule that dimensionless products can be multiplied and divided by other dimensionless groups it can be shown that the groups $\frac{Dgox}{|\vec{v}_T|L}$ and $\frac{Dgwx}{|\vec{v}_T|L}$ can be transformed to $\frac{Dgoy}{W^2|\vec{v}_T|}\frac{L}{}$ and $\frac{Dgwy}{W^2|\vec{v}_T|}\frac{L}{}$

$$\frac{Dgoy\ L}{W^2|\vec{v}_T|} = \frac{Dgox}{|\vec{v}_T|L} \times \frac{L}{W} \times \frac{Dgoy\ L}{Dgox\ W}$$

$$\frac{Dgwy\ L}{W^2|\vec{v}_T|} = \frac{Dgwx}{|\vec{v}_T|L} \times \frac{L}{W} \times \frac{Dgwy\ L}{Dgwx\ W}$$

These scaling groups are more general indicators of the level of transverse dispersion of CO_2.

4.2. Dimensional Analysis

The dimensional analysis approach to derive the scaling groups for a process is based on the Buckingham π-theorem[89] which was presented in 1914. It can be stated in the following words: if an equation is dimensionally homogeneous, it can be rewritten as a relationship among a complete set of dimensionless products. The Buckingham π-theorem and many of its applications are discussed at great length by Langhaar[70].

A number of researchers have used dimensional analysis to determine the scaling groups for several oil recovery processes. Loomis and Crowell[90], and Demetre[91] determined the scaling groups for immiscible flow of two phases (oil-water). Greenkorn[92,93] obtained the dimensionless groups necessary for deriving the scaling laws for miscible flow of two fluids. Apparently scaling groups for immiscible displacement of oil by water and carbon dioxide have not been published.

The variables which control the immiscible displacement of heavy oil from a horizontal reservoir by carbon dioxide and water considering mass transfer are:

1. Geometry

   a) Length and width of the system. For a five-spot pattern

these are equal.

b) Thickness of the system.

2. Sand Characteristics

a) Morphology. It depends upon whether the sand is consolidated or unconsolidated.

b) Absolute permeability (single-fluid permeability).

c) Porosity.

3. Variables which Depend Upon the Interaction Oil-CO_2-Water-Sand

a) Effective permeability to oil at gas and water saturations ahead of the flood front.

b) Effective permeability to gas at average gas saturation behind of the flood front.

c) Effective permeability to water at average water saturation behind the flood front.

d) Oil-water Leverett J-function.

e) Gas-oil Leverett J-function.

f) Dispersion coefficient of CO_2 into oil.

g) Dispersion coefficient of CO_2 into water.

4. Fluid Properties

a) Viscosity of carbon dioxide.

b) Viscosity of oil saturated with carbon dioxide.

c) Viscosity of water saturated with carbon dioxide.

d) Density of carbon dioxide.

e) Density of oil saturated with carbon dioxide.

f) Density of water saturated with carbon dioxide.

g) Water-oil interfacial tension.

h) Gas-oil interfacial tension.

5. Other

a) Time.

b) Superficial or total velocity.

c) Gravity.

d) Volume of water and carbon dioxide slugs.

Table 1 shows a resumé of the symbols, dimensions, and description of the variables which control the displacement.

Comments: 1) the superficial velocity is assumed to be constant. This is an arbitrary assumption but according to Geerstma et al.[94] it does not affect the model scales.

2) It is well known that the gravitational forces are proportional to the factor $\Delta\rho g$ (difference in the density gravity products of the fluids), then the density of fluids and gravity occur in the combinations $g\Delta\rho_{wo}$ and $g\Delta\rho_{og}$.

3) The inertial effects will be considered in the derivation of the scaling groups, so that the densities of injection fluids must appear in the Reynolds number groups.

4) The end effects as variables are not included. Later on, it is explained why in the experiments it is not necessary to take them into account.

The derivation of the scaling groups by dimensional analysis is presented in Appendix E. Any manipulation of the π-terms obtained in the Appendix E is permissible provided that a complete set of π-terms

TABLE 1

VARIABLES WHICH CONTROL THE DISPLACEMENT PROCESS

Symbol	Dimensions	Description
L,W,H	[L]	Length, Width, and Height of the System
ϕ	Dimensionless	Porosity
M	Dimensionless	Morphology
K	$[L^2]$	Absolute Permeability
Krg(Sg*), Kro(Sg*,Sw*), Krw(Sw*)	Dimensionless	Relative Permeabilities to CO_2, Oil and Water
μ_o, μ_w, μ_g	$[ML^{-1}t^{-1}]$	Viscosities of Oil and Water Saturated with CO_2 and CO_2, Respectively
ρ_g, ρ_w	$[ML^{-3}]$	Densities of CO_2 and Water Saturated with CO_2, Respectively
$(\rho_o - \rho_g)g = g\Delta\rho_{og}$	$[ML^{-2}t^{-2}]$	Density of Oil Saturated with CO_2 Minus Density of CO_2 Multiplied by Gravity Acceleration
$(\rho_w - \rho_o)g = g\Delta\rho_{wo}$	$[ML^{-2}t^{-2}]$	Density of Water Saturated with CO_2 Minus Density of Oil Saturated with CO_2 Multiplied by Gravity Acceleration
σ_{go}, σ_{ow}	$[Mt^{-2}]$	Gas-Oil and Oil-Water Interfacial Tensions
J(Sw*), J(Sg*)	Dimensionless	Oil-Water and Gas-Oil Leverett J-functions
Dgox, Dgoy, Dgoz	$[L^2t^{-1}]$	Dispersion Coefficients of CO_2 into Oil in x, y, and z Directions

TABLE 1 (Continued)

Symbol	Dimensions	Descriptions
Dgwx, Dgwy, Dgwz	$[L^2t^{-1}]$	Dispersion Coefficients of CO_2 into Water in x, y, and z Directions
t	[t]	Time
V	$[Lt^{-1}]$	Superficial or Total Velocity
Vw*	Dimensionless	Slug Volume of Water Divided by the Hydrocarbon Pore Volume (HCPV)
Vg*	Dimensionless	Slug Volume of CO_2 Divided by the Hydrocarbon Pore Volume (HCPV)

contains every variable at least once. Applying the rule mentioned previously that π-terms (dimensionless groups) can be multiplied and divided by other π-terms the following new dimensionless groups are obtained:

$$\pi_1^{-1} = L/W \tag{31}$$

$$\pi_2^{-1} = L/H \tag{32}$$

$$\pi_4\pi_5^{-1}\pi_{23}\pi_{22}^{-1} = \frac{Krw(Sw^*)\mu_o}{Kro(Sg^*,Sw^*)\mu_w} \tag{33}$$

$$\pi_4\pi_{21}\pi_{22}^{-1} = \frac{Krg(Sg^*)\mu_o}{Kro(Sg^*,Sw^*)\mu_g} \tag{34}$$

$$\pi_8\pi_3\pi_{18}^{-1} = \frac{gK\Delta\rho_{og}}{V\mu_g} \tag{35}$$

$$\pi_9\pi_3\pi_5^{-1}\pi_{18}^{-1} = \frac{gK\Delta\rho_{wo}}{V\mu_w} \tag{36}$$

$$\pi_{10}\pi_3^{\frac{1}{2}}\pi_{19}\pi_{18}^{-1} = \frac{\sigma_{go}\sqrt{K\phi}}{L\mu_g V} \tag{37}$$

$$\pi_{11}\pi_5^{-1}\pi_3^{\frac{1}{2}}\pi_{19}\pi_{18}^{-1} = \frac{\sigma_{ow}\sqrt{K\phi}}{L\mu_w V} \tag{38}$$

$$\pi_{13}\pi_1^{-2}\pi_{18}^{-1} = \frac{Dgoy\ L}{W^2 V} \tag{39}$$

$$\pi_{16}\pi_1^{-2}\pi_{18}^{-1} = \frac{Dgwy\ L}{W^2 V} \tag{40}$$

$$\pi_{13}\pi_{12}^{-1}\pi_1^{-1} = \frac{Dgoy\ L}{Dgox\ W} \tag{41}$$

$$\pi_{14}\pi_{12}^{-1}\pi_2^{-1} = \frac{Dgoz\ L}{Dgox\ H} \tag{42}$$

$$\pi_{16}\pi_{15}^{-1}\pi_1^{-1} = \frac{Dgwy\ L}{Dgwx\ W} \tag{43}$$

$$\pi_{17}\pi_{15}^{-1}\pi_2^{-1} = \frac{Dgwz\ L}{Dgwx\ H} \tag{44}$$

$$\pi_3^{\frac{1}{2}}\pi_{18}\pi_6 = \frac{\rho_g\ V\sqrt{K}}{\mu_g} \tag{45}$$

$$\pi_3^{\frac{1}{2}}\pi_{18}\pi_7\pi_5^{-1} = \frac{\rho_w\ V\sqrt{K}}{\mu_w} \tag{46}$$

$$\pi_{26}^{-1}\pi_{27} = \frac{Vw^*}{Vg^*} \tag{47}$$

Thus, the scaling groups derived by dimensional analysis are:

$$\frac{L}{W},\ \frac{L}{H},\ \frac{Krw(Sw^*)\mu_o}{Kro(Sg^*,Sw^*)\mu_w},\ \frac{Krg(Sg^*)\mu_o}{Kro(Sg^*,Sw^*)\mu_g},\ \frac{gK\Delta\rho_{og}}{V\mu_g},\ \frac{gK\Delta\rho_{wo}}{V\mu_w},$$

$$\frac{\sigma_{go}\sqrt{K\phi}}{L\mu_g V},\ \frac{\sigma_{ow}\sqrt{K\phi}}{L\mu_w V},\ \frac{Dgoy\ L}{W^2 V},\ \frac{Dgwy\ L}{W^2 V},\ \frac{Dgoy\ L}{Dgox\ W},\ \frac{Dgoy\ L}{Dgox\ W},\ \frac{Dgoz\ L}{Dgox\ H},$$

$$\frac{Dgwy\ L}{Dgwx\ W},\ \frac{Dgwz\ L}{Dgwx\ H},\ \frac{\rho_g\ V\sqrt{K}}{\mu_g},\ \frac{\rho_w\ V\sqrt{K}}{\mu_w},\ \frac{Vw^*}{Vg^*},\ \phi,\ M,\ Krg(Sg^*),$$

$$Kro(Sg^*,Sw^*),\ Krw(Sw^*),\ J(Sg^*),\ \text{and}\ J(Sw^*)$$

Table 2 shows a comparison of the scaling groups derived by inspectional and dimensional analyses. It can be seen that for three-dimensional immiscible displacement of heavy oil by carbon dioxide and water the total number of scaling groups is twenty six. Dimensional analysis yielded five scaling groups more than inspectional analysis. The difference between the number of scaling groups derived by the two approaches points out the advantage of using both techniques in deriving a set of dimensionless groups. Dimensionless analysis gives the correct number of groups for the process variables, but does not relate them physically. Inspectional analysis, based upon a mathematical model

does have more physical sense, but does not contain all the scaling groups such as Reynolds numbers, volumetric ratio of slugs, morphology factor, porosity factor, etc. (see Table 2).

4.3. Scaling of Unstable Displacements

Immiscible displacement of oil by carbon dioxide may become unstable due to macroscopic bypassing in the form of viscous fingering, when viscous forces dominate capillary, gravity, and diffusive forces depending fundamentally on injection flow rate, mobility ratio and transverse length of the system for horizontal reservoirs. Chuoke et al.[94] pointed out that for unstable displacements a properly scaled experiment also requires a scaling group which accounts for the flood front instabilities. They presented a dimensionless group to scale properly an unstable displacement of oil by water. Later, Peters and Flock[95], and Bentsen[96] extended the theory of Chuoke et al.[94] to obtain a dimensionless group and its critical value for predicting the onset of instability during immiscible displacement in porous media.

Peters and Flock[95] delineated more precisely the three regions in which to consider the scaling requirements for instability identified by Chuoke et al.[94]. For $\lambda c/D > 1.71$ (ratio of characteristic wave length to core diameter) the displacement is stable, i.e. no fingers occur; therefore, no additional scaling is necessary to account for instability. For $\lambda c/D < 0.20$ the displacement is unstable, the oil recovery is low but it does not depend on velocity. Again, strict scaling is not required to ensure similarity in recovery behaviour between model and prototype. But, for $0.2 < \lambda c/D < 1.71$, where the

TABLE 2

COMPARISON BETWEEN THE SCALING GROUPS
DERIVED BY INSPECTIONAL AND DIMENSIONAL ANALYSES

Number	Scaling Group	Derived by Inspectional Analysis	Derived by Dimensional Analysis	Name
1	L/W	Yes	Yes	Geometric Factor
2	L/H	Yes	Yes	Geometric Factor
3	$\frac{Krg(Sg^*)\mu_o}{Kro(Sg^*,Sw^*)\mu_w}$	Yes	Yes	Gas-Oil Ratio of Viscous Forces
4	$\frac{Krw(Sw^*)}{Kro(Sg^*,Sw^*)\mu_w}$	Yes	Yes	Water-Oil Ratio of Viscous Forces
5	$\frac{\vec{g}K\Delta\rho_{og}}{V\mu_g}$	Yes	Yes	Gas-Oil Ratio of Gravitational Forces to Viscous Forces
6	$\frac{\vec{g}K\Delta\rho_{wo}}{V\mu_w}$	Yes	Yes	Water-Oil Ratio of Gravitational Forces to Viscous Forces
7	$\frac{\sigma_{go}\sqrt{K\phi}}{L\mu_g V}$	Yes	Yes	Gas-Oil Ratio of Capillary Forces to Viscous Forces
8	$\frac{\sigma_{ow}\sqrt{K\phi}}{L\mu_w V}$	Yes	Yes	Water-Oil Ratio of Capillary Forces to Viscous Forces
9	$\frac{Dgoy\ L}{W^2\lvert\vec{v}_T\rvert}$	Yes	Yes	Gas in Oil Transverse Dispersion Scaling Group (or Ratio of Convection Time to Transverse Dispersion Time)
10	$\frac{Dgwy\ L}{W^2\lvert\vec{v}_T\rvert}$	Yes	Yes	Gas in Water Transverse Dispersion Scaling Group (or Ratio of Convection Time to Transverse Dispersion Time)
11	$\frac{Dgoy\ L}{Dgox\ W}$	Yes	Yes	X-Y Gas in Oil Dispersion Similarity Group

TABLE 2 (Continued)

Number	Scaling Group	Derived by Inspectional Analysis	Derived by Dimensional Analysis	Name
12	$\frac{Dgoz\ L}{Dgox\ H}$	Yes	Yes	X-Z Gas in Oil Dispersion Similarity Group
13	$\frac{Dgwy\ L}{Dgwx\ W}$	Yes	Yes	X-Y Gas in Water Dispersion Similarity Group
14	$\frac{Dgwz\ L}{Dgwx\ H}$	Yes	Yes	X-Z Gas in Water Dispersion Similarity Group
15	$\frac{\rho_g \sqrt{K}\ V}{\mu_g}$	No	Yes	Reynolds Number for Gas
16	$\frac{\rho_w \sqrt{K}\ V}{\mu_w}$	No	Yes	Reynolds Number for Water
17	Vw*	No	Yes	Water-Gas Ratio of Slug Volumes
18	ϕ	No	Yes	Porosity Factor
19	M	No	Yes	Morphology Factor
20	Krg(Sg*)	Yes	Yes	Gas Relative Permeability Factor
21	Kro(Sg*,Sw*)	Yes	Yes	Oil Relative Permeability Factor
22	Krw(Sw*)	Yes	Yes	Water Relative Permeability Factor
23	J(Sg*)	No	Yes	Gas-Oil Leverett J-Function Factor
24	J(Sw*)	No	Yes	Oil-Water Leverett J-Function Factor
25	$\frac{dJ(Sg^*)}{dSg^*}$	Yes	No	Gas-Oil Leverett J-Function Slope Factor
26	$\frac{dJ(Sw^*)}{dSw^*}$	Yes	No	Oil-Water Leverett J-Function Slope Factor

recovery is seriously affected by the variations in the value $\lambda c/D$, the similarity group that accounts for flood front instabilities should have the same value in model and prototype. For heavy oil recovery by carbon dioxide and water the mobility ratio is much higher than unity and the displacement in rectangular models and prototypes is likely to be dominated by viscous fingering. If such is the case, recovery is insensitive to variations in the value of $\lambda c/D$, and therefore, it is not necessary to have an additional scaling group to ensure dynamic similarity between the model and the prototype.

The relative importance of transverse dispersion in a displacement with mass transfer is characterized by the dimensionless transverse dispersion group $(D_T L / W^2 V)$, which is the ratio of convection time to transverse dispersion time. Gardner and Ypma[97] used this dimensionless group for delineating the boundary between stable and unstable miscible displacements of light oil by carbon dioxide. They concluded that if carbon dioxide - crude core floods are conducted at low values of $D_T L/W^2 V$ (< 0.04) a recovery efficiency characteristic of a completely unstable displacement is obtained, whereas if conducted at high values of $D_T L/W^2 V$ (> 0.5) a recovery efficiency characteristic of a stable displacement is observed. A transition zone occurs in which displacements are neither completely unstable nor completely stable.

5. RELAXATION OF SCALING REQUIREMENTS

It is well known that it is virtually impossible to satisfy all the scaling groups involved in a recovery process. However, in any particular application, e.g. heavy oil recovery, not all of the scaled parameters are important. Consequently, it is necessary to know which scaling groups may be relaxed and what errors are introduced.

5.1. Structure of Porous Medium

According to Geertsma et al.[98] the structure of the porous medium can be scaled by the coefficient $L/\sqrt{K}$ and the morphology factor, M. Considering that the length of a reservoir may be scaled down by a geometric factor of 300, then constancy of $L/\sqrt{K}$ would entail that the model permeability be

$$K_M = \frac{L_M^2}{L_P^2} K_P = \frac{K_P}{90000}$$

or a permeability 9×10^4 times lower in the model than in the prototype. This condition cannot be fulfilled. Geertsma, et al.[98] pointed out that it is plausible to assume that $L/\sqrt{K}$ may be deleted if the average diameter of the pores is much smaller than the smallest dimension of the reservoir which is the case for the majority of reservoirs. This factor could have great effect in very narrow slim tube models.

When the sand in both prototype and model is unconsolidated the morphology scaling factor is believed to have the same value in the prototype as in the model.

5.2. Inertial Forces

As pointed out by Geertsma et al.[98] when the flow is to be slow (laminar flow) in the model and in the prototype the influence of the inertial forces is not significant, so that the Reynolds number scaling group can be left out of consideration.

To know the flow regime, it is necessary to calculate the Reynolds number for flow through porous media (ratio of inertial to viscous forces). According to McFarland and Dranchuk[99] two approaches have been used to calculate the Reynolds number at the point of transition to turbulent flow. One uses the grain diameter as the characteristic length and the other uses the product KF_B, K being absolute permeability and F_B inertial resistance coefficient. McFarland and Dranchuk as well as Geertsma[100] recommended the use of KF_B as the length parameter in the Reynolds number. As the determination of F_B requires special flow experiments, Geertsma[100] introduced an empirical relationship which correlates F_B with permeability and porosity and permits the derivation of an expression to calculate the Reynolds number in porous media as a function of ϕ and K. For gases it has the following form:

$$Re \simeq 0.005 \frac{\rho_g V\sqrt{K}}{\mu_g \phi^{5.5}} \qquad (48)$$

Provided the practical applicability of Darcy's law occurs at $Re < 0.1$, Geertsma[100] concluded that it is permissible to use Darcy's law for

$$V < \frac{20\, \mu_g \phi^{5.5}}{\rho_g \sqrt{K}} \qquad (49)$$

This inequality is valid only for 100 percent liquid or gas saturations. The effect of increasing the liquid saturation in a two-phase flow system is to increase the gas turbulence[101]. According to this, for gas flow in porous media with oil and water saturations, the above relationship may be modified replacing ϕ by ϕSg and K by K Krg. Then, inequality 49 becomes:

$$V < \frac{20\ \mu_g (\phi Sg)^{5.5}}{\rho_g \sqrt{K\ Krg}} \qquad (50)$$

The application of this inequality to the injection of CO_2 gas at 5.5 MPag & 21.1°C (ρ_g = 160 Kg/m^3 from Equation 60, and μ_g = 0.02 mPa·s from Uyehara and Watson's method) into unconsolidated sand packs with the following average properties:

Absolute peremeability = 12.2 Darcies

Porosity = 43.7%

Relative permeability to CO_2 (at Sg = 0.02) = 0.1

(taken from heavy oil-CO_2 relative permeability curves for unconsolidated porous medium[12])

results in the criterion that the average superficial velocity of CO_2 has to be less than 2.74 m/d in order to avoid visco-inertial effects. This indicates that under the above gas and sand properties, laminar flow conditions for CO_2 are likely to be encountered in unconsolidated porous media at not very high velocities, and therefore, it is not necessary to maintain appropriate scaling for the visco-inertial forces.

5.3. Capillary Forces, Relative Permeabilities, and Wettability

One of the most difficult requirements to scale a physical model is that the capillary pressure and relative permeability relationships should be the same functions of saturation in the model and the prototype. The difficulty arises because in the majority of cases the two or three-phase relative permeability curves applicable to a reservoir under operating conditions (i.e. CO_2 and water displacing heavy oil) are unknowns, and also because we do not know how to create a desired set of relative permeability properties for the model.

In dealing with highly viscous oil recovery from unconsolidated sands, it has been pointed out by Pujol and Boberg[102] that capillary forces do not need to be scaled. For medium viscosity oils (less [redacted] 10000 mPa.s), unscaled capillary pressures resulted in the prediction of slightly optimistic (less than 5% HCPV) oil recovery by continuous steam injection. Demetre et al.[88] concluded that breakthrough recovery in immiscible displacement at large values of mobility ratio is only a weak function of the capillary number, provided the displacement is stable. Flock et al.[103] obtained similar results for the immiscible displacement of viscous oil by water (μ_o/μ_w = 292). In conclusion, for heavy oils the ratio of capillary to viscous forces is so low that unscaled capillary pressures have negligible effect on the oil recovery behaviour.

Rock wettability is another very difficult but important factor to scale. Although often the exact wettability characteristics of the prototype are not known, it seems that if a rock system is allowed to cure for a reasonable period of time in contact with the native oil and water, a reasonable state of wettability and/or surface equilibrium can

be obtained in the model comparable to that of the prototype[104]. Recently Morrow[105] showed that wettability alteration by crude, from strongly water-wet to weakly water-wet, occurred by deposition of a tenacious film, probably a monolayer of asphaltenes, after allowing the cores (Berea, sandstone) saturated with oil and water to stand for 24 hours.

5.4. Dispersion of Carbon Dioxide into Oil and Water

Bear[106] and Marle[107] showed that for isotropic media the dispersion tensor has only two distinct components. If any orthonormal system of axes is selected in which the first axis x is parallel to the flow, the components on the second and third axes of the matrix must be equal for reasons of symmetry. Thus $\bar{\bar{D}}go$ and $\bar{\bar{D}}gw$ may be written,

$$\bar{\bar{D}}go = \begin{pmatrix} D_{Lgo} & 0 & 0 \\ 0 & D_{Tgo} & 0 \\ 0 & 0 & D_{Tgo} \end{pmatrix}, \quad \bar{\bar{D}}gw = \begin{pmatrix} D_{Lgw} & 0 & 0 \\ 0 & D_{Tgw} & 0 \\ 0 & 0 & D_{Tgw} \end{pmatrix}$$

where D_{Lgo} and D_{Lgw} are the longitudinal dispersion coefficient of gas in oil and water, and D_{Tgo} and D_{Tgw} are the transverse dispersion coefficient of gas in oil and water.

Therefore, the carbon dioxide in oil and water dispersion similarity groups $\frac{Dgoy\ L}{Dgox\ W}$, $\frac{Dgoz\ L}{Dgox\ H}$, $\frac{Dgwy\ L}{Dgwx\ W}$, $\frac{Dgwz\ L}{Dgwx\ H}$, and the ratios of convection time to transverse dispersion time $\frac{Dgoy\ L}{W^2|\vec{v}_T|}$, $\frac{Dgwy\ L}{W^2|\vec{v}_T|}$ may be reduced to

$\frac{D_{Tgo}\ L}{D_{Lgo}\ W}$, $\frac{D_{Tgw}\ L}{D_{Lgw}\ W}$ Ratios of transverse to longitudinal dispersion of CO_2 in oil and water

and

$\frac{D_{Tgo}\,L}{D_{Lgo}\,W}$, $\frac{D_{Tgw}\,L}{D_{Lgw}\,W}$ — Ratios of convection time to transverse dispersion time of CO_2 in oil and water.

5.5. End Effects

According to Engelberts and Klinkenberg[108] the capillary forces can be expected to influence the results of unscaled laboratory experiments in a more direct way called end effects. The end effects, which may be characteristic of laboratory model behaviour and may not exist in the prototype, are due to a discontinuity in capillary properties at the outflow end of the core. This discontinuity occurs when the fluids pass abruptly from the rock, a region of finite capillary pressure, into an open receiving well, where capillary pressure vanishes. Because of the capillary forces existing within the core, the rock tends to retain the wetting phase at the outflow end. This results in an increase of the wetting phase saturation at the outflow boundary.

In order to analyze the influence of end effects on three-phase displacements, two systems were analyzed: gas-oil and water-oil.

5.5.1. Gas-Oil System

Ridings et al.[109] presented experimental and calculated behaviour of dissolved-gas-drive systems considering end effects. The oil recovery was plotted as a function of the scaling group $LV\mu_o$ (cm × cm × mPa.s/s). They showed that if

$LV\mu_o \leq 1.0$ gas-oil end effects are significant and recovery is decreased

and if

$LV\mu_o > 1.0$ gas-oil end effects are negligible.

For example, when μ_o = 1032 mPa.s, $V = 3.5 \times 10^{-4}$ cm/s (0.3 m/d) and L = 45.7 cm, the value of $LV\mu_o$ is 16.1 which is greater than 1.0. This example shows that in the case of dissolved-gas-drive of viscous oils in not very short models, the end effects are negligible.

5.5.2. Water-Oil System

Kyte and Rapoport[110] pointed out that the outlet end effects in water-wet cores is that they not only result in an excessive wetting phase saturation at the outflow face, but that they also cause an undue delay in the appearance of water in the produced effluent. They presented experimental results for light oil recoveries at water breakthrough and at water arrival as functions of the scaling coefficient $LV\mu_w$.

For the study of heavy oil-water systems, Equation 51 taken from Amyx et al.[111] may be rearranged to observe the effect of oil viscosity since its effects cannot be seen in the Kyte and Rapoport's scaling coefficient.

For two phase, horizontal, laminar flow,

$$\frac{dSw}{dL} = \frac{1}{A}\left(\frac{q_w\mu_w}{Kw} - \frac{q_o\mu_o}{Ko}\right)\frac{1}{dPc/dSw} \qquad (51)$$

This equation can be rearranged to yield,

$$dL = \frac{1}{V\mu_o} \times \frac{Ko(dPc/dSw)}{f_w\left(1 + \frac{Kq}{Kw}\frac{\mu_w}{\mu_o}\right) - 1}\, dSw \qquad (52)$$

where

$$f_w = \frac{q_w}{q_o + q_w} \quad \text{and} \quad V = (q_o + q_w)/A$$

The distance ΔL, where the water saturation increases with increasing distance, can be determined by integrating Equation 53

$$\Delta L = \frac{1}{V \mu_o} \int_{Swi}^{1-Sor} \frac{Ko(dPc/dSw)}{fw\left(1 + \frac{Ko\ \mu_w}{Kw\ \mu_o}\right) - 1} dSw \qquad (53)$$

This equation shows that for flow of heavy oil and water in unconsolidated porous media where the capillary pressure is low in comparison with the relatively high pressure drops involved in heavy oil displacements, the distance ΔL is small and the end effects are negligible due to the high viscosity of heavy oils.

For displacement of light oil by water through strongly water-wet alundum cores, Kyte and Rapoport[110] found that the scaling coefficient $LV\mu_w$ ($cm^2 \times$ mPa.s/min) must be greater than unity in order that the end effects do not affect oil recovery. Although the end effects are worse when displacing light oil through sandstone cores than those when displacing heavy oil through unconsolidated sand packs, the application of Kyte and Rapoport's scaling coefficient to the following conditions: L = 45.7 cm, V = 0.021 cm/min (0.3 m/d), and μ_w = 1 mPa.s, yields a value of 0.96 $cm^2 \times$ mPa.s/min which is very close to the limit given by the aforementioned researchers.

5.6. Scaling Groups After Relaxation

After relaxing the capillary and inertial forces, the scaling groups for heavy oil displacement from unconsolidated sands by carbon dioxide and water and taking into account the mass transfer among fluids are:

$$\frac{L}{H}, \frac{L}{W}, Mwo, Mgo, \frac{\vec{g}K\Delta\rho_{og}}{V\mu_g}, \frac{\vec{g}K\Delta\rho_{wo}}{V\mu_w}, \frac{Vw^*}{Vg^*}, \frac{D_{Tgo}\,L}{W^2V}, \frac{D_{Tgw}\,L}{W^2V},$$

$$\frac{D_{Tgo}\,L}{D_{Lgo}\,W}, \frac{D_{Tgw}\,L}{D_{Lgw}\,W}, \phi, M$$

Scaled physical models can be classified in two types: high pressure and low pressure models. A high pressure model was chosen in order to simulate accurately the mass transfer between CO_2 and the reservoir fluids, the chemistry of the process, and the in situ formation of emulsions.

Considering that model and prototype have the same morphology, the same fluids and are operated at the same conditions of pressure and temperature the following equalities must be maintained:

$$\frac{(L/H)_M}{(L/H)_P} = \frac{(L/W)_M}{(L/W)_P} = \frac{(K/V)_M}{(K/V)_P} = \frac{(Vw^*/Vg^*)_M}{(Vw^*/Vg^*)_P} = \frac{(D_{Tgo}\,L/W^2V)_M}{(D_{Tgo}\,L/W^2V)_P}$$

$$= \frac{(D_{Tgw}\,L/W^2V)_M}{(D_{Tgw}\,L/W^2V)_P} = \frac{(D_{Tgo}\,L/D_{Lgo}\,W)_M}{(D_{Tgo}\,L/D_{Lgo}\,W)_P}$$

$$= \frac{(D_{Tgw}\,L/D_{Lgw}\,W)_M}{(D_{Tgw}\,L/D_{Lgw}\,W)_P} = 1 \qquad (54)$$

These equalities permitted choosing the dimensions of the model,

the injection flow rates, and the slug volumes of carbon dioxide and brine in order to obtain approximate similarity in recovery between the model and prototype. However, heterogeneities and leakage of fluids out of the pilot volume are responsible for lower recovery in the prototype than in a scaled model.

6. OPERATING POLICY VARIATIONS

Basically two CO_2/brine processes were studied. The slug CO_2 process and the WAG process. Variations in operational policy for the slug CO_2 process included changes in injection flow rates of carbon dioxide and brine and their effect on oil recovery. A carbon dioxide slug volume of 20% HCPV was chosen on the basis of experimental results reported by Wang[5] on the effect of slug size on heavy oil recovery using the slug CO_2 process and on the basis of results of the first runs, which showed that the oil recovery from CO_2 injection was already near its asymptotic limit when a 20% HCPV CO_2 slug had been injected. Maintaining a constant slug volume, the injection flow rate was changed from 19 to 306 cm^3/hr. Flow velocities in a five-spot pattern vary significantly from near the wellbore to midway between wells and therefore a problem arises in selecting the appropriate superficial velocity for calculating the scaling factors. The following formula suggested by Stalkup[112] was used:

$$V = \frac{5Q}{\sqrt{2}\,HL} \tag{55}$$

It assumes that the proper width for calculating an average superficial velocity is one-fifth the distance between wells. Using this equation the range of superficial velocities that corresponds to the above injection flow rates was 0.18 - 2.9 m/d. This broad range of velocities permitted the study of the effect of the viscous, diffusive, and gravitational forces on slug CO_2 process for heavy oil recovery.

The model superficial velocity and its equivalent flow rate to

scale down the ratio of viscous forces to gravitational forces between the model and the prototype may be calculated by means of the following relationship when using the prototype fluids and unconsolidated sand in the model:

$$V_M = V_P \times \frac{K_M}{K_P} \qquad (56)$$

In order to apply Equation 56 it is necessary to know the superficial velocity of the fluids in the prototype. A small range of prototype superficial velocity (0.09 - 0.36 m/d) was chosen. The prototype flow rates equivalent to the above velocities are 0.12 - 0.36 HCPV/year. These compare favorably with 0.19 HCPV/year which was the flow rate recommended by the National Petroleum Council of USA[113] for displacement of light oils by carbon dioxide.

Considering that the molecular diffusion coefficients of CO_2 in water and oil are of the same order of magnitude[25,26], the requirements for scaling longitudinal and transverse dispersions including the effect of molecular diffusion become,

$$\frac{\left(\frac{D_{Tgo}\,L}{W^2 V}\right)_M}{\left(\frac{D_{Tgo}\,L}{W^2 V}\right)_P} = \frac{\left(\frac{D_{Tgo}\,L}{D_{Lgo}\,W}\right)_M}{\left(\frac{D_{Tgo}\,L}{D_{Lgo}\,W}\right)_P} = 1 \qquad (57)$$

where D_{Lgo} and D_{Tgo} are the longitudinal and transverse dispersion coefficients which can be calculated using the equations given by Perkins and Johnston[79]:

$$D_{Tgo} = \frac{Do}{F\phi} + 0.015\ V dp\ \sigma m, \qquad \frac{V dp\ \sigma m}{Do} < 10^4 \tag{58}$$

and

$$D_{Lgo} = \frac{Do}{F\phi} + 0.5\ V dp\ \sigma m, \qquad \frac{V dp\ \sigma m}{Do} < 50 \tag{59}$$

For unconsolidated sands $1/F\phi \simeq 0.7$ and σm depends on the average particle diameter[112].

The scaling group $D_{Tgo}\ L/W^2V$ is an indicator of the level of transverse dispersion of CO_2 in a porous medium saturated with oil and water. It is the ratio of the time for a small unit volume of CO_2 to be convected through the length of the porous medium (L/V) to the time to be dispersed across the width of the porous medium (W^2/D_{Tgo}). Low values of $(D_{Tgo}\ L/W^2V)_M$, which correspond to high superficial velocities, are believed to be most representative of unstable field-scale immiscible CO_2 flooding processes. For high model superficial velocities the lateral dispersion scaling factor becomes,

$$\lim_{V\to\infty}\left(\frac{D_{Tgo}\ L}{W^2V}\right)_M = \lim_{V\to\infty}\left(\frac{Do\ L}{F\phi W^2V}\right)_M + \lim_{V\to\infty}\left(\frac{0.0157\ dp\ \sigma m\ L}{W^2}\right)_M$$

$$= \frac{0.0157\ dp\ \sigma m\ L}{W^2}$$

This is the convective component of the lateral dispersion scaling group.

The scaling group $D_{Tgo}\ L/D_{Lgo}\ W$ is the ratio of the transverse dispersion velocity to the longitudinal dispersion velocity. Replacing D_{Tgo} and D_{Lgo} by the expressions given by Perkins and Johnston (Equations 58 and 59), the ratio of transverse to longitudinal dispersion similarity group is scaled down by using a low model velocity equal to the

prototype velocity.

Exact scaling of longitudinal and transverse dispersion groups, geometric similarity, chemical similarity, and ratio of viscous to gravitational forces simultaneously in an experimental model is impractically large laboratory models and long experiment times. For that reason it was decided to run the experiments at different superficial velocities from a low value of 0.18 m/d similar to reservoir superficial velocities to a maximum of 2.9 m/d achieved with the model injection facilities. At low velocities it is possible to scale down simultaneously geometric similarity, ratio of viscous forces, ratio of viscous to gravitational forces, and chemical similarity, while at high velocities it is possible to scale down simultaneously geometric similarity, ratio of viscous forces, lateral dispersion similarity group, and chemical similarity.

For the water-alternate-gas (WAG) process the variations in operational policy included the optimization of WAG ratios (slug volume of brine/slug volume of CO_2) for secondary and tertiary recovery of Aberfeldy-Lloydminster heavy oil. The superficial velocities for these runs were chosen applying the ratio of gravitational to viscous forces scaling group. The total volume of CO_2 injected was maintained constant and equal to the slug of CO_2 injected in the slug CO_2 process runs (20% HCPV). This permitted the comparison of the CO_2 requirements needed to recover a cubic metre of oil in both processes.

In addition to examining various brine-carbon dioxide injection strategies for recovering heavy oil, the effect of oil viscosity and type of sand used in packing the model cavity on recovery and CO_2

requirement was investigated.

All the runs were carried out at an average pressure of 5.5 MPag and at room temperature (21 - 23°C). A subcritical rather than a supercritical CO_2 pressure (> 7.4 MPa) was chosen since the actual pressure of the Aberfeldy-Lloydminster reservoirs is of the order of 3.4 MPa. As the model temperature was 21-23°C, lower than the CO_2 critical temperature (31.1°C), the carbon dioxide was in the gaseous phase at pressures below 5.9 MPag.

7. EXPERIMENTAL APPARATUS

A schematic diagram of the apparatus used in this research is shown in Figure 4. The main components are the physical model (Plate 1), the fluid injection (Plate 2), production (Plate 3), and the data acquisition systems.

7.1. High Pressure Physical Model

7.1.1. General Design

Utilization of the physical scaling groups led to a set of rules for the construction of the high pressure physical model. The prototype considered was a shallow, thin, horizontal, unconsolidated sandstone reservoir with rock and fluid properties similar to the average properties of the Aberfeldy field in the Lloydminster area. Table 3[114] summarizes the properties of the prototype. Based on information about the pattern configurations that are often used in horizontal carbon dioxide floods in the United States[9,115] and on the different flood patterns that have been used in Lloydminster area[116,117], it was thought that 6.4 ha (64750 m^2) 5-spot patterns probably represented a reasonable spacing for Lloydminster carbon dioxide projects, allowing a quadrant to be isolated and modelled as a small element of symmetry that may represent overall project behaviour.

7.1.2. Steel Pressure Vessel

The basic structural element is a steel flanged rectangular pressure vessel. The size of the model was selected as large as was

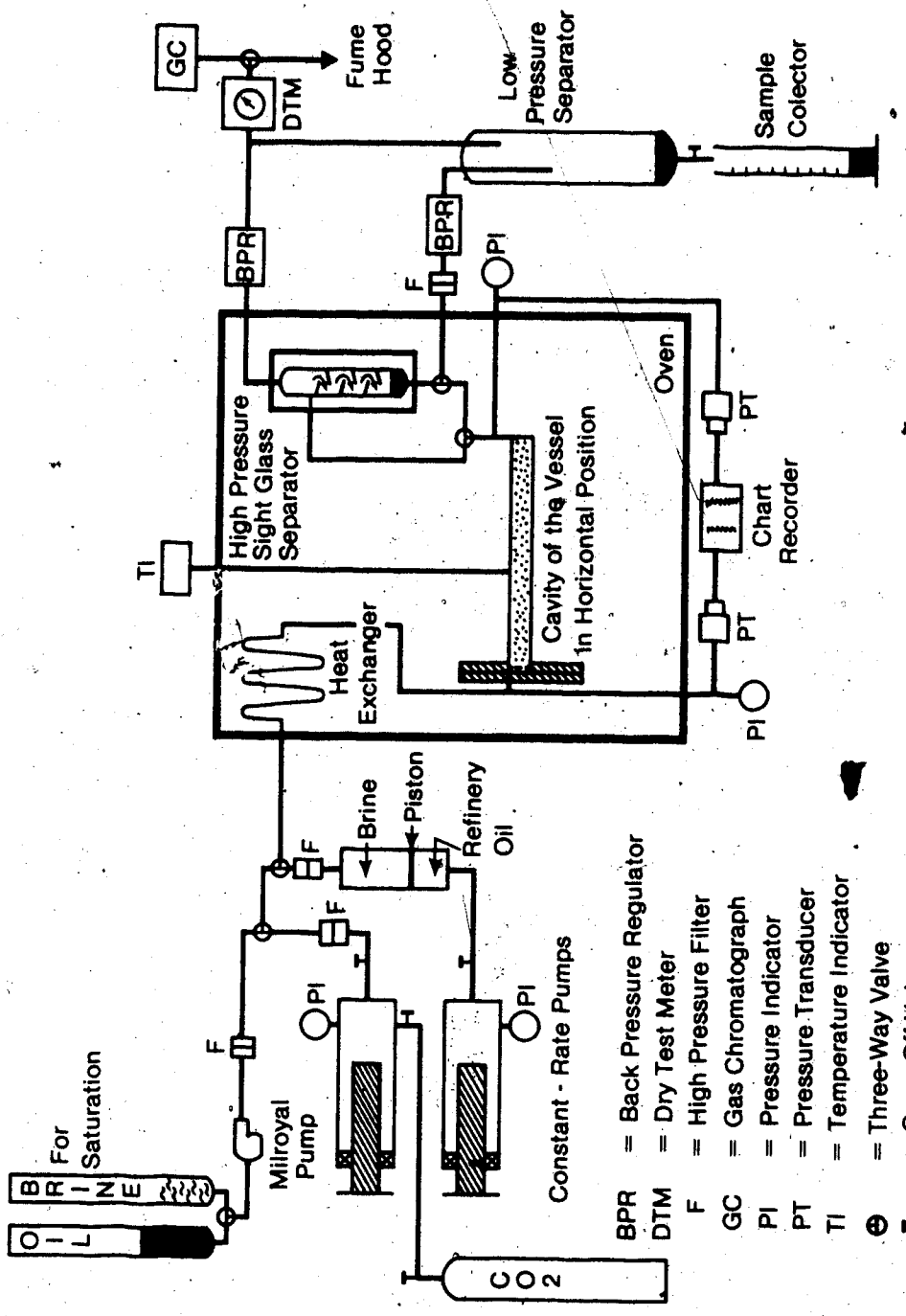


Figure 4 Schematic Diagram of the Physical Model

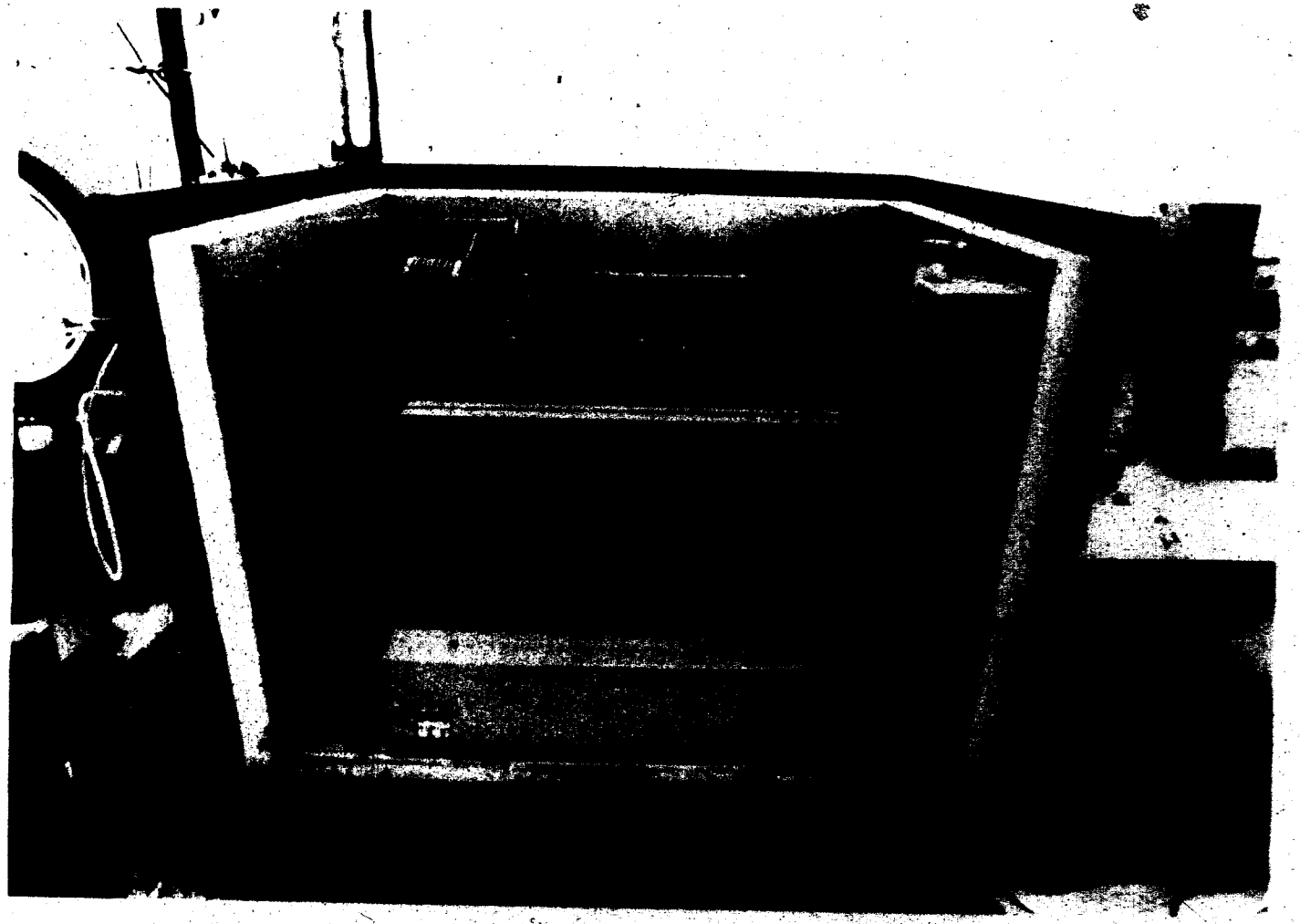


Plate 1. Rectangular, High Pressure Vessel and Sight Glass Equipped High Pressure Separator.



Plate 2. High Pressure Fluid Injection System.



Plate 3. Model and Fluid Production System.

TABLE 3

ROCK AND FLUID PROPERTIES OF THE PROTOTYPE

Aberfeldy-Lloydminster thin reservoir	
Horizontal, unconsolidated marine sand	
Net sand (thickness)	6.1 m
Pattern size (5-spot)	6.4 ha
Porosity	35%
Permeability	1 - 3 Darcies
Oil Saturation	87%
Gas Saturation	0%
Depth	500 - 600 m
Reservoir Temperature	21° - 22°C
Oil Gravity	15 - 17°API
Oil Viscosity	1000 - 5000 mPa.s
Original Solution GOR	9 sm^3/m^3

possible within the constraints of the oven space and time available to perform the experiments. Selecting $L_M = W_M = 1.5$ ft (0.457 m) the thickness of the model cavity was determined by the geometric scaling factor

$$H_M = \frac{0.457\ m}{127.23\ m/6.1\ m} = 0.022\ m\ (2.2\ cm)$$

In order for the vessel to withstand pressures up to 10 MPa

at 100°C, it was necessary to pay special attention to its design. This was done by following the rules in Appendix 13 (Vessels of Noncircular Cross Section) of the ASME Boiler and Pressure Vessel Code Section VIII - Division 1[118]. The rules of that Appendix apply to the walls and parts of the vessel subject to pressure stresses including reinforcing. Considering that rectangular vessels exhibit a tendency to bulge under internal fluid pressure, it was necessary to place reinforcing members on the outside of the vessel which were attached to the plates of the vessel by welding on each side of the reinforcing member. The design characteristics such as distance between reinforcing members, number, shape, size, and thickness of the reinforcing members, thickness of the walls of the vessel, and membrane, bending and total stresses were given to Dominion Bridge, in Calgary, who constructed the steel vessel. Figure 5 shows two cross sections of the vessel which is shown in Photographic Plate 1. An important characteristic of the model is that it can be rotated to perform horizontal, vertical, and inclined floods. At the highest pressure considered (10 MPa), the maximum deflection of the vessel walls will be less than 0.01 mm. The pressure vessel has been operated free of mechanical problems at 5-6 MPag pressure for two years. The main characteristics of the high pressure vessel are listed in Table 4.

7.1.3. Injection and Production Wells

For horizontal floods the model has nine wells which permit the simulation of different types of patterns such as 5-spot, 9-spot, and line drive. The wells were designed in such a way that they can go within or outside of the sand depending on the type of pattern used.

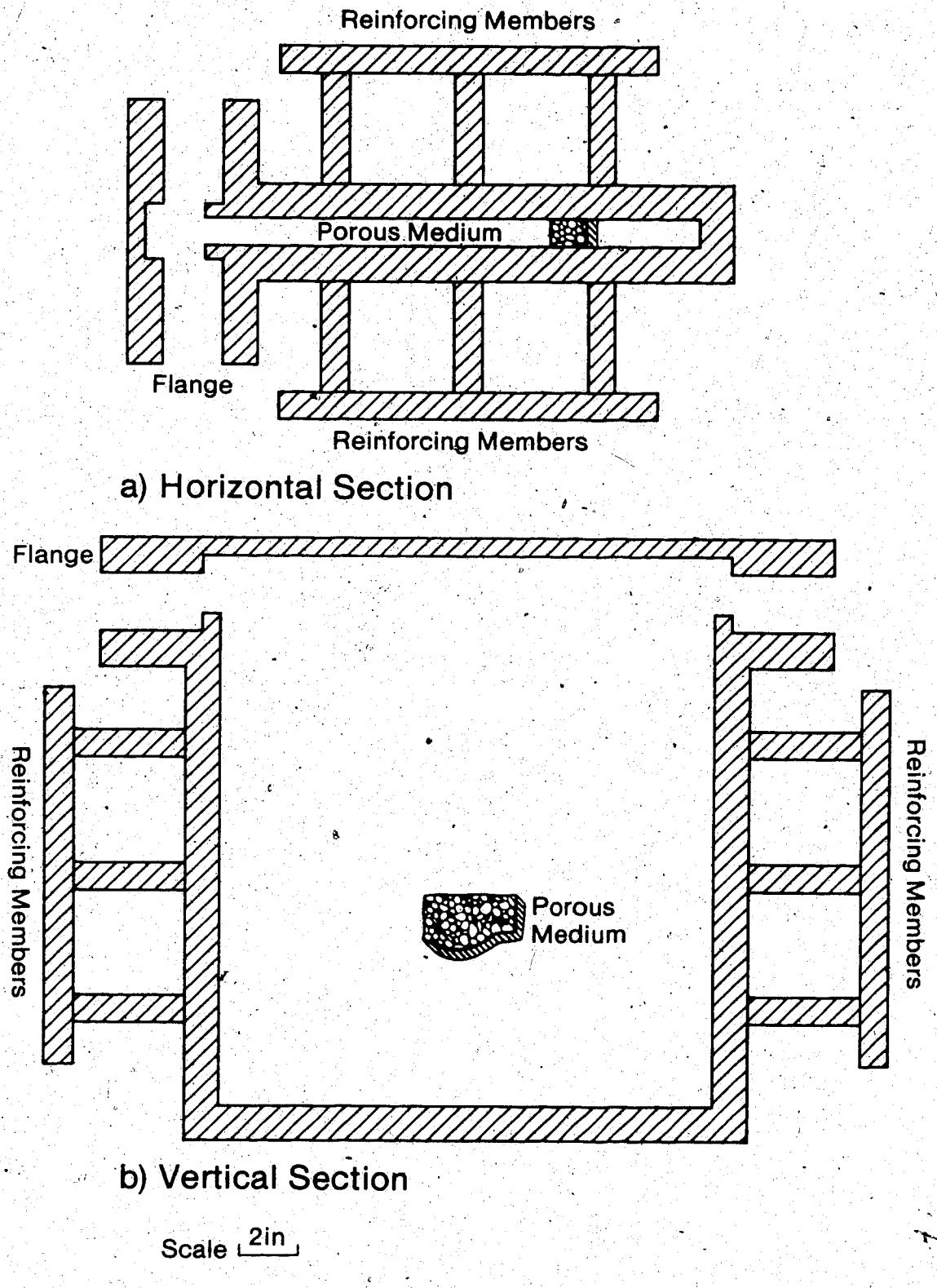


Figure 5 Cross Sections of the High Pressure Vessel

TABLE 4

CHARACTERISTICS OF THE HIGH PRESSURE VESSEL

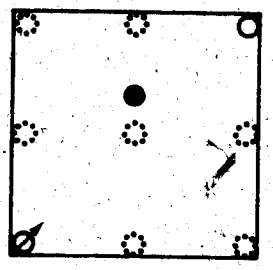
- Rectangular shape 45.7 cm × 45.7 cm × 2.2 cm
- Three reinforcing members
- Maximum internal pressure: 10 MPa
- Maximum deflections of walls at 10 MPa < 0.01 mm
- Weight ~ 1 Tonne
- Number of wells available: 9
- Possible patterns to simulate: 5-spot, 9-spot, line drive
- The central well permits the simulation of cyclic injection
- The model can be rotated for horizontal, inclined, or vertical floods

---

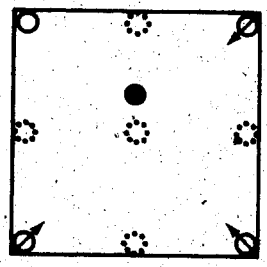
Figure 6 shows the location of the wells for each pattern. The wells were made of stainless steel 1/8" (3 mm) tubing with small holes (0.055 mm diameter) perforated all over (see Plate 1 for position of wells).

For vertical floods the model has two wells. These have the same diameter as the wells for horizontal floods but with the difference that they can have different intervals perforated in order to study the effect of selective well completions on the recovery under gravitational effects.

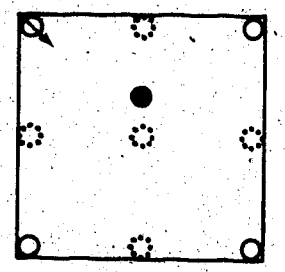
In addition to the production and injection wells, the model has another well with a thermistor inserted to measure the temperature of the porous medium in the position shown in Figure 6. Thermistors are



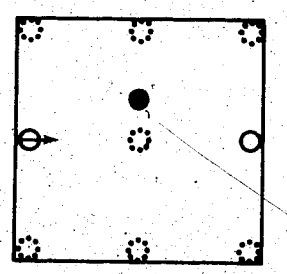
Quarter of
five - spot



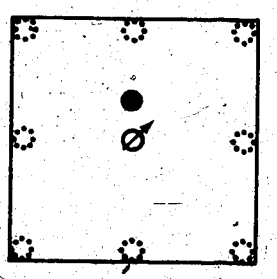
Quarter of normal
nine - spot



Quarter of inverted
nine - spot



Direct Line Drive
d/a = 1



Injection - Production
well to simulate a
huff-n-puff process

Ø Injection Well

O Production Well

◌ Dummy Well (out of the porous medium)

● Well with a thermistor inserted to measure
the temperature of the porous medium.

Figure 6 Pattern Arrangements for Horizontal Floods. Also Central Well to Simulate the Huff-n-Puff Process

basically semiconductors which exhibit rapid and extremely large changes in resistance for relatively small changes in temperature. They are more accurate than thermocouples for temperatures up to 100°C.

7.1.4. Fluid Injection and Production Systems

As is shown in Figure 4 and Plate 2, a Milroyal positive displacement pump was used for injecting the brine and oil to saturate the porous medium. The brine and oil were filtered using a steel filter located upstream of the model.

Two dual, constant rate, screw type, high pressure pumps (Plate 2) built in the Department of Mineral Engineering at the University of Alberta, were used to inject the carbon dioxide and brine into the porous medium to recover the oil. The injection rate could be controlled by varying the pump speed. As dry CO_2 is not corrosive, the carbon dioxide could be displaced directly by the piston pump into the model. However, as the brine is very corrosive, it was preferred to put it in a high pressure steel cylinder with a floating piston to obviate the need for mercury within the system. The pump cylinder was filled with a refinery oil which pushed the floating piston, and brine into the model.

A heat exchanger located in between the pressure filters and the injection wells was designed to heat the injection fluids to the oven temperature before entering the model. It consisted of a stainless steel slim wall tube 5 m in length and 0.635 cm internal diameter.

The effluents from the model were separated in a two-stage separation system. The first stage consisted of a high pressure, sight glass separator with baffles (Plate 2) and the second stage consisted of

a glass separator operating at atmospheric pressure (Plate 3). The tops of both separators were connected to a dry test meter (DTM) to measure the amount of gas produced (Plate 3). Liquids were removed from the second separator and were collected in graduated cylinders. At low production rates (low superficial velocities) it was not necessary to use the high pressure separator and the production fluids were bypassed to the atmospheric separator (see Figure 4).

All valves, fittings, and connections were of stainless steel (1/8 in, 3 mm) to prevent corrosion and to exercise precise control of the production and injection fluid volumes.

7.1.5. Oven

The pressure vessel, the heat exchanger, and the high pressure separator were placed in an oven of dimensions 76 × 76 × 103 cm. The oven permits the operator to maintain the temperature of the model, heat exchanger, and high pressure separator at a constant level. The oven temperature is controlled by an Omega temperature controller according to the desired temperature of the porous medium (Figure 4 and Plate 1).

7.1.6. Data Acquisition System

To control the pressure of the production wells, automatic back pressure regulators (BPR) were located at the gas stream end of the high pressure regulator and upstream of the low pressure separator. Two Heise pressure gauges were used to measure the pressure of the wells, and two pressure transducers connected to a chart recorder provided the injection and production pressure histories for each run.

The temperature of the porous medium was measured with a thermistor

and recorded by an Omega temperature controller with an accuracy of ±1°C or ±1°F depending on the scale chosen.

The cumulative volume of the gas produced was measured by a dry test meter (DTM) with an accuracy of 10 cm^3 at room conditions.

To know the possible vaporization of hydrocarbons by the carbon dioxide, gas samples were taken from the downstream side of the DTM for chromatographic analysis (Figure 4).

7.2. Diffusion Cell

An attempt to observe whether the CO_2 diffusive forces were able to overcome the gravitational forces was made by setting up an experimental apparatus, which is shown in Figure 7. The diffusion cell which is similar to that used by Denoyelle and Bardon[26] consisted of a high pressure coreholder made of a stainless steel cylinder fitted with two flanges. The cell was placed in the vertical position and its top flange was connected to a high pressure CO_2 cylinder. Carbon dioxide pressure in the top part of the cell was measured using a Heise pressure gauge. The bottom flange of the diffusion cell was equipped with a high pressure valve which permitted the taking of samples of oil for determining the concentration of diffused CO_2 in the bottom of the oil column at the end of the experiment. Knowing the CO_2 concentration in the oil sample, an approximate value of the molecular diffusion coefficient of CO_2 into oil was estimated.

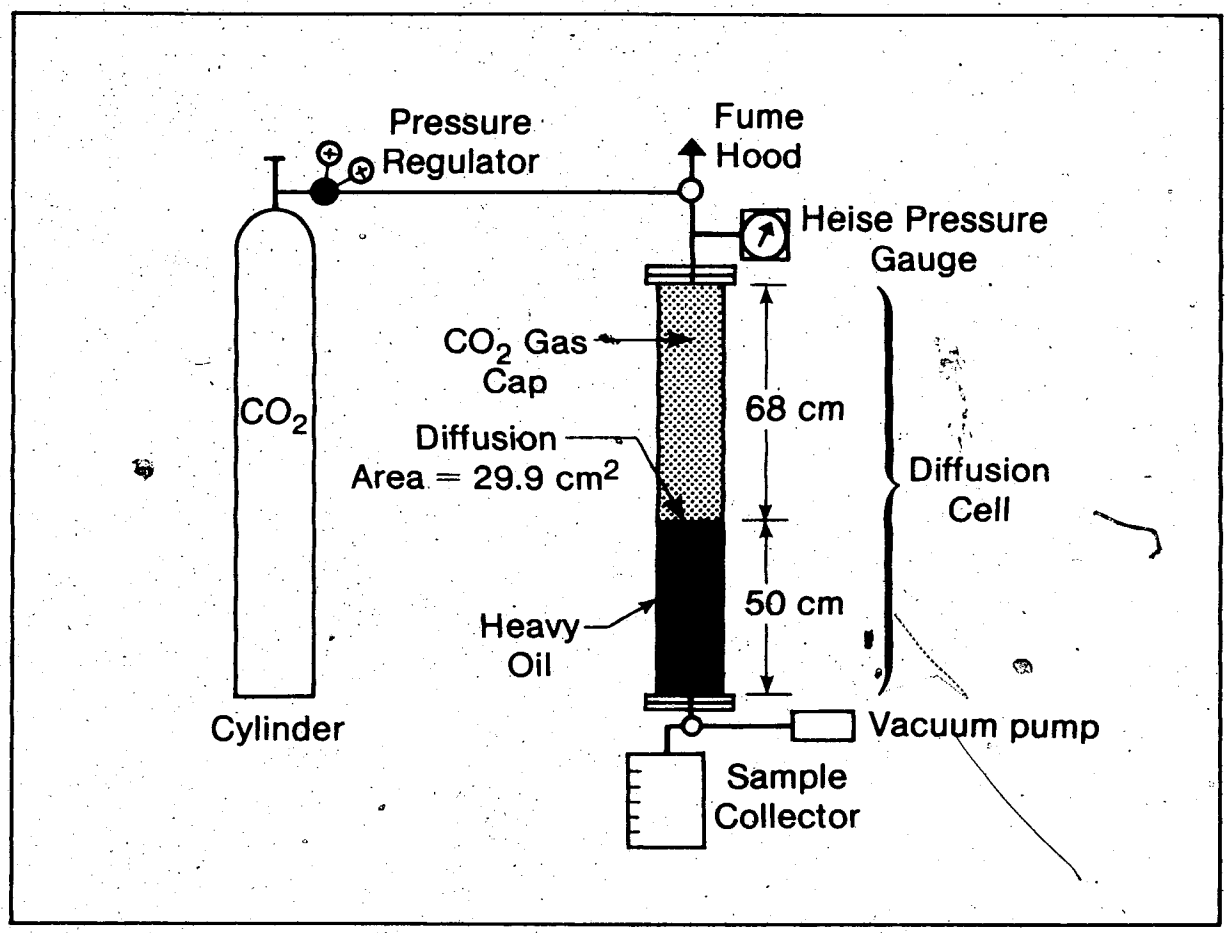


Figure 7 Schematic Diagram of the Diffusion Cell

8. MATERIALS, EXPERIMENTAL PROCEDURES, AND DATA PROCESSING

8.1. Fluids

In all displacement tests and diffusion experiments commercial grade carbon dioxide (99.5% purity) was used. The displacement tests were conducted using reservoir water to create an irreducible brine saturation, as well as two samples of viscous crude oil from the Aberfeldy, Lloydminster area. The same reservoir water (jointly with CO_2) was used to recover the oil from the porous medium.

As the oil samples received from the field had more than 10% vol. of water it was necessary to dehydrate them. The water was separated from the oil in an oil dryer by gravity and by adding four drops of de-emulsifier (used by Husky Oil Co. in Lloydminster area) for each litre of sample. The oil dryer consisted of a metal cylinder, provided with rotating paddles, and equipped with two heating jackets to raise the temperature of the oil-water mixture to 40°C. The water was drained from the oil dryer sump weekly until no more free water was produced. At this point, a sample of oil was taken for water and sand content analyses. Drying a sample of oil (20 litres) took between one and two months depending on the volume of emulsified oil in the water-oil mixture.

A summary of the average properties of the dried oil and brine samples is shown in Table 5.

8.2. Unconsolidated Sand

Two types of sand were used in the model; unconsolidated sand

TABLE 5

PROPERTIES OF OIL AND WATER USED IN THE MODEL

	Sample 1	Sample 2
CRUDE OIL		
Density, kg/m^3 @ 0 MPag & 23°C	952.8	970.2
Viscosity, mPa.s @ 0 MPag & 23°C	1032	4681
Water content, % Vol.	0.25	1.0
Sand content, % Weight	< 0.5	1.0
Molecular weight, g/gmol	425	460
RESERVOIR WATER		
Density, kg/m^3 @ 23°C	1047	
Viscosity, mPa.s @ 23°C	1.14	
pH @ 23°C	7.5 - 8.1	
Water analysis:		
Total solids, ppm	77200	
Hardness, ppm	8997	
Sulphates, ppm	41122	
Alkalinity, ppm	60	
Iron, ppm	67.5	
Calcium, ppm	1971	
Magnesium, ppm	990	
Sodium, ppm	19850	
Potassium, ppm	3610	
Salt, ppm	67851	
Nature of Alkalinity	Bicarbonate of calcium and magnesium	

produced with the oil (tank sand) in the Aberfeldy field and Ottawa silica sand. The Aberfeldy tank sand was cleaned in coreholders using solvents. The Ottawa silica sand was used as received from the supplier.

Figure 8 shows a comparison of the grain size distribution of the sand produced with the oil, of a core sample from Sparky-Aberfeldy, and of the Ottawa silica sand. It can be seen from Figure 8 that the tank sand and the core sample show little difference in the particle size analyses. However the Ottawa silica sand shows a smaller amount of fines than the other two sand samples.

The Ottawa silica sand and the tank sand samples were analyzed by x-ray analysis to determine the bulk mineralogy of the two sands. Table 6 reveals that quartz is the major portion of both sands but the Aberfeldy tank sand has a greater clay content than Ottawa silica sand. Also the Aberfeldy tank sand has minor to trace amounts of orthoclase, which is a potasssium- aluminum silicate of the feldspar group. As expected, the Ottawa silica sand has less clay content than the Aberfeldy tank sand. It can also be seen in Table 6 that the kaolin group mineral was the major constituent of the clay content of the Aberfeldy tank sand and that the type of clay present in the Ottawa silica sand is possibly illite/smectite.

Although the clay mineral content of both sands represents a small percentage of the total matrix, its presence has been recognized as being very important in the stabilization of oil-water emulsions.

8.3. Aberfeldy Tank Sand Cleaning Procedure

The Aberfeldy tank sand was cleaned in coreholders using two different procedures, which permitted observation of the effect of solvents

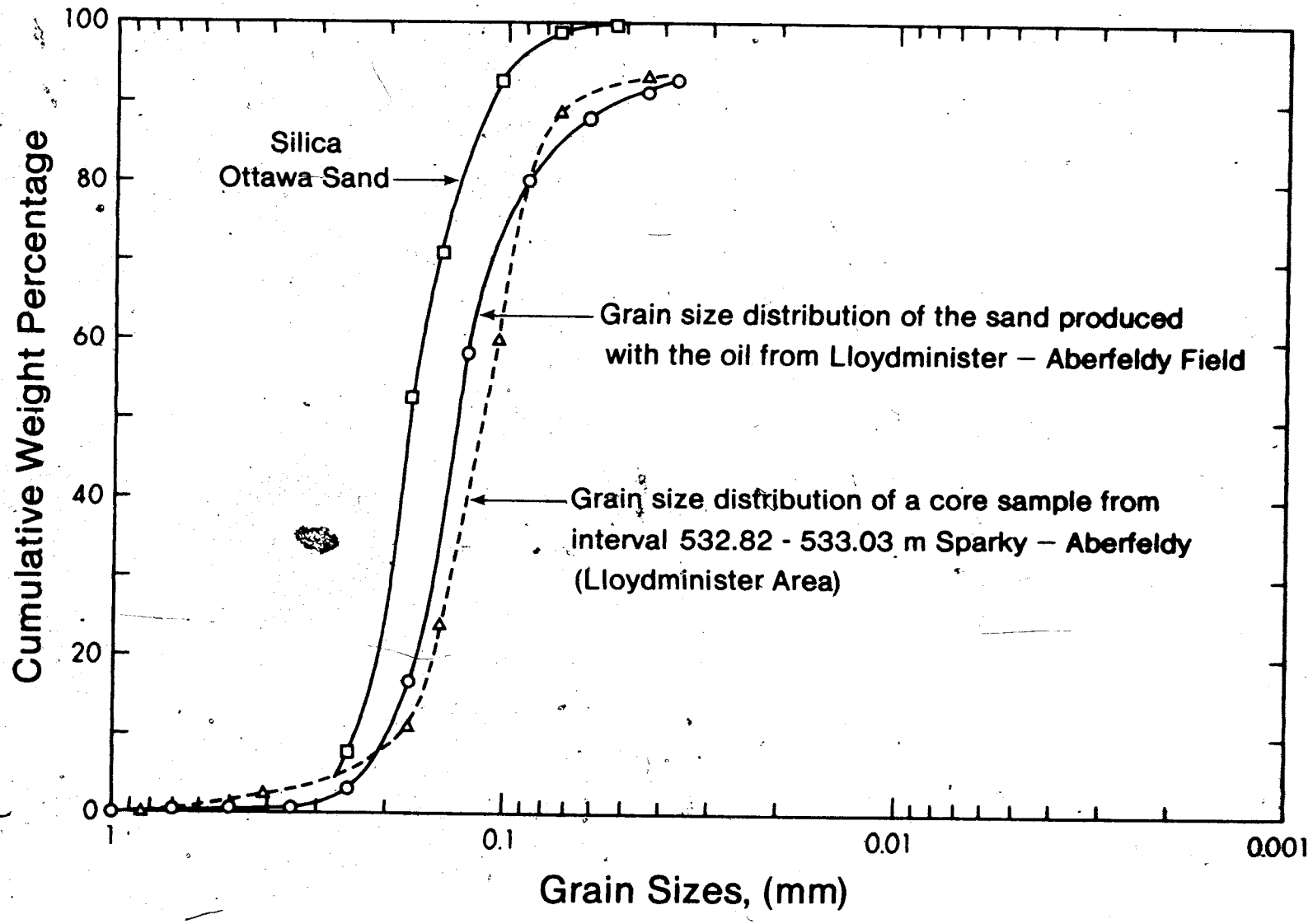


Figure 8 Particle Size Analysis of Three Sand Samples

TABLE 6

BULK MINERALOGY OF THE SANDS USED IN THE EXPERIMENTS*

Sand	QZ	OR	C	Type of Clay
Ottawa Silica Sand	M	-	t	Possibly Illite/Smectite
Aberfeldy-Lloyd. Tank Sand	M	mt	mt	Kaolin Group Mineral and Possibly Chlorite and Illite

QZ = Quartz, OR = Orthoclase, C = Clays

M = Major, mt = minor to trace, t = trace

M > mt > t

*Made by the Department of Geology, University of Alberta

on the wettability of sand and on the recovery behaviour. Two steel coreholders (120 cm × 30 cm^2 volume) with flanges were packed with tank sand as received and were connected in series. In the first procedure, toluene was injected to displace the oil, then the toluene was driven out by isopropyl alcohol and this was displaced by distilled water; after that, the sand was dried by injecting air for several hours. In the second procedure, only toluene was injected into the coreholders, and then the toluene was evaporated by injecting air.

To clean the sand required for a run (12 Kg), 8 litres of toluene in each one of the two procedures and 5 litres of isopropyl alcohol in the first procedure were used. The time consumed by the two procedures was 15 and 7 days, respectively.

8.4. Diffusion of CO_2 into Oil at High Pressure

The following experimental procedure was followed in the diffusion experiments:

8.4.1. The diffusion cell (Figure 7) was evacuated for 24 hours.

8.4.2. Oil was injected into the diffusion cell to obtain an oil column of 50 cm.

8.4.3. The rest of the cell was filled with carbon dioxide at 5.5 MPag. The gas space allowed room for the swelling of the oil and maintained a CO_2 concentration of 100% at the gas-oil interface.

8.4.4. Five times a day, CO_2 from a cylinder was injected into the cell to maintain a constant pressure in the gas phase, while gas diffused into the oil.

8.4.5. The oil-CO_2 system was left at high pressure for 8 days.

8.4.6. At the end of the experiment two samples of 500 cm^3 were taken from the bottom valve.

8.4.7. From the first sample, the variation of cumulative weight of liberated CO_2 with time was obtained.

8.4.8. From the second one, the variation of the foam viscosity with time was determined using a Brookfield LV digital viscometer.

8.5. Packing, Saturation, and Model Cleaning Procedures

The wet packing technique was used to obtain packs with consistent properties. With the model in the vertical position, it was partially filled with distilled water to a height of 10 cm. The distilled water was followed by sand and the model was vibrated with an

air vibrator. During the packing process, a constant 10 cm head of distilled water was kept above the sand (see Figure 9). A 10 cm tall filling lid with a shape similar to that of the vessel cavity was used to maintain the same head of distilled water at the end of the packing process after the model had been filled with sand. Following that, the model was vibrated for several hours. The packing process took approximately 3 hours. The model vibration during and after packing eliminated the trapping of air by sand.

After packing the model with sand, the packing lid was replaced by the flange plate and the model was tested for leaks at a pressure of 6 MPa. The distilled water was then displaced miscibly by reservoir water, which flowed from the bottom to the top as shown in Figure 9. After determining the pore volume and the permeability of sandpack following procedures explained later, oil was injected using the three wells at the top of the vertically positioned model (see Figure 9) to create an irreducible water saturation in the porous medium. After that, the model was repressured with oil up to 3.45 MPag to simulate the actual pressure of the Aberfeldy reservoirs in Lloydminster area. At this point the sandpack was ready for carbon dioxide injection.

At the end of each run, the oil, brine, and sand remaining in the model were removed with a metal scraper. When most of the sand was removed, the interior walls of the vessel cavity were cleaned with varsol and water. All wells and the flange plate were also cleaned with varsol and tolune. Great care was taken about the cleanliness of the wells in order to avoid plugging of the well perforations.

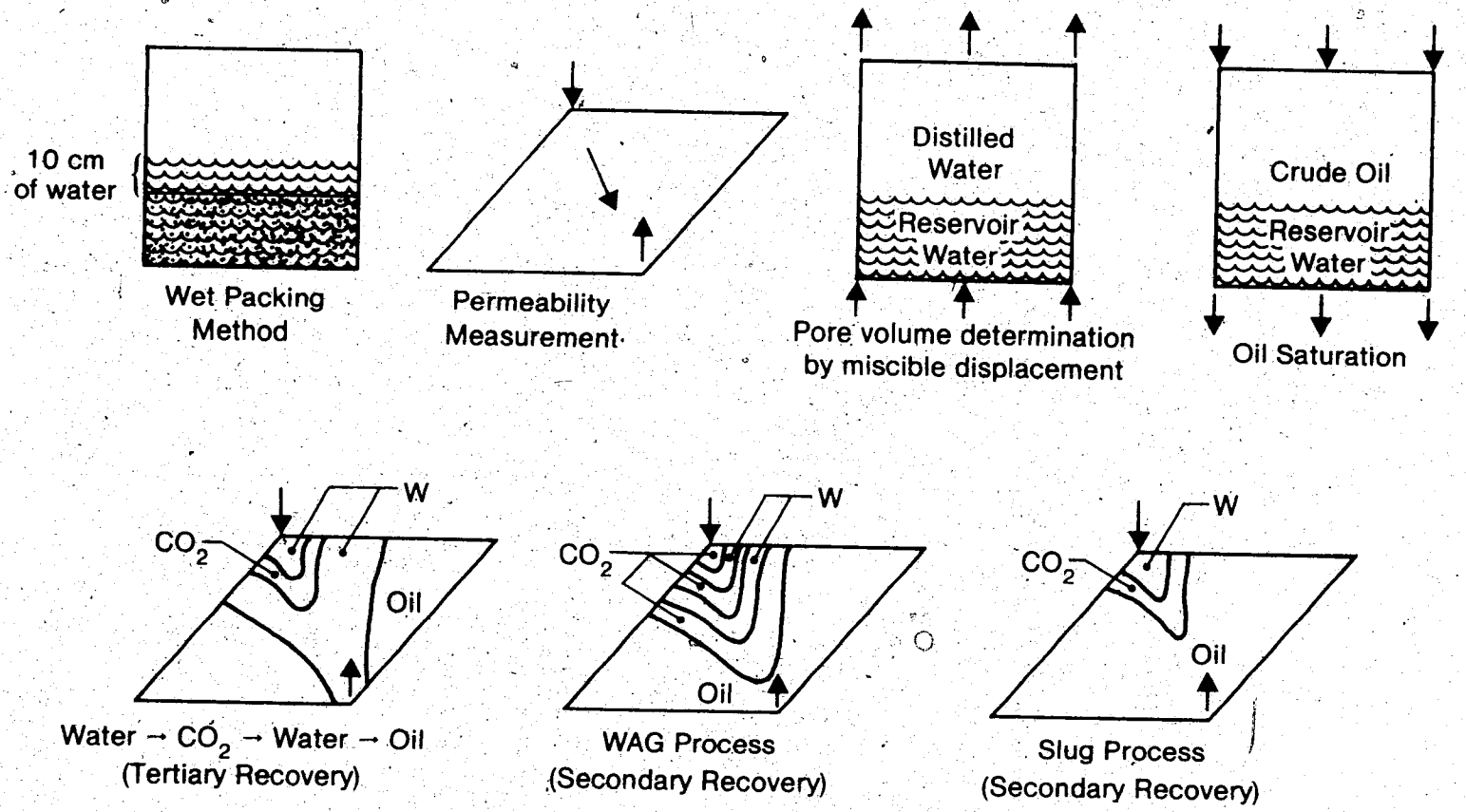


Figure 9 Steps of Displacement Experiment Procedure

8.6. Porosity and Permeability Measurements

The pore volume and porosity of the sandpacks were determined by the miscible displacement method. In this method, the distilled water used in the wet packing of the sand was displaced vertically by reservoir water. Refractive indices of distilled and reservoir water mixtures were measured using an Abbé refractometer, and a plot of refractive index versus percentage of reservoir water in the mixture was made (Figure 10). Volumes of effluent samples were collected and their refractive indices were measured. Entering Figure 10 with the mixture refractive index, the percentage of reservoir water in the mixture was determined and then a plot of percent displacing fluid in the effluent versus cumulative volume produced was made (Figure 11). The areas above and below the S-shaped curve were balanced using a planimeter and the pore volume was determined. The porosity was calculated by dividing the pore volume by the volume of the vessel cavity. For reliable results with this method it is necessary that viscous and gravitational instabilities do not occur during the displacement. These two conditions were met in the vertical miscible displacement of distilled water by reservoir water since the heavier reservoir water was injected from the bottom and the mobility ratio was slightly less than one.

The absolute permeability of the sandpacks was determined by placing the model in horizontal position and by flowing reservoir water at various flow rates in a quarter of 5-spot pattern as shown in Figure 9. The pressure drops between injection and production wells were recorded with a Heise pressure gauge. Muskat's flow equation[119] for a 5-spot geometry was then used to calculate the absolute permeability. After

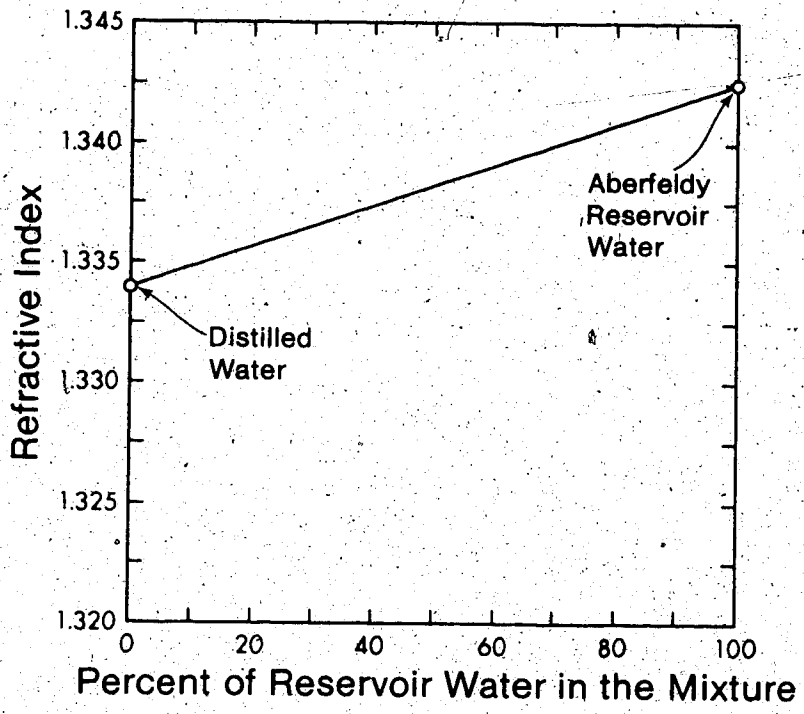


Figure 10 Refractive Indices of Aberfeldy Reservoir Water-Distilled Water Mixtures

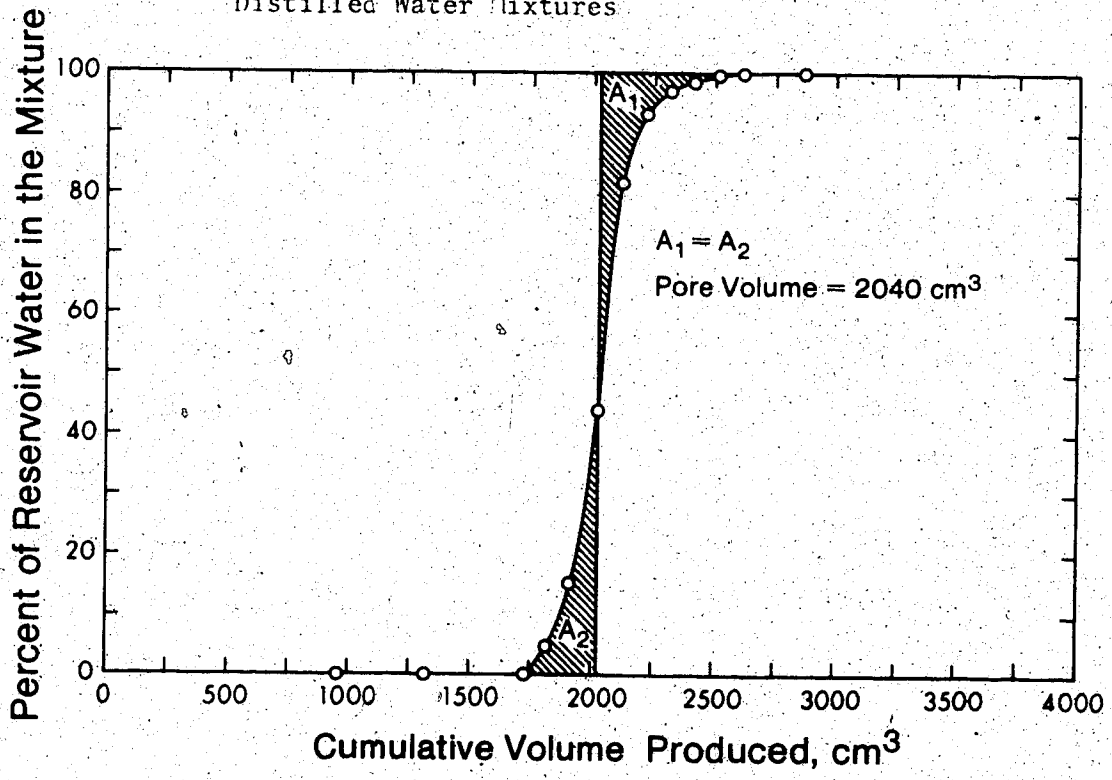


Figure 11 Determination of Pore Volume by Miscible Displacement. Run 7.

that, oil was injected into the top of the vertically positioned model to create an irreducible water saturation in the porous medium. Having the porous medium saturated with oil and water, more oil was injected to pressurize the model up to 3.45 MPag to simulate the actual pressure of the Aberfeldy reservoirs in Lloydminster.

8.7. Experimental Procedure for the Displacement Tests

To start a run, the high pressure separator was filled with CO_2 at 5.5 MPag. The model pressure was then increased to the test pressure (5.5 MPag) by injecting carbon dioxide with the production well closed and the two back pressure regulators were set to control the pressure of the production well at 5.5 MPag. Once the run pressure was reached in the model, subcritical carbon dioxide and brine were injected into the model at a constant flow rate from the screw-driven pumps and according to the injection scheme selected for the run. For all the CO_2/brine floods, the pressure was controlled at 5.5 MPag and the temperature at 21-23°C. Up to CO_2 breakthrough, the produced oil went directly to the low pressure separator. Later, the two or three-phase production (when also injecting brine) was switched to the high pressure separator. The high pressure separator was only used in the runs at the high superficial velocities. At low superficial velocities (less than 1.5 m/d) the atmospheric pressure separator was adequate to separate the gas from oil and brine.

Carbon dioxide breakthrough was detected by observing the first production of CO_2 in the atmospheric pressure separator and the initial movement of the gas meter needle. The brine breakthrough was detected

by analyzing small emulsion effluent samples (10-20 cm^3) for brine content since free brine did not breakthrough before the emulsion. The brine content of the emulsion was determined by adding 50 cm^3 of toluene to the sample and centrifuging the mixture at 3000 rev. min^{-1} for 20 minutes.

During the runs, the pressures of the injection and production wells were logged, the production liquids were collected, and the volume of gas was measured.

The following CO_2/brine injection processes were investigated:

8.7.1. CO_2 Slug Process

In this process, a carbon dioxide slug of 20% HCPV (Hydrocarbon Pore Volume = $\Delta x \Delta y \Delta z \phi So$) was driven by brine (see Figure 9) to a water-oil ratio (WOR) of approximately 20 m^3/m^3. Most of the runs using this process were conducted with the porous medium at irreducible water saturation. A few tertiary recovery runs were also carried out injecting the slugs of CO_2 and brine after a brineflood.

8.7.2. Brine-Alternating-CO_2 Slugs (WAG Process)

In this case, small slugs of CO_2 and brine were injected alternately until a total amount of 20% HCPV CO_2 was injected. Brine was then injected continuously until the process was terminated at a producing WOR of approximately 20 m^3/m^3. Several WAG ratios (brine slug volume/CO_2 slug volume) were investigated for secondary and tertiary recovery of Aberfeldy-Lloydminster heavy oil.

8.7.3. Brineflood

Several brinefloods were conducted in order to know whether the CO_2/brine injection processes were able to recover additional oil with respect to that recovered by brine alone. The brinefloods were conducted by injecting brine continuously at an appropriate pumping rate until a WOR of 20 m^3/m^3 was attained. Breakthrough was detected as explained above.

8.8. Oil-Water Separation

In the subordinate phase of the floods, pure brine drops were produced between slugs of water-in-oil emulsions. The emulsions were broken down by adding one drop of de-emulsifier (the same as used when drying the oil) per 200 cm^3 of sample and putting the mixture in a thermostatic bath at 70°C for 24 hours.

8.9. Additional Tests

After the brine breakthrough occurred, a sample of oil and brine produced was carefully analyzed for:

8.9.1. Brine pH using an Accumet digital pH meter.

8.9.2. Interfacial tension between oil and brine using a Du-Nouy tensiometer.

8.9.3. Water content of emulsion by dissolving the hydrocarbon phase of the emulsion in toluene and then centrifuging the mixture at 3000 rev. min^{-1} for 20 min.

8.9.4. Viscosity of emulsion using a Brookfield LV digital viscometer with UL adaptor for small samples.

8.10. Interfacial Tension of Oil - CO_2 Saturated Brine at Different Pressures

The objective of these experimental tests was to measure the interfacial tension between Aberfeldy heavy oil and brine saturated with CO_2 at pressures of 0, 2.76, 3.44, .4.14, 4.83, 5.59, and 5.79 MPag, and at the room temperature of 23°C using a pendent drop apparatus. A Detailed description of this apparatus and its general use were recently presented by Flock et al.[120]. For the present tests the pendent drop cell was filled with brine, and then the brine was saturated with CO_2 by injecting carbon dioxide at high pressure into the cell. As a result of mass transfer between the CO_2 and brine, the pressure decreased continuously. For ten hours, each hour the mixture of brine-CO_2 was repressurized injecting more CO_2 into the cell to increase the pressure to the initial value again. The cell was left overnight at high pressure. On the following day the pressure was increased again, and this procedure was continued each hour until the pressure drop in one hour was less than 0.02 MPa. The saturation procedure took approximately 20-30 hours for each pressure test. After saturating the reservoir water with CO_2, an oil drop was forced through the oil inlet port (a needle) into the bulk fluid. The drop formed was left suspended, in some instances, for 20 minutes before taking the picture, in order to ensure equilibrium between the phases. Maintaining the pressure constant, several pictures were taken at equal number of drops changing the contact time, in order to have an average of the interfacial tension values over time.

The density difference between the phases is required to calculate

the interfacial tension by the pendent drop method. The oil density was measured using a Parr DMA 60 densitometer. The density of the CO_2 saturated brine was estimated using experimental data on carbon dioxide solubility in water. Solubility of CO_2 in water at specific pressures and temperatures was obtained from the chart presented by Dodds et al.[121]. This solubility was corrected for the salt content of water on the basis of experimental data obtained by Crawford et al.[122]. Converting the CO_2 solubility factor into mass fraction of CO_2 in brine, the density of the CO_2 saturated brine was readily calculated.

8.11. Study of Mechanically Prepared Emulsions

As the volume of emulsion samples obtained from the runs was not large enough for a rheological study, it was decided to prepare some emulsions by mixing in a blender Aberfeldy crude oil with reservoir water (basic pH) and with effluent water from the runs (acidic pH) at volumetric water percentages of 25 and 60%. The emulsions were prepared in approximately 300 cm^3 batches. To prepare water in oil emulsions, oil was first placed in the blender and then water was gradually added to the oil while mixing at a speed around 2000 rev min^{-1}. The emulsions were mixed for 20 minutes with some stops to allow the trapped or entrained air to rise out of the emulsion as recommended by Steinborn and Flock[123]. At the end of blending, the emulsions were placed in a separatory funnel and allowed to stand for 24 hours. Two small emulsion samples, one from the bottom and the other from the top of the separatory funnel, were then taken for water content analysis.

Observation of emulsion droplet distribution on a microscope slide

permitted the emulsion type, water-in-oil or oil-in-water, to be determined. Several photographs were taken while observing the emulsions on the Leitz Wetzlar microscope, and these are discussed later.

Finally, the rheology of the emulsions was studied using a Brookfield LV digital viscometer. Dow corning calibration fluids were used to caribrate the viscometer prior to the viscosity measurements.

8.12. Data Processing

In order to extract meaningful information from the physical model, the data were processed using a computer program. The program made the material balance on oil, water, and CO_2. It also calculated the water-oil ratios, gas-oil ratios, carbon dioxide retention, carbon dioxide required to produce an unit volume of oil, oil recovery, and oil produced-fluid injected ratio (OPFIR).

The carbon dioxide material balance used the Starling equation of state[124] for CO_2 to calculate the moles of CO_2 injected and produced. This equation of state has the following general form:

$$P = \rho RT + \left(BoRT - Ao - \frac{Co}{T^2} + \frac{Do}{T^3} - \frac{Eo}{T^4}\right)\rho^2 + \left(b\rho R - a - \frac{d}{T}\right)\rho^3$$

$$+ \alpha\left(a + \frac{d}{T}\right)\rho^6 + \frac{c\rho^3}{T^2}\left(1 + \gamma\rho^2\right)\exp\left(-\gamma\rho^2\right) \qquad (60)$$

A new set of constants were derived to use the equation in SI units. For P in MPa, T in °K and ρ in Kg-mol/m^3 the following constants apply:

Bo = 0.024588	Ao = 0.176976	Co = 2.451876E04
Do = 188.348169E04	Eo = 2.631556E04	b = 0.003781
a = 0.009434	d = 0.055761	α = 0.961229E-04
c = 1419.7888	γ = 0.006421	R = 0.008314

To determine the molar density of CO_2 using the above equation, a trial and error procedure with an acceleration approach was used. According to Starling[124] his equation predicts experimental density data with an average uncertainty of 1.0%.

9. PRESENTATION AND DISCUSSION OF RESULTS

The first part of this chapter presents and discusses the results of experimental work done on the main mechanisms of Aberfeldy heavy oil recovery by immiscible CO_2/brine injection. The mechanisms studied include solution and diffusion of CO_2 in heavy oils, interfacial tension between heavy oil and carbonated brine, and in situ emulsification of oil.

The second part contains the results obtained using the rectangular, high pressure model constructed, which was used in the investigation of different CO_2/brine injection strategies for recovering Aberfeldy-Lloydminster heavy oil. The use of scaling groups derived in the theoretical part of this study to correlate experimental results is also presented.

9.1. Solution and Diffusion of CO_2 into Aberfeldy Heavy Oil

As was shown in the literature review chapter, solution and diffusion of gases in liquids are governed by different mass transfer mechanisms. While solution is related to the attractive van der Waal-London forces between the molecules of substances under consideration, diffusion is proportional to the concentration gradient of the gas being diffused. However, the two mass transfer mechanisms are found acting simultaneously when gases and liquids are brought into contact and it is quite difficult to differentiate them. The PVT studies of gas-oil mixtures made under strong agitation and/or circulation to reach a pseudo-equilibrium are basically representative of the solution mass

transfer mechanism. To account for diffusion of gases into liquids, it is necessary to leave the two fluids in contact for long periods of time without any agitation. The solubility and diffusivity of CO_2 into two Aberfeldy oil samples were investigated separately in this study.

9.1.1. Properties of Aberfeldy Heavy Oil Saturated with CO_2

The solution of CO_2 in samples 1 and 2 of Aberfeldy crude oil and its effect on oil viscosity and swelling factors was studied at various pressures and at a constant temperature of 21-21.5°C. For sample 1, the Simon and Graue correlations[18] were used. For sample 2, experimental values were obtained by Alberta Research Council[125] using a high pressure rotovisco viscometer with a static mixer and pump attached.

The Simon and Graue correlations[18] were developed from experimental data determined by measuring the properties of mixtures of CO_2 and nine different oils with API gravities from 11.9 to 33.3. Properties predicted by the correlations had average errors, with respect to experimental values, of 2% for solubility, 0.5% for swelling factor, and 12% for viscosity.

Values of CO_2 solubility and swelling factors versus saturation pressure of CO_2 mixture for two Aberfeldy oil samples are shown in Figure 12. As expected, the solubility of CO_2 and the swelling factor increased slightly with decreasing oil density. At conditions of pressure and temperature of 5.5 MPag and 21-21.5°C, about 86 and 76 sm^3 CO_2/m^3 oil were required to saturate the two samples of oil. The corresponding swelling factors of the two crude oils at the same conditions were 1.17 and 1.14, respectively. These values indicate that

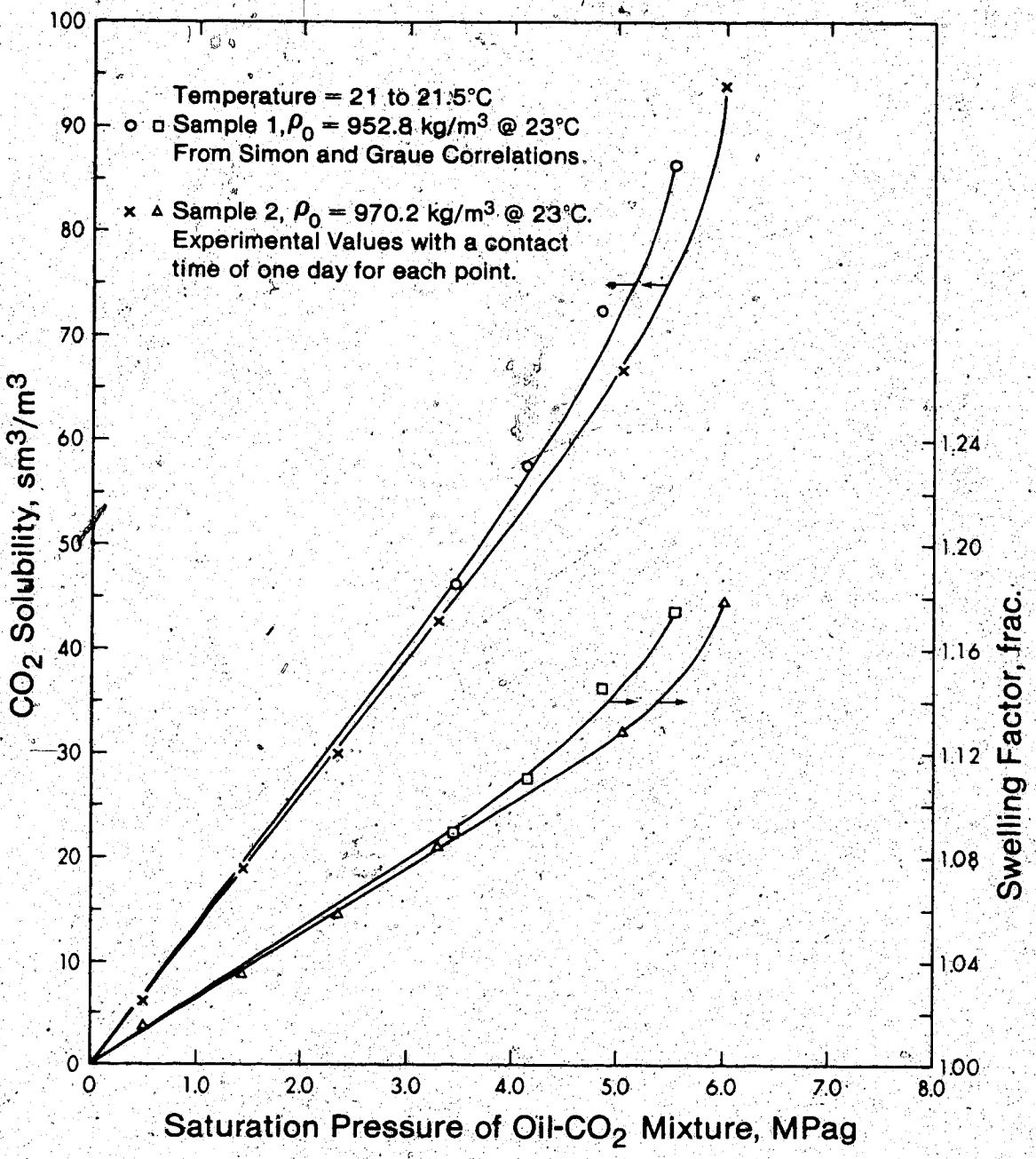


Figure 12 Effect of Pressure on CO_2 Solubility and Swelling Factor of Two Aberfeldy Heavy Oil Samples

17 and 14% volume expansion of Aberfeldy oil samples can be expected at reservoir conditions in a subcritical CO_2 injection project.

Because of the high solubility of CO_2 gas in Aberfeldy heavy oil, the viscosity decreased considerably from 1080 and 4900 mPa.s for the gas-free oil samples at 21-21.5°C to 47 and 82 mPa.s when the two heavy oils were saturated at the same temperature with subcritical carbon dioxide at 5.5 MPag, which represent 95.6 and 98.3% reductions in viscosity for the two samples, respectively (see Figure 13).

Figure 13 also shows a comparison of viscosity reduction by solution of carbon dioxide and by temperature increase. The effect of temperature on viscosity of the two gas-free heavy oil samples was obtained using the Brookfield LV digital viscometer at atmospheric pressure. It can be seen in that figure that the aforementioned reductions in viscosity by subcritical carbon dioxide may also be obtained by heating the oil samples to a temperature of approximately 90°C.

9.1.2. Molecular Diffusion of CO_2 into Aberfeldy Heavy Oil

Using the diffusion cell shown in Figure 7 the heavy oil samples 1 and 2 with viscosities of 1032 and 4831 mPa.s at 23°C were tested for molecular diffusion of carbon dioxide at 5.5 MPag and 21-23°C (laboratory temperature). For approximately eight days, a gas space of CO_2 was left in contact with a 50 cm column of oil without any mechanical agitation. At the end of this period an oil sample was taken by the bottom valve of the diffusion cell. In both cases the samples had the appearance of an unstable foam with oil being the external phase and carbon dioxide coming out from the oil slowly. This finding showed that the diffusive forces were able to overcome partially the gravitational

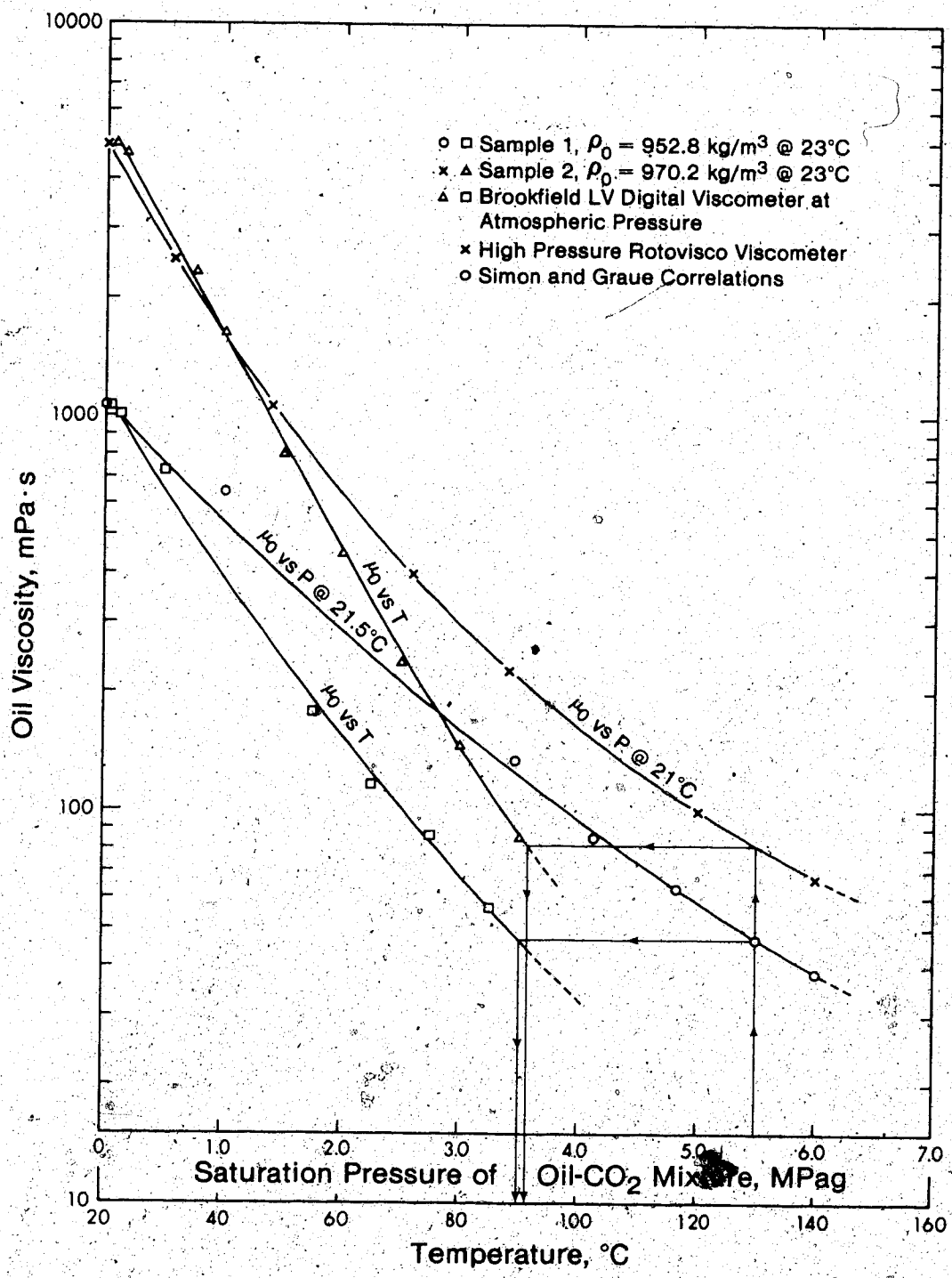


Figure 13 Effect of CO_2 Solubility and Temperature on Two Aberfeldy Heavy Oil Samples

forces, which is important from the point of view of field application.

The oil samples with diffused CO_2 in the oil were tested for changes in viscosity and weight with time. Figure 14 shows the change of the foam viscosity with time. It can be seen that initially the foam had a viscosity more than twice the original oil viscosity. The viscosity decreased rapidly and the foam disappeared at 2 and 3 hours after taking the sample depending on oil viscosity. The more viscous the oil the longer the time for the foam to disappear. At that time the oil samples had approximately the same viscosity as the original crude oils. Since the viscosity measurements had to be taken at small time intervals, it was impossible to study any non-Newtonian behaviour of the foams.

The foam formed due to expansion when the bottom valve of the diffusion cell was opened, while the pressure of the oil-CO_2 mixture dropped to zero. Inside the diffusion cell, the oil-CO_2 mixture had lower viscosity than the oil alone. Foam formation is likely to occur in a field project, and it could be necessary to use a defoamer[21,68] under such conditions.

The sample weight difference immediately after taking it, and when the variation of the sample weight (in one hour) was less than 0.01%, permitted making an estimate of the initial weight percentage of CO_2 in the foam, which was 1.89% for sample 1 and 0.77% for sample 2, while the corresponding molar percents were 15.7 and 7.5%, respectively. Molecular weights of 425 for sample 1 and 460 for sample 2 were determined from Hougen and Watson's chart of isoproperties[126]. In order to use that chart it was necessary to determine the kinematic viscosity of

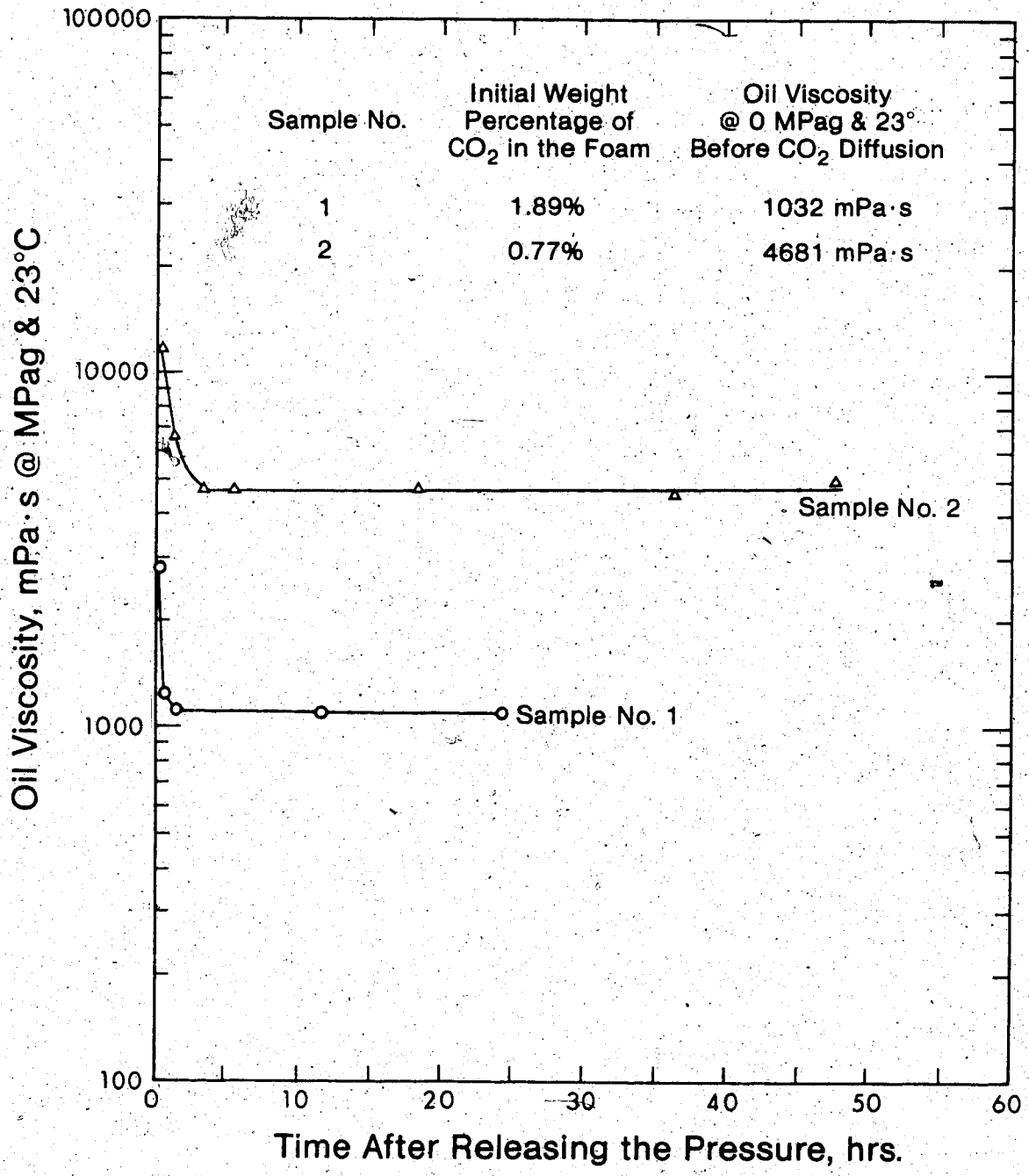


Figure 14 Changes of Viscosity of Heavy Oil-CO_2 Foam Formed by Releasing the Pressure After Diffusion of CO_2 at 23°C & 5.5 MPag During Eight Days

the oil samples at 50°C on the basis of their absolute viscosities and densities at the same temperature.

Rough estimates of the molecular diffusion coefficient of carbon dioxide into the two heavy oil samples at 5.5 MPag and 21-23°C were obtained by applying Fick's law of diffusion which can be written, in finite difference form, as follows:

$$Do = -\frac{1}{A \times \frac{\Delta C}{\Delta L}} \times \frac{\Delta G}{\Delta t} \qquad (61)$$

The assumptions made in applying the above equation are:

1. After eight days of diffusion, the molar flux of carbon dioxide was invariant (i.e. it did not change with time).
2. The concentration gradient in the small column of oil was linear.
3. Convection induced by density changes and pressure gradients at the beginning of the experiment was negligible.

Although various diffusion experiments were run, Table 7 shows the results of two which are considered to be the most representative, and the most precise. It can be seen in the table that the molecular diffusion coefficients obtained for samples 1 and 2 were 3.59E - 05 and 2.56E - 05 cm^2/s, respectively. These values are higher than those reported by Davis et al.[23] for oils of lower viscosity at atmospheric conditions, but they are of the same order of magnitude as the molecular diffusion coefficient of CO_2 in heavy oils obtained by Denoyelle and Bardon[26]. The reduction in the molecular diffusion of CO_2 with increasing oil viscosity is in accordance with the behaviour observed by

TABLE 7

DATA AND RESULTS OF THE MOLECULAR DIFFUSION EXPERIMENTS

	Oil Sample No. 1	Oil Sample No. 2
Oil Density, Kg/m^3 @ 0 MPag & 23°C	952.8	970.2
Oil Viscosity, mPa.s @ 0 MPag & 23°C	1032	4681
Molecular Weight, g/g mol	425	460
Internal Cross Sectional Area of the Diffusion Cell, cm^2	31.67	31.67
Length of the Oil Column, cm	50.0	50.0
Diffusion Time, hrs	166	188
Weight of Oil in the Foam Sample, g	109.22	225.35
Weight of CO_2 in the Foam Sample, g	2.1	1.74
Weight Percent of CO_2 in the Foam Sample, %	1.89	0.77
Concentration Gradient of CO_2, g mol/cm^3 × cm	-7.02E - 05	-7.23E - 05
Molar Flux of CO_2, g mol/s	7.987E - 08	5.843E - 08
Molecular Diffusion Coefficient, cm^2/s	3.59E - 05	2.56E - 05

various researchers[23,24,25] using oils of lower viscosity.

An example showing the calculation of the molecular diffusion is included in Appendix F.

Although the diffusion of carbon dioxide in heavy oils is certainly high, the amount of diffused CO_2 is not high enough to produce a large reduction in oil viscosity. The molar fraction of CO_2

in Aberfeldy oil samples obtained by diffusion represented less than 20% of that obtained by solution with mechanical agitation. From Figure 13 the reduction in the viscosity of the Aberfeldy oil samples produced by 0.1 molar fraction of diffused CO_2 in oil, which can be also achieved saturating the oil samples at a pressure of approximately 0.5 MPag, represents less than 50% of the gas-free oil viscosities. From Figure 12, the increase in oil expansion produced by the same molar fraction of CO_2 in oil is less than 2%.

9.2. Heavy Oil - Carbonated Brine Interfacial Tensions

An important finding, not reported before, was the lowering of interfacial tension (IFT) between heavy oil external emulsion and acidic brine produced during the subordinate phase (after brine breakthrough) of the runs. The measurements were carried out at laboratory conditions using the Du Noüy tensiometer and are presented as functions of the brine pH and brine content of emulsions in Table 8 and Figure 15. The in situ reaction, at high pressures, of carbon dioxide and brine (both used as displacing agents) lowered the pH of the injected brine from 7.3 - 8.0 to 5.4 - 6.5. On the other hand, the brine produced from a brineflood had a pH of almost 7. The brine pH was measured with an Accumet digital pH meter which was standardized with buffer solutions prior to all measurements. It can be seen from Table 8 and Figure 15 that low interfacial tensions were obtained at pH values lower than 6 and at high brine content of the brine-in-oil emulsions. As the effluent emulsions were seen to be unstable, the presence of free brine drops could affect the interfacial tension measurements and could

TABLE 8

INTERFACIAL TENSIONS OF OIL EXTERNAL EMULSION - BRINE PRODUCED DURING THE CO_2/BRINE FLOODS

(Du Noüy Tensiometer)

Run No.	Sample No.	Pore Volume* Injected, fracc.	pH of Brine	Brine Content of the Emulsion, % Vol.	Interfacial Tension mN/m
7	12	0.67	6.55	51.0	9.7
8	14	1.26	5.79	75.0	2.9
9	17	1.86	5.37	53.3	1.8
10	18	0.31	5.80	--	2.0
11	17	0.77	6.93	55.0	19.4**
12	14	0.61	6.19	13.1	6.4
13	9	0.47	5.90	60.0	13.9
15	24	0.90	5.60	50.1	7.0
16	24	1.05	5.72	35.0	7.0
17	24	0.95	5.70	50.0	10.8
18	26	1.37	5.70	60.2	6.6
19	25	2.48	5.87	60.0	7.6
20	9	0.45	6.56	10.1	26.9**
20	35	2.03	5.60	20.0	14.1
21	12	0.36	6.97	9.8	30.3**
25	33	1.23	6.26	12.0	19.7

*Pore volume injected at the moment of taking the sample.

**Samples taken from brinefloods.

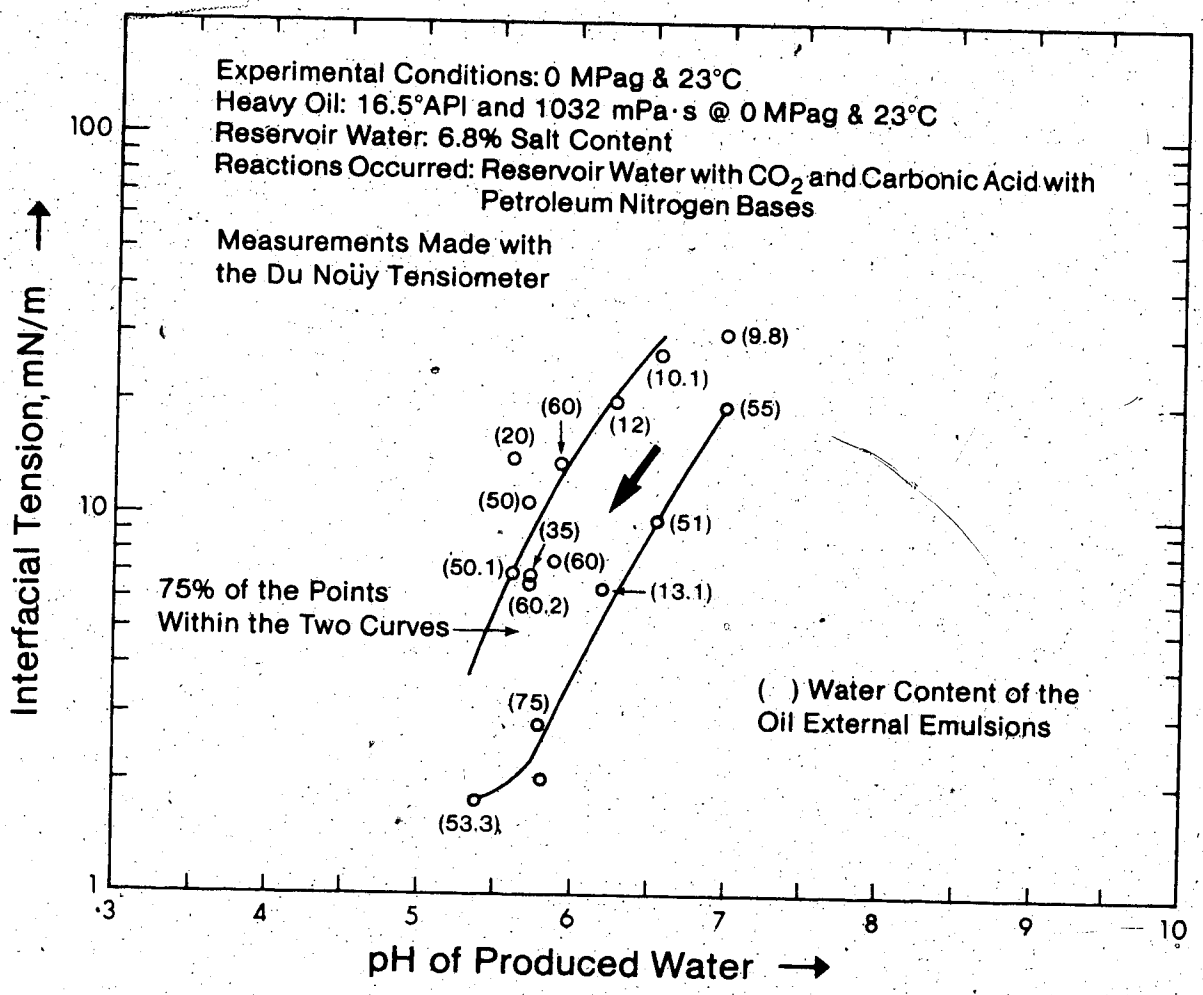


Figure 15 Interfacial Tensions of Oil External Emulsion - Brine Produced During the CO_2/Brine Floods

be in part responsible for the low interfacial tension values. Nevertheless, Figure 15 shows a defined trend which indicates a decrease in interfacial tension with decreasing pH of the effluent reservoir water from the runs. It can also be seen from Table 8 that the IFT's between brine-in-oil emulsions and brine (pH $\sim$ 7) from three brinefloods had a high value of 20 - 30 mN/m and the oil also contained a certain volume of emulsified brine (10 - 50% vol.). The lowering of interfacial tension may produce a small decrease in capillary pressure and in situ emulsification of the oil is likely to occur which improves oil recovery.

To be sure that the IFT lowering was not caused totally by the presence of free brine drops of the unstable emulsions produced in the subordinate phase of the runs, another type of IFT measurements was carried out. In this case, the interfacial tension between dried Aberfeldy oil (sample 1, μ_o = 1032 mPa.s at 23°C) and reservoir water saturated with CO_2 at pressures of 2.76, 3.44, 4.14, 4.83, 5.59, and 5.79 MPag and temperature of 23°C were measured using the pendent drop apparatus. The procedure used in these tests was explained in Chapter 8, Section 8.10 of this study. An example of the time required to saturate the reservoir water with carbon dioxide is shown in Figure 16. As can be seen from Table 9 and Figure 17, the interfacial tensions between dried Aberfeldy oil and reservoir water saturated with CO_2 measured with the pendent drop apparatus were in general higher than those for oil external emulsion - acidic brine (effluents from the runs) obtained with the Du Noüy tensiometer. However the IFT of dried Aberfeldy oil appeared to decrease with increasing carbonation pressure of reservoir water. This finding shows that a decrease in interfacial tension

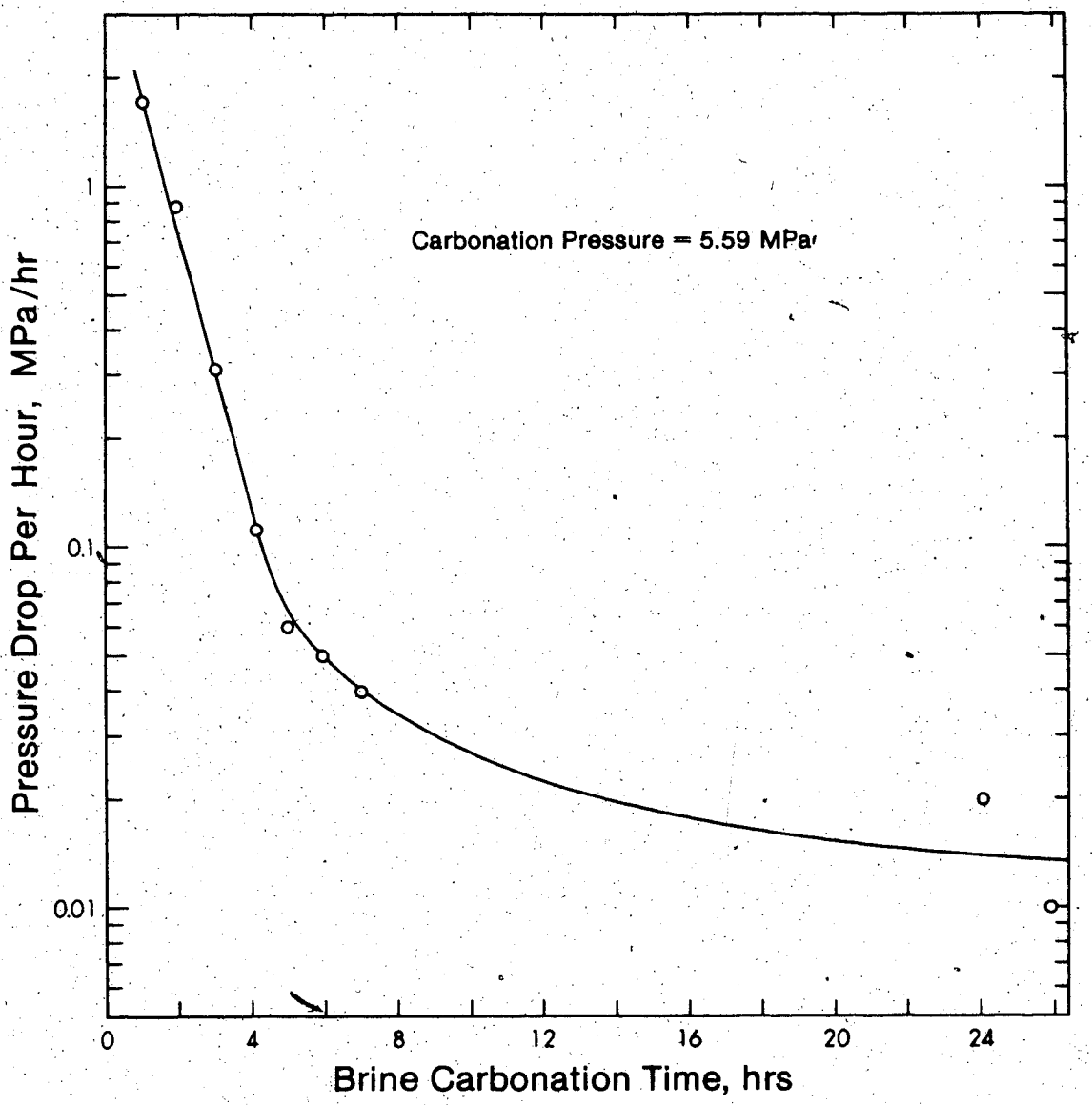


Figure 16 Time Required to Saturate the Reservoir Water with CO_2 at 5.59 MPag & 23°C

TABLE 9

INTERFACIAL TENSION OF HEAVY OIL - RESERVOIR WATER SATURATED WITH CO_2 AT DIFFERENT PRESSURES

(Pendent Drop Apparatus)

Carbonation Pressure MPag	Temperature °C	Solubility of* CO_2 in Brine, $gCO_2/100g$ brine	Density of Brine** Saturated with CO_2, g/cm^3	Density*** of CO_2, g/cm^3	Density† Difference g/cm^3	D(e)†† cm	$\frac{1}{H}$†††	Interfacial Tension, mN/m
0	24.0	–	1.0650	–	0.1128	0.4010	1.41508	25.15
2.76	23.5	2.51	1.0404	0.0615	0.0882	0.4585	1.37028	24.90
3.44	22.9	2.99	1.0364	0.0819	0.0842	0.4543	1.29209	22.0
4.14	23.0	3.53	1.0322	0.1046	0.0800	0.5960	0.84434	23.51
4.83	22.8	4.20	1.0274	0.1335	0.0752	0.5612	0.84112	19.52
5.59	23.0	4.53	1.0265	0.1761	0.0743	0.3968	1.31549	15.08
5.79	23.0	4.57	1.0268	0.1913	0.0746	0.5044	0.78594	14.62

*Estimated from experimental data presented by Dodds et al.[121] and Crawford et al.[122].

**Calculated by the equation $\rho_{W\text{-}CO_2} = X_{CO_2}\rho_{CO_2} + (1 - X_{CO_2})\rho_W$ where X_{CO_2} is the weight fraction of CO_2 in the mixture.

***Determined by the Starling's equation of State[124].

†Density of brine saturated with CO_2 minus density of oil.

††Maximum diameter of the drops.

†††Shape factor of the drops obtained from tables presented by Ambwani and Tomlinson[127].

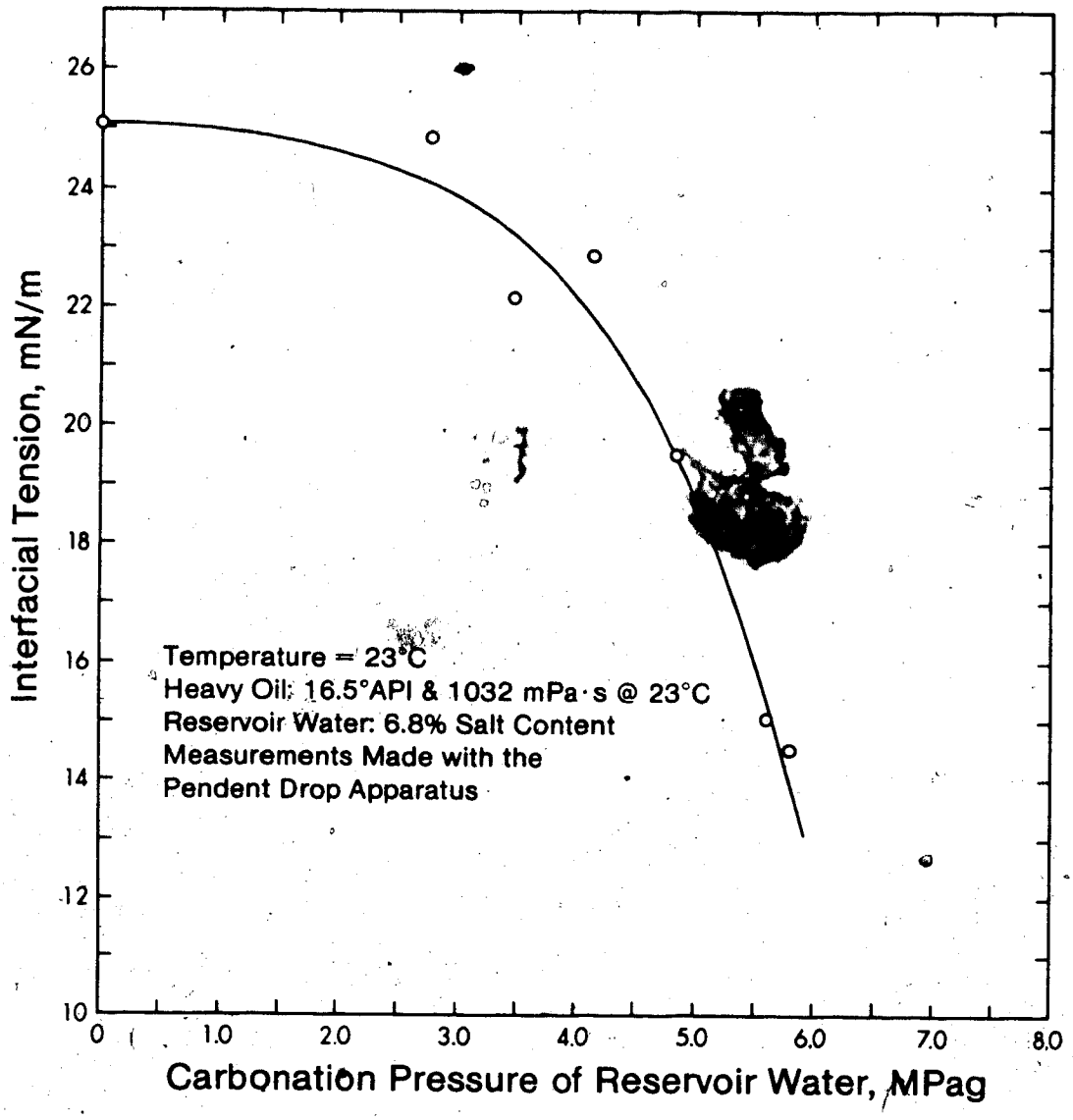


Figure 17 Effect of Carbon Dioxide on the Interfacial Tension Between Heavy Oil and Reservoir Water From Aberfeldy Field, Lloydminster Area

of heavy oil really occurs in immiscible CO_2/brine floods.

Positively charged nitrogen compounds resulting from the action of carbonic acid on the nitrogen bases of Aberfeldy heavy oil may constitute the surfactants which concentrate at the oil-water interface and produce the lowering of interfacial tension. The structure of different nitrogen bases such as vanadyl and nickel porphyrins, pyridine, and quinoline found in heavy oils by several researchers[129,130] are shown in Figure 18. Hodgson et al.[128] reported that Lloydminster crude oil has 220 ppm of vanadyl porphyrin and 20 ppm of nickel porphyrin. Dunning et al.[130] isolated 275 ppm of free porphyrins from a 14°API oil which reacted with hydrochloric acid to form solutions that showed a milk-white fluorescence under ultraviolet light indicating the formation of soaps. Also, Goncharov et al.[129] isolated nitrogen bases from crude oils of various deposits in the U.S.S.R. It was established by the Russian investigators that compounds of quinoline and acridine series represented a large part of concentrates of nitrogen bases in those crude oils. Some researchers[38,39] have also observed reduction of interfacial tension between Lloydminster crude oil and hydrochloric and sulfuric acid solutions indicating that natural surfactants were produced.

9.3. In Situ Emulsification of Aberfeldy Crude Oil

Production of viscous gasified emulsions was observed after brine breakthrough in the displacement of Aberfeldy heavy oil by carbon dioxide and brine. Heating the emulsions to 70°C for 24 hours and chemical treatment in the form of emulsion breaker were sufficient

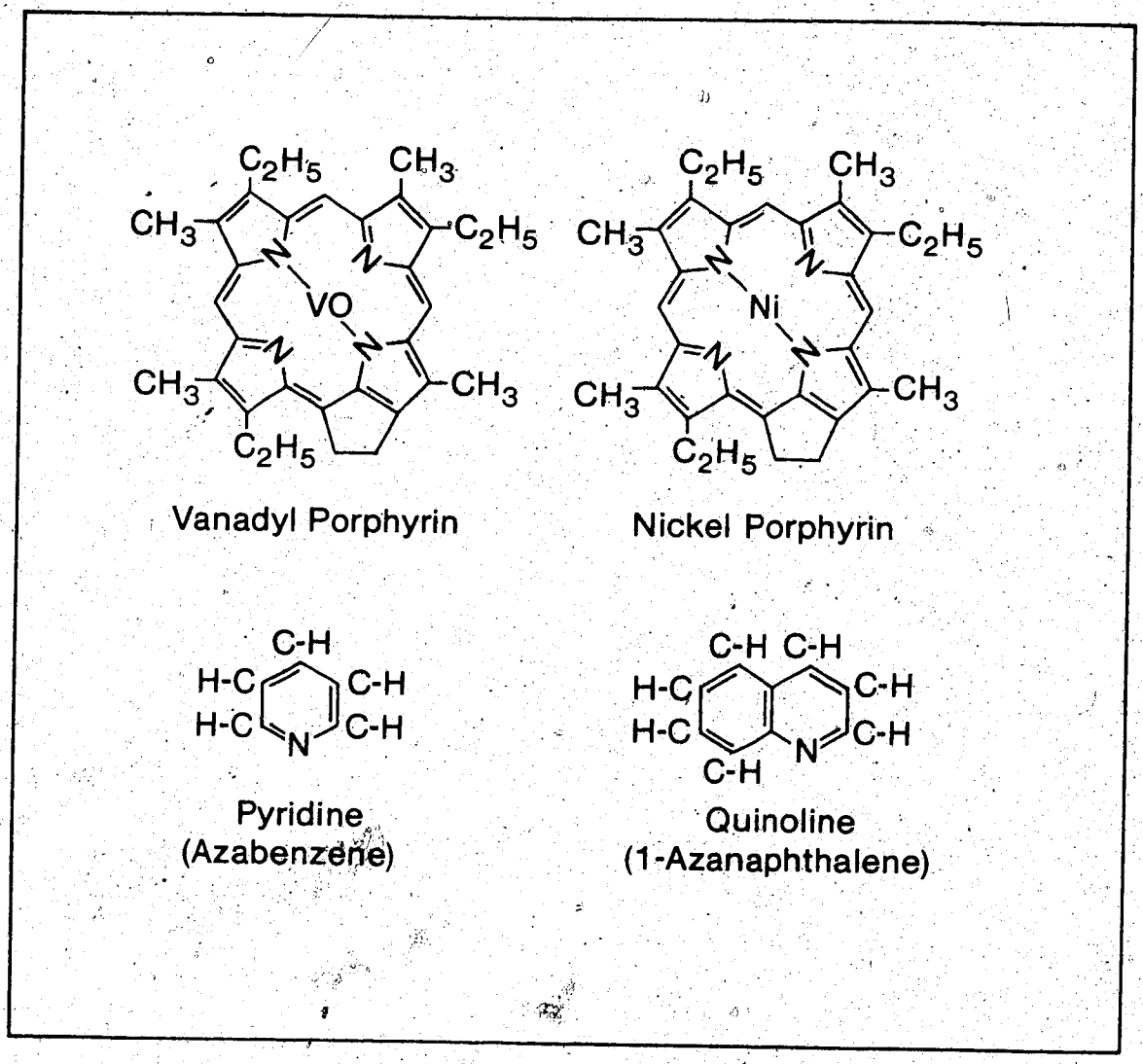


Figure 18 Structure of Some Nitrogen Bases Found in Heavy Oils

to break down the emulsions produced. These emulsions are believed to be formed in situ rather than in the production facilities outside of the porous medium. There are several papers in the petroleum literature which show that under certain conditions emulsions do form in porous media. For instance, using a Jegurson cell packed with glass beads, Mar and Singhal[131] showed that emulsions can be formed during the injection of water and steam into an oil-saturated porous medium. Also, several investigators[132,133] have reported the in situ emulsification of heavy oil as an important recovery mechanism of the caustic flooding process.

Some evidence of the in situ formation of acidic brine in oil emulsions was obtained in this research, as noted below:

a. The subordinate phase of the CO_2/brine floods was characterized by the production of viscous gasified brine-in-oil emulsions. Later in the life of the floods, free brine drops were produced between slugs of emulsion. Pure brine did not breakthrough before the emulsion in any of the runs.

In almost all runs, an emulsion sample - after 24 hours of settling at room temperature - was analyzed for acidic brine content and viscosity. The brine content was found to depend on the place from which emulsion was taken. Thus the samples taken from the separatory funnel bottom had an average brine content of 60% by volume with some free drops of brine and those taken from the top contained 20-25% of brine by volume without free brine. As the emulsion samples were small in volume, the UL adaptor of the Brookfield LV digital viscometer had to be used for the viscosity

measurements. However, the maximum viscosity that can be measured with this adaptor is only 2000 mPa.s at the lowest speed of 3 rev. min^{-1}. All the emulsions had a viscosity greater than the viscosity of the constituents: heavy oil and brine. Some of them were twice as viscous as clean Aberfeldy crude oil.

Visual observation of the emulsions as well as the fact that the viscosity of the emulsions had been greater than that of the oil viscosity show that the emulsions produced during the floods were brine-in-oil type.

b. Pressure fluctuations in the injection and production wells were observed after brine breakthrough in the CO_2/brine floods in comparison with almost no fluctuations of pressure in the brinefloods. Figure 19 shows the pressure drop between injection and production wells as a function of cumulative volume of fluid injected for five runs using Ottawa silica sandpacks. It can be observed that at the beginning of the brinefloods the pressure drop was as high as 0.30-0.54 MPa depending on the brine superficial velocity (see Figure 19), but it declined smoothly during the subordinate phase of brinefloods to a low value, less than 0.1 MPa. The pressure drop curves for secondary heavy oil recovery by a slug of CO_2 driven by brine and by alternate slugs of CO_2 and brine show high pressure fluctuations after the brine breakthrough. The higher the superficial velocity of the fluids in the porous medium the more pronounced the pressure fluctuations. Curve 8 (for Run 8), at the highest superficial velocity (2.9 m/d), shows pressure fluctuations as high as 0.1 MPa, while curve 6 for Run 6 at the lowest

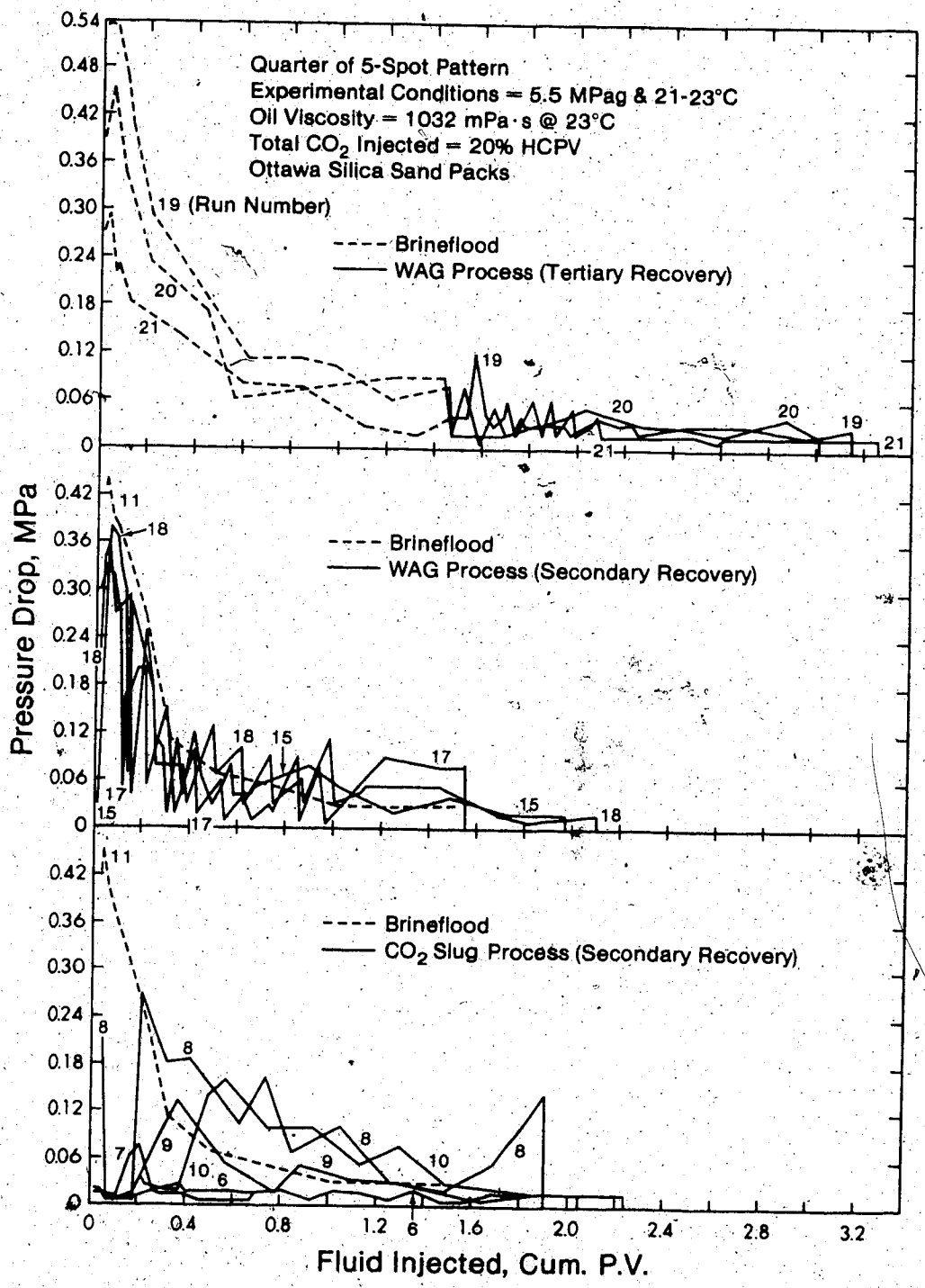
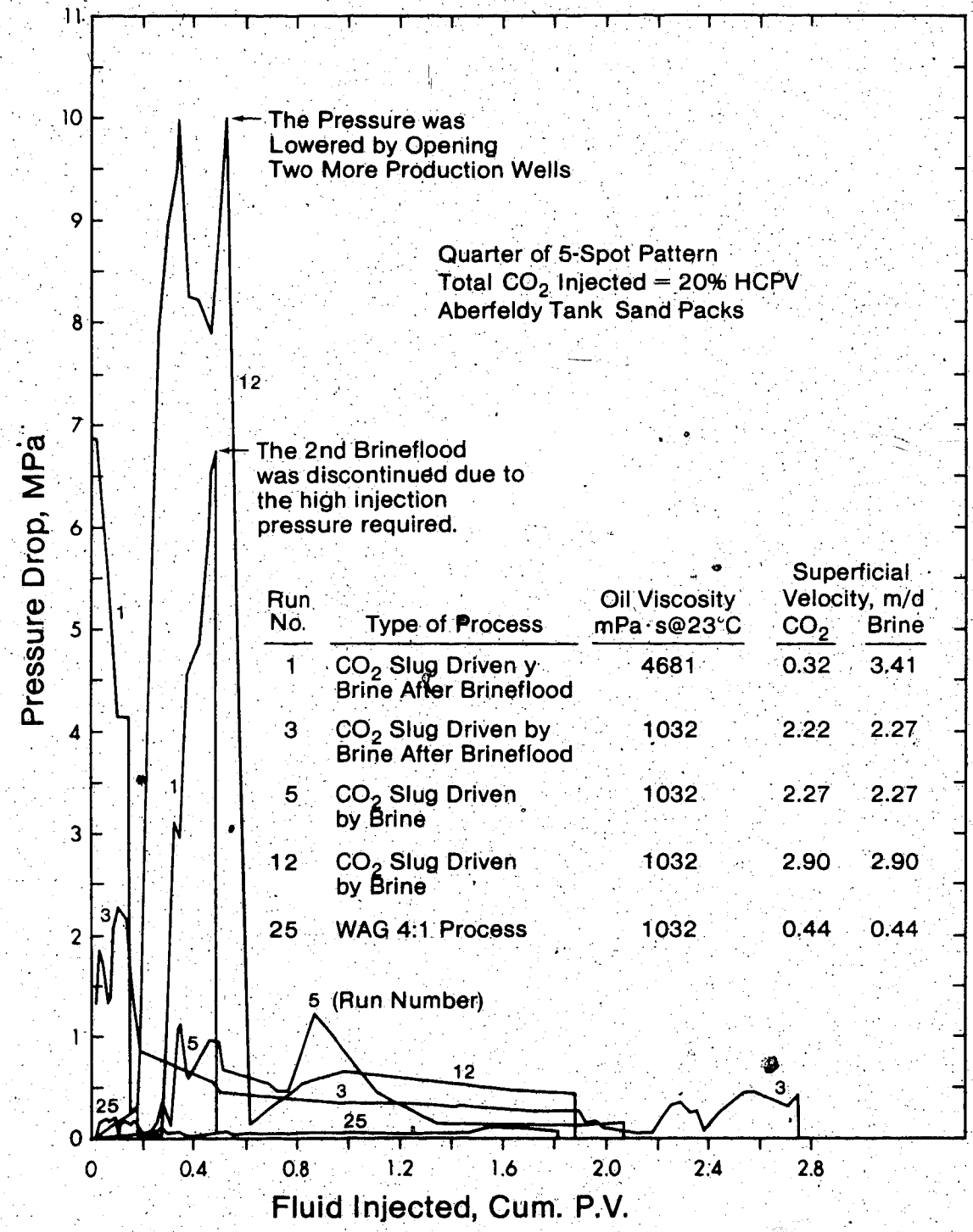


Figure 19 Pressure Drop Versus Fluid Injected for Different Processes Using Ottawa Silica Sand

superficial velocity (0.18 m/d) shows pressure fluctuations less than 0.01 MPa. The pressure drop curves 19,20, and 21 for the tertiary recovery experiments (Runs 19,20, and 21) also show fluctuations when the CO_2 slug injection started (after a brineflood). It was observed that the pressure drop increased when emulsion slugs were being produced, and decreased when, in turn, free brine drops were being produced. The low pressure drop observed during the injection of the 20% HCPV slug of CO_2 (i.e. Curves 7,8,9, and 10 of Figure 19) was caused by the mass transfer between CO_2 and reservoir fluids, which slowed down the displacement of oil. The peak shown by Curve 8 was observed after the back pressure regulators were set.

As is shown in Figure 20 the pressure drops were higher for the runs where the Aberfeldy tank sand cleaned with solvents was used. This behaviour can be accounted for by the higher amount of fines in Aberfeldy tank sand in comparison with Ottawa silica sand that gave low sandpack permeability. Very high pressure drops were observed for the Aberfeldy tank sandpacks when the average superficial velocity of the fluids was higher than 2.27 m/d. Run 1 (Curve 1, Figure 20) had to be discontinued when the brine to drive the slug of CO_2 was injected at a high flow rate (superficial velocity of 3.41 m/d). The pressure drop required to displace the bank of tertiary oil (4681 mPa.s of viscosity) increased sharply to almost 7 MPag when it was decided to discontinue the run. A similar problem arose in Run 12 at a high superficial velocity of 2.9 m/d. In this case the pressure drop could be lowered from 10 to 0.6 MPa by opening two more production wells. It was



Run No.	Type of Process	Oil Viscosity mPa·s@23°C	Superficial Velocity, m/d CO_2	Superficial Velocity, m/d Brine
1	CO_2 Slug Driven y Brine After Brineflood	4681	0.32	3.41
3	CO_2 Slug Driven by Brine After Brineflood	1032	2.22	2.27
5	CO_2 Slug Driven by Brine	1032	2.27	2.27
12	CO_2 Slug Driven by Brine	1032	2.90	2.90
25	WAG 4:1 Process	1032	0.44	0.44

Figure 20. Pressure Drop Versus Fluid Injected for Different Processes Using Aberfeldy Tank Sand

possible that the corner production well was plugged by the fines in the Aberfeldy tank sand.

Because of the very high pressure drops at high superficial velocities jointly with the very long time consumed by the cleaning procedure, it was decided to use Ottawa silica sand in most of the runs rather than Aberfeldy tank sand.

In the basis of the previous discussion of the two emulsification phenomena observed, the mechanism of in situ formation of brine-in-oil emulsions in immiscible displacement of heavy oil by CO_2/brine injection can be visualized as follows:

a. Fingering of the brine into the swollen carbonated oil, which still had a much lower mobility than brine, led to the formation of large brine droplets inside the oil.
b. The reduction of interfacial tension between the oil and the acidic brine broke down the droplets into small, more stable brine droplets.
c. Acid media can produce absorbed membranous skins at the oil/brine interface. These skins are believed to be formed by basic nitrogen containing groups[134] and finely divided particles (clays and fine sand) regardless of their composition[135]. The skins acted as physical barriers which partially prevented the coalescence of the dispersed droplets. Strassner[40] found that the rigid interfacial skins formed by asphaltenes are strongest in acid pH.

9.4. Rheology of Mechanically Prepared Emulsions

Depending on different factors, oil-water emulsions can have Newtonian or non-Newtonian behaviour[123]. It is very important to know

the rheological behaviour of emulsions in order to choose the appropriate mass transport equations that apply to emulsion flow through porous media. For this reason it was decided to determine the rheological properties of emulsions formed when carbonated brine was mixed with Aberfeldy heavy oil. This study had to be done using emulsions mechanically prepared in a blender utilizing effluent carbonated brine with slight acid pH from the displacement experiments, reservoir water with slight basic pH, and clean Aberfeldy oil, since the volume of emulsion samples produced in the runs was not large enough to conduct a complete rheological study in the Brookfield LV digital viscometer.

Figure 21 shows the rheology of six emulsions, four were prepared using oil sample 1 and two using oil sample 2. It can be seen that all of them show an apparent viscosity relatively constant over the range of shear rates which is characteristic of Newtonian fluids. The average viscosity of the emulsions depended on the oil sample viscosity, on the brine content, and on the brine pH. As expected, it was observed that the higher the brine content, the higher the emulsion viscosity. The Aberfeldy emulsions prepared with both oil samples at low water content (25% vol.) displayed an increase in viscosity with decreasing brine pH, which could have been caused by the strongest interfacial films formed at the brine-oil interfaces in acid pH. The small difference in pH (7.32 - 7.1) of the brines used in preparing Aberfeldy emulsions with 60% vol. disperse brine concentrations was unable to produce any appreciable viscosity change.

The Newtonian behaviour of the emulsions with low brine

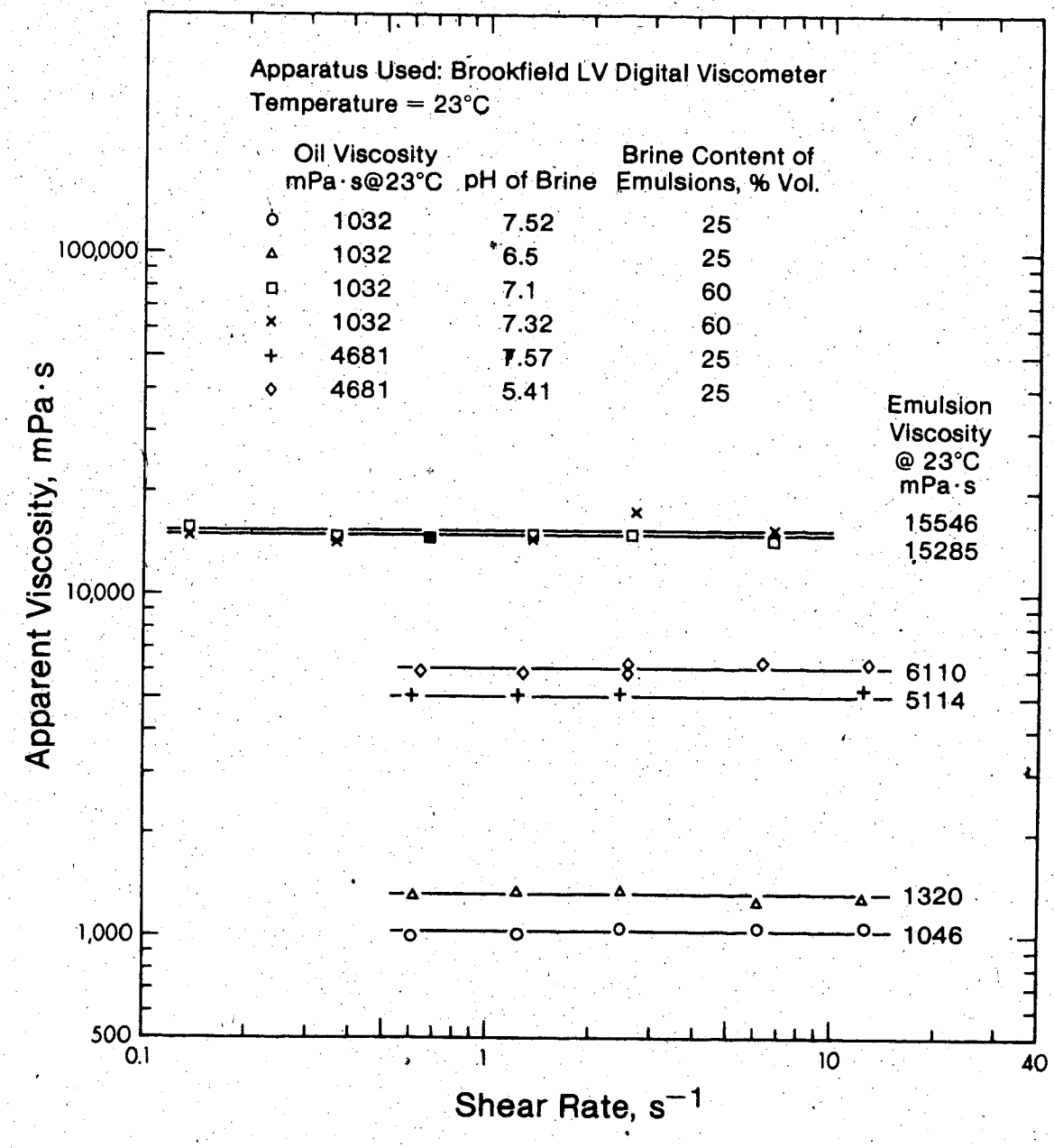


Figure 21 Rheology of Mechanically Prepared Emulsions

concentrations was expected, but the Newtonian behaviour of the emulsions with 60% vol. brine content was unexpected. Two reasons may explain this: first, the emulsions were unstable in nature and after a few days of settling, the formation of two phases with different amount of brine was observed; and second, the range of shear rates was small. Steinborn and Flock[123] observed non-Newtonian behaviour of Cold Lake and Epping water-in-oil emulsions at shear rates higher than $10s^{-1}$.

Although the fact that all emulsions had average viscosities higher than those of the dried oil samples indicates that the emulsions were brine-in-oil type, a better definition of the emulsion type created was obtained by observing the emulsion on a microscope slide. Plates 4-9 show pictures of the emulsions taken after 24 hours of settling with a magnification factor of 740X. All of them display brine droplets within the continuous oil phase indicating that the emulsions were brine-in-oil type, which corresponds to the observation made on the basis of the emulsion viscosity measurements.

It can be also seen from the plates that the brine droplet sizes of the emulsions prepared with effluent brine from the CO_2/brine floods (Plates 4,6, and 8) are smaller than those for the emulsions prepared with reservoir brine of slightly alkaline pH. This leads one to conclude that the acidic brine emulsions are less unstable than the corresponding basic emulsions.

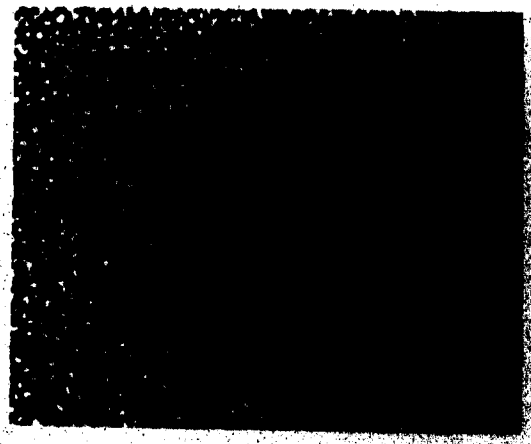


Plate 4. 60% brine-in-oil Aberfeldy emulsion.
Brine pH = 7.1. Oil sample 1.



Plate 5. 40% brine-in-oil Aberfeldy emulsion.
Brine pH = 7.56. Oil sample 1.

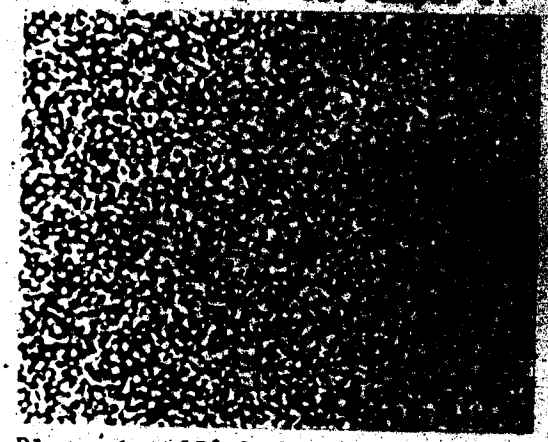


Plate 6. 25% brine-in-oil Aberfeldy emulsion.
Brine pH = 6.5. Oil sample 1.

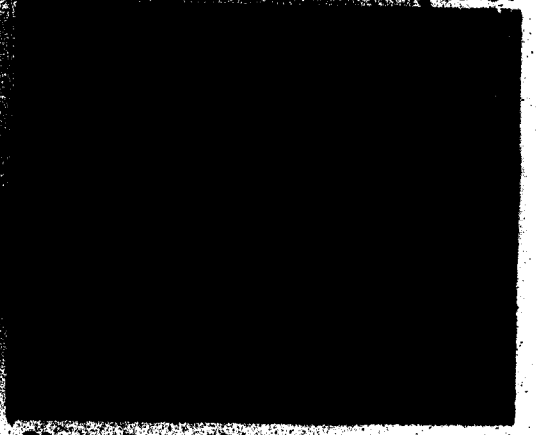


Plate 7. 25% brine-in-oil Aberfeldy emulsion.
Brine pH = 7.5. Oil sample 1.

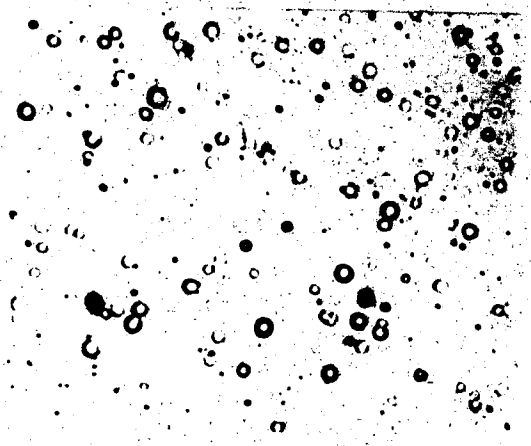


Plate 8. 25% brine-in-oil Aberfeldy emusion.
Brine pH = 5.41. Oil sample 2.

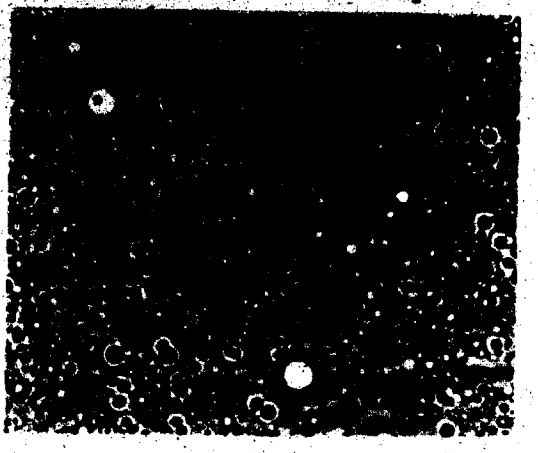


Plate 9. 25% brine-in-oil Aberfeldy emulsion.
Brine pH = 7.56. Oil sample 2.

9.5. Sandpack Properties

The properties of the sandpacks are listed in Table 10. Two types of unconsolidated sand were used: Aberfeldy tank sand (Runs 1-5, 12, and 25) and Ottawa silica sand (Runs 5-11, and 13-24). While the Ottawa silica sand was used as received, the Aberfeldy tank sand was cleaned with solvents. For Runs 2 and 3 the tank sand was cleaned with toluene, isopropyl alcohol, and distilled water, and for Runs 1,5,12, and 25 the tank sand was only cleaned with toluene. In Run 4, tank sand from Run 3 cleaned with toluene, isopropyl alcohol, and distilled water was reused. With some exceptions, the Aberfeldy tank sandpacks had lower absolute permeabilities than the Ottawa silica sandpacks because of the greater amount of clays and sand fines contained in the former. As the vessel was very heavy ($\sim$ 1 tonne), it was difficult to vibrate the whole vessel, and for that reason the porosity of almost all the sandpacks was over 40%.

Examination of Table 10 reveals that the irreducible water saturation obtained in the Aberfeldy tank sandpacks cleaned with toluene, isopropyl alcohol and distilled water was higher than that obtained in the rest of sandpacks, showing that the presence of isopropyl alcohol in cleaning the Aberfeldy tank sand tended to shift the sand wettability toward the water wet situation. It seems that the combination toluene-isopropyl alcohol desorbed more polar materials from the grain surfaces than toluene alone.

An unusually high irreducible water saturation of 26.4% was obtained when the Aberfeldy tank sand from Run 3 was reused in Run 4. According to the experiments carried out by Grist et al.[136] toluene

TABLE 10

CHARACTERISTICS OF UNCONSOLIDATED SANDPACKS

Run No.	Type of Sand	Pore Volume cm^3	HCPV* cm^3	Porosity %	Permeability Darcies	Irreducible Water Sat., %	Initial Oil Sat., %
1	Aberfeldy Tank Sand**	2092.0	1959.0	43.7	—	6.4	93.6
2	Aberfeldy Tank Sand***	2059.0	1689.3	43.0	—	18.0	82.0
3	Aberfeldy Tank Sand***	2149.3	1751.3	44.9	10.1	18.5	81.5
4	Aberfeldy Tank Sand†	2058.0	1514.0	43.0	10.6	26.4	73.6
5	Aberfeldy Tank Sand**	2107.0	1860.5	44.0	7.4	11.7	88.3
6	Ottawa Silica Sand	2065.0	1839.0	43.1	24.2	11.4	88.6
7	Ottawa Silica Sand	2092.0	1899.0	43.7	15.4	9.9	90.1
8	Ottawa Silica Sand	2180.0	1984.0	45.5	15.4	9.0	91.0
9	Ottawa Silica Sand	2186.0	1990.0	45.7	16.7	9.0	91.0
10	Ottawa Silica Sand	2250.0	1973.0	47.0	17.9	12.3	87.7
11	Ottawa Silica Sand	1850.0	1634.0	38.7	8.7	11.7	88.3
12	Aberfeldy Tank Sand**	2296.0	2109.0	48.0	4.9	8.1	91.9

TABLE 10 (Continued)

CHARACTERISTICS OF UNCONSOLIDATED SANDPACKS

Run No.	Type of Sand	Pore Volume cm^3	HCPV* cm^3	Porosity %	Permeability Darcies	Irreducible Water Sat., %	Initial Oil Sat., %
13	Ottawa Silica Sand	2083.0	1825.0	43.5	11.9	12.4	87.6
14	Ottawa Silica Sand	1965.0	1734.0	41.1	10.9	11.7	88.3
15	Ottawa Silica Sand	2069.0	1839.0	43.2	11.7	11.1	88.9
16	Ottawa Silica Sand	2123.0	1883.0	44.4	14.9	11.3	88.7
17	Ottawa Silica Sand	2043.0	1789.0	42.7	12.7	12.4	87.6
18	Ottawa Silica Sand	2093.0	1837.0	43.7	14.1	12.2	87.8
19	Ottawa Silica Sand	2142.0	1836.0	44.7	13.8	14.3	85.7
20	Ottawa Silica Sand	2148.0	1931.0	44.9	14.8	10.1	89.9
21	Ottawa Silica Sand	2065.0	1820.0	43.1	9.2	11.9	88.1
22	Ottawa Silica Sand	2004.0	1784.0	41.9	9.6	11.0	89.0
23	Ottawa Silica Sand	2013.0	1794.0	42.1	9.3	10.9	89.1

TABLE 10 (Continued)

CHARACTERISTICS OF UNCONSOLIDATED SANDPACKS

Run No.	Type of Sand	Pore Volume cm^3	HCPV* cm^3	Porosity %	Permeability Darcies	Irreducible Water Sat., %	Initial Oil Sat., %
24	Ottawa Silica Sand	2107.0	1877.0	44.0	11.5	10.9	89.1
25	Aberfeldy Tank Sand**	2068.0	1815.0	43.2	4.5	12.2	87.8

*Hydrocarbon Pore Volume

**Cleaned with Toluene

***Cleaned with Toluene, Isopropyl Alcohol, and Distilled Water

†Reused from Run 3 and cleaned with Tol., IA, and Dist. Water.

extraction may not alter core wettability to any great extent, but if this is followed by extended periods of brine soaking, or alcohol extraction, the core is likely to become strongly water-wet. This was found to be the case for the Aberfeldy tank sand reused in Run 4.

Considering that the irreducible water saturation is related to grain wettability, it can be concluded from Table 10 that the Ottawa silica sand is slightly more water-wet than the Aberfeldy tank sand cleaned with toluene alone, and less water-wet than the Aberfeldy tank sand cleaned with toluene, isopropyl alcohol and distilled water. Figure 22 shows that 76% of sandpacks had a low irreducible water saturation in the range of 9 to 13%, indicating that possible Aberfeldy tank sand cleaned with toluene alone and Ottawa silica sand has a mixed or intermediate wettability when it is brought in contact with Aberfeldy reservoir water and heavy oil for a period of time longer than 24 hours. Wettability changes induced by heavy crude oils are related to the oil polar compounds concentrated in the resins and asphaltenes which adsorb on the rock surface. Recently, Collins and Melrose[137] conducted a study of adsorption of asphaltenes and water on reservoir rock minerals. They concluded that the presence of a thin film of water adsorbed on the clay mineral surfaces reduces but does not eliminate the adsorption of asphaltenes.

The average irreducible water saturation for 21 sandpacks (excluding the sandpacks of the first four runs) was 11.2%, which is close to the initial water saturation (13%) of Aberfeldy reservoirs. This may be a fair indication that the capillary forces in the model and prototype are of the same order of magnitude.

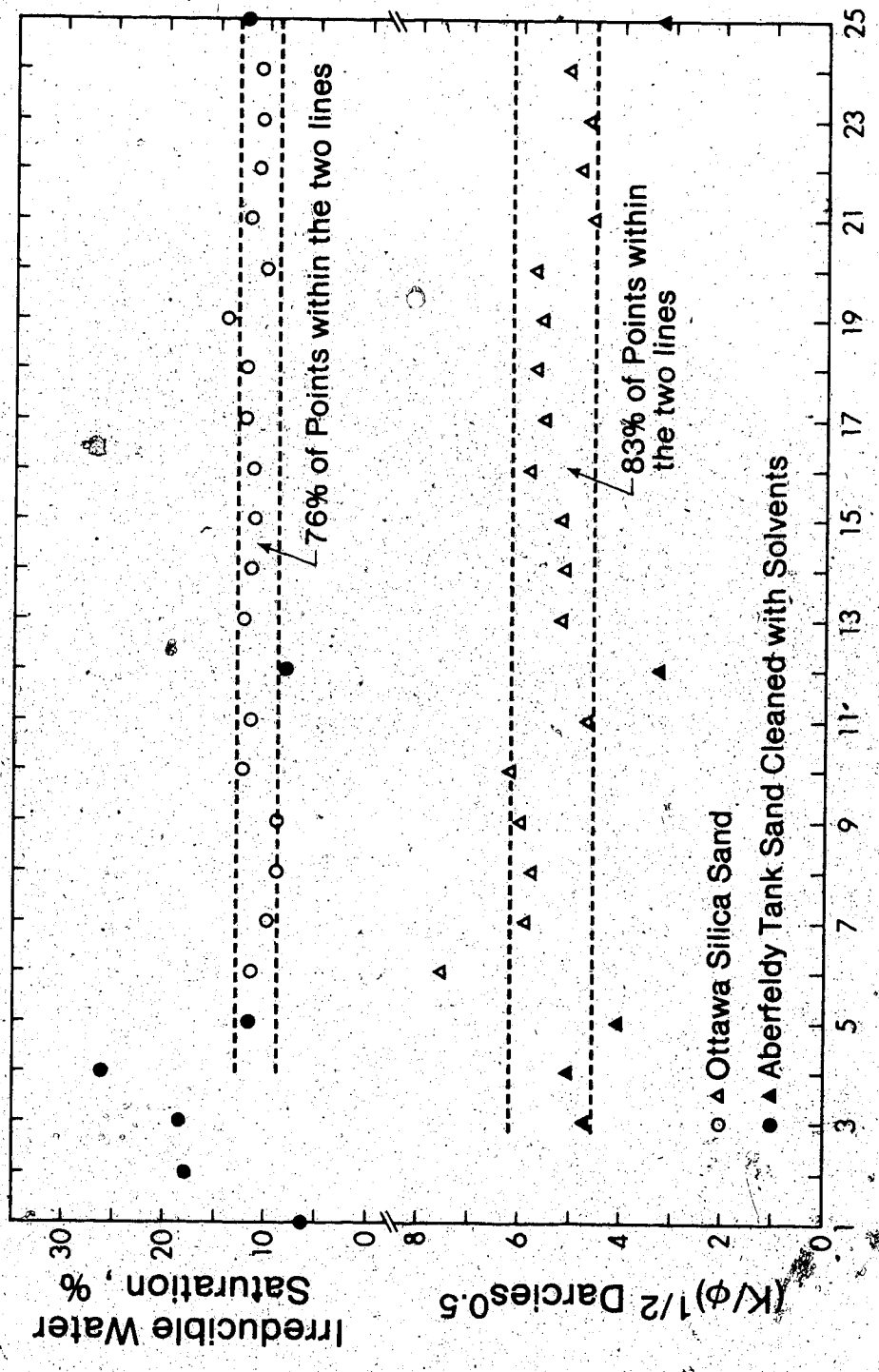


Figure 22 Comparison of Pack Properties

Figure 22 also shows the factor $(K/\phi)^{1/2}$ for all sandpacks, which is a part of the Leverett J-function (Equation D-2) and is related to the petrophysical structure of the sandpacks. It can be seen that there is certain degree of consistency in the $(K/\phi)^{1/2}$ factors obtained.

9.6. Displacement Results

Twenty four displacement tests were carried out to study the recovery of Aberfeldy heavy oil (1000 - 5000 mPa.s) by different immiscible CO_2/brine injection processes. The production histories of all runs are given in Appendix G (tabulated form) and Appendix H (graphical form). The tables and graphs show the variation of oil recovery, oil produced-fluid injected ratio, average and injection/production pressures, water and gas-oil ratios with the amount of CO_2 and brine injected. Also a summary of displacements is shown in Table 11. Because of plugging of the production well, Run 2 had to be discontinued early during brine injection and for that reason it was not recorded in Table 11. In all the CO_2/brine floods the following parameters were maintained constant:

Volume of CO_2 = 20% HCPV

Production well pressure $\sim$ 5.5 MPag

Temperature $\sim$ 21-23°C

Pattern = Confined quarter of 5-spot.

9.6.1. Heavy Oil Recovery by Immiscible CO_2 Injection

Runs 5-10, 12, and 24 were started injecting subcritical

TABLE 11

SUMMARY OF DISPLACEMENT TESTS

Average Experimental Conditions = 5.5 MPag & 22°C

Run No.	Experiment Description*	Oil Sample No.	Superficial Velocity, m/d CO_2	Superficial Velocity, m/d Brine	Oil Recovery, % HCPV By Brine-flood	Oil Recovery, % HCPV By CO_2/Brine	Oil Recovery, % HCPV By Blow-down	Oil Recovery, % HCPV Total
1	CO_2 Slug Driven by Brine After Brine Flood	2	0.38	3.41	1.7	5.1	4.0	10.8**
3	CO_2 Slug Driven by Brine After Brineflood	1	2.22	2.27	45.3	17.5	7.7	70.5
4	CO_2 Slug Driven by Brine After Brineflood	1	2.31	2.31	54.4	9.4	3.8	67.6
5	CO_2 Slug Driven by Brine	1	2.27	2.27	–	53.5	1.5	55.0
6	CO_2 Slug Driven by Brine	1	0.18	0.18	–	35.9	3.3	39.2
7	CO_2 Slug Driven by Brine	1	0.20	0.20	–	26.4	–	26.4
8	CO_2 Slug Driven by Brine	1	2.90	2.90	–	36.6	1.7	38.3

TABLE 11 (Continued)

SUMMARY OF DISPLACEMENT TESTS

Average Experimental Conditions = 5.5 MPag & 22°C

Run No.	Experiment Description*	Oil Sample No.	Superficial Velocity, m/d CO_2	Superficial Velocity, m/d Brine	Oil Recovery, % HCPV By Brine-flood	Oil Recovery, % HCPV By CO_2/Brine	Oil Recovery, % HCPV By Blow-down	Oil Recovery, % HCPV Total
9	CO_2 Slug Driven By Brine	1	1.66	1.05	–	32.3	1.2	33.5
10	CO_2 Slug Driven By Brine	1	0.72	2.32	–	44.6	1.3	45.9
11	Brineflood	1	—	0.87	32.4	–	–	32.4
12	CO_2 Slug Driven By Brine	1	2.90	2.90	–	50.4	0.5	50.9
13	WAG 1:1 Process†	1	1.15	1.15	–	37.1	1.5	38.6
14	WAG 1:1 Process	1	1.16	1.16	–	37.2	2.2	39.4
15	WAG 3:1 Process	1	1.16	1.16	–	38.0	4.3	42.3
16	WAG 4:1 Process	1	1.44	1.44	–	44.6	2.9	47.5
17	WAG 5:1 Process	1	1.16	1.16	–	44.1	2.3	46.4
18	WAG 6:1 Process	1	1.47	1.47	–	41.2	2.0	43.2
19	WAG 4:1 Process After Brineflood	1	1.43	1.43	35.2	11.6	1.9	48.7
20	WAG 1:1 Process After Brineflood	1	1.44	1.44/	35.5	9.3	3.2	48.0
21	WAG 6:1 Process After Brineflood	1	0.88	0.88	33.8	10.8	1.7	46.3

TABLE 11 (Continued)

SUMMARY OF DISPLACEMENT TESTS

Average Experimental Conditions = 5.5 MPag & 22°C

Run No.	Experiment Desription*	Oil Sample No.	Superficial Velocity, m/d CO_2	Superficial Velocity, m/d Brine	Oil Recovery, % HCPV By Brine-flood	Oil Recovery, % HCPV By CO_2/ Brine	Oil Recovery, % HCPV By Blow-down	Oil Recovery, % HCPV Total
22	WAG 4:1 Process After Brineflood	2	0.87	0.87	17.1	8.0	2.6	27.7
23	WAG 4:1 Process	2	0.87	0.87°	–	18.5	3.7	22.2
24	CO_2 Slug Driven By Brine	2	1.16	1.16	–	19.8	3.0	22.8
25	WAG 4:1 Process	1	0.44	0.44	–	42.3	1.6	43.9

*Total CO_2 injected in all the CO_2/Brinefloods = 20% HCPV (Hyd. Pore Vol.)

**Only in this run the brine was injected with the Milroyal pump. In the rest, the brine was injected with the constant flow rate pump.

†CO_2 slug volumes = 4% HCPV for Run 13
= 2% HCPV for Runs 14-23 and 25.

(5.5 MPag, 21-23°C) carbon dioxide continuously until a 20% HCPV slug volume had been injected. A subcritical pressure rather than a supercritical one was chosen since the actual pressure of the Aberfeldy-Lloydminster reservoirs is of the order of 3.45 MPa and also because the mass transfer between CO_2 and heavy oils is greater when the CO_2 is in gas rather than in liquid phase. As the reservoir temperature of the prototype is 21-22°C, less than the critical temperature of CO_2 (31.1°C), the carbon dioxide will be in gas phase at pressures lower than 5.9 MPag.

It can be seen in Table 12 and Figures H4-H9, H11, and H23 (presented in Appendix H) that in all the runs where a slug of CO_2 was injected, the CO_2 breakthrough occurred very rapidly (after injecting less than 0.15% HCPV) and the average recovery at this point was 1% HCPV. This shows that the viscous forces completely dominated the carbon dioxide injection and that viscous instability occurred because of the high CO_2-oil mobility ratio. The diffusive and gravitational forces played a much less important role in the displacement.

After the injection of 20% HCPV carbon dioxide, only 3% (average of 8 runs) of the original oil in place was recovered. At that stage of the displacement the gas-oil ratio was of the order of 1000 sm^3 CO_2/m^3 oil and the oil produced-fluid injected ratio (OPFIR), for seven out of eight runs, was less than 0.25 indicating that a very low recovery (less than 5% HCPV) would have been obtained if a straight CO_2 injection had been continued up to an economic limit of gas-oil ratio (viz. 7000 sm^3/m^3 in this work). These results show that

TABLE 12

VISCOUS OIL RECOVERY PERFORMANCE DURING THE CONTINUOUS INJECTION OF A 20% HCPV SLUG OF SUBCRITICAL CO_2

Experimental Conditions: 5.5 MPag & 21-23°C

Run No.	Type of Sand	Superficial Velocity, m/d CO_2	Superficial Velocity, m/d Brine	Recovery at CO_2 B.T. % HCPV	Recovery % HCPV	Maximum GOR During Slug Injection sm^3/m^3
5	Aberfeldy* Tank Sand	2.27	2.27	0.8	2.3	735.8
6	Ottawa Silica Sand	0.18	0.18	1.2	2.6	256.3
7	Ottawa Silica Sand	0.20	0.20	1.0	6.5	109.2
8	Ottawa Silica Sand	2.90	2.90	0.7	2.4	3767.0
9	Ottawa Silica Sand	1.66	1.05	0.7	2.0	533.7
10	Ottawa Silica Sand	0.72	2.32	0.8	2.8	869.6
12	Aberfeldy** Tank Sand	2.90	2.90	0.8	1.7	507.6
24	Ottawa Silica Sand	1.16	1.16	2.2	3.7	1009.0

*Cleaned with toluene, isopropyl alcohol and distilled water.

**Cleaned with toluene.

the straight (or continuous) CO_2 injection process under subcritical conditions is not applicable to conventional viscous oils of the Aberfeldy-Lloydminster type. As is shown in Figure H10, brine injection alone yields a higher recovery than the straight CO_2 injection.

Another negative factor in straight CO_2 injection under subcritical conditions was the low OPFIR's obtained. As can be seen from Figures H4-H9, H11, and H23, the oil produced-fluid (CO_2) injected ratios during the injection of the 20% HCPV slug volume of CO_2 in 8 runs averaged a value of 0.35 before the CO_2 breakthrough. During the primary phase of CO_2 gas injection mass transfer between CO_2 and reservoir fluids takes place by the solution and diffusion mechanisms. This is the reason the voidage balance is so low, thus yielding low oil production rates. Simultaneously with mass transfer, carbon dioxide begins to establish a carbon dioxide phase saturation in the porous medium. When the CO_2 saturation is above its critical value and it is continuous from well to well, the CO_2 breakthrough occurs and the OPFIR's start decreasing as the free carbon dioxide production increases. As CO_2 has a much higher mobility than viscous oils, the gas-oil ratios increase rapidly and the invaded porous medium with a small carbon dioxide saturation acts as a thief zone. Depending on the level of mass transfer between CO_2 and oil, the production of free CO_2 may range from moderate to very high during the subordinate phase of the displacement.

In conclusion, up to CO_2 breakthrough the immiscible displacement of heavy oil by subcritical carbon dioxide is dominated by viscous forces, and mass transfer betweeen CO_2 and oil does not appear to play an

important role. It can make itself felt during the subordinate phase of the CO_2 injection by increasing the heavy oil recovery by 2-3 percentiles, but the displacement is still dominated by the viscous forces.

9.6.2. Visualization of Displacement Type

Based upon low recoveries of heavy oils by CO_2 injection in cylindrical sandpacks, several authors[3,4,14] have indicated that the displacement of heavy oil (< 20° API) by CO_2 at practical injection pressures (< 20.6 MPag) is immiscible. But they have failed to give more conclusive evidence other than a low recovery, which is not by itself a sufficient criterion to demonstrate that a displacement is of the immiscible type. Offeringa and van der Poel[138] showed that when the displacement is dominated by viscous fingering, the breakthrough recoveries obtained in miscible displacements are equal to those obtained in immiscible displacements at the same viscosity ratio.

In this research two additional manifestations (with respect to the low recovery criterion), which show that the displacement of Aberfeldy-Lloydminster heavy oil by carbon dioxide at subcritical conditions is immiscible type were observed:

a. After the CO_2 breakthrough a clear gas-oil interface was observed at 5.5 MPag in the high pressure separator sight glass, which is shown in Figure 4 and Plate 1. As expected, chromatographic analysis of the gas phase only showed the presence of carbon dioxide and traces of methane and ethane as components, because CO_2 was injected at subcritical conditions and dead heavy oil samples of high molecular weight (> 420 g/gmol) were used in the runs. The

simulated distillations of the two oil samples are shown in Figure 23. It can be seen from that figure that the volume of extractable hydrocarbons (C_5 - C_{30}) by the carbon dioxide is too low to generate miscibility by multiple contacts in shallow reservoirs. High supercritical pressures (> 27.6 MPa) would be required to compress the CO_2 to a dense fluid, which could solubilize the C_5 - C_{30} content of heavy oils[34]. But such pressures are impractical for recovering heavy oil from shallow, unconsolidated reservoirs.

b. PVT laboratory tests on CO_2 - Aberfeldy heavy oil mixtures carried out by Alberta Research Council[125] showed that at gas-oil ratios greater than 80 sm^3/m^3 and at pressures higher than 6 MPag, two immiscible liquid phases were formed: a carbon dioxide-rich phase which floated on top of the heavy oil phase and a saturated heavy oil phase. The liquid CO_2 was not miscible with the heavy oil at 21.5°C and 10 MPa (maximum pressure tested).

9.6.3. Rate-Dependence of CO_2 and Brine Breakthrough Oil Recoveries

In order to observe the effect of the diffusive and gravitational forces on the heavy oil recovery by immiscible carbon dioxide slug (20% HCPV) and brine injection, the superficial velocity of the fluids was varied from 0.18 to 2.9 m/d, which corresponds to the minimum and maximum flow rates achieved with the model injection system. This range covers reservoir fluid velocities (< 0.4 m/d). The time duration of the runs was from 10.15 to 0.57 days. That means that there was plenty of time for the diffusive and gravitational forces to influence the behaviour of the displacement.

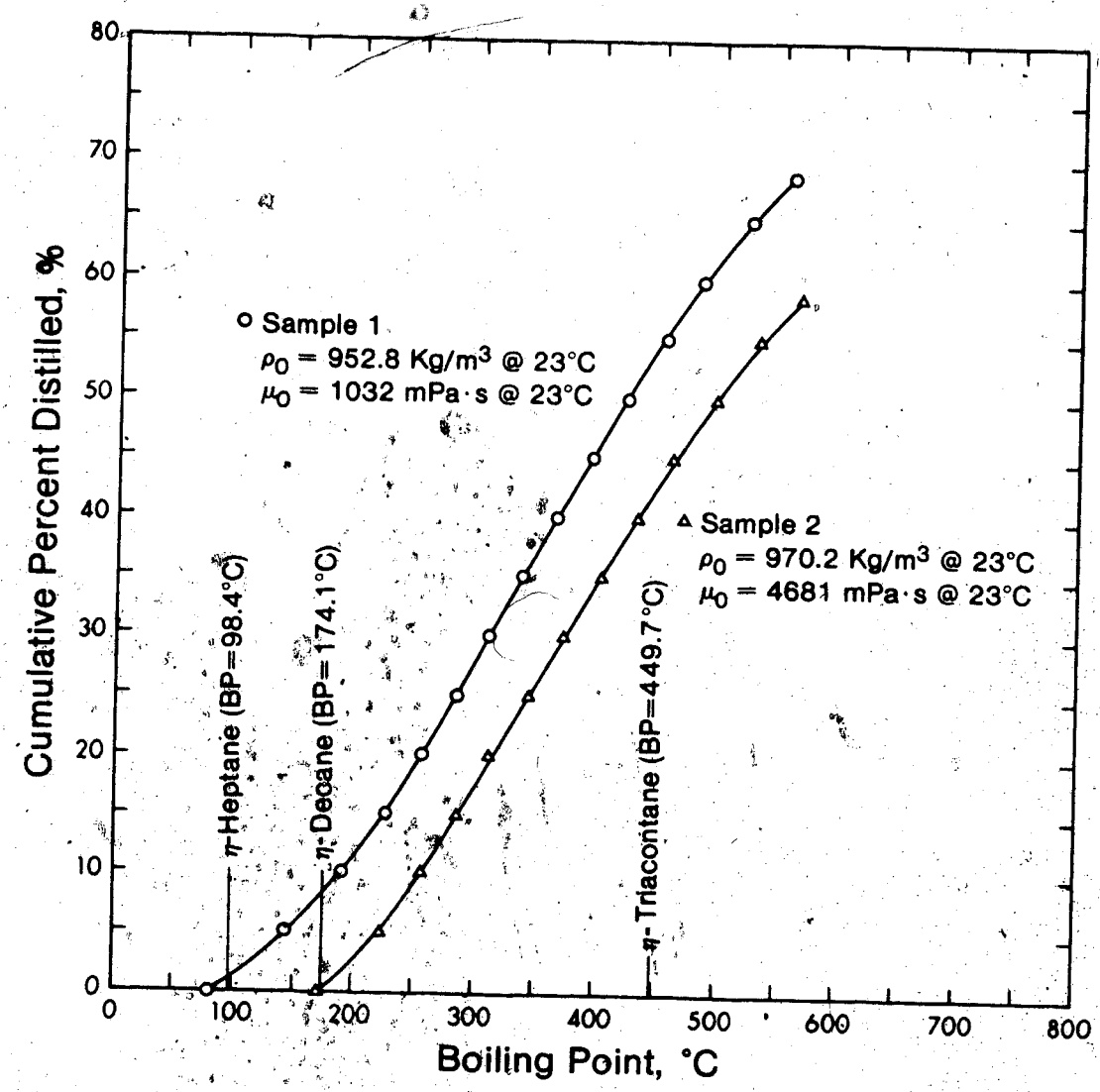


Figure 23 Simulated Distillations of Two Aberfeldy-Lloydminster Heavy Oil Samples

Based upon the results of seven runs (Table 13), Figure 24 was prepared. The results show that CO_2 and brine breakthrough oil recoveries in the CO_2 slug process are rate dependent. While the CO_2 breakthrough oil recovery decreases with increasing injection rate, the brine breakthrough oil recovery increases.

9.6.3.1. Oil Recovery at CO_2 Breakthrough

A very small decrease in the CO_2 breakthrough oil recovery from 1.2 to 0.7% HCPV was observed as the CO_2 superficial velocity increased from 0.18 to 2.9 m/d. This decrease in recovery is thought to be caused by the effect of the diffusive forces rather than by the effect of the gravitational forces. If the rate dependence of the CO_2 breakthrough oil recovery was caused by the gravitational forces the curves for oil recovery versus model/prototype ratios of gravitational forces to viscous forces for carbon dioxide injection (Figure 25) would have shown negative rather than positive slopes. In view of this, it was thought that better results could be obtained by plotting CO_2 breakthrough oil recovery versus the scaling groups which take into account the transverse and longitudinal dispersions of CO_2 into oil as is shown in Figures 26 and 27. To calculate the transverse and longitudinal dispersion factors D_{Tgo} and D_{Lgo} for model and prototype, the following values of d_p and σ_m were used:

Ottawa silica sandpacks: $d_p = 0.0177$ cm and $\sigma_m = 5.5$

Aberfeldy tank sandpacks and prototype: $d_p = 0.01$ cm and $\sigma_m = 8.0$

Figure 26, which only shows the CO_2 breakthrough oil recoveries achieved

TABLE 13

EFFECT OF SUPERFICIAL VELOCITY ON CARBON DIOXIDE AND BRINE BREAKTHROUGH OIL RECOVERIES

Process: 20% HCPV slug of CO_2 (at 5.5 MPag & 21-23°C) driven by brine

Do = 3.59 E-05 cm^2/s (Oil Sample No. 1)

Sandpacks: Runs 5 and 12 Aberfeldy Tank Sand, d_p = 0.01 cm, σ_m = 8

Runs 6-11 Ottawa Silica Sand, d_p = 0.018 cm, σ_m = 5.5

Run No.	Superficial Velocity, m/d CO_2	Brine	Recovery at CO_2 B.T., %HCPV	Recovery at Brine B.T., %HCPV	$(\frac{D_{Tgo}L^*}{W^2V})_M \times 10^3$	$(\frac{D_{Tgo}L^*}{D_{Lgo}W})_M$	$(\frac{D_{Tgo}L}{W^2V})_M / (\frac{D_{Tgo}L^*}{W^2V})_P$		
							V_p =0.09	0.18	0.36m/d
5	2.27	2.27	0.8	15.6	0.24	0.22	13.9	27.5	55.0
6	0.18	0.18	1.2	7.9	2.67	0.72	156.8	312.8	617.6
7	0.20	0.20	1.0	7.7	2.41	0.70	141.4	281.3	556.8
8	2.90	2.90	0.7	11.9	0.20	0.16	11.6	23.0	45.6
9	1.66	1.05	0.7	11.7	0.32	0.24	18.8	37.4	74.1
10	0.72	2.32	0.8	12.2	0.69	0.40	40.7	81.0	160.3
12	2.90	2.90	0.8	15.8	0.19	0.18	11.2	22.2	44.4

*Calculated using the superficial velocity of the carbon dioxide.

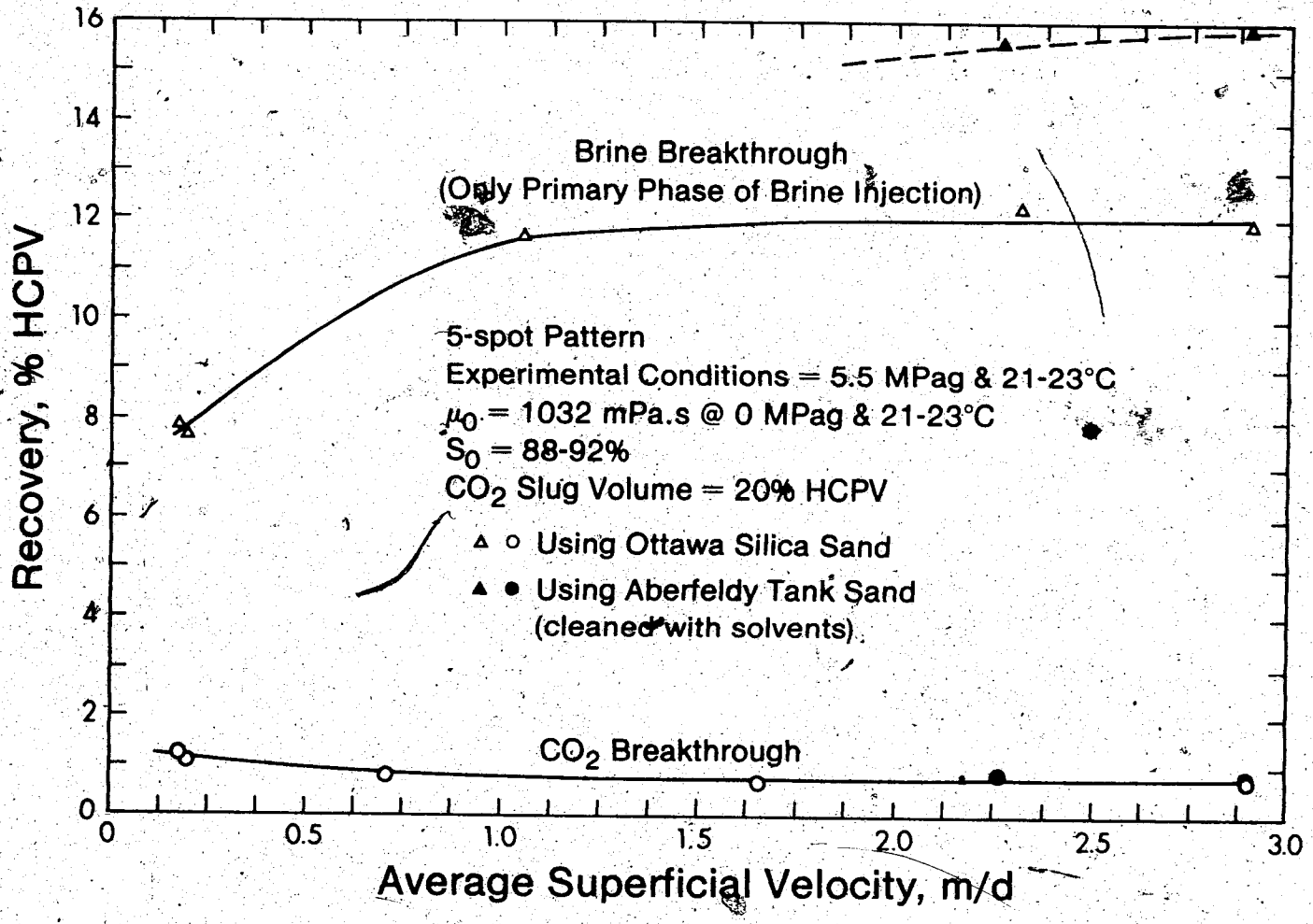


Figure 24 Rate Dependence of CO_2 and Brine Breakthrough Oil Recoveries of Heavy Oil in Immiscible Carbon Dioxide Slug Process

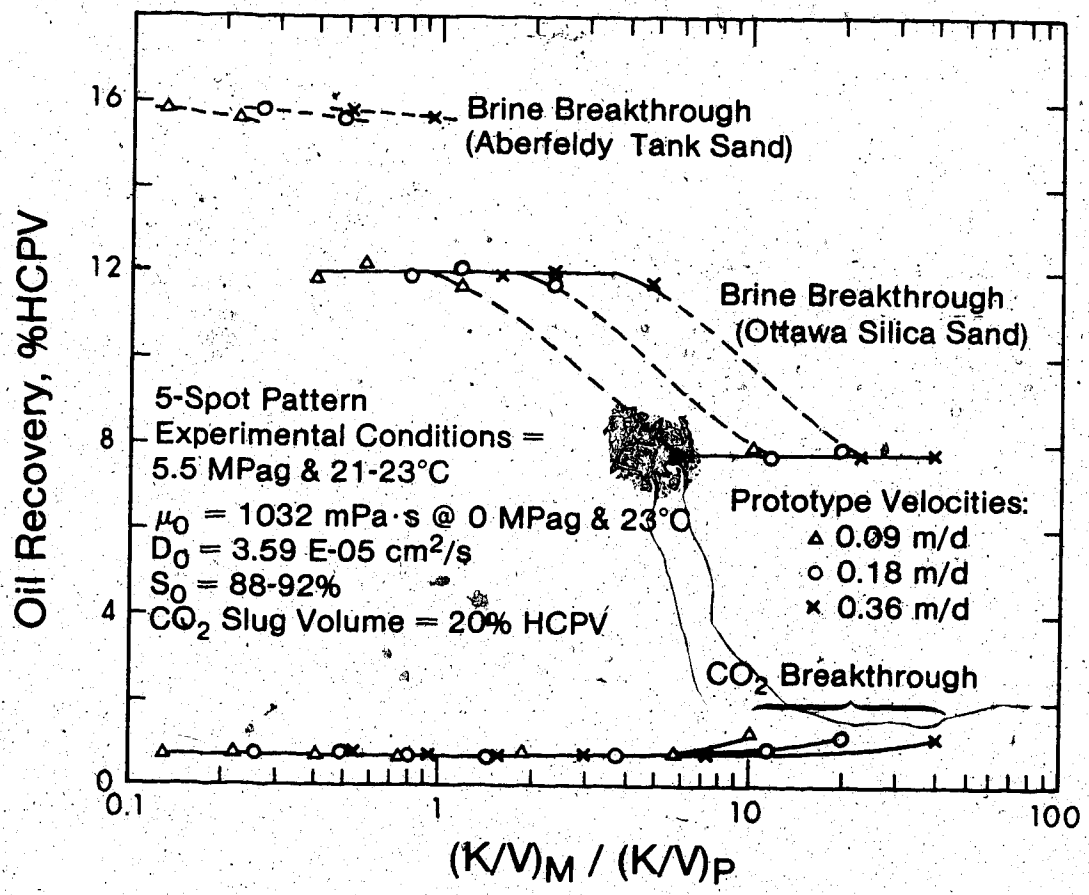


Figure 25 CO_2 and Brine Breakthrough Oil Recoveries as a Function of Model/Prototype Ratios of Gravitational Forces to Viscous Forces

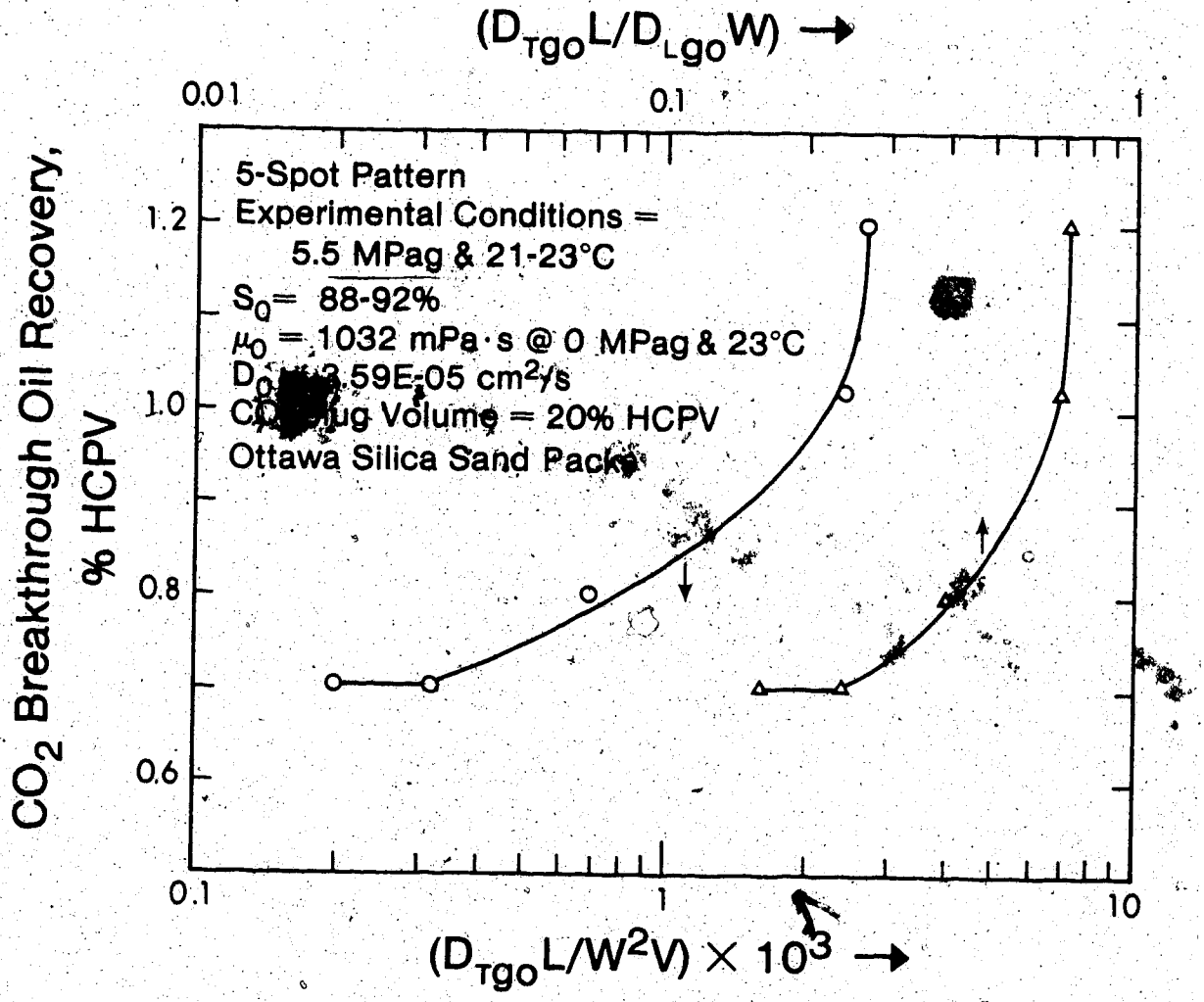


Figure 26 Effect of Transverse and Longitudinal Dispersion on CO_2 Breakthrough Oil Recovery. Ottawa Silica Sand Packs

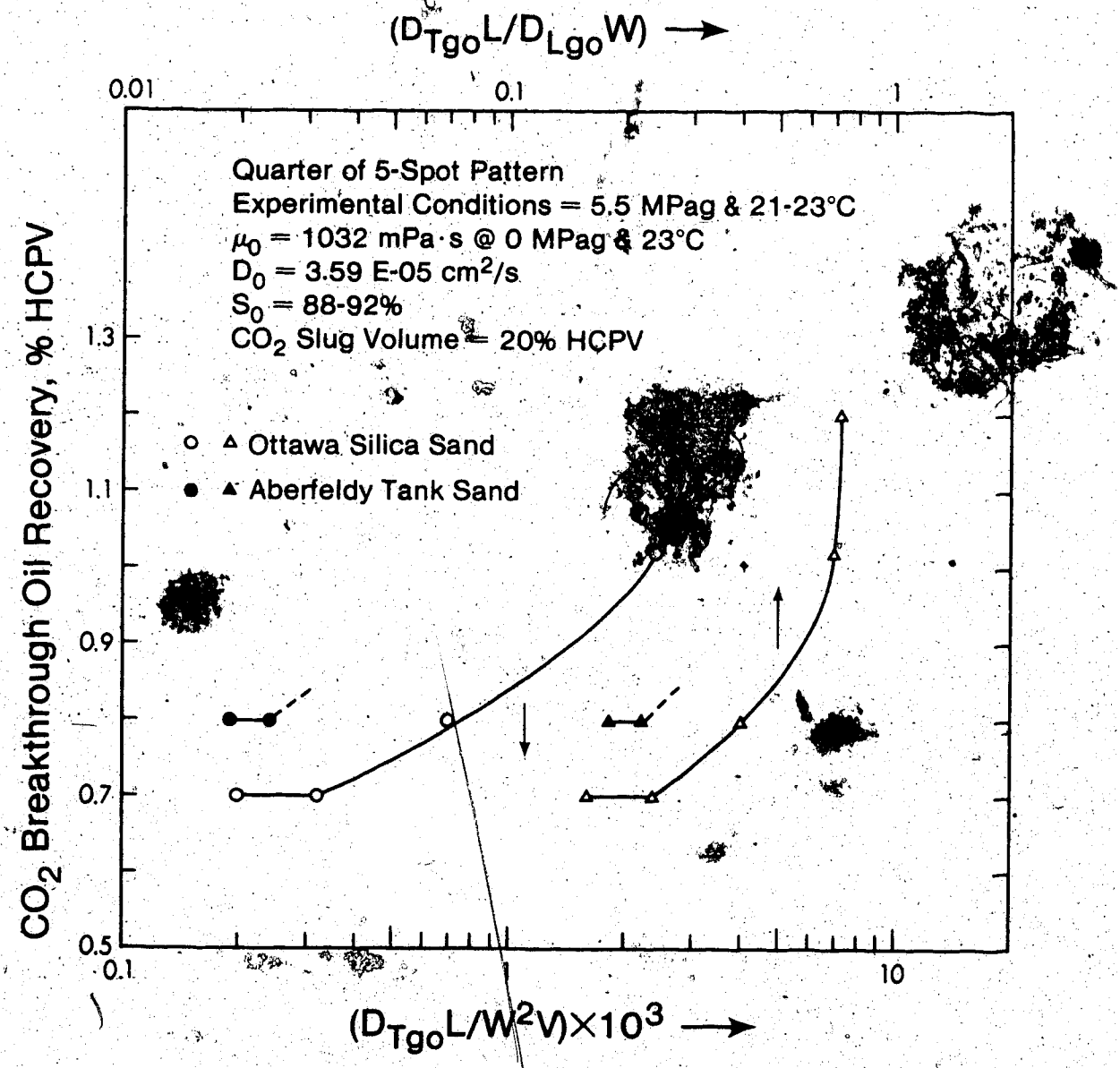


Figure 27 Effect of Transverse and Longitudinal Dispersion on CO_2 Breakthrough Oil Recovery. Ottawa Silica and Aberfeldy Tank Sand Packs

in the Ottawa silica sandpacks indicates that for immiscible displacement of viscous oils by carbon dioxide at very high mobility ratios, the CO_2 breakthrough oil recovery remains relatively constant as long as the dimensionless transverse dispersion scaling group $(D_{Tgo}L/W^2V)$ is below a value of 0.32E - 03. Above this value, transverse dispersion makes itself felt and the oil recovery at CO_2 breakthrough increases with increasing transverse dispersion. The inclusion of the breakthrough recoveries obtained in Aberfeldy tank sandpacks as shown in Figure 27 only produced a little change in the CO_2 breakthrough oil recoveries at low values of $(D_{Tgo}L/W^2V)$.

The very low recoveries at CO_2 breakthrough obtained in the experiments show that for values of the transverse dispersion scaling group less than 2.7E - 03, immiscible displacement of viscous oil by carbon dioxide was unstable. It is possible that at higher values of $(D_{Tgo}L/W^2V)$ the displacement still remains unstable. Although Gardner and Ypma[97] found that at very high values of the transverse dispersion group (> 0.5) a recovery efficiency of light oil by CO_2 characteristic of a stable displacement was observed by them, the immiscible displacement of heavy oil by carbon dioxide in rectangular models and field projects is likely to be unstable since the low dispersion of CO_2 in heavy oils as compared with that in light oils and the high value of W (width) in scaled models and field projects give the transverse dispersion group a low value characteristic of unstable displacement. At this point it is important to keep in mind that oil viscosity is taken into account on the transverse-dispersion scaling group through the molecular diffusion of CO_2 into oil which decreases

with increasing viscosity. High values of the transverse scaling group are likely to be obtained in laboratory unscaled experiments when long tubes of small diameter are used.

Figures 26 and 27 also show a plot of CO_2 breakthrough oil recovery versus the scaling group (D_{TgoL}/D_{LgoW}), which simultaneously accounts for the effect of transverse and longitudinal dispersion. As lateral dispersion plays a more important role than longitudinal dispersion since the lateral area of the fingers is much greater than the frontal area, the graphs in Figures 26 and 27 have the same trend.

In conclusion, it appears that dispersion of CO_2 into heavy oils is insufficient to damp out the fingers in immiscible displacement of oil by CO_2 dominated by viscous forces. However, while in miscible displacement dispersion may affect negatively the recovery since it is responsible for dilution of solvent slugs and loss of miscibility, in immiscible displacement of heavy oil by CO_2 it becomes a beneficial factor for oil recovery, as can be seen from Figures 26 and 27.

9.6.3.2. Comparison Between Levels of Dispersion in Model and Prototype

Figure 28, giving the Ottawa silica sandpack results, and Figure 29, giving the Ottawa silica and Aberfeldy tank sandpack results, show the CO_2 breakthrough oil recovery as a function of model/prototype transverse dispersion scaling group. Three prototype velocities (0.09, 0.18, and 0.36 m/d) were chosen to calculate the prototype transverse dispersion scaling group. Although some runs were performed at the highest superficial velocity that could be achieved with the model injection system, it was not possible to scale down the CO_2.

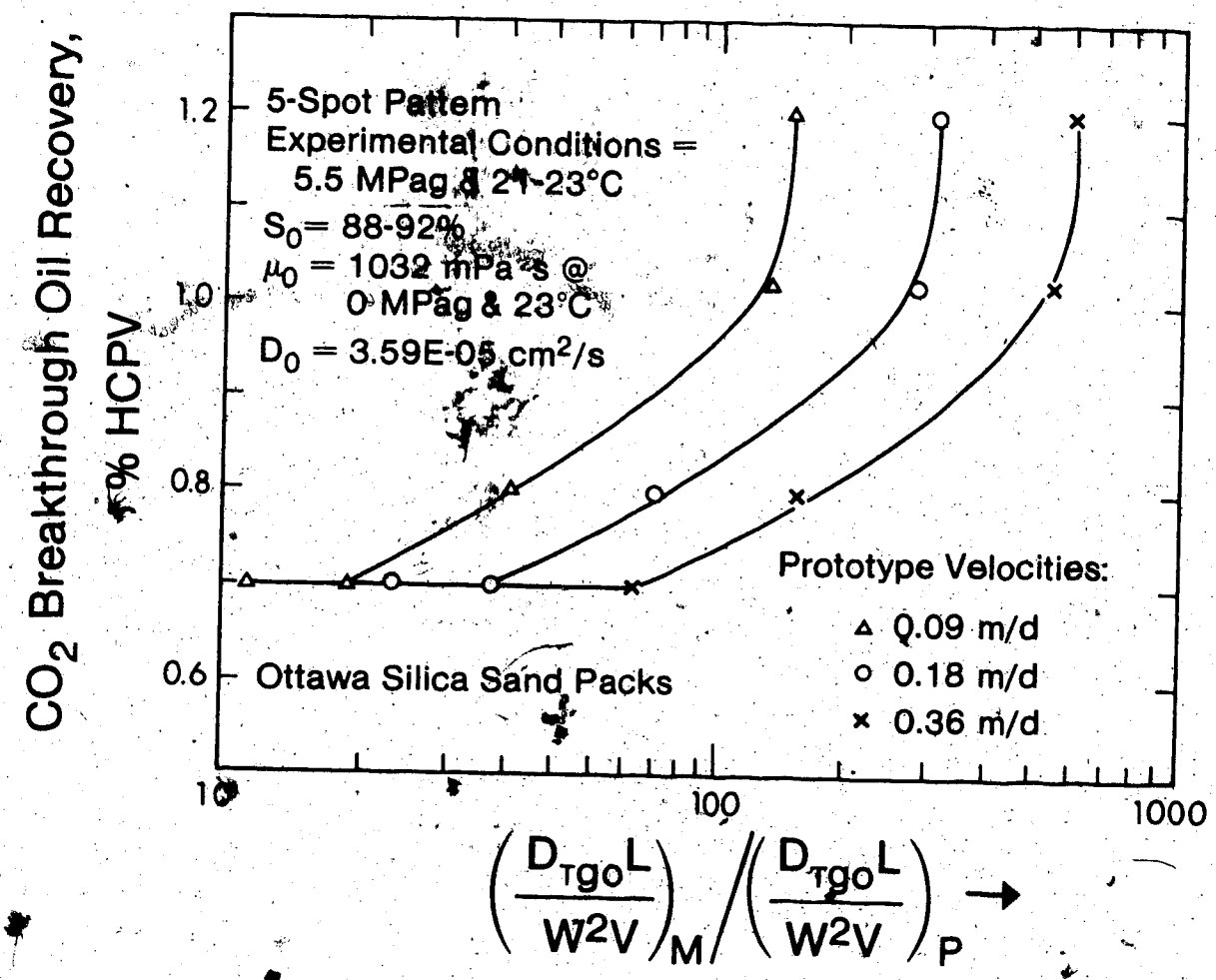


Figure 28 CO_2 Breakthrough Oil Recovery as a Function of Model/Prototype Transverse Dispersion Scaling Group. Ottawa Silica Sand Packs

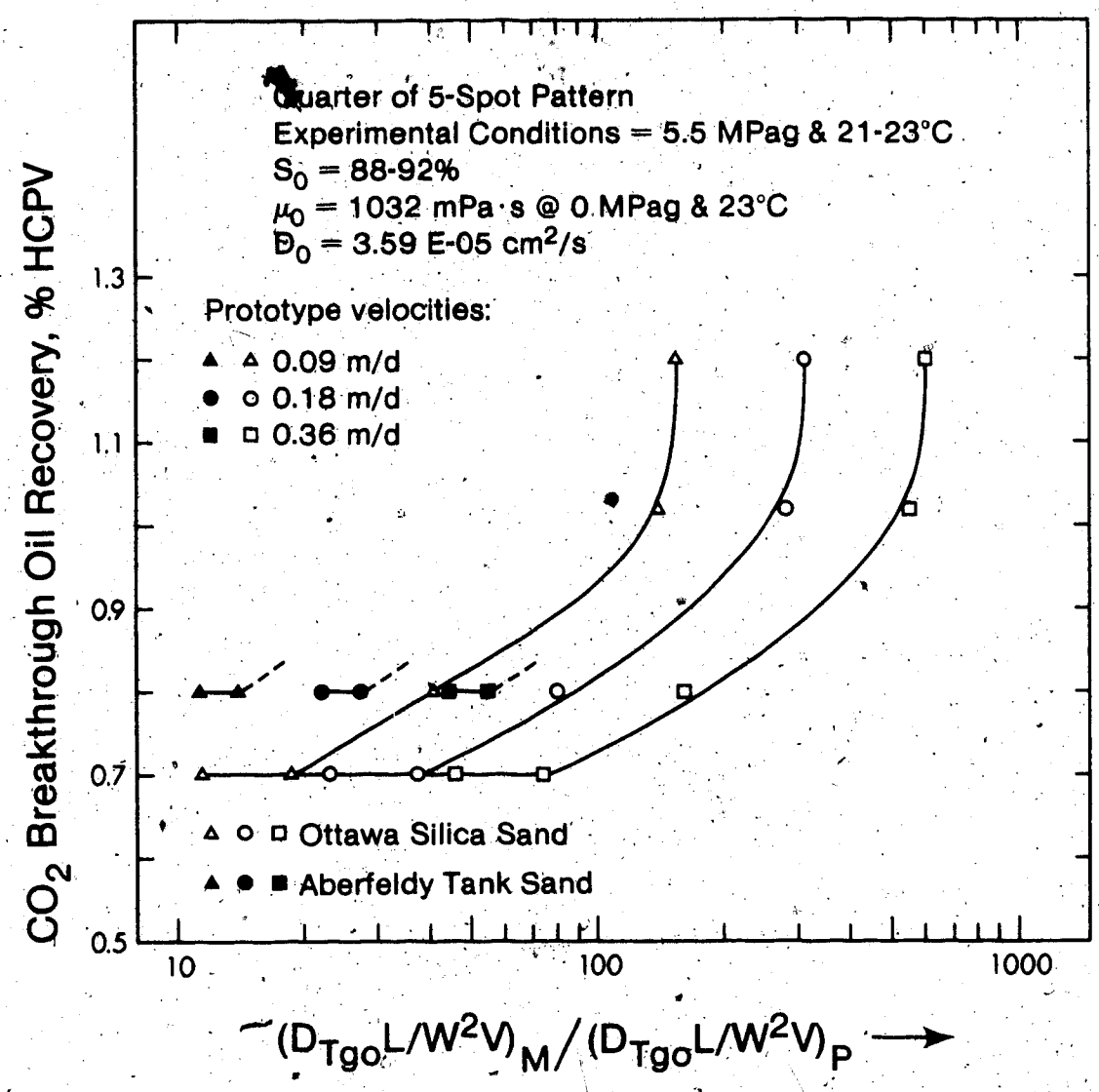


Figure 29 CO_2 breakthrough Oil Recovery as a Function of Model/ Prototype Transverse Dispersion Scaling Group. Ottawa Silica and Aberfeldy Tank Sand Packs

dispersion level of the prototype in the model. Depending on model velocity, the level of CO_2 dispersion into the oil in the model was 10 to 600 times higher than that in the prototype. However, it seems that at values of the model/prototype transverse dispersion scaling group lower than 30 for a prototype velocity of 0.18 m/d the CO_2 breakthrough oil recovery remains constant at a low value of 0.75% HCPV. Therefore, it is possible to assume that the oil recovery at CO_2 breakthrough in a field application of the subcritical CO_2 slug process in Aberfeldy-Lloydminster reservoirs would be of the order of 0.7-0.8% HCPV for a confined 5-spot pattern. This finding agrees with the very rapid CO_2 breakthrough that has occurred in field projects of immiscible displacement of heavy oils[21].

The small increase in CO_2 breakthrough oil recovery observed in Runs 5 and 12 where Aberfeldy tank sand was used, could have been caused by the greater amount of fines in that sand, which increased the convective component of the transverse dispersion factor.

9.6.3.3. Oil Recovery at Brine Breakthrough

As a result of higher viscosity of the brine and in situ emulsification, the brine displaced the CO_2 saturated oil much more efficiently than the carbon dioxide alone. Depending on the superficial velocity, the oil recovery at brine breakthrough was 7 to 11% HCPV more than that obtained at CO_2 breakthrough when using Ottawa silica sand, and 14 to 15% HCPV when using Aberfeldy tank sand (see Figure 24).

An increase of four percentiles in brine breakthrough oil recovery can be observed in Figure 24 when the superficial velocity

increased from 0.18 to 2.9 m/d. This behaviour is opposite to that observed during the carbon dioxide slug injection. The increase in brine breakthrough oil recovery with increasing velocity could have been caused by the reduced gravitational segregation of the brine and the in situ emulsification of the oil.

Figure 25 shows the brine breakthrough oil recovery as a function of model/prototype ratios of gravitational to viscous forces which are listed in Table 14. Values of K_p = 1.2 Darcies and V_p = 0.09, 0.18, and 0.36 m/d were used to calculate the $(K/V)_p$ values for the prototype. It can be seen that when the prototype ratio of gravitational forces to viscous forces was scaled down in the model, the recovery achieved was as high as 12% HCPV, which remained almost constant for values of $(K/V)_M/(K/V)_p$ from 0.4 to 1.6 for a prototype velocity of 0.18 m/d. At higher values of model/prototype ratios of gravitational to viscous forces, the brine breakthrough oil recovery fell to 7.8% HCPV. Although it is well known that when gravitational segregation occurs in a horizontal reservoir the oil recovery increases with increasing injection rate since gravity segregation requires some time to make itself felt, it has been shown by Crane et al.[139] and Craig et al.[71] that for high mobility ratios the volumetric sweep efficiency at breakthrough is low and varies very little with the ratio of gravitational to viscous forces. For this reason, it is thought that the increase in brine breakthrough oil recovery from 7.8 to 12% HCPV could have been caused partially by another phenomenon rather than by the gravitational forces alone.

As was discussed in Section 9.3 a new recovery mechanism is

TABLE 14

VALUES OF $(K/V)_M/(K/V)_p$ FOR VARIOUS CARBON DIOXIDE AND BRINE SUPERFICIAL VELOCITIES

Process: 20% HCPV Slug of CO_2 (at 5.5 MPag & 21-23°C) Driven by Brine
Oil Viscosity: 1032 mPa.s @ 0 MPag & 23°C
Sandpacks: Runs 5 and 12 Aberfeldy Tank Sand
Runs 6 - 11 Ottawa Silica Sand

Run No.	Superficial Velocity, m/d		$[(K/V)_M/(K/V)_p]_{CO_2}$			$[(K/V)_M/(K/V)_p]_{Brine}$		
	CO_2	Brine	V_p = 0.09	0.18	0.36 m/d	V_p = 0.09	0.18	0.36 m/d
5	2.27	2.27	0.24	0.49	0.98	0.24	0.49	0.98
6	0.18	0.18	10.08	20.17	40.33	10.08	20.17	40.33
7	0.20	0.20	5.78	11.55	23.10	5.78	11.55	23.10
8	2.90	2.90	0.40	0.80	1.59	0.40	0.80	1.59
9	1.66	1.05	0.75	1.51	3.02	1.19	2.39	4.77
10	0.72	2.32	1.86	3.73	7.46	0.58	1.16	2.31
12	2.90	2.90	0.13	0.25	0.51	0.13	0.25	0.51

visualized in this research which accounts for the in situ emulsification of Aberfeldy-Lloydminster heavy oil occurring during the CO_2/brine injection. The in situ formation of acidic brine-in-oil emulsions could improve oil recovery in the following ways:

a. As an increase in viscosity was the most pronounced physical change observed in the in situ emulsification of Aberfeldy heavy oil, the viscous acidic crude oil emulsions could block flow and induce a high pressure gradient in the region where they formed. The high pressure gradient, in turn, could partially overcome the capillary forces, already a little decreased by low interfacial tension so that a reduction in the residual oil saturation could be achieved. Also a possible shift in the relative permeability ratios towards a less favourable water mobility could have occurred. Sankur et al.[14] indicated that the relative permeability curves measured after a tertiary viscous oil recovery by continuous injection of CO_2 were significantly different from those prior to CO_2 injection.

b. In situ emulsification also decreased the tendency of the brine to finger through the carbonated heavy oil. Emulsified droplets lowered the effective permeability in the brine flow channels and forced the brine to invade regions that otherwise had been by-passed, improving volumetric sweep efficiency and breakthrough oil recovery.

According to the aforementioned mechanisms, the higher brine breakthrough oil recoveries obtained in Runs 5 and 12 (see Figures 24 and 25) can be explained by the improvement in the emulsification

mechanism produced by the greater amount of clay and sand fines contents of the Aberfeldy tank sand than of the Ottawa silica sand. Also, as the sand fines reduce the pore throats of the sandpacks, higher injection pressures were necessary to displace the emulsion bank through the Aberfeldy tank sandpacks.

To conclude, besides the reduced negative effect of the gravitational forces already discussed, the increase in brine breakthrough oil recovery with increasing superficial velocity may be explained in part by the increase in the mixing intensity produced by high flow rates, which improves oil emulsification.

9.6.4. Stabilizing Effect of CO_2 on the Brine Front

It was explained that the CO_2-oil mass transfer at 5.6 Mpa and 21-22°C produces a moderate expansion (17-14%) but a very high viscosity reduction (96-98%) in the Aberfeldy heavy oil samples used in this study. As a result of the expansion and viscosity reduction of oil by carbon dioxide, the brine displaced the swollen oil much more efficiently, than in the experimental test where brine was injected without the preflush with CO_2. Also, the higher viscosity of the moderated, acidic emulsions than that of the slightly basic emulsions could play an important role in the CO_2 stabilizing effect.

Table 15 shows that under different conditions of superficial velocity, the brine breakthrough oil recovery was higher when the injected brine followed a slug of CO_2. Depending on the superficial velocity, the increase in brine breakthrough oil recovery due to the preflush with CO_2 ranged from 1 to 6% HCPV for oil sample 1

TABLE 15

EFFECT OF CARBON DIOXIDE ON HEAVY OIL RECOVERY AT BRINE BREAKTHROUGH

Run No.	Oil Sample No.	Experiment Description	Superficial Velocity, m/d CO_2	Superficial Velocity, m/d Brine	Brine Breakthrough Recovery, %HCPV	Brine Breakthrough Brine Injected, %PV*
11	1	Brineflood	—	0.87	6.5	8.5
6	1	20%HCPV Slug of CO_2 Driven by Brine	0.18	0.18	7.9	9.2
7	1	20%HCPV Slug of CO_2 Driven by Brine	0.20	0.20	7.7	8.1
8	1	20%HCPV Slug of CO_2 Driven by Brine	2.90	2.90	11.9	14.0
9	1	20%HCPV Slug of CO_2 Driven by Brine	1.66	1.05	11.7	19.2
10	1	20%HCPV Slug of CO_2 Driven by Brine	0.72	2.32	12.2	13.7
22	2	Brineflood	—	0.87	3.9	4.7
24	2	20%HCPV Slug of CO_2 Driven by Brine	0.44	0.44	4.5	6.3

*Only primary phase of brine injection.

(1032 mPa.s viscosity) and 0.6% HCPV for oil sample 2 (4681 mPa.s viscosity). The increase in brine breakthrough oil recovery produced by the CO_2 slug injection prior to the brineflood can also be observed in Figure 30. Although this increase in recovery is not very substantial it does show that the carbon dioxide slug, instead of opening channels where the brine could finger more rapidly, tried to stabilize the brine front, first, decreasing the oil mobility, and second, reducing the brine mobility by emulsification.

9.6.5. Overall Recovery for the CO_2 Slug Process

As the effect of the superficial velocity on the CO_2 and brine breakthrough oil recoveries was opposite, it is interesting to examine what is the global effect of the superficial velocity on the final heavy oil recovery for the immiscible carbon dioxide slug process when the slug volume remains constant. At the end of the runs, the model was blown down (pressure released to atmospheric pressure), after a water-oil ratio higher than 20 m^3/m^3 had been achieved.

Table 16 shows that the overall or final recovery of oil sample 1 for the carbon dioxide slug process ranged from 33.5 to 55% HCPV depending on the superficial velocity of CO_2 and brine and the type of sandpack used. The highest recoveries were obtained in Runs 5 and 12 in which Aberfeldy tank sand was used to pack the model. Also, the heavy oil sample 1 was displaced at a high superficial velocity in these runs. The 4.1 perecentiles of recovery difference between Runs 5 and 12 may be explained by the fact that the Aberfeldy tank sand cleaned with toluene, isopropyl alcohol and distilled water was more water-wet

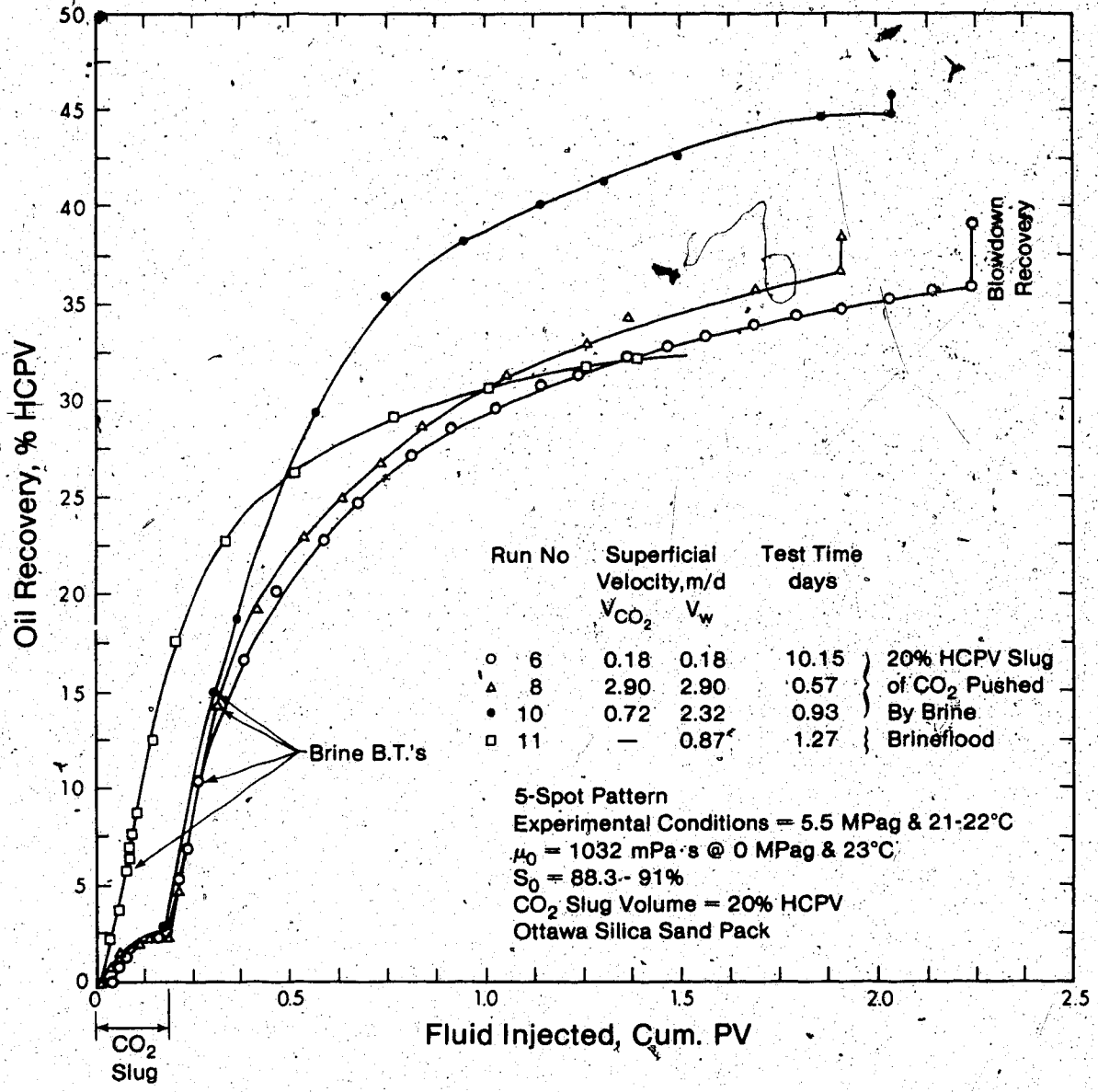


Figure 30 Effect of Superficial Velocity on the Production History of the CO_2 Slug Process

TABLE 16

SUMMARY OF BASIC ECONOMIC PARAMETERS FOR SECONDARY RECOVERY OF HEAVY OIL BY INJECTION OF A 20% HCPV SLUG OF CO_2 DRIVEN BY BRINE

Run No.	Oil Sample	Superficial Velocity, m/d CO_2	Brine	Final Recovery %HCPV*	Extra Recovery %HCPV**	Blowdown Recovery %HCPV**	%Final Rec.	CO_2 Retention %***	CO_2 Required sm^3/m^3 ****
5	1	2.27	2.27	55.0	9.7	1.5	2.7	37.0	192.2
6	1	0.18	0.18	39.2	6.7	3.3	8.4	54.2	267.5
7°	1	0.20	0.20	26.4	—	—	—	84.0	—
8	1	2.90	2.90	38.3	5.8	1.7	4.4	25.2	283.6
9	1	1.66	1.05	33.5	1.0	1.2	3.6	64.8	934.9
10	1	0.72	2.32	45.9	13.4	1.3	2.8	20.4	142.9
12	1	2.90	2.90	50.9	5.6	0.5	1.0	75.6	379.1
24	2	1.16	1.16	22.8	5.7	3.0	13.2	31.4	318.6

* Includes the blowdown recovery. Total fluid injected $\sim$ 2PV and final WOR $\sim$ 20 m^3/m^3.

** Extra Recovery = Final Recovery - Brineflood Recovery (BFR). BFR = 45.3% for Runs 5 and 12 (Aberfeldy Tank sand), BFR = 32.5% for Runs 6-10 (Ottawa Silica Sand), and BFR = 17.1% for Run 24.

*** Percentage of the total carbon dioxide injected left in the porous medium.

**** Cubic metres of carbon dioxide required to produce an extra cubic metre of oil (in basis of the extra oil recovery).

° This run had to be discontinued when the WOR was 7.1 due to a problem in the injection system.

than the same tank sand cleaned with toluene alone. The model/prototype ratios of gravitational forces to viscous forces for both runs were less than 1.0 (Table 14), falling in the range, where according to Figure 24, the recovery remains almost constant while varying the ratio of gravitational to viscous forces.

A lower overall recovery was obtained in Runs 6-10 where Ottawa silica sand was used. It can be seen in Table 16 that the maximum recovery obtained in Runs 6-10 corresponded to Run 10. In this run, the model was operated at a low CO_2 superficial velocity of 0.72 m/d and a high brine superficial velocity of 2.32 m/d. This was done in order to examine the effect of combining a low CO_2 injection rate with a high brine injection rate on the final recovery. It seems that the combination of injection flow rates produced the expected results. The low CO_2 superficial velocity yielded the beneficial effect of the diffusive forces and, in turn, the high brine superficial velocity improved the recovery by increasing the emulsification mechanism and decreasing the ratio of gravitational forces to viscous forces.

It can be seen in Figure 30 that the overall recovery in Runs 6 and 8 with very different superficial velocities was almost the same with a recovery difference less than one percentile, although the difference of oil recovery at brine breakthrough was as high as 4 percentiles. The superficial velocity and test time for Runs 6 and 8 were 0.18 m/d - 10.15 days, and 2.9 m/d - 0.57 days, respectively. Since both runs were carried out at the same conditions of pressure, temperature, CO_2 slug volume, and CO_2/oil ratio of viscous forces, the decrease in recovery difference between the two runs during the

subordinate phase may be explained by the transverse dispersion of carbon dioxide which is particularly effective at a high superficial velocity and therefore, it could have increased the amount of oil contacted by the CO_2 during the subordinate phase.

Comparing the overall results of Runs 6, 8, and 10 it may be concluded that it is better to operate a carbon dioxide slug project at the lowest and highest practical injection flow rates of carbon dioxide and brine, respectively.

Although the preflush with carbon dioxide prior to brine injection produced a stabilizing effect on the brine front, the mass transfer between CO_2 and reservoir fluids delayed the oil production as can be seen from Figure 30. The brine and CO_2/brine flood recovery curves are parallel during the first quarter of the experiments, which is the most important part. Only late in the subordinate phase of the CO_2 slug process an improvement in recovery with respect to the brineflood recovery was observed.

9.6.6. Injection of Alternate Slugs of CO_2 and Brine

The major disadvantage of the use of carbon dioxide in recovering heavy oil is its very high mobility in comparison with the low mobility of viscous oils. As was discussed before, continuous CO_2 injection and the injection of a slug of CO_2 driven by water are inefficient processes for heavy oil recovery because of the rapid production of a large part of

the CO_2 injected. A practical way to decrease high production of carbon dioxide in field projects[21,68] is to inject alternately small slugs of CO_2 and water.

The purpose of this part of this research was to provide information on the effectiveness of the WAG process to recover Aberfeldy-Lloydminster heavy oil. Ten equal size CO_2 slugs separated by brine slugs at different volumetric brine-CO_2 slug ratios were injected into the porous medium until a total of 20% HCPV of CO_2 had been injected. Then the CO_2 slugs were followed by brine injection until the producing water-oil ratio exceeded 20 m^3/m^3. In order to compare the effectiveness of the WAG process with the CO_2 slug process, the same total amount of CO_2 at the same pressure and temperature conditions was injected in both cases. The injection flow rate for the WAG floods was calculated using Equation 56 to scale down the ratio of viscous to gravitational forces of the prototype. This scaling group yields moderate injection flow rates, which can be achieved in high pressure models saturated with oil and water of the prototype. Choosing a moderate injection flow rate for the WAG floods the following scaling groups were completely satisfied:

*Geometric factors.

*Morphology factor.

*Ratio of gravitational forces to viscous forces.

*Ratio of viscous forces.

*Water-Gas ratio of slug volumes.

While the following groups were only partially satisfied:

*Ratio of capillary to viscous forces.

*Ratio of convection time to transverse dispersion time.

As the fluids of the prototype were used in the model, chemical similarity was also satisfied.

Two types of experimental tests were carried out using the WAG process. One with the porous medium at irreducible water saturation, which is referred to as a secondary recovery test, and the other with the porous medium at a high mobile water saturation (after waterflooding) which is referred to as a tertiary recovery test.

9.6.6.1. Effect of the WAG Ratio on Secondary Oil Recovery

The effect of varying the WAG ratio from 1:1 to 6:1 on secondary heavy oil recovery is shown in Figure 31. Several interesting features can be observed in this figure. The most important, from the point of view of field application, is that the delay in production observed during the injection of the large slug of CO_2, in the CO_2 slug driven by brine floods, disappeared in the WAG floods at high WAG ratios. However, a certain delay in oil production is still evident for the WAG 1:1 process with respect to brineflooding. The recovery curves of Figure 32 show clearly the positive effect of dividing a large slug of CO_2 into several small ones on the oil production response of the CO_2/brine injection process. Although the CO_2-oil and CO_2-brine mass transfers still try to produce a delay in oil production as is observed in Figures H13-H17 which show a reduction in OPFIR during the injection of the CO_2 slugs, the liquid-liquid immiscible displacement of the swollen

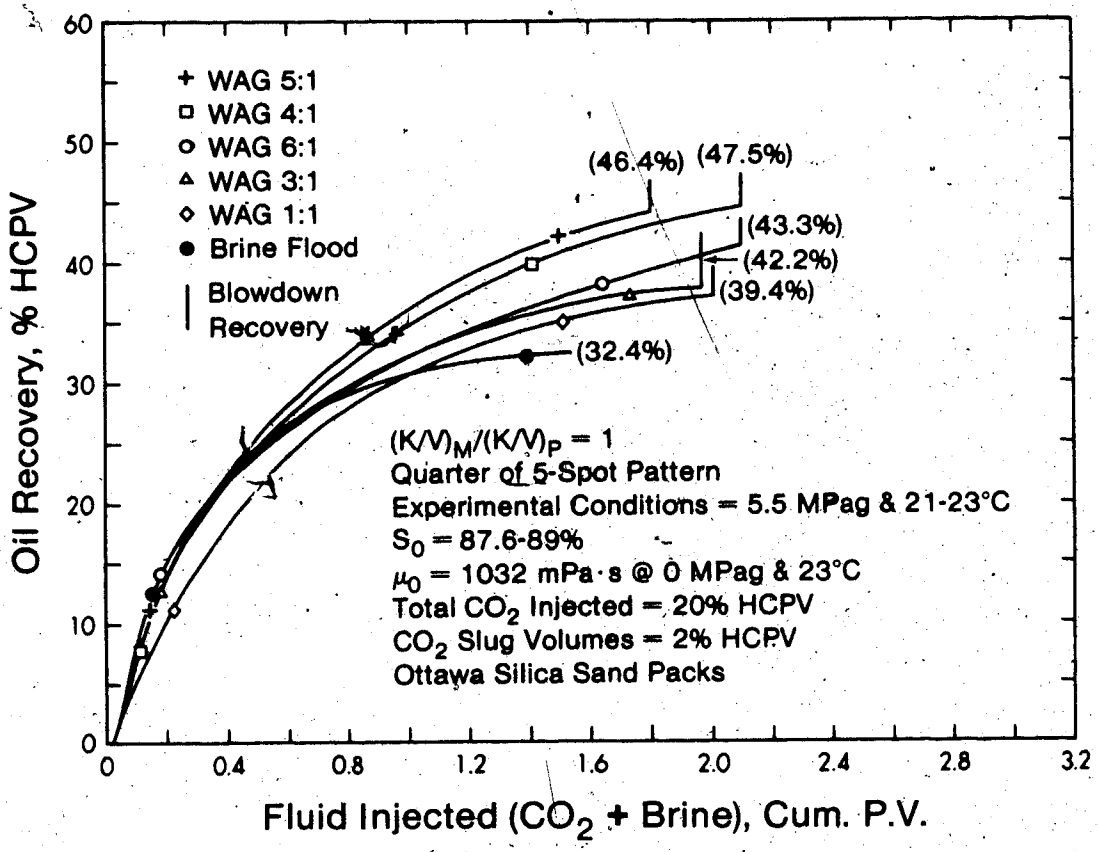


Figure 31 Effect of the WAG Ratio on Production Histories of Secondary Heavy Oil Recovery Floods

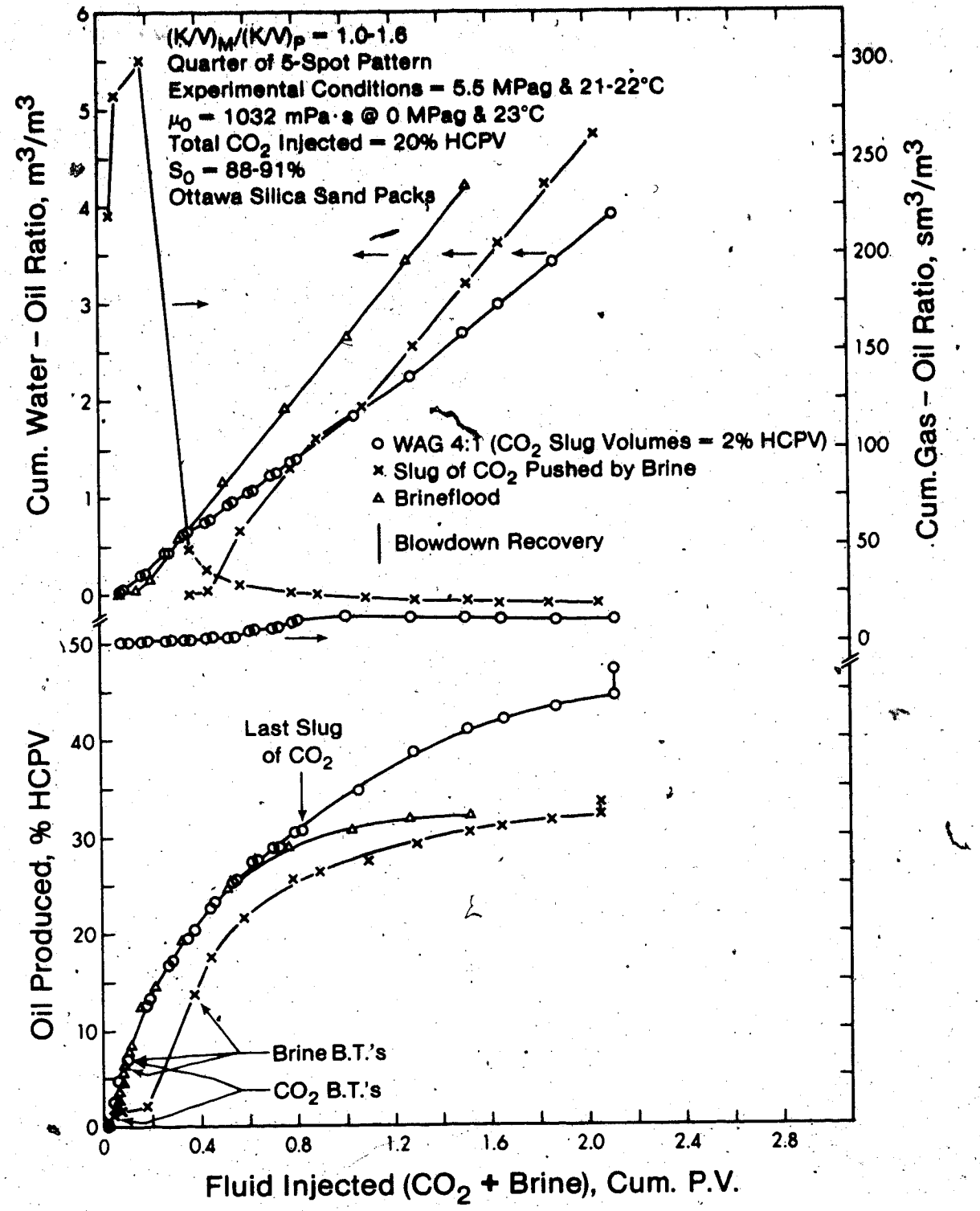


Figure 32 Comparison of the WAG 4:1 and Slug CO_2 Processes with Brineflood. Secondary Recovery of 1032 mPa.s Oil.

oil by brine decreases notably the oil production delay and increases the oil production-fluid injected ratio. At low WAG ratios, the volume of brine injected between the CO_2 slugs is not large enough to eliminate the oil production delay generated by carbon dioxide in gaseous phase.

Another important aspect that can be seen from Figures 31 and 32 is that the extra oil recovery with respect to brineflood recovery for the alternate injection of CO_2/brine slug process is higher than that for the CO_2 slug process. As can be seen in Table 17 the extra recovery of oil sample 1 (1032 mPa.s viscosity) using the WAG process at different brine: CO_2 ratios ranged from 6-15% HCPV.

Runs 13 and 14 were carried out at the same WAG 1:1 ratio but at different CO_2 slug volumes: 4% HCPV (five slugs) and 2% HCPV (ten slugs), respectively. The effect of CO_2 slug volume on heavy oil recovery using the WAG process was not noticeable as the final recovery difference for the two runs was only 0.8% HCPV (see Table 17). In view of these results it was decided to perform all the WAG floods using a constant CO_2 slug volume of 2% HCPV.

9.6.6.2. Optimal WAG Ratio

Based upon numerical simulation studies, Reid and Robinson[68] reported that a WAG injection ratio of 1:1 was selected as the optimum for the Lick Creek Meakin Sand Unit Immiscible CO_2/Waterflood Project. Low WAG ratios have been used also in miscible CO_2/water flooding[140,141] as recommended by numerical simulation results. The experimental results show that high rather than low WAG ratios should be chosen to optimize the Aberfeldy heavy oil recovery by subcritical CO_2/brine

TABLE 17

SUMMARY OF BASIC ECONOMIC PARAMETERS FOR SECONDARY RECOVERY OF HEAVY OIL USING THE WAG PROCESS

Total CO_2 Injected = 20% HCPV. CO_2 Slug volumes = 2% HCPV (4% HCPV only for Run 13)

Run No.	Volumetric Ratio of Brine/CO_2 Slugs	Oil Sample No.	Superficial Velocity of CO_2 and Brine, m/d	Final Recovery % HCPV *	Extra Recovery % HCPV**	Blowdown % HCPV	Recovery % Final Rec.	CO_2 Retention % ***	CO_2 Required sm^3/m^3 ****
13	1:1	1	1.15	38.6	6.1	1.5	1.5	68.8	252.1
14	1:1	1	1.16	39.4	6.9	2.2	5.6	49.0	286.2
15	3:1	1	1.16	42.3	9.8	4.3	10.2	74.4	196.6
16	4:1	1	1.44	47.5	15.0	2.9	6.1	67.5	131.5
17	5:1	1	1.16	46.4	13.9	2.3	5.0	53.5	142.3
18	6:1	1	1.47	43.2	10.7	2.0	4.6	61.3	163.0
23	4:1	2	0.87	22.2	5.1	3.7	16.7	75.2	388.0
25	4:1	1	0.44	44.0	11.5	1.6	3.6	94.7	168.4

* Includes the blowdown recovery. Total fluid injected $\sim$ 2PV and final WOR $\sim$ 20 m^3/m^3.

** Extra Recovery = Final Recovery - Brineflood Recovery (BFR). BFR = 32.5% for Runs 13-18 and 25
BFR = 17.1% for Run 23.

*** Percentage of the total carbon dioxide injected left in the porous medium.

**** Cubic metres of CO_2 required to produce an extra cubic metre of oil (in basis of the extra oil recovery).

injection.

Figure 33 summarizes the overall oil recoveries at different WAG ratios ($V_W^*/V_{CO_2}^*$) obtained by injection of alternate slugs of CO_2 and brine. Two more points were included in that figure: one corresponds to the slug CO_2 process (as brine is not injected between the CO_2 slugs, $V_W^*/V_{CO_2}^* = 0$) and the other corresponds to brineflooding (as slugs of CO_2 are not injected, $V_W^*/V_{CO_2}^* = \infty$). It can be seen that the 4:1 WAG injection ratio was optimal among five tested because more heavy oil was produced over approximately the same volume of CO_2 and brine injected. The WAG 4:1 ratio yielded a final recovery of 47.5% HCPV and 15.0% HCPV of extra recovery over brineflood. In turn, the WAG 1:1 ratio was the worst with a final recovery of 39.4% HCPV and an extra recovery of 6.9% HCPV. Table 17 and Figure 33 show that the WAG 5:1 ratio response was very close to that of the WAG 4:1 corroborating that in the case of secondary recovery high WAG injection ratios yield better results than low WAG injection ratios.

Figure 34 shows that the WAG injection ratio also had a considerable effect on the cumulative water-oil and gas-oil ratios. These ratios indicate the cumulative volumes of water (m^3) and carbon dioxide (sm^3) produced per cubic metre of oil recovered. Low cumulative WOR's and GOR's reduce the fluid handling costs of a field project and are also indicative of the mobility control of the displacing fluids. It is seen from that figure that the lowest cumulative GOR corresponded to the WAG 4:1 flood indicating that this WAG ratio was the most efficient in controlling the carbon dioxide production.

Many years ago, Caudle and Dyes[57] presented the main mechanism

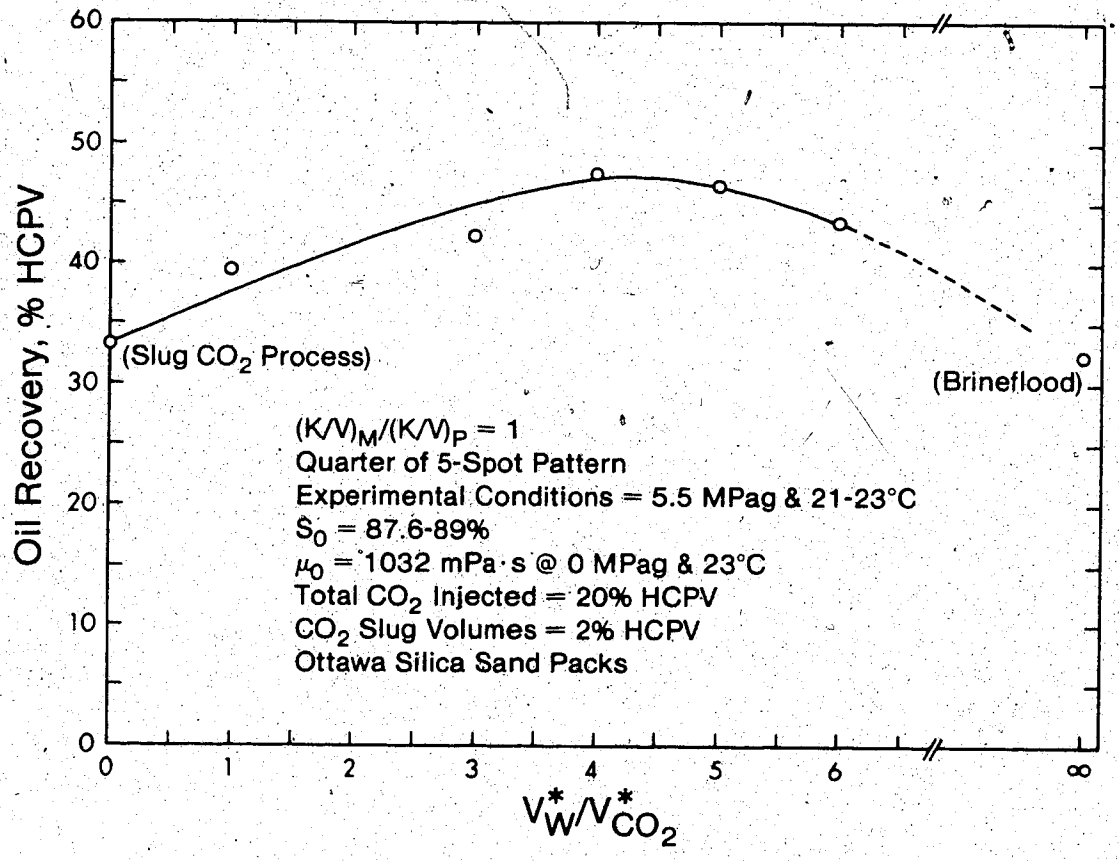


Figure 33 Optimal WAG Ratio for Secondary Recovery of Heavy Oil

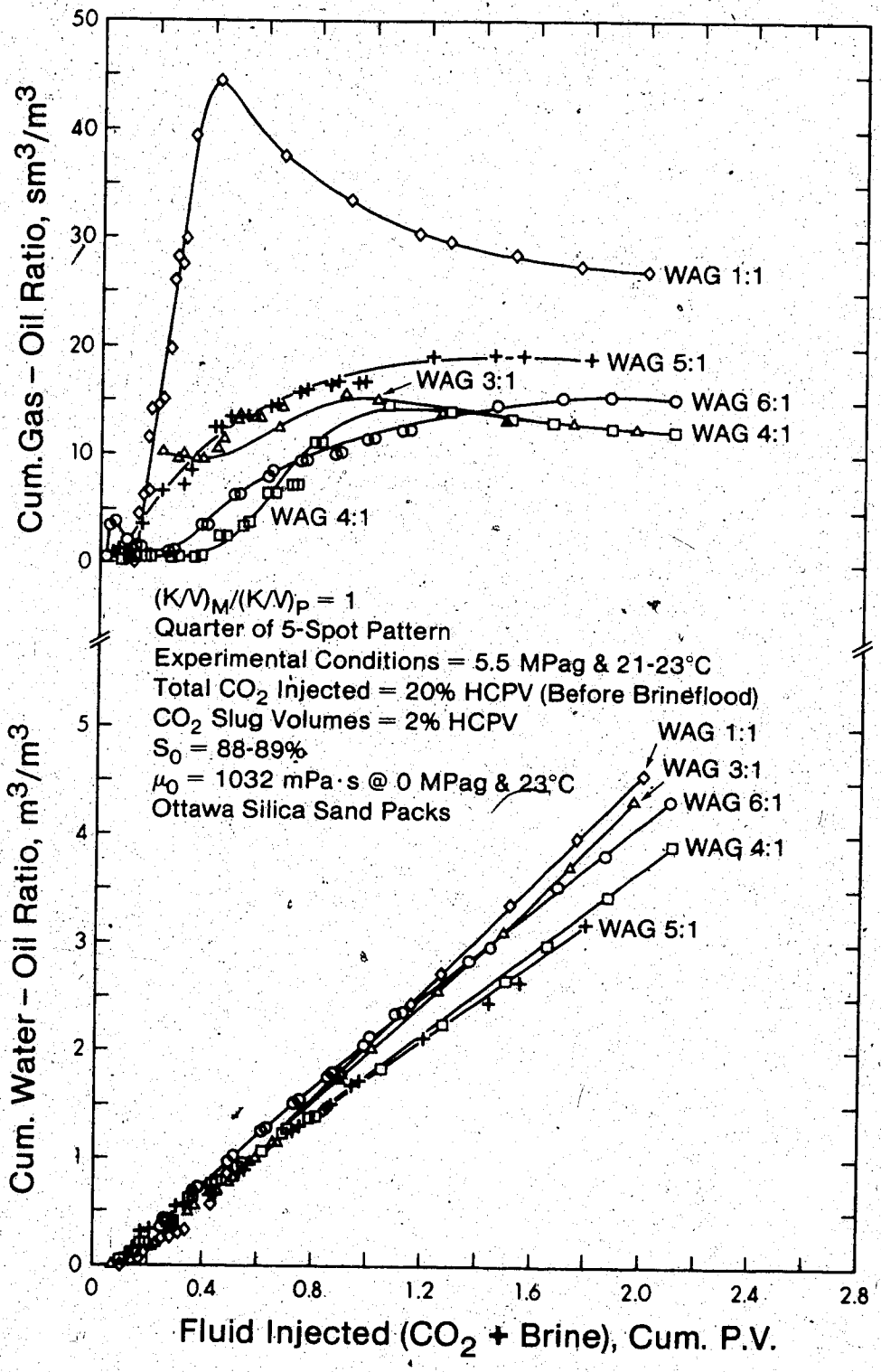


Figure 34 Effect of WAG Ratio on Cumulative Water-Oil and Gas-Oil Ratios of Immiscible Displacement of Heavy Oil

of the WAG process, which may be explained for CO_2/brine injection as follows. The presence of brine in the CO_2 invaded zone lowers the relative permeability to carbon dioxide and decreases its mobility, so that the injected brine interferes with the flow of carbon dioxide to discourage its rapid production. Thus, the CO_2 mobility depends on the brine slug volumes. If the brine slugs are of equal or smaller volumes than the CO_2 slugs, the brine is unable to control effectively the CO_2 mobility and a large production of CO_2 occurs. This phenomenon was observed when a WAG 1:1 ratio was used to displace the Aberfeldy heavy oil. From Figure 34 the steady increase of cumulative GOR during the injection of the CO_2 slugs in the WAG 1:1 flood is evident. The cumulative GOR reached a maximum, and when the injection of the CO_2 slugs was terminated the cumulative GOR started decreasing as the CO_2 production diminished. Maximum peaks of cumulative GOR were also observed in the WAG 3:1 and 4:1 floods, and with smaller slope change by the WAG 5:1 and 6:1 floods. As expected, the volume of fluid injected to achieve the maximum cumulative gas-oil ratio increased with increasing WAG ratio.

It is apparent from Figure 34 that a low cumulative water-oil ratio may be achieved using an optimal WAG injection ratio of 4:1 or 5:1. The cumulative WOR curves for the WAG 4:1 and 5:1 were very similar. But as the cumulative GOR was higher for the WAG 5:1 than for the WAG 4:1 flood, the latter is believed to be the optimum for a field application of the WAG process in Aberfeldy-Lloydminster reservoirs.

It can be also seen in Figure 34 that the maximum cumulative WOR was obtained by the WAG 1:1 flood. These results point out that the optimal WAG injection ratio is the one that is able to control

simultaneously the mobility of the carbon dioxide as well as the mobility of the brine.

Another factor that corroborates the choice of the WAG 4:1 ratio as optimal for field application is its low CO_2 requirement, viz. the standard cubic metres of CO_2 required to produce a cubic metre of oil. From Table 17, the minimum CO_2 required for secondary recovery of Aberfeldy heavy oil appears to be 131.5 sm^3/m^3 for the WAG 4:1 process.

9.6.7. WAG Process Versus CO_2 Slug Process

One of the objectives of this study was to select the best CO_2/brine injection strategy for the recovery of viscous oil from shallow, thin reservoirs. It is evident from Figure 32 that the WAG process is superior to the CO_2 slug process in recovering Aberfeldy heavy oil. Considering that the three experimental tests shown in Figure 32 were carried out at moderate superficial velocities, which permit simulation of the ratio of gravitational to viscous forces of the prototype in the model, the recovery difference achieved between the WAG 4:1 and the CO_2 slug processes injecting the same amount of CO_2 was as high as 14% HCPV, almost the same as the extra recovery (15% HCPV) of the WAG 4:1 process over brineflood recovery. It was also mentioned earlier that the continuous injection of subcritical CO_2 (without brine injection) was unable to recover more than 5% of the original heavy oil in situ. These experimental results show that the carbon dioxide injection strategy has a significant effect on heavy oil recovery.

As in all CO_2/brine injection runs the same amount of CO_2 was injected, the recovery difference can be accounted for by the effectiveness of the different processes in controlling CO_2 production. From Figure 32

the high production of CO_2 at the beginning of the CO_2 slug process can be seen. The cumulative gas-oil ratio versus fluid injected curve shows a maximum point at the end of slug injection and a sharp decrease in cumulative GOR with increasing volume of brine injected. This behaviour is similar to that observed in Figure 34 for the WAG process at low brine: CO_2 ratios. The cumulative GOR curve for the WAG 4:1 process shows that in this process excellent production control of free CO_2 occurred during the first 0.5 fraction of pore volume injected. Then, the cumulative GOR was observed to increase slightly to a value of 25 sm^3/m^3, remaining almost constant thereafter. This cumulative GOR is approximately half of that observed at the end of the CO_2 slug process.

The cumulative water-oil ratio also shows the beneficial effect of choosing a good CO_2/brine injection strategy. As expected, the cumulative WOR curves presented in Figure 32 show that the carbon dioxide reduced significantly the production of brine. The cumulative WOR curves of the WAG 4:1 and the CO_2 slug processes were shifted to the right by the CO_2. The flow of free CO_2 in the zone invaded by the brine and the in situ formation of brine-in-oil emulsions reduced brine mobility.

The earlier brine breakthrough observed in the WAG process came about because of the initial volume of CO_2 injected was smaller in the WAG than in the CO_2 slug process. But later in the subordinate phase, the better brine mobility control produced by the CO_2 slugs resulted in a low cumulative WOR of the WAG process.

A global comparison of average economic parameters for secondary heavy oil recovery using the CO_2 slug and WAG processes is shown in Table 18. In addition to higher recovery achieved with the WAG process,

TABLE 18

COMPARISON OF AVERAGE ECONOMIC PARAMETERS FOR SECONDARY HEAVY OIL RECOVERY USING THE SLUG CO_2 AND WAG PROCESSES

Experimental Conditions = 5.5 MPag & 21-23°C
Oil Viscosity = 1032 mPa.s @ 23°C
Total CO_2 Injected = 20% HCPV
Ottawa Silica Sand Packs

	CO_2 Slug Process	WAG Process
Run Numbers	6, 8, 9, 10	13, 14, 15, 16, 17, 18
Average Total Recovery, % HCPV	39.2	42.9
Average CO_2 Retentions, %	41.1	62.3
Average CO_2 Required, sm^3/m^3	406.0	194.7

this process required approximately half as much CO_2 to recover a cubic metre of oil as the slug CO_2 process. Also the average CO_2 retention, which indicates the percentage of CO_2 injected that reacts with oil and brine, and that remains in the sandpack at the termination of a flood, was higher in the WAG than in the CO_2 slug process. This finding is supported by the lower production of CO_2 in the former process.

9.6.8. Conventional Brinefloods

A series of conventional brinefloods was carried out varying the injection rate, oil viscosity, and the type of sand. Brineflood was also a step prior to performing the tertiary runs using carbon dioxide. The results of eight brinefloods are summarized in Table 19. With the exception of Run 1, where the brine was injected with a Milroyal pump,

TABLE 19

RESULTS OF CONVENTIONAL BRINEFLOODS

Run No.	Type of Sand	Oil Sample No.	Superficial* Velocity, m/d	$\frac{(K/V)_M}{(K/V)_p}$	$(Isr)_M$**	Brine Breakthrough Recovery % HCPV	Brine Breakthrough Brine Injected % PV	Final Recovery % HCPV
1	Aberfeldy Tank Sand	2	3.41	—	—	1.0	2.5	1.7
3	Aberfeldy Tank Sand	1	2.27	0.5	545	3.3	4.2	45.3
4	Aberfeldy Tank Sand	1	2.31	0.5	533	2.4	6.8	54.4
11	Ottawa Silica Sand	1	0.87	1.0	245	6.5	8.5	32.4
19	Ottawa Silica Sand	1	1.43	1.0	235	8.4	7.9	35.2
20	Ottawa Silica Sand	1	1.44	1.0	237	8.9	9.0	35.5
21	Ottawa Silica Sand	1	0.88	1.0	234	8.7	8.3	33.8
22	Ottawa Silica Sand	2	0.87	1.0	1081	3.9	4.7	17.1

*Average superficial velocity calculated by Equation 55[112].

**$(Isr)_p = 0.19 \times 10^8$ for oil sample 1, and $(Isr)_p = 0.92 \times 10^8$ for oil sample 2.

all runs used a continuous displacement constant-flow rate pump. It is thought that the discontinuous displacement of the Milroyal pump could produce greater viscous instabilities in Run 1 and for that reason the oil recovery was very low. The oil displacement by water through porous materials is governed by nonlinear partial differential equations and therefore any small perturbation can produce large disturbances of the displacement front.

As the Aberfeldy heavy oil has a viscosity higher than 1000 mPa.s at 23°C, the immiscible displacement of this oil by brine in the reservoir or in a rectangular model is likely to be unstable. The following instability number proposed initially by Peters and Flock,[95] and modified by Bentsen,[96] was used to form an idea of the type of displacement achieved in the model.

$$Isr = \frac{\mu_w V(M-1-Ng)}{Kwor\ \sigma_e} \times \frac{M^{5/3}+1}{(M+1)(M^{1/3}+1)^2} \times \frac{4H^2W^2}{(H^2+W^2)} \qquad (62)$$

For horizontal displacement of viscous oil ($\mu_o \geq 1000$ mPa.s) by water, it is permissible to make the following simplifications with less than 0.1% of error:

$$M - 1 - Ng \simeq M$$

and

$$\frac{M^{5/3}+1}{(M+1)(M^{1/3}+1)^2} \simeq \frac{M^{5/3}+1}{M(M^{1/3}+1)^2}$$

finally, Equation 62 may be rewritten as follows:

$$Isr = \frac{4H^2W^2\mu_W V(M^{5/3}+1)}{(H^2+W^2)Kwor\ \sigma_e(M^{1/3}+1)^2} \qquad (63)$$

where σ_e is an effective or pseudo-interfacial tension and Kwor is the effective permeability to water at residual oil saturation.

Assuming, as did Peters and Flock,[95] that the effective interfacial tension is directly proportional to the water-oil interfacial tension, σ, then

$$\sigma_e = C\sigma \qquad (64)$$

where C is a wettability number, which is believed to be related to the wetting characteristics of the porous medium.

Using a value of σ_e = 7442 mN/m found by Peters and Flock[95] for displacement of Dow Corning oil by water (σ = 24.3 mN/m) through Ottawa sandpacks (80 - 120 mesh), the effective interfacial tension for the brinefloods (σ = 25.5 mN/m, an average of three values, Table 8) may be calculated as follows:

$$\sigma_e = 7442 \times \frac{25.5}{24.3} = 7809.4 \text{ mN/m}.$$

Finally taking, as did Demetre et al.[88], Kwor = K and $M = \mu_o/\mu_W$ and placing the following values into Equation 63:

W = 45.7 cm, L = 2.2 cm, σ_e = 7809.4 mN/m, and μ_W = 1.15 mPa.s

Equations 65 and 66 were obtained:

For oil sample 1 (μ_o = 1032 mPa.s):

$$Isr = 0.02115 \times 10^8 \frac{V \ (cm/s)}{K \ (Darcies)} \qquad (65)$$

and for oil sample 2 (μ_o = 4682 mPa.s):

$$Isr = 0.10305 \times 10^8 \frac{V \ (cm/s)}{K \ (Darcies)} \qquad (66)$$

Using Equations 65 and 66 the values of Isr that appear in Table 19 were calculated.

As the values of Isr for the immiscible displacement of Aberfeldy oil sample 1 by brine where in the range $\pi^2 < Isr \leq 900$ the displacement was unstable (transition region).[88] In turn, the instability number for the displacement of Aberfeldy oil sample 2 by brine (Run 22) was 1081 and the displacement was again unstable but located in the pseudo-stable region.[88]

It can be seen from Table 19 that brine breakthrough oil recovery increased with decreasing value of the instability number, which is a characteristic of unstable displacements in the transition zone[88,95]. For approximately the same instability number, a lower brine breakthrough oil recovery was achieved in the experiments than in those reported by Demetre et al.[88]. The difference could be due to the different geometries of the models used.

Waterflooding has been carried out in most of the major Lloydminster reservoirs since the mid-1960's with very poor efficiency, in the case of viscous oils. Adams[116] showed that recovery at water breakthrough has been less than 2% HCPV. The difference in recovery

between model and prototype may be due to the lack of homogeneity of the reservoir and the difference of values of Isr for model and prototype unstable displacements. While the model displacements of Aberfeldy oil sample 1 by brine was unstable, transition zone (π^2 < Isr < 900), the prototype displacement is likely to be pseudo-stable (Isr > 900) because of the width of the pattern (127.2 m). In the pseudo-stable zone the breakthrough recoveries are lower than in the transition zone and appear to be independent of the instability number. In conclusion, changing from the prototype-size system to the model-size system resulted in the unstable flow-regime changing from pseudo-stable to transition zone.

It is evident from Table 19 that the brine breakthrough oil recoveries for the Aberfeldy tank sandpacks were lower than those for the Ottawa silica sandpacks and that the opposite was true for the final recoveries. These were higher for the Aberfeldy tank sandpacks. The lower brine breakthrough recoveries for the Aberfeldy tank sandpacks may be explained by the higher values of Isr for these runs and the fact that viscous forces completely dominated the primary phase of brine injection, and sand wettability had a much smaller effect on breakthrough recovery. On the other hand, the higher final recoveries for the Aberfeldy tank sandpacks can be explained on the basis of a recent study carried out by Morrow et al.[105]. They observed that the miscroscopic displacement efficiencies and reductions in residual oil by water were higher for cores pre-exposed to crude oil and flushed with solvents (usually toluene) than for fresh cores. It seems that the adsorption on grain surfaces of polar materials from asphaltenes and resins, resistant

to toluene, improved the displacement of oil from pore bodies with trapping of oil commonly occurring in pore throats. The same phenomenon may have occurred in the recovery of oil sample 1 by brine from Aberfeldy sandpacks cleaned with solvents. It is seen from Figure 35 that higher recoveries were achieved in the model by flooding the Aberfeldy tank sandpacks with a large volume of brine, and the water-oil ratio curves were shifted to the right. This indicates that the Aberfeldy tank sandpacks had a lower relative permeability to brine than the Ottawa silica sandpacks. It is also interesting to observe that the special wettability characteristics of the reused Aberfeldy tank sandpack cleaned with toluene, isopropyl alcohol, and distilled water permitted oil flow at very low water-oil ratios during the subordinate phase of the brineflood (Run 4).

Finally, Figure 35 also shows that under the same operating conditions, brinefloods carried out using Ottawa silica sand to pack the model yielded similar recovery and WOR curves, while brinefloods performed in Aberfeldy tank sandpacks cleaned with solvents yielded very different recovery and WOR curves.

9.6.9. Mobilization of Viscous Residual Oil

To determine if subcritical carbon dioxide was able to displace viscous residual oil, several tertiary floods were carried out using the WAG and the CO_2 slug processes. Previous work in this area has been performed by various authors[5,13,14] using less viscous oils and tubes packed with unconsolidated sand.

A summary of the tertiary runs is presented in Table 20, and the

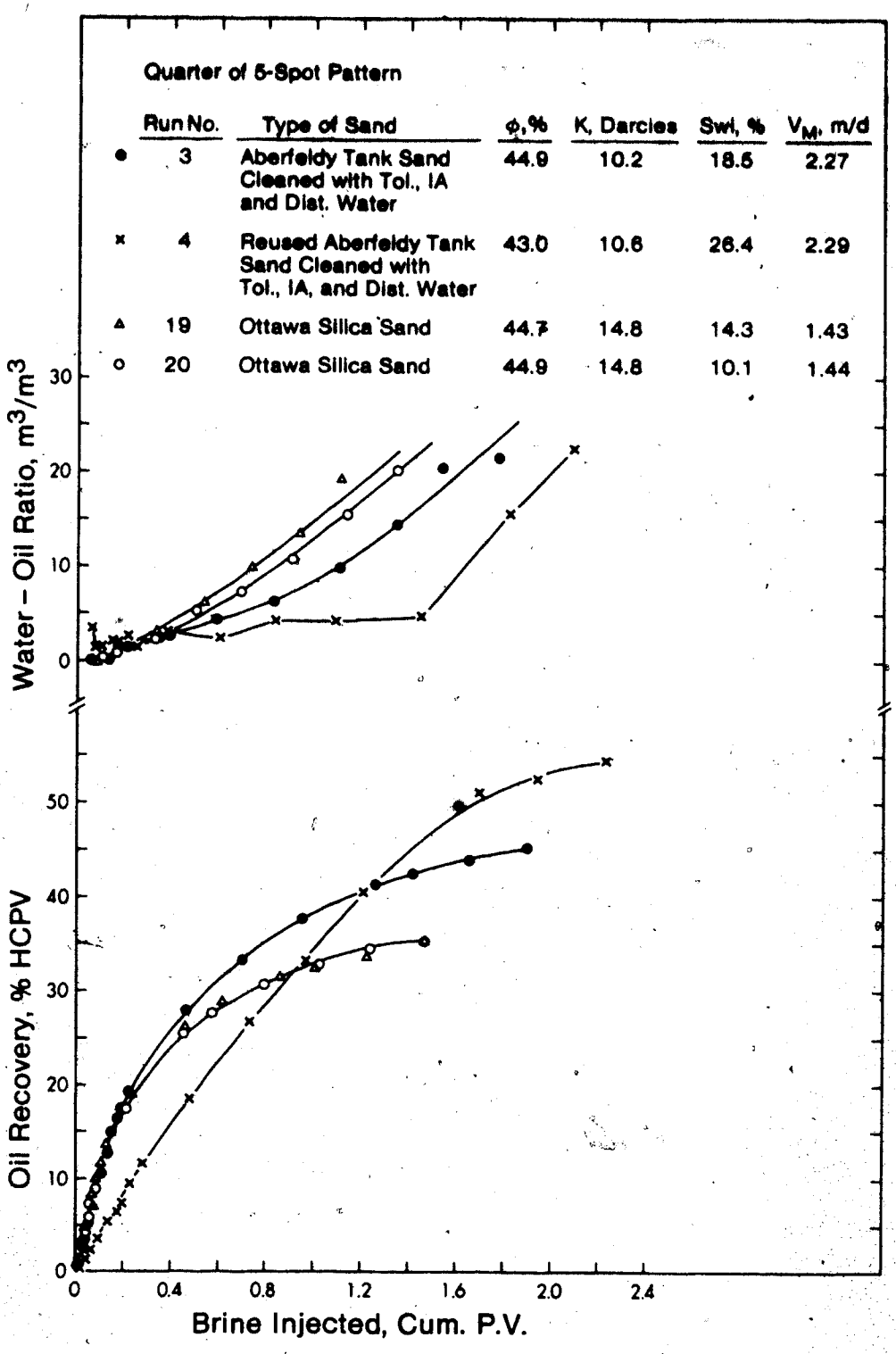


Figure 35. Effect of Type of Sand on the Brineflood Performance of Heavy Oil (1032 mPa.s @ 23°C)

TABLE 20

SUMMARY OF BASIC ECONOMIC PARAMETERS FOR TERTIARY RECOVERY OF HEAVY OIL BY INJECTION OF CO_2 AND BRINE

Run No.	Experiment Description	Total CO_2 Injected % HCPV	Oil Sample No.	Superficial Velocity, m/d		Tertiary Recovery*		Blowdown Recovery		CO_2 Retention % ***	CO_2 Required sm^3/m^3****
				CO_2	Brine	%HCPV	%Oil Left ABF**	%HCPV	%Tert. Rec.		
1	CO_2 Slug Driven by Brine	3.6	2	0.38	3.41	9.1	9.3	4.0	44.0	32.4	38.0
3	CO_2 Slug Driven by Brine	20.0	1	2.22	2.27	25.3	46.1	7.7	30.4	62.9	120.8
4	CO_2 Slug Driven by Brine	20.0	1	2.31	2.31	13.2	29.0	3.8	28.8	32.7	264.2
19	WAG 4:1 Process	20.0	1	1.43	1.43	13.5	20.9	1.9	14.1	63.7	145.0
20	WAG 1:1 Process	20.0	1	1.44	1.44	12.5	19.3	3.2	25.6	64.9	163.2
21	WAG 6:1 Process	20.0	1	0.88	0.88	12.6	19.0	1.7	13.5	50.4	154.1
22	WAG 4:1 Process	20.0	2	0.87	0.87	10.6	12.8	2.6	24.5	45.4	188.8

*Includes the blowdown recovery. Final WOR $\simeq$ 20 m^3/m^3.

**ABF = After Brineflood.

***Percentage of the total CO_2 injected left in the porous medium.

****Cubic metres of CO_2 required to produce a cubic metre of tertiary recovery.

individual production histories in graphical and tabulated forms can be found in Appendices G and H, respectively. Figures 36 and 37 show the oil recovery as a function of cumulative fluid injected for Runs 19-21 using three different WAG injection ratios 1:1, 4:1 and 6:1. These runs were performed using oil sample 1, Ottawa silica sand, and ten CO_2 slugs of 2% HCPV each. As was indicated earlier, moderate injection flow rates were chosen in order to scale down the dimensionless groups given in Section 9.6.6. In these runs, CO_2 breakthrough occurred after injecting 6 - 14.7% HCPV of CO_2 and the recovery at that point was less than 2.5% HCPV. The high volume of CO_2 injected after CO_2 breakthrough again indicates the good mobility control of CO_2 produced by the brine slugs in the WAG process as compared with the CO_2 slug process.

It was found that the oil recoveries for the three WAG ratios were very close. They ranged from 12.6 to 13.5% of hydrocarbon pore volume before brineflooding or 19 to 20.9% of hydrocarbon pore volume after brine flooding (see Table 20). As can be seen from Figure 38, the WAG 4:1 process yielded only one percent more recovery than either the 1:1 or 6:1 WAG processes.

Although there was no apparent difference in oil recovery for various WAG ratios, there was a measurable effect on the cumulative gas-oil and water-oil ratios (see Figure 39). Maximum cumulative GOR values similar to those observed in the WAG secondary floods were shown by the cumulative GOR histories of the WAG tertiary floods. It is also seen from Figure 39 that the WAG 4:1 tertiary flood has the lowest final cumulative GOR. This indicates that less production of CO_2 per cubic metre of oil occurred in this run than in the WAG 1:1 and 6:1

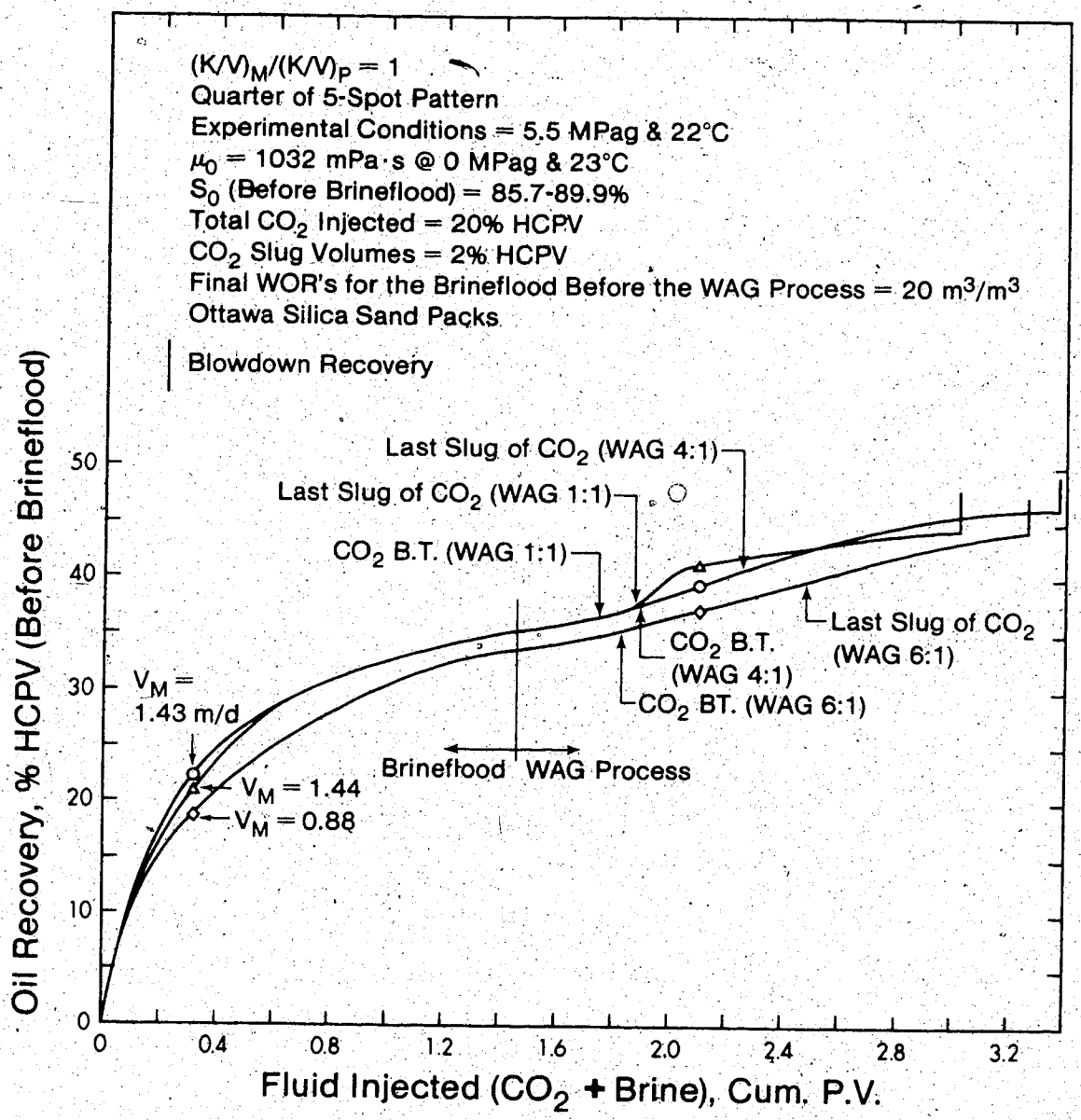


Figure 36 Increase of Heavy Oil Recovery by Injection of Brine Alternated with Subcritical CO_2 after Brineflooding.

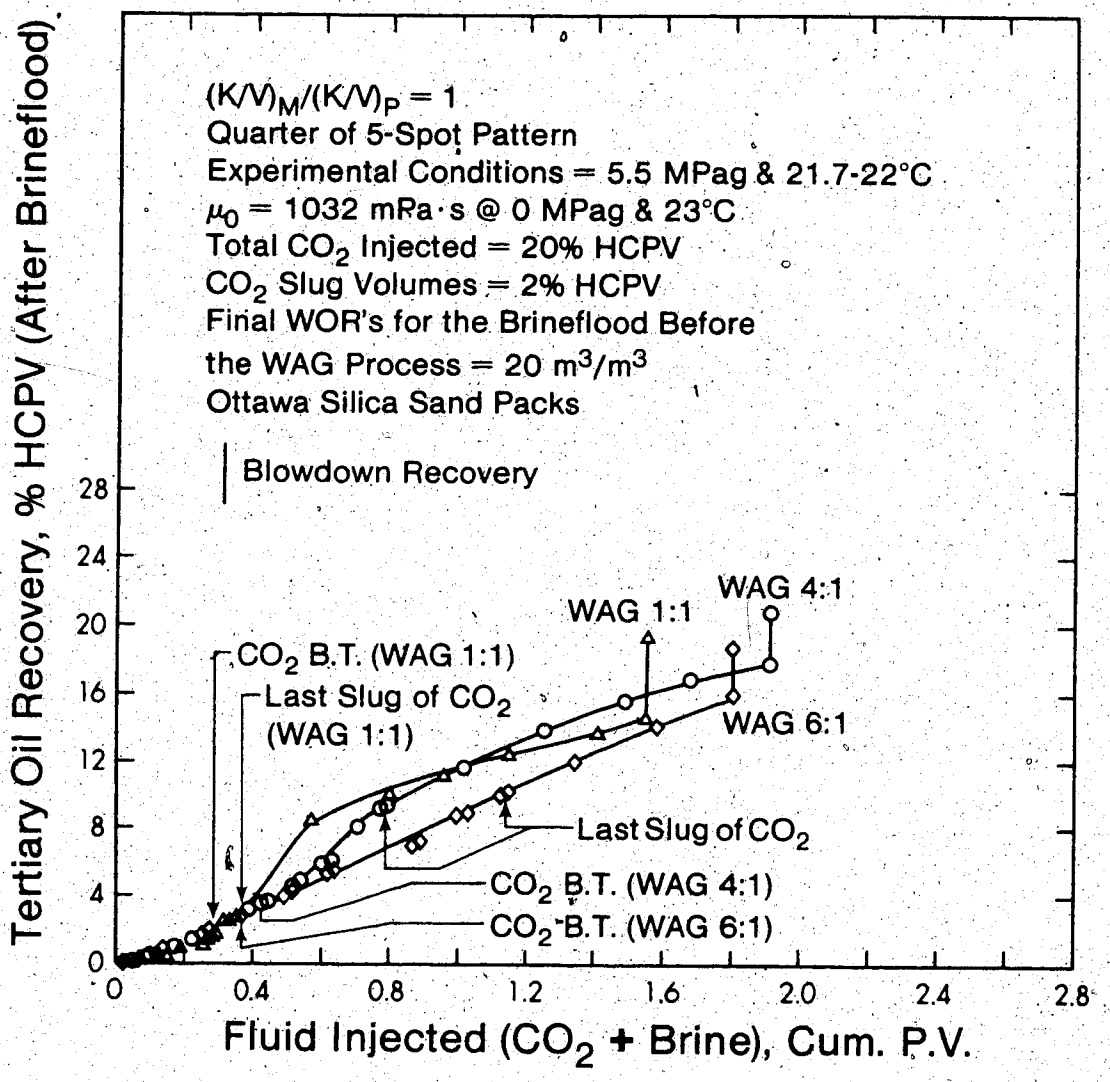


Figure 37 Effect of WAG Ratio on Production Histories of Tertiary Heavy Oil Recovery Floods

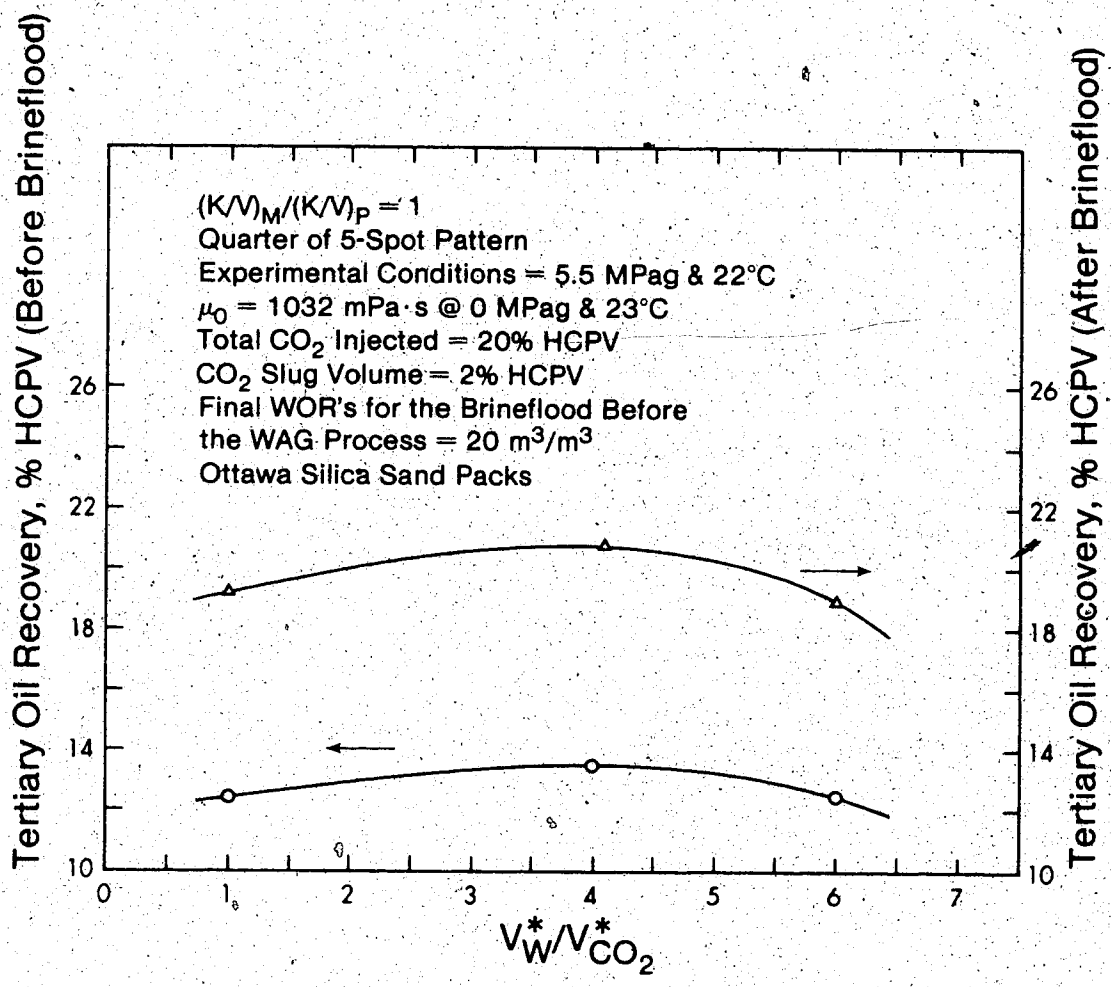


Figure 38 Effect of WAG Ratio on Tertiary Heavy Oil Recovery

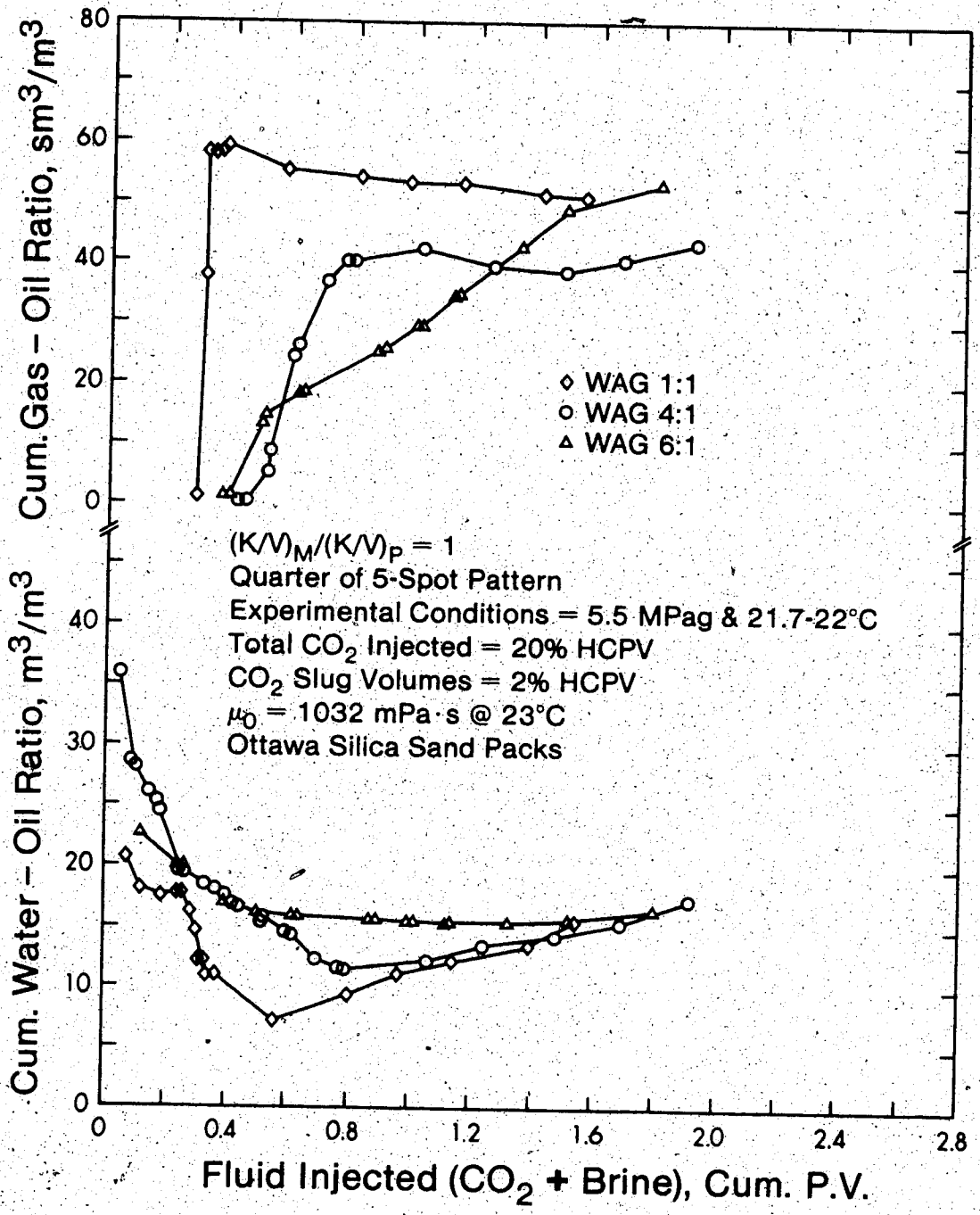


Figure 39 Effect of WAG Ratio on Cumulative Water-Oil and Gas-Oil Ratios of Tertiary Recovery of Heavy Oil

tertiary floods, and therefore the WAG 4:1 ratio was the best among the WAG ratios tested in controlling the high mobility of CO_2 in the porous medium. It is apparent from Figure 39 that the WAG tertiary floods had the same final cumulative WOR. However, the WAG 1:1 ratio yielded higher reductions in cumulative WOR and higher oil flow rates during the production of the oil bank.

A clear indication that subcritical CO_2 injection mobilized residual heavy oil is given by the increase of oil produced-fluid injected ratio (OPFIR) during the oil bank production observed in the production histories of the WAG tertiary floods (Figures H18-H20). The higher increase in OPFIR corresponded to the WAG 1:1 tertiary flood. However, the OPFIR for this run decreased rapidly after the production of the oil bank, which did not occur in the WAG 4:1 and 6:1 tertiary floods. Earlier, injection of the small slugs of CO_2 and brine in Run 20 (WAG 1:1 ratio) could have produced higher OPFIR's during the oil bank production.

The production histories of the WAG tertiary recovery runs had the following common features:

1) During the first quarter of CO_2/brine injection, low production of oil at high water-oil ratios was observed. High production of brine before the CO_2 breakthrough enables the carbon dioxide to contact residual oil.
2) Oil bank production started at moderate water-oil ratios at the same time as the carbon dioxide breakthrough occurred. This type of behaviour has been also observed in miscible field projects of tertiary recovery of light oils by carbon dioxide[9,142]. The mechanism

of oil bank formation may be visualized as follows. Mass transfer between CO_2 and oil swells the oil and reduces drastically its viscosity. The swollen oil forms a bank with higher saturation than the residual oil saturation, which moves through the porous medium along with brine and free CO_2. The in situ emulsification of the crude oil already explained (Section 9.3) may increase the volumetric sweep efficiency and reduce brine mobility.

3) The ratio of the volumes of the CO_2 and brine slugs had an important effect on oil bank formation. At high WAG ratios (i.e. 6:1) the over injection of brine produced a high water saturation at and behind the carbon dioxide front, and only a small increase in oil production rate was observed. In turn, at low WAG ratios (i.e. 1:1) the small slugs of brine did not control efficiently the production of CO_2 and high gas-oil ratios occurring after CO_2 breakthrough. However, the oil bank was produced at lower water-oil ratios than those in the tertiary WAG 4:1 and 6:1 floods.

4) After producing the oil bank the water-oil ratio started increasing again until it reached a value similar to that obtained at the end of secondary brineflooding.

As can be seen from Table 20 and Figures H2 and H3, unexpectedly high tertiary recoveries were achieved in Runs 3 and 4, for the CO_2 slug process. The recoveries ranged from 46.1 to 29% HCPV (after brineflooding). These two runs were carried out using oil sample 1 and Aberfeldy tank sand. It is thought that the wettability characteristics of these sandpacks, combined with the emulsification mechanism improved by the high superficial velocity used in these runs, were responsible for

the above-mentioned unusual recoveries.

Two oil banks were observed in Runs 3 and 4 (see Figures H2 and H3). The first occurred after CO_2 breakthrough, characterized by moderate oil production flow rates, high gas-oil ratios and very low water-oil ratios, and the second was observed some time after starting the brine injection to push the CO_2 slug through the porous medium. This oil bank showed higher oil flow rates than the former, low gas-oil ratios and moderate water-oil ratios.

The tertiary and secondary recovery production histories of Runs 16 and 19 using Aberfeldy oil sample 1, Ottawa silica sand, and the WAG 4:1 process are compared in Figure 40. The overall recovery was similar for secondary (CO_2 + brine) and secondary (brine) - tertiary (CO_2 + brine) conditions. The pore volume injected (CO_2 + brine) in the tertiary flood (after brineflooding) was also almost the same as the pore volume injected in the secondary flood. This indicates that to achieve the same level of recovery it is necessary to inject a much greater volume of brine under the combination secondary (brine) - tertiary (CO_2 + brine) condition than under secondary (CO_2 + brine) condition alone.

Figure 41 shows a comparison of the effect of the scaling group $V_W^*/V_{CO_2}^*$ (WAG ratio) on tertiary and secondary heavy oil recoveries by CO_2/brine injection. It can be seen that although the WAG ratio had a greater effect on secondary than on tertiary recovery, the optimum WAG ratio is 4:1 for both cases.

9.6.10. Blowdown Recovery

As explained earlier, blowdown recovery is the oil recovered upon

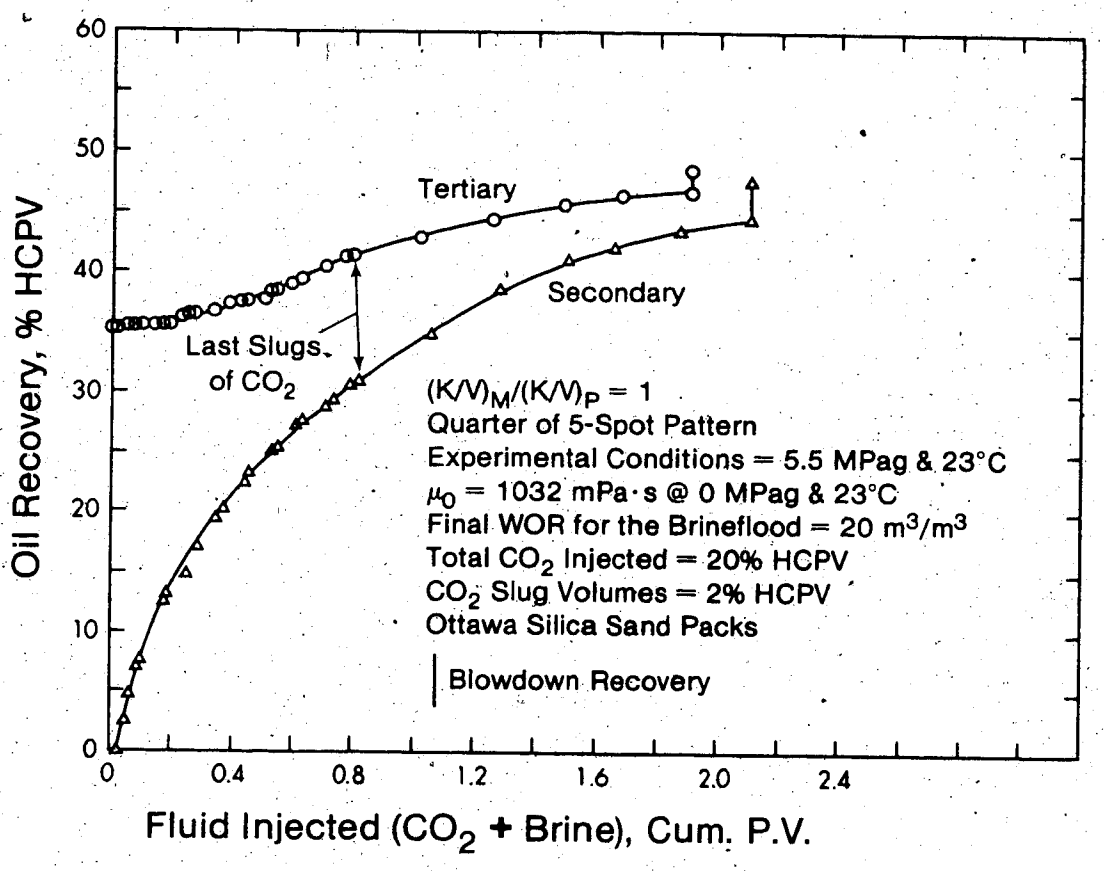


Figure 40 Comparison of Secondary and Tertiary Heavy Oil Recovery Using the WAG 4:1 Process

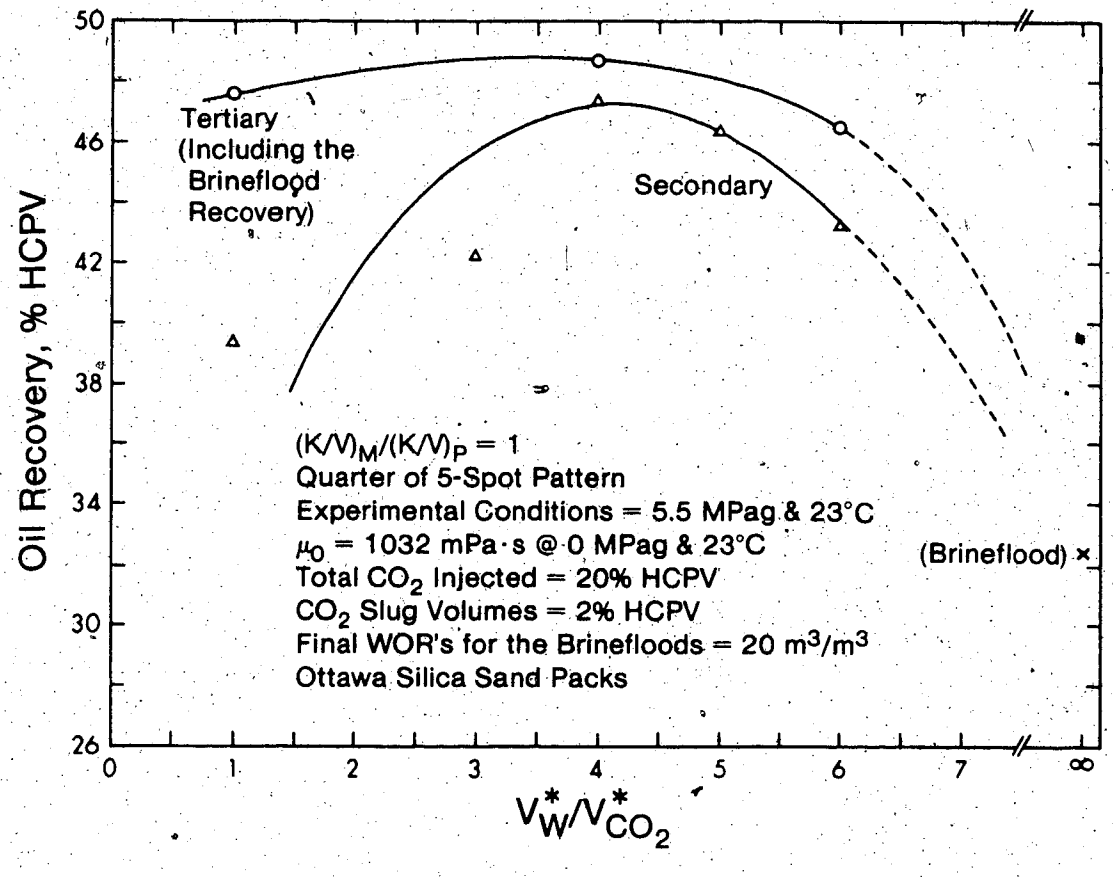


Figure 41 Optimal WAG Ratios for Secondary and Tertiary Recovery of Heavy Oil

the termination of a flood, when the reservoir pressure is depleted to a low value. The main drive mechanism is the expansion of oil, water, and free and dissolved carbon dioxide remaining in the reservoir after the injection of CO_2 and brine is stopped.

Blowdown recovery as a function of pressure for different CO_2/brine injection strategies is depicted in Figure 42. The three curves show the same hyperbolic shape indicating that the strategy used to inject the CO_2 and brine into the porous medium did not have any appreciable effect on the variation of blowdown recovery with pressure and therefore the same production mechanism applies for the strategies tested.

The blowdown recovery performance of 17 runs is presented in Figure 43. This figure shows a very good correlation between blowdown recovery and molar volume of CO_2. The pressure ($\sim$ 1.0 MPag) at which a sharp increase in recovery occurred corresponds to a very high increase in the molar volume of carbon dioxide. This behaviour was expected since the expansion of carbon dioxide is much higher than that of oil and brine. Also, as the CO_2 is more compressible than natural gas and nitrogen and therefore more expansive when pressure is released, the blowdown recovery in natural gas and nitrogen floods should be less than that in carbon dioxide flood for the same initial pressure, temperature, fluid saturations and crude oil composition.

The scattering shown by the points in Figure 43 may be due to the slight difference in the final fluid saturations at the beginning of the blowdown phases.

As pressures lower than 1-2 MPag are very difficult to achieve in heavy oil reservoirs under economical conditions, the blowdown recovery

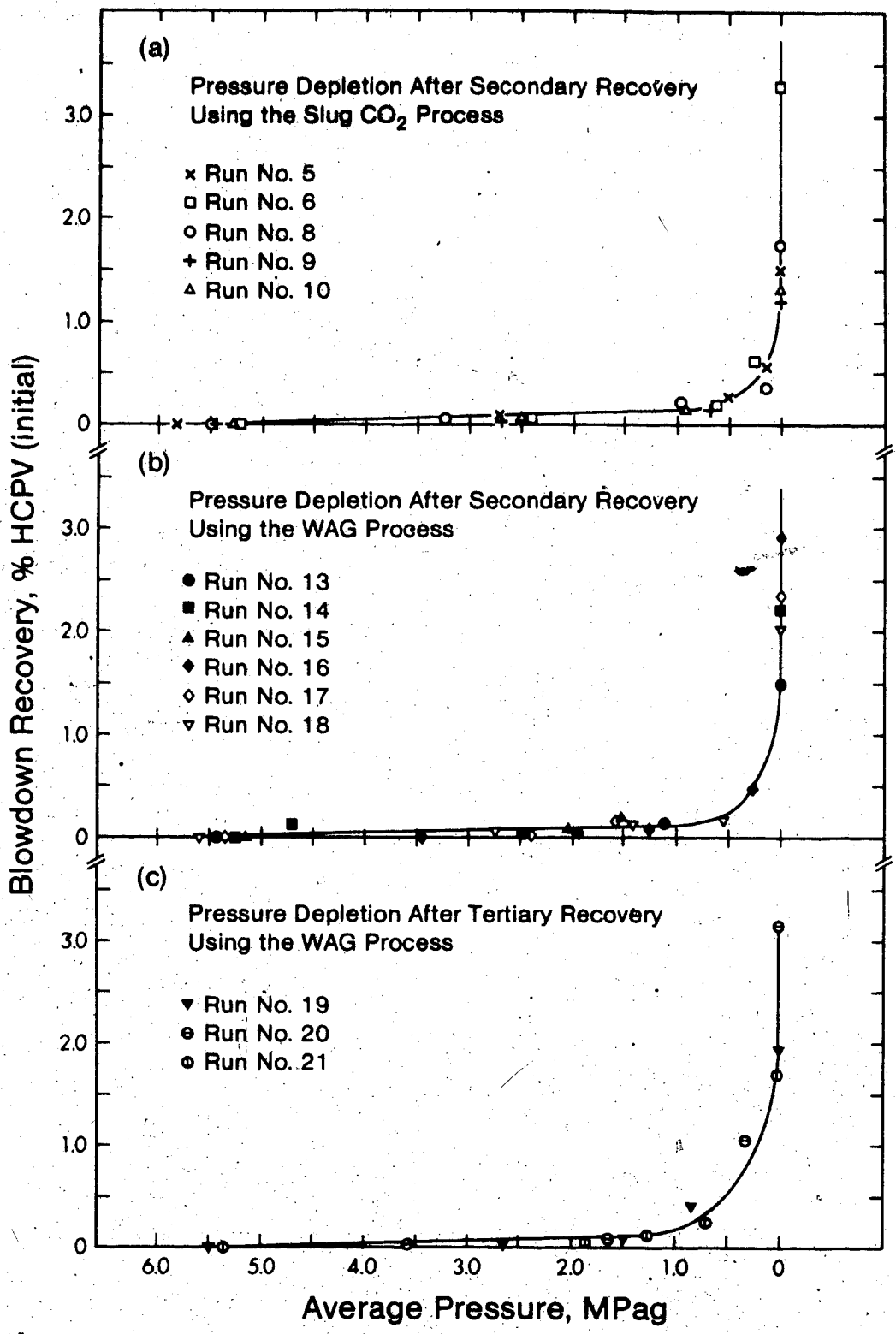


Figure 42 Variation of Recovery with Pressure During the Blowdown Stage of Heavy Oil (1032 mPa.s at 23°C) Displacements

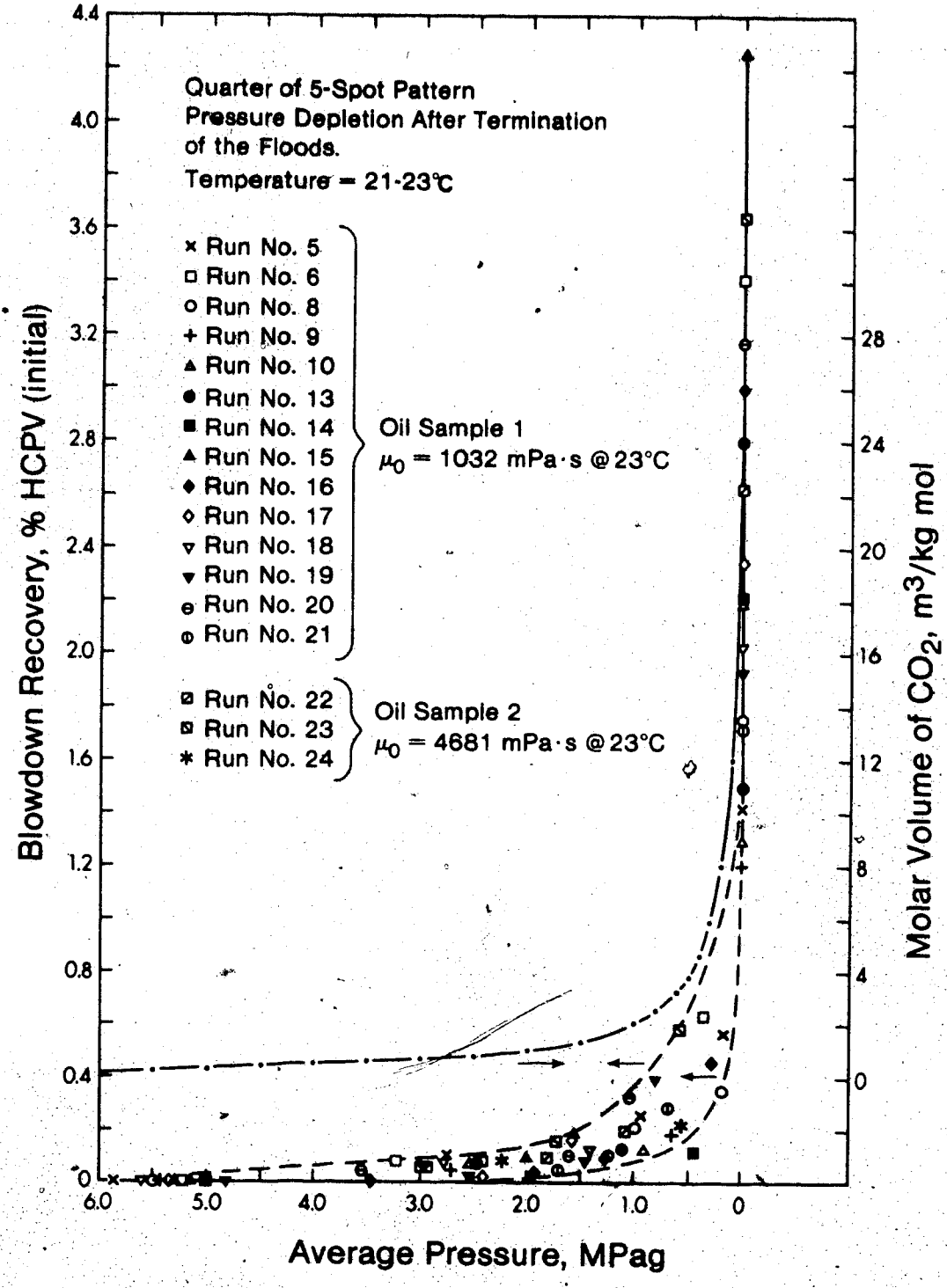


Figure 43 Effect of Pressure on Blowdown Recovery and Molar Volume of CO_2

in the prototype is likely to be lower than 0.5% of the original oil in place.

It can be seen from Table 20 that the tertiary oil production in the blowdown stage accounted for 13.5 - 40% (excluding Run 1) of the total tertiary oil production. In turn, the secondary oil production in the blowdown stage accounted for a lower percentage (less than 10%) of the total secondary oil production of the runs using Aberfeldy oil sample 1 (see Tables 16 and 17). The high percentage of the total tertiary recovery accounted for in the blowdown phase diminishes the economics of a field tertiary heavy oil project using subcritical CO_2 and brine in the Lloydminster area.

A sharp decline in the water-oil ratio was observed during the blowdown phase of all runs. Figures 44 and 45 show that the water-oil ratio decreased from 20-25 m^3/m^3 to less than 5 m^3/m^3. Because the average water saturation remaining in the porous medium upon the termination of a secondary recovery flood is lower than that in a tertiary recovery flood, the reduction in water-oil ratio during the blowdown stage was higher in the former than in the latter floods (see Figure 44). This important WOR decrease indicates that carbon dioxide displaced heavy oil somewhat preferentially even though a high water (mobile) saturation existed in the porous medium. It is interesting to note that a significant decrease in water production has also characterized carbon dioxide well stimulation field tests[22].

Because of CO_2 expansion during pressure depletion of the model, the gas-oil ratio increased with decreasing pressure. This behaviour, which was opposite to that observed for the water-oil ratio, can be seen

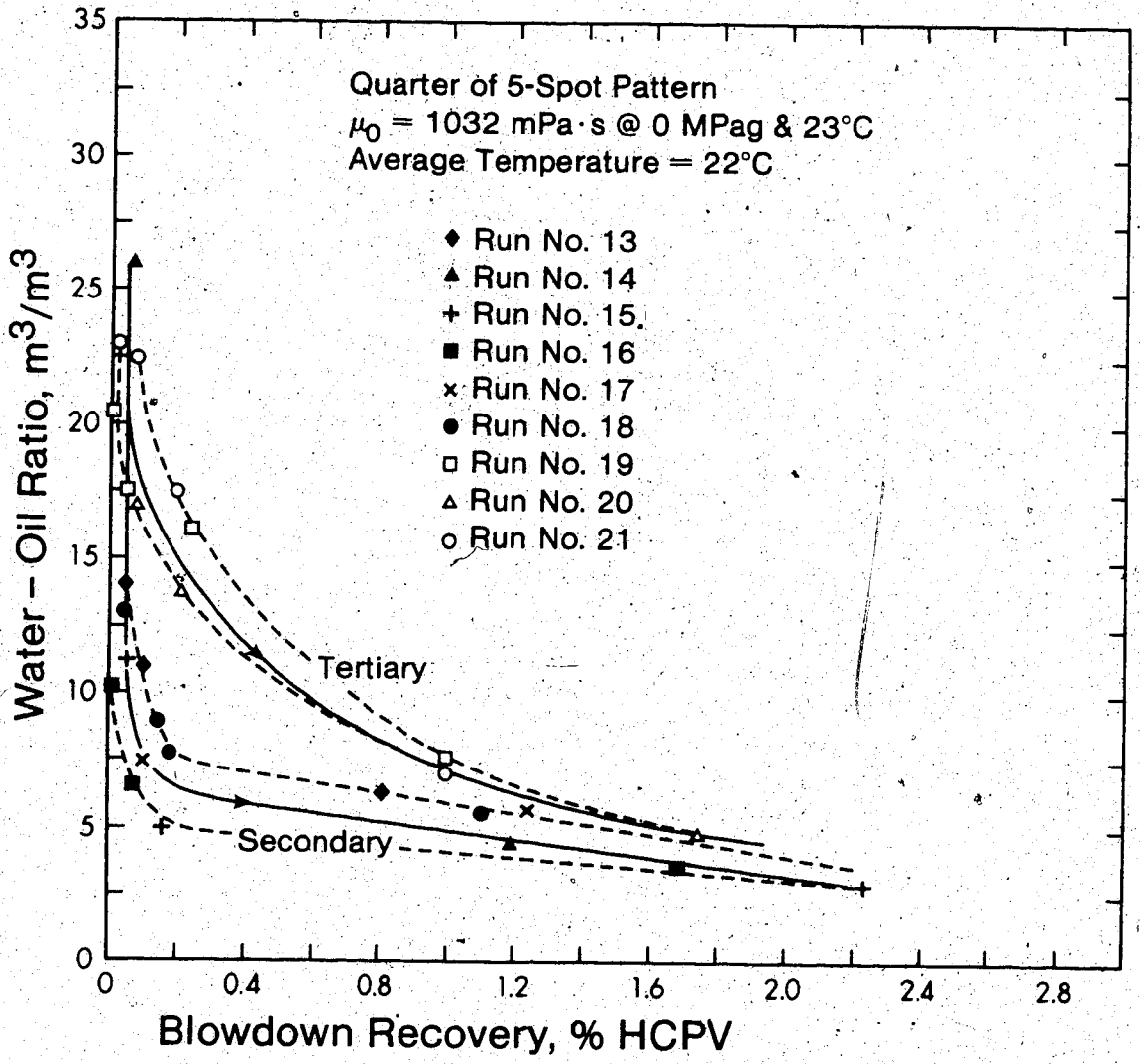


Figure 44 Variation of Water-Oil Ratio During the Blowdown Stage of the Displacements Using the WAG Process

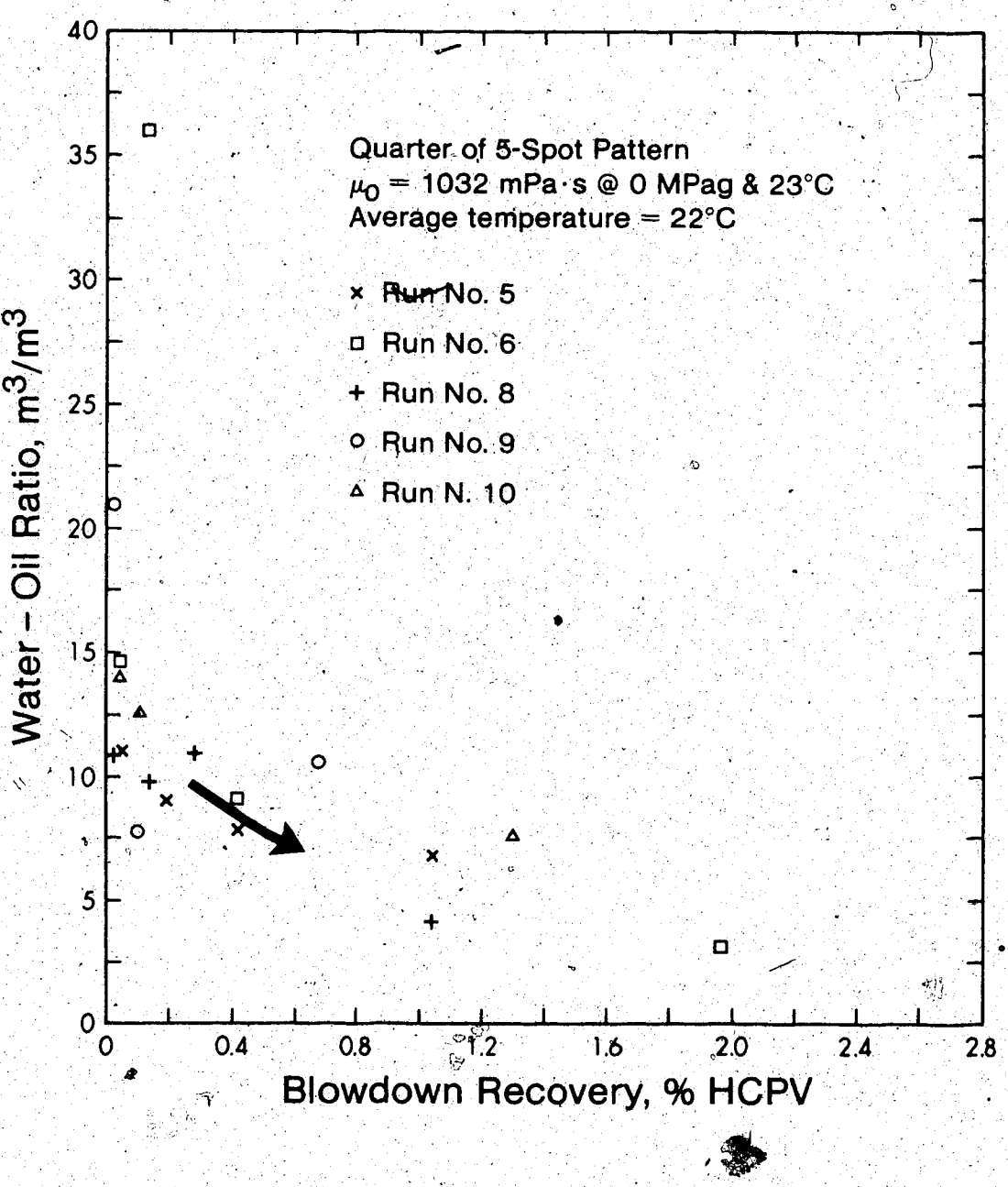


Figure 45 Variation of Water-Oil Ratio During the Blowdown Stage of Secondary Recovery Displacements Using the CO_2 Slug Process

in Figures H15 - H22. Some runs showed only a small increase in GOR during the blowdown stage since almost all free CO_2 had been produced before termination of the flood.

9.6.11. Effect of Oil Viscosity

Although the majority of the runs were carried out using Aberfeldy oil sample 1 (1032 mPa.s viscosity), several runs were performed using Aberfeldy oil sample 2 (4681 mPa.s viscosity) in order to examine the effect of oil viscosity on heavy oil recovery by CO_2/brine injection. The total amount of CO_2 injection was kept constant (20% HCPV).

It is seen from Figures 46-48 that for the different CO_2/brine injection strategies tested the recovery was higher for the less viscous oil. Nevertheless, the secondary recovery of oil sample 2 using the CO_2 slug and WAG processes were very similar indicating that for a very viscous oil the CO_2/brine injection strategy has no significant effect on recovery. As a result of this phenomenon, the decrease secondary oil recovery with increasing oil viscosity was higher for the WAG process (25% HCPV) than for the CO_2 slug process (11% HCPV) (see Figures 46 and 47).

The stabilizing effect on the brine front produced by a CO_2 preflush prior to brine injection was also observed in Run 24 where a 20% HCPV slug of CO_2 was driven by brine. It can be seen from Figure 49 that brine breakthrough was delayed by the preflush of CO_2. While for the conventional brineflood the brine broke through at 4.7% PV injected and the recovery at this point was 3.5% HCPV, for the CO_2 slug process the brine broke through at 6.3% PV injected and the recovery

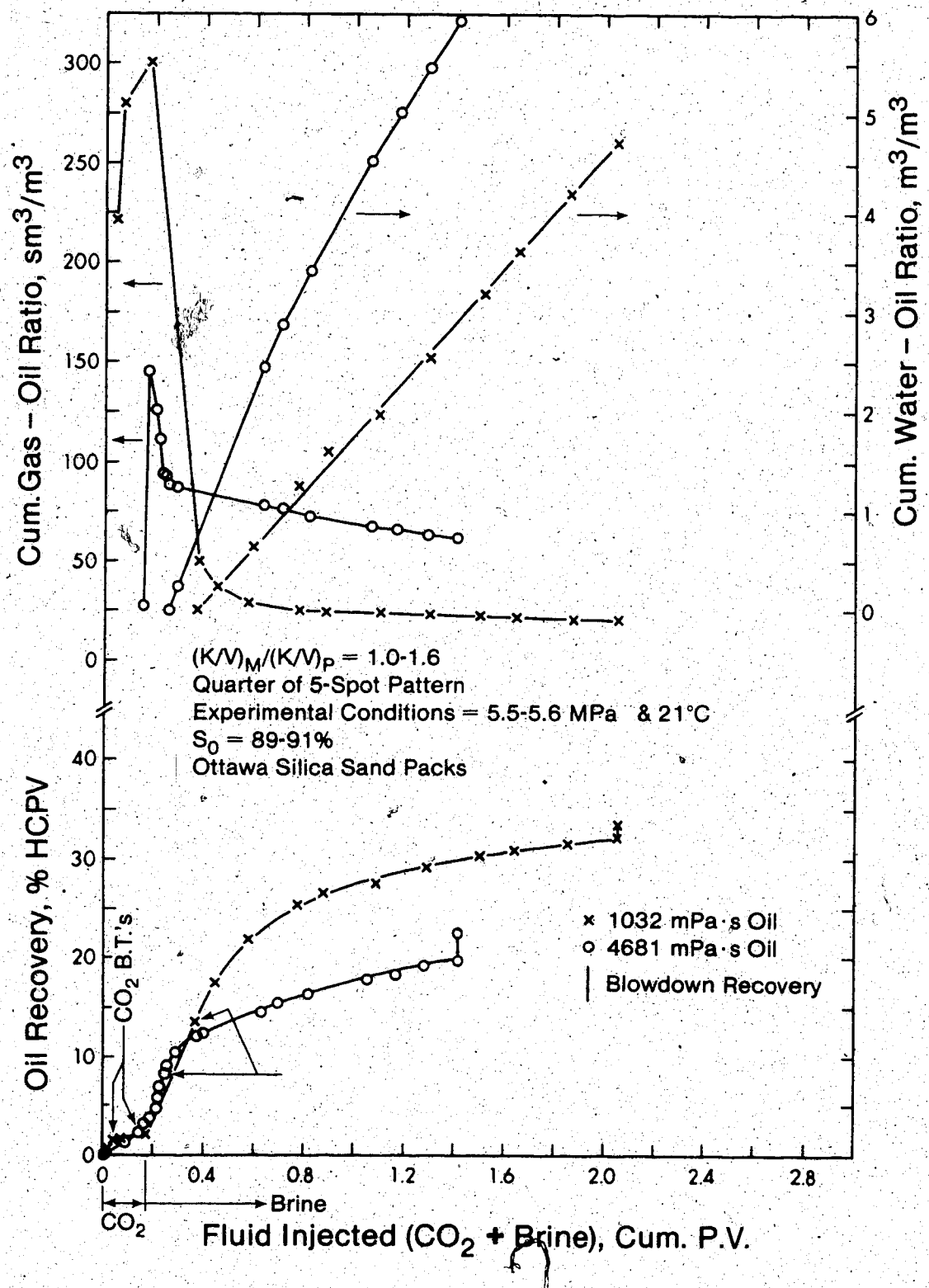


Figure 46 Effect of Viscosity on Heavy Oil Recovery by a 20% HCPV Slug of Subcritical CO_2 Driven by Brine

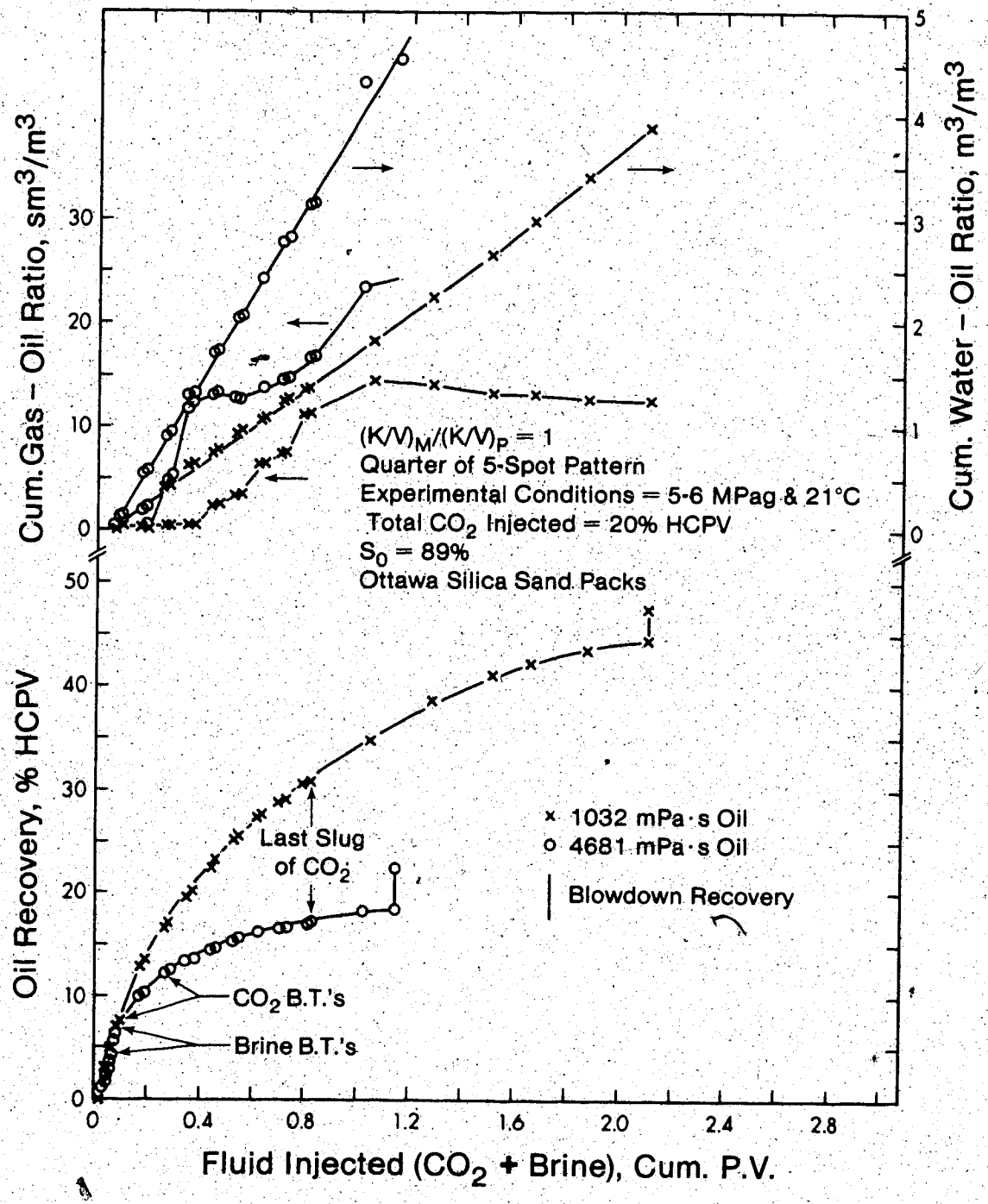


Figure 47 Effect of Viscosity on Heavy Oil Recovery Using the WAG 4:1 Process (CO_2 Slug Volumes = 2% HCPV)

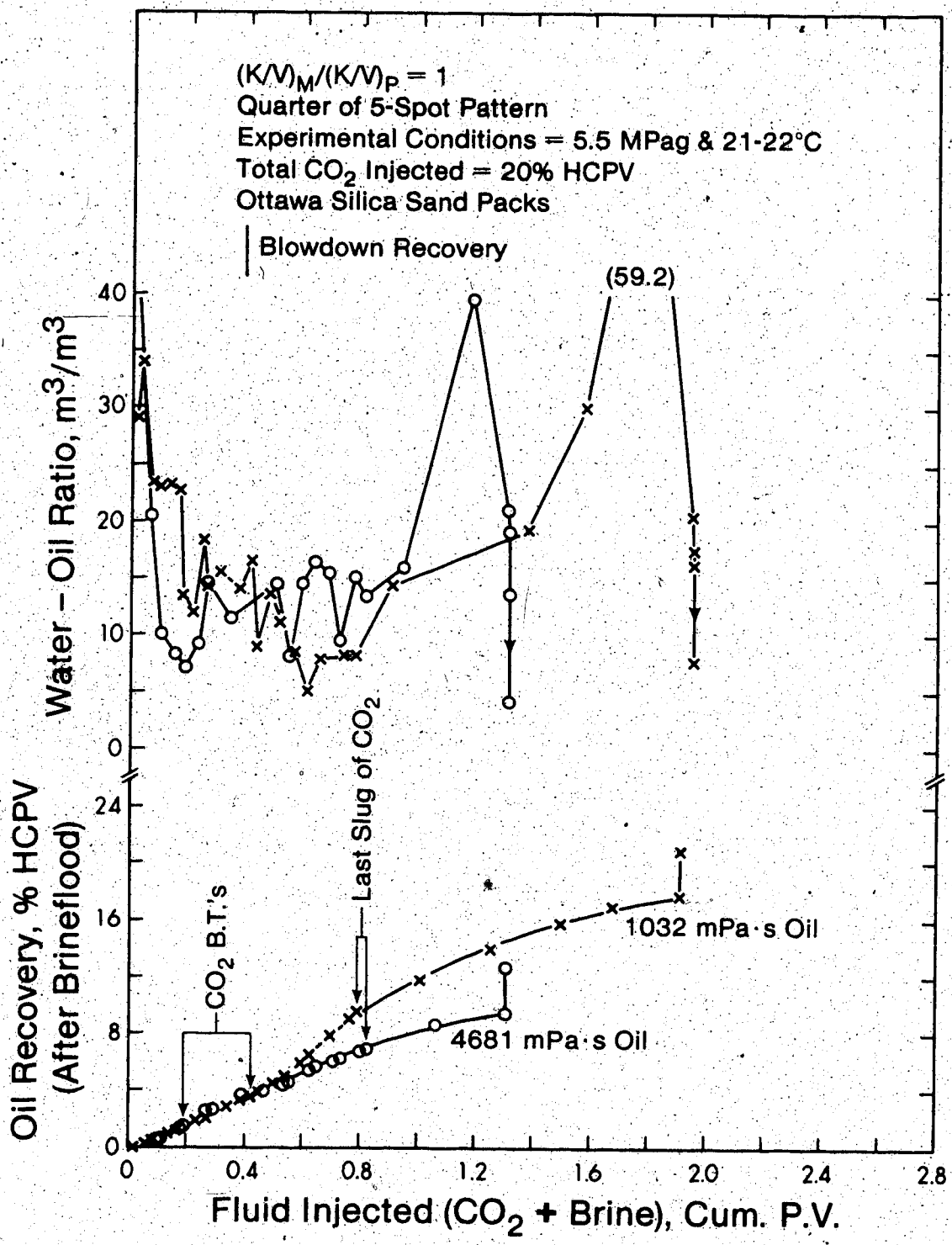


Figure 48 Effect of Viscosity on Tertiary Recovery of Heavy Oil Using the WAG 4:1 Process (CO_2 Slug Volumes = 2% HCPV)

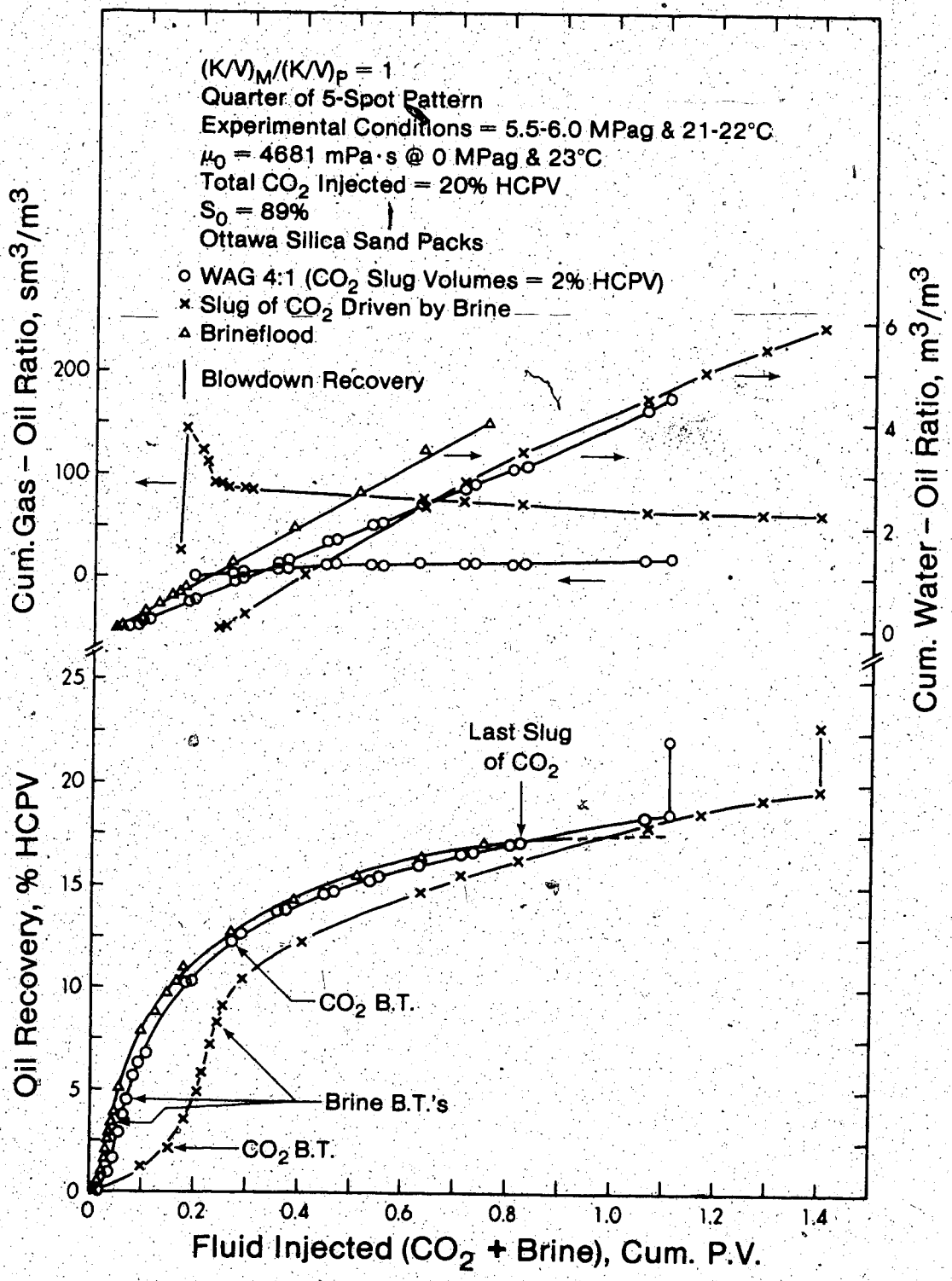


Figure 49 Comparison of WAG 4:1 and CO_2 Slug Processes with Brineflooding for Secondary Recovery of 4681 mPa.s Oil

by brine injection at this point was 4.5% HCPV. Although this brine-breakthrough delay was less noticeable than that for the less viscous oil, it still shows that the mass transfer between CO_2 and oil improved the flow properties of the 4681 mPa.s oil.

Much higher cumulative water-oil and gas-oil ratios were observed when the oil sample 2 was used in the experiments (see Figures 46 and 47). However, lower values of GOR were observed in Run 24 (4681 mPa.s oil) than in Run 9 (1032 mPa.s oil) during the injection of the carbon dioxide slug. This unexpected result is explained by the higher injection pressure required to displace the more viscous oil through the porous medium, and therefore a greater volume of CO_2 was dissolved in the oil.

Figure 48 shows that the WAG 4:1 process was also able to mobilize some residual sample 2 oil. The tertiary recovery of 4681 mPa.s oil was approximately 12% HCPV (after brineflooding), eight percentiles less than the tertiary recovery of the 1032 mPa.s oil achieved under the same experimental conditions. It can be observed in the same figure that subcritical CO_2 injection reduced the water-oil ratio from a high value of 30-40 m^3/m^3 to a value of 10-15 m^3/m^3. After the injection of the CO_2 slug the WOR increased again to 40 m^3/m^3 and then decreased drastically during the blowdown phase.

Finally, a smaller increase in oil produced-fluid injected ratio was observed in tertiary recovery of oil sample 2 (Run 22, Figure H21) as compared with that observed in the tertiary recovery of oil sample 1 (Run 19, Figure H18).

As was expected, the secondary and tertiary recovery efficiencies of Aberfeldy oil sample 2 were much lower than those of Aberfeldy oil

sample 1, indicating that an increase in viscosity of the crude oil and a decrease in CO_2-oil mass transfer and in oil mobility causes a marked reduction in heavy oil recovery by immiscible CO_2/brine injection.

A comparison of the recovery efficiencies of 4681 mPa.s oil yielded by injection of brine, a slug of CO_2 driven by brine, and alternate slugs of CO_2 and brine is shown in Figure 49. It is evident that the improvement in recovery over brineflooding obtained by CO_2/brine injection was achieved mainly in the blowdown stage of the floods. This indicates that gas drive was the main mechanism aided by carbon dioxide to the brine drive mechanism in the subcritical CO_2/brine injection to recover the more viscous oil.

The characteristics of the cumulative water-oil and gas-oil ratio curves as well as the delay in oil (sample 2) recovery observed in Figure 49 for the CO_2 slug process are similar to those shown in Figure 32 for oil sample 1, (see Section 9.6.6.1).

9.6.12. Basic Economic Parameters

In addition to extra oil recovery over brineflood recovery and cumulative gas-oil and water-oil ratios, the following economic parameters: CO_2 required to produce a cubic metre of oil and retention of CO_2 in the porous medium were also evaluated in this study.

9.6.12.1. CO_2 Requirement

Some economic parameters for secondary heavy oil recovery by injection of a 20% HCPV slug of CO_2 driven by brine are given in Table 16. For six out of seven runs the carbon dioxide required in

standard cubic metres to produce an extra cubic metre of Aberfeldy crude oil (over the oil produced by brineflooding) was lower than 400 sm^3/m^3. As can be seen in Table 17 the WAG process required a smaller amount of CO_2 to produce an extra cubic metre of oil than the CO_2 slug process. The CO_2 requirement for the WAG secondary runs ranged from 131.5 (WAG 4:1) to 286.2 sm^3/m^3 (WAG 1:1). A comparison of the two processes indicates that the CO_2 slug process required twice as much CO_2 as the WAG process and the total secondary recovery averaged almost 4 percentiles higher for the WAG than for the CO_2 slug process (see Table 18).

A higher amount of CO_2 to recover a cubic metre of oil was required for tertiary recovery (145 sm^3/m^3) than for secondary recovery (131.5 sm^3/m^3) using the same WAG 4:1 ratio which is thought to be the best WAG ratio, among those tested, for Aberfeldy oil. However, Table 20 shows that the CO_2 required for WAG 1:1 and 6:1 tertiary floods was only slightly higher than that for the WAG 4:1 tertiary flood. It can be seen in Table 17 that the effect of WAG ratio on CO_2 required was more pronounced for secondary than for tertiary recovery of Aberfeldy oil sample 1. A summary of the beneficial effect of the WAG 4:1 process on the recovery of the two Aberfeldy oil samples is shown in Figure 50.

A clear comparison of economic parameters for tertiary oil recovery using the WAG and the slug CO_2 processes could not be made since different types of sands were used in the WAG (Ottawa silica sand) and CO_2 slug (Aberfeldy tank sand) floods.

Although only a few runs were performed using Aberfeldy oil

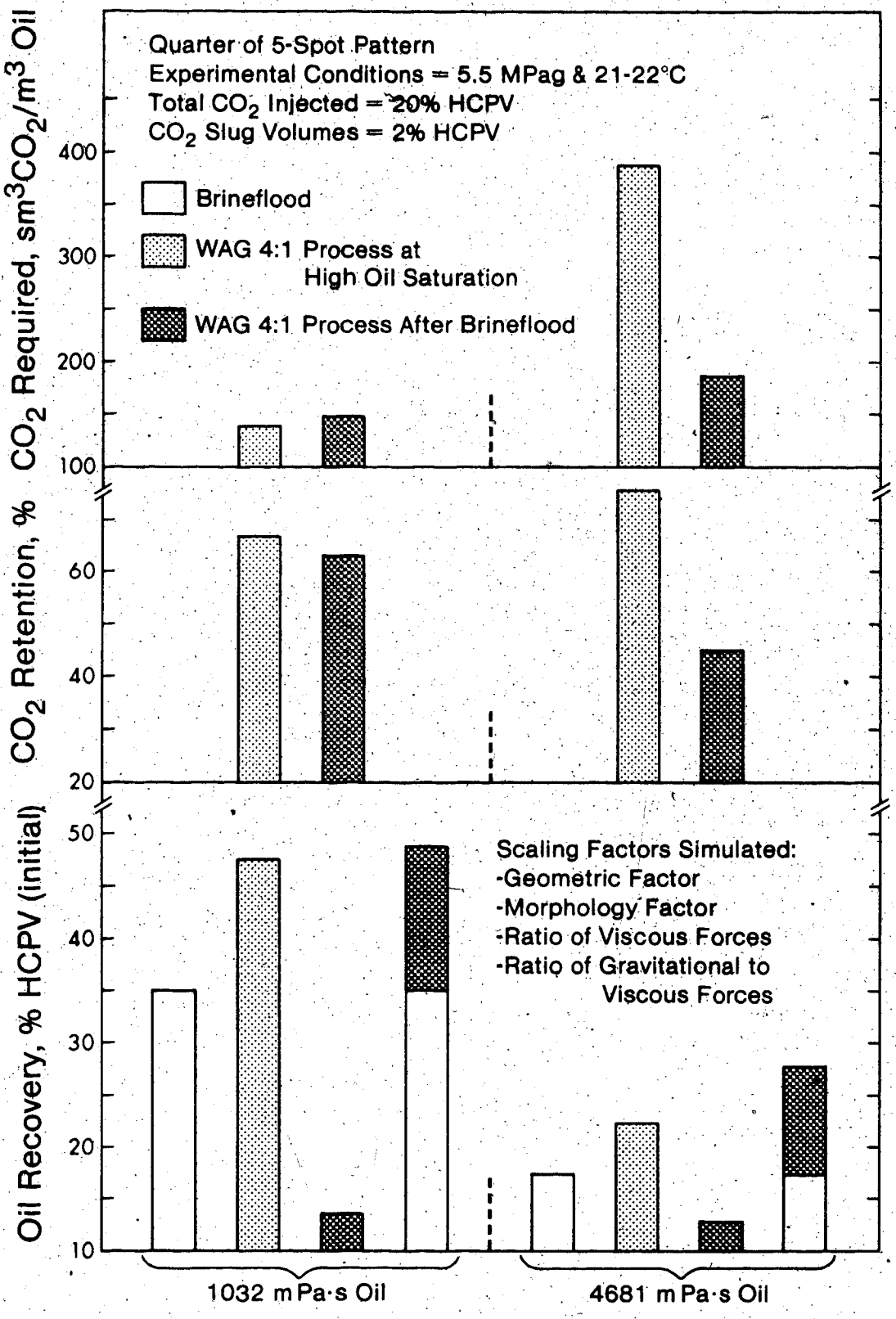


Figure 50 Comparison of Economic Parameters for Secondary and Tertiary Recovery of Two Viscous Oils Using the WAG 4:1 Process

sample 2, Figure 50 shows that the amount of CO_2 per sm^3 oil required to recover this crude oil was higher than that to recovery Aberfeldy oil sample 1. This indicates that the higher the oil viscosity the larger will be the requirement of CO_2.

Since the scaled physical model does not account for heterogeneities of the prototype and CO_2 leakoff outside of the patterns, the values of CO_2 required obtained in this study have to be adjusted upward to a value of approximately $1000 \cdot sm^3/m^3$ for a field application. This value represents the CO_2 requirement in field projects[9,21] of immiscible displacement of heavy oil by CO_2 and water.

The low experimental ($< 400\ sm^3/m^3$) and field ($\sim 1000\ sm^3/m^3$) requirements of CO_2 for immiscible displacement of heavy oil by CO_2 and brine as compared with the high CO_2 requirement for miscible displacement of light oils ($1500 - 3000\ sm^3/m^3$) is due to the fact that the mole fraction of CO_2 in the CO_2-oil mixture required to saturate a heavy oil with CO_2 is lower than that to achieve miscibility between CO_2 and oil. Also, the CO_2 required for immiscible displacement of heavy oil is much lower than the air requirement ($2500 - 3000\ sm^3/m^3$) for in situ combustion projects.

Finally, Figure 51 shows that high extra heavy oil recovery was achieved when carbon dioxide was used efficiently. High extra recoveries correspond to low requirements of CO_2 to produce an extra cubic metre of heavy oil.

9.6.12.2. CO_2 Retention

CO_2 retention measures the percentage of CO_2 injected that

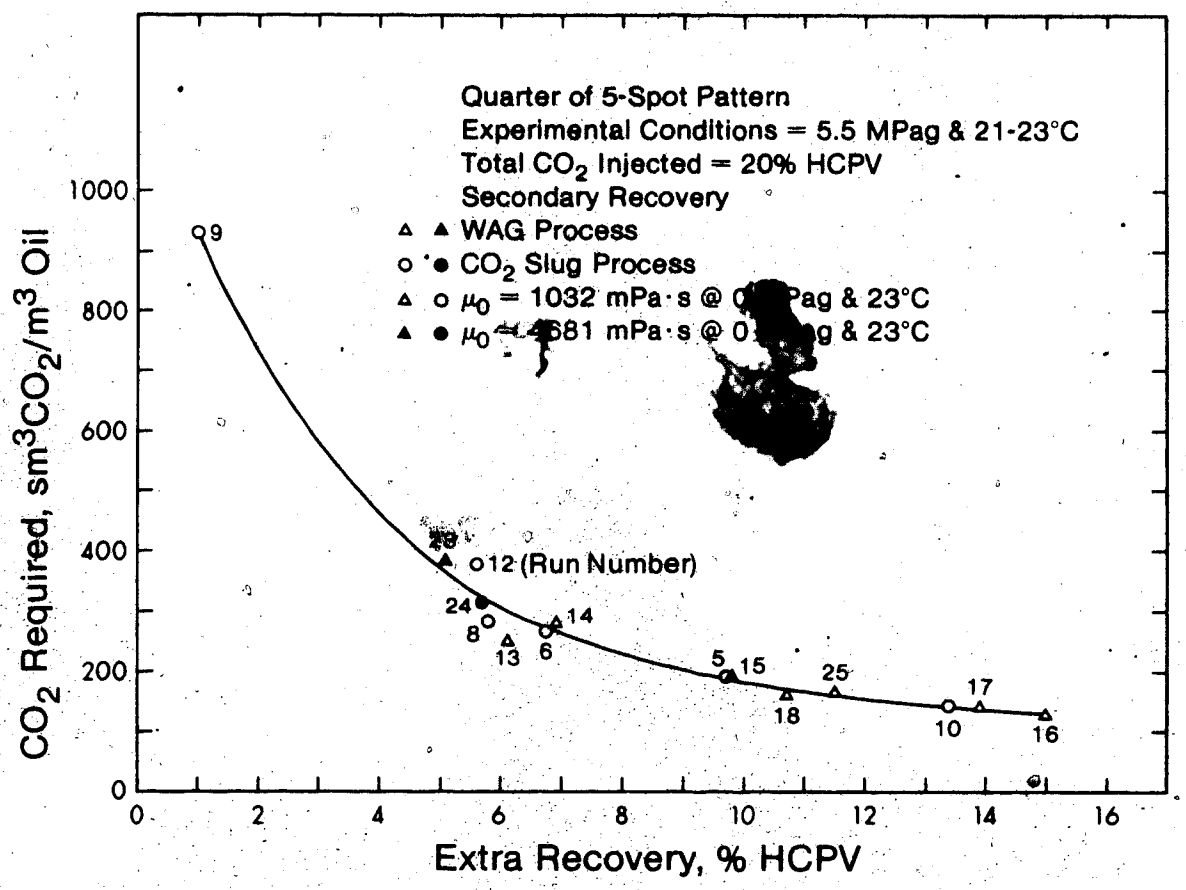


Figure 51 Carbon Dioxide Required to Displace Heavy Oil Using CO_2 Slug and WAG Processes

reacts with oil and brine, and that remains in the porous medium at the termination of a flood. Table 18 shows that for secondary recovery, the higher the CO_2 retention, the higher will be the overall recovery. Thus, the average CO_2 retention of the secondary WAG floods was 20% higher than that of the CO_2 slug floods. Although in a waterflooded sand, large amounts of CO_2 may be consumed by the brine to lower its pH, high increase in CO_2 retention in the WAG tertiary run was not evident as compared with that for the WAG secondary runs (see Tables 17 and 20). In general good oil recoveries were achieved where the CO_2 retention was higher than 60%. This means that in the prototype it may be possible to recycle 40% of the total volume of CO_2 required to recover the heavy oil.

Figure 52 shows the effect of CO_2 retention on blowdown recovery. It is seen in the lower part of Figure 52 that high blowdown recovery corresponded to high CO_2 retention in the porous medium. It can also be observed in the upper part of the same figure, on the average CO_2 retention and the blowdown recovery of the WAG secondary runs were higher than those for the CO_2 slug secondary runs.

9.6.12.3. Prototype/Model Time Scale

Writing Equation D-29 for prototype and model, the time scale ratio is given by

$$\frac{\tau_P}{\tau_M} = \frac{\left(\frac{Vt}{\phi L(1 - Sor - Swi)}\right)_P}{\left(\frac{Vt}{\phi L(1 - Sor - Swi)}\right)_M} = 1 \qquad (67)$$

Assuming that $(1 - Sor - Swi)$ is the same for the model and

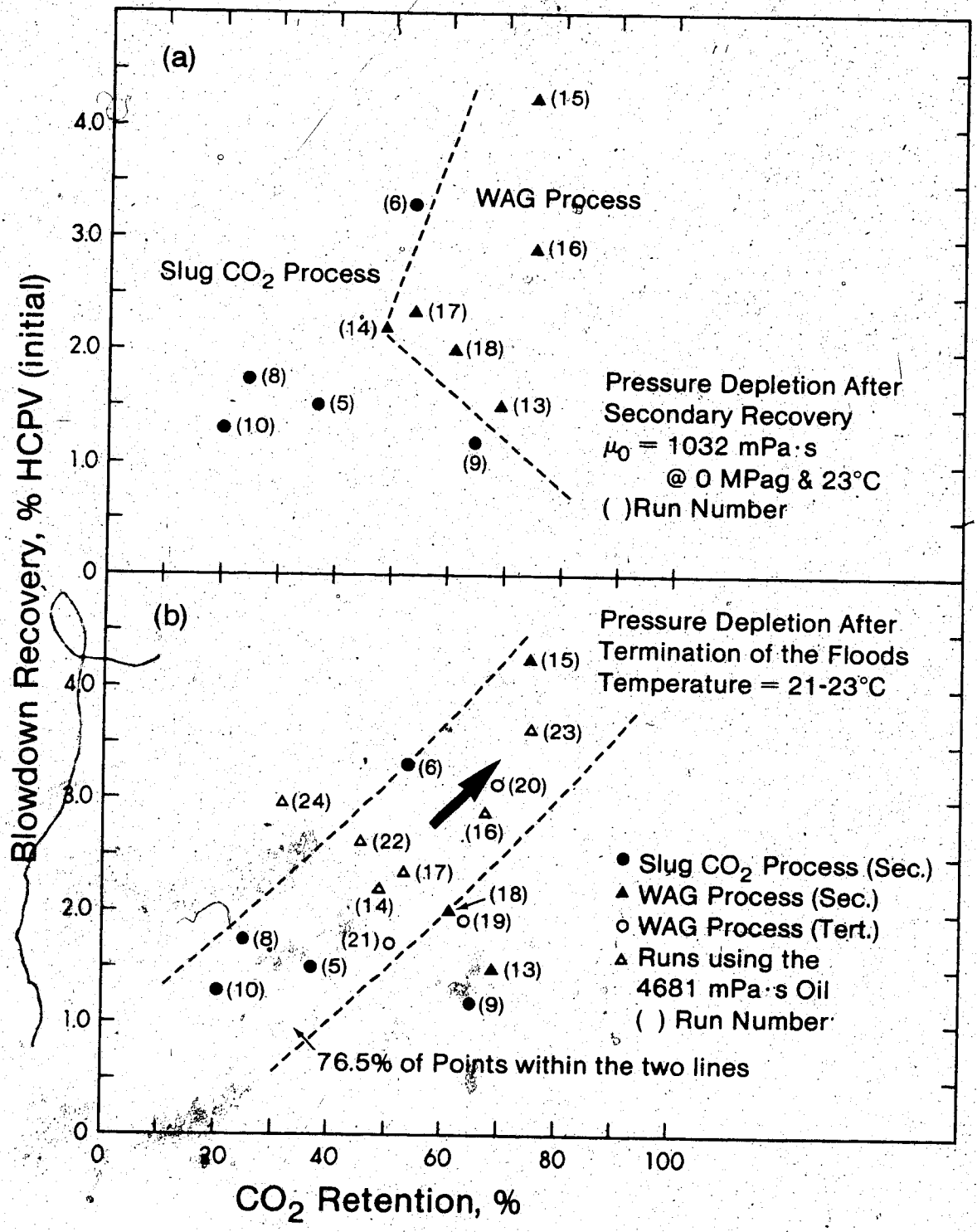


Figure 52 Effect of CO_2 Retention on Blowdown Recovery

prototype, Equation 67 can be written as follows:

$$\frac{\tau_P}{\tau_M} = \frac{L_M \phi_M V_P t_P}{L_P \phi_P V_M t_M} = 1. \tag{68}$$

From Equation 68 the prototype time, t_p can be expressed in terms of known parameters,

$$t_p = \frac{L_P \phi_P V_M}{L_M \phi_M V_P} t_M . \tag{69}$$

This equation was used to calculate the prototype time scale depicted in Figure 53 for a possible field application of the WAG 4:1 process before or after brineflooding in a uniform reservoir:

The following common features can be observed from Figure 53:

1) Most of the blowdown recovery was achieved early in the blowdown stage.
2) A WAG 4:1 secondary project may have a flood life two years longer than that of a brineflood in the same reservoir and at the same injection rate.
3) A WAG tertiary flood after brineflooding may have a flood life similar to that of a WAG secondary flood.
4) Obviously, the higher the oil viscosity the higher the viscous instability of the displacement, leading to a shorter flood life.

The above observations are limited by the fact that the model simulated a homogeneous reservoir.

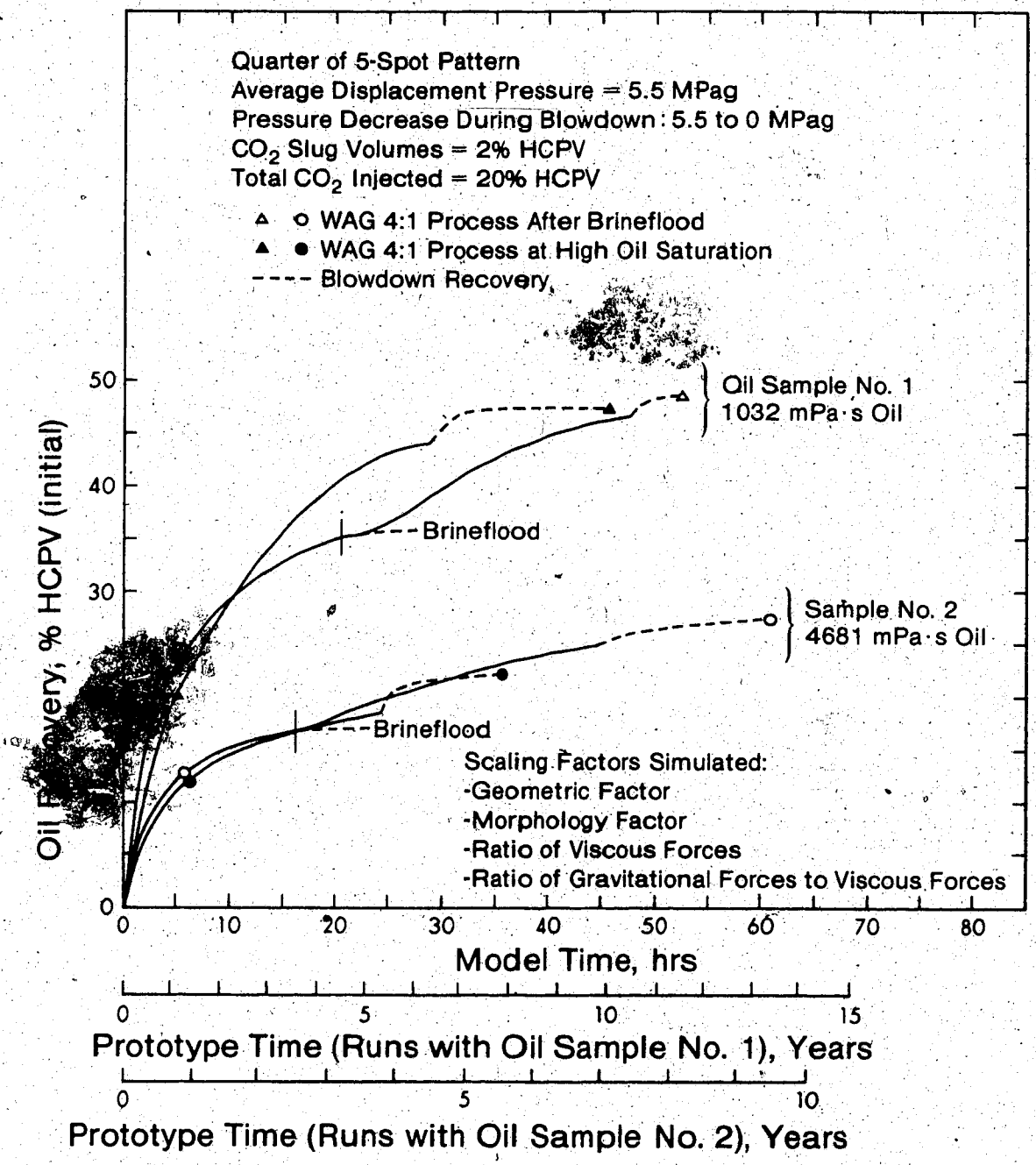


Figure 53 Secondary and Tertiary Oil Recovery Versus Model and Prototype Times. WAG 4:1 Process

9.6.13. Production of Sand Fines and Clay Minerals

Some production of sand fines and clay minerals was observed late in the subordinate phase of brine injection. It is believed that the following factors were responsible for this:

1) Aberfeldy tank sand and Ottawa sand have around 10% and less than 1% weight of grain sizes lower than 0.05 mm, respectively.
2) The diameter of the well perforations in the model was 0.05 mm.
3) The dried Aberfeldy oil samples had 0.5 - 1% vol. of sand and clay. As explained by Ignasiak et al.[143] the asphaltene fraction concentrates in large measure the oil wet clay minerals present in heavy oils. This difficulty suggests that the clay minerals have a high affinity for certain crude oil components.

In this study, sand fines and clay minerals were found associated with heavy ends (probably asphaltenes and resins) resembling a dark-yellow sludge. This sludge is a well dispersed sandfines-clay minerals/heavy ends/acidic brine mixture. After 24 hours of heating at 70°C, three phases were observed in the effluent sample collectors: dried oil at the top, dark-brown sludge at the interface oil-acidic brine and clear acidic brine at the bottom. The relative volume of the sludge was, in all runs, less than 10% of the total sample volume, and the most severe conditions for sludge formation appeared to be high volume of brine injection (tertiary oil recovery) and high fines content of the sand (Aberfeldy tank sand). As most of the sludge was brine, this was considered part of the volume of brine produced for the water-oil ratio calculations.

Clay minerals carry a permanent negative charge in their structural

framework. This positive charge deficiency may be balanced by the adsorption of positively charged organic ions. A good example could be the great difficulty in removing the fine clay associated with Athabasca bitumen[143]. According to Hill,[144] besides the clays, all inorganic minerals of extreme fineness also have a small cation exchange capacity, as a result of broken bonds around their edges. These materials include silica fines and silt. Bowman[145] also concluded in his study on molecular and interfacial properties of Athabasca tar sands that in oil-water systems, finely divided particles are capable of strongly stabilizing emulsions, regardless of their composition.

It seems that the slightly acid pH of the effluent brine and the type of cations present had a strong effect on the dispersion characteristics of the sludge in the brine. The Aberfeldy reservoir water used to push the CO_2 slug through the porous medium had a slightly alkaline pH due to the presence of 60 ppm of bicarbonate of calcium and magnesium (see Table 5). At high pressure the carbon dioxide reacted with the brine to lower its pH to a value of 5.4-6.5 and to precipitate small amounts of Ca, Mg, and Fe carbonates.

To observe the characteristics of the solids found in the sludge, some sludge samples from Runs 5, 7, 10, and 22 were analyzed. In all cases, a 2 cm^3 sludge sample was mixed with 18 cm^3 of dichloromethane. The mixture was centrifuged for one hour at 3000 rev min^{-1}. The dichloromethane acquired a dark color and the mixture of solids and some organic materials floated in between layers of brine and dichloromethane. The dichloromethane dissolved most of the organic

materials and the remaining solids had a texture similar to the sand fine/clay mineral mixture present in the dried oil used in the runs.

No plugging problem was encountered during the production of the sludge late in the subordinate phase of brine injection. Accumulation of sludge in the production well and tubing was not observed when washing the wells at the termination of the runs.

The presence of sludge in the aqueous phase of some effluent samples is a problem different from asphaltene flocculation observed in miscible displacement of light oil by carbon dioxide at high pressure.[51] Two factors can help avoid the flocculation of asphaltenes in immiscible displacement of heavy oil by CO_2: 1) the high amount of resins in heavy oils ($\sim$ 25 - 40%) acts as a strong peptizing agent for the colloidally dispersed asphaltene particles and protect them from any acid,[146]; 2) low molar fraction of CO_2 in the mixture heavy oil-CO_2 at the relatively low pressures of the immiscible displacement of oil by CO_2. The asphaltene solubility in an oil decreases with increasing amounts of gas dissolved in the oil.[147]

Several researchers[145,148] have found that the degree of dispersion of silt/clay/bitumen/water sludges is determined by the level of pH of the water. Speight and Moschopedis[148] found that a GCOS (Great Canadian Oil Sands) sludge with 22% solids formed a thick viscous mud when the water pH was lowered from 8.0 - 8.5 to 6.0. Variation in the water pH causes a change on the mineral particle surfaces by ion adsorption, thus affecting flocculation. In order to see the effect of brine pH on the settling characteristics of the sludge produced in Run 22, two samples with solid-organic complexes

(sludge) floating on the top of acidic brine were mixed with NaOH to pH levels of 9.8 and 10.4. At pH = 9.8 the sludge settled down in 15 min. and at pH = 10.4 in 30 min. These results show that, by adjusting the brine pH, it may be possible to overcome the sludge settling problem in a possible CO_2/brine injection project in the Lloydminster area.

Sand production is a major production problem in the Lloydminster area. Upon well completion the sand cut is as high as 30-40% vol. of gross production, after which the sand cut gradually decreases with time to approximately 1%. Numerous sand control techniques have failed to eliminate sand production and the operating companies have preferred to produce the sand rather than attempting to exclude it from the wellbore.

9.6.14. Reproducibility of Displacement Results

In order to test the reproducibility of displacement results, a pair of brineflooding runs were performed under identical operating conditions, using Ottawa sandpacks. The results are depicted in Figure 54. It can be seen that the reproducibility of the final recovery was within 0.3% HCPV. It is evident from Figure 35 that the reproducibility of displacement results was not good when Aberfeldy tank sand cleaned with solvents was used in packing the model.

Two secondary recovery floods (Runs 13 and 14) were carried out using the WAG 1:1 process and Ottawa silica sandpacks. The operating conditions were identical with the exception that the volume of CO_2 slugs was 2% HCPV in Run 14 and 4% HCPV in Run 13, but injecting the same total amount of CO_2 and maintaining the ratio of gravitational forces to viscous forces and the water-CO_2 ratio of slug volumes constant. As shown in Figure 55 the reproducibility of recovery was within 1%.

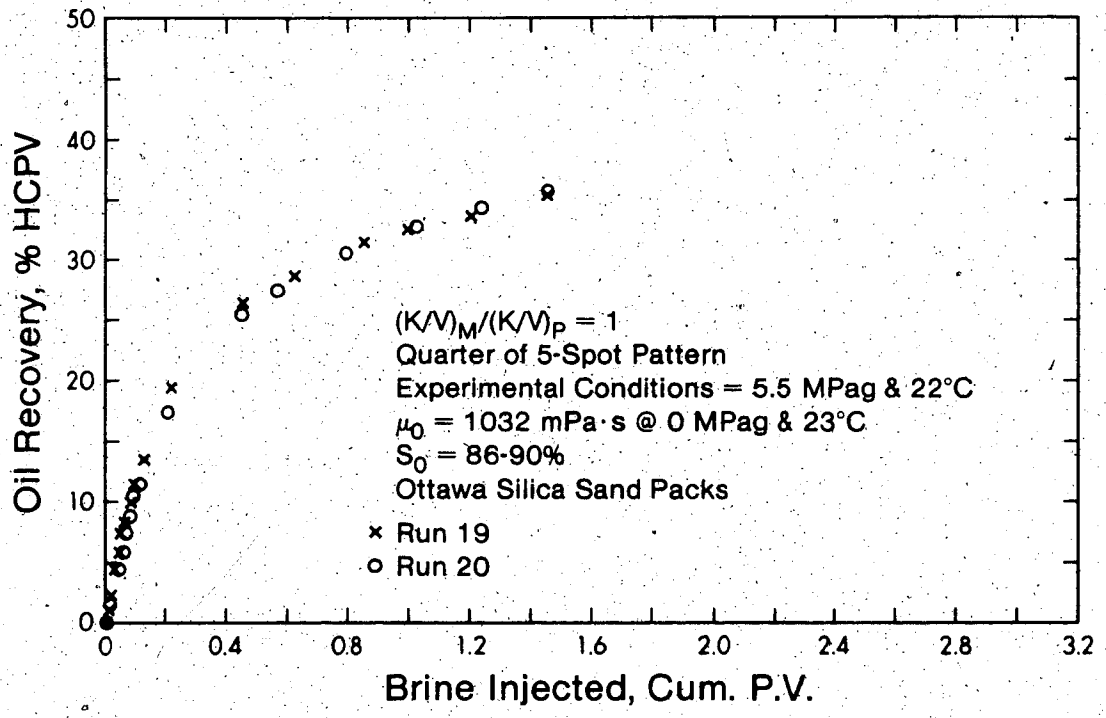


Figure 54 Reproducibility of Brinefloods Conducted Under Identical Conditions

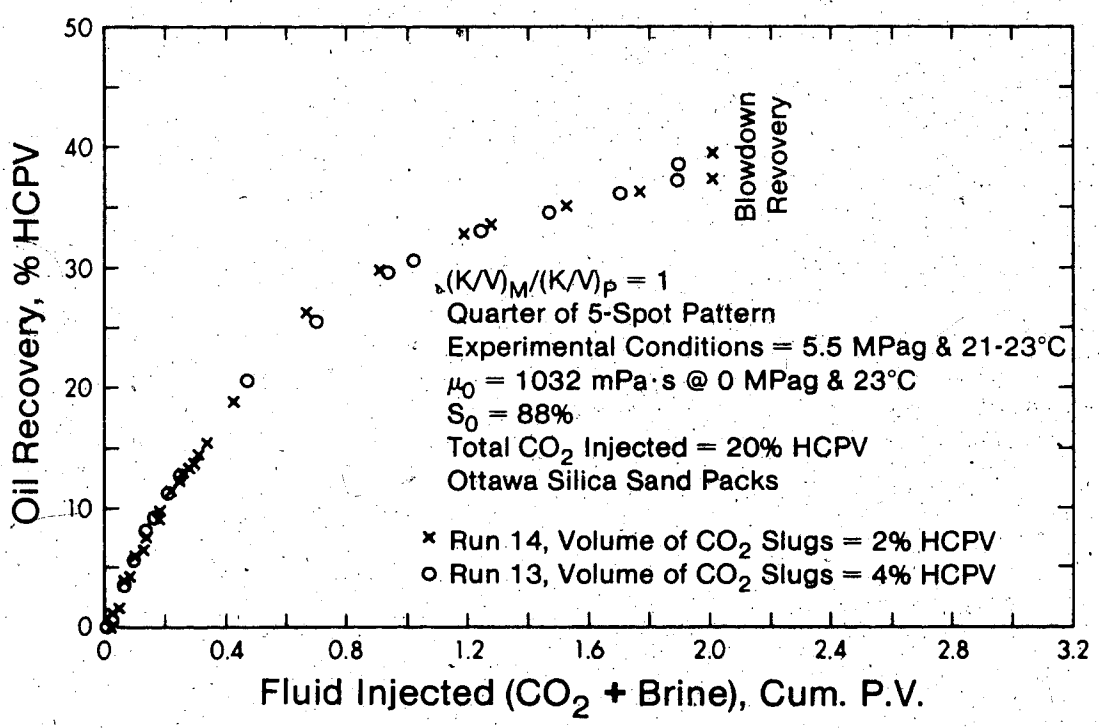


Figure 55 Reproducibility of the WAG 1:1 Process Varying Only the Volume of the CO_2 Slugs

The difference in recovery in both pairs of runs is within normal experimental errors.

10. CONCLUSIONS

This chapter presents the main conclusions drawn from this theoretical and experimental study on the immiscible displacement of heavy oil by subcritical CO_2 and brine. The conclusions follow approximately the same order as the list of objectives outlined in Chapter 2. Moreover, the conclusions may apply only to a prototype with geometric characteristics and sand-fluid properties similar to those used in this study.

1. On the basis of dimensional and inspectional analyses and after relaxing the capillary and inertial forces, the set of scaling groups to scale an immiscible displacement of heavy oil by CO_2 and water, taking into account the mass transfer among the phases was found to be:

   L/H, L/W, Mwo , Mgo , $\vec{g}K\Delta\rho_{og}/V\mu_g$, $\vec{g}K\Delta\rho_{wo}/V\mu_w$, Vw^*/Vg^*,

   $D_{Tgo}L/W^2V$, $D_{Tgw}L/W^2V$, $D_{Tgo}L/D_{Lgo}W$, $D_{Tgw}L/D_{Lgw}W$, ϕ , M

2. If model and prototype have the same morphology, the same fluids, and are operated at the same conditions of pressure and temperature, the requirements for scaling after relaxing the diffusive forces become

$$\frac{(L/H)_M}{(L/H)_P} = \frac{(L/W)_M}{(L/H)_P} = \frac{(K/V)_M}{(K/V)_P} = \frac{(Vw^*/Vg^*)_M}{(Vw^*/Vg^*)_P} = 1$$

3. A high pressure rectangular model, which was able to simulate different types of horizontal and inclined patterns for isothermal

displacement of oil was designed and constructed. It is concluded that this facility is suitable for simulating reservoir performance and provides a useful tool to develop a strategy for oil recovery.

4. Mass transfer between subcritical CO_2 and two Aberfeldy heavy oil samples by the solution and diffusion mechanisms was found to be very high. Saturation of the oil samples with CO_2 at 5.5 MPag & 21-21.5°C caused a moderate oil expansion ($\sim$ 15%) and significantly decreased the oil viscosity (> 95%). Molecular diffusion was also high ($\sim$ 3E - 05 cm^2/s at 5.5 MPag & 21-23°C), but the small amount of diffused CO_2 was not enough to produce a large reduction of oil viscosity.
5. Evidence of in situ formation of unstable brine-in-oil emulsions was obtained from the experimental results. The mass transfer between CO_2 and heavy oil and the in situ emulsification mechanism had a stabilizing effect on the brine front when the brine followed a slug of CO_2.
6. Subcritical carbon dioxide injection by itself was not an effective heavy oil displacing agent and the continuous CO_2 injection process is believed to be inapplicable to highly viscous oils. Conventional waterflooding may yield a higher recovery.
7. The highest extra oil recovery for the CO_2 slug process was achieved when the model was operated at low and high injection rates of carbon dioxide and brine, respectively.
8. The subcritical CO_2 slug (20% HCPV) process for secondary heavy oil recovery has the following disadvantages with respect to the WAG process: 1) longer oil production delay and higher production

of free CO_2 during the injection of the slug of CO_2; 2) lower overall recovery; and 3) higher CO_2 requirement.

9. The WAG ratio had a considerable effect on the secondary recovery performance of heavy oil (1032 mPa.s viscosity). The 4:1 WAG ratio was the best among five tested. The basic economic parameters of this WAG process were: an extra recovery of 15% HCPV over brineflood; a CO_2 requirement of 131.5 sm^3 to produce an extra cubic metre of oil; and a production of 32.5% of the CO_2 injected.

10. An increase in oil viscosity and therefore a decrease in CO_2-oil mass transfer and in oil mobility caused a marked increase in CO_2 requirement and a reduction in heavy oil recovery by immiscible CO_2/brine injection. For the more viscous oil (4681 mPa.s), the improvements in recovery over waterflooding was achieved mainly in the blowdown phase of the floods.

11. In all WAG tertiary floods there was a clear indication that subcritical CO_2/brine injection mobilized residual heavy oil and that an oil bank started to be produced at moderate water-oil ratios at the same time as CO_2 breakthrough.

12. Although there was no apparent difference in tertiary oil recovery by changing the WAG ratio, there was a measurable effect on the cumulative gas-oil and water-oil ratios of the floods. The 4:1 WAG ratio yielded the highest final recovery, the lowest cumulative GOR, and also the lowest CO_2 requirement.

13. From the point of view of field application, it is more efficient to start injecting the CO_2 when the reservoir has a high oil saturation. However, a secondary process (CO_2/brine) yields the

same overall recovery as a combination of secondary (brine) - tertiary (CO_2/brine) processes.

14. The main drive mechanism for the blowdown phase was observed to be the high expansion of the carbon dioxide when decreasing the model pressure.

15. The significant decrease in brine production that characterized the blowdown phase of all floods and the oil bank production stage of the tertiary recovery floods indicates that carbon dioxide displaced heavy oil somewhat preferentially to brine.

11. RECOMMENDATIONS FOR FURTHER STUDIES

The following studies should be undertaken to complement the present one:

1. The effect of pressure (6 - 10 MPa) on the efficiency of the WAG process should be evaluated with a view of comparing the effectiveness of subcritical CO_2 injection in recovering heavy oil.
2. The effect of slug size of CO_2 on the economic factors of heavy oil recovery is another task that should be undertaken.
3. Addition of a small amount of surfactant to the water to generate a foam with CO_2 in the porous medium should increase the mobility control of water and CO_2 and better results should be achieved. This idea should be tested.
4. As the subcritical CO_2/brine injection was observed to be able to mobilize residual heavy oil, there exists a possibility of using the WAG process for tertiary recovery of moderately viscous oils after steamflooding which should be studied.
5. The experimental data obtained in this study should be used in "calibrating" a compositional simulator which should take into account the changes of CO_2 - heavy oil mass transfer with pressure and time and the in situ formation of water-in-oil emulsions.

REFERENCES

1. Leonard, J.: "Annual Production Report," The Oil and Gas Journal, April 2, 1984, 83-105.

2. Beeson, D.M. and Ortloff, G.D.: "Laboratory Investigation of the Water Driven Carbon Dioxide Process for Oil Recovery," Trans. AIME, Vol. 216, 1959, 388-391.

3. Harvey, A.H. and Henry, R.L.: "A Laboratory Investigation of Oil Recovery Displacement with Carbon Dioxide and Hydrogen Sulfide," Paper SPE 6983, Soc. Pet. Eng. of AIME.

4. Rojas, G.: "Heavy Oil Recovery by CO_2 Injection. Laboratory Results and Field Tests," University of Oriente, Ven., Nov. 1981 (in Spanish).

5. Wang, G.C.: "Study of Carbon Dioxide Method for Enhanced Heavy Oil Recovery in Alabama," School of Mines and Energy Development, The University of Alabama, Oct. 1982.

6. Dosher, T.M. and Gharib, S.: "Physically Scaled Model Studies Simulating the Displacement of Residual Oil by Miscible Fluids," Soc. Pet. Eng. Jour., June 1983, 440-446.

7. Dickerson, L.R. and Crawford, G.W.: "Lab. Tests Show that CO_2 Scores Highest in Reducing Oil Viscosity," The Oil and Gas Journal, Feb. 22, 1960, 96-98.

8. Welker, J.R. and Dunlop, D.D.: "Physical Properties of Carbonated Oils," Jour. Pet. Tech., Aug. 1963, 873-876.

9. McRee, B.C.: "CO_2: How It Works Where It Works," Pet. Eng. Intl., Nov. 1977, 52-63.

10. Miller, J.S. and Jones, R.A.: "Physical Characteristics of Heavy Oil After CO_2 Saturation are Studied in DOE Tests," The Oil and Gas Journal, July 6, 1981, 135-145.

11. Kamath, K.I., Comberiati, J.R. and Zamerilli, A.M.: "The Role of Reservoir Temperature in CO_2 Flooding," Paper presented at the 5th Annual DOE Symposium on Enhanced Oil and Gas Recovery, Tulsa, Okla., Aug. 22-24, 1979.

12. Spivak, A. and Chima, C.M.: "Mechanisms of Immiscible CO_2 Injection in Heavy Oil Reservoirs, Wilmington Field, CA.," Paper SPE 12667 presented at the 1984 California Regional Meeting, Long Beach, CA., April 11-13, 1984.

13. Sankur, V. and Emanuel, A.S.: "A Laboratory Study of Heavy Oil Recovery with CO_2 Injection," Paper SPE 11962 presented at the 1983 California Regional Meeting, Ventura, CA., March 23-25.

14. Sankur, V., Creek, J.L., DiJulio, S.S. and Emanuel, A.S.: "A Laboratory Study of Wilmington Tar Zone CO_2 Injection Project," Paper SPE 12751 presented at the 1984 California Regional Meeting, Long Beach, CA., April 11-13.

15. Beecher, C.E. and Parkhurst, I.P.: "Effect of Dissolved Gas Upon the Viscosity and Surface Tension of Crude Oils," Petroleum Development and Technology in 1926, Pet. Div. AIME, 51-69.

16. Clark, N.J., Roberts, T.G. and Lindner, J.D.: "Engine Exhaust Gas Boots Heavy Oil Recovery," Pet. Eng., Aug. 1964, 43-47.

17. Davison, K.: "Inert Gas Boots Recovery From Heavy Oil Reservoirs," World Oil, March 1967, 98-105.

18. Simon, R. and Graue, D.J.: "Generalized Correlation for Predicting Solubility, Swelling and Viscosity Behaviour of CO_2-Crude Oil Systems," Jour. Pet. Tech., Jan. 1965, 102-106.

19. Jacobs, F.A., Donnelly, J.K., Stanislav, J. and Svrcek, N.Y.: "Viscosity of Gas Saturated Bitumen," Jour. Can. Pet. Tech., Oct.-Dec. 1980, 46-50.

20. Svrcek, W.Y. and Mehrotra, A.K.: "Gas Solubility, Viscosity and Density Measurements for Athabasca Bitumen," Jour. Can. Pet. Tech., July-Aug. 1982, 31-38.

21. Saner, W.B. and Patton, J.T.: "CO_2 Recovery of Heavy Oil: The Wilmington Field Test," Paper SPE 12082 presented at the 58th Annual Technical Conference and Exhibition, San Francisco, CA., Oct. 5-8, 1983.

22. Patton, J.T., Sigmund, P., Evans, B., Ghose, S. and Weinbrandt, D.: "Carbon Dioxide Well Stimulation: Part 2 - Design of Aminoil's North Bolsa Strip Project," Jour. Pet. Tech., Aug. 1982, 1805-1810.

23. Davies, G.A., Ponter, A.B. and Craine, K.: "The Diffusion of Carbon Dioxide in Organic Liquids," Can. Jour. Chem. Eng., Dec. 1967, 372-376.

24. Rajan, S.M. and Goren, S.L.: "Gas Absorption by Drops Traveling on a Vertical Wire," AIChE Jour., Jan. 1967, 91-96.

25. McManamey, W.J. and Woollen, J.M.: "The Diffusivity of Carbon Dioxide in Some Organic Liquids at 25°C and 50°C," AIChE Jour., May 1973, 667-669.

26. Denoyelle, L. and Bardon, C.: "Diffusivity of Carbon Dioxide into Reservoir Fluids," Paper CIM 115-15:.30 presented at the 86th CIM Annual General Meeting, Ottawa, April 17, 1984.

27. Schmidt, T., Leshchyshyn, T.H. and Putagunta, V.R.: "Diffusivity of Carbon Dioxide into Athabasca Bitumen," Paper CIM 82-33-100 presented at the 33rd Annual Technical Meeting of the Petroleum Society of CIM, Calgary, Alta., June 6-9, 1982.

28. Mungan, N.: "Carbon Dioxide Flooding - Fundamentals," Jour. Can. Pet. Tech., Jan. - March 1981, 87-92.

29. Barder, B.E., Fox, R.L. and Stosur, J.J.: "The Potential of Down Hole Steam Generation to the Recovery of Heavy Oils," Presented at the UNITAR First International Conference on the Future of Heavy Crude and Tar Sand, Edmonton, 1979. McGraw-Hill, Inc., 369-377.

30. Killesreiter, H.: "Competing Effect of Temperature and Dissolved Gas on the Viscosity of Petroleum," Erdol Kohle Erdgas Petrochem., Sept. 1982, 428-431.

31. Goss, M.J. and Exall, D.I.: "Experimental Investigations of the Transport Mechanisms Controlling In Situ Recovery From Heavy Oil Sands," The Oil Sands of Canada - Venezuela 1977, CIM Special Volume 17, 327-333.

32. Prausnitz, J.M. and Benso, P.R.: "Solubility of Liquids in Compressed Hydrogen, Nitrogen and Carbon Dioxide," AIChE Jour., June 1959, 161-164.

33. Holm, L.W. and Josendal, V.A.: "Effect of Oil Composition on Miscible-Type Displacement by Carbon Dioxide," Soc. Pet. Eng. Jour., Feb. 1982, 87-98.

34. Holm, L.W.: "CO_2 Flooding; Its Time Has Come," Distinguished Author Series, Jour. Pet. Tech., Dec. 1982, 2739-2745.

35. Rosman, A. and Zana, E.: "Experimental Studies of Low IFT Displacement by CO_2 Injection," Paper SPE 6723 presented at the 52nd Annual Fall Technical Conference and Exhibition, Denver, Col., Oct. 9-12, 1977.

36. Katz, D.L., Moore, R.R. and Trainer, R.P.: "Surface Tension of Crude Oils Containing Dissolved Gases," SPE Reprint Series No. 15, Phase Behaviour, published by the SPE-AIME, 1981 Edition, 285-294.

37. Breston, J.N. and Macfarlane, R.M.: "The Effect of a Number of Variables on Oil Recovery from Cores when Flooded with Carbonated Water and Liquid CO_2," Producers Monthly, Nov. 1952, 36-45.

38. Farouq Ali, S.M., Figueroa, J.M., Azuaje, E.A. and Farquharson, R.G.: "Recovery of Lloydminster and Morichal Crudes by Caustic, Acid and Emulsion Floods," Jour. Can. Pet. Tech., Jan. - March, 1979.

39. Scott, G.R., Collins, H.N. and Flock, D.L.: "Improving Waterflood Recovery of Viscous Crude Oils by Chemical Control," Jour. Can. Pet. Tech., Oct.-Dec. 1965, 243-251.

40. Strassner, J.E.: "Effect of pH on Interfacial Films and Stability of Crude Oil-Water Emulsions," Jour. Pet. Tech., March 1968, 303-312.

41. Holm, L.W. and Josendal, V.A.: "Mechanisms of Oil Displacement by Carbon Dioxide," Jour. Pet. Tech., Dec. 1974, 1427-1436.

42. Guaiquirian, L.C., Arismendi, S.J. and Rojas, G.: "Heavy Oil Recovery by Repressuring - Depletion Technique Using Supercritical CO_2," Proc. VI J. Tec. Pet. SVIP, Maracaibo, Oct. 30-Nov. 3, 1979 (in Spanish).

43. Holm, L.W.: "Carbon Dioxide Solvent Flooding for Increased Oil Recovery," Trans. AIME, Vol. 216, 1959, 225-231.

44. Klins, M.A. and Farouq Ali, S.M.: "Heavy Oil Production by Carbon Dioxide Injection," Jour. Can. Pet. Tech., Sept.-Oct. 1982, 64-72.

45. Bardon, Ch., Behar, E. and Topkaya, I.: "Laboratory Studies for CO_2 Injection as an Immiscible Application in a Heavy Oil Reservoir in Turkey," Presented at the UNITAR 2nd International Conference on the Future of Heavy Crude and Tar Sand, Caracas, 1982. McGraw-Hill, Inc., 853-868.

46. Henry, R.L.: "A Laboratory Study of Carbon Dioxide and Hydrogen Sulfide Miscible Injection in an Oil-Filled Porous Medium," Ph.D. Dissertation, University of Missouri-Rolla, 1977.

47. Holm, L.W. and O'Brien, L.J.: "Carbon Dioxide Test at the Mead-Strawn Field," Jour. Pet. Tech., April 1971, 431-442.

48. Omole, O. and Osoba, J.S.: "Carbon Dioxide - Dolomite Rock Iteration During CO_2 Flooding Process," Paper No. 83-34-17 presented at the 34th Annual Technical Meeting of Petroleum Society of CIM, Banff, Alta., May 10-13, 1983.

49. Graue, D.J. and Blevins, T.R.: "SACROC Tertiary CO_2 Pilot Project," Paper SPE 7090 presented at the 5th Symposium on Improved Methods for Oil Recovery, SPE-AIME, Tulsa, Okla., April 16-19, 1978.

50. Strausz, O.P. "Some Recent Advances in the Chemistry of Oil Sand Bitumen," presented at the UNITAR first International Conference on the Future of Heavy Crude and Tar Sand, Edmonton, 1979. McGraw-Hill, Inc., 187-194.

51. Graue, D.J. and Zana, E.T.: "Study of a Possible CO_2 Flood in Rangely Field," Jour. Pet. Tech., July 1981, 1312-1318.

52. Stalkup, F.I. Jr.: "Status of Miscible Displacement," Jour. Pet. Tech., April 1983, 815-826.

53. Holm, L.W.: "CO_2 Requirements in CO_2 Slug and Carbonated Water Oil Recovery Processes," Producers Monthly, Dec. 1963, 16-28.

54. Pontious, S.B. and Tham, M.J.: "North Cross (Devonian) Unit CO_2 Flood Review of Flood Performance and Numerical Simulation Model," Jour. Pet. Tech., Dec. 1978.

55. West Growth Petroleums LTD.: "Carbon-Dioxide Flood Enhanced Recovery Scheme Retlaw Mannville "V" Pool," Application No.820333 Submitted to Energy Resources Conservation Board of Alberta, Appendix B, April 1982.

56. Sayegh, S.G. and Maini, B.B.: "Laboratory Evaluation of the CO_2 Huff-n-Puff Process for Heavy Oil Reservoirs," Jour. Can. Pet. Tech., May-June 1984, 29-36.

57. Caudle, B.H. and Dyes, A.B.: "Improving Miscible Displacement by Gas-Water Injection," Trans. AIME, Vol. 213, 1958, 281-284.

58. Stone, H.L.: "Vertical Conformance in an Alternating Water-Miscible Gas Flood," Paper SPE-11130 presented at the 57th Annual Fall Technical Conference and Exhibition of the SPE-AIME, New Orleans, LA., Sept. 26-29, 1982.

59. Blackwell, R.J., Terry, W.M., Rayne, J.R., Lindley, D.C. and Henderson, J.R.: "Recovery of Oil by Displacement with Water-Solvent Mixtures," Trans. AIME, Vol. 219, 1960, 293-300.

60. Warner, H.R. Jr.: "An Evaluation of Miscible CO_2 Flooding in Waterflood Sandstone Reservoirs," Jour. Pet. Tech., Oct. 1977, 1339-1346.

61. Ko, S.C.M. and Stanton, P.M.: "Tertiary Recovery Potential of CO_2 Flooding in Joffre Viking Pool, Alberta," Paper No. 83-34-18 presented at the 34th Annual Technical Meeting of the Petroleum Society of CIM, Banff, Alta., May 10-13, 1983.

62. Shelton, J.L. and Schneider, F.N.: "The Effects of Water Injection on Miscible Flooding Methods Using Hydrocarbons and Carbon Dioxide," Soc. Pet. Eng. Jour., June 1975, 217-226.

63. Saxon, J. Jr., Breston, J.N. and Macfarlane, R.M.: "Increased Oil Recovery from Long Core Water Floods by Preliminary Gas Injection," Producers Monthly, Jan. 1951, 7-17.

64. Holmgren, C.R. and Morse, R.A.: "Effect of Free Gas Saturation on Oil Recovery by Water Flooding," Trans. AIME, Vol. 192, 1951, 135-140.

65. Kyte, J.R., Stanclift, R.J. Jr., Stephan, S.C. Jr. and Rapoport, L.A.: "Mechanism of Water Flooding in the Presence of Free Gas," Trans. AIME, Vol. 207, 1956, 215-221.

66. Craig, F.F. Jr.: "The Reservoir Engineering Aspects of Waterflooding," Monograph Volume 3, SPE-AIME, 1971, 39-43.

67. Gil, J.R. and Rebolledo, R.R.: "Experimental Study on Heavy Oil Recovery Using Alternate Slugs of Supercritical CO_2 and Water," Petroleum Engineering Thesis, University of Oriente, March 1980 (in Spanish).

68. Reid, T.B. and Robinson, H.J.: "Lick Creek Meaking Sand Unit Immiscible CO_2/Waterflood Project," Jour. Pet. Tech., Sept. 1981, 1723-1729.

69. Patton, J.T., Coats, K.H. and Spence, K.: "Carbon Dioxide Well Stimulation: Part 1 - A Parametric Study," Jour. Pet. Tech. Aug. 1982, 1798-1804.

70. Langhaar, H.L.: "Dimensional Analysis and Theory of Models," John Wiley and Sons, Inc., New York, 1951.

71. Craig, F.F. Jr., Sanderling, J.L., Moore, D.W. and Geffen, T.M.: "A Laboratory Study of Gravity Segregation in Frontal Drives," Trans. AIME, Vol. 210, 1957, 275-282.

72. Farouq Ali, S.M., Donohue, D.A.T. and Stahl, C.D.: "Fluid Flow in Porous Media - Problems in Relating Experiments to Field Projects," 7th World Petroleum Congress, Vol. 3, Mexico, 1967, 159-168.

73. Hildebrand, J.H.: "Solubility of Non-Electrolytes," Reinhold Publishing Corp., 1936.

74. Hildebrand, J.H., Prausnitz, J.M. and Scott, R.L.: "Regular and Related Solutions," van Nostrand Reinhold Co., New York, 1970.

75. Bird, R.B., Stewart, W.E. and Lightfoot, E.N.: "Transport Phenomena," John Wiley and Sons, Inc., New York, 1960.

76. Reid, R.C., Prausnitz, J.M. and Sherwood, T.K.: "The Properties of Gases and Liquids," McGraw-Hill Book Co., New York, 1977.

77. Crank, J.: "The Mathematics of Diffusion," Oxford at the Clarendon Press, 1967.

78. Sherwood, T.K., Pigford, R.L. and Willke, Ch.R.: "Mass Transfer," McGraw-Hill Book Co., New York, 1975.

79. Perkins, F.M. Jr. and Johnston, O.C.: "A Review of Diffusion and Dispersion in Porous Media," Soc. Pet. Eng. Jour., March 1963, 70-84.

80. Stone, H.L.: "Probability Model for Estimating Three-Phase Relative Permeability," Jour. Pet. Tech., Feb.1970, 214-218.

81. Leverett, M.C. and Lewis, W.B.: "Steady Flow of Gas-Oil-Water Mixtures Through Unconsolidated Sands," Trans. AIME, Vol. 142, 1941, 107-120.

82. Collins, R.E.: "Flow of Fluids Through Porous Materials," Penn Well Co., Tulsa, Okla., 1961.

83. Farouq Ali, S.M.: "Elements of Reservoir Modelling," University of Alberta, 1980.

84. Perkins, F.M. Jr. and Collins, R.E.: "Scaling Laws for Laboratory Flow Models of Oil Reservoirs," Trans. AIME, 219, 383-385.

85. Leverett, M.C.: "Capillary Behaviour in Porous Solids," Trans. AIME, Vol. 142, 1941, 159-172.

86. Rose, W.R. and Bruce, W.A.: "Evaluation of Capillary Character in Petroleum Reservoir Rock," Trans. AIME, Vol. 186, 1949, 127-142.

87. Ridings, R.L., Dalton, R.L., Greene, H.W., Kyte, J.R. and Naumann, V.O.: "Experimental and Calculated Behaviour of Dissolved-Gas-Drive Systems," Soc. Pet. Eng. Jour., March 1963, 41-48.

88. Demetre, G.P., Bentsen, R.G. and Flock, D.L.: "A Multi-Dimensional Approach to Scaled Immiscible Fluid Displacement," Jour. Can. Pet. Tech., July-Aug. 1982, 49-60.

89. Buckingham, E.: "On Physically Similar Systems; Illustrations of the Use of Dimensional Equations," Phys. Rev., Vol. IV, No. 4, 1914.

90. Loomis, A.G. and Crowell, D.C.: "Theory and Application of Dimensional and Inspectional Analysis to Model Study of Fluid Displacements in Petroleum Reservoirs," U.S. Bureau of Mines, Reports of Investigations, No. 6546, 1964.

91. Demetre, G.P.: "Scaling and Instability of Simultaneous Flow in Porous Media," M.Sc. Thesis, Department of Mineral Engineering, University of Alberta, 1980.

92. GreenKorn, R.A.: "Flow Models and Scaling Laws for Flow Through Porous Media," Ind. Eng. Chem., March 1964, 32-37.

93. GreenKorn, R.A.: "Flow Phenomena in Porous Media," Marcel Dekker, Inc., New York, 1983.

94. Chuoke, R.L., van Meurs, P. and van der Poel, C.: "The Instability of Slow, Immiscible, Viscous Liquid-Liquid Displacements in Permeable Media," Trans. AIME, Vol. 216, 1959, 188-194.

95. Peters, E.J. and Flock, D.L.: "The Onset of Instability During Two-Phase Immiscible Displacement in Porous Media," Soc. Pet. Eng. Jour., April 1981, 249-258.

96. Bentsen, R.G.: "A New Approach to Instability Theory in Porous Media," Dept. of Mineral Engineering, University of Alberta, Edmonton, 1984.

97. Gardner, J.W. and Ypma, J.G.J.: "An Investigation of Phase Behaviour-Macroscopic Bypassing Interaction CO_2 Flooding," Paper SPE/DOE 10686, presented at the 1982 SPE/DOE Third Joint Symposium on Enhanced Oil Recovery, Tulsa, Okla., April 4-7, 1982.

98. Geertsma, J., Croes, G.A. and Schwartz, N.: "Theory of Dimensionally Scaled Models of Petroleum Reservoirs," Trans. AIME, Vol. 207, 1956, 118-127.

99. McFarland, J.D. and Dranchuk, P.M.: "Visualization of the Transition to Turbulent Flow in Porous Media," Jour. Can. Pet. Tech., April-June, 1976, 71-78.

100. Geertsma, J.: "Estimating the Coefficients of Inertial Resistance in Fluid Flow Through Porous Media," Soc. Pet. Eng. Jour., Oct. 1974, 445-450.

101. Wong, S.W.: "Effect of Liquid Saturation on Turbulence Factors for Gas-Liquid Systems," Jour. Can. Pet. Tech., Oct.-Dec., 1970, 274-278.

102. Pujol, L. and Boberg, T.C.: "Scaling Accuracy of Laboratory Steam Flooding Models," Paper SPE 4191, presented at the 1972 California Regional Meeting, Bakersfield, Nov. 8-10.

103. Flock, D.L., Peters, E.J., Baird, H., Wiborg, R. and Kloepfer, J.: "The Influence of Frontal Instabilities During Viscous Oil Displacements," The Oil Sands of Canada-Venezuela, 1977, CIM Special Volume No. 17, 380-385.

104. Flock, D.L.: "Physical Modelling for Oil Sands - Relevance and Limitations," Department of Mineral Engineering, University of Alberta, Dec. 1976.

105. Morrow, N.R., Lim, H.T. and Ward, J.S.: "Effect of Crude-Oil-Induced Wettability Changes on Oil Recovery," Paper SPE 13215, presented at the 59th Annual Technical Conference and Exhibition held in Houston, Texas, Sept. 16-19, 1984.

106. Bear, J.: "Dynamics of Fluids in Porous Media," American Elsevier Publishing Co. Inc., New York, 1972.

107. Marle, C.M.: "Multiphase Flow in Porous Media," Editions Technip, Paris, 1981.

108. Engelberts, W.F. and Klinkenberg, L.J.: "Laboratory Experiments on the Displacement of Oil by Water from Packs of Granular Material," Proceedings of the 3rd World Petroleum Congress, Section II, 1951, 544-554.

109. Ridings, R.L., Dalton, R.L., Greene, H.W., Kyte, J.R. and Naumann, V.O.: "Experimental and Calculated Behaviour of Dissolved-Gas-Drive Systems," Soc. Pet. Eng. Jour., March 1963, 41-48.

110. Kyte, J.R. and Rapoport, L.A.: "Linear Waterflood Behaviour and End Effects in Water-Wet Porous Media," Trans. AIME, Vol. 213, 1958, 423-426.

111. Amyx, J.W., Bass, D.M. Jr. and Whiting, R.L.: "Petroleum Reservoir Engineering. Physical Properties," McGraw-Hill Book Co., New York, 1960.

112. Stalkup, F.I. Jr.: "Miscible Displacement," Monograph Volume 8, SPE-AIME, 1983.

113. _____: "Enhanced Oil Recovery, EOR," National Petroleum Council, Dec. 1976.

114. Chaibi, K.: "Private Communication," 1983.

115. Khatib, A.L., Earlougher, R.C. and Kantar, K.: "CO_2 Injection as an Immiscible Application for Enhanced Recovery in Heavy Oil Reservoirs," Paper SPE 9928 presented at the 1981 California Regional Meeting, Bakersfield, Calif., March 25-26, 1981, 461-471.

116. Adams, D.M.: "Experiences with Waterflooding Lloydminster Heavy-Oil Reservoirs," Jour. Pet. Tech., Aug. 1982, 1643-1650.

117. Jameson, C.E.: "The Lloydminster Heavy Oil Area," Jour. Can. Pet. Tech., July-Sept. 1973, 17-20.

118. _____: "Vessel of Noncircular Cross Section," ASME Boiler and Pressure Vessel Code Section VIII, Division 1, Appendix 13, 1980, 461-490.

119. Muskat, M.: "Physical Principles of Oil Production," McGraw-Hill Book Co., New York, 1949.

120. Flock, D.L., Lee, T.H. and Gibeau, J.P.: "The Effect of Temperatures on the Interfacial Tension of Heavy Crude Oils Using the Pendent Drop Apparatus," Paper No. 84-35-33 presented at the 35th Annual Technical Meeting of the Petroleum Society of CIM, Calgary, June 10-13, 1984.

121. Dodds, W.S., Stutzman, L.F. and Sollami, B.J.: "Carbon Dioxide Solubility in Water," Chem. Eng. Data Series, Vol. 1, No. 1, 1956, 92-94.

122. Crawford, H.R., Neil, G.H., Bucy, B.J. and Crawford, P.B.: "Carbon Dioxide - An Multipurpose Additive for Effective Well Stimulation," Jour. Pet. Tech., March 1963, 237-242.

123. Steinborn, R. and Flock, D.L.: "The Rheology of Heavy Crude Oils and Their Emulsions," Jour. Can Pet. Tech., Sept.-Oct. 1983, 39-52.

124. Starling, K.E.: "Fluid Thermodynamic Properties for Light Petroleum Systems," Gulf Publishing Co., 1973.

125. Briggs, J.P. and Puttagunta, V.R.: "The Effect of Carbon Dioxide on the Viscosity of Lloydminster Aberfeldy Oil at Reservoir Temperature," Alberta Research Council, Oil Sands Department, Edmonton, Alta., Jan. 1984.

126. Hougen, O.A. and Watson, K.M.: "Chemical Process Principles," John Willey and Sons, Inc., New York, 1961.

127. Ambwani, D.S. and Tomlinson, F.: "Pendent Drop Technique for Measuring Liquid Boundary Tensions," Surface and Colloid Science, Vol. 11 - Expiremental Methods, Plenum Press, 1979, 93-119.

128. Hodgson, G.W., Peake, E. and Baker, B.L.: "The Origin of Petroleum Porphyrins: The Position of the Athabasca Oil Sands," The K.A. Clark Volume Published by Alberta Research Council, Oct. 1963, 75-100.

129. Goncharov, I.V. et al.: "Study of Nitrogen Bases of Crude Oils by Mass-Spectrometry," Petroleum Chemistry, Vol. 21, No. 3, 1981, 173-179.

130. Dunning, H.N., Moore, J.W. and Denekas, M.O.: "Interfacial Activities and Porphyrin Contents of Petroleum Extracts," Ind. Eng. Chem., August 1953, 1759-1765.

131. Mar, A. and Singhal, A.K.: "In Situ Emulsification During the Injection of Water and Steam into an Oil-Saturated Model Porous Medium," Research Note RN-10, Petroleum Recovery Institute, May 1979.

132. Jennings, H.Y. Jr., Johnson, C.E. Jr. and McAuliffe, C.D.: "A Caustic Waterflooding Process for Heavy Oils," Jour. Pet. Tech. Dec. 1974, 1344-1352.

133. Dranchuk, P.M., Scott, J.D. and Flock, D.L.: "Effect of Addition of Certain Chemicals on Oil Recovery During Waterflooding," Jour. Can. Pet. Tech., July-Sept. 1974, 27-36.

134. Jones, T.J., Neustadter, E.L., and Whittingham, K.P.: "Water-in-Crude Oil Emulsion Stability and Emulsion Destabilization by Chemical Demulsifiers," Jour. Can. Pet. Tech., April-June, 1978, 100-108.

135. Gewers, C.W.W.: "Colloid and Surface Chemical Problems in Non-Conventional Heavy Oil Recovery," Jour. Can. Pet. Tech., April-June 1968, 85-90.

136. Grist, D.M., Langley, G.O. and Neustadter, E.L.: "The Dependence of Water Permeability on Core Cleaning Methods in the Case of Some Sandstone Samples," Jour. Can. Pet. Tech., April-June 1975, 48-52.

137. Collins, S.H. and Melrose, J.C.: "Adsorption of Asphaltenes and Water on Reservoir Rock Minerals," Paper SPE 11800 presented at the Internation Symposium on Oilfield and Geothermal Chemistry held in Denver, CO., June 1-3, 1983.

138. Oferinga, J. and van der Poel, C.: "Displacement of Oil from Porous Media by Miscible Liquids," Trans. AIME, Vol. 201, 1954, 310-316.

139. Crane, F.E., Kendall, H.A. and Gardner, G.H.F.: "Some Experiments on the Flow of Miscible Fluids of Unequal Density through Porous Media," Soc. Pet. Eng. Jour., Vol. 3, No. 4, 1963, 277.

140. Kane, A.V.: "Performance Review of a Large-Scale CO_2-WAG Enhanced Recovery Project, SACROC Unit Kelly-Snyder Field," Jour. Pet. Tech., Feb. 1979, 217-231.

141. Desch, J.B., Larsen, W.K. Lindsay, R.F. and Nettle, R.L.: "Enhanced Oil Recovery by CO_2 Miscible Displacement in the Little Knife Field, Billings County, North Dakota," Jour. Pet. Tech., Sep. 1984, 1592-1602.

142. Hansen, P.W.: "A CO_2 Tertiary Pilot/Little Creek Field, Mississippi," Paper SPE 6747, presented at the 52nd Annual Fall Technical Conference and Exhibition, SPE-AIME, Denver, Col., Oct. 9-12, 1977.

143. Ignasiak, T.M., Kotlyar, L., Longstaffe, F.J., Strausz, O.P., and Montgomery, D.S.: "Separation and Characterization of Clay from Athabasca Asphaltene," Fuel, March 1983, 353-362.

144. Hill, D.G.: "Clay Stabilization - Criteria for Best Performance," Paper CIM 82-33-20 presented at the 33rd Annual Technical Meeting of the Petroleum Society of CIM, Calgary, June 6-9, 1982.

145. Bowman, C.W.: "Molecular and Interfacial Properties of Athabasca Tar Sands," 7th World Petroleum Congress, Vol. 3, 583-604.

146. Lichaa, P.M.: "Asphaltene Deposition Problem in Venezuelan Crudes - Usage of Asphaltenes in Emulsion Stability," The Oil Sands of Canada - Venezuela, CIM Special Volume 17, 1977, 609-624.

147. Hirschberg, A., de Jong, L.N.J., Schipper, B.A., and Meyers, J.G.: "Influence of Temperature and Pressure on Asphaltenes Flocculation," Paper SPE 11202 presented at the 57th Annual Fall Technical Conference and Exhibition of the SPE-AIME, New Orleans, LA., Sept. 26-29, 1982.

148. Speight, J.G. and Moschopedis, S.E.: "Factors Affecting Bitumen Recovery by the Hot Water Process," Fuel Processing Technology Vol. 1, 1977/1978, 261-268.

149. Jameson, C.E.: "The Lloydminster Heavy Oil Area," Jour. Can. Pet. Tech., July-Sept. 1973, 17-19.

APPENDIX A

MASS BALANCE

MASS BALANCE

A mass balance will be considered about a small control volume as shown in Figure A1 with length Δx, width Δy, and height Δz. For all phases a mass balance can be written as follows:

Output - input + net change over time in the control volume = 0

1. Carbon Dioxide Equation

Output - input = mass of free, dissolved, and dispersed carbon dioxide leaving - mass of free, dissolved, and dispered carbon dioxide entering during Δt.

Net change over Δt = mass of free, dissolved, and dispersed carbon dioxide at $t + \Delta t$ - mass of free, dissolved, and dispersed carbon dioxide at t.

Thus considering three dimensions, the mass balance for carbon dioxide is given by:

$$\left[(Ng)_{x+\Delta x} + (Ng)_{y+\Delta y} + (Ng)_{z+\Delta x}\right]\Delta t - \left[(Ng)_x + (Ng)_y + (Ng)_z\right]\Delta t$$
$$+ \left[\phi_{t+\Delta t}\,\Delta x\Delta y\Delta z\left(\frac{Sg\,\rho_g}{Mg} + \frac{Rso\,So\,\rho^*_g}{Bo\,Mg} + \frac{So\,Cgo\,\rho_g}{Mg} + \frac{Rsw\,Sw\,\rho^*_g}{Bw\,Mg} + \frac{Sw\,Cgw\,\rho_g}{Mg}\right)_{t+\Delta t}\right.$$
$$\left. - \phi_t\,\Delta x\Delta y\Delta z\left(\frac{Sg\,\rho_g}{Mg} + \frac{Rso\,So\,\rho^*_g}{Bo\,Mg} + \frac{So\,Cgo\,\rho_g}{Mg} + \frac{Rsw\,Sw\,\rho^*_g}{Bw\,Mg} + \frac{Sw\,Cgw\,\rho_g}{Mg}\right)_t\right]$$
$$= 0 \qquad (A\text{-}1)$$

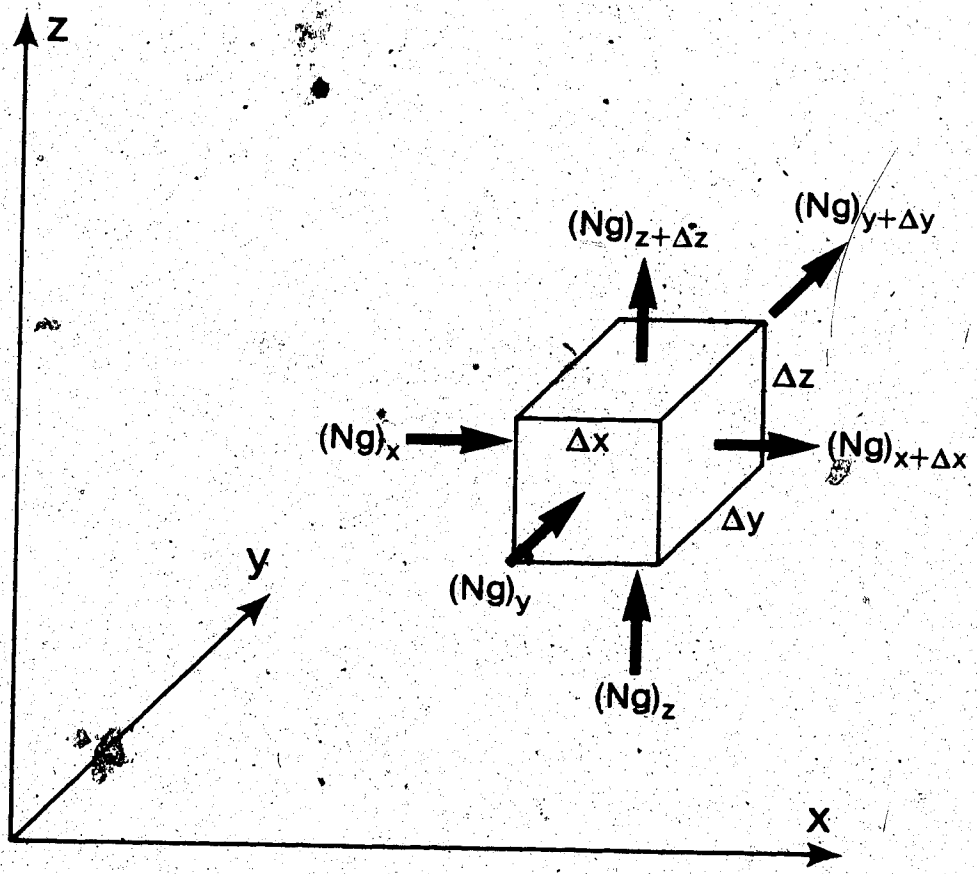


Figure A1 Control Volume for Mass Balance of Carbon Dioxide

Rearranging terms and taking the limits as Δt, Δx, Δy, and Δz go to zero:

$$\left(\frac{\partial Ngx}{\partial x}\right)\Delta x + \left(\frac{\partial Ngy}{\partial y}\right)\Delta y + \left(\frac{\partial Ngz}{\partial z}\right)\Delta z + Vb\,\frac{\partial}{\partial t}\left[\phi\left(\frac{Sg\,\rho_g}{Mg} + \frac{Rso\,So\,\rho_g^*}{Bo\,Mg} + \frac{So\,Cgo\,\rho_g}{Mg} + \frac{Rsw\,Sw\,\rho_g}{Bw\,Mg} + \frac{Sw\,Cgw\,\rho_g}{Mg}\right)\right] = 0 \quad \text{(A-2)}$$

where

$$Ngx = \frac{v'_{gx}\,\rho_g\,Ax}{Mg} + \frac{Rso\,v'_{ox}\,Ax\,\rho_g^*}{Bo\,Mg} + \frac{Ggox\,\rho_g}{Mg} + \frac{Rsw\,v'_{wx}\,Ax\,\rho_g^*}{Bw\,Mg} + \frac{Ggwx\,\rho_g}{Mg} \quad \text{(A-3)}$$

|→free CO_2→|←dissolved and dispersed→|←dissolved and dispersed→|

CO_2 in oil CO_2 in water

For Ngy and Ngz replace x by y and by z respectively in Equation A-3.

Replacing the expressions for Ngx, Ngy, and Ngz into Equation A-2, one obtains:

$$\frac{\partial}{\partial x}\left(\frac{v'_{gx}\,\rho_g\,Ax}{Mg} + \frac{Rso\,v'_{ox}\,\rho_g^*\,Ax}{Bo\,Mg} + \frac{Ggox\,\rho_g}{Mg} + \frac{Rsw\,v'_{wx}\,\rho_g^*\,Ax}{Bw\,Mg} + \frac{Ggwx\,\rho_g}{Mg}\right)\Delta x$$
$$+ \frac{\partial}{\partial y}\left(\frac{v'_{gy}\,\rho_g\,Ay}{Mg} + \frac{Rso\,v'_{oy}\,\rho_g^*\,Ay}{Bo\,Mg} + \frac{Ggoy\,\rho_g}{Mg} + \frac{Rsw\,v'_{wy}\,\rho_g^*\,Ay}{Bw\,Mg} + \frac{Ggwy\,\rho_g}{Mg}\right)\Delta y$$
$$+ \frac{\partial}{\partial z}\left(\frac{v'_{gz}\,\rho_g\,Az}{Mg} + \frac{Rso\,v'_{oz}\,\rho_g^*\,Az}{Bo\,Mg} + \frac{Ggoz\,\rho_g}{Mg} + \frac{Rsw\,v'_{wz}\,\rho_g^*\,Az}{Bw\,Mg} + \frac{Ggwz\,\rho_g}{Mg}\right)\Delta z$$
$$+ V_b\,\frac{\partial}{\partial t}\left[\phi\left(\frac{Sg\,\rho_g}{Mg} + \frac{Rso\,So\,\rho_g^*}{Bo\,Mg} + \frac{Rsw\,Sw\,\rho_g^*}{Bw\,Mg} + \frac{So\,Cgo\,\rho_g}{Mg} + \frac{Sw\,Cgw\,\rho_g}{Mg}\right)\right] = 0 \quad \text{(A-4)}$$

Substituting $\rho_g = \rho_g^*/Bg$ and $\Delta x Ax = \Delta y Ay = \Delta z Az = V_b$ into Equation A-4 the three-dimensional equation of mass conservation for carbon dioxide is obtained. This equation takes into account solution

and dispersion of CO_2 in oil and water at reservoir conditions.

$$\frac{\partial}{\partial x}\left(\frac{v'_{gx}}{Bg}+\frac{Rso\ v'_{ox}}{Bo}+\frac{Ggox}{Ax\ Bg}+\frac{Rsw\ v'_{wx}}{Bw}+\frac{Ggwx}{Ax\ Bg}\right)$$
$$+\frac{\partial}{\partial y}\left(\frac{v'_{gy}}{Bg}+\frac{Rso\ v'_{oy}}{Bo}+\frac{Ggoy}{Bg\ Ay}+\frac{Rsw\ v'_{wy}}{Bw}+\frac{Ggwy}{Ay\ Bg}\right)$$
$$+\frac{\partial}{\partial z}\left(\frac{v'_{gz}}{Bg}+\frac{Rso\ v'_{oz}}{Bo}+\frac{Ggoz}{Bg\ Az}+\frac{Rsw\ v'_{wz}}{Bw}+\frac{Ggwz}{Az\ Bg}\right)$$
$$+\frac{\partial}{\partial t}\left[\phi\left(\frac{Sg}{Bg}+\frac{Rso\ So}{Bo}+\frac{Rsw\ Sw}{Bw}+\frac{So\ Cgo}{Bg}+\frac{Sw\ Cgw}{Bg}\right)\right]=0 \qquad \text{(A-5)}$$

For two phases (oil and carbon dioxide) this equation can be written

$$\frac{\partial}{\partial x}\left(\frac{v'_{gx}}{Bg}+\frac{Rso\ v'_{ox}}{Bo}+\frac{Ggox}{Ax\ Bg}\right)+\frac{\partial}{\partial y}\left(\frac{v'_{gy}}{Bg}+\frac{Rso\ v'_{oy}}{Bo}+\frac{Ggoy}{Bg\ Ay}\right)$$
$$+\frac{\partial}{\partial z}\left(\frac{v'_{gz}}{Bg}+\frac{Rso\ v'_{oz}}{Bo}+\frac{Ggoz}{Az\ Bg}\right)+\frac{\partial}{\partial t}\left[\phi\left(\frac{Sg}{Bg}+\frac{Rso\ So}{Bo}+\frac{So\ Cgo}{Bg}\right)\right]=0 \qquad \text{(A-6)}$$

Oil and Water Equations

The three-dimensional equations of mass conservation for oil and water are much simpler than that for carbon dioxide. They can be derived using a similar procedure to the above. In this case the equations are given by:

$$\frac{\partial}{\partial x}\left(\frac{v'_{ox}}{Bo}\right)+\frac{\partial}{\partial y}\left(\frac{v'_{oy}}{Bo}\right)+\frac{\partial}{\partial z}\left(\frac{v'_{oz}}{Bo}\right)+\frac{\partial}{\partial t}\left(\frac{\phi So}{Bo}\right)=0 \qquad \text{(A-7)}$$

$$\frac{\partial}{\partial x}\left(\frac{v'_{wx}}{Bw}\right)+\frac{\partial}{\partial y}\left(\frac{v'_{wy}}{Bw}\right)+\frac{\partial}{\partial z}\left(\frac{v'_{wz}}{Bw}\right)+\frac{\partial}{\partial t}\left(\frac{\phi Sw}{Bw}\right)=0 \qquad \text{(A-8)}$$

APPENDIX B

DERIVATION OF THE FRACTIONAL FLOW EQUATION OF CARBON DIOXIDE

DERIVATION OF THE FRACTIONAL FLOW EQUATION OF CARBON DIOXIDE

Rewriting Equations 9 to 11, and 17 to 19:

$$\vec{v}'_g = - \frac{\bar{\bar{K}}\, Krg}{\mu_g} (\nabla Pg - \rho_g \vec{g}) \qquad (B\text{-}1)$$

$$\vec{v}'_o = - \frac{\bar{\bar{K}}\, Kro}{\mu_o} (\nabla Po - \rho_o \vec{g}) \qquad (B\text{-}2)$$

$$\vec{v}'_w = - \frac{\bar{\bar{K}}\, Krw}{\mu_w} (\nabla Pw - \rho_w \vec{g}) \qquad (B\text{-}3)$$

$$\vec{v}_g = - \frac{\bar{\bar{K}}\, Krg}{\mu_g} (\nabla Pg - \rho_g \vec{g}) - \bar{\bar{D}}go \nabla Cgo - \bar{\bar{D}}gw \nabla Cgw \qquad (B\text{-}4)$$

$$So + Sw + Sg = 1 \qquad (B\text{-}5)$$

$$Pcow(Sw) = Po - Pw \qquad (B\text{-}6)$$

$$Pcgo(Sg) = Pg - Po \qquad (B\text{-}7)$$

The velocities of oil and water are those obtained by Darcy's law, therefore $\vec{v}'_o = \vec{v}_o$ and $\vec{v}'_w = \vec{v}_w$.

From Equations B-2 to B-4

$$\nabla Po = - \frac{\mu_o \vec{v}_o}{\bar{\bar{K}}\, Kro} + \rho_o \vec{g} \qquad (B\text{-}8)$$

$$\nabla Pw = - \frac{\mu_w \vec{v}_w}{\bar{\bar{K}}\, Krw} + \rho_w \vec{g} \qquad (B\text{-}9)$$

$$\nabla Pg = - \frac{\mu_g \vec{v}_g}{\bar{\bar{K}}\, Krg} + \rho_g \vec{g} - \frac{\bar{\bar{D}}go\, \mu_g}{\bar{\bar{K}}\, Krg} \nabla Cgo - \frac{\bar{\bar{D}}gw\, \mu_g}{\bar{\bar{K}}\, Krg} \nabla Cgw \qquad (B\text{-}10)$$

Combining Equations B-6, B-8 and B-9, and Equations B-7, B-8 and B-10, results in:

$$\nabla P_{cow} = \nabla P_o - \nabla P_w = -\frac{\mu_o \vec{v}_o}{\bar{\bar{K}}\, K_{ro}} + \rho_o \vec{g} + \frac{\mu_w \vec{v}_w}{\bar{\bar{K}}\, K_{rw}} - \rho_w \vec{g} \qquad \text{(B-11)}$$

and

$$\nabla P_{cgo} = \nabla P_g - \nabla P_o = -\frac{\mu_g \vec{v}_g}{\bar{\bar{K}}\, K_{rg}} + \rho_g \vec{g} - \frac{\bar{\bar{D}}_{go}\, \mu_g}{\bar{\bar{K}}\, K_{rg}} \nabla C_{go}$$

$$- \frac{\bar{\bar{D}}_{gw}\, \mu_g}{\bar{\bar{K}}\, K_{rg}} \nabla C_{gw} + \frac{\mu_o \vec{v}_o}{\bar{\bar{K}}\, K_{ro}} - \rho_o \vec{g} \qquad \text{(B-12)}$$

Equation B-12 may be rearranged to yield

$$\frac{\mu_o \vec{v}_o}{\bar{\bar{K}}\, K_{ro}} - \frac{\mu_g \vec{v}_g}{\bar{\bar{K}}\, K_{rg}} = \vec{g}(\rho_o - \rho_g) + \nabla P_{cgo} + \frac{\bar{\bar{D}}_{go}\, \mu_g}{\bar{\bar{K}}\, K_{rg}} \nabla C_{go} + \frac{\bar{\bar{D}}_{gw}\, \mu_g}{\bar{\bar{K}}\, K_{rg}} \nabla C_{gw} \qquad \text{(B-13)}$$

Assuming that the fluids at reservoir conditions are incompressible and immiscible, the phase velocities can be related through equation

$$\vec{v}_o = \vec{v}_T - \vec{v}_w - \vec{v}_g \qquad \text{(B-14)}$$

Combining Equations B-13 and B-14, results in:

$$\frac{\mu_o}{\bar{\bar{K}}\, K_{ro}} (\vec{v}_T - \vec{v}_w - \vec{v}_g) - \frac{\mu_g \vec{v}_g}{\bar{\bar{K}}\, K_{rg}} = \vec{g}\, \Delta\rho_{og} + \nabla P_{cog}$$

$$+ \frac{\bar{\bar{D}}_{go}\, \mu_g}{\bar{\bar{K}}\, K_{rg}} \nabla C_{go} + \frac{\bar{\bar{D}}_{gw}\, \mu_g}{\bar{\bar{K}}\, K_{rg}} \nabla C_{gw} \qquad \text{(B-15)}$$

where

$$\Delta \rho_{og} = \rho_o - \rho_g$$

Equation B-15 may be written as:

$$\frac{\mu_o \vec{v}_w}{\bar{\bar{K}} K_{ro}} + \left(\frac{\mu_o}{\bar{\bar{K}} K_{ro}} + \frac{\mu_g}{\bar{\bar{K}} K_{rg}} \right) \vec{v}_g - \frac{\mu_o \vec{v}_T}{\bar{\bar{K}} K_{ro}} = -\vec{g} \Delta \rho_{og} - \nabla P_{cgo}$$

$$- \frac{\bar{\bar{D}}_{go} \mu_g}{\bar{\bar{K}} K_{rg}} \nabla C_{go} - \frac{\bar{\bar{D}}_{gw} \mu_g}{\bar{\bar{K}} K_{rg}} \nabla C_{gw} \qquad \text{(B-16)}$$

From this equation

$$\vec{v}_w = \vec{v}_T - \frac{\left(\frac{\mu_o}{K_{ro}} + \frac{\mu_g}{K_{rg}} \right)}{\left(\frac{\mu_o}{K_{ro}} \right)} \vec{v}_g - \frac{\bar{\bar{K}} K_{ro}}{\mu_o} \left(\vec{g} \Delta \rho_{og} + \nabla P_{cgo} \right.$$

$$\left. + \frac{\bar{\bar{D}}_{go} \mu_g}{\bar{\bar{K}} K_{rg}} \nabla C_{go} + \frac{\bar{\bar{D}}_{gw} \mu_g}{\bar{\bar{K}} K_{rg}} \nabla C_{gw} \right) \qquad \text{(B-17)}$$

Combining Equation B-11 and B-14 another equation which relates $\vec{v}_w$, $\vec{v}_g$, and $\vec{v}_T$ is obtained

$$\left(\frac{\mu_o}{\bar{\bar{K}} K_{ro}} + \frac{\mu_w}{\bar{\bar{K}} K_{rw}} \right) \vec{v}_w - \frac{\mu_o}{\bar{\bar{K}} K_{ro}} \vec{v}_T + \frac{\mu_o}{\bar{\bar{K}} K_{ro}} \vec{v}_g = \nabla P_{cow} + \vec{g} \Delta \rho_{wo} \qquad \text{(B-18)}$$

where

$$\Delta \rho_{wo} = \rho_w - \rho_o$$

Substituting Equation B-17 into B-18 and solving for $\vec{v}_g$ results in:

$$\vec{v}_g = \left\{ \vec{v}_T - \frac{\bar{\bar{K}}\, Krw}{\mu_w} \left(1 + \frac{Kro\ \mu_w}{Krw\ \mu_o}\right)\left(\vec{g}\,\Delta\rho_{og} + \nabla Pcgo + \frac{\bar{\bar{D}}go\ \mu_g}{\bar{\bar{K}}\, Krg} \nabla Cgo + \frac{\bar{\bar{D}}gw\ \mu_g}{\bar{\bar{K}}\, Krg} \nabla Cgw\right) - \frac{\bar{\bar{K}}\, Krw}{\mu_w} \nabla Pcow - \frac{\bar{\bar{K}}\, Krw\, \vec{g}}{\mu_w} \Delta\rho_{wo} \right\} \left(1 + \frac{Krw\ \mu_g}{Krg\ \mu_w} + \frac{Kro\ \mu_g}{Krg\ \mu_o}\right)^{-1} \qquad \text{(B-19)}$$

Defining

$$Fg = \left(1 + \frac{Krw\ \mu_g}{Krg\ \mu_w} + \frac{Kro\ \mu_g}{Krg\ \mu_o}\right)^{-1} \qquad \text{(B-20)}$$

and dividing Equation B-19 by the superficial velocity $|\vec{v}_T|$, one obtains:

$$\vec{f}_g = \frac{\vec{v}_g}{|\vec{v}_T|} = \left\{ \left(\vec{v}_T - \frac{\bar{\bar{K}}\, Krw}{\mu_w} \left(1 + \frac{Kro\ \mu_w}{Krw\ \mu_o}\right)\left(\vec{g}\,\Delta\rho_{og} + \nabla Pcgo + \frac{\bar{\bar{D}}go\ \mu_g}{\bar{\bar{K}}\, Krg} \nabla Cgo + \frac{\bar{\bar{D}}gw\ \mu_g}{\bar{\bar{K}}\, Krg} \nabla Cgw\right) - \frac{\bar{\bar{K}}\, Krw}{\mu_w} \nabla Pcow - \frac{\bar{\bar{K}}\, Krw\, \vec{g}\,\Delta\rho_{wo}}{\mu_w} \right\} \frac{Fg}{|\vec{v}_T|} \qquad \text{(B-21)}$$

Because of the gas-oil capillary pressure is function of gas saturation and the oil-water capillary pressure is function of water saturation the following relations hold

$$\nabla Pcgo = \frac{dPcgo}{dSg} \nabla Sg \qquad \text{(B-22)}$$

and

$$\nabla Pcow = \frac{dPcow}{dSw} \nabla Sw \qquad \text{(B-23)}$$

Substituting Equations B-22 and B-23 into Equation B-21 results in:

$$\vec{f}_g = \left(\vec{v}_T - \frac{\bar{\bar{K}}\, Krw}{\mu_w} \left(1 + \frac{Kro\ \mu_w}{Krw\ \mu_o} \right) \vec{g}\, \Delta \rho_{og} - \vec{g}\, \Delta \rho_{wo}\, \frac{\bar{\bar{K}}\, Krw}{\mu_w} \right) \frac{Fg}{|\vec{v}_T|}$$

$$- \left(\left(1 + \frac{Kro\ \mu_w}{Krw\ \mu_o} \right) \frac{dPcgo}{dSg}\, \nabla Sg - \frac{dPcow}{dSw}\, \nabla Sw \right) \frac{\bar{\bar{K}}\, Krw\, Fg}{\mu_w |\vec{v}_T|}$$

$$- \left(1 + \frac{Kro\ \mu_w}{Krw\ \mu_o} \right) (\bar{\bar{D}}go\ \nabla\ Cgo + \bar{\bar{D}}gw\, \nabla\, Cgw)\, \frac{Krw\ \mu_g}{Krg\ \mu_w}\, \frac{Fg}{|\vec{v}_T|} \qquad \text{(B-24)}$$

APPENDIX C

DERIVATION OF EQUATIONS 24, 25, AND 26

DERIVATION OF EQUATIONS 24, 25, AND 26

Equation 5 can be written as follows

$$\nabla \cdot \left(\frac{\vec{v}_g}{Bg} \right) + \nabla \cdot \left(\frac{Rso\ \vec{v}_o}{Bo} \right) + \nabla \cdot \left(\frac{Rsw\ \vec{v}_w}{Bw} \right)$$

$$= - \frac{\partial}{\partial t} \left[\phi \left(\frac{Sg}{Bg} + \frac{Rso\ So}{Bo} + \frac{Rsw\ Sw}{Bw} + \frac{Cgo\ So}{Bg} + \frac{Cgw\ Sw}{Bg} \right) \right] \qquad (C\text{-}1)$$

The following vectorial operations hold

$$\nabla \cdot \left(\frac{\vec{v}_g}{Bg} \right) = \frac{1}{Bg} \nabla \cdot \vec{v}_g + \frac{d(1/Bg)}{dPg} \nabla Pg \cdot \vec{v}_g \qquad (C\text{-}2)$$

$$\nabla \cdot \left(\frac{Rso\ \vec{v}_o}{Bo} \right) = \frac{Rso}{Bo} \nabla \cdot \vec{v}_o + \frac{d(Rso/Bo)}{dPo} \nabla Po \cdot \vec{v}_o \qquad (C\text{-}3)$$

$$\nabla \cdot \left(\frac{Rsw\ \vec{v}_w}{Bw} \right) = \frac{Rsw}{Bw} \nabla \cdot \vec{v}_w + \frac{d(Rsw/Bw)}{dPw} \nabla Pw \cdot \vec{v}_w \qquad (C\text{-}4)$$

Substituting Equations C-2 to C-4 into Equation C-1 results in:

$$\frac{1}{Bg} \nabla \cdot \vec{v}_g + \frac{d(1/Bg)}{dPg} \nabla Pg \cdot \vec{v}_g + \frac{Rso}{Bo} \nabla \cdot \vec{v}_o + \frac{d(Rso/Bo)}{dPo} \nabla Po \cdot \vec{v}_o + \frac{Rsw}{Bw} \nabla \cdot \vec{v}_w$$

$$+ \frac{d(Rsw/Bw)}{dPw} \nabla Pw \cdot \vec{v}_w = - \frac{\partial}{\partial t} \left(\frac{\phi Sg}{Bg} \right) - \frac{\partial}{\partial t} \left(\frac{\phi Rso\ So}{Bo} \right) - \frac{\partial}{\partial t} \left(\frac{\phi Rsw\ Sw}{Bw} \right)$$

$$- \frac{\partial}{\partial t} \left(\frac{\phi So\ Cgo}{Bg} \right) - \frac{\partial}{\partial t} \left(\frac{\phi Sw\ Cgw}{Bg} \right) \qquad (C\text{-}5)$$

Dividing Equation C-5 by $|\vec{v}_T|$, it may be written as follows:

$$\frac{1}{Bg}\nabla\cdot\vec{f}_g + \frac{d(1/Bg)}{dPg}\nabla Pg\cdot\vec{f}_g + \frac{Rso}{Bo}\nabla\cdot\vec{f}_o + \frac{d}{dPo}\left(\frac{Rso}{Bo}\right)\nabla Po\cdot\vec{f}_o$$

$$+ \frac{Rsw}{Bw}\nabla\cdot\vec{f}_w + \frac{d(Rsw/Bw)}{dPw}\nabla Pw\cdot\vec{f}_w$$

$$= -\frac{1}{|\vec{v}_T|}\frac{\partial}{\partial t}\left(\frac{\phi\, Sg}{Bg}\right) - \frac{1}{|\vec{v}_T|}\frac{\partial}{\partial t}\left(\frac{\phi\, So\, Rso}{Bo}\right) - \frac{1}{|\vec{v}_T|}\frac{\partial}{\partial t}\left(\frac{\phi\, Sw\, Rsw}{Bw}\right)$$

$$- \frac{1}{|\vec{v}_T|}\frac{\partial}{\partial t}\left(\frac{\phi\, So\, Cgo}{Bg}\right) - \frac{1}{|\vec{v}_T|}\frac{\partial}{\partial t}\left(\frac{\phi\, Sw\, Cgw}{Bg}\right) \qquad \text{(C-6)}$$

Following a procedure similar to the above, the continuity equations for oil and water (Equations 7 and 8) may be written as:

$$\frac{1}{Bo}\nabla\cdot\vec{f}_o + \frac{d(1/Bo)}{dPo}\nabla Po\cdot\vec{f}_o = -\frac{1}{|\vec{v}_T|}\frac{\partial}{\partial t}\left(\frac{\phi\, So}{Bo}\right) \qquad \text{(C-7)}$$

and

$$\frac{1}{Bw}\nabla\cdot\vec{f}_w + \frac{d(1/Bw)}{dPw}\nabla Pw\cdot\vec{f}_w = -\frac{1}{|\vec{v}_T|}\frac{\partial}{\partial t}\left(\frac{\phi\, Sw}{Bw}\right) \qquad \text{(C-8)}$$

APPENDIX D

DERIVATION OF THE DIMENSIONLESS FORM OF THE FRACTIONAL FLOW AND CONTINUITY EQUATIONS

DERIVATION OF THE DIMENSIONLESS FORM OF THE FRACTIONAL FLOW AND CONTINUITY EQUATIONS

An approach similar to that of Perkins and Collins[84], is used in the derivation of the dimensionless form of the necessary equations for describing the immiscible heavy oil displacement by carbon dioxide and water considering mass transfer.

When the porous medium is isotropic the absolute permeability tensor takes a constant value $\overline{\overline{K}} = K$ and Equation 20 may be written in the following expanded form:

$$\vec{f}_g = \left[\frac{\vec{v}_T}{|\vec{v}_T|} - \frac{K\ Krw}{|\vec{v}_T|\mu_w}\left(1 + \frac{Kro\ \mu_w}{Krw\ \mu_o}\right)\vec{g}\,\Delta\rho_{og} - \frac{\vec{g}\,\Delta\rho_{wo}\ K\ Krw}{|\vec{v}_T|\mu_w}\right] Fg$$

$$- \left[\frac{1}{|\vec{v}_T|}\left(1 + \frac{Kro\ \mu_w}{Krw\ \mu_o}\right)\frac{dPcgo}{dSg}\left(\frac{\partial Sg}{\partial x}\vec{i} + \frac{\partial Sg}{\partial y}\vec{j} + \frac{\partial Sg}{\partial z}\vec{k}\right)\right.$$

$$\left. - \frac{1}{|\vec{v}_T|}\frac{dPcow}{dSw}\left(\frac{\partial Sw}{\partial x}\vec{i} + \frac{\partial Sw}{\partial y}\vec{j} + \frac{\partial Sw}{\partial z}\vec{k}\right)\right]\frac{K\ Krw\ Fg}{\mu_w}$$

$$- \frac{1}{|\vec{v}_T|}\left(1 + \frac{Kro\ \mu_w}{Krw\ \mu_o}\right)\left[Dgox\ \frac{\partial Cgo}{\partial x}\vec{i} + Dgoy\ \frac{\partial Cgo}{\partial y}\vec{j}\right.$$

$$+ Dgoz\ \frac{\partial Cgo}{\partial z}\vec{k} + Dgwx\ \frac{\partial Cgw}{\partial x}\vec{i} + Dgwy\ \frac{\partial Cgw}{\partial y}\vec{j}$$

$$\left. + Dgwz\ \frac{\partial Cgw}{\partial z}\vec{k}\right)\frac{Krw\ \mu_g}{Krg\ \mu_w}\ Fg \qquad (D\text{-}1)$$

Capillary Pressure Model

For clean, unconsolidated sands the Leverett J-function[85] is successful in correlating capillary pressure data for water-oil systems.

$$J(Sw) = \frac{Pcow(Sw)}{\sigma_{ow}} \left(\frac{K}{\phi}\right)^{\frac{1}{2}} \qquad (D\text{-}2)$$

According to derivation from Poiseuille and Darcy's equations the term $(K/\phi)^{\frac{1}{2}}$ is related to the average pore radius of the porous system being studied.

The original Leverett J-function (Equation D-2) considers that the contact angle is substantially zero which is true for strongly water wet porous media.[86] When the contact angle is greater than zero, the modified Leverett J-function by Rose and Bruce[86] applies

$$J(Sw) = \frac{Pcow\ (Sw)}{\sigma_{ow} \cos\theta} \left(\frac{K}{\phi}\right)^{\frac{1}{2}} \qquad (D\text{-}3)$$

The gas-oil capillary pressure is considered a function of gas saturation only[80]. However, some authors[87] consider that the gas-oil capillary pressure is a function of both saturation and pressure. The dependence of capillary pressure on pressure is due to the variation of interfacial tension between oil and gas with pressure. Because of the lack of information of the effect of pressure on gas-oil capillary pressure, it will be assumed that gas-oil capillary pressure depends on gas saturation only. Thus the Leverett J-function for gas-oil systems may be written as:

$$J(Sg) = \frac{Pcgo\ (Sg)}{\sigma_{go}} \left(\frac{K}{\phi}\right)^{\frac{1}{2}} \qquad (D\text{-}4)$$

To introduce a certain degree of uniformity in relative permeabilities and capillary pressures for the variety of porous media

encountered in oil reservoirs, Collins[82] defined a modified saturation function for water-oil systems as follows:

$$Sw^* = \frac{Sw - Swi}{1-Swi-Sor} \qquad (D\text{-}5)$$

For three phases, Stone[80] defined the normalized saturation for oil and gas in the following form:

$$So^* = \frac{So - Sor}{1-Swi-Sor} \qquad (D\text{-}6)$$

and

$$Sg^* = \frac{Sg}{1-Swi-Sor} \qquad (D\text{-}7)$$

In the definition of Sg^*, the critical gas saturation is assumed to be zero.

Using the above definitions of Sw^* and Sg^*, the Leverett J-functions may be expressed as follows:

$$J(Sw^*) = \frac{Pcow(Sw^*)}{\sigma_{ow}} \left(\frac{K}{\phi}\right)^{\frac{1}{2}} \qquad (D\text{-}8)$$

and

$$J(Sg^*) = \frac{Pcgo(Sg^*)}{\sigma_{go}} \left(\frac{K}{\phi}\right)^{\frac{1}{2}} \qquad (D\text{-}9)$$

The relative permeabilities as functions of normalized saturations may be written:

$$Krw(Sw^*) = \frac{Kw\ (Sw^*)}{K} \qquad (D\text{-}10)$$

$$Krg(Sg^*) = \frac{Kg\ (Sg^*)}{K} \qquad (D\text{-}11)$$

$$Kro(Sg^*, Sw^*) = \frac{Ko(Sg^*, Sw^*)}{K} \qquad (D\text{-}12)$$

The transformation of Equation D-1 to a dimensionless form is accomplished by dividing each of the original variable in the equation by some reference quantity of the same dimensions as follows (after Perkins and Collins[84], and Demetre et al[88]).

$$\xi = x/L \qquad (D\text{-}13)$$

$$\theta = y/W \qquad (D\text{-}14)$$

$$\lambda = z/H \qquad (D\text{-}15)$$

$$Cgo^* = Cgo/C' \qquad (D\text{-}16)$$

$$Cgw^* = Cgw/C'' \qquad (D\text{-}17)$$

The dimensionless forms for Sw, So, and Sg are given by Equations D-5, D-6, and D-7 respectively, and for Pcow and Pcgo by Equations D-8 and D-9.

By definition Cgo and Cgw are dimensionless, then $C' = C'' = 1$.

Substitution of the dimensionless variables into Equation D-1 yields

$$\vec{f}_g = \left[\frac{\vec{v}_T}{|\vec{v}_T|} - \frac{\vec{g}\,K\,Krw(Sw^*)}{\mu_w\,|\vec{v}_T|}\,\Delta\rho_{og}\left(1 + \frac{Kro(Sg^*, Sw^*)\mu_w}{Krw(Sw^*)\mu_o}\right) - \frac{\vec{g}\,\Delta\rho_{wo}\,K\,Krw(Sw^*)}{|\vec{v}_T|\,\mu_w}\right] Fg$$

$$+ \left[\left(1 + \frac{Kro(Sg^*, Sw^*)\mu_w}{Krw(Sw^*)\mu_o}\right)\frac{\sigma_{go}\,K\,Krw(Sw^*)}{\mu_w|\vec{v}_T|L(K/\phi)^{\frac{1}{2}}}\frac{dJ(Sg^*)}{dSg^*}\left(\frac{\partial Sg^*}{\partial \xi}\vec{i}\right.\right.$$

$$\left.\left. + \frac{L}{W}\frac{\partial Sg^*}{\partial \theta}\vec{j} + \frac{L}{H}\frac{\partial Sg^*}{\partial \lambda}\vec{k}\right) - \frac{\sigma_{ow}\,K\,Krw(Sw^*)}{\mu_w|\vec{v}_T|L(K/\phi)^{\frac{1}{2}}}\frac{dJ(Sw^*)}{dSw^*}\right] \times$$

$$\times \left(\frac{\partial Sw^*}{\partial \xi} \vec{i} + \frac{L}{W} \frac{\partial Sw^*}{\partial \theta} \vec{j} + \frac{L}{H} \frac{\partial Sw^*}{\partial \lambda} \vec{k} \right) \Bigg] Fg - \frac{1}{|\vec{v_T}|} \left(1 + \frac{Kro(Sg^*, Sw^*)\mu_w}{Krw(Sw^*)\mu_o} \right)$$

$$\times \frac{Dgox}{L} \left(\frac{\partial Cgo}{\partial \xi} \vec{i} + \frac{Dgoy}{Dgox} \frac{L}{W} \frac{\partial Cgo}{\partial \theta} \vec{j} + \frac{Dgoz}{Dgox} \frac{L}{H} \frac{\partial Cgo}{\partial \lambda} \vec{k} \right) Fg \times \frac{Krw(Sw^*)\mu_g}{Krg(Sg^*)\mu_w}$$

$$- \frac{1}{|\vec{v_T}|} \left(1 + \frac{Kro(Sg^*, Sw^*)\mu_w}{Krw(Sw^*)\mu_o} \right) \frac{Dgwx}{L} \left(\frac{\partial Cgw}{\partial \xi} \vec{i} + \frac{Dgwy}{Dgwx} \frac{L}{W} \frac{\partial Cgw}{\partial \theta} \vec{j} \right.$$

$$\left. + \frac{Dgwz}{Dgwx} \frac{L}{H} \frac{\partial Cgw}{\partial \lambda} \vec{k} \right) Fg \times \frac{Krw(Sw^*)\mu_g}{Krg(Sg^*)\mu_w} \qquad \text{(D-18)}$$

Defining the ratio of the water to the oil mobility, Mwo, and the ratio of the gas to the oil mobility, Mgo, in the same manner as was done by Craig et al.[71], one obtains

$$\text{Water-oil mobility ratio, } Mwo = \frac{Krw(Sw^*)\,\mu_o}{Kro(Sg^*, Sw^*)\mu_w} \qquad \text{(D-19)}$$

$$\text{Gas-oil mobility ratio, } Mgo = \frac{Krg(Sg^*)\,\mu_o}{Kro(Sg^*, Sw^*)\mu_g} \qquad \text{(D-20)}$$

For displacement of oil by water and gas, $Krw(Sw^*)$ and $Krg(Sg^*)$ are evaluated at average saturations of water and gas behind of the flood front, and $Kro(Sg^*,Sw^*)$ at average saturations ahead of the flood front.

According to the above definitions of Mwo and Mgo, it can be shown that

$$\frac{Krw(Sw^*)}{\mu_w} \left(1 + \frac{Kro(Sg^*, Sw^*)\mu_w}{Krw(Sw^*)\mu_o} \right) = \frac{Krg(Sg^*)}{\mu_g} \left(\frac{1+Mwo}{Mgo} \right) \qquad \text{(D-21)}$$

and

$$\frac{Krw(Sw^*)\mu_g}{Krg(Sg^*)\mu_w}\left(1+\frac{Kro(Sg^*,Sw^*)\mu_w}{Krw(Sw^*)\mu_o}\right)=\left(\frac{1+Mwo}{Mgo}\right) \qquad \text{(D-22)}$$

Substituting Equations D-19 to D-22 [illegible]

$$\vec{f}_g=\left[\frac{\vec{v}_T}{|\vec{v}_T|}\left[\frac{\vec{g}\,K\,Krg(Sg^*)}{\mu_g|\vec{v}_T|}\,\Delta\rho_{og}\left(\frac{1+Mwo}{Mgo}\right)-\frac{\vec{g}\,\Delta\rho_{ow}\,K\,Krw(Sw^*)}{|\vec{v}_T|\,\mu_w}\right]Fg\right.$$

$$+\left[\left(\frac{1+Mwo}{Mgo}\right)\frac{\sigma_{go}\,K\,Krg(Sg^*)}{|\vec{v}_T|L\mu_g(K/\phi)^{\frac{1}{2}}}\frac{dJ(Sg^*)}{dSg^*}\left(\frac{\partial Sg^*}{\partial\xi}\vec{i}+\frac{L}{W}\frac{\partial Sg^*}{\partial\theta}\vec{j}+\frac{L}{H}\frac{\partial Sg^*}{\partial\lambda}\vec{k}\right)\right.$$

$$\left.\left.-\frac{\sigma_{ow}\,K\,Krw(Sw^*)}{|\vec{v}_T|L\mu_w(K/\phi)^{\frac{1}{2}}}\frac{dJ(Sw^*)}{dSw^*}\left(\frac{\partial Sw^*}{\partial\xi}\vec{i}+\frac{L}{W}\frac{\partial Sw^*}{\partial\theta}\vec{j}+\frac{L}{H}\frac{\partial Sw^*}{\partial\lambda}\vec{k}\right)\right]Fg\right.$$

$$-\left(\frac{1+Mwo}{Mgo}\right)\frac{Dgox}{|\vec{v}_T|L}\left(\frac{\partial Cgo}{\partial\xi}\vec{i}+\frac{Dgoy}{Dgox}\frac{L}{W}\frac{\partial Cgo}{\partial\theta}\vec{j}+\frac{Dgoz}{Dgox}\frac{L}{H}\frac{\partial Cgo}{\partial\lambda}\vec{k}\right)Fg$$

$$-\left(\frac{1+Mwo}{Mgo}\right)\frac{Dgwx}{|\vec{v}_T|L}\left(\frac{\partial Cgw}{\partial\xi}\vec{i}+\frac{Dgwy}{Dgwx}\frac{L}{W}\frac{\partial Cgw}{\partial\theta}\vec{j}+\frac{Dgwz}{Dgwx}\frac{L}{H}\frac{\partial Cgw}{\partial\lambda}\vec{k}\right)Fg \qquad \text{(D-23)}$$

Now, the following additional dimensionless groups are defined:

Vector of oil-gas gravity number, $\vec{N}gog=\dfrac{\vec{g}\,K\,\Delta\rho_{og}}{|\vec{v}_T|\,\mu_g}$ (D-24)

Vector of water-oil gravity number, $\vec{N}gwo=\dfrac{\vec{g}\,K\,\Delta\rho_{wo}}{|\vec{v}_T|\,\mu_w}$ (D-25)

Linear gas-oil capillary number, $Ncgo=\dfrac{\sigma_{go}\sqrt{K\phi}}{|\vec{v}_T|\,\mu_g\,L}$ (D-26)

Linear oil-water capillary number, $Ncow=\dfrac{\sigma_{ow}\sqrt{K\phi}}{|\vec{v}_T|\,\mu_w\,L}$ (D-27)

By making use of these definitions, Equation D-23 becomes

$$\vec{f}_g = \left[\frac{\vec{v}_T}{|\vec{v}_T|} - Krg(Sg^*)\vec{N}gog\left(\frac{1+Mwo}{Mgo}\right) - Krw(Sw^*)\vec{N}gwo\right] Fg$$

$$+ \left[Krg(Sg^*)Ncgo\left(\frac{1+Mwo}{Mgo}\right)\frac{dJ(Sg^*)}{dSg^*}\left(\frac{\partial Sg}{\partial \xi}\vec{i} + \frac{L}{W}\frac{\partial Sg^*}{\partial \theta}\vec{j} + \frac{L}{H}\frac{\partial Sg^*}{\partial \lambda}\vec{k}\right)\right.$$

$$\left. - Krw(Sw^*)Ncow\frac{dJ(Sw^*)}{dSw^*}\left(\frac{\partial Sw^*}{\partial \xi}\vec{i} + \frac{L}{W}\frac{\partial Sw^*}{\partial \theta}\vec{j} + \frac{L}{H}\frac{\partial Sw^*}{\partial \lambda}\vec{k}\right)\right] Fg$$

$$- \left(\frac{1+Mwo}{Mgo}\right)\frac{Dgox}{|\vec{v}_T|L}\left(\frac{\partial Cgo}{\partial \xi}\vec{i} + \frac{Dgoy}{Dgox}\frac{L}{W}\frac{\partial Cgo}{\partial \theta}\vec{j} + \frac{Dgoz}{Dgox}\frac{L}{H}\frac{\partial Cgo}{\partial \lambda}\vec{k}\right) Fg$$

$$- \left(\frac{1+Mwo}{Mgo}\right)\frac{Dgwx}{|\vec{v}_T|L}\left(\frac{\partial Cgw}{\partial \xi}\vec{i} + \frac{Dgwy}{Dgwx}\frac{L}{W}\frac{\partial Cgw}{\partial \xi}\vec{j} + \frac{Dgwz}{Dgwx}\frac{L}{H}\frac{\partial Cgw}{\partial \lambda}\vec{k}\right) Fg \quad (D\text{-}28)$$

In order to obtain the complete set of scaling groups by dimensional analysis, it is necessary to put Equations 18-20 in dimensionless form by defining dimensionless time in the same form as was defined by Perkins and Collins[84].

$$\tau = \frac{|\vec{v}_T|t}{\phi L(1-Sor-Swi)} \quad (D\text{-}29)$$

ξ, θ, λ, So*, Sg*, and Sw* will have the same definitions as above. The remaining variables $f_{g\xi}$, $f_{g\theta}$, $f_{g\lambda}$, Rso, Rsw, Bo, Bw, Bg, ϕ, Cgo, and Cgw are dimensionless and they do not need to be changed. It is also not necessary to define a dimensionless quantity for pressure because the model will be operated at the same high pressure of the prototype and because in the terms of Equation 24 which have pressure as variable, the pressure appears in the numerator and denominator, therefore the reference quantity would be cancelled.

Substituting the expressions for ξ, θ, λ, So*, Sg*, Sw*, and τ into Equation 18 yields

$$\frac{1}{Bg}\left(\frac{1}{L}\frac{\partial f_{g\xi}}{\partial \xi}+\frac{1}{W}\frac{\partial f_{g\theta}}{\partial \theta}+\frac{1}{H}\frac{\partial f_{g\lambda}}{\partial \lambda}\right)+\left(\frac{f_{g\xi}}{L}\frac{\partial Pg}{\partial \xi}+\frac{f_{g\theta}}{W}\frac{\partial Pg}{\partial \theta}+\frac{f_{g\lambda}}{H}\frac{\partial Pg}{\partial \lambda}\right)\frac{d(1/Bg)}{dPg}$$

$$+\frac{Rso}{Bo}\left(\frac{1}{L}\frac{\partial f_{o\xi}}{\partial \xi}+\frac{1}{W}\frac{\partial f_{o\theta}}{\partial \theta}+\frac{1}{H}\frac{\partial f_{o\lambda}}{\partial \lambda}\right)+\left(\frac{f_{o\xi}}{L}\frac{\partial Po}{\partial \xi}+\frac{f_{o\theta}}{W}\frac{\partial Po}{\partial \theta}+\frac{f_{o\lambda}}{H}\frac{\partial Po}{\partial \lambda}\right)\frac{d}{dPo}\left(\frac{Rso}{Bo}\right)$$

$$+\frac{Rsw}{Bw}\left(\frac{1}{L}\frac{\partial f_{w\xi}}{\partial \xi}+\frac{1}{W}\frac{\partial f_{w\theta}}{\partial \theta}+\frac{1}{H}\frac{\partial f_{w\lambda}}{\partial \lambda}\right)+\left(\frac{f_{w\xi}}{L}\frac{\partial Pw}{\partial \xi}+\frac{f_{w\theta}}{W}\frac{\partial Pw}{\partial \theta}+\frac{f_{w\lambda}}{H}\frac{\partial Pw}{\partial \lambda}\right)\frac{d}{dPw}\left(\frac{Rsw}{Bw}\right)$$

$$=-\frac{1}{L}\frac{\partial}{\partial \tau}\left(\frac{Sg^*}{Bg}\right)-\frac{1}{L}\frac{\partial}{\partial \tau}\left(\frac{Rso\ So^*}{Bo}\right)-\frac{Sor}{L(1-Sor-Swi)}\frac{\partial}{\partial \tau}\left(\frac{Rso}{Bo}\right)-\frac{1}{L}\frac{\partial}{\partial \tau}\left(\frac{Rsw\ Sw^*}{Bw}\right)$$

$$-\frac{Swi}{L(1-Sor-Swi)}\frac{\partial}{\partial \tau}\left(\frac{Rsw}{Bw}\right)-\frac{1}{L}\frac{\partial}{\partial \tau}\left(\frac{Cgo\ So^*}{Bg}\right)-\frac{Sor}{L(1-Sor-Swi)}\frac{\partial}{\partial \tau}\left(\frac{Cgo}{Bg}\right)$$

$$-\frac{1}{L}\frac{\partial}{\partial \tau}\left(\frac{Cgw\ Sw^*}{Bg}\right)-\frac{Swi}{L(1-Sor-Swi)}\frac{\partial}{\partial \tau}\left(\frac{Cgw}{Bg}\right) \qquad \text{(D-30)}$$

The right hand side (RHS) of Equation D-30 can be written in the following form:

$$RHS=-\frac{1}{LBg}\frac{\partial Sg^*}{\partial \tau}-\frac{Sg^*}{L}\frac{d}{dPg}\left(\frac{1}{Bg}\right)\frac{\partial Pg}{\partial \tau}-\frac{Rso}{LBo}\frac{\partial So^*}{\partial \tau}-\frac{So^*}{L}\frac{d}{dPo}\left(\frac{Rso}{Bo}\right)\frac{\partial Po}{\partial \tau}$$

$$-\frac{Sor}{L(1-Sor-Swi)}\frac{d}{dPo}\left(\frac{Rso}{Bo}\right)\frac{\partial Po}{\partial \tau}-\frac{Rsw}{LBw}\frac{\partial Sw^*}{\partial \tau}-\frac{Sw^*}{L}\frac{d}{dPw}\left(\frac{Rsw}{Bw}\right)\frac{\partial Pw}{\partial \tau}$$

$$-\frac{Swi}{L(1-Sor-Swi)}\frac{d}{dPw}\left(\frac{Rsw}{Bw}\right)\frac{\partial Pw}{\partial \tau}-\frac{1}{LBg}\frac{\partial}{\partial \tau}(Cgo\ So^*)-\frac{Cgo\ So^*}{L}\frac{d}{dPg}\left(\frac{1}{Bg}\right)\frac{\partial Pg}{\partial \tau}$$

$$-\frac{Sor}{LBg(1-Sor-Swi)}\frac{\partial Cgo}{\partial \tau}-\frac{Sor\ Cgo}{L(1-Sor-Swi)}\frac{d}{dPg}\left(\frac{1}{Bg}\right)\frac{\partial Pg}{\partial \tau}-\frac{1}{LBg}\frac{\partial}{\partial \tau}(Cgw\ Sw^*)$$

$$-\frac{Cgw\ Sw^*}{L}\frac{d}{dPg}\left(\frac{1}{Bg}\right)\frac{\partial Pg}{\partial \tau}-\frac{Swi}{LBg(1-Sor-Swi)}\frac{\partial Cgw}{\partial \tau}-\frac{Swi\ Cgw}{L(1-Sor-Swi)}\frac{d}{dPg}\left(\frac{1}{Bg}\right)\frac{\partial Pg}{\partial \tau}$$

Multiplying Equation D-30 by L and substituting the above expansion of its RHS, this equation takes the form:

$$\frac{1}{Bg}\left(\frac{\partial f_{g\xi}}{\partial \xi}+\frac{L}{W}\frac{\partial f_{g\theta}}{\partial \theta}+\frac{L}{H}\frac{\partial f_{g\lambda}}{\partial \lambda}\right)+\left(f_{g\xi}\frac{\partial Pg}{\partial \xi}+\frac{L}{W}f_{g\theta}\frac{\partial Pg}{\partial \theta}+\frac{L}{H}f_{g\lambda}\frac{\partial Pg}{\partial \lambda}\right)\frac{d}{dPg}\left(\frac{1}{Bg}\right)$$

$$+\frac{Rso}{Bo}\left(\frac{\partial f_{o\xi}}{\partial \xi}+\frac{L}{W}\frac{\partial f_{o\theta}}{\partial \theta}+\frac{L}{H}\frac{\partial f_{o\lambda}}{\partial \lambda}\right)+\left(f_{o\xi}\frac{\partial Po}{\partial \xi}+\frac{L}{W}f_{o\theta}\frac{\partial Po}{\partial \theta}+\frac{L}{H}f_{o\lambda}\frac{\partial Po}{\partial \lambda}\right)$$

$$\times\frac{d}{dPo}\left(\frac{Rso}{Bo}\right)+\frac{Rsw}{Bw}\left(\frac{\partial f_{w\xi}}{\partial \xi}+\frac{L}{W}\frac{\partial f_{w\theta}}{\partial \theta}+\frac{L}{H}\frac{\partial f_{w\lambda}}{\partial \lambda}\right)+\left(f_{w\xi}\frac{\partial Pw}{\partial \xi}+\frac{L}{W}f_{w\theta}\frac{\partial Pw}{\partial \theta}\right.$$

$$\left.+\frac{L}{H}f_{w\lambda}\frac{\partial Pw}{\partial \lambda}\right)\frac{d}{dPw}\left(\frac{Rsw}{Bw}\right)$$

$$=-\frac{1}{Bg}\frac{\partial Sg^*}{\partial \tau}-\left(Sg^*+Cgo\,So^*+\frac{Sor\;Cgo}{1-Sor-Swi}+Cgw\,Sw^*+\frac{Swi\;Cgw}{1-Sor-Swi}\right)\frac{d}{dPg}\left(\frac{1}{Bg}\right)\frac{\partial Pg}{\partial \tau}$$

$$-\frac{Rso}{Bo}\frac{\partial So^*}{\partial \tau}-\left(So^*+\frac{Sor}{1-Sor-Swi}\right)\frac{d}{dPo}\left(\frac{Rso}{Bo}\right)\frac{\partial Po}{\partial \tau}-\frac{Rsw}{Bw}\frac{\partial Sw^*}{\partial \tau}$$

$$-\left(Sw^*+\frac{Swi}{1-Sor-Swi}\right)\frac{d}{dPw}\left(\frac{Rsw}{Bw}\right)\frac{\partial Pw}{\partial \tau}-\frac{1}{Bg}\frac{\partial}{\partial \tau}\left(Cgo\,So^*\right)-\frac{Sor}{Bg(1-Sor-Swi)}\frac{\partial Cgo}{\partial \tau}$$

$$-\frac{1}{Bg}\frac{\partial}{\partial \tau}\left(Cgw\,Sw^*\right)-\frac{Swi}{Bg(1-Sor-Swi)}\frac{\partial Cgw}{\partial \tau} \qquad \text{(D-31)}$$

It turns out (after some algebra) the continuity equations for oil and water become

$$\frac{1}{Bo}\left(\frac{\partial f_{o\xi}}{\partial \xi}+\frac{L}{W}\frac{\partial f_{o\theta}}{\partial \theta}+\frac{L}{H}\frac{\partial f_{o\lambda}}{\partial \lambda}\right)+\left(f_{o\xi}\frac{\partial Po}{\partial \xi}+\frac{L}{W}f_{o\theta}\frac{\partial Po}{\partial \theta}+\frac{L}{H}f_{o\lambda}\frac{\partial Po}{\partial \lambda}\right)\frac{d}{dPo}\left(\frac{1}{Bo}\right)$$

$$=-\frac{1}{Bo}\frac{\partial So^*}{\partial \tau}-\left(So^*+\frac{Sor}{1-Sor-Swi}\right)\frac{d}{dPo}\left(\frac{1}{Bo}\right)\frac{\partial Po}{\partial \tau} \qquad \text{(D-32)}$$

and

$$\frac{1}{Bw}\left(\frac{\partial f_{w\xi}}{\partial \xi}+\frac{L}{W}\frac{\partial f_{w\theta}}{\partial \theta}+\frac{L}{H}\frac{\partial f_{w\lambda}}{\partial \lambda}\right)+\left(f_{w\xi}\frac{\partial Pw}{\partial \xi}+\frac{L}{W}f_{w\theta}\frac{\partial Pw}{\partial \theta}+\frac{L}{H}f_{w\lambda}\frac{\partial Pw}{\partial \lambda}\right)\frac{d}{dPw}\left(\frac{1}{Bw}\right)$$

$$=-\frac{1}{Bw}\frac{\partial Sw^*}{\partial \tau}-\left(Sw^*+\frac{Swi}{1-Sor-Swi}\right)\frac{d}{dPw}\left(\frac{1}{Bw}\right)\frac{\partial Pw}{\partial \tau} \qquad \text{(D-33)}$$

APPENDIX E

DERIVATION OF THE SCALING GROUPS BY DIMENSIONAL ANALYSIS

DERIVATION OF THE SCALING GROUPS BY DIMENSIONAL ANALYSIS

The variables involved in the immiscible displacement of heavy oil by carbon dioxide and water, considering mass transfer are given by the following equation:

$$f(L, W, H, \phi, M, K, Krg, Kro, Krw, \mu_g, \mu_o, \mu_w, \rho_g, \rho_w, g\Delta\rho_{og}, g\Delta\rho_{wo}, \sigma_{go}, \sigma_{ow}, J(Sg^*), J(Sw^*), Dgox, Dgoy, Dgoz, Dgwx, Dgwy, Dgwz, V, t, Vg^*, Vw^*) = 0 \quad (E\text{-}1)$$

Applying the principle of dimensional homogeneity and using the mass (M), length (L), time (t) system, results in:

$$M^oL^ot^o \underline{d} L^{K_1} W^{K_2} H^{K_3} \phi^o M^o K^{K_4} Krg^o Kro^o Krw^o \mu_g^{K_5} \mu_o^{K_6} \mu_w^{K_7} \rho_g^{K_8} \rho_w^{K_9} (g\Delta\rho_{og})^{K_{10}} (g\Delta\rho_{wo})^{K_{11}} \sigma_{go}^{K_{12}} \sigma_{ow}^{K_{13}} (J(Sg^*))^o (J(Sw^*))^o Dgox^{K_{14}} Dgoy^{K_{15}} Dgoz^{K_{16}} Dgwx^{K_{17}} Dgwy^{K_{18}} Dgwz^{K_{19}} V^{K_{20}} t^{K_{21}} Vg^{*o} Vw^{*o} \quad (E\text{-}2)$$

where $K_1, K_2, \ldots K_{21}$ are constants, the exponents of the dimensionless variables ϕ, M, Krg, Kro, Krw, Vg*, and Vw* are zero, and $\underline{d}$ means dimensionally equal.

Introducing the dimensions of the variables (Table 1) into the above equation yields

$$M^{0}L^{0}t^{0} \doteq (L)^{K_1}(L)^{K_2}(L)^{K_3}(L^2)^{K_4}(ML^{-1}t^{-1})^{K_5}(ML^{-1}t^{-1})^{K_6}(ML^{-1}t^{-1})^{K_7}$$
$$(ML^{-3})^{K_8}(ML^{-3})^{K_9}(ML^{-2}t^{-2})^{K_{10}}(ML^{-2}t^{-2})^{K_{11}}(Mt^{-2})^{K_{12}}(Mt^{-2})^{K_{13}}$$
$$(L^2t^{-1})^{K_{14}}(L^2t^{-1})^{K_{15}}(L^2t^{-1})^{K_{16}}(L^2t^{-1})^{K_{17}}(L^2t^{-1})^{K_{18}}$$
$$(L^2t^{-1})^{K_{19}}(Lt^{-1})^{K_{20}}(t)^{K_{21}} \qquad \text{(E-3)}$$

Equating the exponents of M, L, and t on both sides of Equation E-3, the following system of equations is obtained:

$$M: \quad K_5 + K_6 + K_7 + K_8 + K_9 + K_{10} + K_{11} + K_{12} + K_{13} = 0 \qquad \text{(E-4)}$$

$$L: \quad K_1 + K_2 + K_3 + 2K_4 - K_5 - K_6 - K_7 - 3K_8 - 3K_9$$
$$- 2K_{10} - 2K_{11} + 2K_{14} + 2K_{15} + 2K_{16} + 2K_{17}$$
$$+ 2K_{18} + 2K_{19} + K_{20} = 0 \qquad \text{(E-5)}$$

$$t: \quad -K_5 - K_6 - K_7 - 2K_{10} - 2K_{11} - 2K_{12} - 2K_{13} - K_{14} - K_{15}$$
$$- K_{16} - K_{17} - K_{18} - K_{19} - K_{20} + K_{21} = 0 \qquad \text{(E-6)}$$

This system of equations may be written in the following matrix form:

$$A\vec{K} = 0 \qquad \text{(E-7)}$$

where A is the dimensional matrix[93] given by

$$A = \begin{bmatrix} 0 & 0 & 0 & 0 & 1 & 1 & 1 & 1 & 1 & 1 & 1 & 1 & 1 & 0 & 0 & 0 & 0 & 0 & 0 & 0 & 0 \\ 1 & 1 & 1 & 2 & -1 & -1 & -1 & -3 & -3 & -2 & -2 & 0 & 0 & 2 & 2 & 2 & 2 & 2 & 2 & I & 0 \\ 0 & 0 & 0 & 0 & -1 & -1 & -1 & 0 & 0 & -2 & -2 & -2 & -2 & -1 & -1 & -1 & -1 & -1 & -1 & -1 & 1 \end{bmatrix} \qquad \text{(E-8)}$$

and the solution vector $\vec{K}$ may be written as:

$$\vec{K} = \begin{bmatrix} K_1 \\ K_2 \\ \cdot \\ \cdot \\ \cdot \\ K_{19} \\ K_{20} \\ K_{21} \end{bmatrix} \qquad \text{(E-9)}$$

Buckingham[89] pointed out that the number of dimensionless groups (or products) in a complete set is equal to the total number of variables minus the number of fundamental dimensions, e.g. mass, length, and time. That is true in most cases, however it is better to use the following Langhaar's theorem[70] that is more general: "the number of dimensionless products in a complete set is equal to the total number of variables minus the rank of their dimensional matrix." He also stated that the rank of a matrix may be defined as: "if a matrix contains a non zero determinant of order γ, and if all determinants of order greater than γ that the matrix contains have the value zero, the rank of the matrix is said to be γ".

For the above dimensional matrix its rank is 3, since the highest order of the determinant for the matrix is 3. It may easily be shown that the determinant formed from the columns number 12, 20, and 21 is different from zero. Thus, there are 3 equations and 21 unknowns. In mathematical terminology this system of equations is "under-determined". Such a system of equations possesses an infinite number of solutions. A possible solution is to express any three of the coefficients in terms of the others. For example

$$K_1 = - K_2 - K_3 - 2K_4 + K_5 + K_6 + K_7 + 3K_8 + 3K_9 + 2K_{10}$$
$$+ 2K_{11} - 2K_{14} - 2K_{15} - 2K_{16} - 2K_{17} - 2K_{18}$$
$$- 2K_{19} - K_{20} \qquad \text{(E-10)}$$

$$K_5 = - K_6 - K_7 - K_8 - K_9 - K_{10} - K_{11} - K_{12} - K_{13} \qquad \text{(E-11)}$$

$$K_{21} = K_5 + K_6 + K_7 + 2K_{10} + 2K_{11} + 2K_{12} + 2K_{13} + K_{14}$$
$$+ K_{15} + K_{16} + K_{17} + K_{18} + K_{19} + K_{20} \qquad \text{(E-12)}$$

The variables L (with K_1 as exponent), μ_g (with K_5 as exponent), and t (with K_{21} as exponent) were chosen because these variables are considered to play an important role in the process. Really, one can choose any three.

Replacing K_5 from Equation E-11 into Equations E-10 and E-13 yields the following system of equations which is easier to handle.

$$K_1 = - K_2 - K_3 - 2K_4 + 2K_8 + 2K_9 + K_{10} + K_{11} - K_{12} - K_{13}$$
$$- 2K_{14} - 2K_{15} - 2K_{16} - 2K_{17} - 2K_{18} - 2K_{19} - K_{20} \qquad \text{(E-13)}$$

$$K_5 = - K_6 - K_7 - K_8 - K_9 - K_{10} - K_{11} - K_{12} - K_{13} \qquad \text{(E-14)}$$

$$K_{21} = - K_8 - K_9 + K_{10} + K_{11} + K_{12} + K_{13} + K_{14} + K_{15} + K_{16}$$
$$+ K_{17} + K_{18} + K_{19} + K_{20} \qquad \text{(E-15)}$$

Substituting Equations E-13, E-14, and E-15 into Equation E-2 yields:

$$M^{o}L^{o}t^{o} \stackrel{d}{=} L^{(-K_2-K_3-2K_4+2K_8+2K_9+K_{10}+K_{11}-K_{12}-K_{13}-2K_{14}-2K_{15}-2K_{16}-2K_{17}-2K_{18}-2K_{19}-K_{20})}$$
$$\times W^{K_2} H^{K_3} \phi^{o} M^{o} K^{K_4} Krg^{o} Kro^{o} Krw^{o} \mu_g^{(-K_6-K_7-K_8-K_9-K_{10}-K_{11}-K_{12}-K_{13})} \mu_o^{K_6}$$
$$\times \mu_w^{K_7} \rho_g^{K_8} \rho_w^{K_9} (g\Delta\rho_{og})^{K_{10}} (g\Delta\rho_{wo})^{K_{11}} \sigma_{go}^{K_{12}} \sigma_{ow}^{K_{13}} (J(Sg^*))^{o} (J(Sw^*))^{o}$$
$$\times Dgox^{K_{14}} Dgoy^{K_{15}} Dgoz^{K_{16}} Dgwx^{K_{17}} Dgwy^{K_{18}} Dgwz^{K_{19}} V^{K_{20}}$$
$$\times t^{(-K_8-K_9+K_{10}+K_{11}+K_{12}+K_{13}+K_{14}+K_{15}+K_{16}+K_{17}+K_{18}+K_{19}+K_{20})} Vg^{*o} Vw^{*o} \qquad \text{(E-16)}$$

Putting together terms with the same exponent results in:

$$M^{o}L^{o}t^{o} \stackrel{d}{=} (L^{-1}W)^{K_2} (L^{-1}H)^{K_3} (L^{-2}K)^{K_4} (\mu_g^{-1}\mu_o)^{K_6} (\mu_g^{-1}\mu_w)^{K_7} (L^2\mu_g^{-1}\rho_g t^{-1})^{K_8}$$
$$\times (L^2\mu_g^{-1}\rho_w t^{-1})^{K_9} (L\mu_g^{-1} g\Delta\rho_{og} t)^{K_{10}} (Lg\Delta\rho_{wo}\, g^{-1} t)^{K_{11}}$$
$$\times (L^{-1}\mu_g^{-1}\sigma_{go} t)^{K_{12}} (L^{-1}\mu_g^{-1}\sigma_{ow} t)^{K_{13}} (L^{-2} Dgox\, t)^{K_{14}} (L^{-2} Dgoy\, t)^{K_{15}}$$
$$\times (L^{-2} Dgoz\, t)^{K_{16}} (L^{-2} Dgwx\, t)^{K_{17}} (L^{-2} Dgwy\, t)^{K_{18}} (L^{-2} Dgwz\, t)^{K_{19}}$$
$$\times (L^{-1}Vt)^{K_{20}} \phi^{o} M^{o} Krg^{o} Kro^{o} Krw^{o} (J(Sg^*))^{o} (J(Sw^*))^{o} Vg^{*o} Vw^{*o} \qquad \text{(E-17)}$$

The following π-terms are obtained from Equation E-17:

$$\pi_1 = W/L \qquad \text{(E-18)}$$

$$\pi_2 = H/L \qquad \text{(E-19)}$$

$$\pi_3 = K/L^2 \qquad \text{(E-20)}$$

$$\pi_4 = \mu_o/\mu_g \qquad \text{(E-21)}$$

$$\pi_5 = \mu_w/\mu_g \quad \text{(E-22)}$$

$$\pi_6 = L^2\rho_g/\mu_g t \quad \text{(E-23)}$$

$$\pi_7 = L^2\rho_w/\mu_g t \quad \text{(E-24)}$$

$$\pi_8 = Lg\,\Delta\rho_{og}t/\mu_g \quad \text{(E-25)}$$

$$\pi_9 = Lg\,\Delta\rho_{wo}t/\mu_g \quad \text{(E-26)}$$

$$\pi_{10} = \sigma_{go}t/L\mu_g \quad \text{(E-27)}$$

$$\pi_{11} = \sigma_{ow}t/L\mu_g \quad \text{(E-28)}$$

$$\pi_{12} = Dgox\ t/L^2 \quad \text{(E-29)}$$

$$\pi_{13} = Dgoy\ t/L^2 \quad \text{(E-30)}$$

$$\pi_{14} = Dgoz\ t/L^2 \quad \text{(E-31)}$$

$$\pi_{15} = Dgwx\ t/L^2 \quad \text{(E-32)}$$

$$\pi_{16} = Dgwy\ t/L^2 \quad \text{(E-33)}$$

$$\pi_{17} = Dgwz\ t/L^2 \quad \text{(E-34)}$$

$$\pi_{18} = Vt/L \quad \text{(E-35)}$$

$$\pi_{19} = \phi \quad \text{(E-36)}$$

$$\pi_{20} = M \quad \text{(E-37)}$$

$$\pi_{21} = Krg \quad \text{(E-38)}$$

$$\pi_{22} = Kro \quad \text{(E-39)}$$

$$\pi_{23} = Krw \quad \text{(E-40)}$$

$$\pi_{24} = J(Sg^*) \quad \text{(E-41)}$$

$$\pi_{25} = J(Sw^*) \qquad \text{(E-42)}$$

$$\pi_{26} = Vg^* \qquad \text{(E-43)}$$

$$\pi_{27} = Vw^* \qquad \text{(E-44)}$$

APPENDIX F

CALCULATION EXAMPLE OF THE MOLECULAR DIFFUSION COEFFICIENT

Data:

Sample 2

Δt = diffusion time = 676800 s

m_o = weight of oil in the foam = 225.35 g

m_{CO_2} = weight of CO_2 in the foam = 1.74 g

A = internal cross sectional area of the diffusion cell

= 31.67 cm^2

ΔL = length of the oil column = 50 cm

M_o = molecular weight of oil = 460 g/g mol

M_{CO_2} = molecular weight of CO_2 = 44 g/g mol

Calculations:

1. The initial molar fraction of CO_2 in the foam can be expressed as

$$x_{CO_2} = \frac{m_{CO_2}/M_{CO_2}}{m_o/M_o + m_{CO_2}/M_{CO_2}} = \frac{1}{1 + \frac{M_{CO_2}\, m_o}{M_o\, m_{CO_2}}} \qquad \text{(F1)}$$

Replacing the data in Equation F1 a value of x_{CO_2} = 0.075 (7.5%) was obtained.

2. The specific volume of the oil-CO_2 mixture at 5.5 MPag and 22°C can be calculated as

$$\nu_f = \nu_o x_o + \nu_{CO_2} x_{CO_2} \quad \text{at 5.5 MPag \& 22°C} \qquad \text{(F2)}$$

$$\nu_o = \frac{1}{\rho_o} = 1.03 \text{ cm}^3/\text{g} \text{ (from Table 5)}$$

ν_{CO_2} = 6.075 cm^3/g (from Reference 124).

Substituting the values of ν_o, x_o, ν_{CO_2}, and x_{CO_2} in Equation F2 the specific volume of the foam at diffusion conditions was obtained,

$$\nu_f = 1.408 \text{ cm}^3/\text{g}$$

3. The concentration gradient of CO_2 in the oil, may be expressed as

$$\frac{\Delta C}{\Delta L} = \frac{1}{\Delta L} (C_2 - C_1) \qquad \text{(F3)}$$

where

C_2 = concentration of CO_2 in the sample taken, g mol/cm^3

C_1 = concentration of CO_2 at the gas-oil contact, g mol/cm^3

$$C_2 = \frac{m_{CO_2}/M_{CO_2}}{m_f \nu_f} \qquad \text{(F4)}$$

and

$$C_1 = \frac{1}{\nu_{CO_2} M_{CO_2}} \qquad \text{(F5)}$$

Replacing Equations F4 and F5 in Equation F3, the following equation was obtained to calculate $\Delta C/\Delta L$:

$$\frac{\Delta C}{\Delta L} = \frac{1}{\Delta L}\left(\frac{m_{CO_2}}{m_f \nu_f M_{CO_2}} - \frac{1}{\nu_{CO_2} M_{CO_2}}\right) \qquad \text{(F6)}$$

From Equation F6

$$\frac{\Delta C}{\Delta L} = -0.0000723 \frac{\text{g mol}}{\text{cm}^3 \times \text{cm}}$$

(The negative sign indicates that the CO_2 concentration decreases with distance.)

4. Molar flux of carbon dioxide, $\Delta G/\Delta t$.

$$\frac{\Delta G}{\Delta t} = \frac{m_{CO_2}/M_{CO_2}}{\Delta t} . \qquad (F7)$$

From Equation F7

$$\frac{\Delta G}{\Delta t} = 5.843E-08 \ \frac{g\ mol}{s} .$$

5. Substituting $\Delta C/\Delta L$, $\Delta G/\Delta t$, and A in Equation 61 of Chapter 9 an approximate value of the molecular diffusion coefficient was obtained

$$Do = 2.56E-05 \ cm^2/s .$$

APPENDIX G

PRODUCTION HISTORIES OF ALL RUNS IN TABULATED FORM

TABLE G1

RESULTS OF RUN 1

PORE VOLUME=0.2092E+04 CM3
HYDROCARBON PORE VOLUME=0.1959E+04 CM3
POROSITY=0.4370E+02%
IRREDUCIBLE WATER SATURATION=0.6400E+01%
INITIAL OIL SATURATION=0.9360E+02%
CARBON DIOXIDE RETENTION=0.3241E+02 %
CARBON DIOXIDE REQUIRED=0.3799E+02 SM3/M3

PI,MPAG	PP,MPAG	GI,CM3	WI,CM3	VFI/PV	NP,CM3	%R	GOR,SM3/M3	WOR,M3/M3	OPFIR,M3/M3
0.6895E+01	0.0	0.0	0.1500E+02	0.7170E-02	0.1500E+02	0.7657E+00	0.0	0.0	0.1000E+01
0.6895E+01	0.0	0.0	0.5200E+02	0.2486E-01	0.2000E+02	0.1021E+01	0.0	0.1140E+02	0.1351E+00
0.5516E+01	0.0	0.0	0.1500E+03	0.7170E-01	0.2400E+02	0.1225E+01	0.0	0.1725E+02	0.4082E-01
0.4137E+01	0.0	0.0	0.2275E+03	0.1087E+00	0.2850E+02	0.1455E+01	0.0	0.1622E+02	0.5806E-01
0.4137E+01	0.0	0.0	0.3015E+03	0.1441E+00	0.3250E+02	0.1659E+01	0.0	0.1750E+02	0.5405E-01
0.5619E+01	0.5330E+01	0.2234E+02	0.3015E+03	0.1548E+00	0.3251E+02	0.1660E+01	0.0	0.0	0.4476E-03
0.5688E+01	0.5157E+01	0.3234E+02	0.3015E+03	0.1596E+00	0.4150E+02	0.2118E+01	0.0	0.1112E+00	0.8990E+00
0.5757E+01	0.5206E+01	0.4674E+02	0.3015E+03	0.1665E+00	0.5150E+02	0.2629E+01	0.7299E+02	0.0	0.6944E+00
0.5654E+01	0.5640E+01	0.5104E+02	0.3015E+03	0.1685E+00	0.5450E+02	0.2782E+01	0.1622E+03	0.0	0.6977E+00
0.5206E+01	0.5192E+01	0.6994E+02	0.3015E+03	0.1776E+00	0.6750E+02	0.3446E+01	0.3743E+02	0.0	0.6878E+00
0.5392E+01	0.5378E+01	0.6994E+02	0.3903E+03	0.2200E+00	0.7052E+02	0.3600E+01	0.5639E+02	0.7616E+01	0.3401E-01
0.5585E+01	0.5564E+01	0.6994E+02	0.5015E+03	0.2732E+00	0.7250E+02	0.3701E+01	0.8602E+02	0.1162E+02	0.1781E-01
0.6550E+01	0.3447E+01	0.6994E+02	0.6015E+03	0.3210E+00	0.7950E+02	0.4058E+01	0.8110E+02	0.1157E+02	0.7000E-01
0.5861E+01	0.2896E+01	0.6994E+02	0.6515E+03	0.3449E+00	0.8350E+02	0.4262E+01	0.2028E+03	0.1225E+02	0.8000E-01
0.6068E+01	0.1517E+01	0.6994E+02	0.7215E+03	0.3783E+00	0.9200E+02	0.4696E+01	0.6679E+02	0.8706E+01	0.1214E+00
0.5516E+01	0.6895E+00	0.6994E+02	0.8015E+03	0.4166E+00	0.9700E+02	0.4952E+01	0.2433E+02	0.1800E+02	0.6250E-01

University of Alberta

TABLE G1 (CONTINUED)

RESULTS OF RUN 1

PI,MPAG	PP,MPAG	GI,CM3	WI,CM3	VFI/PV	NP,CM3	%R	GOR,SM3/M3	WOR,M3/M3	OPFIR,M3/M3
0.6412E+01	0.4826E+00	0.6994E+02	0.8815E+03	0.4548E+00	0.1040E+03	0.5309E+01	0.1738E+02	0.1071E+02	0.8750E-01
0.6895E+01	0.3447E+00	0.6994E+02	0.9165E+03	0.4715E+00	0.1220E+03	0.6228E+01	0.4055E+01	0.3167E+01	0.5143E+00
0.6895E+01	0.1724E+00	0.6994E+02	0.9415E+03	0.4835E+00	0.1330E+03	0.6789E+01	0.1475E+02	0.1545E+01	0.4400E+00
0.1603E+01	0.1034E-01	0.6994E+02	0.9415E+03	0.4835E+00	0.2020E+03	0.1031E+02	0.1352E+01	0.1884E+00	
0.1462E+01	0.0	0.6994E+02	0.9415E+03	0.4835E+00	0.2110E+03	0.1077E+02	0.0	0.1111E+00	

PI=INJECTION PRESSURE
PP=PRODUCTION PRESSURE
GI=CUMULATIVE VOLUME OF CO2 INJECTED
WI=BRINE INJECTED
VFI=TOTAL VOLUME OF FLUID INJECTED
PV=PORE VOLUME OF SAND PACK
NP=CUMULATIVE VOLUME OIL PRODUCED
%R=RECOVERY PERCENT
GOR=GAS-OIL RATIO
WOR=WATER-OIL RATIO
OPFIR=OIL PRODUCED-FLUID INJECTED RATIO

University of Alberta

TABLE G2

RESULTS OF RUN 3

PORE VOLUME=0.2149E+04 CM3
HYDROCARBON PORE VOLUME=0.1751E+04 CM3
POROSITY=0.4490E+02%
IRREDUCIBLE WATER SATURATION=0.1850E+02%
INITIAL OIL SATURATION=0.8150E+02%
ABSOLUTE PERMEABILITY=0.1015E+02 DARCIES
CARBON DIOXIDE RETENTION=0.6293E+02 %
CARBON DIOXIDE REQUIRED=0.1208E+03 SM3/M3

PI,MPAG	PP,MPAG	GI,CM3	WI,CM3	VFI/PV	NP,CM3	%R	GOR,SM3/M3	WOR,M3/M3	OPFIR,M3/M3
0.1310E+01	0.0	0.0	0.3900E+02	0.1815E-01	0.1300E+02	0.7423E+00	0.0	0.0	0.3333E+00
0.1862E+01	0.0	0.0	0.7900E+02	0.3676E-01	0.5000E+02	0.2855E+01	0.0	0.0	0.9250E+00
0.1724E+01	0.0	0.0	0.9000E+02	0.4187E-01	0.5730E+02	0.3272E+01	0.0	0.2740E+00	0.6636E+00
0.1310E+01	0.0	0.0	0.1300E+03	0.6048E-01	0.9030E+02	0.5156E+01	0.0	0.3030E+00	0.8250E+00
0.2068E+01	0.0	0.0	0.1880E+03	0.8747E-01	0.1323E+03	0.7554E+01	0.0	0.1905E+00	0.7241E+00
0.2275E+01	0.0	0.0	0.2390E+03	0.1112E+00	0.1793E+03	0.1024E+02	0.0	0.1064E+00	0.9216E+00
0.2151E+01	0.0	0.0	0.2850E+03	0.1326E+00	0.2253E+03	0.1286E+02	0.0	0.1087E+00	0.1000E+01
0.1517E+01	0.0	0.0	0.3330E+03	0.1549E+00	0.2613E+03	0.1492E+02	0.0	0.4167E+00	0.7500E+00
0.9308E+00	0.0	0.0	0.3790E+03	0.1763E+00	0.2858E+03	0.1632E+02	0.0	0.1184E+01	0.5326E+00
0.8481E+00	0.0	0.0	0.4290E+03	0.1996E+00	0.3028E+03	0.1729E+02	0.0	0.2059E+01	0.3400E+00
0.8274E+00	0.0	0.0	0.5030E+03	0.2340E+00	0.3368E+03	0.1923E+02	0.0	0.1647E+01	0.4595E+00
0.5861E+00	0.0	0.0	0.1018E+04	0.4736E+00	0.4898E+03	0.2797E+02	0.0	0.2222E+01	0.2971E+00
0.4275E+00	0.0	0.0	0.1523E+04	0.7086E+00	0.5848E+03	0.3339E+02	0.0	0.4368E+01	0.1881E+00
0.3310E+00	0.0	0.0	0.2068E+04	0.9622E+00	0.6638E+03	0.3790E+02	0.0	0.6101E+01	0.1450E+00
0.3172E+00	0.0	0.0	0.2718E+04	0.1265E+01	0.7238E+03	0.4133E+02	0.0	0.9967E+01	0.9231E-01
0.3034E+00	0.0	0.0	0.3068E+04	0.1427E+01	0.7468E+03	0.4264E+02	0.0	0.1426E+02	0.6571E-01

University of Alberta

TABLE G2 (CONTINUED)

RESULTS OF RUN 3

PI,MPAG	PP,MPAG	GI,CM3	WI,CM3	VFI/PV	NP,CM3	%R	GOR,SM3/M3	WOR,M3/M3	OPFIR,M3/M3
0.2896E+00	0.0	0.0	0.3578E+04	0.1665E+01	0.7698E+03	0.4396E+02	0.0	0.2070E+02	0.4510E-01
0.2896E+00	0.0	0.0	0.4078E+04	0.1897E+01	0.7928E+03	0.4527E+02	0.0	0.2178E+02	0.4600E-01
0.5619E+01	0.5516E+01	0.0	0.4136E+04	0.1924E+01	0.7928E+03	0.4527E+02	0.0	0.0	0.1724E-03
0.5668E+01	0.5516E+01	0.8100E+02	0.4136E+04	0.1962E+01	0.7965E+03	0.4548E+02	0.0	0.1024E+02	0.4556E-01
0.5702E+01	0.5585E+01	0.1200E+03	0.4136E+04	0.1980E+01	0.8040E+03	0.4591E+02	0.3101E+03	0.4000E+00	0.1923E+00
0.5744E+01	0.5723E+01	0.4250E+03	0.4136E+04	0.2122E+01	0.8450E+03	0.4825E+02	0.1239E+03	0.2439E+00	0.1344E+00
0.4999E+01	0.4964E+01	0.5400E+03	0.4136E+04	0.2176E+01	0.8525E+03	0.4868E+02	0.2275E+03	0.0	0.6522E-01
0.5585E+01	0.5378E+01	0.5400E+03	0.4210E+04	0.2210E+01	0.8525E+03	0.4868E+02	0.0	0.0	0.1361E-03
0.5964E+01	0.5654E+01	0.5400E+03	0.4306E+04	0.2255E+01	0.8585E+03	0.4902E+02	0.1898E+03	0.0	0.6207E-01
0.5482E+01	0.5151E+01	0.5400E+03	0.4381E+04	0.2290E+01	0.8865E+03	0.5062E+02	0.2106E+02	0.2036E+01	0.3733E+00
0.5068E+01	0.4826E+01	0.5400E+03	0.4464E+04	0.2328E+01	0.9143E+03	0.5221E+02	0.6039E+02	0.1583E+01	0.3349E+00
0.5033E+01	0.4758E+01	0.5400E+03	0.4530E+04	0.2359E+01	0.9466E+03	0.5405E+02	0.4512E+02	0.1641E+01	0.4894E+00
0.4344E+01	0.4296E+01	0.5400E+03	0.4596E+04	0.2390E+01	0.9766E+03	0.5576E+02	0.4225E+02	0.1000E+01	0.4545E+00
0.4792E+01	0.4551E+01	0.5400E+03	0.4711E+04	0.2443E+01	0.1006E+04	0.5725E+02	0.4096E+02	0.2500E+01	0.2261E+00
0.4861E+01	0.4516E+01	0.5400E+03	0.4816E+04	0.2492E+01	0.1025E+04	0.5853E+02	0.3601E+02	0.3422E+01	0.2143E+00
0.3758E+01	0.3344E+01	0.5400E+03	0.4906E+04	0.2534E+01	0.1045E+04	0.5968E+02	0.3593E+02	0.4750E+01	0.2222E+00
0.4413E+01	0.3999E+01	0.5400E+03	0.5020E+04	0.2587E+01	0.1063E+04	0.6067E+02	0.3536E+02	0.3857E+01	0.1535E+00
0.4309E+01	0.4006E+01	0.5400E+03	0.5296E+04	0.2715E+01	0.1082E+04	0.6181E+02	0.3535E+02	0.1293E+02	0.7174E-01
0.3241E+01	0.2820E+01	0.5400E+03	0.5375E+04	0.2752E+01	0.1090E+04	0.6223E+02	0.3028E+02	0.1253E+02	0.9494E-01
0.3075E+01	0.3034E+01	0.5400E+03	0.5494E+04	0.2807E+01	0.1101E+04	0.6284E+02	0.2647E+02	0.1023E+02	0.8908E-01

University of Alberta

TABLE G2 (CONTINUED)

RESULTS OF RUN 3

PI,MPAG	PP,MPAG	GI,CM3	WI,CM3	VFI/PV	NP,CM3	%R	GOR,SM3/M3	WOR,M3/M3	OPFIR,M3/M3
0.1620E+01	0.1586E+01	0.5400E+03	0.5494E+04	0.2807E+01	0.1103E+04	0.6300E+02	0.2028E+02	0.9643E+01	
0.9377E+00	0.6550E+00	0.5400E+03	0.5494E+04	0.2807E+01	0.1106E+04	0.6317E+02	0.8921E+01	0.6333E+01	
0.6895E+00	0.6895E-01	0.5400E+03	0.5494E+04	0.2807E+01	0.1111E+04	0.6346E+02	0.2920E+01	0.5200E+01	
0.5516E+00	0.0	0.5400E+03	0.5494E+04	0.2807E+01	0.1181E+04	0.6745E+02	0.3707E+00	0.2214E+00	
0.1379E+00	0.0	0.5400E+03	0.5494E+04	0.2807E+01	0.1235E+04	0.7053E+02	0.0	0.4378E+00	

PI=INJECTION PRESSURE
PP=PRODUCTION PRESSURE
GI=CUMULATIVE VOLUME OF CO2 INJECTED
WI=BRINE INJECTED
VFI=TOTAL VOLUME OF FLUID INJECTED
PV=PORE VOLUME OF SAND PACK
NP=CUMULATIVE VOLUME OIL PRODUCED
%R=RECOVERY PERCENT
GOR=GAS-OIL RATIO
WOR=WATER-OIL RATIO
OPFIR=OIL PRODUCED-FLUID INJECTED RATIO

University of Alberta

TABLE G3

RESULTS OF RUN 4

PORE VOLUME=0.2058E+04 CM3
HYDROCARBON PORE VOLUME=0.1514E+04 CM3
POROSITY=0.4300E+02%
IRREDUCIBLE WATER SATURATION=0.2640E+02%
INITIAL OIL SATURATION=0.7360E+02%
ABSOLUTE PERMEABILITY=0.1060E+02 DARCIES
CARBON DIOXIDE RETENTION=0.3274E+02 %
CARBON DIOXIDE REQUIRED=0.2642E+03 SM3/M3

PI,MPAG	PP,MPAG	GI,CM3	WI,CM3	VFI/PV	NP,CM3	%R	GOR,SM3/M3	WOR,M3/M3	OPFIR,M3/M3
0.2482E+00	0.0	0.0	0.7200E+02	0.3498E-01	0.1150E+02	0.7594E+00	0.0	0.0	0.1597E+00
0.2551E+00	0.0	0.0	0.9500E+02	0.4615E-01	0.2400E+02	0.1585E+01	0.0	0.0	0.5435E+00
0.1586E+00	0.0	0.0	0.1400E+03	0.6802E-01	0.3580E+02	0.2364E+01	0.0	0.3644E+01	0.2622E+00
0.2206E+00	0.0	0.0	0.2110E+03	0.1025E+00	0.5830E+02	0.3850E+01	0.0	0.1844E+01	0.3169E+00
0.2620E+00	0.0	0.0	0.2820E+03	0.1370E+00	0.8230E+02	0.5435E+01	0.0	0.1875E+01	0.3380E+00
0.2344E+00	0.0	0.0	0.3420E+03	0.1662E+00	0.1023E+03	0.6756E+01	0.0	0.2150E+01	0.3333E+00
0.2413E+00	0.0	0.0	0.4120E+03	0.2002E+00	0.1253E+03	0.8274E+01	0.0	0.2087E+01	0.3286E+00
0.2206E+00	0.0	0.0	0.4870E+03	0.2366E+00	0.1473E+03	0.9727E+01	0.0	0.2545E+01	0.2933E+00
0.2758E+00	0.0	0.0	0.5710E+03	0.2774E+00	0.1753E+03	0.1158E+02	0.0	0.1536E+01	0.3333E+00
0.1724E+00	0.0	0.0	0.9870E+03	0.4795E+00	0.2803E+03	0.1851E+02	0.0	0.3143E+01	0.2524E+00
0.1620E+00	0.0	0.0	0.1487E+04	0.7224E+00	0.4083E+03	0.2696E+02	0.0	0.2891E+01	0.2560E+00
0.1379E+00	0.0	0.0	0.1987E+04	0.9654E+00	0.5008E+03	0.3307E+02	0.0	0.4378E+01	0.1850E+00
0.1379E+00	0.0	0.0	0.2487E+04	0.1208E+01	0.6128E+03	0.4047E+02	0.0	0.4116E+01	0.2240E+00
0.1379E+00	0.0	0.0	0.3487E+04	0.1694E+01	0.7728E+03	0.5103E+02	0.0	0.4813E+01	0.1600E+00
0.6895E-01	0.0	0.0	0.3987E+04	0.1937E+01	0.7938E+03	0.5242E+02	0.0	0.2252E+02	0.4200E-01
0.6895E-01	0.0	0.0	0.4587E+04	0.2229E+01	0.8238E+03	0.5440E+02	0.0	0.1583E+02	0.5000E-01

University of Alberta

TABLE G3 (CONTINUED)

RESULTS OF RUN 4

PI,MPAG	PP,MPAG	GI,CM3	WI,CM3	VFI/PV	NP,CM3	%R	GOR,SM3/M3	WOR,M3/M3	OPFIR,M3/M3
0.5544E+01	0.5537E+01	0.0	0.4699E+04	0.2283E+01	0.8238E+03	0.5440E+02	0.0	0.0	0.8929E-04
0.5599E+01	0.5578E+01	0.7200E+02	0.4699E+04	0.2318E+01	0.8248E+03	0.5447E+02	0.0	0.4313E+02	0.1375E-01
0.5585E+01	0.5550E+01	0.1350E+03	0.4699E+04	0.2349E+01	0.8298E+03	0.5480E+02	0.1995E+03	0.2800E+01	0.7937E-01
0.5537E+01	0.5530E+01	0.2550E+03	0.4699E+04	0.2407E+01	0.8408E+03	0.5552E+02	0.6503E+03	0.4364E+00	0.9167E-01
0.5599E+01	0.5578E+01	0.3930E+03	0.4699E+04	0.2474E+01	0.8481E+03	0.5601E+02	0.1348E+04	0.5753E+00	0.5290E-01
0.5544E+01	0.5530E+01	0.4950E+03	0.4699E+04	0.2523E+01	0.8531E+03	0.5634E+02	0.1200E+04	0.8000E+00	0.4902E-01
0.5454E+01	0.5447E+01	0.5400E+03	0.4699E+04	0.2545E+01	0.8566E+03	0.5657E+02	0.2642E+03	0.5714E+00	0.7778E-01
0.5564E+01	0.5550E+01	0.5400E+03	0.4771E+04	0.2580E+01	0.8566E+03	0.5657E+02	0.0	0.0	0.1389E-03
0.5633E+01	0.5585E+01	0.5400E+03	0.4901E+04	0.2643E+01	0.8586E+03	0.5670E+02	0.1227E+04	0.1357E+02	0.1531E-01
0.5599E+01	0.5550E+01	0.5400E+03	0.5036E+04	0.2709E+01	0.8686E+03	0.5736E+02	0.9732E+02	0.2200E+01	0.7407E-01
0.5502E+01	0.5482E+01	0.5400E+03	0.5126E+04	0.2753E+01	0.8801E+03	0.5812E+02	0.5642E+02	0.6000E+01	0.1278E+00
0.5550E+01	0.5537E+01	0.5400E+03	0.5202E+04	0.2790E+01	0.8971E+03	0.5924E+02	0.2385E+02	0.4529E+01	0.2237E+00
0.5585E+01	0.5516E+01	0.5400E+03	0.5271E+04	0.2823E+01	0.9263E+03	0.6117E+02	0.8888E+01	0.3271E+01	0.4232E+00
0.5516E+01	0.5482E+01	0.5400E+03	0.5336E+04	0.2855E+01	0.9393E+03	0.6203E+02	0.1248E+02	0.5038E+01	0.2000E+00
0.4861E+01	0.4826E+01	0.5400E+03	0.5400E+04	0.2886E+01	0.9481E+03	0.6261E+02	0.3594E+02	0.8318E+01	0.1375E+00
0.4964E+01	0.4930E+01	0.5400E+03	0.5496E+04	0.2933E+01	0.9529E+03	0.6293E+02	0.6083E+02	0.1854E+02	0.5000E-01
0.5516E+01	0.5413E+01	0.5400E+03	0.5574E+04	0.2970E+01	0.9581E+03	0.6327E+02	0.3431E+02	0.1381E+02	0.6667E-01
0.5192E+01	0.5171E+01	0.5400E+03	0.5751E+04	0.3056E+01	0.9671E+03	0.6386E+02	0.2703E+02	0.1933E+02	0.5085E-01
0.2917E+01	0.2910E+01	0.5400E+03	0.5751E+04	0.3056E+01	0.9681E+03	0.6393E+02	0.8110E+01	0.2000E+02	
0.1800E+01	0.1793E+01	0.5400E+03	0.5751E+04	0.3056E+01	0.9696E+03	0.6403E+02	0.2703E+02	0.1767E+02	

University of Alberta

TABLE G3 (CONTINUED)

RESULTS OF RUN 4

PI,MPAG	PP,MPAG	GI,CM3	WI,CM3	VFI/PV	NP,CM3	%R	GOR,SM3/M3	WOR,M3/M3	OPFIR,M3/M3
0.1386E+01	0.1379E+01	0.5400E+03	0.5751E+04	0.3056E+01	0.9728E+03	0.6424E+02	0.1774E+02	0.9938E+01	
0.9515E+00	0.9377E+00	0.5400E+03	0.5751E+04	0.3056E+01	0.9858E+03	0.6510E+02	0.2183E+02	0.5231E+01	
0.3861E+00	0.3792E+00	0.5400E+03	0.5751E+04	0.3056E+01	0.9968E+03	0.6583E+02	0.9879E+02	0.4318E+01	
0.6895E-01	0.0	0.5400E+03	0.5751E+04	0.3056E+01	0.1024E+04	0.6764E+02	0.1209E+03	0.5109E+01	

PI=INJECTION PRESSURE
PP=PRODUCTION PRESSURE
GI=CUMULATIVE VOLUME OF CO2 INJECTED
WI=BRINE INJECTED
VFI=TOTAL VOLUME OF FLUID INJECTED
PV=PORE VOLUME OF SAND PACK
NP=CUMULATIVE VOLUME OIL PRODUCED
%R=RECOVERY PERCENT
GOR=GAS-OIL RATIO
WOR=WATER-OIL RATIO
OPFIR=OIL PRODUCED-FLUID INJECTED RATIO

University of Alberta

TABLE G4

RESULTS OF RUN 5

PORE VOLUME=0.2107E+04 CM3
HYDROCARBON PORE VOLUME=0.1860E+04 CM3
POROSITY=0.4400E+02%
IRREDUCIBLE WATER SATURATION=0.1170E+02%
INITIAL OIL SATURATION=0.8830E+02%
ABSOLUTE PERMEABILITY=0.7400E+01 DARCIES
CARBON DIOXIDE RETENTION=0.3696E+02 %
CARBON DIOXIDE REQUIRED=0.1922E+03 SM3/M3

PI,MPAG	PP,MPAG	GI,CM3	WI,CM3	VFI/PV	NP,CM3	%R	GOR,SM3/M3	WOR,M3/M3	OPFIR,M3/M3
0.5523E+01	0.5502E+01	0.5500E+02	0.0	0.2610E-01	0.0	0.0	0.0	0.0	0.0
0.5482E+01	0.5468E+01	0.8800E+02	0.0	0.4177E-01	0.1500E+02	0.8063E+00	0.0	0.0	0.4545E+00
0.5544E+01	0.5537E+01	0.1290E+03	0.0	0.6122E-01	0.2000E+02	0.1075E+01	0.1023E+03	0.0	0.1220E+00
0.5502E+01	0.5488E+01	0.2050E+03	0.0	0.9729E-01	0.3050E+02	0.1640E+01	0.4140E+03	0.0	0.1382E+00
0.5447E+01	0.5419E+01	0.3634E+03	0.0	0.1725E+00	0.4290E+02	0.2306E+01	0.7358E+03	0.0	0.7828E-01
0.5516E+01	0.5502E+01	0.3634E+03	0.3500E+02	0.1891E+00	0.4291E+02	0.2307E+01	0.0	0.0	0.2857E-03
0.5619E+01	0.5585E+01	0.3634E+03	0.9500E+02	0.2176E+00	0.8190E+02	0.4403E+01	0.0	0.0	0.6498E+00
0.5688E+01	0.5550E+01	0.3634E+03	0.1395E+03	0.2387E+00	0.1231E+03	0.6617E+01	0.9193E+02	0.0	0.9258E+00
0.5592E+01	0.5275E+01	0.3634E+03	0.1890E+03	0.2622E+00	0.1731E+03	0.9305E+01	0.2109E+02	0.0	0.1010E+01
0.5550E+01	0.5516E+01	0.3634E+03	0.2684E+03	0.2999E+00	0.2511E+03	0.1350E+02	0.1314E+02	0.0	0.9824E+00
0.6647E+01	0.5564E+01	0.3634E+03	0.3118E+03	0.3205E+00	0.2931E+03	0.1576E+02	0.6527E+01	0.0	0.9677E+00
0.6757E+01	0.5654E+01	0.3634E+03	0.3518E+03	0.3394E+00	0.3326E+03	0.1788E+02	0.6940E+01	0.5063E-01	0.9875E+00
0.6667E+01	0.6102E+01	0.3634E+03	0.4140E+03	0.3690E+00	0.3906E+03	0.2100E+02	0.4195E+01	0.1552E+00	0.9325E+00
0.6481E+01	0.5516E+01	0.3634E+03	0.5580E+03	0.4373E+00	0.4771E+03	0.2565E+02	0.4032E+01	0.6474E+00	0.6007E+00
0.6447E+01	0.5516E+01	0.3634E+03	0.6290E+03	0.4710E+00	0.5071E+03	0.2726E+02	0.5001E+01	0.1383E+01	0.4225E+00
0.6205E+01	0.5516E+01	0.3634E+03	0.6870E+03	0.4985E+00	0.5351E+03	0.2876E+02	0.3041E+01	0.1643E+01	0.4828E+00

University of Alberta

TABLE G4 (CONTINUED)

RESULTS OF RUN 5

PI,MPAG	PP,MPAG	GI,CM3	WI,CM3	VFI/PV	NP,CM3	%R	GOR,SM3/M3	WOR,M3/M3	OPFIR,M3/M3
0.6033E+01	0.5516E+01	0.3634E+03	0.1034E+04	0.6632E+00	0.6346E+03	0.3411E+02	0.3260E+01	0.2497E+01	0.2867E+00
0.5861E+01	0.5378E+01	0.3634E+03	0.1107E+04	0.6979E+00	0.6526E+03	0.3508E+02	0.2253E+01	0.3444E+01	0.2466E+00
0.5778E+01	0.5309E+01	0.3634E+03	0.1190E+04	0.7373E+00	0.6716E+03	0.3610E+02	0.2134E+01	0.3474E+01	0.2289E+00
0.6861E+01	0.5654E+01	0.3634E+03	0.1425E+04	0.8488E+00	0.7176E+03	0.3857E+02	0.2645E+01	0.4130E+01	0.1957E+00
0.6102E+01	0.5654E+01	0.3634E+03	0.1905E+04	0.1077E+01	0.8226E+03	0.4422E+02	0.3862E+00	0.3524E+01	0.2188E+00
0.5861E+01	0.5723E+01	0.3634E+03	0.2381E+04	0.1303E+01	0.9026E+03	0.4852E+02	0.0	0.5250E+01	0.1681E+00
0.5964E+01	0.5861E+01	0.3634E+03	0.3581E+04	0.1872E+01	0.9746E+03	0.5239E+02	0.0	0.1558E+02	0.6000E-01
0.5895E+01	0.5723E+01	0.3634E+03	0.3846E+04	0.1998E+01	0.9866E+03	0.5303E+02	0.0	0.2117E+02	0.4528E-01
0.5861E+01	0.5792E+01	0.3634E+03	0.4046E+04	0.2093E+01	0.9946E+03	0.5346E+02	0.0	0.2463E+02	0.4000E-01
0.2737E+01	0.2710E+01	0.3634E+03	0.4046E+04	0.2093E+01	0.9966E+03	0.5357E+02	0.0	0.1150E+02	
0.9239E+00	0.5378E+00	0.3634E+03	0.4046E+04	0.2093E+01	0.9996E+03	0.5373E+02	0.0	0.6500E+01	
0.1655E+00	0.3447E-01	0.3634E+03	0.4046E+04	0.2093E+01	0.1005E+04	0.5403E+02	0.0	0.7818E+01	
0.3447E-01	0.0	0.3634E+03	0.4046E+04	0.2093E+01	0.1023E+04	0.5497E+02	0.0	0.6914E+01	

PI=INJECTION PRESSURE
WI=BRINE INJECTED
NP=CUMULATIVE VOLUME OIL PRODUCED
WOR=WATER-OIL RATIO

PP=PRODUCTION PRESSURE
VFI=TOTAL VOLUME OF FLUID INJECTED
%R=RECOVERY PERCENT
OPFIR=OIL PRODUCED-FLUID INJECTED RATIO

GI=CUMULATIVE VOLUME OF CO2 INJECTED
PV=PORE VOLUME OF SAND PACK
GOR=GAS-OIL RATIO

University of Alberta

TABLE G5

RESULTS OF RUN 6

PORE VOLUME=0.2065E+04 CM3
HYDROCARBON PORE VOLUME=0.1839E+04 CM3
POROSITY=0.4314E+02%
IRREDUCIBLE WATER SATURATION=0.1140E+02%
INITIAL OIL SATURATION=0.8860E+02%
ABSOLUTE PERMEABILITY=0.2425E+02 DARCIES
CARBON DIOXIDE RETENTION=0.5419E+02 %
CARBON DIOXIDE REQUIRED=0.2675E+03 SM3/M3

PI,MPAG	PP,MPAG	GI,CM3	WI,CM3	VFI/PV	NP,CM3	%R	GOR,SM3/M3	WOR,M3/M3	OPFIR,M3/M3
0.5516E+01	0.5495E+01	0.8040E+02	0.0	0.3893E-01	0.0	0.0	0.0	0.0	0.0
0.5530E+01	0.5523E+01	0.1652E+03	0.0	0.8000E-01	0.3126E+02	0.1700E+01	0.0	0.0	0.3686E+00
0.5502E+01	0.5492E+01	0.3335E+03	0.0	0.1615E+00	0.4200E+02	0.2283E+01	0.6385E+03	0.0	0.6381E-01
0.5440E+01	0.5426E+01	0.3679E+03	0.0	0.1782E+00	0.4750E+02	0.2583E+01	0.2563E+03	0.0	0.1599E+00
0.5550E+01	0.5516E+01	0.3679E+03	0.8467E+02	0.2192E+00	0.9730E+02	0.5290E+01	0.6444E+02	0.0	0.5882E+00
0.5544E+01	0.5516E+01	0.3679E+03	0.1121E+03	0.2324E+00	0.1253E+03	0.6812E+01	0.1216E+02	0.0	0.1022E+01
0.5585E+01	0.5564E+01	0.3679E+03	0.1904E+03	0.2703E+00	0.1918E+03	0.1043E+02	0.7256E+01	0.1353E+00	0.8493E+00
0.5592E+01	0.5564E+01	0.3679E+03	0.4224E+03	0.3827E+00	0.3038E+03	0.1652E+02	0.2426E+01	0.1018E+01	0.4828E+00
0.5564E+01	0.5544E+01	0.3679E+03	0.4626E+03	0.4022E+00	0.3233E+03	0.1758E+02	0.0	0.1205E+01	0.4851E+00
0.5564E+01	0.5544E+01	0.3679E+03	0.6036E+03	0.4704E+00	0.3713E+03	0.2019E+02	0.0	0.1979E+01	0.3404E+00
0.5495E+01	0.5482E+01	0.3679E+03	0.6499E+03	0.4929E+00	0.3871E+03	0.2105E+02	0.0	0.2025E+01	0.3413E+00
0.5564E+01	0.5544E+01	0.3679E+03	0.8524E+03	0.5909E+00	0.4211E+03	0.2289E+02	0.0	0.4588E+01	0.1679E+00
0.5516E+01	0.5502E+01	0.3679E+03	0.1031E+04	0.6773E+00	0.4551E+03	0.2474E+02	0.0	0.4176E+01	0.1906E+00
0.5516E+01	0.5495E+01	0.3679E+03	0.1102E+04	0.7116E+00	0.4691E+03	0.2550E+02	0.0	0.4429E+01	0.1980E+00
0.5564E+01	0.5544E+01	0.3679E+03	0.1305E+04	0.8099E+00	0.4971E+03	0.2703E+02	0.0	0.6214E+01	0.1379E+00
0.5447E+01	0.5440E+01	0.3679E+03	0.1539E+04	0.9232E+00	0.5261E+03	0.2860E+02	0.0	0.7138E+01	0.1239E+00

University of Alberta

TABLE G5 (CONTINUED)

RESULTS OF RUN 6

PI,MPAG	PP,MPAG	GI,CM3	WI,CM3	VFI/PV	NP,CM3	%R	GOR,SM3/M3	WOR,M3/M3	OPFIR,M3/M3
0.5516E+01	0.5499E+01	0.3679E+03	0.1756E+04	0.1029E+01	0.5431E+03	0.2953E+02	0.0	0.1265E+02	0.7809E-01
0.5523E+01	0.5509E+01	0.3679E+03	0.1992E+04	0.1143E+01	0.5641E+03	0.3067E+02	0.0	0.1033E+02	0.8906E-01
0.5495E+01	0.5488E+01	0.3679E+03	0.2204E+04	0.1245E+01	0.5771E+03	0.3138E+02	0.0	0.1508E+02	0.6141E-01
0.5495E+01	0.5475E+01	0.3679E+03	0.2458E+04	0.1368E+01	0.5921E+03	0.3219E+02	0.0	0.1600E+02	0.5906E-01
0.5475E+01	0.5468E+01	0.3679E+03	0.2667E+04	0.1470E+01	0.6021E+03	0.3274E+02	0.0	0.1880E+02	0.4780E-01
0.5537E+01	0.5530E+01	0.3679E+03	0.2883E+04	0.1574E+01	0.6131E+03	0.3333E+02	0.0	0.2064E+02	0.5093E-01
0.5399E+01	0.5385E+01	0.3679E+03	0.3119E+04	0.1689E+01	0.6231E+03	0.3388E+02	0.0	0.2250E+02	0.4237E-01
0.5399E+01	0.5385E+01	0.3679E+03	0.3344E+04	0.1797E+01	0.6311E+03	0.3431E+02	0.0	0.2738E+02	0.3559E-01
0.5385E+01	0.5371E+01	0.3679E+03	0.3579E+04	0.1911E+01	0.6391E+03	0.3475E+02	0.0	0.2838E+02	0.3404E-01
0.5378E+01	0.5364E+01	0.3679E+03	0.3818E+04	0.2027E+01	0.6471E+03	0.3518E+02	0.0	0.2925E+02	0.3347E-01
0.5299E+01	0.5285E+01	0.3679E+03	0.4062E+04	0.2145E+01	0.6541E+03	0.3556E+02	0.0	0.3414E+02	0.2865E-01
0.5220E+01	0.5206E+01	0.3679E+03	0.4262E+04	0.2242E+01	0.6591E+03	0.3583E+02	0.0	0.3900E+02	0.2506E-01
0.2427E+01	0.2434E+01	0.3679E+03	0.4262E+04	0.2242E+01	0.6606E+03	0.3592E+02	0.0	0.1467E+02	
0.6757E+00	0.6723E+00	0.3679E+03	0.4262E+04	0.2242E+01	0.6626E+03	0.3602E+02	0.2028E+02	0.3650E+02	
0.3861E+00	0.3792E+00	0.3679E+03	0.4262E+04	0.2242E+01	0.6706E+03	0.3646E+02	0.3548E+02	0.9250E+01	
0.1379E-01	0.0	0.3679E+03	0.4262E+04	0.2242E+01	0.7201E+03	0.3915E+02	0.6504E+02	0.3172E+01	

PI=INJECTION PRESSURE
PP=PRODUCTION PRESSURE
GI=CUMULATIVE VOLUME OF CO2 INJECTED
WI=BRINE INJECTED
VFI=TOTAL VOLUME OF FLUID INJECTED
PV=PORE VOLUME OF SAND PACK
NP=CUMULATIVE VOLUME OIL PRODUCED
%R=RECOVERY PERCENT
GOR=GAS-OIL RATIO
WOR=WATER-OIL RATIO
OPFIR=OIL PRODUCED-FLUID INJECTED RATIO

University of Alberta

TABLE G6

RESULTS OF RUN 7

PORE VOLUME=0.2092E+04 CM3
HYDROCARBON PORE VOLUME=0.1899E+04 CM3
POROSITY=0.4370E+02%
IRREDUCIBLE WATER SATURATION=0.9900E+01%
INITIAL OIL SATURATION=0.9010E+02%
ABSOLUTE PERMEABILITY=0.1540E+02 DARCIES
CARBON DIOXIDE RETENTION=0.8403E+02 %

PI,MPAG	PP,MPAG	GI,CM3	WI,CM3	VFI/PV	NP,CM3	%R	GOR,SM3/M3	WOR,M3/M3	OPFIR,M3/M3
0.5530E+01	0.5523E+01	0.2628E+02	0.0	0.1256E-01	0.0	0.0	0.0	0.0	0.0
0.5509E+01	0.5488E+01	0.5628E+02	0.0	0.2690E-01	0.1950E+02	0.1027E+01	0.0	0.0	0.6500E+00
0.5537E+01	0.5523E+01	0.1463E+03	0.0	0.6992E-01	0.5320E+02	0.2801E+01	0.2816E+02	0.0	0.3744E+00
0.5475E+01	0.5468E+01	0.2473E+03	0.0	0.1182E+00	0.9170E+02	0.4828E+01	0.8847E+01	0.0	0.3812E+00
0.5516E+01	0.5454E+01	0.3799E+03	0.0	0.1816E+00	0.1240E+03	0.6529E+01	0.1092E+03	0.0	0.2436E+00
0.5619E+01	0.5544E+01	0.3799E+03	0.5986E+02	0.2102E+00	0.1655E+03	0.8714E+01	0.9967E+01	0.0	0.6933E+00
0.5585E+01	0.5568E+01	0.3799E+03	0.1693E+03	0.2625E+00	0.2690E+03	0.1416E+02	0.2116E+01	0.4831E-02	0.9459E+00
0.5626E+01	0.5613E+01	0.3799E+03	0.2400E+03	0.2963E+00	0.3205E+03	0.1687E+02	0.1732E+01	0.2816E+00	0.7286E+00
0.5585E+01	0.5571E+01	0.3799E+03	0.4316E+03	0.3878E+00	0.3765E+03	0.1982E+02	0.0	0.2179E+01	0.2924E+00
0.5530E+01	0.5523E+01	0.3799E+03	0.5813E+03	0.4594E+00	0.4045E+03	0.2130E+02	0.0	0.4357E+01	0.1869E+00
0.5406E+01	0.5399E+01	0.3799E+03	0.7412E+03	0.5359E+00	0.4335E+03	0.2282E+02	0.0	0.4586E+01	0.1814E+00
0.5492E+01	0.5485E+01	0.3799E+03	0.1026E+04	0.6719E+00	0.4735E+03	0.2493E+02	0.3852E+01	0.5950E+01	0.1406E+00
0.5482E+01	0.5468E+01	0.3799E+03	0.1085E+04	0.7000E+00	0.4805E+03	0.2530E+02	0.5214E+01	0.7571E+01	0.1190E+00
0.5675E+01	0.5661E+01	0.3799E+03	0.1251E+04	0.7797E+00	0.5005E+03	0.2635E+02	0.3650E+01	0.7100E+01	0.1200E+00

PI=INJECTION PRESSURE
WI=BRINE INJECTED
NP=CUMULATIVE VOLUME OIL PRODUCED
WOR=WATER-OIL RATIO

PP=PRODUCTION PRESSURE
VFI=TOTAL VOLUME OF FLUID INJECTED
%R=RECOVERY PERCENT
OPFIR=OIL PRODUCED-FLUID INJECTED RATIO

GI=CUMULATIVE VOLUME OF CO2 INJECTED
PV=PORE VOLUME OF SAND PACK
GOR=GAS-OIL RATIO

University of Alberta

TABLE G7

RESULTS OF RUN 8

PORE VOLUME=0.2180E+04 CM3
HYDROCARBON PORE VOLUME=0.1984E+04 CM3
POROSITY=0.4550E+02%
IRREDUCIBLE WATER SATURATION=0.9000E+01%
INITIAL OIL SATURATION=0.9100E+02%
ABSOLUTE PERMEABILITY=0.1541E+02 DARCIES
CARBON DIOXIDE RETENTION=0.2522E+02 %
CARBON DIOXIDE REQUIRED=0.2836E+03 SM3/M3

PI,MPAG	PP,MPAG	GI,CM3	WI,CM3	VFI/PV	NP,CM3	%R	GOR,SM3/M3	WOR,M3/M3	OPFIR,M3/M3
0.5537E+01	0.5537E+01	0.1989E+02	0.0	0.9124E-02	0.0	0.0	0.0	0.0	0.0
0.5757E+01	0.5550E+01	0.1022E+03	0.0	0.4690E-01	0.1400E+02	0.7055E+00	0.0	0.0	0.1700E+00
0.5544E+01	0.5537E+01	0.1599E+03	0.0	0.7334E-01	0.3170E+02	0.1598E+01	0.2582E+03	0.0	0.3070E+00
0.5537E+01	0.5530E+01	0.2374E+03	0.0	0.1089E+00	0.3970E+02	0.2001E+01	0.5728E+03	0.0	0.1032E+00
0.5537E+01	0.5530E+01	0.3039E+03	0.0	0.1394E+00	0.4550E+02	0.2293E+01	0.7746E+03	0.0	0.8722E-01
0.5557E+01	0.5550E+01	0.3969E+03	0.0	0.1821E+00	0.4795E+02	0.2416E+01	0.3767E+04	0.0	0.2634E-01
0.5764E+01	0.5495E+01	0.3969E+03	0.9143E+02	0.2240E+00	0.9525E+02	0.4800E+01	0.2743E+02	0.0	0.5173E+00
0.5806E+01	0.5626E+01	0.3969E+03	0.3054E+03	0.3222E+00	0.2838E+03	0.1430E+02	0.1613E+02	0.9549E-01	0.8808E+00
0.5806E+01	0.5619E+01	0.3969E+03	0.5264E+03	0.4235E+00	0.3798E+03	0.1914E+02	0.7603E+01	0.1271E+01	0.4344E+00
0.5654E+01	0.5516E+01	0.3969E+03	0.7604E+03	0.5309E+00	0.4468E+03	0.2251E+02	0.8352E+01	0.2537E+01	0.2863E+00
0.5654E+01	0.5550E+01	0.3969E+03	0.9948E+03	0.6384E+00	0.4968E+03	0.2503E+02	0.1622E+01	0.3640E+01	0.2133E+00
0.5599E+01	0.5430E+01	0.3969E+03	0.1199E+04	0.7320E+00	0.5328E+03	0.2685E+02	0.1352E+01	0.4722E+01	0.1765E+00
0.5585E+01	0.5516E+01	0.3969E+03	0.1444E+04	0.8443E+00	0.5684E+03	0.2864E+02	0.2278E+00	0.5910E+01	0.1454E+00
0.5550E+01	0.5447E+01	0.3969E+03	0.1899E+04	0.1053E+01	0.6214E+03	0.3131E+02	0.1530E+00	0.7491E+01	0.1165E+00
0.5482E+01	0.5447E+01	0.3969E+03	0.2354E+04	0.1262E+01	0.6514E+03	0.3283E+02	0.0	0.1417E+02	0.6593E-01
0.5537E+01	0.5546E+01	0.3969E+03	0.2852E+04	0.1490E+01	0.6794E+03	0.3424E+02	0.0	0.1536E+02	0.5619E-01

University of Alberta

TABLE G7 (CONTINUED)

RESULTS OF RUN 8

PI,MPAG	PP,MPAG	GI,CM3	WI,CM3	VFI/PV	NP,CM3	%R	GOR,SM3/M3	WOR,M3/M3	OPFIR,M3/M3
0.5482E+01	0.5426E+01	0.3969E+03	0.3307E+04	0.1699E+01	0.7064E+03	0.3560E+02	0.0	0.1556E+02	0.5934E-01
0.5482E+01	0.5468E+01	0.3969E+03	0.3765E+04	0.1909E+01	0.7254E+03	0.3655E+02	0.0	0.2289E+02	0.4145E-01
0.3241E+01	0.3241E+01	0.3969E+03	0.3765E+04	0.1909E+01	0.7269E+03	0.3664E+02	0.0	0.1088E+02	
0.9791E+00	0.9791E+00	0.3969E+03	0.3765E+04	0.1909E+01	0.7294E+03	0.3676E+02	0.0	0.9833E+01	
0.1793E+00	0.1448E+00	0.3969E+03	0.3765E+04	0.1909E+01	0.7321E+03	0.3690E+02	0.0	0.1096E+02	
0.0	0.0	0.3969E+03	0.3765E+04	0.1909E+01	0.7601E+03	0.3831E+02	0.0	0.4304E+01	

PI=INJECTION PRESSURE
PP=PRODUCTION PRESSURE
GI=CUMULATIVE VOLUME OF CO2 INJECTED
WI=BRINE INJECTED
VFI=TOTAL VOLUME OF FLUID INJECTED
PV=PORE VOLUME OF SAND PACK
NP=CUMULATIVE VOLUME OIL PRODUCED
%R=RECOVERY PERCENT
GOR=GAS-OIL RATIO
WOR=WATER-OIL RATIO
OPFIR=OIL PRODUCED-FLUID INJECTED RATIO

University of Alberta

TABLE G8

RESULTS OF RUN 9

PORE VOLUME=0.2186E+04 CM3
HYDROCARBON PORE VOLUME=0.1990E+04 CM3
POROSITY=0.4567E+02%
IRREDUCIBLE WATER SATURATION=0.8950E+01%
INITIAL OIL SATURATION=0.9105E+02%
ABSOLUTE PERMEABILITY=0.1675E+02 DARCIES
CARBON DIOXIDE RETENTION=0.6476E+02 %
CARBON DIOXIDE REQUIRED=0.9349E+03 SM3/M3

PI,MPAG	PP,MPAG	GI,CM3	WI,CM3	VFI/PV	NP,CM3	%R	GOR,SM3/M3	WOR,M3/M3	OPFIR,M3/M3
0.5516E+01	0.5516E+01	0.2000E+02	0.0	0.9149E-02	0.0	0.0	0.0	0.0	0.0
0.5599E+01	0.5585E+01	0.4640E+02	0.0	0.2123E-01	0.1390E+02	0.6984E+00	0.0	0.0	0.5265E+00
0.5495E+01	0.5482E+01	0.1101E+03	0.0	0.5034E-01	0.2380E+02	0.1196E+01	0.5337E+03	0.0	0.1555E+00
0.5437E+01	0.5423E+01	0.1701E+03	0.0	0.7779E-01	0.3280E+02	0.1648E+01	0.4415E+03	0.0	0.1500E+00
0.5488E+01	0.5482E+01	0.3986E+03	0.0	0.1823E+00	0.3980E+02	0.2000E+01	0.3939E+03	0.0	0.3063E-01
0.5530E+01	0.5399E+01	0.3986E+03	0.4194E+03	0.3742E+00	0.2728E+03	0.1371E+02	0.5882E+01	0.4292E-01	0.5556E+00
0.5619E+01	0.5516E+01	0.3986E+03	0.5754E+03	0.4456E+00	0.3508E+03	0.1763E+02	0.1040E+00	0.9744E+00	0.5000E+00
0.5654E+01	0.5602E+01	0.3986E+03	0.8643E+03	0.5777E+00	0.4338E+03	0.2180E+02	0.0	0.2446E+01	0.2873E+00
0.5530E+01	0.5516E+01	0.3986E+03	0.1298E+04	0.7762E+00	0.5078E+03	0.2551E+02	0.0	0.5000E+01	0.1706E+00
0.5530E+01	0.5478E+01	0.3986E+03	0.1528E+04	0.8811E+00	0.5298E+03	0.2662E+02	0.0	0.9273E+01	0.9590E-01
0.5516E+01	0.5471E+01	0.3986E+03	0.1986E+04	0.1091E+01	0.5478E+03	0.2752E+02	0.0	0.1150E+02	0.3928E-01
0.5468E+01	0.5437E+01	0.3986E+03	0.2445E+04	0.1301E+01	0.5808E+03	0.2918E+02	0.0	0.1303E+02	0.7191E-01
0.5433E+01	0.5416E+01	0.3986E+03	0.2904E+04	0.1511E+01	0.6056E+03	0.3043E+02	0.0	0.1772E+02	0.5403E-01
0.5340E+01	0.5330E+01	0.3986E+03	0.3202E+04	0.1647E+01	0.6166E+03	0.3098E+02	0.0	0.2618E+02	0.3690E-01
0.5392E+01	0.5378E+01	0.3986E+03	0.3659E+04	0.1856E+01	0.6316E+03	0.3173E+02	0.0	0.2933E+02	0.3279E-01
0.5461E+01	0.5447E+01	0.3986E+03	0.4090E+04	0.2053E+01	0.6436E+03	0.3234E+02	0.0	0.3383E+02	0.2785E-01

University of Alberta

TABLE G8 (CONTINUED)

RESULTS OF RUN 9

PI,MPAG	PP,MPAG	GI,CM3	WI,CM3	VFI/PV	NP,CM3	%R	GOR,SM3/M3	WOR,M3/M3	OPFIR,M3/M3
0.2696E+01	0.2696E+01	0.3986E+03	0.4090E+04	0.2053E+01	0.6446E+03	0.3239E+02	0.0	0.2100E+02	
0.6895E+00	0.6895E+00	0.3986E+03	0.4090E+04	0.2053E+01	0.6466E+03	0.3249E+02	0.0	0.7750E+01	
0.0	0.0	0.3986E+03	0.4090E+04	0.2053E+01	0.6676E+03	0.3354E+02	0.0	0.1057E+02	

PI=INJECTION PRESSURE
PP=PRODUCTION PRESSURE
GI=CUMULATIVE VOLUME OF CO2 INJECTED
WI=BRINE INJECTED
VFI=TOTAL VOLUME OF FLUID INJECTED
PV=PORE VOLUME OF SAND PACK
NP=CUMULATIVE VOLUME OIL PRODUCED
%R=RECOVERY PERCENT
GOR=GAS-OIL RATIO
WOR=WATER-OIL RATIO
OPFIR=OIL PRODUCED-FLUID INJECTED RATIO

University of Alberta

TABLE G9

RESULTS OF RUN 10

PORE VOLUME=0.2250E+04 CM3
HYDROCARBON PORE VOLUME=0.1973E+04 CM3
POROSITY=0.4700E+02%
IRREDUCIBLE WATER SATURATION=0.1230E+02%
INITIAL OIL SATURATION=0.8770E+02%
ABSOLUTE PERMEABILITY=0.1790E+02 DARCIES
CARBON DIOXIDE RETENTION=0.1995E+02 %
CARBON DIOXIDE REQUIRED=0.1421E+03 SM3/M3

PI,MPAG	PP,MPAG	GI,CM3	WI,CM3	VFI/PV	NP,CM3	%R	GOR,SM3/M3	WOR,M3/M3	OPFIR,M3/M3
0.5500E+01	0.5500E+01	0.4345E+02	0.0	0.1931E-01	0.0	0.0	0.0	0.0	0.0
0.5500E+01	0.5480E+01	0.1128E+03	0.0	0.5013E-01	0.1580E+02	0.8007E+00	0.0	0.0	0.2278E+00
0.5530E+01	0.5520E+01	0.1674E+03	0.0	0.7440E-01	0.2760E+02	0.1399E+01	0.6845E+02	0.0	0.2161E+00
0.5545E+01	0.5540E+01	0.2558E+03	0.0	0.1137E+00	0.4040E+02	0.2047E+01	0.2579E+03	0.0	0.1448E+00
0.5380E+01	0.5370E+01	0.3946E+03	0.0	0.1754E+00	0.5520E+02	0.2797E+01	0.8696E+03	0.0	0.1066E+00
0.5560E+01	0.5540E+01	0.3946E+03	0.3073E+03	0.3120E+00	0.2960E+03	0.1500E+02	0.2629E+02	0.4153E-02	0.7836E+00
0.5560E+01	0.5540E+01	0.3946E+03	0.4350E+03	0.3687E+00	0.3705E+03	0.1878E+02	0.3526E+02	0.3490E+00	0.5834E+00
0.5775E+01	0.5635E+01	0.3946E+03	0.7275E+03	0.4987E+00	0.5175E+03	0.2623E+02	0.1194E+02	0.8163E+00	0.5025E+00
0.5680E+01	0.5520E+01	0.3946E+03	0.8800E+03	0.5665E+00	0.5810E+03	0.2944E+02	0.7535E+01	0.1890E+01	0.4164E+00
0.5615E+01	0.5510E+01	0.3946E+03	0.1292E+04	0.7495E+00	0.6990E+03	0.3542E+02	0.7835E+01	0.3072E+01	0.2866E+00
0.5535E+01	0.5430E+01	0.3946E+03	0.1738E+04	0.9479E+00	0.7580E+03	0.3841E+02	0.8522E+01	0.6525E+01	0.1321E+00
0.5480E+01	0.5430E+01	0.3946E+03	0.2171E+04	0.1140E+01	0.7920E+03	0.4014E+02	0.8349E+01	0.1176E+02	0.7852E-01
0.5445E+01	0.5370E+01	0.3946E+03	0.2551E+04	0.1309E+01	0.8185E+03	0.4148E+02	0.1530E+00	0.1472E+02	0.6976E-01
0.5420E+01	0.5390E+01	0.3946E+03	0.2971E+04	0.1496E+01	0.8415E+03	0.4264E+02	0.7228E+01	0.1717E+02	0.5484E-01
0.5380E+01	0.5360E+01	0.3946E+03	0.3798E+04	0.1864E+01	0.8745E+03	0.4432E+02	0.9830E+00	0.2427E+02	0.3986E-01
0.5295E+01	0.5275E+01	0.3946E+03	0.4210E+04	0.2047E+01	0.8805E+03	0.4462E+02	0.4055E+01	0.6683E+02	0.1457E-01

University of Alberta

TABLE G9 (CONTINUED)

RESULTS OF RUN 10

PI,MPAG	PP,MPAG	GI,CM3	WI,CM3	VFI/PV	NP,CM3	%R	GOR,SM3/M3	WOR,M3/M3	OPFIR,M3/M3
0.2500E+01	0.2500E+01	0.3946E+03	0.4210E+04	0.2047E+01	0.8820E+03	0.4470E+02	0.0	0.1400E+02	
0.9000E+00	0.9000E+00	0.3946E+03	0.4210E+04	0.2047E+01	0.8835E+03	0.4477E+02	0.0	0.1267E+02	
0.0	0.0	0.3946E+03	0.4210E+04	0.2047E+01	0.9060E+03	0.4591E+02	0.0	0.7822E+01	

PI=INJECTION PRESSURE
PP=PRODUCTION PRESSURE
GI=CUMULATIVE VOLUME OF CO2 INJECTED
WI=BRINE INJECTED
VFI=TOTAL VOLUME OF FLUID INJECTED
PV=PORE VOLUME OF SAND PACK
NP=CUMULATIVE VOLUME OIL PRODUCED
%R=RECOVERY PERCENT
GOR=GAS-OIL RATIO
WOR=WATER-OIL RATIO
OPFIR=OIL PRODUCED-FLUID INJECTED RATIO

University of Alberta

TABLE G10

RESULTS OF RUN 11

PORE VOLUME=0.1850E+04 CM3
HYDROCARBON PORE VOLUME=0.1634E+04 CM3
POROSITY=0.3870E+02%
IRREDUCIBLE WATER SATURATION=0.1166E+02%
INITIAL OIL SATURATION=0.8834E+02%
ABSOLUTE PERMEABILITY=0.8700E+01 DARCIES

PI,MPAG	PP,MPAG	GI,CM3	WI,CM3	VFI/PV	NP,CM3	%R	GOR,SM3/M3	WOR,M3/M3	OPFIR,M3/M3
0.4800E+00	0.5000E-01	0.0	0.8608E+02	0.4653E-01	0.3460E+02	0.2117E+01	0.0	0.0	0.4020E+00
0.5000E+00	0.6000E-01	0.0	0.9838E+02	0.5318E-01	0.4660E+02	0.2851E+01	0.0	0.0	0.9756E+00
0.5000E+00	0.7000E-01	0.0	0.1120E+03	0.6053E-01	0.5970E+02	0.3653E+01	0.0	0.0	0.9632E+00
0.5000E+00	0.8000E-01	0.0	0.1277E+03	0.6902E-01	0.7620E+02	0.4663E+01	0.0	0.0	0.1051E+01
0.5000E+00	0.9000E-01	0.0	0.1430E+03	0.7729E-01	0.9220E+02	0.5642E+01	0.0	0.0	0.1046E+01
0.4900E+00	0.1000E+00	0.0	0.1567E+03	0.8469E-01	0.1059E+03	0.6480E+01	0.0	0.2190E-01	0.1000E+01
0.4900E+00	0.1000E+00	0.0	0.1706E+03	0.9221E-01	0.1154E+03	0.7061E+01	0.0	0.5263E-01	0.6835E+00
0.4800E+00	0.1000E+00	0.0	0.1842E+03	0.9956E-01	0.1244E+03	0.7612E+01	0.0	0.6667E-01	0.6618E+00
0.4700E+00	0.9000E-01	0.0	0.1996E+03	0.1079E+00	0.1399E+03	0.8560E+01	0.0	0.6452E-01	0.1006E+01
0.4200E+00	0.9000E-01	0.0	0.2752E+03	0.1487E+00	0.2059E+03	0.1260E+02	0.0	0.1667E+00	0.8730E+00
0.3500E+00	0.8000E-01	0.0	0.3835E+03	0.2073E+00	0.2370E+03	0.1450E+02	0.0	0.8682E+00	0.2872E+00
0.1700E+00	0.6000E-01	0.0	0.6074E+03	0.3283E+00	0.3187E+03	0.1950E+02	0.0	0.1812E+01	0.3649E+00
0.1200E+00	0.5000E-01	0.0	0.9560E+03	0.5167E+00	0.4086E+03	0.2500E+02	0.0	0.3226E+01	0.2579E+00
0.9000E-01	0.4000E-01	0.0	0.1419E+04	0.7672E+00	0.4744E+03	0.2903E+02	0.0	0.6581E+01	0.1420E+00
0.7000E-01	0.4000E-01	0.0	0.1879E+04	0.1016E+01	0.5024E+03	0.3074E+02	0.0	0.1536E+02	0.6087E-01
0.7000E-01	0.4000E-01	0.0	0.2343E+04	0.1266E+01	0.5204E+03	0.3184E+02	0.0	0.2517E+02	0.3884E-01
0.7000E-01	0.4000E-01	0.0	0.2805E+04	0.1516E+01	0.5294E+03	0.3239E+02	0.0	0.5033E+02	0.1947E-01

PI=INJECTION PRESSURE
WI=BRINE INJECTED
NP=CUMULATIVE VOLUME OIL PRODUCED
WOR=WATER-OIL RATIO

PP=PRODUCTION PRESSURE
VFI=TOTAL VOLUME OF FLUID INJECTED
%R=RECOVERY PERCENT
OPFIR=OIL PRODUCED-FLUID INJECTED RATIO

GI=CUMULATIVE VOLUME OF CO2 INJECTED
PV=PORE VOLUME OF SAND PACK
GOR=GAS-OIL RATIO

University of Alberta

TABLE G11

RESULTS OF RUN 12

PORE VOLUME=0.2296E+04 CM3
HYDROCARBON PORE VOLUME=0.2109E+04 CM3
POROSITY=0.4800E+02%
IRREDUCIBLE WATER SATURATION=0.8100E+01%
INITIAL OIL SATURATION=0.9190E+02%
ABSOLUTE PERMEABILITY=0.4900E+01 DARCIES
CARBON DIOXIDE RETENTION=0.7663E+02 %
CARBON DIOXIDE REQUIRED=0.3791E+03 SM3/M3

PI,MPAG	PP,MPAG	GI,CM3	WI,CM3	VFI/PV	NP,CM3	%R	GOR,SM3/M3	WOR,M3/M3	OPFIR,M3/M3
0.5500E+01	0.5500E+01	0.3100E+02	0.0	0.1350E-01	0.0	0.0	0.0	0.0	0.0
0.5750E+01	0.5500E+01	0.3427E+03	0.0	0.1493E+00	0.1700E+02	0.8060E+00	0.0	0.0	0.5454E-01
0.5670E+01	0.5400E+01	0.3705E+03	0.0	0.1614E+00	0.2550E+02	0.1209E+01	0.5076E+03	0.0	0.3058E+00
0.5690E+01	0.5340E+01	0.4205E+03	0.0	0.1831E+00	0.3600E+02	0.1707E+01	0.2016E+03	0.0	0.2100E+00
0.8900E+01	0.9000E+00	0.4205E+03	0.2163E+03	0.2774E+00	0.2068E+03	0.9804E+01	0.1880E+02	0.0	0.7896E+00
0.9220E+01	0.3000E+00	0.4205E+03	0.2718E+03	0.3015E+00	0.2567E+03	0.1217E+02	0.0	0.0	0.8991E+00
0.9720E+01	0.3200E+00	0.4205E+03	0.3433E+03	0.3327E+00	0.3115E+03	0.1477E+02	0.0	0.0	0.7664E+00
0.1026E+02	0.3100E+00	0.4205E+03	0.4038E+03	0.3590E+00	0.3700E+03	0.1754E+02	0.0	0.2564E-01	0.9669E+00
0.8720E+01	0.4600E+00	0.4205E+03	0.4618E+03	0.3843E+00	0.4325E+03	0.2050E+02	0.0	0.3200E-01	0.1078E+01
0.8660E+01	0.4400E+00	0.4205E+03	0.5478E+03	0.4217E+00	0.5160E+03	0.2446E+02	0.0	0.2395E-01	0.9709E+00
0.8340E+01	0.4400E+00	0.4205E+03	0.6453E+03	0.4642E+00	0.6030E+03	0.2859E+02	0.0	0.2299E-01	0.8923E+00
0.1020E+02	0.1000E+00	0.4205E+03	0.7759E+03	0.5211E+00	0.7130E+03	0.3380E+02	0.0	0.1818E+00	0.8423E+00
0.9800E+00	0.8600E+00	0.4205E+03	0.9809E+03	0.6104E+00	0.8594E+03	0.4074E+02	0.5567E+01	0.1031E+01	0.7141E+00
0.9700E+00	0.4300E+00	0.4205E+03	0.1454E+04	0.8162E+00	0.9274E+03	0.4397E+02	0.8945E+00	0.6309E+01	0.1439E+00
0.9200E+00	0.2800E+00	0.4205E+03	0.1848E+04	0.9882E+00	0.9654E+03	0.4577E+02	0.4268E+00	0.8211E+01	0.9623E-01
0.9500E+00	0.3600E+00	0.4205E+03	0.2581E+04	0.1307E+01	0.1005E+04	0.4767E+02	0.0	0.1688E+02	0.5459E-01

University of Alberta

TABLE G11 (CONTINUED)

RESULTS OF RUN 12

PI,MPAG	PP,MPAG	GI,CM3	WI,CM3	VFI/PV	NP,CM3	%R	GOR,SM3/M3	WOR,M3/M3	OPFIR,M3/M3
0.7900E+00	0.3200E+00	0.4205E+03	0.3411E+04	0.1669E+01	0.1043E+04	0.4947E+02	0.0	0.2105E+02	0.4578E-01
0.7500E+00	0.3000E+00	0.4205E+03	0.3883E+04	0.1874E+01	0.1063E+04	0.5041E+02	0.0	0.2265E+02	0.4237E-01
0.0	0.0	0.4205E+03	0.3883E+04	0.1874E+01	0.1074E+04	0.5094E+02	0.0	0.8182E+01	

PI=INJECTION PRESSURE
PP=PRODUCTION PRESSURE
GI=CUMULATIVE VOLUME OF CO2 INJECTED
WI=BRINE INJECTED
VFI=TOTAL VOLUME OF FLUID INJECTED
PV=PORE VOLUME OF SAND PACK
NP=CUMULATIVE VOLUME OIL PRODUCED
%R=RECOVERY PERCENT
GOR=GAS-OIL RATIO
WOR=WATER-OIL RATIO
OPFIR=OIL PRODUCED-FLUID INJECTED RATIO

University of Alberta

TABLE G12

RESULTS OF RUN 13

PORE VOLUME=0.2083E+04 CM3
HYDROCARBON PORE VOLUME=0.1825E+04 CM3
POROSITY=0.4350E+02%
IRREDUCIBLE WATER SATURATION=0.1240E+02%
INITIAL OIL SATURATION=0.8760E+02%
ABSOLUTE PERMEABILITY=0.1190E+02 DARCIES
CARBON DIOXIDE RETENTION=0.6885E+02 %
CARBON DIOXIDE REQUIRED=0.2521E+03 SM3/M3

PI,MPAG	PP,MPAG	GI,CM3	WI,CM3	VFI/PV	NP,CM3	%R	GOR,SM3/M3	WOR,M3/M3	OPFIR,M3/M3
0.5500E+01	0.5500E+01	0.1346E+02	0.0	0.6462E-02	0.0	0.0	0.0	0.0	0.0
0.5540E+01	0.5520E+01	0.4400E+02	0.0	0.2112E-01	0.1200E+02	0.6574E+00	0.0	0.0	0.3929E+00
0.5540E+01	0.5520E+01	0.7300E+02	0.0	0.3505E-01	0.1980E+02	0.1085E+01	0.1612E+02	0.0	0.2690E+00
0.5800E+01	0.5540E+01	0.7300E+02	0.7310E+02	0.7014E-01	0.6480E+02	0.3550E+01	0.4506E+01	0.0	0.6156E+00
0.5520E+01	0.5460E+01	0.1460E+03	0.7310E+02	0.1052E+00	0.1078E+03	0.5906E+01	0.1207E+02	0.0	0.5890E+00
0.5640E+01	0.5560E+01	0.1460E+03	0.1461E+03	0.1402E+00	0.1468E+03	0.8043E+01	0.3473E+02	0.1795E+00	0.5342E+00
0.5530E+01	0.5510E+01	0.2190E+03	0.1461E+03	0.1753E+00	0.1678E+03	0.9193E+01	0.1892E+02	0.3810E+00	0.2877E+00
0.5590E+01	0.5540E+01	0.2190E+03	0.2191E+03	0.2103E+00	0.2048E+03	0.1122E+02	0.3945E+02	0.4054E+00	0.5068E+00
0.5530E+01	0.5500E+01	0.2929E+03	0.2191E+03	0.2458E+00	0.2318E+03	0.1270E+02	0.5857E+02	0.5556E+00	0.3653E+00
0.5630E+01	0.5580E+01	0.2929E+03	0.6922E+03	0.4729E+00	0.3754E+03	0.2057E+02	0.2124E+02	0.2029E+01	0.3035E+00
0.5650E+01	0.5600E+01	0.2929E+03	0.1166E+04	0.7005E+00	0.4654E+03	0.2550E+02	0.0	0.4056E+01	0.1898E+00
0.5700E+01	0.5620E+01	0.2929E+03	0.1661E+04	0.9379E+00	0.5384E+03	0.2950E+02	0.0	0.5781E+01	0.1477E+00
0.5620E+01	0.5560E+01	0.2929E+03	0.1834E+04	0.1021E+01	0.5554E+03	0.3043E+02	0.0	0.8765E+01	0.9798E-01
0.5590E+01	0.5530E+01	0.2929E+03	0.2307E+04	0.1248E+01	0.6034E+03	0.3306E+02	0.0	0.9000E+01	0.1015E+00
0.5650E+01	0.5640E+01	0.2929E+03	0.2780E+04	0.1475E+01	0.6344E+03	0.3476E+02	0.0	0.1406E+02	0.6548E-01
0.5545E+01	0.5500E+01	0.2929E+03	0.3264E+04	0.1707E+01	0.6574E+03	0.3602E+02	0.0	0.2030E+02	0.4758E-01

University of Alberta

TABLE G12 (CONTINUED)

RESULTS OF RUN 13

PI,MPAG	PP,MPAG	GI,CM3	WI,CM3	VFI/PV	NP,CM3	%R	GOR,SM3/M3	WOR,M3/M3	OPFIR,M3/M3
0.5490E+01	0.5400E+01	0.2929E+03	0.3668E+04	0.1902E+01	0.6764E+03	0.3706E+02	0.0	0.2105E+02	0.4701E-01
0.2480E+01	0.2480E+01	0.2929E+03	0.3668E+04	0.1902E+01	0.6779E+03	0.3714E+02	0.0	0.1400E+02	
0.1100E+01	0.1100E+01	0.2929E+03	0.3668E+04	0.1902E+01	0.6789E+03	0.3719E+02	0.0	0.1100E+02	
0.0	0.0	0.2929E+03	0.3668E+04	0.1902E+01	0.7039E+03	0.3856E+02	0.0	0.634CE+01	

PI=INJECTION PRESSURE
PP=PRODUCTION PRESSURE
GI=CUMULATIVE VOLUME OF CO2 INJECTED
WI=BRINE INJECTED
VFI=TOTAL VOLUME OF FLUID INJECTED
PV=PORE VOLUME OF SAND PACK
NP=CUMULATIVE VOLUME OIL PRODUCED
%R=RECOVERY PERCENT
GOR=GAS-OIL RATIO
WOR=WATER-OIL RATIO
OPFIR=OIL PRODUCED-FLUID INJECTED RATIO

University of Alberta

TABLE G13

RESULTS OF RUN 14

PORE VOLUME=0.1965E+04 CM3
HYDROCARBON PORE VOLUME=0.1734E+04 CM3
POROSITY=0.4410E+02%
IRREDUCIBLE WATER SATURATION=0.1170E+02%
INITIAL OIL SATURATION=0.8830E+02%
ABSOLUTE PERMEABILITY=0.1090E+02 DARCIES
CARBON DIOXIDE RETENTION=0.4899E+02 %
CARBON DIOXIDE REQUIRED=0.2862E+03 SM3/M3

PI,MPAG	PP,MPAG	GI,CM3	WI,CM3	VFI/PV	NP,CM3	%R	GOR,SM3/M3	WOR,M3/M3	OPFIR,M3/M3
0.5500E+01	0.5500E+01	0.3470E+02	0.0	0.1766E-01	0.0	0.0	0.0	0.0	0.0
0.5900E+01	0.5500E+01	0.3470E+02	0.3540E+02	0.3567E-01	0.2450E+02	0.1413E+01	0.0	0.0	0.6921E+00
0.5540E+01	0.5500E+01	0.6940E+02	0.3540E+02	0.5333E-01	0.3200E+02	0.1845E+01	0.0	0.0	0.2161E+00
0.5760E+01	0.5490E+01	0.6940E+02	0.7010E+02	0.7099E-01	0.6450E+02	0.3719E+01	0.0	0.0	0.9366E+00
0.5540E+01	0.5500E+01	0.1041E+03	0.7010E+02	0.8865E-01	0.7300E+02	0.4209E+01	0.0	0.0	0.2450E+00
0.5640E+01	0.5460E+01	0.1041E+03	0.1053E+03	0.1066E+00	0.1030E+03	0.5939E+01	0.2568E+01	0.1167E+00	0.8523E+00
0.5530E+01	0.5500E+01	0.1400E+03	0.1053E+03	0.1248E+00	0.1102E+03	0.6354E+01	0.0	0.1806E+00	0.2006E+00
0.5640E+01	0.5520E+01	0.1400E+03	0.1400E+03	0.1425E+00	0.1342E+03	0.7738E+01	0.2399E+02	0.2292E+00	0.6916E+00
0.5520E+01	0.5500E+01	0.1747E+03	0.1400E+03	0.1602E+00	0.1397E+03	0.8055E+01	0.5013E+02	0.8182E+00	0.1585E+00
0.5650E+01	0.5530E+01	0.1747E+03	0.1747E+03	0.1778E+00	0.1592E+03	0.9179E+01	0.4866E+02	0.4359E+00	0.5620E+00
0.5530E+01	0.5520E+01	0.2094E+03	0.1747E+03	0.1955E+00	0.1662E+03	0.9583E+01	0.7531E+02	0.5714E+00	0.2017E+00
0.5650E+01	0.5530E+01	0.2094E+03	0.2094E+03	0.2131E+00	0.1872E+03	0.1079E+02	0.1661E+02	0.4286E+00	0.6052E+00
0.5530E+01	0.5520E+01	0.2435E+03	0.2094E+03	0.2305E+00	0.1970E+03	0.1136E+02	0.2069E+02	0.5102E+00	0.2873E+00
0.5440E+01	0.5370E+01	0.2435E+03	0.2441E+03	0.2481E+00	0.2160E+03	0.1245E+02	0.7043E+02	0.5789E+00	0.5476E+00
0.5500E+01	0.5310E+01	0.2790E+03	0.2441E+03	0.2662E+00	0.2250E+03	0.1297E+02	0.1766E+03	0.6667E+00	0.2535E+00
0.5640E+01	0.5550E+01	0.2790E+03	0.2788E+03	0.2839E+00	0.2335E+03	0.1346E+02	0.8110E+02	0.1059E+01	0.2450E+00

University of Alberta

TABLE G13 (CONTINUED)

RESULTS OF RUN 14

PI,MPAG	PP,MPAG	GI,CM3	WI,CM3	VFI/PV	NP,CM3	%R	GOR,SM3/M3	WOR,M3/M3	OPFIR,M3/M3
0.5560E+01	0.5540E+01	0.3140E+03	0.2788E+03	0.3017E+00	0.2390E+03	0.1378E+02	0.7373E+01	0.7273E+00	0.1574E+00
0.5600E+01	0.5540E+01	0.3140E+03	0.3135E+03	0.3193E+00	0.2545E+03	0.1467E+02	0.6488E+02	0.7742E+00	0.4467E+00
0.5510E+01	0.5450E+01	0.3489E+03	0.3135E+03	0.3371E+00	0.2670E+03	0.1540E+02	0.2368E+03	0.8000E+00	0.3582E+00
0.5580E+01	0.5530E+01	0.3489E+03	0.4992E+03	0.4316E+00	0.3279E+03	0.1891E+02	0.6619E+02	0.1529E+01	0.3280E+00
0.5660E+01	0.5500E+01	0.3489E+03	0.9784E+03	0.6754E+00	0.4571E+03	0.2636E+02	0.2027E+02	0.2661E+01	0.2696E+00
0.5550E+01	0.5480E+01	0.3489E+03	0.1451E+04	0.9162E+00	0.5191E+03	0.2993E+02	0.4578E+01	0.6532E+01	0.1311E+00
0.5530E+01	0.5430E+01	0.3489E+03	0.1933E+04	0.1161E+01	0.5691E+03	0.3281E+02	0.0	0.9200E+01	0.1037E+00
0.5330E+01	0.5320E+01	0.3489E+03	0.2173E+04	0.1283E+01	0.5841E+03	0.3368E+02	0.0	0.1347E+02	0.6271E-01
0.5220E+01	0.5190E+01	0.3489E+03	0.2647E+04	0.1524E+01	0.6071E+03	0.3501E+02	0.0	0.1978E+02	0.4852E-01
0.5720E+01	0.5270E+01	0.3489E+03	0.3122E+04	0.1766E+01	0.6301E+03	0.3633E+02	0.0	0.1913E+02	0.4842E-01
0.5110E+01	0.4910E+01	0.3489E+03	0.3597E+04	0.2008E+01	0.6451E+03	0.3720E+02	0.0	0.3067E+02	0.3158E-01
0.4700E+00	0.4700E+00	0.3489E+03	0.3597E+04	0.2008E+01	0.6476E+03	0.3734E+02	0.0	0.2660E+02	
0.0	0.0	0.3489E+03	0.3597E+04	0.2008E+01	0.6836E+03	0.3942E+02	0.0	0.4333E+01	

PI=INJECTION PRESSURE
PP=PRODUCTION PRESSURE
GI=CUMULATIVE VOLUME OF CO2 INJECTED
WI=BRINE INJECTED
VFI=TOTAL VOLUME OF FLUID INJECTED
PV=PORE VOLUME OF SAND PACK
NP=CUMULATIVE VOLUME OIL PRODUCED
%R=RECOVERY PERCENT
GOR=GAS-OIL RATIO
WOR=WATER-OIL RATIO
OPFIR=OIL PRODUCED-FLUID.INJECTED RATIO

University of Alberta

TABLE G14

RESULTS OF RUN 15

PORE VOLUME=0.2069E+04 CM3
HYDROCARBON PORE VOLUME=0.1839E+04 CM3
POROSITY=0.432OE+02%
IRREDUCIBLE WATER SATURATION=0.111OE+02%
INITIAL OIL SATURATION=0.889OE+02%
ABSOLUTE PERMEABILITY=0.117OE+02 DARCIES
CARBON DIOXIDE RETENTION=0.7439E+02 %
CARBON DIOXIDE REQUIRED=0.1966E+03 SM3/M3

PI,MPAG	PP,MPAG	GI,CM3	WI,CM3	VFI/PV	NP,CM3	%R	GOR,SM3/M3	WOR,M3/M3	OPFIR,M3/M3
0.5500E+01	0.5500E+01	0.2490E+02	0.0	0.1203E-01	0.0	0.0	0.0	0.0	0.0
0.5550E+01	0.5520E+01	0.3680E+02	0.0	0.1779E-01	0.1500E+01	0.8155E-01	0.0	0.0	0.1261E+00
0.5840E+01	0.5480E+01	0.3680E+02	0.1104E+03	0.7115E-01	0.1005E+03	0.5464E+01	0.0	0.0	0.8967E+00
0.5570E+01	0.5500E+01	0.6970E+02	0.1104E+03	0.8705E-01	0.1100E+03	0.5981E+01	0.0	0.0	0.2888E+00
0.5810E+01	0.5520E+01	0.6970E+02	0.2208E+03	0.1404E+00	0.2070E+03	0.1125E+02	0.0	0.5155E-01	0.8790E+00
0.5560E+01	0.5520E+01	0.1061E+03	0.2208E+03	0.1580E+00	0.2180E+03	0.1185E+02	0.0	0.4545E-01	0.3022E+00
0.5650E+01	0.5400E+01	0.1061E+03	0.3311E+03	0.2113E+00	0.2665E+03	0.1449E+02	0.0	0.9381E+00	0.4393E+00
0.5410E+01	0.5300E+01	0.1429E+03	0.3311E+03	0.2291E+00	0.2825E+03	0.1536E+02	0.1784E+03	0.9375E+00	0.4342E+00
0.5600E+01	0.5500E+01	0.1429E+03	0.4436E+03	0.2835E+00	0.3245E+03	0.1764E+02	0.6565E+01	0.1071E+01	0.3735E+00
0.5500E+01	0.5480E+01	0.1829E+03	0.4436E+03	0.3028E+00	0.3391E+03	0.1844E+02	0.2333E+02	0.8219E+00	0.3659E+00
0.5530E+01	0.5420E+01	0.1829E+03	0.5555E+03	0.3569E+00	0.3781E+03	0.2056E+02	0.6238E+01	0.1769E+01	0.3485E+00
0.5510E+01	0.5470E+01	0.2196E+03	0.5555E+03	0.3746E+00	0.3827E+03	0.2081E+02	0.0	0.2826E+01	0.1251E+00
0.5560E+01	0.5440E+01	0.2196E+03	0.6659E+03	0.4280E+00	0.4157E+03	0.2260E+02	0.1868E+02	0.2030E+01	0.2989E+00
0.5460E+01	0.5390E+01	0.2564E+03	0.6659E+03	0.4458E+00	0.4267E+03	0.2320E+02	0.5161E+02	0.1727E+01	0.2989E+00
0.5500E+01	0.5470E+01	0.2564E+03	0.7763E+03	0.4991E+00	0.4517E+03	0.2456E+02	0.4963E+02	0.2400E+01	0.2264E+00
0.5500E+01	0.5460E+01	0.2932E+03	0.7763E+03	0.5169E+00	0.4557E+03	0.2478E+02	0.5069E+02	0.4125E+01	0.1087E+00

University of Alberta

TABLE G14 (CONTINUED)

RESULTS OF RUN 15

PI,MPAG	PP,MPAG	GI,CM3	WI,CM3	VFI/PV	NP,CM3	%R	GOR,SM3/M3	WOR,M3/M3	OPFIR,M3/M3
0.5520E+01	0.5440E+01	0.2932E+03	0.8867E+03	0.5703E+00	0.4737E+03	0.2575E+02	0.0	0.4889E+01	0.1630E+00
0.5480E+01	0.5440E+01	0.3300E+03	0.8867E+03	0.5881E+00	0.4767E+03	0.2592E+02	0.0	0.5000E+01	0.8152E-01
0.5460E+01	0.5420E+01	0.3300E+03	0.1018E+04	0.6517E+00	0.5037E+03	0.2739E+02	0.0	0.3481E+01	0.2050E+00
0.5170E+01	0.5120E+01	0.3668E+03	0.1018E+04	0.6695E+00	0.5157E+03	0.2804E+02	0.9597E+02	0.2333E+01	0.3261E+00
0.5000E+01	0.4920E+01	0.3668E+03	0.1499E+04	0.9018E+00	0.5657E+03	0.3076E+02	0.2757E+02	0.7900E+01	0.1041E+00
0.5180E+01	0.5130E+01	0.3668E+03	0.1750E+04	0.1023E+01	0.5897E+03	0.3206E+02	0.1690E+01	0.9292E+01	0.9543E-01
0.5060E+01	0.5040E+01	0.3668E+03	0.2232E+04	0.1256E+01	0.6347E+03	0.3451E+02	0.0	0.9444E+01	0.9340E-01
0.4730E+01	0.4690E+01	0.3668E+03	0.2717E+04	0.1491E+01	0.6637E+03	0.3608E+02	0.0	0.1503E+02	0.5979E-01
0.4670E+01	0.4650E+01	0.3668E+03	0.3202E+04	0.1725E+01	0.6837E+03	0.3717E+02	0.0	0.2350E+02	0.4124E-01
0.5160E+01	0.5140E+01	0.3668E+03	0.3696E+04	0.1964E+01	0.6987E+03	0.3799E+02	0.0	0.3133E+02	0.3037E-01
0.2040E+01	0.2040E+01	0.3668E+03	0.3696E+04	0.1964E+01	0.7007E+03	0.3810E+02	0.0	0.1125E+02	
0.1540E+01	0.1540E+01	0.3668E+03	0.3696E+04	0.1964E+01	0.7022E+03	0.3818E+02	0.0	0.5000E+01	
0.0	0.0	0.3668E+03	0.3696E+04	0.1964E+01	0.7772E+03	0.4226E+02	0.1622E+01	0.2933E+01	

PI=INJECTION PRESSURE
PP=PRODUCTION PRESSURE
GI=CUMULATIVE VOLUME OF CO2 INJECTED
WI=BRINE INJECTED
VFI=TOTAL VOLUME OF FLUID INJECTED
PV=PORE VOLUME OF SAND PACK
NP=CUMULATIVE VOLUME OIL PRODUCED
%R=RECOVERY PERCENT
GOR=GAS-OIL RATIO
WOR=WATER-OIL RATIO
OPFIR=OIL PRODUCED-FLUID INJECTED RATIO

University of Alberta

TABLE G15

RESULTS OF RUN 16

PORE VOLUME=0.2123E+04 CM3
HYDROCARBON PORE VOLUME=0.1883E+04 CM3
POROSITY=0.4440E+02%
IRREDUCIBLE WATER SATURATION=0.1130E+02%
INITIAL OIL SATURATION=0.8870E+02%
ABSOLUTE PERMEABILITY=0.1490E+02 DARCIES
CARBON DIOXIDE RETENTION=0.6754E+02 %
CARBON DIOXIDE REQUIRED=0.1315E+03 SM3/M3

PI,MPAG	PP,MPAG	GI,CM3	WI,CM3	VFI/PV	NP,CM3	%R	GOR,SM3/M3	WOR,M3/M3	OPFIR,M3/M3
0.5500E+01	0.5500E+01	0.3800E+02	0.0	0.1790E-01	0.0	0.0	0.0	0.0	0.0
0.5600E+01	0.5500E+01	0.3800E+02	0.6000E+02	0.4616E-01	0.5125E+02	0.2721E+01	0.0	0.0	0.8542E+00
0.5750E+01	0.5500E+01	0.3800E+02	0.1050E+03	0.6736E-01	0.9255E+02	0.4914E+01	0.0	0.0	0.9178E+00
0.5890E+01	0.5500E+01	0.3800E+02	0.1500E+03	0.8855E-01	0.1324E+03	0.7033E+01	0.1524E+01	0.1692E+00	0.8867E+00
0.5500E+01	0.5460E+01	0.7570E+02	0.1500E+03	0.1063E+00	0.1409E+03	0.7484E+01	0.0	0.5882E-01	0.2255E+00
0.5730E+01	0.5490E+01	0.7570E+02	0.3006E+03	0.1772E+00	0.2438E+03	0.1294E+02	0.9861E+00	0.4280E+00	0.6826E+00
0.5520E+01	0.5470E+01	0.1134E+03	0.3006E+03	0.1950E+00	0.2508E+03	0.1331E+02	0.0	0.6429E+00	0.1857E+00
0.5600E+01	0.7400E+01	0.1134E+03	0.4521E+03	0.2664E+00	0.3169E+03	0.1683E+02	0.0	0.1148E+01	0.4370E+00
0.5530E+01	0.5520E+01	0.1511E+03	0.4521E+03	0.2841E+00	0.3211E+03	0.1705E+02	0.0	0.8333E+00	0.1114E+00
0.5050E+01	0.6880E+01	0.1511E+03	0.6028E+03	0.3551E+00	0.3721E+03	0.1976E+02	0.0	0.1902E+01	0.3384E+00
0.5560E+01	0.5550E+01	0.1888E+03	0.6028E+03	0.3729E+00	0.3791E+03	0.2013E+02	0.0	0.2143E+01	0.1857E+00
0.5650E+01	0.5500E+01	0.1888E+03	0.7535E+03	0.4439E+00	0.4311E+03	0.2289E+02	0.1794E+02	0.1654E+01	0.3451E+00
0.5580E+01	0.5460E+01	0.2265E+03	0.7535E+03	0.4616E+00	0.4374E+03	0.2322E+02	0.1308E+01	0.2581E+01	0.1645E+00
0.5600E+01	0.5480E+01	0.2265E+03	0.9042E+03	0.5326E+00	0.4764E+03	0.2529E+02	0.1643E+02	0.2410E+01	0.2588E+00
0.5540E+01	0.5520E+01	0.2642E+03	0.9042E+03	0.5504E+00	0.4819E+03	0.2559E+02	0.2949E+01	0.1636E+01	0.1459E+00
0.5560E+01	0.5500E+01	0.2642E+03	0.1055E+04	0.6213E+00	0.5209E+03	0.2766E+02	0.4429E+02	0.2667E+01	0.2588E+00

University of Alberta

TABLE G15 (CONTINUED)

RESULTS OF RUN 16

PI,MPAG	PP,MPAG	GI,CM3	WI,CM3	VFI/PV	NP,CM3	%R	GOR,SM3/M3	WOR,M3/M3	OPFIR,M3/M3
0.5580E+01	0.5600E+01	0.3019E+03	0.1055E+04	0.6391E+00	0.5234E+03	0.2779E+02	0.3244E+01	0.3000E+01	0.6631E-01
0.5600E+01	0.5520E+01	0.3019E+03	0.1206E+04	0.7101E+00	0.5454E+03	0.2896E+02	0.1880E+02	0.5455E+01	0.1460E+00
0.5530E+01	0.5520E+01	0.3396E+03	0.1206E+04	0.7278E+00	0.5474E+03	0.2906E+02	0.1216E+02	0.5500E+01	0.5305E-01
0.5600E+01	0.5370E+01	0.3396E+03	0.1356E+04	0.7988E+00	0.5774E+03	0.3066E+02	0.8272E+02	0.3467E+01	0.1991E+00
0.5580E+01	0.5560E+01	0.3773E+03	0.1356E+04	0.8166E+00	0.5799E+03	0.3079E+02	0.9732E+01	0.4400E+01	0.6631E-01
0.5490E+01	0.5450E+01	0.3773E+03	0.1851E+04	0.1049E+01	0.6574E+03	0.3490E+02	0.4311E+02	0.5129E+01	0.1568E+00
0.5210E+01	0.5170E+01	0.3773E+03	0.2344E+04	0.1282E+01	0.7313E+03	0.3883E+02	0.6914E+01	0.5886E+01	0.1498E+00
0.5010E+01	0.4980E+01	0.3773E+03	0.2824E+04	0.1508E+01	0.7733E+03	0.4106E+02	0.1159E+01	0.1060E+02	0.8738E-01
0.4810E+01	0.4790E+01	0.3773E+03	0.3147E+04	0.1660E+01	0.7933E+03	0.4212E+02	0.1622E+01	0.1425E+02	0.6205E-01
0.4620E+01	0.4590E+01	0.3773E+03	0.3596E+04	0.1872E+01	0.8153E+03	0.4329E+02	0.2212E+01	0.1991E+02	0.4892E-01
0.3450E+01	0.3430E+01	0.3773E+03	0.4092E+04	0.2105E+01	0.8403E+03	0.4462E+02	0.6488E+00	0.1900E+02	0.5045E-01
0.1940E+01	0.1920E+01	0.3773E+03	0.4092E+04	0.2105E+01	0.8413E+03	0.4467E+02	0.0	0.1050E+02	
0.1250E+01	0.1250E+01	0.3773E+03	0.4092E+04	0.2105E+01	0.8423E+03	0.4472E+02	0.0	0.6500E+01	
0.2800E+00	0.2800E+00	0.3773E+03	0.4092E+04	0.2105E+01	0.8493E+03	0.4509E+02	0.1274E+02	0.1971E+02	
0.0	0.0	0.3773E+03	0.4092E+04	0.2105E+01	0.8953E+03	0.4754E+02	0.3403E+02	0.3543E+01	

PI=INJECTION PRESSURE
WI=BRINE INJECTED
NP=CUMULATIVE VOLUME OIL PRODUCED
WOR=WATER-OIL RATIO

PP=PRODUCTION PRESSURE
VFI=TOTAL VOLUME OF FLUID INJECTED
%R=RECOVERY PERCENT
OPFIR=OIL PRODUCED-FLUID INJECTED RATIO

GI=CUMULATIVE VOLUME OF CO2 INJECTED
PV=PORE VOLUME OF SAND PACK
GOR=GAS-OIL RATIO

University of Alberta

TABLE G16

RESULTS OF RUN 17

PORE VOLUME=0.2043E+04 CM3
HYDROCARBON PORE VOLUME=0.1789E+04 CM3
POROSITY=0.427OE+02%
IRREDUCIBLE WATER SATURATION=0.127OE+02%
INITIAL OIL SATURATION=0.876OE+02%
ABSOLUTE PERMEABILITY=0.124OE+02 DARCIES
CARBON DIOXIDE RETENTION=0.5353E+02 %
CARBON DIOXIDE REQUIRED=0.1423E+03 SM3/M3

PI,MPAG	PP,MPAG	GI,CM3	WI,CM3	VFI/PV	NP,CM3	%R	GOR,SM3/M3	WOR,M3/M3	OPFIR,M3/M3
0.5520E+01	0.5520E+01	0.3580E+02	0.0	0.1752E-01	0.0	0.0	0.0	0.0	0.0
0.5800E+01	0.5500E+01	0.3580E+02	0.4300E+02	0.3857E-01	0.3100E+02	0.1733E+01	0.0	0.0	0.7209E+00
0.5840E+01	0.5510E+01	0.3580E+02	0.7560E+02	0.5453E-01	0.6050E+02	0.3381E+01	0.2475E+01	0.0	0.9049E+00
0.5800E+01	0.5480E+01	0.3580E+02	0.9800E+02	0.6549E-01	0.8305E+02	0.4641E+01	0.1079E+01	0.1109E-01	0.1007E+01
0.5820E+01	0.5500E+01	0.3580E+02	0.1287E+03	0.8052E-01	0.1159E+03	0.6475E+01	0.2225E+01	0.1524E-01	0.1068E+01
0.5780E+01	0.5500E+01	0.3580E+02	0.1675E+03	0.9951E-01	0.1479E+03	0.8263E+01	0.3548E+01	0.2188E+00	0.8247E+00
0.5770E+01	0.5500E+01	0.3580E+02	0.1789E+03	0.1051E+00	0.1579E+03	0.8822E+01	0.3244E+01	0.3000E+00	0.8772E+00
0.5550E+01	0.5500E+01	0.7160E+02	0.1789E+03	0.1226E+00	0.1643E+03	0.9180E+01	0.2534E+01	0.2500E+00	0.1788E+00
0.5670E+01	0.5500E+01	0.7160E+02	0.2277E+03	0.1465E+00	0.1973E+03	0.1102E+02	0.1303E+02	0.3030E+00	0.6762E+00
0.5690E+01	0.5500E+01	0.7160E+02	0.2935E+03	0.1787E+00	0.2348E+03	0.1312E+02	0.2249E+02	0.7733E+00	0.5699E+00
0.5690E+01	0.5500E+01	0.7160E+02	0.3578E+03	0.2102E+00	0.2646E+03	0.1479E+02	0.7076E+01	0.1174E+01	0.4635E+00
0.5550E+01	0.5500E+01	0.1080E+03	0.3578E+03	0.2280E+00	0.2701E+03	0.1509E+02	0.0	0.1273E+01	0.1511E+00
0.5650E+01	0.5500E+01	0.1080E+03	0.5367E+03	0.3156E+00	0.3451E+03	0.1928E+02	0.8759E+01	0.1280E+01	0.4192E+00
0.5520E+01	0.5500E+01	0.1438E+03	0.5367E+03	0.3331E+00	0.3544E+03	0.1980E+02	0.7151E+02	0.1452E+01	0.2598E+00
0.5620E+01	0.5520E+01	0.1438E+03	0.7156E+03	0.4207E+00	0.4364E+03	0.2439E+02	0.2967E+02	0.9268E+00	0.4584E+00
0.5540E+01	0.5520E+01	0.1796E+03	0.7156E+03	0.4382E+00	0.4408E+03	0.2463E+02	0.0	0.2273E+01	0.1229E+00

University of Alberta

TABLE G16 (CONTINUED)

RESULTS OF RUN 17

PI,MPAG	PP,MPAG	GI,CM3	WI,CM3	VFI/PV	NP,CM3	%R	GOR,SM3/M3	WOR,M3/M3	OPFIR,M3/M3
0.5590E+01	0.5530E+01	0.1796E+03	0.8945E+03	0.5257E+00	0.4794E+03	0.2679E+02	0.2626E+02	0.3264E+01	0.2158E+00
0.5530E+01	0.5520E+01	0.2159E+03	0.8945E+03	0.5435E+00	0.4824E+03	0.2696E+02	0.2703E+01	0.4833E+01	0.8264E-01
0.5570E+01	0.5530E+01	0.2159E+03	0.1073E+04	0.6311E+00	0.5164E+03	0.2886E+02	0.2481E+02	0.3765E+01	0.1901E+00
0.5520E+01	0.5510E+01	0.2517E+03	0.1073E+04	0.6486E+00	0.5219E+03	0.2917E+02	0.1032E+02	0.3545E+01	0.1536E+00
0.5600E+01	0.5570E+01	0.2517E+03	0.1256E+04	0.7379E+00	0.5549E+03	0.3101E+02	0.4178E+02	0.3939E+01	0.1808E+00
0.5520E+01	0.5500E+01	0.2913E+03	0.1256E+04	0.7573E+00	0.5584E+03	0.3120E+02	0.2317E+02	0.6000E+01	0.8838E-01
0.5590E+01	0.5500E+01	0.2913E+03	0.1435E+04	0.8449E+00	0.5804E+03	0.3243E+02	0.3686E+02	0.5909E+01	0.1230E+00
0.5540E+01	0.5530E+01	0.3271E+03	0.1435E+04	0.8624E+00	0.5824E+03	0.3255E+02	0.1622E+02	0.6000E+01	0.5587E-01
0.5560E+01	0.5480E+01	0.3271E+03	0.1614E+04	0.9500E+00	0.6034E+03	0.3372E+02	0.1854E+02	0.7143E+01	0.1174E+00
0.5540E+01	0.5530E+01	0.3629E+03	0.1614E+04	0.9675E+00	[illegible]E+03	0.3383E+02	0.8110E+01	0.8500E+01	0.5587E-01
0.5570E+01	0.5480E+01	0.3629E+03	0.2108E+04	0.1210E+01	[illegible]	0.3800E+02	0.3859E+02	0.5220E+01	0.1508E+00
0.5550E+01	0.5480E+01	0.3629E+03	0.2603E+04	0.1452E+01	[illegible]09E+03	0.4197E+02	0.1942E+02	0.5930E+01	0.1434E+00
0.5530E+01	0.5450E+01	0.3629E+03	0.2821E+04	0.1558E+01	0.7689E+03	0.4297E+02	0.2208E+02	0.1111E+02	0.8283E-01
0.5390E+01	0.5320E+01	0.3629E+03	0.3316E+04	0.1801E+01	0.7889E+03	0.4409E+02	0.1257E+02	0.2375E+02	0.4040E-01
0.2400E+01	0.2400E+01	0.3629E+03	0.3316E+04	0.1801E+01	0.7894E+03	0.4412E+02	0.1622E+02	0.4600E+02	
0.1580E+01	0.1580E+01	0.3629E+03	0.3316E+04	0.1801E+01	0.7919E+03	0.4426E+02	0.2271E+02	0.7400E+01	
0.0	0.0	0.3629E+03	0.3316E+04	0.1801E+01	0.8309E+03	0.4644E+02	0.3390E+02	0.5795E+01	

PI=INJECTION PRESSURE
PP=PRODUCTION PRESSURE
GI=CUMULATIVE VOLUME OF CO2 INJECTED
WI=BRINE INJECTED
VFI=TOTAL VOLUME OF FLUID INJECTED
PV=PORE VOLUME OF SAND PACK
NP=CUMULATIVE VOLUME OIL PRODUCED
%R=RECOVERY PERCENT
GOR=GAS-OIL RATIO
WOR=WATER-OIL RATIO
OPFIR=OIL PRODUCED-FLUID INJECTED RATIO

University of Alberta

TABLE G17

RESULTS OF RUN 18

PORE VOLUME=0.2093E+04 CM3
HYDROCARBON PORE VOLUME=0.1837E+04 CM3
POROSITY=0.4370E+02%
IRREDUCIBLE WATER SATURATION=0.1220E+02%
INITIAL OIL SATURATION=0.8780E+02%
ABSOLUTE PERMEABILITY=0.1410E+02 DARCIES
CARBON DIOXIDE RETENTION=0.6134E+02 %
CARBON DIOXIDE REQUIRED=0.1630E+03 SM3/M3

PI,MPAG.	PP,MPAG	GI,CM3	WI,CM3	VFI/PV	NP,CM3	%R	GOR,SM3/M3	WOR,M3/M3	OPFIR,M3/M3
0.5530E+01	0.5530E+01	0.3670E+02	0.0	0.1753E-01	0.0	0.0	0.0	0.0	0.0
0.5730E+01	0.5500E+01	0.3670E+02	0.2880E+02	0.3129E-01	0.1500E+02	0.8164E+00	0.5407E+00	0.0	0.5208E+00
0.5830E+01	0.5500E+01	0.3670E+02	0.5880E+02	0.4563E-01	0.4300E+02	0.2340E+01	0.5214E+01	0.0	0.9333E+00
0.5850E+01	0.5500E+01	0.3670E+02	0.8920E+02	0.6015E-01	0.7500E+02	0.4082E+01	0.4308E+01	0.1563E-01	0.1053E+01
0.5880E+01	0.5500E+01	0.3670E+02	0.1273E+03	0.7836E-01	0.1012E+03	0.5508E+01	0.6191E+00	0.3053E-01	0.6877E+00
0.5810E+01	0.5500E+01	0.3670E+02	0.1710E+03	0.9924E-01	0.1492E+03	0.8121E+01	0.3379E+00	0.5208E-01	0.1098E+01
0.5830E+01	0.5500E+01	0.3670E+02	0.2041E+03	0.1151E+00	0.1767E+03	0.9617E+01	0.0	0.2545E+00	0.8308E+00
0.5800E+01	0.5500E+01	0.3670E+02	0.2202E+03	0.1227E+00	0.1902E+03	0.1035E+02	0.0	0.3704E+00	0.8385E+00
0.5570E+01	0.5500E+01	0.7400E+02	0.2202E+03	0.1406E+00	0.1989E+03	0.1083E+02	0.0	0.3218E+00	0.2332E+00
0.5780E+01	0.5500E+01	0.7400E+02	0.2586E+03	0.1589E+00	0.2174E+03	0.1183E+02	0.0	0.5946E+00	0.4818E+00
0.5670E+01	0.5500E+01	0.7400E+02	0.4407E+03	0.2459E+00	0.3084E+03	0.1679E+02	0.0	0.1011E+01	0.4997E+00
0.5580E+01	0.5500E+01	0.1107E+03	0.4407E+03	0.2634E+00	0.3174E+03	0.1728E+02	0.0	0.1111E+01	0.2452E+00
0.5580E+01	0.5500E+01	0.1107E+03	0.6655E+03	0.3709E+00	0.3874E+03	0.2109E+02	0.1495E+02	0.2000E+01	0.3114E+00
0.5540E+01	0.5510E+01	0.1474E+03	0.6655E+03	0.3884E+00	0.3919E+03	0.2133E+02	0.0	0.3556E+01	0.1226E+00
0.5620E+01	0.5490E+01	0.1474E+03	0.8857E+03	0.4936E+00	0.4409E+03	0.2400E+02	0.2714E+02	0.3122E+01	0.2225E+00
0.5570E+01	0.5500E+01	0.1877E+03	0.8857E+03	0.5129E+00	0.4446E+03	0.2420E+02	0.1096E+02	0.4324E+01	0.9181E-01

University of Alberta

TABLE G17 (CONTINUED)

RESULTS OF RUN 18

PI,MPAG	PP,MPAG	GI,CM3	WI,CM3	VFI/PV	NP,CM3	%R	GOR,SM3/M3	WOR,M3/M3	OPFIR,M3/M3
0.5600E+01	0.5500E+01	0.1877E+03	0.1106E+04	0.6181E+00	0.4856E+03	0.2643E+02	0.2928E+02	0.3951E+01	0.1862E+00
0.5570E+01	0.5540E+01	0.2243E+03	0.1106E+04	0.6355E+00	0.4906E+03	0.2670E+02	0.7786E+02	0.2800E+01	0.1366E+00
0.5630E+01	0.5540E+01	0.2243E+03	0.1326E+04	0.7408E+00	0.5256E+03	0.2861E+02	0.1622E+02	0.4857E+01	0.1589E+00
0.5570E+01	0.5400E+01	0.2610E+03	0.1326E+04	0.7583E+00	0.5286E+03	0.2877E+02	0.2703E+01	0.4333E+01	0.8174E-01
0.5370E+01	0.5310E+01	0.2610E+03	0.1547E+04	0.8640E+00	0.5596E+03	0.3046E+02	0.2381E+02	0.5710E+01	0.1401E+00
0.5510E+01	0.5480E+01	0.2977E+03	0.1547E+04	0.8815E+00	0.5631E+03	0.3065E+02	0.2085E+02	0.6143E+01	0.9537E-01
0.5540E+01	0.5430E+01	0.2977E+03	0.1780E+04	0.9925E+00	0.5831E+03	0.3174E+02	0.5190E+02	0.1050E+02	0.8606E-01
0.5540E+01	0.5510E+01	0.3347E+03	0.1780E+04	0.1010E+01	0.5851E+03	0.3185E+02	0.1216E+02	0.8500E+01	0.5405E-01
0.5560E+01	0.5520E+01	0.3347E+03	0.2000E+04	0.1115E+01	0.6061E+03	0.3299E+02	0.3128E+02	0.8714E+01	0.9537E-01
0.5550E+01	0.5500E+01	0.3714E+03	0.2000E+04	0.1133E+01	0.6076E+03	0.3307E+02	0.3785E+02	0.1400E+02	0.4087E-01
0.5410E+01	0.5360E+01	0.3714E+03	0.2493E+04	0.1369E+01	0.6565E+03	0.3573E+02	0.4130E+02	0.8611E+01	0.9909E-01
0.5410E+01	0.5360E+01	0.3714E+03	0.2654E+04	0.1445E+01	0.6693E+03	0.3643E+02	0.2598E+02	0.1039E+02	0.7975E-01
0.5550E+01	0.5530E+01	0.3714E+03	0.3153E+04	0.1684E+01	0.7043E+03	0.3833E+02	0.3267E+02	0.1357E+02	0.7007E-01
0.5540E+01	0.5520E+01	0.3714E+03	0.3532E+04	0.1865E+01	0.7393E+03	0.4024E+02	0.1784E+02	0.9571E+01	0.9252E-01
0.5610E+01	0.5590E+01	0.3714E+03	0.4028E+04	0.2102E+01	0.7573E+03	0.4122E+02	0.7659E+01	0.2544E+02	0.3624E-01
0.2760E+01	0.2760E+01	0.3714E+03	0.4028E+04	0.2102E+01	0.7588E+03	0.4130E+02	0.0	0.1333E+02	
0.1400E+01	0.1400E+01	0.3714E+03	0.4028E+04	0.2102E+01	0.7598E+03	0.4135E+02	0.0	0.9000E+01	
0.5700E+00	0.5700E+00	0.3714E+03	0.4028E+04	0.2102E+01	0.7607E+03	0.4140E+02	0.0	0.7778E+01	
0.0	0.0	0.3714E+03	0.4028E+04	0.2102E+01	0.7947E+03	0.4325E+02	0.2051E+02	0.5647E+01	

PI=INJECTION PRESSURE
PP=PRODUCTION PRESSURE
GI=CUMULATIVE VOLUME OF CO2 INJECTED
WI=BRINE INJECTED
VFI=TOTAL VOLUME OF FLUID INJECTED
PV=PORE VOLUME OF SAND PAGK
NP=CUMULATIVE VOLUME OIL PRODUCED
%R=RECOVERY PERCENT
GOR=GAS-OIL RATIO
WOR=WATER-OIL RATIO
OPFIR=OIL PRODUCED-FLUID INJECTED RATIO

University of Alberta

TABLE G18

RESULTS OF RUN 19

PORE VOLUME=0.3142E+04 CM3
HYDROCARBON PORE VOLUME=0.1836E+04 CM3
POROSITY=0.4470E+02%
IRREDUCIBLE WATER SATURATION=0.1430E+02%
INITIAL OIL SATURATION=0.8570E+02%
ABSOLUTE PERMEABILITY=0.1480E+02 DARCIES
CARBON DIOXIDE RETENTION=0.6373E+02 %
CARBON DIOXIDE REQUIRED=0.1450E+03 SM3/M3

PI,MPAG	PP,MPAG	GI,CM3	WI,CM3	VFI/PV	NP,CM3	%R	GOR,SM3/M3	WOR,M3/M3	OPFIR,M3/M3
0.5500E+01	0.5500E+01	0.0	0.1580E+02	0.7376E-02	0.0	0.0	0.0	0.0	0.0
0.6020E+01	0.5500E+01	0.0	0.4040E+02	0.1886E-01	0.2050E+02	0.1117E+01	0.0	0.0	0.8333E+00
0.6030E+01	0.5500E+01	0.0	0.6180E+02	0.2885E-01	0.4150E+02	0.2260E+01	0.0	0.0	0.9813E+00
0.6030E+01	0.5500E+01	0.0	0.8040E+02	0.3754E-01	0.6150E+02	0.3350E+01	0.0	0.0	0.1075E+01
0.6030E+01	0.5500E+01	0.0	0.1048E+03	0.4893E-01	0.8800E+02	0.4793E+01	0.0	0.0	0.1086E+01
0.6030E+01	0.5500E+01	0.0	0.1262E+03	0.5892E-01	0.1097E+03	0.5975E+01	0.0	0.0	0.1014E+01
0.6030E+01	0.5500E+01	0.0	0.1478E+03	0.6900E-01	0.1322E+03	0.7200E+01	0.0	0.0	0.1042E+01
0.6000E+01	0.5500E+01	0.0	0.1702E+03	0.7946E-01	0.1546E+03	0.8420E+01	0.0	0.1339E-01	0.1000E+01
0.5990E+01	0.5500E+01	0.0	0.1999E+03	0.9332E-01	0.1849E+03	0.1007E+02	0.0	0.3960E-01	0.1020E+01
0.5960E+01	0.5500E+01	0.0	0.2305E+03	0.1076E+00	0.2134E+03	0.1162E+02	0.0	0.1404E+00	0.9314E+00
0.5930E+01	0.5520E+01	0.0	0.2734E+03	0.1276E+00	0.2492E+03	0.1357E+02	0.0	0.2514E+00	0.8345E+00
0.5810E+01	0.5520E+01	0.0	0.4790E+03	0.2236E+00	0.3582E+03	0.1951E+02	0.0	0.8991E+00	0.5302E+00
0.5600E+01	0.5520E+01	0.0	0.9757E+03	0.4555E+00	0.4812E+03	0.2621E+02	0.0	0.3065E+01	0.2476E+00
0.5590E+01	0.5480E+01	0.0	0.1344E+04	0.6274E+00	0.5309E+03	0.2892E+02	0.0	0.6485E+01	0.1350E+00
0.5550E+01	0.5440E+01	0.0	0.1839E+04	0.8585E+00	0.5763E+03	0.3139E+02	0.0	0.9837E+01	0.9168E-01
0.5560E+01	0.5460E+01	0.0	0.2144E+04	0.1001E+01	0.5973E+03	0.3253E+02	0.0	0.1348E+02	0.6885E-01

University of Alberta

TABLE [illegible] (CONTINUED)

RESULTS OF RUN [illegible]

PI,MPAG	PP,MPAG	GI,CM3	WI,CM3	VFI/PV	NP,CM3	%R	GOR,SM3/M3	WOR,M3/M3	OPFIR,M3/M3
0.5510E+01	0.5450E+01	0.0	0.2629E+04	0.1227E+01	0.6213E+03	0.3384E+02	0.0	0.1921E+02	0.4948E-01
0.5520E+01	0.5440E+01	0.0	0.3132E+04	0.1462E+01	0.6461E+03	0.3519E+02	0.0	0.1966E+02	0.4930E-01
0.5460E+01	0.5420E+01	0.3670E+02	0.3132E+04	0.1479E+01	0.6464E+03	0.3521E+02	0.0	0.2933E+02	0.8174E-02
0.5590E+01	0.5550E+01	0.3670E+02	0.3206E+04	0.1514E+01	0.6484E+03	0.3532E+02	0.0	0.3400E+02	0.2699E-01
0.5590E+01	0.5550E+01	0.3670E+02	0.3279E+04	0.1548E+01	0.6514E+03	0.3548E+02	0.0	0.2333E+02	0.4115E-01
0.5650E+01	0.5530E+01	0.7340E+02	0.3279E+04	0.1565E+01	0.6519E+03	0.3551E+02	0.0	0.2300E+02	0.1362E-01
0.5530E+01	0.5490E+01	0.7340E+02	0.3381E+04	0.1613E+01	0.6559E+03	0.3572E+02	0.0	0.2313E+02	0.3914E-01
0.5520E+01	0.5480E+01	0.7340E+02	0.3426E+04	0.1634E+01	0.6579E+03	0.3583E+02	0.0	0.2250E+02	0.4474E-01
0.5550E+01	0.5580E+01	0.1101E+03	0.3426E+04	0.1651E+01	0.6589E+03	0.3589E+02	0.0	0.1350E+02	0.2725E-01
0.5500E+01	0.5460E+01	0.1101E+03	0.3523E+04	0.1696E+01	0.6662E+03	0.3629E+02	0.0	0.1208E+02	0.7510E-01
0.5540E+01	0.5480E+01	0.1101E+03	0.3573E+04	0.1719E+01	0.6687E+03	0.3642E+02	0.0	0.1880E+02	0.5030E-01
0.5540E+01	0.5520E+01	0.1468E+03	0.3573E+04	0.1737E+01	0.6697E+03	0.3648E+02	0.0	0.1400E+02	0.2725E-01
0.5520E+01	0.5460E+01	0.1468E+03	0.3720E+04	0.1805E+01	0.6782E+03	0.3694E+02	0.0	0.1547E+02	0.5763E-01
0.5540E+01	0.5520E+01	0.1835E+03	0.3800E+04	0.1860E+01	0.6850E+03	0.3731E+02	0.0	0.1404E+02	0.5862E-01
0.5550E+01	0.5490E+01	0.1835E+03	0.3867E+04	0.1891E+01	0.6906E+03	0.3761E+02	0.2172E+01	0.1146E+02	0.8284E-01
0.5540E+01	0.5520E+01	0.2199E+03	0.3867E+04	0.1908E+01	0.6926E+03	0.3772E+02	0.6082E+01	0.9000E+01	0.5495E-01
0.5550E+01	0.5500E+01	0.2199E+03	0.4014E+04	0.1977E+01	0.7016E+03	0.3821E+02	0.3154E+02	0.1389E+02	0.6122E-01
0.5550E+01	0.5530E+01	0.2566E+03	0.4014E+04	0.1994E+01	0.7036E+03	0.3832E+02	0.1135E+03	0.1100E+02	0.5450E-01
0.5590E+01	0.5560E+01	0.2566E+03	0.4161E+04	0.2062E+01	0.7166E+03	0.3903E+02	0.9358E+02	0.8769E+01	0.8850E-01
0.5550E+01	0.5510E+01	0.2933E+03	0.4161E+04	0.2080E+01	0.7201E+03	0.3922E+02	0.5329E+02	0.5143E+01	0.9537E-01

University of Alberta

TABLE G18 (CONTINUED)

RESULTS OF RUN 19

PI,MPAG	PP,MPAG	GI,CM3	WI,CM3	VFI/PV	NP,CM3	%R	GOR,SM3/M3	WOR,M3/M3	OPFIR,M3/M3
0.5560E+01	0.5530E+01	0.3315E+03	0.4315E+04	0.2169E+01	0.7416E+03	0.4039E+02	0.7356E+02	0.5977E+01	0.1119E+00
0.5640E+01	0.5610E+01	0.3315E+03	0.4462E+04	0.2238E+01	0.7556E+03	0.4115E+02	0.6430E+02	0.8286E+01	0.9530E-01
0.5580E+01	0.5560E+01	0.3682E+03	0.4462E+04	0.2255E+01	0.7576E+03	0.4126E+02	0.2838E+02	0.8000E+01	0.5450E-01
0.5610E+01	0.5580E+01	0.3682E+03	0.4942E+04	0.2479E+01	0.7870E+03	0.4286E+02	0.4414E+02	0.1482E+02	0.6120E-01
0.5610E+01	0.5580E+01	0.3682E+03	0.5446E+04	0.2714E+01	0.8110E+03	0.4417E+02	0.3210E+02	0.2008E+02	0.4769E-01
0.5650E+01	0.5630E+01	0.3682E+03	0.5944E+04	0.2947E+01	0.8360E+03	0.4553E+02	0.3179E+02	0.1920E+02	0.5017E-01
0.5530E+01	0.5500E+01	0.3682E+03	0.6366E+04	0.3144E+01	0.8490E+03	0.4624E+02	0.6675E+02	0.3000E+02	0.3081E-01
0.4840E+01	0.4810E+01	0.3682E+03	0.6861E+04	0.3375E+01	0.8590E+03	0.4679E+02	0.7056E+02	0.592CE+02	0.2021E-01
0.2630E+01	0.2630E+01	0.3682E+03	0.6861E+04	0.3375E+01	0.8595E+03	0.4681E+02	0.0	0.2060E+02	
0.1470E+01	0.1470E+01	0.3682E+03	0.6861E+04	0.3375E+01	0.8605E+03	0.4687E+02	0.4055E+02	0.1750E+02	
0.7000E+00	0.7000E+00	0.3682E+03	0.6861E+04	0.3375E+01	0.8665E+03	0.4719E+02	0.5271E+02	0.1617E+02	
0.0	0.0	0.3682E+03	0.6861E+04	0.3375E+01	0.8945E+03	0.4872E+02	0.1353E+03	0.7643E+01	

PI=INJECTION PRESSURE
PP=PRODUCTION PRESSURE
GI=CUMULATIVE VOLUME OF CO2 INJECTED
WI=BRINE INJECTED
VFI=TOTAL VOLUME OF FLUID INJECTED
PV=PORE VOLUME OF SAND PACK
NP=CUMULATIVE VOLUME OIL PRODUCED
%R=RECOVERY PERCENT
GOR=GAS-OIL RATIO
WOR=WATER-OIL RATIO
OPFIR=OIL PRODUCED-FLUID INJECTED RATIO

University of Alberta

TABLE G19

RESULTS OF RUN 20

PORE VOLUME=0.2148E+04 CM3
HYDROCARBON PORE VOLUME=0.1931E+04 CM3
POROSITY=0.4490E+02%
IRREDUCIBLE WATER SATURATION=0.1010E+02%
INITIAL OIL SATURATION=0.8990E+02%
ABSOLUTE PERMEABILITY=0.1480E+02 DARCIES
CARBON DIOXIDE RETENTION=0.6487E+02 %
CARBON DIOXIDE REQUIRED=0.1632E+03 SM3/M3

PI,MPAG	PP,MPAG	GI,CM3	WI,CM3	VFI/PV	NP,CM3	%R	GOR,SM3/M3	WOR,M3/M3	OPFIR,M3/M3
0.5500E+01	0.5500E+01	0.0	0.1700E+02	0.7914E-02	0.0	0.0	0.0	0.0	0.0
0.5890E+01	0.5500E+01	0.0	0.5620E+02	0.2616E-01	0.2870E+02	0.1486E+01	0.0	0.0	0.7321E+00
0.5930E+01	0.5480E+01	0.0	0.1045E+03	0.4865E-01	0.8420E+02	0.4360E+01	0.0	0.0	0.1149E+01
0.5930E+01	0.5500E+01	0.0	0.1345E+03	0.6262E-01	0.1147E+03	0.5940E+01	0.0	0.0	0.1017E+01
0.5920E+01	0.5500E+01	0.0	0.1626E+03	0.7570E-01	0.1422E+03	0.7364E+01	0.0	0.0	0.9786E+00
0.5880E+01	0.5500E+01	0.0	0.1933E+03	0.8999E-01	0.1722E+03	0.8918E+01	0.0	0.1000E+00	0.9772E+00
0.5850E+01	0.5500E+01	0.0	0.2215E+03	0.1031E+00	0.2002E+03	0.1037E+02	0.0	0.1071E+00	0.9929E+00
0.5840E+01	0.5500E+01	0.0	0.2547E+03	0.1186E+00	0.2227E+03	0.1153E+02	0.0	0.4444E+00	0.6777E+00
0.5760E+01	0.5530E+01	0.0	0.4648E+03	0.2164E+00	0.3327E+03	0.1723E+02	0.0	0.9364E+00	0.5236E+00
0.5700E+01	0.5530E+01	0.0	0.9574E+03	0.4457E+00	0.4918E+03	0.2547E+02	0.0	0.2118E+01	0.3230E+00
0.5550E+01	0.5490E+01	0.0	0.1228E+04	0.5718E+00	0.5348E+03	0.2770E+02	0.0	0.5233E+01	0.1587E+00
0.5540E+01	0.5480E+01	0.0	0.1722E+04	0.8019E+00	0.5948E+03	0.3080E+02	0.0	0.7250E+01	0.1214E+00
0.5600E+01	0.5520E+01	0.0	0.2217E+04	0.1032E+01	0.6368E+03	0.3298E+02	0.0	0.1090E+02	0.8485E-01
0.5610E+01	0.5520E+01	0.0	0.2665E+04	0.1241E+01	0.6638E+03	0.3438E+02	0.0	0.1556E+02	0.6035E-01
0.5560E+01	0.5470E+01	0.0	0.3140E+04	0.1462E+01	0.6858E+03	0.3552E+02	0.0	0.2064E+02	0.4626E-01
0.5540E+01	0.5520E+01	0.4160E+02	0.3140E+04	0.1481E+01	0.6863E+03	0.3554E+02	0.0	0.2200E+02	0.1202E-01

University of Alberta

TABLE G19 (CONTINUED)

RESULTS OF RUN 20

PI,MPAG	PP,MPAG	GI,CM3	WI,CM3	VFI/PV	NP,CM3	%R	GOR,SM3/M3	WOR,M3/M3	OPFIR,M3/M3
0.5570E+01	0.5490E+01	0.8020E+02	0.3218E+04	0.1535E+01	0.6895E+03	0.3571E+02	0.0	0.2250E+02	0.2763E-01
0.5570E+01	0.5560E+01	0.1677E+03	0.3256E+04	0.1594E+01	0.6930E+03	0.3589E+02	0.0	0.1500E+02	0.2776E-01
0.5560E+01	0.5510E+01	0.2063E+03	0.3345E+04	0.1653E+01	0.6987E+03	0.3618E+02	0.0	0.1675E+02	0.4460E-01
0.5540E+01	0.5520E+01	0.2449E+03	0.3423E+04	0.1707E+01	0.7024E+03	0.3637E+02	0.0	0.1914E+02	0.3195E-01
0.5570E+01	0.5550E+01	0.2835E+03	0.3423E+04	0.1725E+01	0.7034E+03	0.3643E+02	0.0	0.1200E+02	0.2591E-01
0.5700E+01	0.5670E+01	0.2835E+03	0.3462E+04	0.1744E+01	0.7064E+03	0.3658E+02	0.1352E+02	0.1000E+02	0.7557E-01
0.5580E+01	0.5540E+01	0.3221E+03	0.3462E+04	0.1762E+01	0.7092E+03	0.3673E+02	0.3070E+03	0.3250E+01	0.7254E-01
0.5570E+01	0.5540E+01	0.3221E+03	0.3498E+04	0.1778E+01	0.7170E+03	0.3713E+02	0.1206E+03	0.3744E+01	0.2179E+00
0.5580E+01	0.5570E+01	0.3607E+03	0.3498E+04	0.1796E+01	0.7176E+03	0.3716E+02	0.4055E+02	0.9833E+01	0.1554E-01
0.5700E+01	0.5670E+01	0.3607E+03	0.3537E+04	0.1814E+01	0.7216E+03	0.3737E+02	0.6488E+02	0.6000E+01	0.1036E+00
0.5610E+01	0.5600E+01	0.3993E+03	0.3537E+04	0.1832E+01	0.7233E+03	0.3746E+02	0.6202E+02	0.5765E+01	0.4404E-01
0.5200E+01	0.5150E+01	0.3993E+03	0.3968E+04	0.2033E+01	0.7928E+03	0.4106E+02	0.5414E+02	0.5288E+01	0.1612E+00
0.4880E+01	0.4850E+01	0.3993E+03	0.4465E+04	0.2264E+01	0.8128E+03	0.4209E+02	0.4623E+02	0.2210E+02	0.4027E-01
0.5000E+01	0.4970E+01	0.3993E+03	0.4812E+04	0.2426E+01	0.8258E+03	0.4277E+02	0.5053E+02	0.2731E+02	0.3741E-01
0.6260E+01	0.6240E+01	0.3993E+03	0.5201E+04	0.2607E+01	0.8418E+03	0.4359E+02	0.3295E+02	0.2144E+02	0.4117E-01
0.3240E+01	0.3200E+01	0.3993E+03	0.5779E+04	0.2876E+01	0.8568E+03	0.4437E+02	0.4163E+02	0.2553E+02	0.2594E-01
0.6240E+01	0.6220E+01	0.3993E+03	0.6081E+04	0.3017E+01	0.8658E+03	0.4484E+02	0.4235E+02	0.5356E+02	0.2978E-01
0.3570E+01	0.3570E+01	0.3993E+03	0.6081E+04	0.3017E+01	0.8668E+03	0.4489E+02	0.8110E+01	0.1100E+02	
0.1600E+01	0.1600E+01	0.3993E+03	0.6081E+04	0.3017E+01	0.8678E+03	0.4494E+02	0.1622E+02	0.1700E+02	
0.1050E+01	0.1050E+01	0.3993E+03	0.6081E+04	0.3017E+01	0.8722E+03	0.4517E+02	0.2765E+02	0.1386E+02	

University of Alberta

TABLE G19 (CONTINUED)

RESULTS OF RUN 20

PI,MPAG	PP,MPAG	GI,CM3	WI,CM3	VFI/PV	NP,CM3	%R	GOR,SM3/M3	WOR,M3/M3	OPFIR,M3/M3
0.0	0.0	0.3993E+03	0.6081E+04	0.3017E+01	0.9267E+03	0.4799E+02	0.8393E+02	0.4752E+01	

PI=INJECTION PRESSURE
PP=PRODUCTION PRESSURE
GI=CUMULATIVE VOLUME OF CO2 INJECTED
WI=BRINE INJECTED
VFI=TOTAL VOLUME OF FLUID INJECTED
PV=PORE VOLUME OF SAND PACK
NP=CUMULATIVE VOLUME OIL PRODUCED
%R=RECOVERY PERCENT
GOR=GAS-OIL RATIO
WOR=WATER-OIL RATIO
OPFIR=OIL PRODUCED-FLUID INJECTED RATIO

University of Alberta

TABLE G20

RESULTS OF RUN 21

PORE VOLUME=0.2065E+04 CM3
HYDROCARBON PORE VOLUME=0.1820E+04 CM3
POROSITY=0.4310E+02%
IRREDUCIBLE WATER SATURATION=0.1190E+02%
INITIAL OIL SATURATION=0.8810E+02%
ABSOLUTE PERMEABILITY=0.9200E+01 DARCIES
CARBON DIOXIDE RETENTION=0.5036E+02 %
CARBON DIOXIDE REQUIRED=0.1541E+03 SM3/M3

PI,MPAG	PP,MPAG	GI,CM3	WI,CM3	VFI/PV	NP,CM3	%R	GOR,SM3/M3	WOR,M3/M3	OPFIR,M3/M3
0.5500E+01	0.5500E+01	0.0	0.1480E+02	0.7167E-02	0.0	0.0	0.0	0.0	0.0
0.5770E+01	0.5500E+01	0.0	0.3680E+02	0.1782E-01	0.2050E+02	0.1126E+01	0.0	0.0	0.9318E+00
0.5770E+01	0.5500E+01	0.0	0.5060E+02	0.2450E-01	0.3400E+02	0.1868E+01	0.0	0.0	0.9783E+00
0.5780E+01	0.5500E+01	0.0	0.6900E+02	0.3341E-01	0.5380E+02	0.2956E+01	0.0	0.0	0.1076E+01
0.5770E+01	0.5480E+01	0.0	0.8430E+02	0.4082E-01	0.7030E+02	0.3863E+01	0.0	0.0	0.1078E+01
0.5770E+01	0.5500E+01	0.0	0.1012E+03	0.4901E-01	0.8760E+02	0.4813E+01	0.0	0.0	0.1024E+01
0.5750E+01	0.5480E+01	0.0	0.1181E+03	0.5719E-01	0.1046E+03	0.5747E+01	0.0	0.0	0.1006E+01
0.5750E+01	0.5500E+01	0.0	0.1365E+03	0.6610E-01	0.1241E+03	0.6819E+01	0.0	0.0	0.1060E+01
0.5740E+01	0.5520E+01	0.0	0.1533E+03	0.7424E-01	0.1411E+03	0.7753E+01	0.0	0.0	0.1012E+01
0.5740E+01	0.5510E+01	0.0	0.1704E+03	0.8252E-01	0.1576E+03	0.8659E+01	0.0	0.1212E+00	0.9649E+00
0.5740E+01	0.5520E+01	0.0	0.1917E+03	0.9283E-01	0.1752E+03	0.9626E+01	0.0	0.2273E+00	0.8263E+00
0.5690E+01	0.5510E+01	0.0	0.2714E+03	0.1314E+00	0.2277E+03	0.1251E+02	0.0	0.5810E+00	0.6587E+00
0.5640E+01	0.5500E+01	0.0	0.7530E+03	0.3646E+00	0.3557E+03	0.1954E+02	0.0	0.2828E+01	0.2658E+00
0.5560E+01	0.5480E+01	0.0	0.1257E+04	0.6085E+00	0.4562E+03	0.2507E+02	0.0	0.4045E+01	0.1996E+00
0.5560E+01	0.5480E+01	0.0	0.1760E+04	0.8523E+00	0.5252E+03	0.2886E+02	0.0	0.6319E+01	0.1371E+00
0.5520E+01	0.5490E+01	0.0	0.2252E+04	0.1090E+01	0.5702E+03	0.3133E+02	0.0	0.9889E+01	0.9154E-01

University of Alberta

TABLE G20 (CONTINUED)

RESULTS OF RUN 21

PI,MPAG	PP;MPAG	GI,CM3	WI,CM3	VFI/PV	NP,CM3	%R	GOR,SM3/M3	WOR,M3/M3	OPFIR,M3/M3
0.5460E+01	0.5440E+01	0.0	0.2738E+04	0.1326E+01	0.6012E+03	0.3303E+02	0.0	0.1481E+02	0.6369E-01
0.5490E+01	0.5450E+01	0.0	0.3019E+04	0.1462E+01	0.6142E+03	0.3375E+02	0.0	0.2038E+02	0.4631E-01
0.5510E+01	0.5490E+01	0.3720E+02	0.3019E+04	0.1480E+01	0.6151E+03	0.3380E+02	0.0	0.2000E+02	0.2419E-01
0.5420E+01	0.5400E+01	0.3720E+02	0.3241E+04	0.1588E+01	0.6231E+03	0.3424E+02	0.0	0.2538E+02	0.3597E-01
0.5490E+01	0.5470E+01	0.7360E+02	0.3241E+04	0.1605E+01	0.6241E+03	0.3429E+02	0.0	0.2500E+02	0.2747E-01
0.5500E+01	0.5480E+01	0.7360E+02	0.3460E+04	0.1711E+01	0.6351E+03	0.3490E+02	0.0	0.1736E+02	0.5037E-01
0.5510E+01	0.5500E+01	0.1100E+03	0.3460E+04	0.1729E+01	0.6361E+03	0.3495E+02	0.0	0.1850E+02	0.2747E-01
0.5500E+01	0.5470E+01	0.1100E+03	0.3678E+04	0.1834E+01	0.6491E+03	0.3566E+02	0.4679E+01	0.1462E+02	0.5952E-01
0.5520E+01	0.5490E+01	0.1464E+03	0.3678E+04	0.1852E+01	0.6505E+03	0.3574E+02	0.2896E+01	0.1607E+02	0.3846E-01
0.5530E+01	0.5500E+01	0.1464E+03	0.3897E+04	0.1958E+01	0.6655E+03	0.3657E+02	0.4055E+02	0.1153E+02	0.6849E-01
0.5540E+01	0.5520E+01	0.1828E+03	0.3897E+04	0.1976E+01	0.6675E+03	0.3668E+02	0.0	0.8500E+01	0.5495E-01
0.5480E+01	0.5440E+01	0.1828E+03	0.4116E+04	0.2082E+01	0.6790E+03	0.3731E+02	0.4513E+02	0.1652E+02	0.5266E-01
0.5510E+01	0.5490E+01	0.2192E+03	0.4116E+04	0.2099E+01	0.6810E+03	0.3742E+02	0.3244E+02	0.1075E+02	0.5495E-01
0.5540E+01	0.5520E+01	0.2556E+03	0.4569E+04	0.2336E+01	0.7073E+03	0.3886E+02	0.4317E+02	0.1558E+02	0.5367E-01
0.5520E+01	0.5500E+01	0.2921E+03	0.4569E+04	0.2354E+01	0.7088E+03	0.3895E+02	0.1622E+02	0.1400E+02	0.4110E-01
0.5490E+01	0.5470E+01	0.2921E+03	0.4793E+04	0.2463E+01	0.7223E+03	0.3969E+02	0.6248E+02	0.1407E+02	0.6024E-01
0.5530E+01	0.5510E+01	0.3285E+03	0.4793E+04	0.2480E+01	0.7233E+03	0.3974E+02	0.1622E+02	0.1600E+02	0.2747E-01
0.5470E+01	0.5460E+01	0.3285E+03	0.5012E+04	0.2586E+01	0.7363E+03	0.4046E+02	0.7299E+02	0.1438E+02	0.5952E-01
0.5520E+01	0.5500E+01	0.3649E+03	0.5012E+04	0.2604E+01	0.7385E+03	0.4058E+02	0.3686E+02	0.9227E+01	0.6044E-01
0.5460E+01	0.5440E+01	0.3649E+03	0.5420E+04	0.2802E+01	0.7605E+03	0.4179E+02	0.9290E+02	0.1650E+02	0.5384E-01

University of Alberta

TABLE G20 (CONTINUED)

RESULTS OF RUN 21

PI,MPAG	PP,MPAG	GI,CM3	WI,CM3	VFI/PV	NP,CM3	%R	GOR,SM3/M3	WOR,M3/M3	OPFIR,M3/M3
0.5400E+01	0.5380E+01	0.3649E+03	0.5923E+04	0.3045E+01	0.7875E+03	0.4327E+02	0.8200E+02	0.1741E+02	0.5373E-01
0.5380E+01	0.5360E+01	0.3649E+03	0.6379E+04	0.3266E+01	0.8115E+03	0.4459E+02	0.8448E+02	0.1817E+02	0.5265E-01
0.1830E+01	0.1850E+01	0.3649E+03	0.6379E+04	0.3266E+01	0.8125E+03	0.4464E+02	0.0	0.2300E+02	
0.1220E+01	0.1220E+01	0.3649E+03	0.6379E+04	0.3266E+01	0.8135E+03	0.4470E+02	0.1135E+03	0.2250E+02	
0.6800E+00	0.6800E+00	0.3649E+03	0.6379E+04	0.3266E+01	0.8168E+03	0.4488E+02	0.3711E+03	0.1748E+02	
0.0	0.0	0.3649E+03	0.6379E+04	0.3266E+01	0.8428E+03	0.4631E+02	0.2165E+03	0.7038E+01	

PI=INJECTION PRESSURE
PP=PRODUCTION PRESSURE
GI=CUMULATIVE VOLUME OF CO2 INJECTED
WI=BRINE INJECTED
VFI=TOTAL VOLUME OF FLUID INJECTED
PV=PORE VOLUME OF SAND PACK
NP=CUMULATIVE VOLUME OIL PRODUCED
%R=RECOVERY PERCENT
GOR=GAS-OIL RATIO
WOR=WATER-OIL RATIO
OPFIR=OIL PRODUCED-FLUID INJECTED RATIO

University of Alberta

TABLE G21

RESULTS OF RUN 22

PORE VOLUME=0.2004E+04 CM3
HYDROCARBON PORE VOLUME=0.1784E+04 CM3
POROSITY=0.4190E+02%
IRREDUCIBLE WATER SATURATION=0.1100E+02%
INITIAL OIL SATURATION=0.8900E+02%
ABSOLUTE PERMEABILITY=0.9600E+01 DARCIES
CARBON DIOXIDE RETENTION=0.4538E+02 %
CARBON DIOXIDE REQUIRED=0.1888E+03 SM3/M3

PI,MPAG	PP,MPAG	GI,CM3	WI,CM3	VFI/PV	NP,CM3	%R	GOR,SM3/M3	WOR,M3/M3	OPFIR,M3/M3
0.5500E+01	0.5500E+01	0.0	0.1560E+02	0.7784E-02	0.0	0.0	0.0	0.0	0.0
0.6500E+01	0.5500E+01	0.0	0.3490E+02	0.1742E-01	0.9700E+01	0.5437E+00	0.0	0.0	0.5026E+00
0.6820E+01	0.5500E+01	0.0	0.4630E+02	0.2310E-01	0.1920E+02	0.1076E+01	0.0	0.0	0.8333E+00
0.6870E+01	0.5500E+01	0.0	0.5550E+02	0.2769E-01	0.2870E+02	0.1609E+01	0.0	0.0	0.1033E+01
0.6880E+01	0.5500E+01	0.0	0.6310E+02	0.3149E-01	0.3680E+02	0.2063E+01	0.0	0.0	0.1066E+01
0.6880E+01	0.5500E+01	0.0	0.7080E+02	0.3533E-01	0.4500E+02	0.2522E+01	0.0	0.0	0.1065E+01
0.6880E+01	0.5500E+01	0.0	0.7850E+02	0.3917E-01	0.5320E+02	0.2982E+01	0.0	0.0	0.1065E+01
0.6870E+01	0.5500E+01	0.0	0.8610E+02	0.4296E-01	0.6190E+02	0.3470E+01	0.0	0.0	0.1145E+01
0.6770E+01	0.5500E+01	0.0	0.9390E+02	0.4686E-01	0.6960E+02	0.3901E+01	0.0	0.1039E+00	0.9872E+00
0.6640E+01	0.5500E+01	0.0	0.1170E+03	0.5838E-01	0.9260E+02	0.5191E+01	0.0	0.2609E+00	0.9957E+00
0.6220E+01	0.5500E+01	0.0	0.2000E+03	0.9980E-01	0.1417E+03	0.7943E+01	0.0	0.7923E+00	0.5916E+00
0.5980E+01	0.5500E+01	0.0	0.2450E+03	0.1223E+00	0.1568E+03	0.8789E+01	0.0	0.1848E+01	0.3356E+00
0.5920E+01	0.5460E+01	0.0	0.2913E+03	0.1454E+00	0.1756E+03	0.9843E+01	0.0	0.1766E+01	0.4060E+00
0.5780E+01	0.5330E+01	0.0	0.3236E+03	0.1615E+00	0.1853E+03	0.1039E+02	0.0	0.2268E+01	0.3003E+00
0.5830E+01	0.5340E+01	0.0	0.3588E+03	0.1790E+00	0.1973E+03	0.1106E+02	0.0	0.2292E+01	0.3409E+00
0.5600E+01	0.5290E+01	0.0	0.5297E+03	0.2643E+00	0.2283E+03	0.1280E+02	0.0	0.4516E+01	0.1814E+00

University of Alberta

TABLE G21 (CONTINUED)

RESULTS OF RUN 22

PI,MPAG	PP,MPAG	GI,CM3	WI,CM3	VFI/PV	NP,CM3	%R	GOR,SM3/M3	WOR,M3/M3	OPFIR,M3/M3
0.5590E+01	0.5220E+01	0.0	0.7760E+03	0.3872E+00	0.2583E+03	0.1448E+02	0.0	0.7333E+01	0.1218E+00
0.5340E+01	0.5260E+01	0.0	0.1022E+04	0.5099E+00	0.2773E+03	0.1554E+02	0.0	0.1200E+02	0.7727E-01
0.5480E+01	0.5320E+01	0.0	0.1272E+04	0.6346E+00	0.2933E+03	0.1644E+02	0.0	0.1563E+02	0.6405E-01
0.5500E+01	0.5310E+01	0.0	0.1519E+04	0.7578E+00	0.3053E+03	0.1711E+02	0.0	0.1967E+02	0.4860E-01
0.5440E+01	0.5380E+01	0.4200E+02	0.1519E+04	0.7787E+00	0.3058E+03	0.1714E+02	0.0	0.6200E+02	0.1190E-01
0.5230E+01	0.5160E+01	0.4200E+02	0.1661E+04	0.8500E+00	0.3118E+03	0.1748E+02	0.0	0.2050E+02	0.4202E-01
0.5470E+01	0.5430E+01	0.7770E+02	0.1661E+04	0.8678E+00	0.3143E+03	0.1762E+02	0.0	0.1000E+02	0.7003E-01
0.5520E+01	0.5430E+01	0.7770E+02	0.1804E+04	0.9390E+00	0.3273E+03	0.1835E+02	0.1435E+02	0.8462E+01	0.9110E-01
0.5500E+01	0.5440E+01	0.1134E+03	0.1804E+04	0.9568E+00	0.3303E+03	0.1851E+02	0.4866E+02	0.7000E+01	0.8403E-01
0.5480E+01	0.5420E+01	0.1134E+03	0.1947E+04	0.1028E+01	0.3423E+03	0.1919E+02	0.1460E+03	0.9167E+01	0.8409E-01
0.5490E+01	0.5420E+01	0.1491E+03	0.1947E+04	0.1046E+01	0.3438E+03	0.1927E+02	0.9191E+02	0.1433E+02	0.4202E-01
0.5540E+01	0.5480E+01	0.1850E+03	0.2132E+04	0.1156E+01	0.3638E+03	0.2039E+02	0.1440E+03	0.1125E+02	0.9029E-01
0.5530E+01	0.5470E+01	0.2207E+03	0.2232E+04	0.1224E+01	0.3643E+03	0.2042E+02	0.6488E+02	0.2400E+02	0.3690E-02
0.5470E+01	0.5440E+01	0.2207E+03	0.2375E+04	0.1295E+01	0.3726E+03	0.2088E+02	0.1446E+03	0.1454E+02	0.5816E-01
0.5540E+01	0.5510E+01	0.2564E+03	0.2375E+04	0.1313E+01	0.3746E+03	0.2100E+02	0.4055E+02	0.8250E+01	0.5602E-01
0.5390E+01	0.5340E+01	0.2564E+03	0.2519E+04	0.1385E+01	0.3872E+03	0.2170E+02	0.4377E+02	0.9794E+01	0.8738E-01
0.5530E+01	0.5500E+01	0.2921E+03	0.2519E+04	0.1403E+01	0.3882E+03	0.2176E+02	0.4055E+02	0.1650E+02	0.2801E-01
0.5530E+01	0.5480E+01	0.2921E+03	0.2662E+04	0.1474E+01	0.3962E+03	0.2221E+02	0.8211E+02	0.1550E+02	0.5606E-01
0.5480E+01	0.5490E+01	0.3278E+03	0.2662E+04	0.1492E+01	0.3984E+03	0.2233E+02	0.4424E+02	0.9455E+01	0.6162E-01
0.5480E+01	0.5490E+01	0.3278E+03	0.2805E+04	0.1563E+01	0.4064E+03	0.2278E+02	0.9732E+02	0.1513E+02	0.5606E-01

University of Alberta

TABLE G21 (CONTINUED)

RESULTS OF RUN 22

PI,MPAG	PP,MPAG	GI,CM3	WI,CM3	VFI/PV	NP,CM3	%R	GOR,SM3/M3	WOR,M3/M3	OPFIR,M3/M3
0.5540E+01	0.5520E+01	0.3635E+03	0.2805E+04	0.1581E+01	0.4079E+03	0.2286E+02	0.5407E+02	0.1333E+02	0.4202E-01
0.5460E+01	0.5430E+01	0.3635E+03	0.3291E+04	0.1824E+01	0.4349E+03	0.2438E+02	0.1123E+03	0.1596E+02	0.5552E-01
0.5090E+01	0.5050E+01	0.3635E+03	0.3786E+04	0.2071E+01	0.4469E+03	0.2505E+02	0.1480E+03	0.3957E+02	0.2424E-01
0.2920E+01	0.2920E+01	0.3635E+03	0.3786E+04	0.2071E+01	0.4479E+03	0.2511E+02	0.7299E+02	0.1900E+02	
0.1800E+01	0.1800E+01	0.3635E+03	0.3786E+04	0.2071E+01	0.4489E+03	0.2516E+02	0.8110E+02	0.2100E+02	
0.1080E+01	0.1080E+01	0.3635E+03	0.3786E+04	0.2071E+01	0.4504E+03	0.2525E+02	0.2866E+03	0.1367E+02	
0.0	0.0	0.3635E+03	0.3786E+04	0.2071E+01	0.4928E+03	0.2768E+02	0.1255E+03	0.4011E+01	

PI=INJECTION PRESSURE
PP=PRODUCTION PRESSURE
GI=CUMULATIVE VOLUME OF CO2 INJECTED
WI=BRINE INJECTED
VFI=TOTAL VOLUME OF FLUID INJECTED
PV=PORE VOLUME OF SAND PACK
NP=CUMULATIVE VOLUME OIL PRODUCED
%R=RECOVERY PERCENT
GOR=GAS-OIL RATIO
WOR=WATER-OIL RATIO
OPFIR=OIL PRODUCED-FLUID INJECTED RATIO

University of Alberta

TABLE G22

RESULTS OF RUN 23

PORE VOLUME=0.2013E+04 CM3
HYDROCARBON PORE VOLUME=0.1794E+04 CM3
POROSITY=0.4210E+02%
IRREDUCIBLE WATER SATURATION=0.1090E+02%
INITIAL OIL SATURATION=0.8910E+02%
ABSOLUTE PERMEABILITY=0.9300E+01 DARCIES
CARBON DIOXIDE RETENTION=0.7521E+02 %
CARBON DIOXIDE REQUIRED=0.3880E+03 SM3/M3

PI,MPAG	PP,MPAG	GI,CM3	WI,CM3	VFI/PV	NP,CM3	%R	GOR,SM3/M3	WOR,M3/M3	OPFIR,M3/M3
0.5505E+01	0.5500E+01	0.3590E+02	0.0	0.1783E-01	0.0	0.0	0.0	0.0	0.0
0.5780E+01	0.5500E+01	0.3590E+02	0.4050E+02	0.3795E-01	0.1880E+02	0.1048E+01	0.0	0.0	0.4642E+00
0.6640E+01	0.5500E+01	0.3590E+02	0.4920E+02	0.4228E-01	0.2910E+02	0.1622E+01	0.0	0.0	0.1184E+01
0.6850E+01	0.5500E+01	0.3590E+02	0.6150E+02	0.4839E-01	0.4010E+02	0.2235E+01	0.0	0.0	0.8943E+00
0.6890E+01	0.5500E+01	0.3590E+02	0.7390E+02	0.5455E-01	0.5260E+02	0.2932E+01	0.0	0.0	0.1008E+01
0.6880E+01	0.5500E+01	0.3590E+02	0.8780E+02	0.6145E-01	0.6710E+02	0.3740E+01	0.0	0.0	0.1043E+01
0.6800E+01	0.5500E+01	0.3590E+02	0.1028E+03	0.6890E-01	0.8240E+02	0.4593E+01	0.0	0.1307E+00	0.1020E+01
0.6570E+01	0.5500E+01	0.3590E+02	0.1256E+03	0.8023E-01	0.1011E+03	0.5635E+01	0.0	0.3209E+00	0.8202E+00
0.6480E+01	0.5500E+01	0.3590E+02	0.1435E+03	0.8912E-01	0.1146E+03	0.6388E+01	0.0	0.5926E+00	0.7542E+00
0.5560E+01	0.5310E+01	0.7180E+02	0.1435E+03	0.1070E+00	0.1211E+03	0.6750E+01	0.0	0.3846E+00	0.1811E+00
0.6050E+01	0.5440E+01	0.7180E+02	0.2909E+03	0.1802E+00	0.1846E+03	0.1029E+02	0.0	0.1331E+01	0.4308E+00
0.5520E+01	0.5440E+01	0.1077E+03	0.2909E+03	0.1980E+00	0.1879E+03	0.1047E+02	0.0	0.1818E+01	0.9192E-01
0.5660E+01	0.5480E+01	0.1077E+03	0.4353E+03	0.2697E+00	0.2219E+03	0.1237E+02	0.2576E+02	0.2765E+01	0.2355E+00
0.5520E+01	0.5450E+01	0.1436E+03	0.4353E+03	0.2876E+00	0.2264E+03	0.1262E+02	0.1262E+02	0.3778E+01	0.1253E+00
0.5630E+01	0.5490E+01	0.1436E+03	0.5788E+03	0.3589E+00	0.2464E+03	0.1373E+02	0.7299E+02	0.5000E+01	0.1394E+00
0.5500E+01	0.5480E+01	0.1795E+03	0.5788E+03	0.3767E+00	0.2471E+03	0.1377E+02	0.2317E+02	0.9714E+01	0.1950E-01

University of Alberta

TABLE G22 (CONTINUED)

RESULTS OF RUN 23

PI,MPAG	PP,MPAG	GI,CM3	WI,CM3	VFI/PV	NP,CM3	%R	GOR,SM3/M3	WOR,M3/M3	OPFIR,M3/M3
0.5650E+01	0.5540E+01	0.1795E+03	0.7223E+03	0.4480E+00	0.2621E+03	0.1461E+02	0.2595E+02	0.8133E+01	0.1045E+00
0.5580E+01	0.5560E+01	0.2154E+03	0.7223E+03	0.4658E+00	0.2631E+03	0.1467E+02	0.1622E+02	0.7000E+01	0.2786E-01
0.5670E+01	0.5550E+01	0.2154E+03	0.8658E+03	0.5371E+00	0.2761E+03	0.1539E+02	0.6862E+01	0.8538E+01	0.9059E-01
0.5570E+01	0.5550E+01	0.2513E+03	0.8658E+03	0.5549E+00	0.2786E+03	0.1553E+02	0.3244E+01	0.4000E+01	0.6964E-01
0.5580E+01	0.5510E+01	0.2513E+03	0.1010E+04	0.6266E+00	0.2876E+03	0.1603E+02	0.3695E+02	0.1367E+02	0.6237E-01
0.5560E+01	0.5540E+01	0.2872E+03	0.1154E+04	0.7157E+00	0.2966E+03	0.1653E+02	0.3424E+02	0.1439E+02	0.5017E-01
0.5570E+01	0.5550E+01	0.3231E+03	0.1154E+04	0.7336E+00	0.2986E+03	0.1664E+02	0.8110E+01	0.6500E+01	0.5571E-01
0.5650E+01	0.5560E+01	0.3231E+03	0.1298E+04	0.8053E+00	0.3056E+03	0.1703E+02	0.9153E+02	0.1729E+02	0.4851E-01
0.5560E+01	0.5540E+01	0.3592E+03	0.1298E+04	0.8232E+00	0.3096E+03	0.1726E+02	0.1419E+02	0.5000E+01	0.1108E+00
0.5450E+01	0.5410E+01	0.3592E+03	0.1781E+04	0.1063E+01	0.3296E+03	0.1837E+02	0.1042E+03	0.2200E+02	0.4139E-01
0.5420E+01	0.5380E+01	0.3592E+03	0.1871E+04	0.1108E+01	0.3326E+03	0.1854E+02	0.7299E+02	0.2833E+02	0.3322E-01
0.2970E+01	0.2970E+01	0.3592E+03	0.1871E+04	0.1108E+01	0.3336E+03	0.1860E+02	0.5677E+02	0.1700E+02	
0.1730E+01	0.1730E+01	0.3592E+03	0.1871E+04	0.1108E+01	0.3356E+03	0.1871E+02	0.4055E+01	0.5500E+01	
0.5900E+00	0.5900E+00	0.3592E+03	0.1871E+04	0.1108E+01	0.3431E+03	0.1912E+02	0.3893E+02	0.6133E+01	
0.0	0.0	0.3592E+03	0.1871E+04	0.1108E+01	0.3981E+03	0.2219E+02	0.3377E+02	0.[illegible]	

PI=INJECTION PRESSURE
PP=PRODUCTION PRESSURE
GI=CUMULATIVE VOLUME OF C[illegible]CTED
WI=BRINE INJECTED
VFI=TOTAL VOLUME OF FLUID INJECTED
PV=PORE VOLUME OF SAND PACK
NP=CUMULATIVE VOLUME OIL PRODUCED
%R=RECOVERY PERCENT
GOR=GAS-OIL RATIO
WOR=WATER-OIL RATIO
OPFIR=OIL PRODUCED-FLUID INJECTED RATIO

University of Alberta

TABLE G23

RESULTS OF RUN 24

PORE VOLUME=0.2107E+04 CM3
HYDROCARBON PORE VOLUME=0.1877E+04 CM3
POROSITY=0.4400E+02%
IRREDUCIBLE WATER SATURATION=0.1090E+02%
INITIAL OIL SATURATION=0.8910E+02%
ABSOLUTE PERMEABILITY=0.1150E+02 DARCIES
CARBON DIOXIDE RETENTION=0.3142E+02 %
CARBON DIOXIDE REQUIRED=0.3186E+03 SM3/M3

PI,MPAG	PP,MPAG	GI,CM3	WI,CM3	VFI/PV	NP,CM3	%R	GOR,SM3/M3	WOR,M3/M3	OPFIR,M3/M3
0.5510E+01	0.5500E+01	0.2660E+02	0.0	0.1262E-01	0.0	0.0	0.0	0.0	0.0
0.5510E+01	0.5500E+01	0.1877E+03	0.0	0.8908E-01	0.2250E+02	0.1199E+01	0.0	0.0	0.1397E+00
0.5670E+01	0.5600E+01	0.3148E+03	0.0	0.1494E+00	0.4200E+02	0.2238E+01	0.2079E+01	0.0	0.1534E+00
0.5820E+01	0.5480E+01	0.3415E+03	0.0	0.1621E+00	0.6150E+02	0.3277E+01	0.8401E+02	0.0	0.7303E+00
0.5640E+01	0.5520E+01	0.3767E+03	0.0	0.1788E+00	0.7000E+02	0.3729E+01	0.1009E+04	0.0	0.2415E+00
0.5580E+01	0.5480E+01	0.3767E+03	0.5720E+02	0.2059E+00	0.9270E+02	0.4939E+01	0.6002E+02	0.0	0.3969E+00
0.5700E+01	0.5500E+01	0.3767E+03	0.8220E+02	0.2178E+00	0.1112E+03	0.5924E+01	0.4691E+02	0.0	0.7400E+00
0.5710E+01	0.5490E+01	0.3767E+03	0.1088E+03	0.2304E+00	0.1337E+03	0.7123E+01	0.7930E+01	0.0	0.8459E+00
0.5670E+01	0.5490E+01	0.3767E+03	0.1335E+03	0.2421E+00	0.1547E+03	0.8242E+01	0.8573E+02	0.4762E-01	0.8502E+00
0.5640E+01	0.5480E+01	0.3767E+03	0.1581E+03	0.2538E+00	0.1722E+03	0.9174E+01	0.3985E+02	0.4000E+00	0.7114E+00
0.5610E+01	0.5510E+01	0.3767E+03	0.1[illegible]E+03	0.2946E+00	0.1952E+03	0.1040E+02	0.8427E+02	0.1870E+01	0.2678E+00
0.5640E+01	0.5570E+01	0.3767E+03	0.4710E+03	0.4023E+00	0.2326E+03	0.1239E+02	0.7555E+02	0.5257E+01	0.1648E+00
0.5630E+01	0.5530E+01	0.3767E+03	0.9578E+03	0.6334E+00	0.2776E+03	0.1479E+02	0.4318E+02	0.9667E+01	0.9244E-01
0.5600E+01	0.5540E+01	0.3767E+03	0.1132E+04	0.7159E+00	0.2911E+03	0.1551E+02	0.2403E+02	0.1181E+02	0.7763E-01
0.5600E+01	0.5540E+01	0.3767E+03	0.1359E+04	0.8238E+00	0.3066E+03	0.1633E+02	0.9941E+01	0.1339E+02	0.6816E-01
0.5560E+01	0.5510E+01	0.3767E+03	0.1858E+04	0.1061E+01	0.3356E+03	0.1788E+02	0.1538E+02	0.1624E+02	0.5814E-01

University of Alberta

TABLE G23 (CONTINUED)

RESULTS OF RUN 24

PI,MPAG	PP,MPAG	GI,CM3	WI,CM3	VFI/PV	NP,CM3	%R	GOR,SM3/M3	WOR,M3/M3	OPFIR,M3/M3
0.5520E+01	0.5480E+01	0.3767E+03	0.2100E+04	0.1175E+01	0.3489E+03	0.1859E+02	0.8537E+01	0.1735E+02	0.5496E-01
0.5570E+01	0.5520E+01	0.3767E+03	0.2345E+04	0.1292E+01	0.3614E+03	0.1925E+02	0.5190E+01	0.1828E+02	0.5106E-01
0.5490E+01	0.5430E+01	0.3767E+03	0.2582E+04	0.1404E+01	0.3719E+03	0.1981E+02	0.7724E+01	0.2167E+02	0.4425E-01
0.2220E+01	0.2220E+01	0.3767E+03	0.2582E+04	0.1404E+01	0.3734E+03	0.1989E+02	0.1622E+02	0.1567E+02	0.1500E+02
0.6600E+00	0.6600E+00	0.3767E+03	0.2582E+04	0.1404E+01	0.3759E+03	0.2003E+02	0.0	0.7800E+01	0.2500E+02
0.0	0.0	0.3767E+03	0.2582E+04	0.1404E+01	0.4279E+03	0.2280E+02	0.5459E+01	0.3365E+01	0.5200E+03

PI=INJECTION PRESSURE
PP=PRODUCTION PRESSURE
GI=CUMULATIVE VOLUME OF CO2 INJECTED
WI=BRINE INJECTED
VFI=TOTAL VOLUME OF FLUID INJECTED
PV=PORE VOLUME OF SAND PACK
NP=CUMULATIVE VOLUME OIL PRODUCED
%R=RECOVERY PERCENT
GOR=GAS-OIL RATIO
WOR=WATER-OIL RATIO
OPFIR=OIL PRODUCED-FLUID INJECTED RATIO

University of Alberta

TABLE G24

RESULTS OF RUN 25

PORE VOLUME=0.2068E+04 CM3
HYDROCARBON PORE VOLUME=0.1815E+04 CM3
POROSITY=0.4320E+02%
IRREDUCIBLE WATER SATURATION=0.1220E+02%
INITIAL OIL SATURATION=0.8780E+02%
ABSOLUTE PERMEABILITY=0.4500E+01 DARCIES
CARBON DIOXIDE RETENTION=0.9473E+02 %
CARBON DIOXIDE REQUIRED=0.1684E+03 SM3/M3

PI,MPAG	PP,MPAG	GI,CM3	WI,CM3	VFI/PV	NP,CM3	%R	GOR,SM3/M3	WOR,M3/M3	OPFIR,M3/M3
0.5500E+01	0.5500E+01	0.3630E+02	0.0	0.1755E-01	0.0	0.0	0.0	0.0	0.0
0.5670E+01	0.5500E+01	0.3630E+02	0.3370E+02	0.3385E-01	0.2100E+02	0.1157E+01	0.0	0.0	0.6231E+00
0.5680E+01	0.5500E+01	0.3630E+02	0.5290E+02	0.4313E-01	0.4050E+02	0.2231E+01	0.0	0.0	0.1016E+01
0.5680E+01	0.5480E+01	0.3630E+02	0.7510E+02	0.5387E-01	0.6400E+02	0.3526E+01	0.0	0.0	0.1059E+01
0.5690E+01	0.5500E+01	0.3630E+02	0.9430E+02	0.6315E-01	0.8350E+02	0.4601E+01	0.0	0.0	0.1016E+01
0.5690E+01	0.5510E+01	0.3630E+02	0.1196E+03	0.7539E-01	0.1100E+03	0.6061E+01	0.0	0.0	0.1047E+01
0.5680E+01	0.5480E+01	0.3630E+02	0.1452E+03	0.8777E-01	0.1380E+03	0.7603E+01	0.0	0.0	0.1094E+01
0.5540E+01	0.5520E+01	0.7260E+02	0.1452E+03	0.1053E+00	0.1495E+03	0.8237E+01	0.0	0.0	0.3168E+00
0.5650E+01	0.5500E+01	0.7260E+02	0.1698E+03	0.1172E+00	0.1665E+03	0.9174E+01	0.0	0.0	0.6911E+00
0.5660E+01	0.5470E+01	0.7260E+02	0.1867E+03	0.1254E+00	0.1840E+03	0.1014E+02	0.0	0.0	0.1036E+01
0.5650E+01	0.5480E+01	0.7260E+02	0.2051E+03	0.1343E+00	0.2027E+03	0.1117E+02	0.0	0.0	0.1016E+01
0.5670E+01	0.5510E+01	0.7260E+02	0.2207E+03	0.1418E+00	0.2207E+03	0.1216E+02	0.0	0.0	0.1154E+01
0.5650E+01	0.5490E+01	0.7260E+02	0.2381E+03	0.1502E+00	0.2362E+03	0.1301E+02	0.5232E+00	0.0	0.8908E+00
0.5650E+01	0.5500E+01	0.7260E+02	0.2541E+03	0.1580E+00	0.2527E+03	0.1392E+02	0.4915E+00	0.0	0.1031E+01
0.5670E+01	0.5500E+01	0.7260E+02	0.2718E+03	0.1665E+00	0.2687E+03	0.1480E+02	0.5069E+00	0.1875E+00	0.9040E+00
0.5570E+01	0.5470E+01	0.7260E+02	0.2904E+03	0.1755E+00	0.2807E+03	0.1547E+02	0.6758E+00	0.6667E+00	0.6452E+00

University of Alberta

TABLE G24 (CONTINUED)

RESULTS OF RUN 25

PI,MPAG	PP,MPAG	GI,CM3	WI,CM3	VFI/PV	NP,CM3	%R	GOR,SM3/M3	WOR,M3/M3	DPFIR,M3/M3
0.5530E+01	0.5440E+01	0.1089E+03	0.2904E+03	0.1931E+00	0.2912E+03	0.1604E+02	0.7724E+00	0.4762E+00	0.2893E+00
0.5560E+01	0.5480E+01	0.1089E+03	0.3602E+03	0.2268E+00	0.3225E+03	0.1777E+02	0.2591E+00	0.8786E+00	0.4484E+00
0.5560E+01	0.5470E+01	0.1089E+03	0.4356E+03	0.2633E+00	0.3519E+03	0.1939E+02	0.8276E+00	0.1541E+01	0.3899E+00
0.5520E+01	0.5460E+01	0.1452E+03	0.4356E+03	0.2809E+00	0.3614E+03	0.1991E+02	0.8537E+00	0.1053E+01	0.2617E+00
0.5550E+01	0.5480E+01	0.1452E+03	0.5808E+03	0.3511E+00	0.4004E+03	0.2206E+02	0.6238E+00	0.2487E+01	0.2686E+00
0.5560E+01	0.5530E+01	0.1815E+03	0.5808E+03	0.3686E+00	0.4029E+03	0.2220E+02	0.3244E+01	0.5200E+01	0.6887E-01
0.5500E+01	0.5460E+01	0.1815E+03	0.7260E+03	0.4388E+00	0.4259E+03	0.2347E+02	0.1763E+01	0.5174E+01	0.1584E+00
0.5550E+01	0.5530E+01	0.2181E+03	0.7260E+03	0.4565E+00	0.4271E+03	0.2353E+02	0.6758E+01	0.4833E+01	0.3279E-01
0.5140E+01	0.5090E+01	0.2181E+03	0.8712E+03	0.5267E+00	0.4476E+03	0.2466E+02	0.8703E+01	0.5951E+01	0.1412E+00
0.5560E+01	0.5540E+01	0.2544E+03	0.8712E+03	0.5443E+00	0.4483E+03	0.2470E+02	0.0	0.1143E+01	0.1928E-01
0.5070E+01	0.5040E+01	0.2544E+03	0.1019E+04	0.6160E+00	0.4658E+03	0.2566E+02	0.6025E+01	0.7200E+01	0.1181E+00
0.5[illegible]0E+01	0.5540E+01	0.2907E+03	0.1019E+04	0.6335E+00	0.4678E+03	0.2577E+02	0.0	0.1500E+01	0.5510E-01
0.4970E+01	0.4950E+01	0.2907E+03	0.1165E+04	0.7037E+00	0.4788E+03	0.2638E+02	0.5161E+01	0.1100E+02	0.7576E-01
0.5580E+01	0.5570E+01	0.3270E+03	0.1165E+04	0.7213E+00	0.4798E+03	0.2644E+02	0.0	0.2000E+01	0.2755E-01
0.5590E+01	0.5560E+01	0.3270E+03	0.1310E+04	0.7915E+00	0.5038E+03	0.2776E+02	0.0	0.6792E+01	0.1653E+00
[illegible]E+01	0.5410E+01	0.3633E+03	0.1310E+04	0.8090E+00	0.5040E+03	0.2777E+02	0.0	0.5000E+01	0.5510E-02
[illegible]E+01	0.4520E+01	0.3633E+03	0.1677E+04	0.9865E+00	0.5960E+03	0.3284E+02	0.6171E+01	0.2989E+01	0.2507E+00
[illegible]E+01	0.2780E+01	0.3633E+03	0.2179E+04	0.1229E+01	0.6856E+03	0.3777E+02	0.4707E+01	0.4714E+01	0.1784E+00
[illegible]370E+01	0.3340E+01	0.3633E+03	0.2681E+04	0.1472E+01	0.7136E+03	0.3932E+02	0.1014E+02	0.1596E+02	0.5575E-01
0.3500E+00	0.2400E+00	0.3633E+03	0.2863E+04	0.1560E+01	0.7306E+03	0.4025E+02	0.0	0.1147E+02	0.9377E-01

University of Alberta

TABLE G24 (CONTINUED)

RESULTS OF RUN 25

PI,MPAG	PP,MPAG	GI,CM3	WI,CM3	VFI/PV	NP,CM3	%R	GOR,SM3/M3	WOR,M3/M3	OPFIR,M3/M3
0.1790E+01	0.1700E+01	0.3633E+03	0.3366E+04	0.1803E+01	0.7566E+03	0.4169E+02	0.6238E+00	0.1977E+02	0.5167E-01
0.3000E+01	0.2920E+01	0.3633E+03	0.3795E+04	0.2011E+01	0.7686E+03	0.4235E+02	0.2028E+01	0.3100E+02	0.2794E-01
0.0	0.0	0.3633E+03	0.3795E+04	0.2011E+01	0.7973E+03	0.4393E+02	0.8477E+00	0.9223E+01	

PI=INJECTION PRESSURE
PP=PRODUCTION PRESSURE
GI=CUMULATIVE VOLUME OF GAS INJECTED
WI=BRINE INJECTED
VFI=TOTAL VOLUME OF FLUID INJECTED
PV=PORE VOLUME OF SAND PACK
NP=CUMULATIVE VOLUME OIL PRODUCED
%R=RECOVERY PERCENT
GOR=GAS-OIL RATIO
WOR=WATER-OIL RATIO
OPFIR=OIL-PRODUCED-FLUID INJECTED RATIO

University of Alberta

APPENDIX H

PRODUCTION HISTORIES OF ALL RUNS IN GRAPHICAL FORM

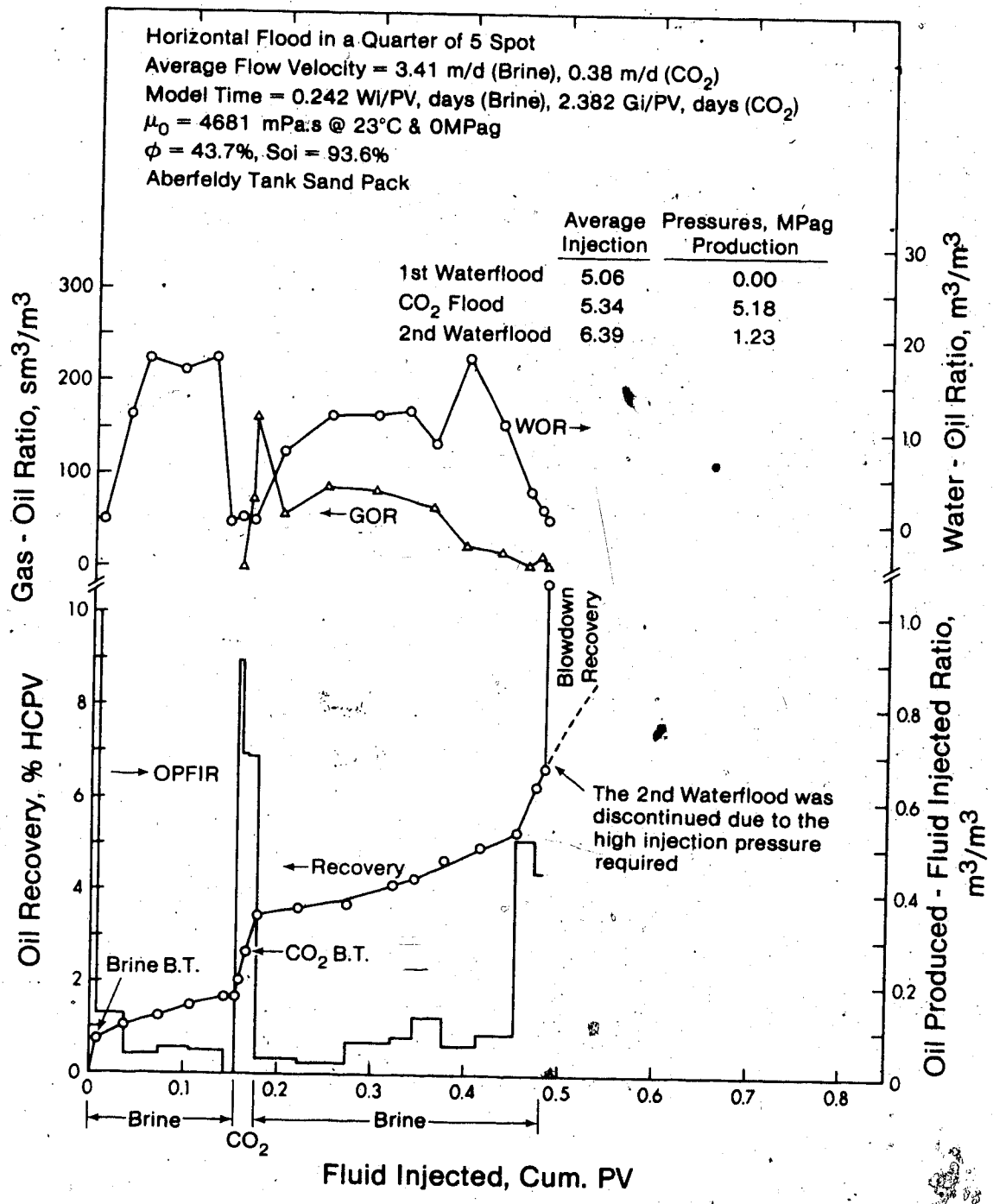


Figure III Production History of Run 1

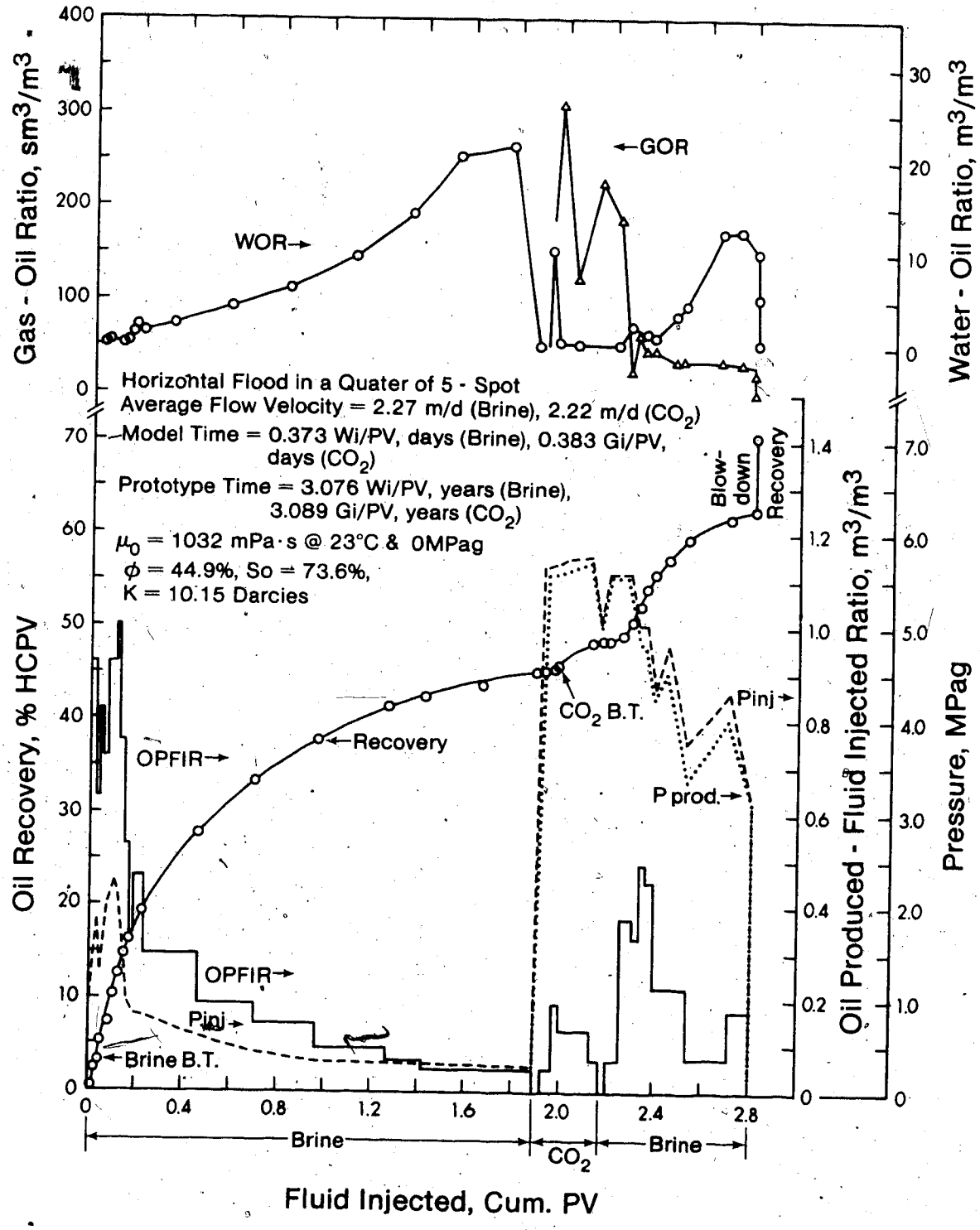


Figure H2 Production History of Run 3

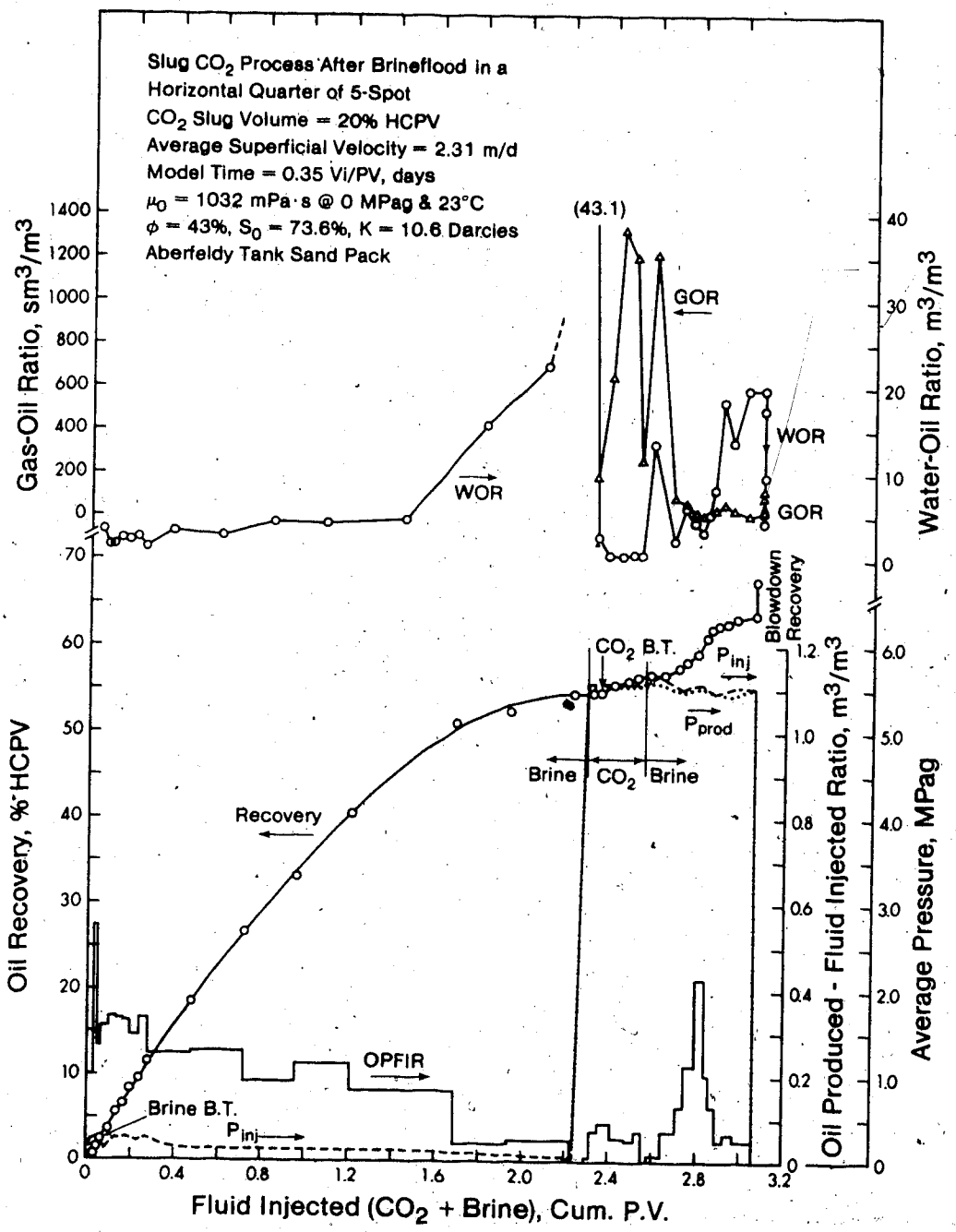


Figure 113 Production History of Run 4

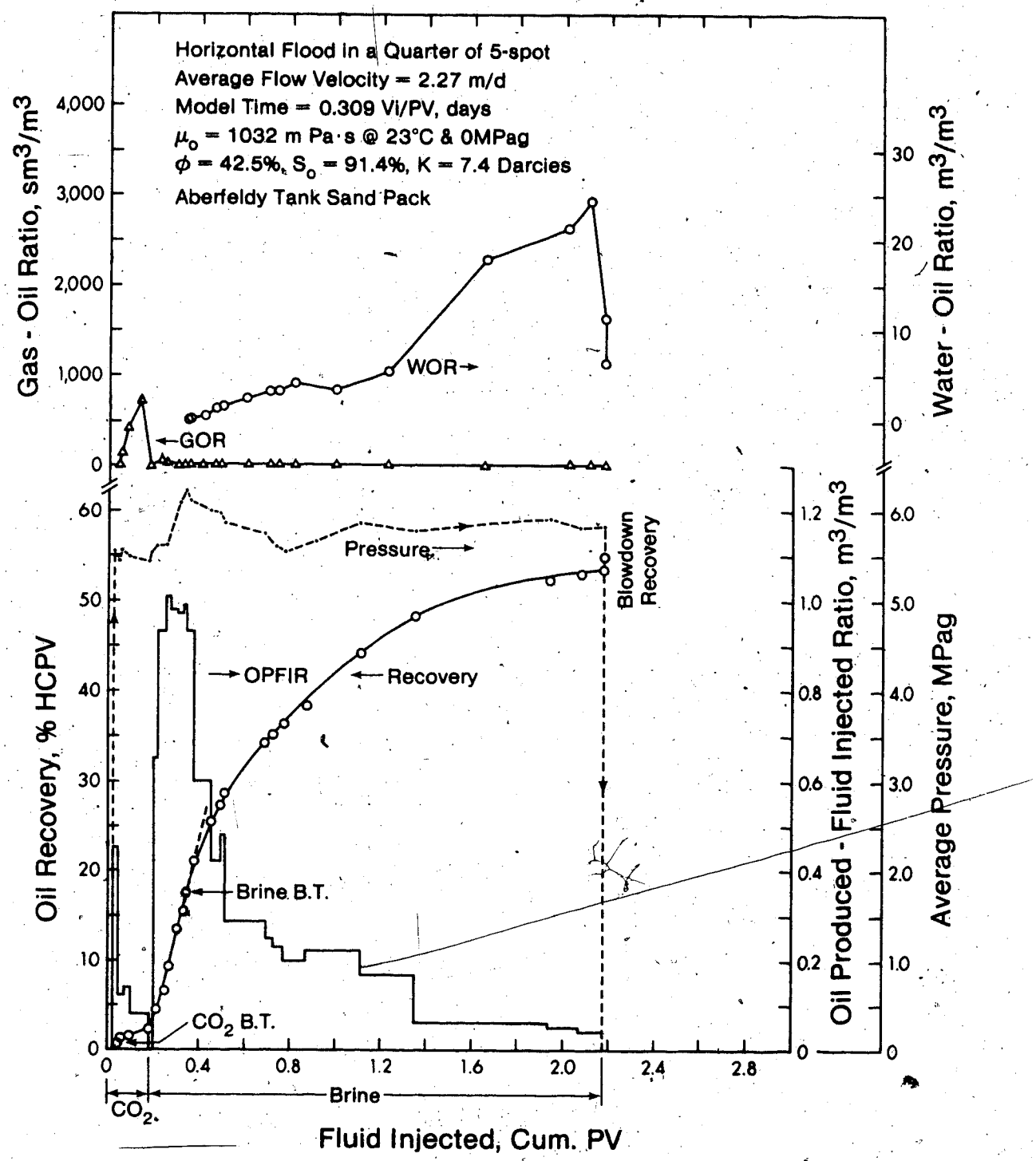


Figure 114 Production History of Run 5

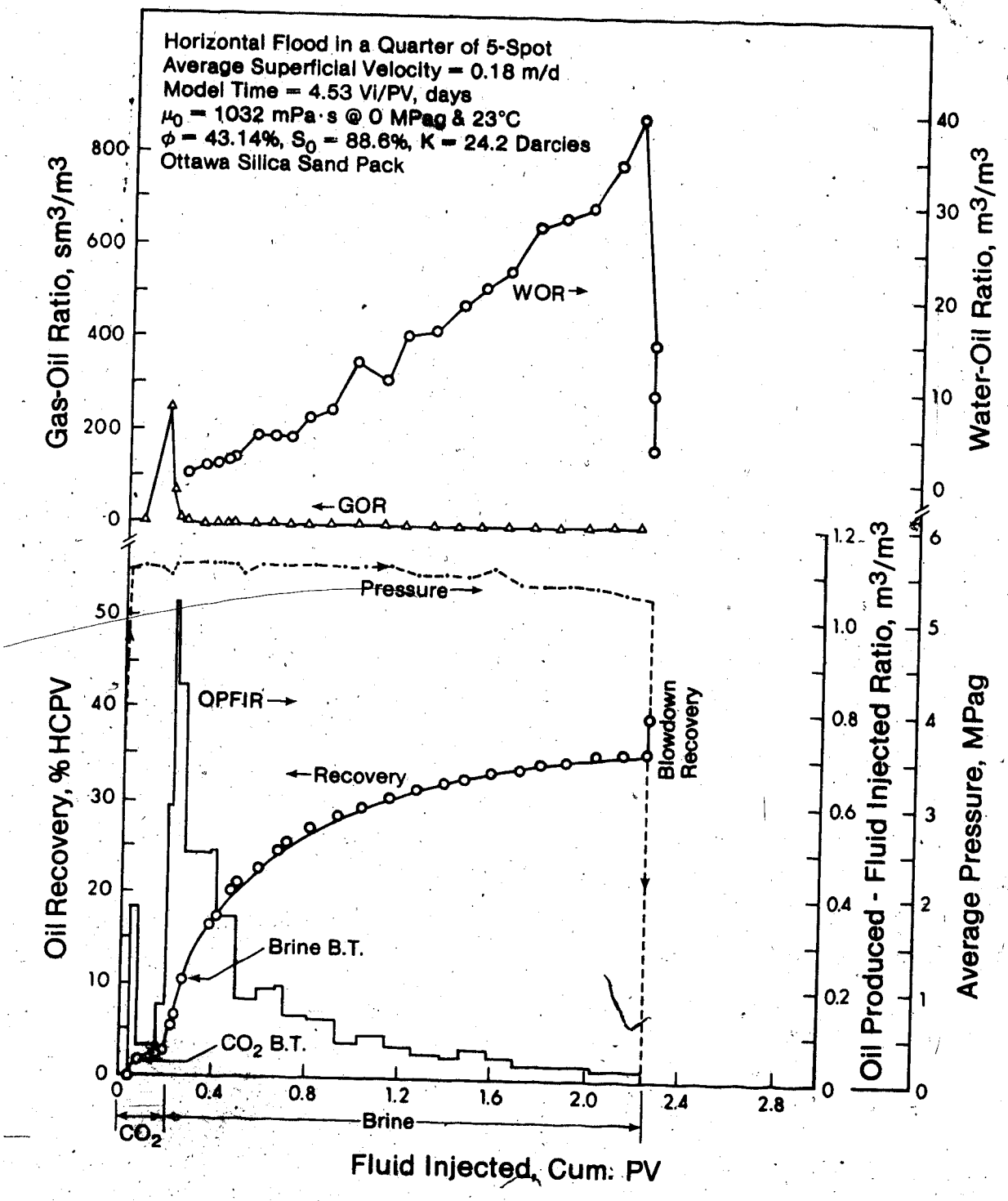


Figure H5 Production History of Run 6

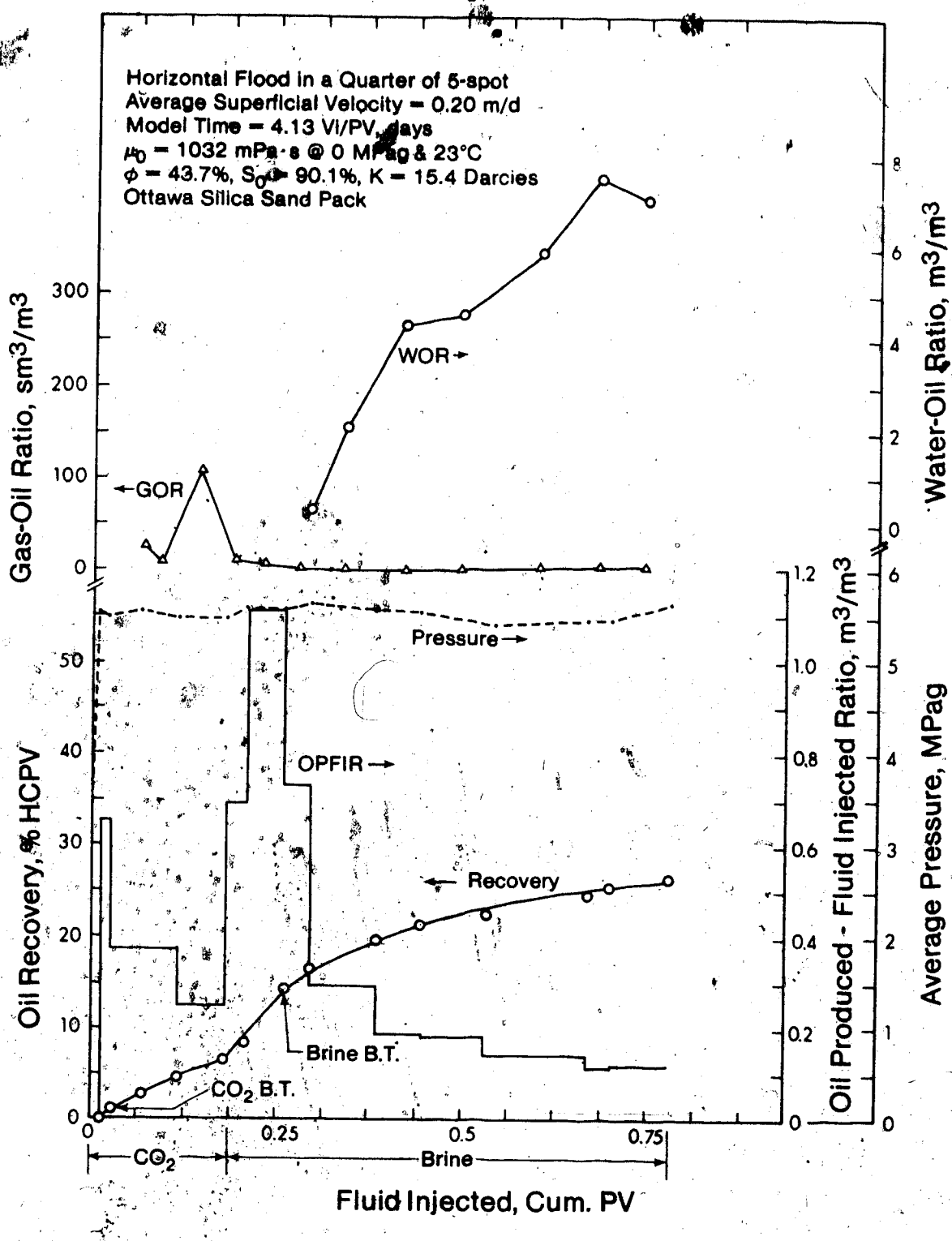


Figure H6 Production History of Run 7

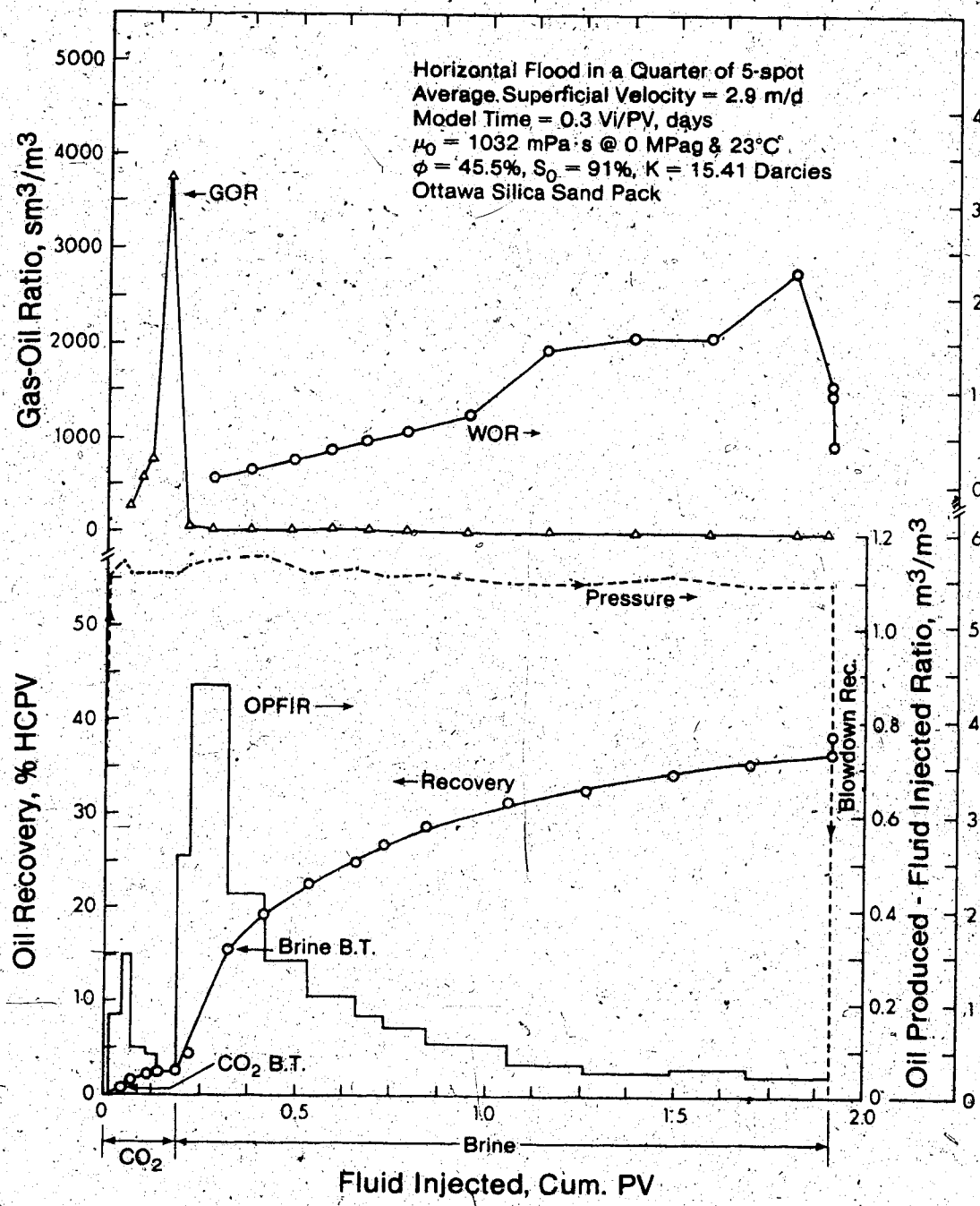


Figure 117 Production History of Run 8

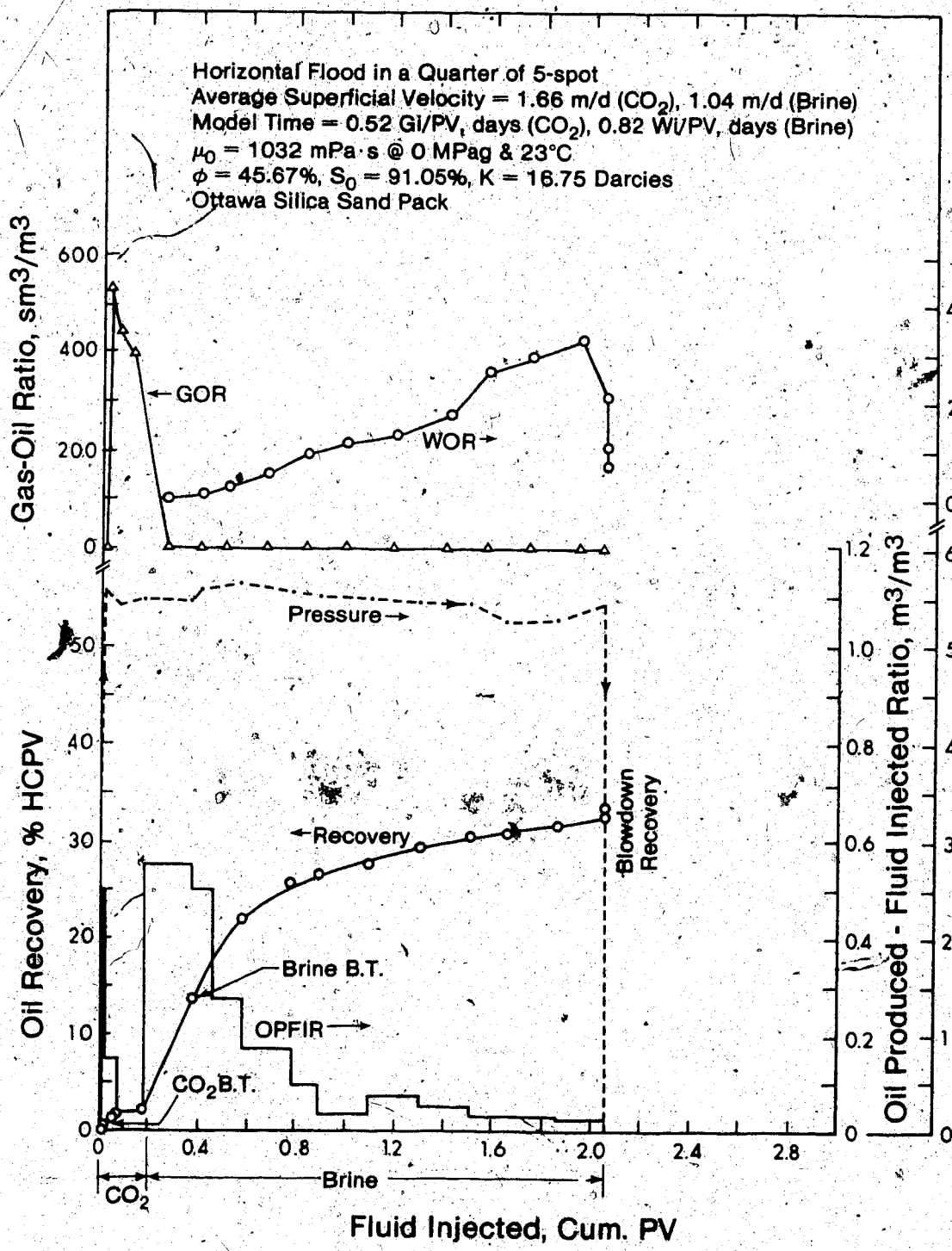


Figure 118 Production History of Run 9

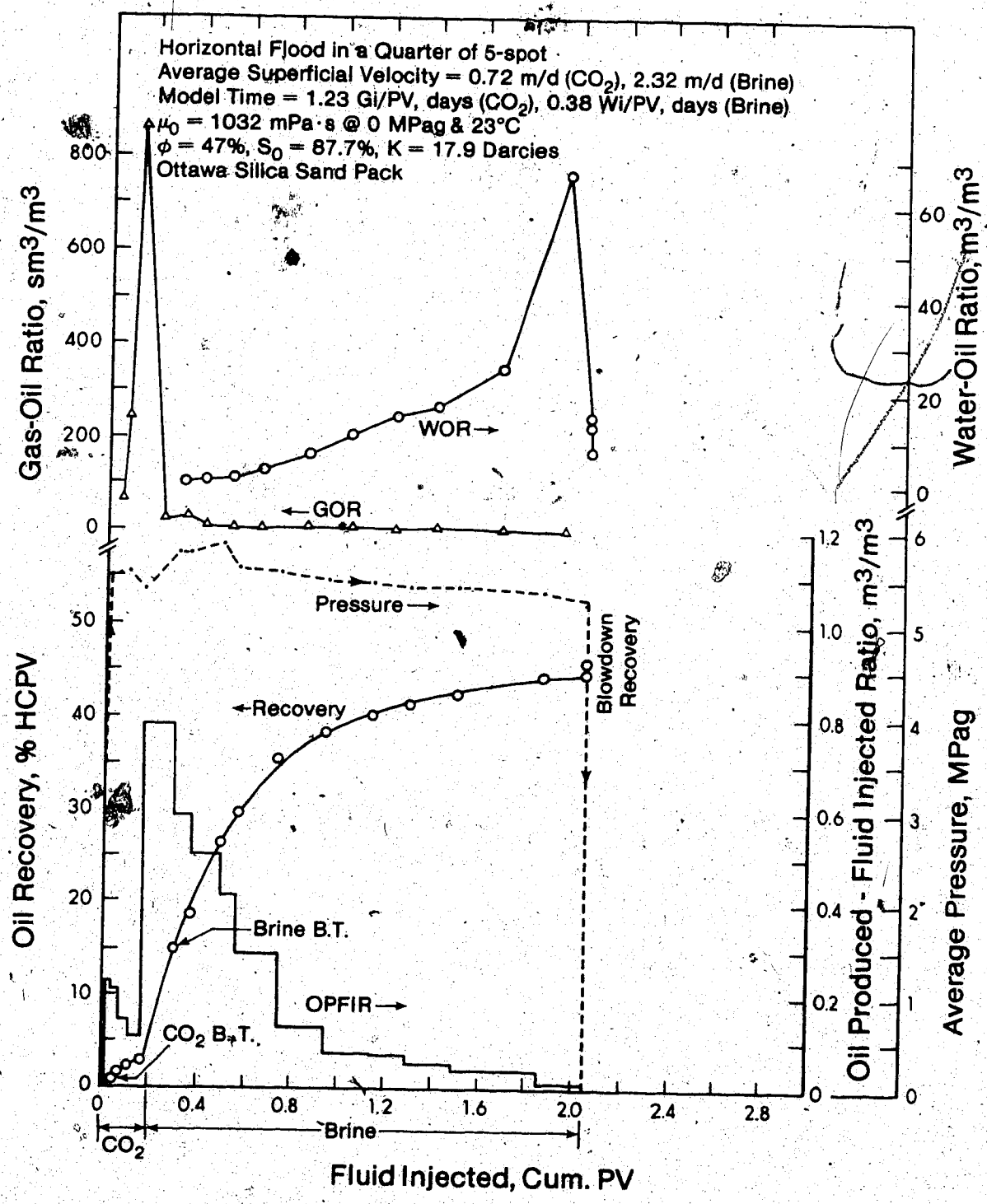


Figure H9 Production History of Run 10

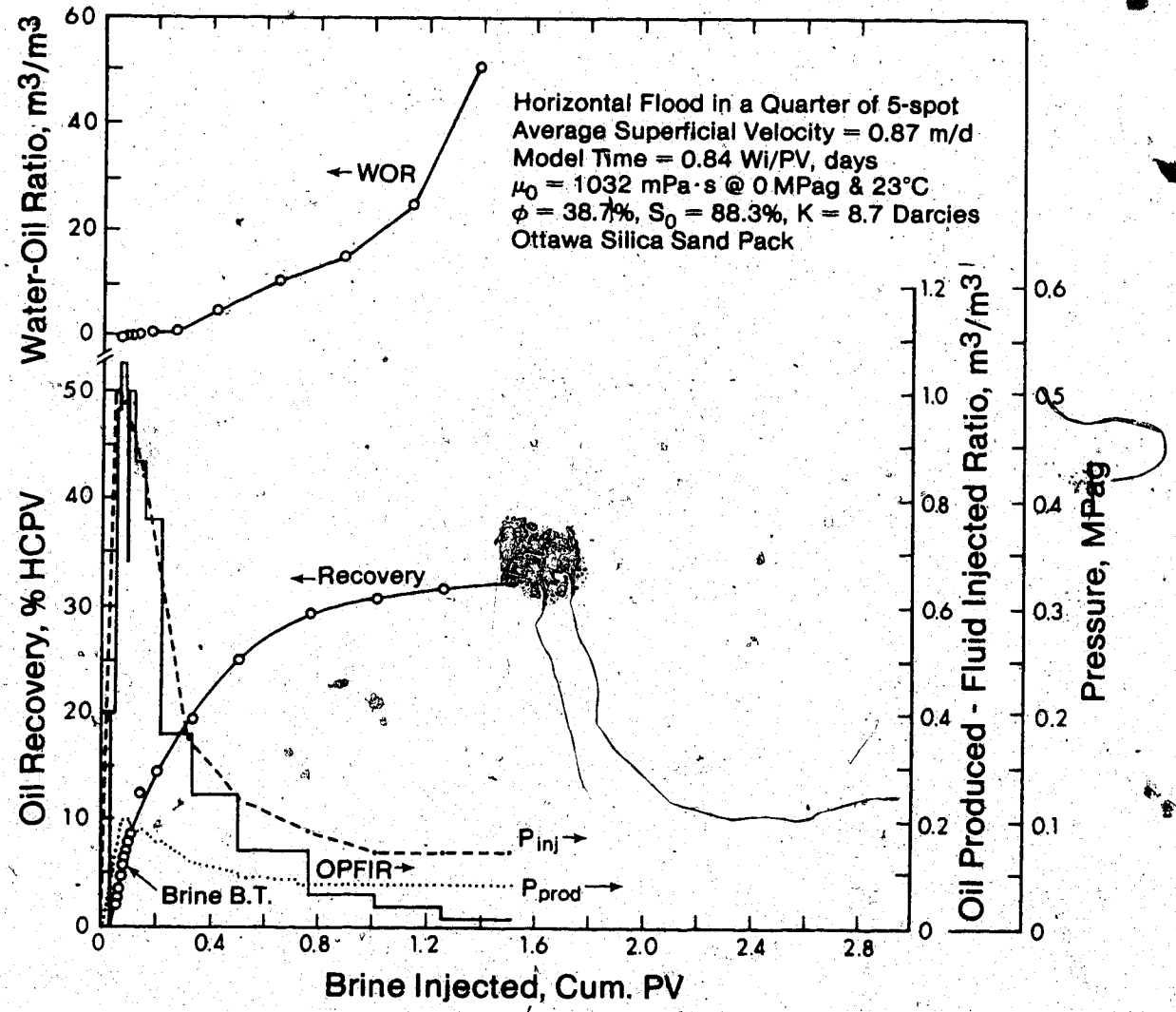


Figure H10 Production History of Run 11

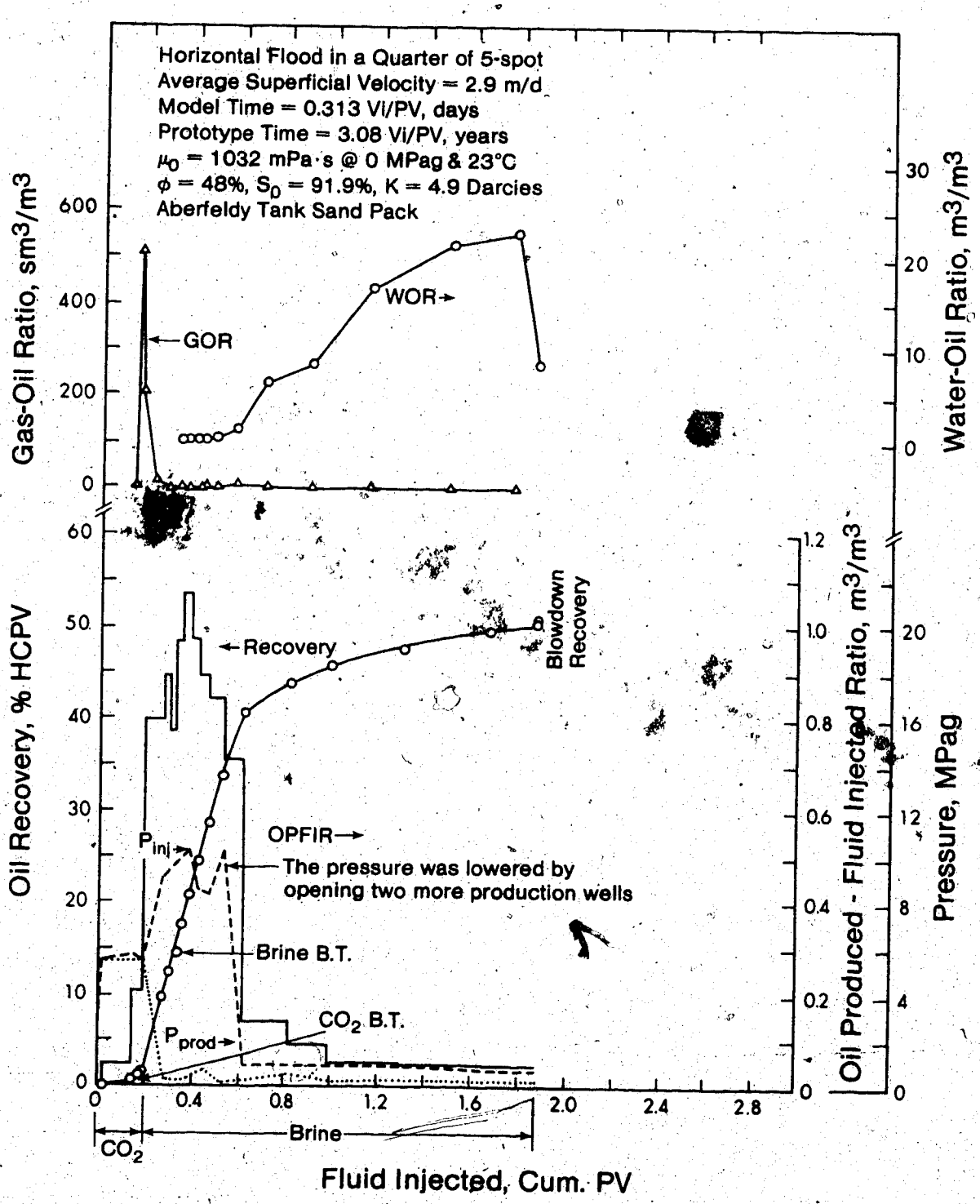


Figure H11 Production History of Run 12

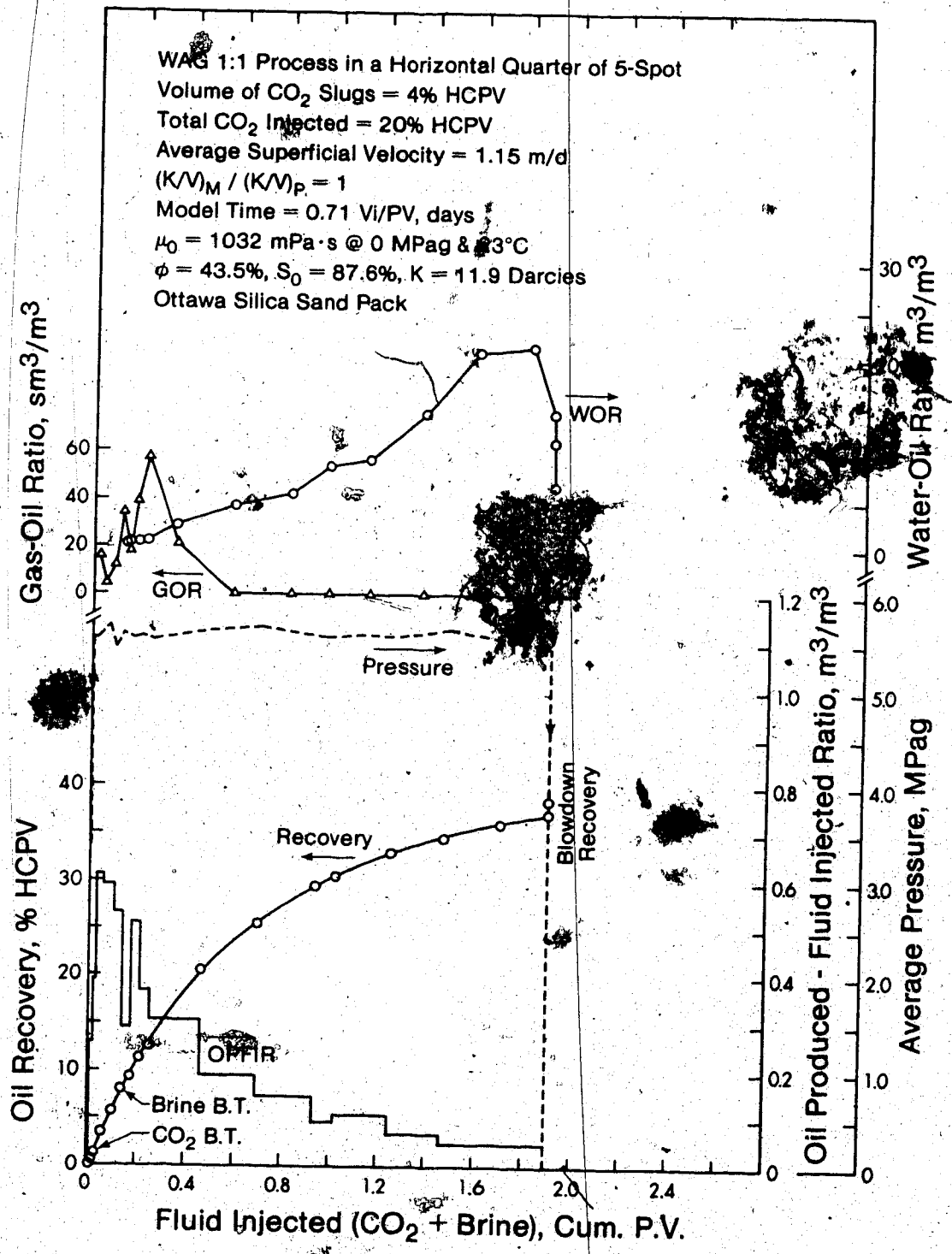


Figure H12 Production History of Run 13

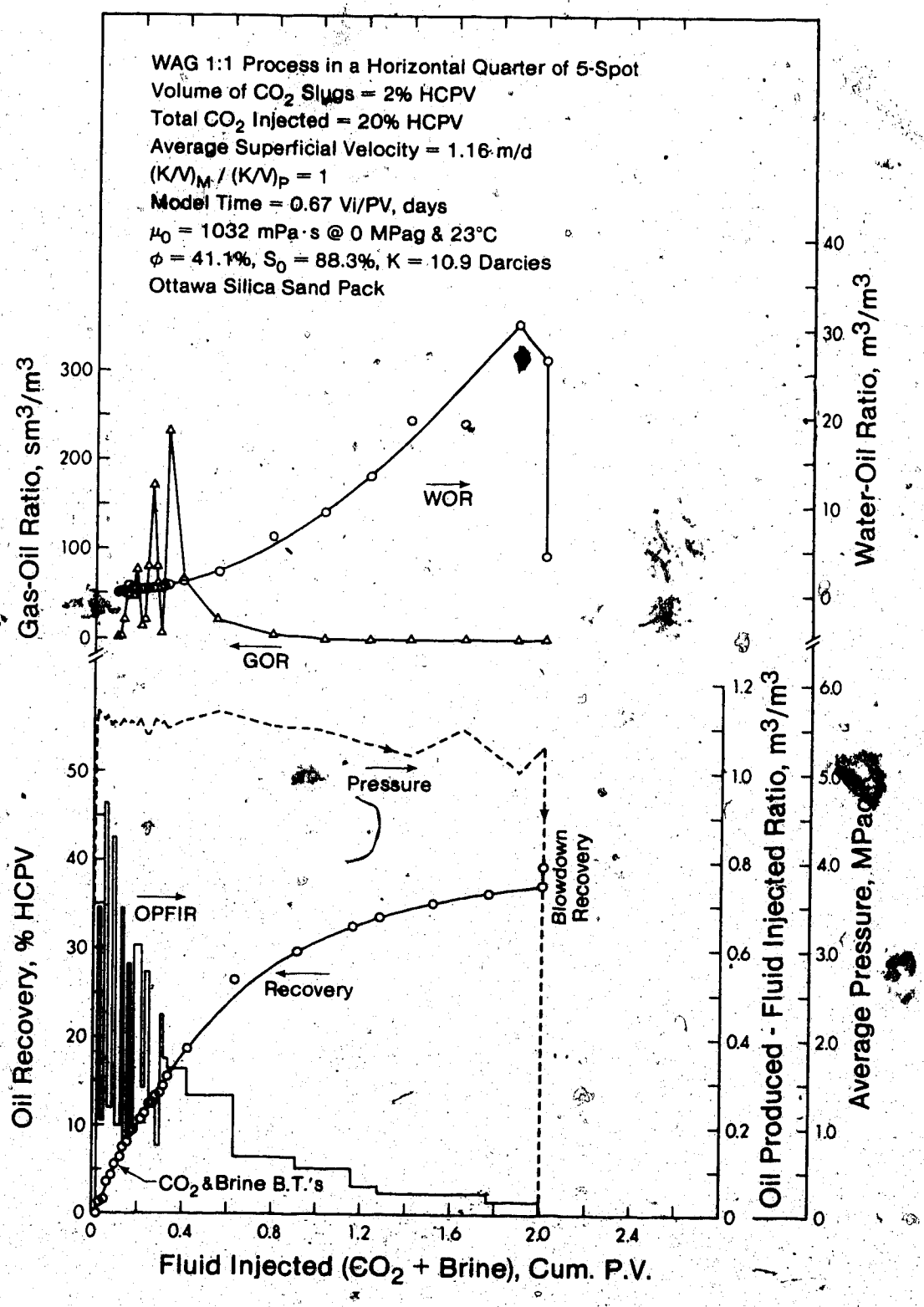


Figure H13 Production History of Run 14

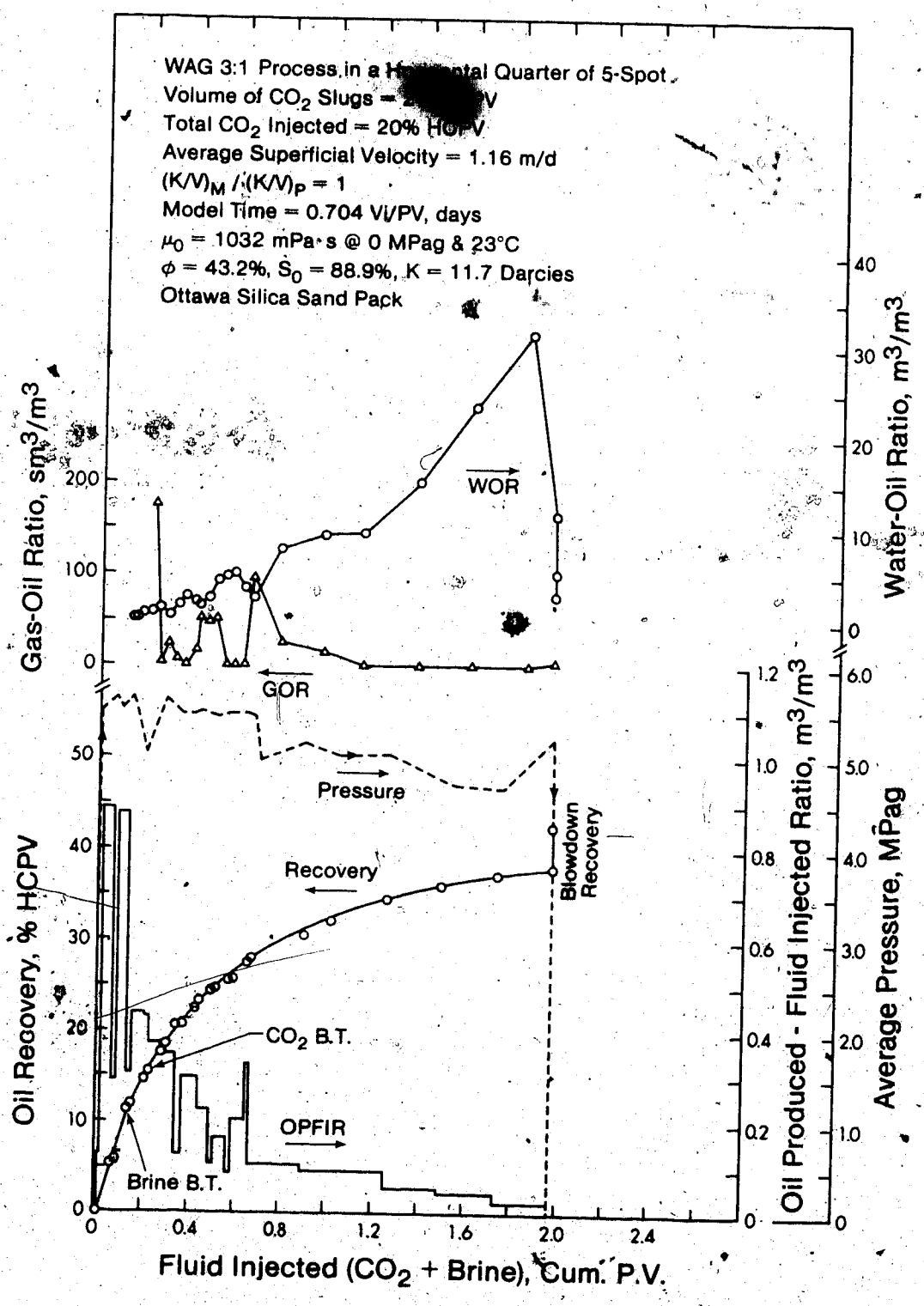


Figure H14 . Production History of Run 15

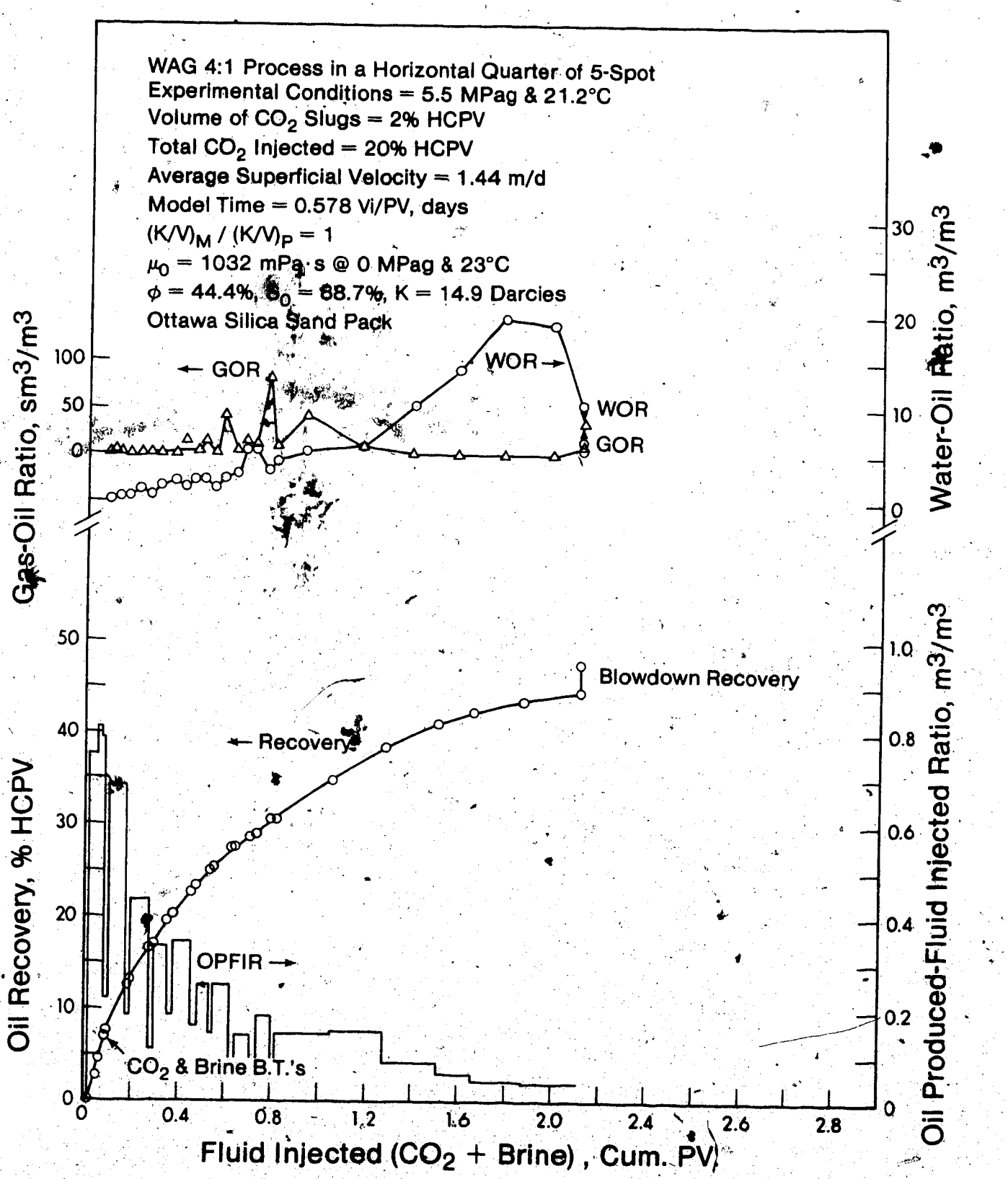


Figure H15 Production History of Run 16

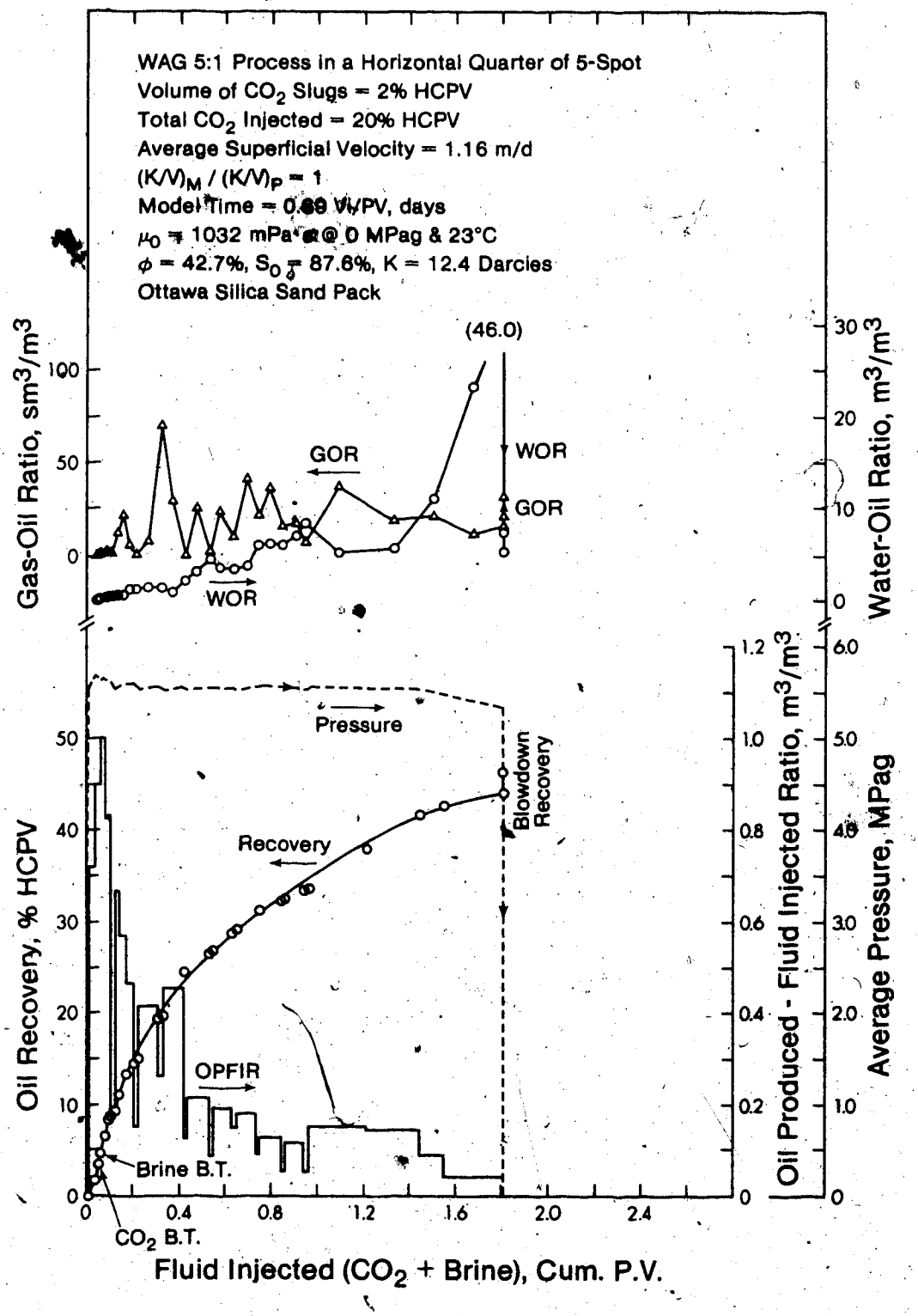


Figure 116 Production History of Run 17

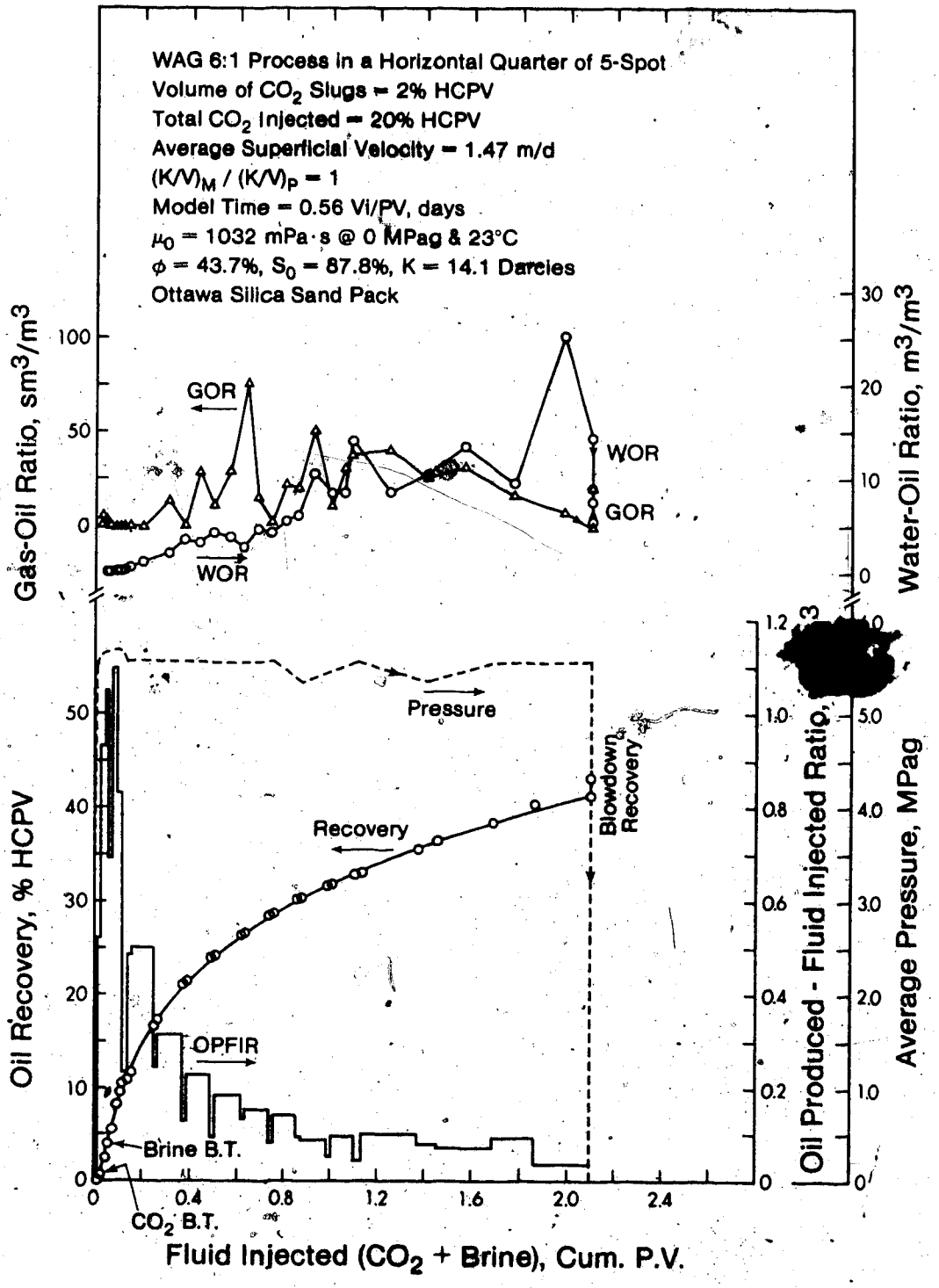


Figure H17 Production History of Run 18

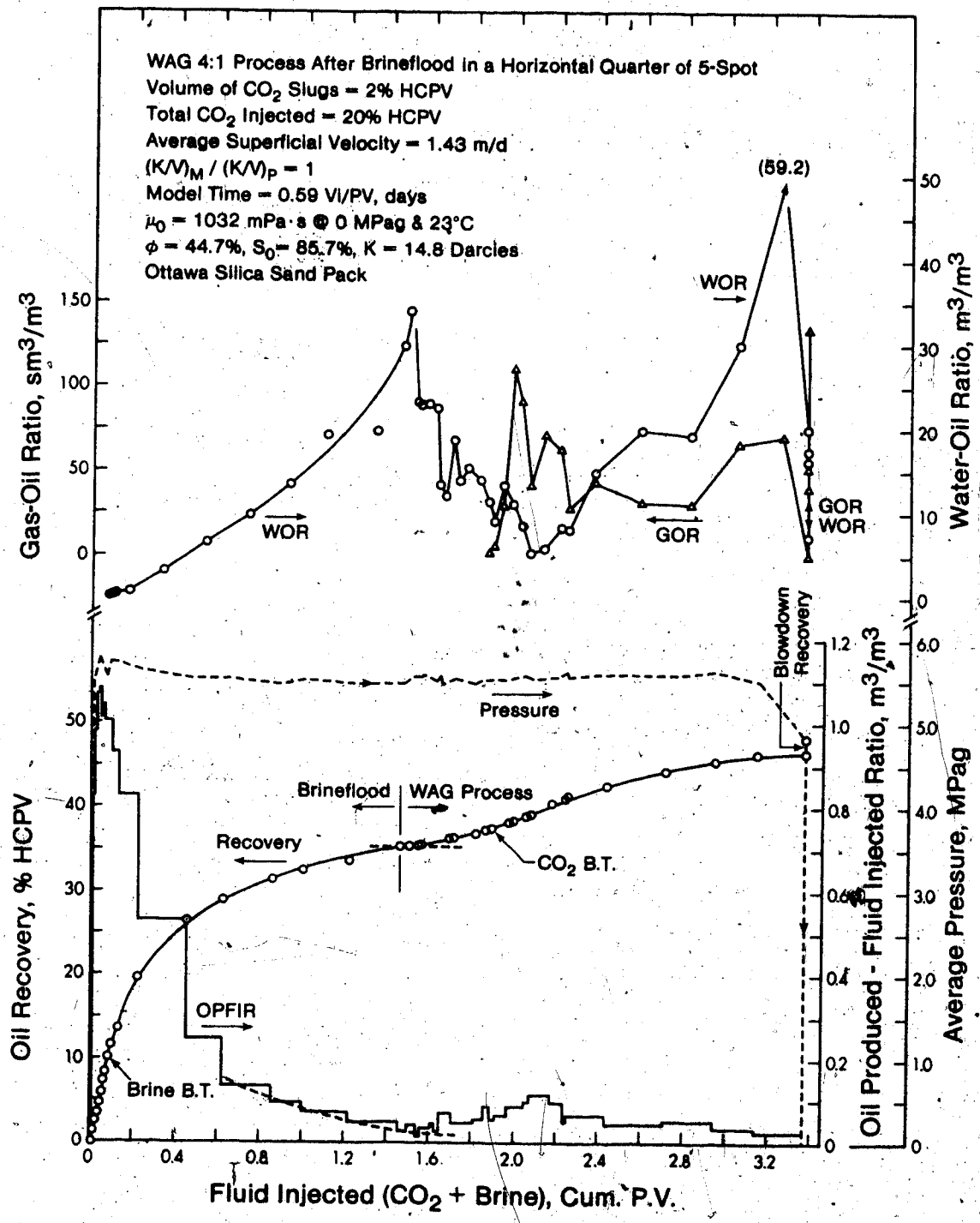


Figure H18 Production History of Run 19

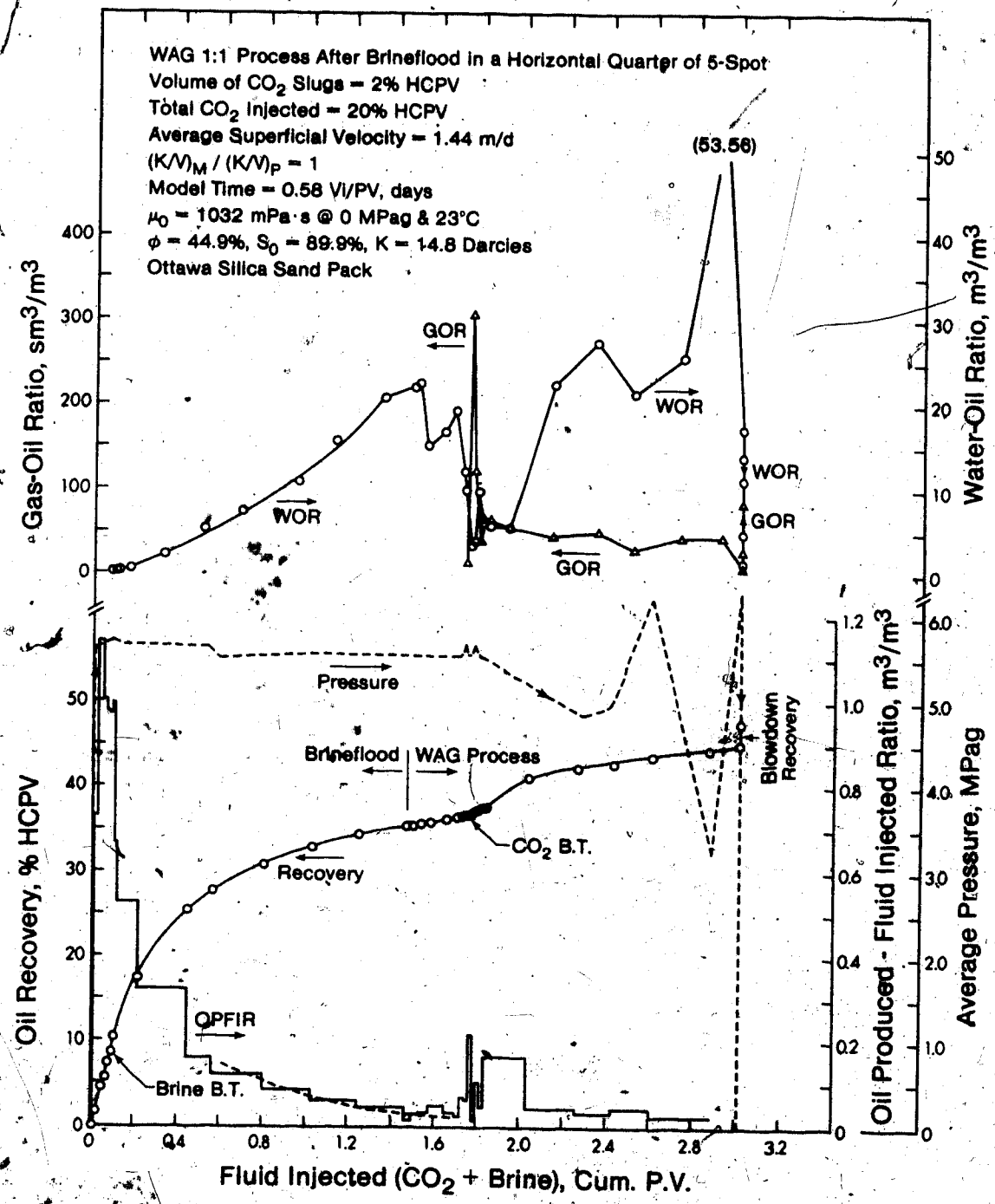


Figure H10 Production History of Run 20

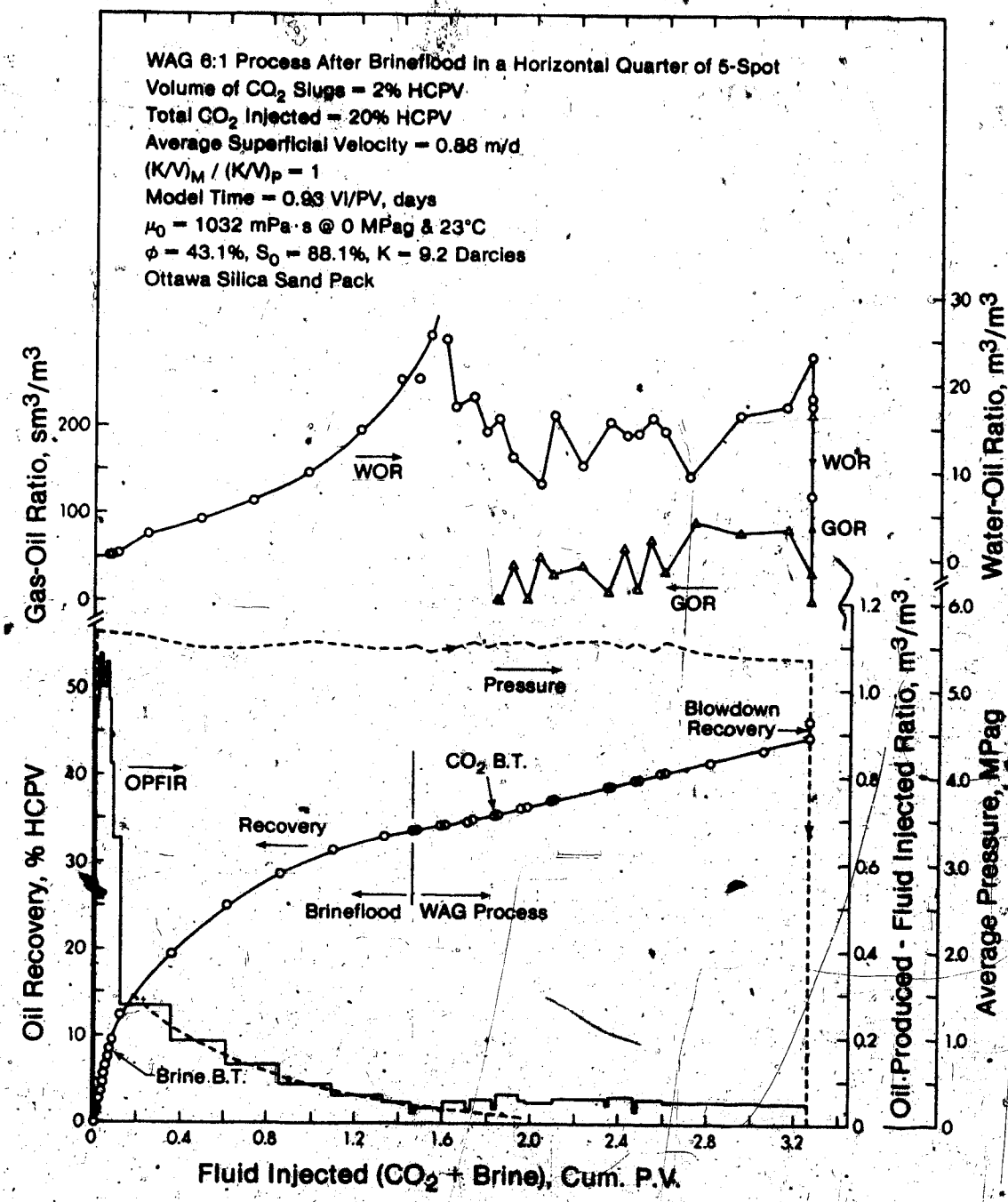


Figure H20 Production History of Run 21

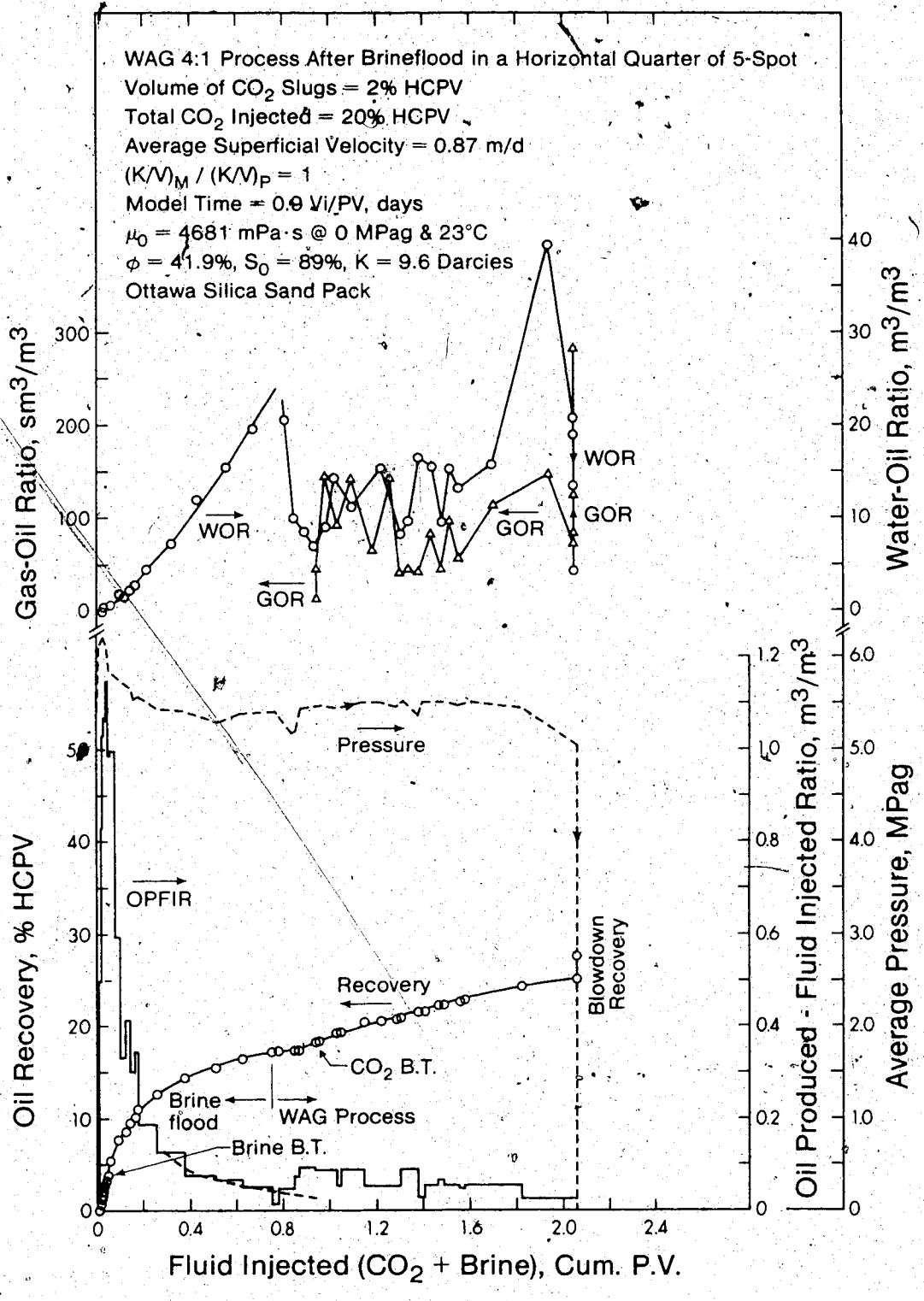


Figure H21 Production History of Run 22

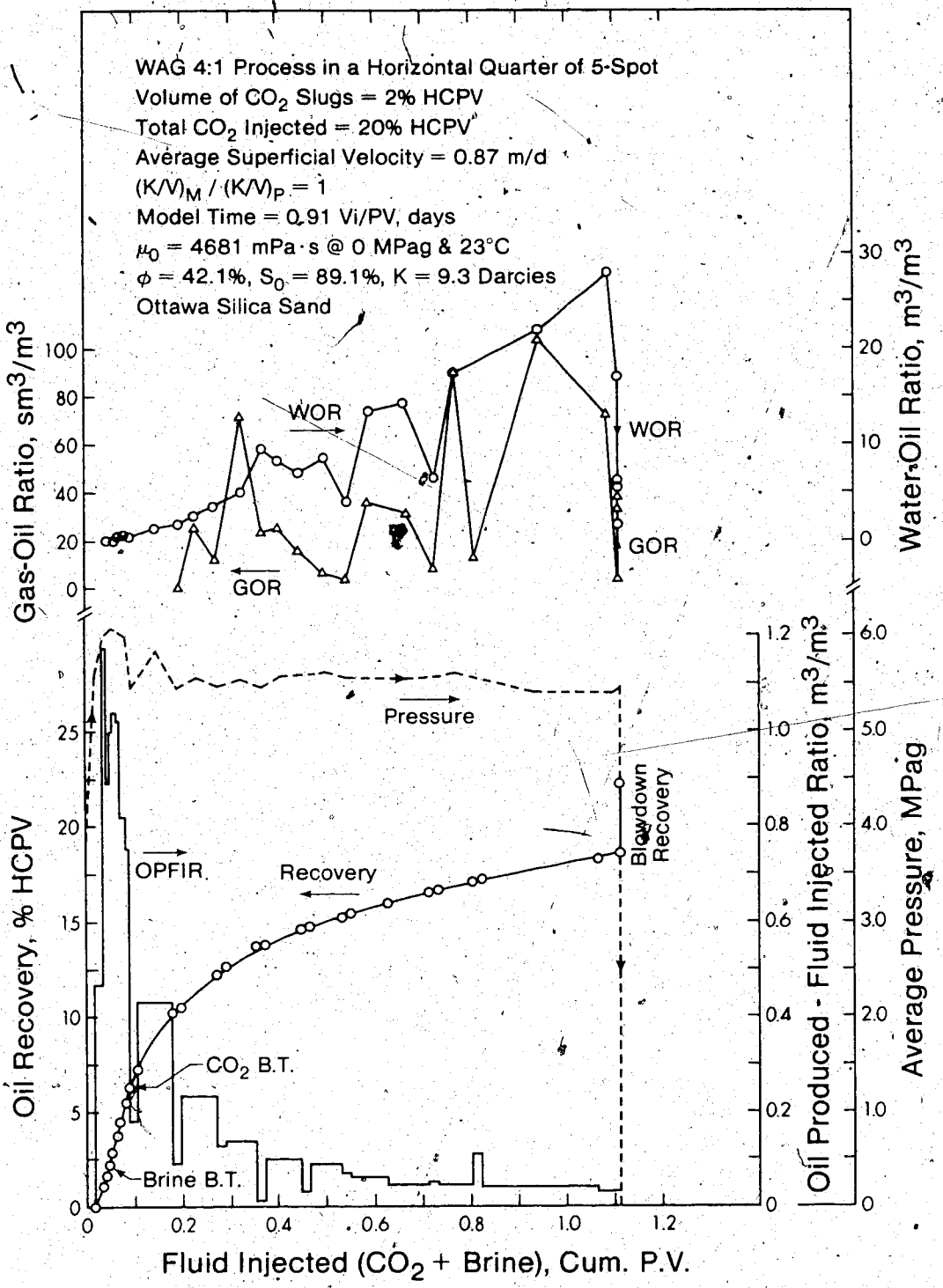


Figure H22 Production History of Run 23

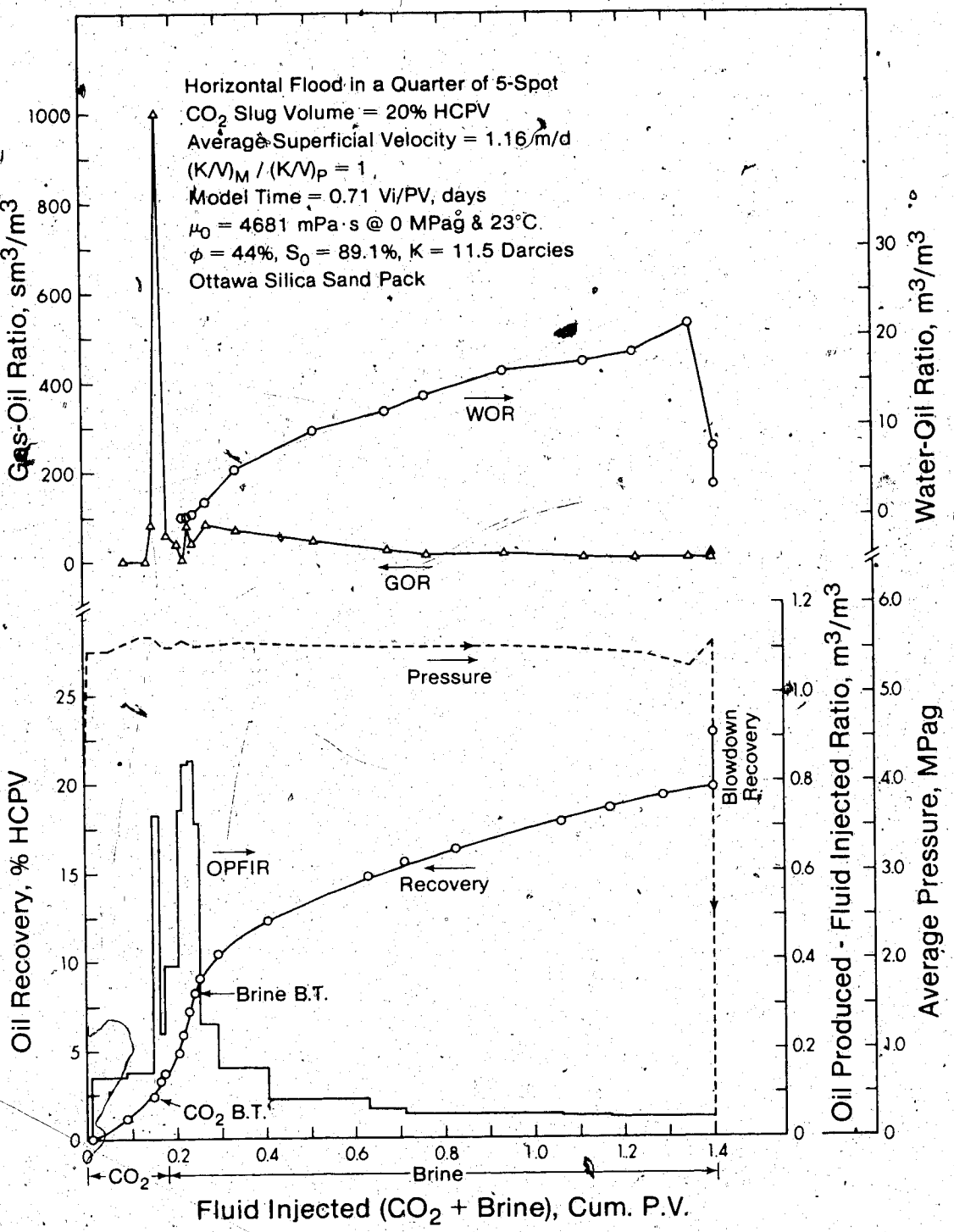


Figure H23 Production History of Run 24

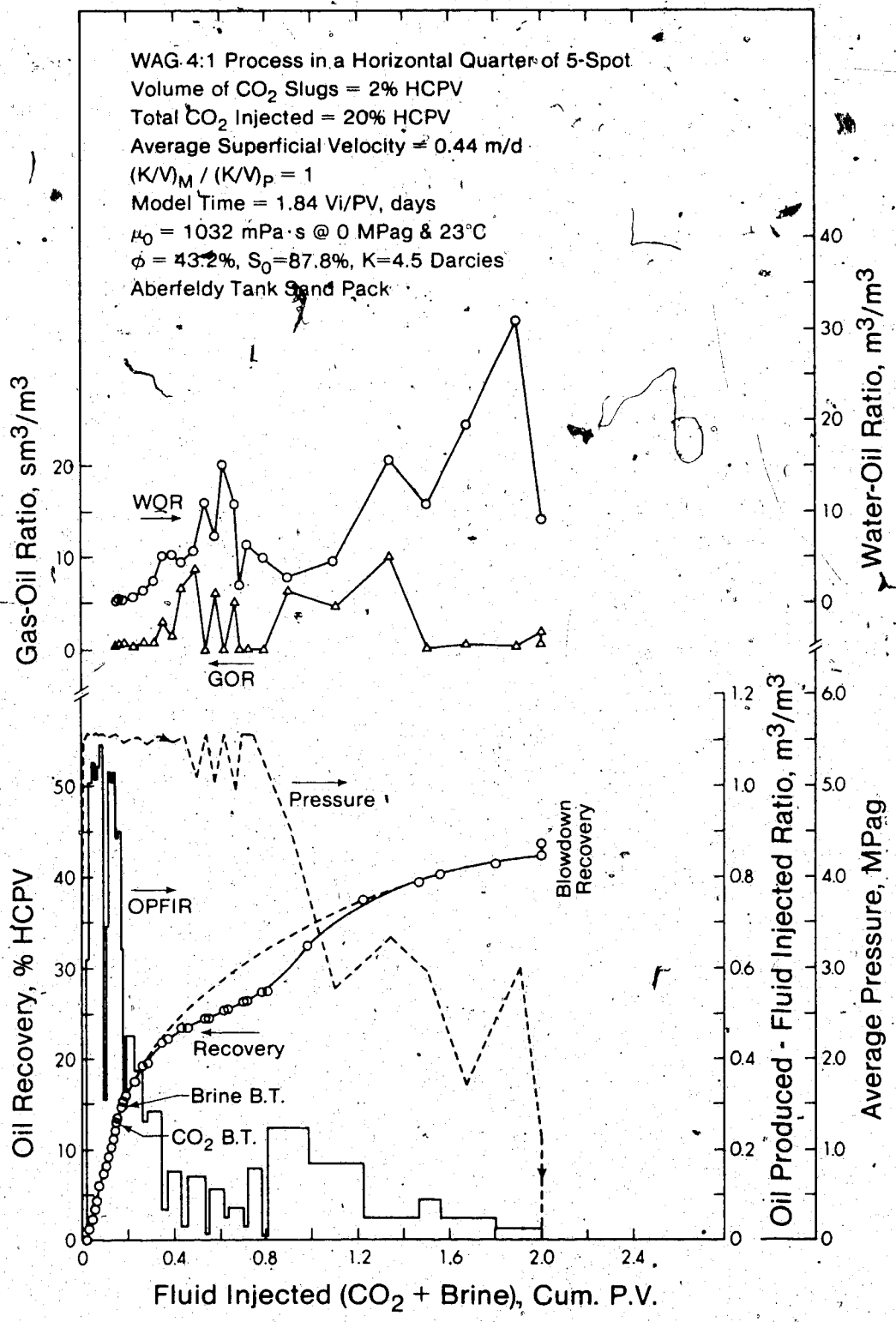


Figure H24 Production History of Run 25